Biological and Medical Physics, Biomedical Engineering

Philipp O.J. Scherer
Sighart F. Fischer

Theoretical Molecular Biophysics

Second Edition

Springer

BIOLOGICAL AND MEDICAL PHYSICS, BIOMEDICAL ENGINEERING

BIOLOGICAL AND MEDICAL PHYSICS, BIOMEDICAL ENGINEERING

The fields of biological and medical physics and biomedical engineering are broad, multidisciplinary and dynamic. They lie at the crossroads of frontier research in physics, biology, chemistry, and medicine. The Biological and Medical Physics, Biomedical Engineering Series is intended to be comprehensive, covering a broad range of topics important to the study of the physical, chemical and biological sciences. Its goal is to provide scientists and engineers with textbooks, monographs, and reference works to address the growing need for information.

Books in the series emphasize established and emergent areas of science including molecular, membrane, and mathematical biophysics; photosynthetic energy harvesting and conversion; information processing; physical principles of genetics; sensory communications; automata networks, neural networks, and cellular automata. Equally important will be coverage of applied aspects of biological and medical physics and biomedical engineering such as molecular electronic components and devices, biosensors, medicine, imaging, physical principles of renewable energy production, advanced prostheses, and environmental control and engineering.

More information about this series at http://www.springer.com/series/3740

Philipp O.J. Scherer · Sighart F. Fischer

Theoretical Molecular Biophysics

Second Edition

Springer

Philipp O.J. Scherer
Physikdepartment T38
Technische Universität München
Garching
Germany

Sighart F. Fischer
Physikdepartment T38
Technische Universität München
Garching
Germany

ISSN 1618-7210 ISSN 2197-5647 (electronic)
Biological and Medical Physics, Biomedical Engineering
ISBN 978-3-662-55670-2 ISBN 978-3-662-55671-9 (eBook)
DOI 10.1007/978-3-662-55671-9

Library of Congress Control Number: 2017948199

This Springer imprint is published by Springer Nature
The registered company is Springer-Verlag GmbH Germany
The registered company address is: Heidelberger Platz 3, 14197 Berlin, Germany

Preface to the Second Edition

The first edition of this book was based on a two-semester course at the physics department of TU München. Approximately, one-third of this edition is new. We tried to give a larger overview over the physical concepts which are applicable to biological systems including established models as well as more recent developments. The major changes are as follows:

The chapter on continuum solvent models contains a discussion of the time dependence of the reaction field after rapid excitation which is useful to understand ultrafast time-resolved experiments on Stokes shift and relaxation processes. The discussion of ion transport includes also models for cooperativity in ion channel kinetics. Here we concentrate on the famous MWC and KNF models for ligand-gated ion channels. In connection with electron transfer theory we present a simple model for the mutual interaction with the medium polarization and discuss the interplay between charge delocalization and self-trapping. Harmonic normal mode approximation and nonadiabatic interactions are discussed in more detail. A new chapter is devoted to intramolecular electronic transitions. The coupling to the radiation field is treated as well with the semiclassical as the quantum mechanical method and the Einstein coefficients for absorption and emission are derived. The chapter ends with an overview of radiationless processes. The chapter on crossing between states has been rewritten and extended. We begin with wavepacket motion for a free particle and a harmonic oscillator, and discuss the classical approximation of nuclear motion. We discuss the adiabatic to diabatic transformation and the definition of quasidiabatic states. The semiclassical approximation to one-dimensional curve crossing leads systematically to the famous Landau–Zener model. The chapter ends with an introduction to conical intersections and the linear vibronic coupling model as a simple example. Two new chapters were added about specific biological systems. First, we discuss charge transfer processes in DNA and describe the contributions of diffusive hopping and superexchange over bridge states. Second, we present rather new models on the photosynthetic reaction center and discuss the possible importance of heterogeneous superexchange and coupled proton motion. We would like to thank Dr. Wolfgang Dietz for his contributions to this chapter, which replaces a rather

short one of the first edition. The molecular motor models include more recent ideas concerning ratchet models and localized reactions. Finally, we added two new chapters to the appendix on the classical approximation of quantum motion and on the complex cotangent function.

Garching, Germany
April 2017

Philipp O.J. Scherer
Sighart F. Fischer

Preface to the First Edition

Biophysics deals with biological systems, such as proteins, which fulfill a variety of functions in establishing living systems. While the biologist uses mostly a phenomenological description, the physicist tries to find the general concepts to classify the materials and dynamics which underly specific processes. The phenomena span a wide range, from elementary processes, which can be induced by light excitation of a molecule, to the communication of living systems. Thus, different methods are appropriate to describe these phenomena. From the point of view of the physicist, this may be continuum mechanics to deal with membranes, hydrodynamics to deal with transport through vessels, bioinformatics to describe evolution, electrostatics to deal with aspects of binding, statistical mechanics to account for temperature and to learn about the role of the entropy, and last but not least quantum mechanics to understand the electronic structure of the molecular systems involved. As can be seen from the title, Molecular Biophysics, this book will focus on systems for which sufficient information on the molecular level is available. Compared to crystallized standard materials studied in solid-state physics, the biological systems are characterized by very big unit cells containing proteins with thousands of atoms. In addition, there is always a certain amount of disorder, so that the systems can be classified as complex. Surprisingly, the functions like a photocycle or the folding of a protein are highly reproducable indicating a paradox situation in relation to the concept of maximum entropy production. It may seem that a proper selection in view of the large diversity of phenomena is difficult, but exactly this is also the challenge taken up within this book. We try to provide basic concepts, applicable to biological systems or soft matter in general. These include entropic forces, phase separation, cooperativity, and transport in complex systems, like molecular motors. We also provide a detailed description for the understanding of elementary processes like electron, proton, and energy transfer, and show how nature is making use of them for instance in photosynthesis. Prerequisites for the reader are a basic understanding in the fields of mechanics, electrostatics, quantum mechanics, and statistics. This means the book is for graduate students, who want to specialize in the field of biophysics. As we try to derive all equations in detail, the book may also be useful to physicists or chemists who are interested in applications of statistical

mechanics or quantum mhemistry to biological systems. The book is the outcome of a course presented by the authors as a basic element of the newly established graduation branch 'Biophysics' in the Physics Department of the Technische Universitaet Muenchen.

The authors would like to thank Dr. Florian Dufey and Dr. Robert Raupp–Kossmann for their contributions during the early stages of the evolving manuscript.

Garching, Germany
August 2009

Philipp O.J. Scherer
Sighart F. Fischer

Contents

Part I
Statistical Mechanics of Biopolymers

Chapter 1
Random Walk Models for the Conformation

In this chapter we study simple statistical models for the entropic forces which are due to the large number of conformations characteristic for biopolymers like DNA or proteins (Fig. 1.1). First we discuss the freely jointed chain model. We evaluate the statistical distribution of end to end distances and discuss the force-extension relation. Then we study a two component model of a polymer chain which is composed of two types of units, which may interconvert. Interactions between the segments are included and explain the appearance of a very flat force-extension relationship, where a small force may lead to much larger changes in length than without interaction.

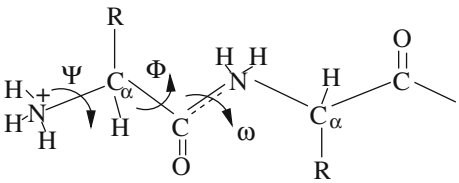

Fig. 1.1 Conformation of a protein. The relative orientation of two successive protein residues can be described by three angles (Ψ, Φ, ω). For a real protein the ranges of these angles are restricted by steric interactions, which are neglected in simple models

1.1 The Freely Jointed Chain

We consider a three-dimensional chain (Fig. 1.2) consisting of M units. The configuration can be described by a point in a 3(M+1)-dimensional space

$$(\mathbf{r}_0, \mathbf{r}_2 \ldots \mathbf{r}_M). \tag{1.1}$$

P.O.J. Scherer and S.F. Fischer, *Theoretical Molecular Biophysics*,
Biological and Medical Physics, Biomedical Engineering,
DOI 10.1007/978-3-662-55671-9_1

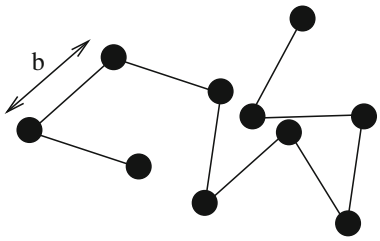

Fig. 1.2 Freely jointed chain with constant bond length b

The M bond vectors

$$\mathbf{b}_i = \mathbf{r}_i - \mathbf{r}_{i-1} \tag{1.2}$$

have a fixed length $|\mathbf{b}_i| = b$ and are randomly oriented . This can be described by a distribution function

$$P(\mathbf{b}_i) = \frac{1}{4\pi b^2}\delta(|b_i| - b). \tag{1.3}$$

Since the different units are independent, the joint probability distribution factorizes

$$P(\mathbf{b}_1 \ldots \mathbf{b}_M) = \prod_{i=1}^{M} P(\mathbf{b_i}). \tag{1.4}$$

There is no excluded volume interaction between any two monomers. Obviously the end-to-end distance

$$\mathbf{R} = \sum_{i=1}^{N} \mathbf{b}_i \tag{1.5}$$

has an average value of $\overline{\mathbf{R}} = 0$ since

$$\overline{\mathbf{R}} = \sum \overline{\mathbf{b}_i} = M \int \mathbf{b_i} P(\mathbf{b}_i) = 0. \tag{1.6}$$

The second moment is

$$\overline{R^2} = \overline{\left(\sum_i \mathbf{b}_i \sum_j \mathbf{b}_j \right)} = \sum_{i,j} \overline{\mathbf{b}_i \mathbf{b}_j} \tag{1.7}$$

$$= \sum_i \overline{b_i^2} + \sum_{i \neq j} \overline{\mathbf{b}_i \mathbf{b}_j} = Mb^2.$$

1.1.1 Entropic Elasticity

The distribution of the end-to-end vector is

$$P(\mathbf{R}) = \int P(\mathbf{b}_1 \dots \mathbf{b}_M)\delta\left(\mathbf{R} - \sum \mathbf{b}_i\right) d^3b_1 \dots d^3b_M. \tag{1.8}$$

This integral can be evaluated by replacing the delta function by the Fourier integral

$$\delta(\mathbf{R}) = \frac{1}{(2\pi)^3}\int \mathrm{e}^{-\mathrm{i}\mathbf{k}\mathbf{R}} d^3k \tag{1.9}$$

which gives

$$P(\mathbf{R}) = \int d^3k \mathrm{e}^{-\mathrm{i}\mathbf{k}\mathbf{R}} \prod_{i=1}^{M}\left(\int \frac{1}{4\pi b^2}\delta(|\mathbf{b}_i| - b)\mathrm{e}^{\mathrm{i}\mathbf{k}\mathbf{b}_i} d^3b_i\right). \tag{1.10}$$

The inner integral can be evaluated in polar coordinates

$$\int \frac{1}{4\pi b^2}\delta(|\mathbf{b}_i| - b)\mathrm{e}^{\mathrm{i}\mathbf{k}\mathbf{b}_i} d^3b_i \tag{1.11}$$

$$= \int_0^{2\pi} d\phi \int_0^{\infty} b_i^2 db_i \frac{1}{4\pi b^2}\delta(|b_i| - b)\int_0^{\pi} \sin\theta d\theta \mathrm{e}^{\mathrm{i}kb_i\cos\theta}.$$

The integral over θ gives

$$\int_0^{\pi} \sin\theta d\theta \mathrm{e}^{\mathrm{i}kb_i\cos\theta} = \frac{2\sin kb_i}{kb_i} \tag{1.12}$$

and hence

$$\begin{aligned}\int \frac{1}{4\pi b^2}\delta(|\mathbf{b}_i| - b)\mathrm{e}^{\mathrm{i}\mathbf{k}\mathbf{b}_i} d^3b_i &= 2\pi\int_0^{\infty} db_i \frac{1}{4\pi b^2}\delta(b_i - b)b_i^2\frac{2\sin kb_i}{kb_i} \\ &= \frac{\sin kb}{kb}\end{aligned} \tag{1.13}$$

and finally we have

$$P(\mathbf{R}) = \frac{1}{(2\pi)^3}\int d^3k \mathrm{e}^{-\mathrm{i}\mathbf{k}\mathbf{R}}\left(\frac{\sin kb}{kb}\right)^M. \tag{1.14}$$

The function

$$\left(\frac{\sin kb}{kb}\right)^M \tag{1.15}$$

has a very sharp maximum at $kb = 0$. For large M, it can be approximated quite accurately by a Gaussian

$$\left(\frac{\sin kb}{kb}\right)^M \approx \mathrm{e}^{-M\frac{1}{6}k^2b^2} \tag{1.16}$$

which gives

$$P(\mathbf{R}) \approx \frac{1}{(2\pi)^3}\int d^3k\mathrm{e}^{-\mathrm{i}\mathbf{k}\mathbf{R}}\mathrm{e}^{-\frac{M}{6}k^2b^2} = \left(\frac{3}{2\pi b^2 M}\right)^{3/2}\mathrm{e}^{-3R^2/(2b^2M)}. \tag{1.17}$$

We consider $\mathbf{R}$ as a macroscopic variable. The free energy is (no internal degrees of freedom, $E = 0$)

$$F = -TS = -k_BT\ln P(\mathbf{R}) = \frac{3R^2}{2b^2M}k_BT + \text{const.} \tag{1.18}$$

The quadratic dependence on L is very similar to a Hookean spring. For a potential energy

$$V = \frac{k_s}{2}x^2 \tag{1.19}$$

the probability distribution of the coordinate is

$$P(x) = \sqrt{\frac{k_s}{2\pi k_bT}}\mathrm{e}^{-k_sx^2/2k_BT} \tag{1.20}$$

which gives a free energy of

$$F = -k_BT\ln P = \text{const} + \frac{k_sx^2}{2}. \tag{1.21}$$

By comparison, the apparent spring constant is

$$k_s = \frac{3k_BT}{Mb^2}\,. \tag{1.22}$$

1.1.2 Force–Extension Relation

We consider now a chain with one fixed end and an external force acting in x-direction at the other end (Fig. 1.3) [1].

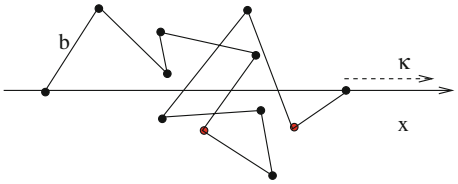

Fig. 1.3 Freely jointed chain with external force

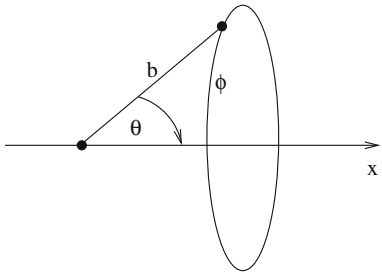

Fig. 1.4 Projection of the bond vector

The projection of the i-th segment onto the x-axis has a length of (Fig. 1.4)

$$b_i = -b\cos\theta \in [-b, b]. \tag{1.23}$$

We discretize the continuous range of b_j by dividing the interval $[-b, b]$ into n bins of width $\Delta b = \frac{2b}{n}$ corresponding to the discrete values $l_i,\ i = 1 \ldots n$. The chain members are divided into n groups according to their bond projections b_j. The number of units in each group is denoted by M_i so that

$$\sum_{i=1}^{n} M_i = M \tag{1.24}$$

and the end-to-end length is

$$\sum_{i=1}^{n} l_i M_i = L. \tag{1.25}$$

The probability distribution is

$$P(\theta, \phi)d\theta d\phi = \frac{\sin(\theta)d\theta d\phi}{4\pi}. \tag{1.26}$$

Since we are only interested in the probability of the l_i , we integrate over ϕ

$$P(\theta)d\theta = \frac{\sin(\theta)d\theta}{2} \tag{1.27}$$

and transform variables to have

$$P(l)dl = P(-b\cos\theta)d(-b\cos\theta) = \frac{1}{2b}d(-b\cos\theta) = \frac{1}{2b}dl. \tag{1.28}$$

The canonical partition function is

$$Z(L, M, T) = \sum_{\{M_i\}\sum M_i l_i = L} \frac{M!}{\prod_j M_j!} \prod_i z_i^{M_i} = \sum_{\{M_i\}} M! \prod_i \frac{z_i^{M_i}}{M_i!}. \tag{1.29}$$

The $z_i = z$ are the independent partition functions of the single units which we assume as independent of i. The degeneracy factor $\frac{M!}{\prod M_i!}$ counts the number of microstates for a certain configuration $\{M_i\}$. The summation is only over configurations with a fixed end-to-end length. This makes the evaluation rather complicated. Instead, we introduce a new partition function by considering an ensemble with fixed force and fluctuating length

$$\Delta(\kappa, M, T) = \sum_L Z(L, M, T)\mathrm{e}^{\kappa L/k_B T}. \tag{1.30}$$

Approximating the logarithm of the sum by the logarithm of the maximum term we see that

$$-k_B T \ln \Delta = -k_B T \ln Z - \kappa L \tag{1.31}$$

($-\kappa L$ corresponds to $+pV$) gives the Gibbs free enthalpy

$$G(\kappa, M, T) = F - \kappa L. \tag{1.32}$$

In this new ensemble the summation over L simplifies the partition function

$$\begin{aligned}\Delta &= \sum_{\{M_i\}} \mathrm{e}^{\kappa \sum M_i l_i/k_B T} M! \prod \frac{z^{M_i}}{M_i!} \\ &= \sum_{\{M_i\}} M! \prod \frac{(z\mathrm{e}^{\kappa l_i/k_B T})^{M_i}}{M_i!} \\ &= \left(\sum z\mathrm{e}^{\kappa l_i/k_B T}\right)^M = \xi(\kappa, T)^M.\end{aligned} \tag{1.33}$$

Now returning to a continuous distribution of $l_i = -b\cos\theta$ we have to evaluate

$$\xi = \int_{-b}^{b} P(l)dl \quad z\mathrm{e}^{\kappa l/k_B T} = z\frac{\sinh t}{t} \tag{1.34}$$

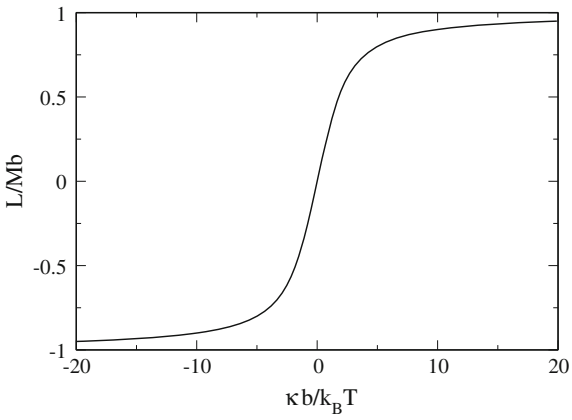

Fig. 1.5 Force - extension relation

with

$$t = \frac{\kappa b}{k_B T}. \tag{1.35}$$

From

$$dG = -SdT - Ld\kappa \tag{1.36}$$

we find (Fig. 1.5)

$$\begin{aligned} L &= -\frac{\partial G}{\partial \kappa}|_T \\ &= \frac{\partial}{\partial \kappa}\left(Mk_BT \ln\left(\frac{z}{\frac{\kappa b}{k_B T}} \sinh \frac{\kappa b}{k_B T} \right)\right) \\ &= Mk_BT \left(-\frac{1}{\kappa} + \frac{b}{k_B T} \coth\left(\frac{\kappa b}{k_B T} \right)\right) = Mb\mathfrak{L}\left(\frac{\kappa b}{k_B T} \right) \end{aligned}$$

with the Langevin function

$$\mathfrak{L}(x) = \coth(x) - \frac{1}{x}. \tag{1.37}$$

1.2 Two Component Model

A one-dimensional random walk model can be applied to a polymer chain which is composed of two types of units (named α and β) , which may interconvert (Fig. 1.6). This model is for instance applicable to the *dsDNA* $\rightarrow$ *SDNA* transition or the

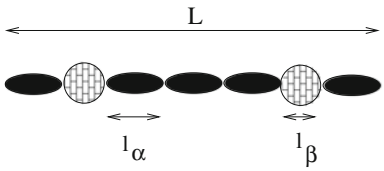

Fig. 1.6 Two component model

α-Helix $\rightarrow$ random coil transition of proteins which show up as a plateau in the force-extension curve [1, 2].

We follow the treatment given in [1] which is based on an explicit evaluation of the partition function. Alternatively, the two component model can be mapped onto a one-dimensional Ising model, which can be solved by the transfer matrix method [3, 4]. We assume that of the overall M units M_α are in the α-configuration and $M - M_\alpha$ are in the β-configuration. The lengths of the two conformers are l_α and l_β, respectively.

1.2.1 Force-Extension Relation

The total length is given by

$$L = M_\alpha l_\alpha + (M - M_\alpha) l_\beta = M_\alpha (l_\alpha - l_\beta) + M l_\beta. \tag{1.38}$$

The number of configurations with length L is given by

$$\Omega(L) = \Omega\left(M_\alpha = \frac{L - M l_\beta}{l_\alpha - l_\beta}\right) = \frac{M!}{\left(\frac{L - M l_\beta}{l_\alpha - l_\beta}\right)! \left(\frac{M l_\alpha - L}{l_\alpha - l_\beta}\right)!}. \tag{1.39}$$

From the partition function

$$Z = z_\alpha^{M_\alpha} z_\beta^{M - M_\alpha} \Omega = z_\alpha^{\frac{L - M l_\beta}{l_\alpha - l_\beta}} z_\beta^{\frac{M l_\alpha - L}{l_\alpha - l_\beta}} \Omega \tag{1.40}$$

application of Stirling's approximation gives for the free energy

$$\begin{aligned} F &= -k_B T \ln Z \\ &= -k_B T \frac{L - M l_\beta}{l_\alpha - l_\beta} \ln z_\alpha - k_B T \frac{M l_\alpha - L}{l_\alpha - l_\beta} \ln z_\beta - k_B T \, (M \ln M - M) \\ &= -k_B T \left\{ -\left(\frac{L - M l_\beta}{l_\alpha - l_\beta}\right) \ln \left(\frac{L - M l_\beta}{l_\alpha - l_\beta}\right) + \left(\frac{L - M l_\beta}{l_\alpha - l_\beta}\right) \right. \\ &\quad \left. - \left(\frac{M l_\alpha - L}{l_\alpha - l_\beta}\right) \ln \left(\frac{M l_\alpha - L}{l_\alpha - l_\beta}\right) + \left(\frac{M l_\alpha - L}{l_\alpha - l_\beta}\right) \right\}. \end{aligned} \tag{1.41}$$

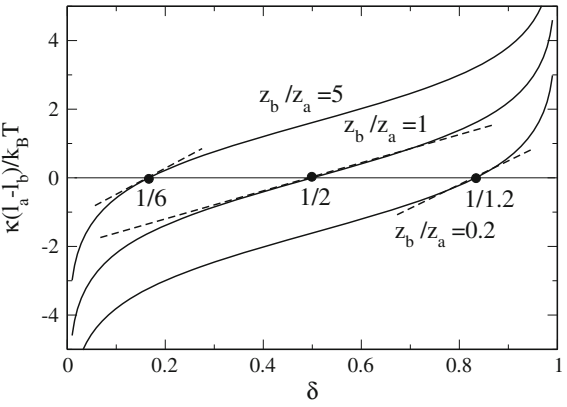

Fig. 1.7 Force - extension relation for the 2-component model

The derivative of the free energy gives the force-extension relation (Fig. 1.7)

$$\kappa = \frac{\partial F}{\partial L} = \frac{k_B T}{l_\alpha - l_\beta} \ln\left(\frac{M l_\beta - L}{L - M l_\alpha}\right) + \frac{k_B T}{l_\alpha - l_\beta} \ln \frac{z_\beta}{z_\alpha}. \tag{1.42}$$

This can be written as a function of the fraction of segments in the α-configuration

$$\delta = \frac{M_\alpha}{M} = \frac{L - M l_\beta}{M(l_\alpha - l_\beta)} \tag{1.43}$$

in the somewhat simpler form

$$\kappa \frac{l_\alpha - l_\beta}{k_B T} = \ln \frac{\delta}{1-\delta} + \ln \frac{z_\beta}{z_\alpha}. \tag{1.44}$$

The mean extension for zero force is obtained by solving $\kappa(L) = 0$

$$\overline{L}_0 = M\left(\frac{z_\alpha l_\alpha + z_\beta l_\beta}{z_\alpha + z_\beta}\right) \tag{1.45}$$

$$\delta_0 = \frac{\bar{L}_0 - M l_\beta}{M(l_\alpha - l_\beta)} = \frac{z_\alpha}{z_\alpha + z_\beta}. \tag{1.46}$$

Taylor series expansion around $\overline{L}_0$ gives the linearized force–extension relation

$$\begin{aligned}\kappa &= \frac{\partial F}{\partial L} \\ &= \frac{k_B T}{M(l_\alpha - l_\beta)^2} \frac{(z_\alpha + z_\beta)^2}{z_\alpha z_\beta}(L - \bar{L}_0) + \cdots \\ &\approx \frac{k_B T}{l_\alpha - l_\beta} \frac{(z_\alpha + z_\beta)^2}{z_\alpha z_\beta}(\delta - \delta_0) \\ &= \frac{k_B T}{l_\alpha - l_\beta} \frac{1}{\delta_0(1 - \delta_0)}(\delta - \delta_0). \end{aligned} \tag{1.47}$$

1.2.2 Two Component Model with Interactions

We now consider additional interaction between neighboring units. We introduce the interaction energies $w_{\alpha\alpha}$, $w_{\alpha\beta}$, $w_{\beta\beta}$ for the different pairs of neighbors and the numbers $N_{\alpha\alpha}$, $N_{\alpha,\beta}$, $N_{\beta\beta}$ of such interaction terms. The total interaction energy is then

$$W = N_{\alpha\alpha} w_{\alpha\alpha} + N_{\alpha\beta} w_{\alpha\beta} + N_{\beta\beta} w_{\beta\beta}. \tag{1.48}$$

The numbers of pair interactions are not independent from the numbers of units M_α, M_β. Consider insertion of an additional α-segment into a chain. Figure 1.8 counts the possible changes in interaction terms. In any case, by insertion of an α-segments the expression $2N_{\alpha\alpha} + N_{\alpha\beta}$ increases by 2.

Similarly, insertion of an extra β-segment increases $2N_{\beta\beta} + N_{\alpha\beta}$ by 2 (Fig. 1.9).

Fig. 1.8 Insertion of an α-segment

α ↓	M_α	M_β	$N_{\alpha\alpha}$	$N_{\alpha\beta}$	$N_{\beta\beta}$	$2N_{\alpha\alpha}+N_{\alpha\beta}$
αα	+1		+1			+2
αβ	+1		+1			+2
βα	+1		+1			+2
ββ	+1			+2	−1	+2

Fig. 1.9 Insertion of a β-segment

β ↓	M_α	M_β	$N_{\alpha\alpha}$	$N_{\alpha\beta}$	$N_{\beta\beta}$	$2N_{\beta\beta}+N_{\alpha\beta}$
αα		+1	−1	+2		+2
αβ		+1			+1	+2
βα		+1			+1	+2
ββ		+1			+1	+2

Fig. 1.10 Determination of the constants

	N_α	N_β	$N_{\alpha\alpha}$	$N_{\alpha\beta}$	$N_{\beta\beta}$	$2N_{\alpha\alpha}+N_{\alpha\beta}-2N_\alpha$	$2N_{\beta\beta}+N_{\alpha\beta}-2N_\beta$
α α	2	0	1	0	0	−2	0
β β	0	2	0	0	1	0	−2
α β	1	1	0	1	0	−1	−1
α α	2	0	2	0	0	0	0
β β	0	2	0	0	2	0	0
α β	1	1	0	2	0	0	0

This shows that there are linear relationships of the form

$$\begin{aligned} 2N_{\alpha\alpha} + N_{\alpha\beta} &= 2M_\alpha + c_1 \\ 2N_{\beta\beta} + N_{\alpha\beta} &= 2M_\beta + c_2. \end{aligned} \tag{1.49}$$

The two constants depend on the boundary conditions as can be seen from an inspection of the shortest possible chains with 2 segments (Fig. 1.10). They are zero for periodic boundaries and will, therefore, be neglected in the following, since the numbers M_α, M_β are much larger.

We substitute

$$N_{\alpha\alpha} = M_\alpha - \frac{1}{2}N_{\alpha\beta} \tag{1.50}$$

$$N_{\beta\beta} = M_\beta - \frac{1}{2}N_{\alpha\beta} \tag{1.51}$$

$$w = w_{\alpha\alpha} + w_{\beta\beta} - 2w_{\alpha\beta} \tag{1.52}$$

to have the interaction energy

$$\begin{aligned} W &= w_{\alpha\alpha}\left(M_\alpha - \frac{1}{2}N_{\alpha\beta}\right) + w_{\beta\beta}\left(M_\beta - \frac{1}{2}N_{\alpha\beta}\right) + w_{\alpha\beta}N_{\alpha\beta} \\ &= w_{\alpha\alpha}M_\alpha + w_{\beta\beta}(M - M_\alpha) - \frac{w}{2}N_{\alpha\beta}. \end{aligned} \tag{1.53}$$

The canonical partition function is

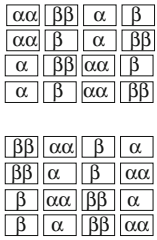

Fig. 1.11 Degeneracy factor g. The possible 8 configurations are shown for $M = 4$, $M_\alpha = 3$, $M_\beta = 3$, $N_{\alpha\beta} = 3$

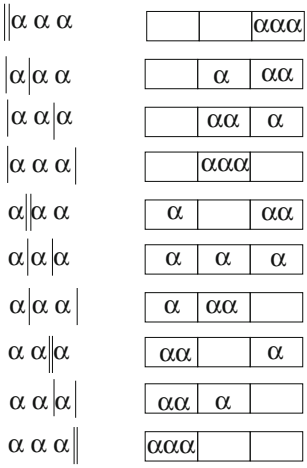

Fig. 1.12 Distribution of three segments over three blocks. This is equivalent to the arrangement of three segments and two border lines

$$
\begin{aligned}
Z(M_\alpha, T) &= z_\alpha^{M_\alpha} z_\beta^{M_\beta} \sum_{N_{\alpha\beta}} g(M_\alpha, N_{\alpha\beta}) \mathrm{e}^{-W(N_{\alpha\beta})/k_B T} \\
&= \left(z_\alpha \mathrm{e}^{-w_{\alpha\alpha}/k_B T}\right)^{M_\alpha} \left(z_\beta \mathrm{e}^{-w_{\beta\beta}/k_B T}\right)^{(M-M_\alpha)} \sum_{N_{\alpha\beta}} g(M_\alpha, N_{\alpha\beta}) \mathrm{e}^{N_{\alpha\beta} w/2k_B T}.
\end{aligned}
\tag{1.54}
$$

The degeneracy factor g will be evaluated in the following. Figure 1.11 shows an example.

The chain can be divided into blocks containing only α-segments (α-blocks) or only β-segments (β-blocks). The number of boundaries between α-blocks and β-blocks obviously is given by $N_{\alpha\beta}$. Let $N_{\alpha\beta}$ be an odd number. Then there are $(N_{\alpha\beta} + 1)/2$ blocks of each type (We assume that $N_{\alpha\beta}$, M_α, M_β are large numbers and neglect small differences of order 1 for even $N_{\alpha\beta}$). In each α-block there is at least one α-segment. The remaining $M_\alpha - (N_{\alpha\beta} + 1)/2$ α-segments have to be distributed over the $(N_{\alpha\beta} + 1)/2$ α-blocks (Fig. 1.12).

Therefore we need the number of possible ways to arrange $M_\alpha - (N_{\alpha\beta} + 1)/2$ segments and $(N_{\alpha\beta} - 1)/2$ walls which is given by the number of ways to distribute the $(N_{\alpha\beta} - 1)/2$ walls over the total of $M_\alpha - 1$ objects which is given by

$$\frac{(M_\alpha - 1)!}{\left(\frac{N_{\alpha\beta}-1}{2}\right)!\left(M_\alpha - \frac{N_{\alpha\beta}+1}{2}\right)!} \approx \frac{M_\alpha!}{\left(\frac{N_{\alpha\beta}}{2}\right)!\left(M_\alpha - \frac{N_{\alpha\beta}}{2}\right)!}. \tag{1.55}$$

The same consideration for the β-segments gives another factor of

$$\frac{(M - M_\alpha)!}{\left(\frac{N_{\alpha\beta}}{2}\right)!\left(M - M_\alpha - \frac{N_{\alpha\beta}}{2}\right)!}. \tag{1.56}$$

Finally, there is an additional factor of 2 because the first block can be of either type. Hence for large numbers we find

$$g(M_\alpha, N_{\alpha\beta}) = 2\frac{(M_\alpha)!}{\left(\frac{N_{\alpha\beta}}{2}\right)!\left(M_\alpha - \frac{N_{\alpha\beta}}{2}\right)!}\frac{(M - M_\alpha)!}{\left(\frac{N_{\alpha\beta}}{2}\right)!\left(M - M_\alpha - \frac{N_{\alpha\beta}}{2}\right)!}. \tag{1.57}$$

We look for the maximum summand of Z as a function of $N_{\alpha\beta}$. The corresponding number will be denoted as $N^*_{\alpha\beta}$ and is determined from the condition

$$0 = \frac{\partial}{\partial N_{\alpha\beta}} \ln\left(g(M_\alpha, N_{\alpha\beta})\mathrm{e}^{\frac{wN_{\alpha\beta}}{2k_BT}}\right) = \frac{w}{2k_BT} + \frac{\partial}{\partial N_{\alpha\beta}} \ln g(M_\alpha, N_{\alpha\beta}). \tag{1.58}$$

Stirling's approximation gives

$$0 = \frac{w}{2k_BT} + \frac{1}{2}\ln\left(M_\alpha - \frac{N^*_{\alpha\beta}}{2}\right) + \frac{1}{2}\ln\left(M - M_\alpha - \frac{N^*_{\alpha\beta}}{2}\right) - \ln\left(\frac{N^*_{\alpha\beta}}{2}\right) \tag{1.59}$$

or

$$0 = \frac{w}{k_BT} + \ln\left(\frac{(M_\alpha - \frac{N^*_{\alpha\beta}}{2})(M - M_\alpha - \frac{N^*_{\alpha\beta}}{2})}{(\frac{N^*_{\alpha\beta}}{2})^2}\right). \tag{1.60}$$

Taking the exponential gives

$$\left(M_\alpha - \frac{N^*_{\alpha\beta}}{2}\right)\left(M - M_\alpha - \frac{N^*_{\alpha\beta}}{2}\right) = \mathrm{e}^{-w/k_BT}\left(\frac{N_{\alpha\beta}}{2}\right)^2. \tag{1.61}$$

Introducing the relative quantities

$$\delta = \frac{M_\alpha}{M} \qquad \gamma = \frac{N^*_{\alpha\beta}}{2M} \tag{1.62}$$

we have to solve the quadratic equation

$$(\delta - \gamma)(1 - \delta - \gamma) = \gamma^2\mathrm{e}^{-\frac{w}{k_BT}}. \tag{1.63}$$

The solutions are

$$\gamma = \frac{-1 \pm \sqrt{(1-2\delta)^2 + 4\mathrm{e}^{-w/k_BT}\delta(1-\delta)}}{2(\mathrm{e}^{-w/k_BT}-1)}. \tag{1.64}$$

Series expansion in w/k_BT gives

$$\begin{aligned}\gamma &= \frac{k_BT}{2w} + \frac{1}{4} + \frac{w}{24k_BT} + \cdots \\ &\cdots \pm \left(-\frac{k_BT}{2w} + \delta(1-\delta) - \frac{1}{4} + \left((\delta-\delta^2)^2 - \frac{1}{24}\right)\frac{w}{k_BT}\right) + \cdots\end{aligned} \tag{1.65}$$

The - alternative diverges for $w \to 0$ whereas the + alternative

$$\gamma = \delta(1-\delta) + (\delta-\delta^2)^2\frac{w}{k_BT} - \delta^2\left(\frac{1}{2}(1-\delta)^2 + 2\delta(\delta-1)^3\right)\frac{w}{k_BT}\cdots \tag{1.66}$$

approaches the value

$$\gamma_0 = \delta - \delta^2 \tag{1.67}$$

which is the only solution of the interactionless case

$$(\delta-\gamma_0)(1-\delta-\gamma_0) = \gamma_0^2 \to \delta(1-\delta) - \gamma = 0. \tag{1.68}$$

For $N^*_{\alpha\beta}$ we obtain approximately

$$N^*_{\alpha\beta} = 2M\left(\delta(1-\delta) + (\delta-\delta^2)^2\frac{w}{k_BT} + \cdots\right). \tag{1.69}$$

Let us now apply the maximum term method, which approximates the logarithm of a sum by the logarithm of the maximum summand

$$\begin{aligned}F &= -k_BT\ln Z(M_\alpha, T) \\ &\approx -k_BTM_\alpha\ln z_\alpha - k_BT(M-M_\alpha)\ln z_\beta + M_\alpha w_{\alpha\alpha} + (M-M_\alpha)w_{\beta\beta} \\ &\quad -k_BT\ln g(M_\alpha, N^*_{\alpha\beta}) - \frac{wN^*_{\alpha\beta}}{2}.\end{aligned} \tag{1.70}$$

The force-length relation (Fig. 1.13) is now obtained from

$$\begin{aligned}\kappa &= \frac{\partial F}{\partial L} = \frac{\partial F}{\partial M_\alpha}\frac{\partial\left(\frac{L-Ml_\beta}{l_\alpha-l_\beta}\right)}{\partial L} = \frac{1}{l_\alpha-l_\beta}\frac{\partial F}{\partial M_\alpha} \\ &= \frac{1}{l_\alpha-l_\beta}\left(-k_BT\ln z_\alpha + k_BT\ln z_\beta + w_{\alpha\alpha} - w_{\beta\beta} - k_BT\frac{\partial}{\partial M_\alpha}\ln g\right) \\ &\quad + \frac{1}{l_\alpha-l_\beta}\frac{\partial N^*_{\alpha\beta}}{\partial M_\alpha}\frac{\partial}{\partial N^*_{\alpha\beta}}\left(-k_BT\ln g - \frac{wN^*_{\alpha\beta}}{2}\right).\end{aligned} \tag{1.71}$$

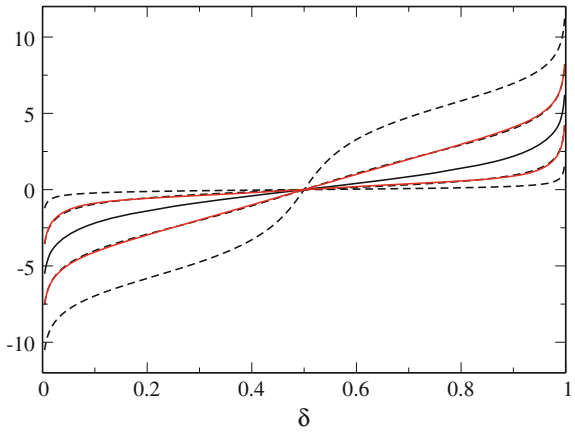

Fig. 1.13 Force - length relation for the interacting two-component model. *Dashed curves:* exact results for $w/k_BT = 0, \pm 2, \pm 5$. *Solid curves:* series expansion (1.73) which gives a good approximation for $|w/k_BT| < 2$

The last part vanishes due to the definition of $N^*_{\alpha\beta}$. Now using Stirling's formula we find

$$\frac{\partial}{\partial M_\alpha} \ln g = \ln \frac{M_\alpha}{M - M_\alpha} + \ln \frac{M - M_\alpha - \frac{N^*_{\alpha\beta}}{2}}{M_\alpha - \frac{N^*_{\alpha\beta}}{2}} = \ln \frac{\delta}{1-\delta} + \ln \frac{1-\delta-\gamma}{\delta-\gamma} \quad (1.72)$$

and substituting γ we have finally

$$\kappa \frac{(l_\alpha - l_\beta)}{k_BT} = \ln \frac{z_\beta e^{-w_{\beta\beta}/k_BT}}{z_\alpha e^{-w_{\alpha\alpha}/k_BT}} - \ln \frac{(1-\delta)}{\delta} + \left(2\delta - 1\right)\frac{w}{k_BT} + \delta\left(3\delta - 2\delta^2 - 1\right)\left(\frac{w}{k_BT}\right)^2. \quad (1.73)$$

Linearization now gives

$$\delta_0 = \frac{z_\alpha e^{-w_{\alpha\alpha}/k_BT}}{z_\alpha e^{-w_{\alpha\alpha}/k_BT} + z_\beta e^{-w_{\beta\beta}/k_BT}}$$

$$\kappa = \frac{k_BT}{l_\alpha - l_\beta} \frac{1}{\delta_0(1-\delta_0)}(\delta - \delta_0) + \frac{w}{k_BT}\left(2\delta_0 - 1\right) + \left(\frac{w}{k_BT}\right)^2 (3\delta_0^2 - \delta_0 - 2\delta_0^3) + \left(2\frac{w}{k_BT} + \left(\frac{w}{k_BT}\right)^2 \left(6\delta_0 - 6\delta_0^2 - 1\right)\right)(\delta - \delta_0). \quad (1.74)$$

For negative w, a small force may lead to much larger changes in length than with no interaction. This explains, for example, how in proteins huge channels may open

although the acting forces are quite small. In the case of Myoglobine, this is how the penetration of oxygen in the protein becomes possible.

Problems

1.1 Gaussian Polymer Model

The simplest description of a polymer is the Gaussian polymer model which considers a polymer to be a series of particles joined by Hookean springs

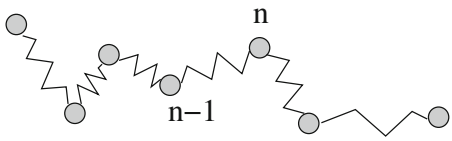

(a) The vector connecting monomers n-1 and n obeys a Gaussian distribution with average zero and variance

$$\left\langle (\mathbf{r}_n - \mathbf{r}_{n-1})^2 \right\rangle = b^2.$$

Determine the distribution function $P(\mathbf{r}_n - \mathbf{r}_{n-1})$ explicitly.
(b) Assume that the distance vectors $\mathbf{r}_n - \mathbf{r}_{n-1}$ are independent and calculate the distribution of end-to-end vectors $P(\mathbf{r}_N - \mathbf{r}_0)$.
(c) Consider now a polymer under the action of a constant force κ in x-direction. The potential energy of a conformation is given by

$$V = \sum_{n=1}^{N} \frac{f}{2} (\mathbf{r}_n - \mathbf{r}_{n-1})^2 - \kappa (x_N - x_0)$$

and the probability of this conformation is

$$P \sim \mathrm{e}^{-V/k_B T}.$$

Determine the effective spring constant f.
(d) Find the most probable configuration by searching for the minimum of the energy

$$\frac{\partial V}{\partial x_n} = \frac{\partial V}{\partial y_n} = \frac{\partial V}{\partial z_n} = 0.$$

Calculate the length of the polymer for the most probable configuration (according to the maximum term method the average value coincides with the most probable value in the thermodynamic limit).

1.2 Three-Dimensional Polymer Model

Consider a model of a polymer in three-dimensional space consisting of N links of length b. The connection of the links i and $i+1$ is characterized by the two angles ϕ_i and θ_i. The vector $\mathbf{r}_i$ can be obtained from the vector $\mathbf{r}_1$ through application of a series of rotation matrices[1]

$$\mathbf{r}_i = R_1 R_2 \ldots R_{i-1} \mathbf{r}_1$$

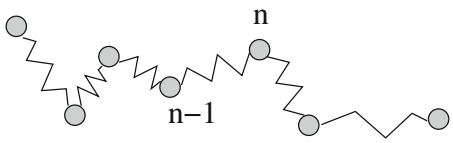

with

$$\mathbf{r}_1 = \begin{pmatrix} 0 \\ 0 \\ b \end{pmatrix} \qquad R_i = R_z(\phi_i) R_y(\theta_i) = \begin{pmatrix} \cos\phi_i & \sin\phi_i & 0 \\ -\sin\phi_i & \cos\phi_i & 0 \\ 0 & 0 & 1 \end{pmatrix} \begin{pmatrix} \cos\theta_i & 0 & -\sin\theta_i \\ 0 & 1 & 0 \\ \sin\theta_i & 0 & \cos\theta_i \end{pmatrix}.$$

Calculate the mean square of the end-to-end distance $\left\langle \left(\sum_{i=1}^{N} \mathbf{r}_i \right)^2 \right\rangle$ for the following cases:

(a) The averaging $\langle \cdots \rangle$ includes averaging over all angles ϕ_i and θ_i.
(b) The averaging $\langle \cdots \rangle$includes averaging over all angles ϕ_i while the angles θ_i are held fixed at a common value θ.
(c) The averaging $\langle \cdots \rangle$includes averaging over all angles ϕ_i while the angles θ_i are held fixed at either $\theta_{2i+1} = \theta_a$ or $\theta_{2i} = \theta_b$ depending on whether the number of the link is odd or even.
(d) How large must N be, so that it is a good approximation to keep only terms which are proportional to N?
(e) What happens in the second case if θ is chosen as very small (wormlike chain)?

Hint: Show first that after averaging over the ϕ_i the only terms of the matrix which have to be taken into account are the elements $(R_i)_{33}$. The appearing summations can be expressed as geometric series.

[1]The rotation matrices act in the laboratory fixed system (xyz). Transformation into the coordinate system of the segment (x'y'z') changes the order of the matrices. For instance $\mathbf{r}_2 = R(y,\theta_1)R(z,\phi_1)\mathbf{r}_1 = R(z,\phi_1)R(y',\theta_1)R^{-1}(z,\phi_1)R(z,\phi_1)\mathbf{r}_1 = R(z,\phi_1)R(y',\theta_1)\mathbf{r}_1$ (This is sometimes discussed in terms of active and passive rotations).

1.3 Two-Component Model

We consider the two-component model of a polymer chain which consists of M segments of two different types α, β (internal degrees of freedom are neglected). The number of configurations with length L is given by the Binomial distribution

$$\Omega(L, M, T) = \frac{M!}{M_\alpha!(M - M_\alpha)!} \qquad L = M_\alpha l_\alpha + (M - M_\alpha) l_\beta.$$

(a) Make use of the asymptotic expansion[2] of the logarithm of the Gamma function

$$\ln(\Gamma(z + 1)) = (\ln z - 1)z + \ln(\sqrt{2\pi}) + \frac{1}{2}\ln z + \frac{1}{12z} + O(z^{-3})$$

$$N! = \Gamma(N + 1)$$

to calculate the leading terms of the force-extension relation which is obtained from

$$\kappa = \frac{\partial}{\partial L}\Big(- k_B T \ln \Omega(L, M, T)\Big).$$

Discuss the error of Stirling's approximation for $M = 1000$ and $l_\beta / l_\alpha = 2$.

(b) Now switch to an ensemble with constant force κ . The corresponding partition function is

$$Z(\kappa, M, T) = \sum_L \mathrm{e}^{\kappa L / k_B T} \Omega(L, M, T).$$

Calculate the first two moments of the length

$$\overline{L} = -\frac{\partial}{\partial \kappa}(-k_B T \ln Z) = Z^{-1} k_B T \frac{\partial}{\partial \kappa} Z$$

$$\overline{L^2} = Z^{-1}(k_B T)^2 \frac{\partial^2}{\partial \kappa^2} Z$$

and discuss the relative uncertainty $\sigma = \frac{\sqrt{\overline{L^2} - \overline{L}^2}}{\overline{L}}$. Determine the maximum of σ.

[2] Several asymptotic expansions can be found in [5] .

Chapter 2
Flory–Huggins Theory for Biopolymer Solutions

In the early 1940s, Paul Flory [6] and Maurice Huggins [7], both working independently, developed a theory based upon a simple lattice model that could be used to understand the nonideal nature of polymer solutions. They consider a lattice model where the lattice sites are chosen to be the size of a solvent molecule and where all lattice sites are occupied by one molecule [1]. The mixing entropy and free energy of a polymer solution are evaluated. The appearance of unstable regions and the transition between a homogeneous and a two-phase system are discussed.

2.1 Monomeric Solution

As the simplest example, consider the mixing of a low-molecular-weight solvent (component α) with a low-molecular-weight solute (component β). The solute molecule is assumed to be the same size as a solvent molecule and therefore every lattice site is occupied by one solvent molecule or by one solute molecule at a given time (Fig. 2.1).

The increase in entropy ΔS_m due to mixing of solvent and solute is given by

$$\Delta S_m = k_B \ln \Omega = k_B \ln \left(\frac{N!}{N_\alpha! N_\beta!} \right) \tag{2.1}$$

where $N = N_\alpha + N_\beta$ is the total number of lattice sites. Using Stirling's approximation leads to

P.O.J. Scherer and S.F. Fischer, *Theoretical Molecular Biophysics*,
Biological and Medical Physics, Biomedical Engineering,
DOI 10.1007/978-3-662-55671-9_2

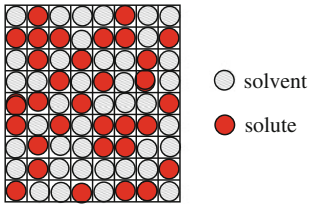

Fig. 2.1 Two-dimensional Flory–Huggins lattice

$$\begin{aligned}\Delta S_m &= k_B(N\ln N - N - N_\alpha \ln N_\alpha + N_\alpha - N_\beta \ln N_\beta + N_\beta)\\ &= k_B(N\ln N - N_\alpha \ln N_\alpha - N_\beta \ln N_\beta)\\ &= -k_B N_\alpha \ln\frac{N_\alpha}{N} - k_B N_\beta \ln\frac{N_\beta}{N}.\end{aligned} \tag{2.2}$$

Inserting the volume fractions

$$\phi_\alpha = \frac{N_\alpha}{N_\alpha + N_\beta} \qquad \phi_\beta = \frac{N_\beta}{N_\alpha + N_\beta} \tag{2.3}$$

the mixing entropy can be written in the well-known form

$$\Delta S_m = -N k_B(\phi_\alpha \ln\phi_\alpha + \phi_\beta \ln\phi_\beta). \tag{2.4}$$

Neglecting boundary effects (or using periodic b.c.) the number of nearest neighbor pairs is (c is the coordination number)

$$N_{nn} = N\frac{c}{2}. \tag{2.5}$$

These are divided into

$$\begin{aligned}N_{\alpha\alpha} &= \frac{N_\alpha c}{2}\phi_\alpha = \frac{N\phi_\alpha^2 c}{2} \quad N_{\beta\beta} = \frac{N_\beta c}{2}\phi_\beta = \frac{N\phi_\beta^2 c}{2}\\ N_{\alpha\beta} &= N\phi_\alpha\phi_\beta\, c.\end{aligned} \tag{2.6}$$

The average interaction energy is

$$\overline{w} = \frac{1}{2}Nc\phi_\alpha^2 w_{\alpha\alpha} + \frac{1}{2}Nc\phi_\beta^2 w_{\beta\beta} + Nc\phi_\alpha\phi_\beta w_{\alpha\beta} \tag{2.7}$$

which after the substitution

$$w_{\alpha\beta} = \frac{1}{2}(w_{\alpha\alpha} + w_{\beta\beta} - w) \tag{2.8}$$

becomes

$$\begin{aligned}\overline{w} &= -\frac{1}{2}Nc\phi_\alpha\phi_\beta w \\ &= +\frac{1}{2}Nc\phi_\alpha(\phi_\alpha w_{\alpha\alpha} + \phi_\beta w_{\alpha\alpha}) + \frac{1}{2}Nc\phi_\beta(\phi_\beta w_{\beta\beta} + \phi_\alpha w_{\beta\beta})\end{aligned} \tag{2.9}$$

and since $\phi_\alpha + \phi_\beta = 1$

$$\overline{w} = -\frac{1}{2}Nc\phi_\alpha\phi_\beta w + \frac{1}{2}Nc(\phi_\alpha w_{\alpha\alpha} + \phi_\beta w_{\beta\beta}). \tag{2.10}$$

Now the partition function is

$$\begin{aligned}Z &= z_\alpha^{N_\alpha} z_\beta^{N_\beta} \mathrm{e}^{-N_\alpha c w_{\alpha\alpha}/2k_BT} \mathrm{e}^{-N_\beta c w_{\beta\beta}/2k_BT} \mathrm{e}^{N_\alpha N_\beta c w/2Nk_BT} \frac{N!}{N_\alpha! N_\beta!} \\ &= (z_\alpha \mathrm{e}^{-cw_{\alpha\alpha}/2k_BT})^{N_\alpha} (z_\beta \mathrm{e}^{-cw_{\beta\beta}/2k_BT})^{N_\beta} \mathrm{e}^{N_\alpha N_\beta c w/2Nk_BT} \frac{N!}{N_\alpha! N_\beta!}.\end{aligned} \tag{2.11}$$

The free energy is

$$\begin{aligned}F &= -k_BT \ln Z = -N_\alpha k_BT \ln z_\alpha - N_\beta k_BT \ln z_\beta \\ &= +N_\alpha \frac{c}{2} w_{\alpha\alpha} + N_\beta \frac{c}{2} w_{\beta\beta} - \frac{N_\alpha N_\beta c w}{2N} + Nk_BT(\phi_\alpha \ln \phi_\alpha + \phi_\beta \ln \phi_\beta).\end{aligned} \tag{2.12}$$

For the pure solvent the free energy is

$$F(N_\alpha = N, N_\beta = 0) = -N_\alpha k_BT \ln z_\alpha + N_\alpha \frac{c}{2} w_{\alpha\alpha} \tag{2.13}$$

and for the pure solute

$$F(N_\alpha = 0, N_\beta = N) = -N_\beta k_BT \ln z_\beta + N_\beta \frac{c}{2} w_{\beta\beta} \tag{2.14}$$

hence, the change in free energy is

$$\Delta F_m = -\frac{N_\alpha N_\beta c w}{2N} + Nk_BT(\phi_\alpha \ln \phi_\alpha + \phi_\beta \ln \phi_\beta) \tag{2.15}$$

with the energy change (van Laar heat of mixing)

$$\Delta E_m = -\frac{N_\alpha N_\beta c w}{2N} = -N\frac{cw}{2}\phi_\alpha\phi_\beta = Nk_BT\chi\phi_\alpha\phi_\beta. \tag{2.16}$$

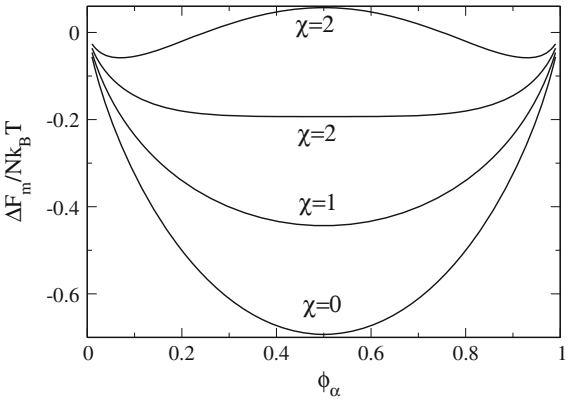

Fig. 2.2 Free energy change $\Delta F/Nk_BT$ of a binary mixture with interaction

The last equation defines the Flory interaction parameter (Fig. 2.2)

$$\chi = -\frac{cw}{2k_BT}. \tag{2.17}$$

For $\chi > 2$ the free energy has two minima and two stable phases exist. This is seen from solving

$$\begin{aligned} 0 &= \frac{\partial \Delta F}{\partial \phi_\alpha} = Nk_BT \frac{\partial}{\partial \phi_\alpha} \left(\chi \phi_\alpha (1-\phi_\alpha) + \phi_\alpha \ln \phi_\alpha + (1-\phi_\alpha)\ln(1-\phi_\alpha)\right) \\ &= Nk_BT \left(\chi(1-2\phi_\alpha) + \ln \frac{\phi_\alpha}{1-\phi_\alpha}\right). \end{aligned} \tag{2.18}$$

This equation has as one solution $\phi_\alpha = 1/2$. This solution becomes unstable for $\chi > 2$ as can be seen from the sign change of the second derivative

$$\frac{\partial^2 \Delta F}{\partial \phi_\alpha^2} = Nk_BT \left(\frac{1 - 2\chi\phi_\alpha + 2\chi\phi_\alpha^2}{\phi_\alpha^2 - \phi_\alpha}\right) = Nk_BT(4 - 2\chi). \tag{2.19}$$

2.2 Polymeric Solution

Now consider N_β polymer molecules which consist of M units and hence occupy a total of MN_β lattice sites. The volume fractions are (Fig. 2.3)

$$\phi_\alpha = \frac{N_\alpha}{N_\alpha + MN_\beta} \qquad \phi_\beta = \frac{MN_\beta}{N_\alpha + MN_\beta} \tag{2.20}$$

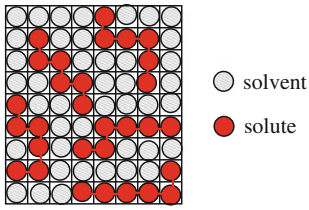

Fig. 2.3 Lattice model for a polymer

and the number of lattice sites is

$$N = N_\alpha + M N_\beta. \tag{2.21}$$

The entropy is given by

$$\Delta S = \Delta S_m + \Delta S_d = k_B \ln \Omega(N_\alpha, N_\beta). \tag{2.22}$$

It consists of the mixing entropy and a contribution due to the different conformations of the polymers (disordering entropy). The latter can be eliminated by subtracting the entropy for $N_\alpha = 0$

$$\Delta S_m = \Delta S - \Delta S_d = k_B \frac{\ln \Omega(N_\alpha, N_\beta)}{\ln \Omega(0, N_\beta)}. \tag{2.23}$$

In the following we will calculate $\Omega(N_\alpha, N_\beta)$ in an approximate way. We use a mean-field method where one polymer after the other is distributed over the lattice, taking into account only the available volume but not the configuration of all the other polymers. Under that conditions Ω factorizes

$$\Omega = \frac{1}{N_\beta!} \prod_{i=1}^{N_\beta} \nu_i \tag{2.24}$$

where ν_i counts the number of possibilities to put the i-th polymer onto the lattice. It will be calculated by adding one segment after the other and counting the number of possible ways

$$\nu_{i+1} = \prod_{s=1}^{M} n_s^{i+1}. \tag{2.25}$$

The first segment of the (i+1)-th polymer molecule can be placed onto

$$n_1^{i+1} = N - i M \tag{2.26}$$

lattice sites (Fig. 2.4).

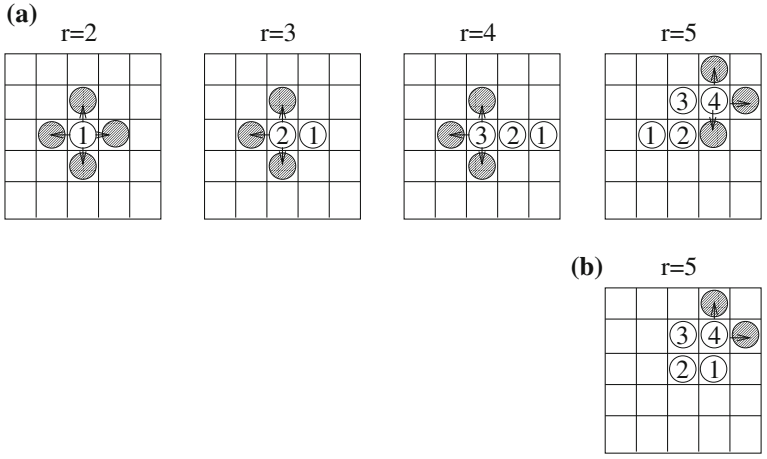

Fig. 2.4 Available positions. The second segment can be placed onto four, the third segment onto three positions. For the following segments it is assumed that they can also be placed onto three positions (**a**). Configurations like (**b**) are neglected

The second segment has to be placed on a neighboring position. Depending on the coordination number of the lattice there are c possible neighboring sites. But only a fraction of

$$f = 1 - \frac{iM}{N} \tag{2.27}$$

is unoccupied. Hence, for the second segment we have

$$n_2^{i+1} = c\left(1 - \frac{iM}{N}\right). \tag{2.28}$$

For the third segment only $c - 1$ neighboring positions are available

$$n_3^{i+1} = (c-1)\left(1 - \frac{iM}{N}\right). \tag{2.29}$$

For the following segments $r = 4 \ldots M$, we assume that the number of possible sites is the same as for the third segment. This introduces some error since for some configurations the number is reduced due to the excluded volume. This error, however, is small compared to the crudeness of the whole model. Multiplying all the factors we have

$$v_{i+1} = (N - iM)c(c-1)^{M-2}\left(1 - \frac{iM}{N}\right)^{M-1}$$
$$\approx (N - iM)^M \left(\frac{c-1}{N}\right)^{M-1} \tag{2.30}$$

and the entropy is

$$\Delta S = k_B \ln\left[\frac{1}{N_\beta!}\prod_{i=1}^{N_\beta}(N - iM)^M \left(\frac{c-1}{N}\right)^{M-1}\right] \tag{2.31}$$

$$= -kN_{B\beta}\ln N_\beta + k_B N_\beta + k_B N_\beta (M-1)\ln\left(\frac{c-1}{N}\right) + k_B M\sum_{i=1}^{N_\beta}\ln(N - iM). \tag{2.32}$$

The sum will be approximated by an integral

$$\sum_{i=1}^{N_\beta}\ln(N - iM) \approx \int_0^{N_\beta}\ln(N - Mx)dx = \left(x - \frac{N}{M}\right)(\ln(N - Mx) - 1)\Big|_0^{N_\beta}$$
$$= -\frac{N_\alpha}{M}(\ln N_\alpha - 1) + \frac{N}{M}(\ln N - 1). \tag{2.33}$$

Finally we get

$$\Delta S = -k_B N_\beta \ln N_\beta + k_B N_\beta + k_B N_\beta (M-1)\ln\left(\frac{c-1}{N}\right)$$
$$+k_B(N\ln N - N + N_\alpha - N_\alpha \ln N_\alpha). \tag{2.34}$$

The disorder entropy is obtained by substituting $N_\alpha = 0$ and $N = MN_\beta$

$$\Delta S_d = \Delta S(N_\alpha = 0)$$
$$= -k_B N_\beta \ln N_\beta + k_B N_\beta + k_B N_\beta (M-1)\ln\left(\frac{c-1}{MN_\beta}\right)$$
$$+k_B(MN_\beta \ln MN_\beta - MN_\beta). \tag{2.35}$$

The mixing entropy is given by the difference (Fig. 2.5)

$$\Delta S_m = \Delta S - \Delta S_d$$
$$= k_B(N\ln N - N + N_\alpha - N_\alpha \ln N_\alpha - MN_\beta \ln MN_\beta + MN_\beta)$$
$$+k_B N_\beta (M-1)(\ln MN_\beta - \ln N)$$
$$= k_B\left(N\ln N - N_\alpha \ln N_\alpha - MN_\beta \ln MN_\beta + MN_\beta \ln MN_\beta\right.$$
$$\left.-MN_\beta \ln N - N_\beta \ln MN_\beta + N_\beta \ln N\right)$$

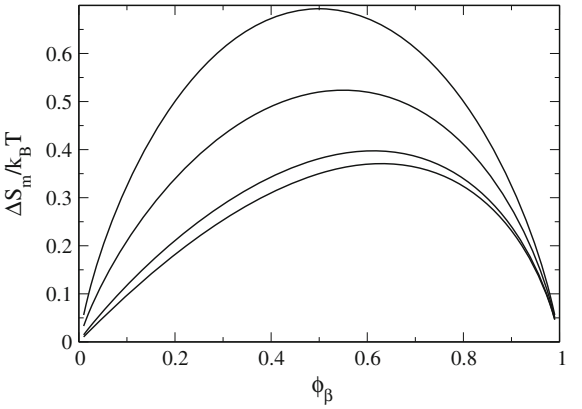

Fig. 2.5 Mixing entropy. $\Delta S_m/Nk_B$ is shown as a function of ϕ_β for M = 1, 2, 10, 100

$$= -k_B \left(N_\alpha \ln \frac{N_\alpha}{N} + N_\beta \ln \frac{MN_\beta}{N} \right) = -k_B N_\alpha \ln \phi_\alpha - k_B N_\beta \ln \phi_\beta$$

$$= -Nk_B \left(\phi_\alpha \ln \phi_\alpha + \frac{\phi_\beta}{M} \ln \phi_\beta \right). \tag{2.36}$$

In comparison with the expression for a solution of molecules without internal flexibility we obtain an extra contribution to the entropy of

$$-N_\beta k_B \ln \frac{MN_\beta}{N} + N_\beta k_B \ln \frac{N_\beta}{N} = -N_\beta k_B \ln M. \tag{2.37}$$

Next, we calculate the change of energy due to mixing, ΔE_m. $w_{\alpha\alpha}$is the interaction energy between nearest-neighbor solvent molecules, $w_{\beta\beta}$ between nearest-neighbor polymer units (not chemically bonded) and $w_{\alpha\beta}$ between one solvent molecule and one polymer unit. The probability that any site is occupied by a solvent molecule is ϕ_α and by a polymer unit is ϕ_β. We introduce an effective coordination number $\overline{c}$ which takes into account that a solvent molecule has c neighbors whereas a polymer segment interacts only with c-2 other molecules. Then

$$N_{\alpha\alpha} = \overline{c}\phi_\alpha \frac{N_\alpha}{2} \qquad N_{\beta\beta} = M\overline{c}\phi_\beta \frac{N_\beta}{2} \tag{2.38}$$

$$N_{\alpha\beta} = \overline{c}\phi_\alpha N_\beta. \tag{2.39}$$

In the pure polymer, $\phi_\beta = 1$ and $N_{\beta\beta} = M\overline{c}N_\beta/2$, whereas in the pure solvent $N_{\alpha\alpha} = \overline{c}N_{\alpha/2}$. The energy change is

$$\begin{aligned}\Delta E_m &= \bar{c} w_{\alpha\alpha} \phi_\alpha \frac{N_\alpha}{2} + w_{\beta\beta} M \bar{c} \phi_\beta \frac{N_\beta}{2} + w_{\alpha\beta} M \bar{c} \phi_\alpha N_\beta \\ &\quad - w_{\alpha\alpha} \bar{c} \frac{N_\alpha}{2} - w_{\beta\beta} M \bar{c} \frac{N_\beta}{2} \\ &= -\bar{c} w_{\alpha\alpha} \frac{N_\alpha}{2} \phi_\beta - \bar{c} M w_{\beta\beta} \frac{N_\beta}{2} \phi_\alpha + w_{\alpha\beta} M \bar{c} \phi_\alpha N_\beta \\ &= \left(w_{\alpha\beta} - \frac{w_{\alpha\alpha} + w_{\beta\beta}}{2} \right) \bar{c} N \phi_\alpha \phi_\beta \\ &= -\frac{w}{2} \bar{c} N \phi_\alpha \phi_\beta \\ &= N k_B T \chi \phi_\alpha \phi_\beta \end{aligned} \tag{2.40}$$

with the Flory interaction parameter

$$\chi = -\frac{w \bar{c}}{2 k_B T}. \tag{2.41}$$

For the change in free energy we find (Figs. 2.6, 2.7 and 2.8)

$$\frac{\Delta F_m}{N k_B T} = \frac{\Delta E_m}{N k_B T} - \frac{\Delta S_m}{N k_B} = \phi_\alpha \ln \phi_\alpha + \frac{\phi_\beta}{M} \ln \phi_\beta + \chi \phi_\alpha \phi_\beta. \tag{2.42}$$

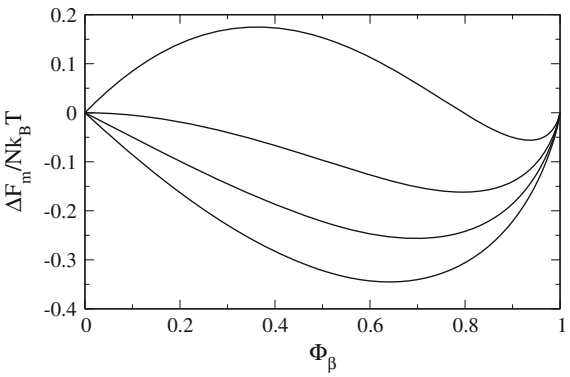

Fig. 2.6 Free energy as a function of solute concentration. $\Delta F_m / N k_B T$ is shown for M = 1000 and $\chi = 0.1, 0.5, 1.0, 2.0$

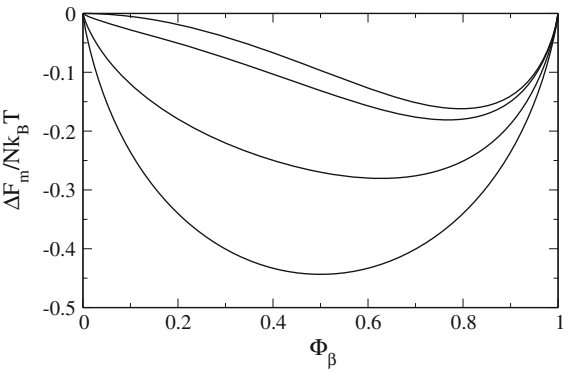

Fig. 2.7 Free energy as a function of solute concentration. $\Delta F_m/Nk_BT$ is shown for $\chi = 1.0$ and M = 1, 2, 10, 1000

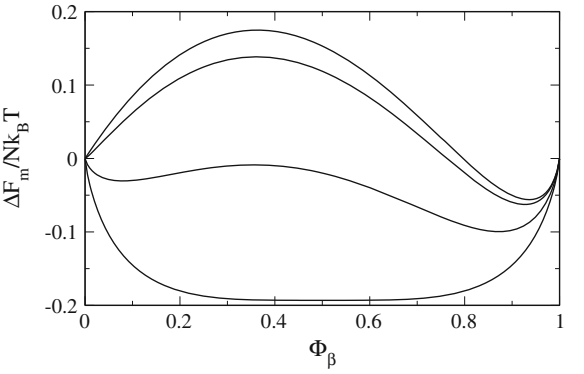

Fig. 2.8 Free energy as a function of solute concentration. $\Delta F_m/Nk_BT$ is shown for $\chi = 2.0$ and M = 1, 2, 10, 1000

2.3 Phase Transitions

2.3.1 Stability Criterion

In equilibrium the free energy (if volume is constant) has a minimum value. Hence a homogeneous system becomes unstable and separates into two phases if the free energy of the two-phase system is lower, i.e., the following equation can be fulfilled

$$\Delta F_m(\phi_\beta, N) > \Delta F_m(\phi_\beta^{'}, N') + \Delta F_m(\phi_\beta^{''}, N - N'). \tag{2.43}$$

But since $\Delta F_m = N\Delta f_m(\phi_\beta)$ is proportional to N, this condition becomes

$$N\Delta f_m(\phi_\beta) > N'\Delta f_m(\phi_\beta') + (N - N')\Delta f_m(\phi_\beta''). \tag{2.44}$$

Since the total numbers N_α,N_β are conserved we have

$$N\phi_\beta = N'\phi_\beta' + (N - N')\phi_\beta'' \tag{2.45}$$

or

$$N' = N\frac{\phi_\beta - \phi''_\beta}{\phi'_\beta - \phi''_\beta} \qquad (N - N') = N\frac{\phi'_\beta - \phi_\beta}{\phi'_\beta - \phi''_\beta}. \tag{2.46}$$

But since N as well as $(N - N')$ should be positive numbers there are two possible cases as follows:

$$\phi'_\beta - \phi''_\beta > 0 \qquad \phi_\beta - \phi''_\beta > 0 \qquad \phi'_\beta - \phi_\beta > 0 \tag{2.47}$$

$$\phi'_\beta - \phi''_\beta < 0 \qquad \phi_\beta - \phi''_\beta < 0 \qquad \phi'_\beta - \phi_\beta < 0 \tag{2.48}$$

which means that either $\phi'_\beta < \phi_b < \phi''_\beta$ or $\phi'_\beta > \phi_b > \phi''_\beta$. By renaming we always can choose the order

$$\phi'_\beta < \phi_\beta < \phi''_\beta. \tag{2.49}$$

The stability criterion becomes (Fig. 2.9)

$$\Delta f_m(\phi_\beta) > \frac{\phi''_\beta - \phi_\beta}{\phi''_\beta - \phi'_\beta}\Delta f_m(\phi'_\beta) + \frac{\phi_\beta - \phi'_\beta}{\phi''_\beta - \phi'_\beta}\Delta f_m(\phi''_\beta) \tag{2.50}$$

which can be written with the abbreviation

$$h' = \phi_\beta - \phi'_\beta \qquad h'' = \phi''_\beta - \phi_\beta \tag{2.51}$$

as

$$\frac{\Delta f(\phi_\beta - h') - \Delta f(\phi_\beta)}{h'} + \frac{\Delta f(\phi_\beta + h'') - \Delta f(\phi_\beta)}{h''} < 0 \tag{2.52}$$

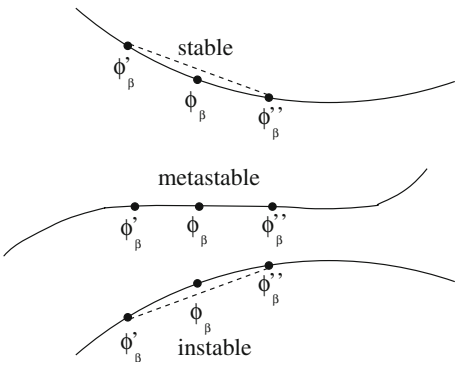

Fig. 2.9 Stability criterion for the free energy

but that means the curvature has to be negative or locally

$$\frac{\partial^2 \Delta f(\phi_\beta)}{\partial \phi_\beta^2} < 0. \tag{2.53}$$

2.3.2 Critical Coupling

Instabilities appear above a certain value of $\chi = \chi_c(M)$. To find this critical value we have to look for the metastable case with

$$0 = \frac{\partial^2}{\partial^2 \phi_b} \Delta f(\phi_b) = \frac{1}{1-\phi_b} + \frac{1}{M\phi_b} - 2\chi. \tag{2.54}$$

In principle, the critical χ value can be found from solving this quadratic equation for ϕ_b and looking for real roots in the range $0 \leq \phi_\beta \leq 1$. Here, however a simpler strategy can be applied. At the boundaries of the interval [0, 1] of possible ϕ_b-values the second derivative is positive

$$\frac{\partial^2}{\partial^2 \phi_b} \Delta f(\phi_b) \to \frac{1}{M\phi_b} > 0 \quad for \quad \phi_b \to 0 \tag{2.55}$$

$$\frac{\partial^2}{\partial^2 \phi_b} \Delta f(\phi_b) \to \frac{1}{1-\phi_b} > 0 \quad for \quad \phi_b \to 1. \tag{2.56}$$

Hence, we look for a minimum of the second derivative, i.e., we solve

$$0 = \frac{\partial^3}{\partial^3 \phi_b} \Delta f(\phi_b) = \frac{1}{(1-\phi_b)^2} - \frac{1}{M\phi_b^2}. \tag{2.57}$$

This gives immediately

$$\phi_{bc} = \frac{1}{1+\sqrt{M}}. \tag{2.58}$$

Above the critical point the minimum of the second derivative is negative. Hence we are looking for a solution of

$$\frac{\partial^2}{\partial^2 \phi_b} \Delta f(\phi_b) = \frac{\partial^3}{\partial^3 \phi_b} \Delta f(\phi_b) = 0. \tag{2.59}$$

Inserting ϕ_{bc} into the second derivative gives

$$0 = 1 + \frac{1}{M} + \frac{2}{\sqrt{M}} - 2\chi \tag{2.60}$$

which determines the critical value of χ

$$\chi_c = \frac{(1+\sqrt{M})^2}{2M} = \frac{1}{2} + \frac{1}{\sqrt{M}} + \frac{1}{2M}. \tag{2.61}$$

From $dF = -SdT + \mu_\alpha dN_\alpha + \mu_\beta dN_\beta$ we obtain the change of the chemical potential as

$$\mu_\alpha - \mu_\alpha^0 = \Delta\mu_\alpha = \frac{\partial \Delta F}{\partial N_\alpha}|_{N_\beta,T} = \left(\frac{\partial N}{\partial N_\alpha}\frac{\partial}{\partial N} + \frac{\partial \phi_\beta}{\partial N_\alpha}\frac{\partial}{\partial \phi_\beta}\right) N\Delta f(\phi_\beta) \tag{2.62}$$

$$= \Delta f(\phi_\beta) - \phi_\beta \Delta f'(\phi_\beta) = k_B T\left(\ln(1-\phi_\beta) + \left(1 - \frac{1}{M}\right)\phi_\beta + \chi\phi_\beta^2\right). \tag{2.63}$$

Now the derivatives of $\Delta\mu_\alpha$ are

$$\frac{\partial}{\partial \phi_\beta}\Delta\mu_\alpha = -\phi_\beta \Delta f''(\phi_\beta) \tag{2.64}$$

$$\frac{\partial^2}{\partial \phi_\beta^2}\Delta\mu_\alpha = -\Delta f''(\phi_\beta) - \phi_\beta \Delta f'''(\phi_\beta). \tag{2.65}$$

Hence the critical point can also be found by solving

$$\frac{\partial^2}{\partial \phi_\beta^2}\Delta\mu_\alpha = \frac{\partial}{\partial \phi_\beta}\Delta\mu_\alpha = 0. \tag{2.66}$$

Employing the ideal gas approximation

$$\mu = k_B T\ \ln(p) + \text{const} \tag{2.67}$$

this gives for the vapor pressure (Figs. 2.10 and 2.11)

$$\frac{p_\alpha}{p_\alpha^0} = \mathrm{e}^{(\mu_\alpha - \mu_\alpha^0)/k_B T} = (1-\phi_\beta)\mathrm{e}^{\chi\phi_\beta^2 + (1-1/M)\phi_\beta} \tag{2.68}$$

and since the exponential is a monotonous function another condition for the critical point is

$$\frac{\partial}{\partial \phi_\beta}\frac{p_\alpha}{p_\alpha^0} = \frac{\partial^2}{\partial^2 \phi_\beta}\frac{p_\alpha}{p_\alpha^0} = 0. \tag{2.69}$$

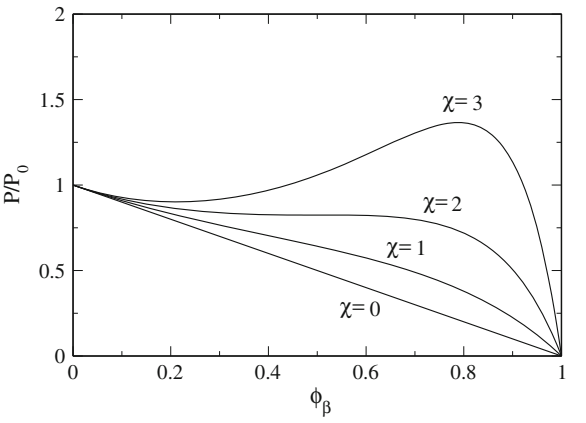

Fig. 2.10 Vapor pressure of a binary mixture with interaction (M = 1)

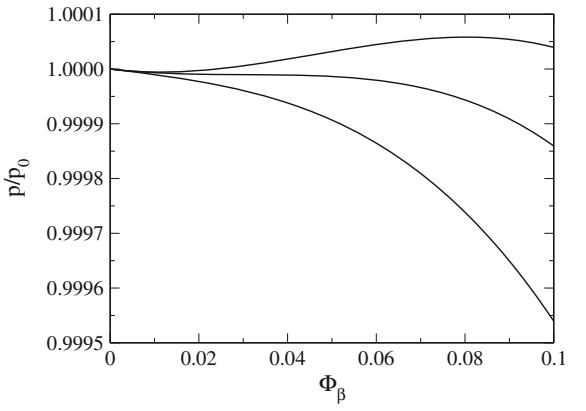

Fig. 2.11 Vapor pressure of a polymer solution with interaction for $M = 1000$, $\chi = 0.5, 0.532, 0.55$

2.3.3 Phase Diagram

In the simple Flory–Huggins theory the interaction parameter is proportional to $\frac{1}{T}$. Hence we can write it as

$$\chi = \frac{T_0 \chi_0}{T} \tag{2.70}$$

and discuss the free energy change as a function of ϕ_β and T:

$$\Delta F = N k_B T \left((1 - \phi_\beta) \ln(1 - \phi_\beta) + \frac{\phi_\beta}{M} \ln \phi_\beta \right) + N k_B T_0 \chi_0 \phi_\beta (1 - \phi_\beta) \tag{2.71}$$

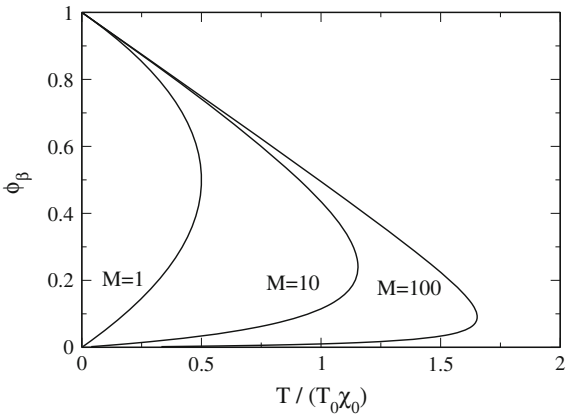

Fig. 2.12 Spinodal curve

The turning points follow from

$$0 = \frac{\partial^2}{\partial \phi_\beta^2} \Delta F = N k_B \left(\frac{T}{1-\phi_\beta} + \frac{T}{M \phi_\beta} - 2 T_0 \chi_0 \right) \tag{2.72}$$

as

$$\phi_{\beta,TP} = \frac{1}{2} + \frac{T(1-M) \pm \sqrt{T^2(M-1)^2 + 4T_0\chi_0 M (T_0\chi_0 M - T - 4MT)}}{4T_0\chi_0 M}. \tag{2.73}$$

This defines the spinodal curve which separates the unstable from the metastable region (Fig. 2.12).

Which is the minimum free energy of a two-phase system? The free energy takes the form

$$\Delta F = \Delta F^1 + \Delta F^2 = N^1 k_B T \Delta f(\phi_\beta^1) + N^2 k_B T \Delta f(\phi_\beta^2) \tag{2.74}$$

with

$$N^j = N_\alpha^j + M N_\beta^j \qquad \phi_\beta^j = \frac{M N_\beta^j}{N^j}. \tag{2.75}$$

The minimum free energy can be found from the condition that exchange of solvent or solute molecules between the two phases does not change the free energy, i.e., the chemical potentials in the two phases are the same

$$0 = d\Delta F = \left(\frac{\partial \Delta F^1}{\partial N_\alpha^1} - \frac{\partial \Delta F^2}{\partial N_\alpha^2} \right) dN_\alpha + \left(\frac{\partial \Delta F^1}{\partial N_\beta^1} - \frac{\partial \Delta F^2}{\partial N_\beta^2} \right) dN_\beta \tag{2.76}$$

$$0 = \mu_\alpha^1 - \mu_\alpha^2 = \mu_\beta^1 - \mu_\beta^2 \tag{2.77}$$

or

$$0 = \left(\Delta f^1 - \phi_\beta^1 \frac{\partial}{\partial \phi_\beta^1} \Delta f^1 \right) - \left(\Delta f^2 - \phi_\beta^2 \frac{\partial}{\partial \phi_\beta^2} \Delta f^2 \right) \tag{2.78}$$

$$0 = \left(\Delta f^1 + (1 - \phi_\beta^1) \frac{\partial}{\partial \phi_\beta^1} \right) \Delta f^1 - \left(\Delta f^2 + (1 - \phi_\beta^2) \frac{\partial}{\partial \phi_\beta^2} \Delta f^2 \right). \tag{2.79}$$

From the difference of these two equations, we find

$$\frac{\partial \Delta f^1}{\partial \phi_\beta^1} = \frac{\partial \Delta f^2}{\partial \phi_\beta^2} \tag{2.80}$$

and hence the slope of the free energy has to be the same for both phases. Inserting into the first equation then gives

$$\Delta f^1 - \Delta f^2 = (\phi_\beta^1 - \phi_\beta^2) \Delta f' \tag{2.81}$$

which shows that the concentrations of the two phases can be found by the well-known "common tangent" construction (Fig. 2.13).

These so called binodal points give the border to the stable one-phase region. Between spinodal and binodal the system is metastable. It is stable in relation to small fluctuations since the curvature of the free energy is positive. It is, however, unstable against larger scale fluctuations (Fig. 2.14).

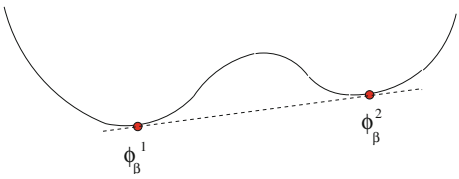

Fig. 2.13 Common tangent construction

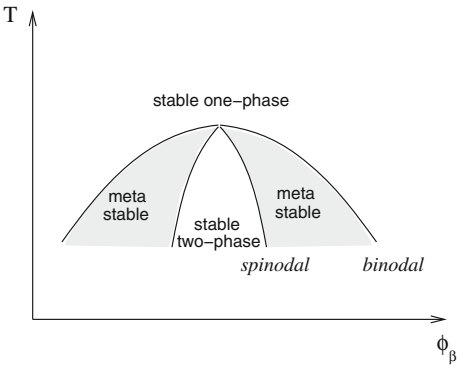

Fig. 2.14 Phase diagram

Problems

2.1 Osmotic pressure of a Polymer solution

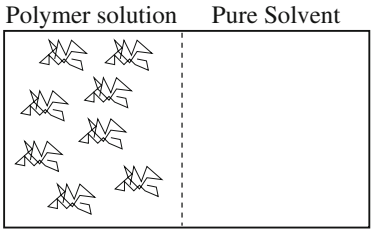

Calculate the osmotic pressure $\Pi = P - P'$ for the Flory–Huggins model of a polymer solution The difference of the chemical potential of the solvent

$$\mu_\alpha(P,T) - \mu_\alpha^0(P,T) = \frac{\partial \Delta F_m}{\partial N_\alpha}\Big|_{N_\beta,T}$$

can be obtained from the free energy change

$$\Delta F_m = N k_B T \left(\phi_\alpha \ln \phi_\alpha + \frac{\phi_\beta}{M} \ln \phi_\beta + \chi \phi_\alpha \phi_\beta\right)$$

and the osmotic pressure is given by

$$\mu_\alpha^0(P',T) - \mu_\alpha^0(P,T) = -\Pi \frac{\partial \mu_\alpha^0}{\partial P}.$$

Taylor series expansion gives the virial expansion of the osmotic pressure as a series of powers of ϕ_β. Truncate after the quadratic term and discuss qualitatively the dependence on the interaction parameter χ (and hence also on temperature).

2.2 Polymer mixture

Consider a mixture of two types of polymers with chain lengths M_1 and M_2 and calculate the mixing free energy change ΔF_m. Determine the critical values ϕ_c and χ_c. Discuss the phase diagram for the symmetrical case $M_1 = M_2$.

Part II
Protein Electrostatics and Solvation

Chapter 3
Implicit Continuum Solvent Models

Since an explicit treatment of all solvent atoms and ions is not possible in many cases, the effect of the solvent on the protein has to be approximated by implicit models which replace the large number of dynamic solvent modes by a continuous medium [8–10] and treat the solvent as a dielectric continuum. We discuss the Born model of a point charge in the center of a cavity and its extension for a general charge distribution. The solvation energy of a dipole is evaluated, together with its time dependence for the case of a simple Debye solvent.

3.1 Potential of Mean Force

In solution a protein occupies a conformation γ with the probability given by the Boltzmann factor

$$P(X,Y) = \frac{\mathrm{e}^{-U(X,Y)}}{\int dX dY \mathrm{e}^{-U(X,Y)}} \tag{3.1}$$

where X stands for the coordinates of the protein (including the protonation state) and Y for the coordinates of the solvent. The potential energy can be formally split into three terms

$$U(X,Y) = U_{prot}(X) + U_{solv}(Y) + U_{prot,solv}(X,Y). \tag{3.2}$$

The mean value of a physical quantity which depends only on the protein coordinates $Q(X)$ is

$$\overline{Q} = \int dX dY \quad Q(X)P(X,Y) = \int dX \quad Q(X)\widetilde{P}(X) \tag{3.3}$$

P.O.J. Scherer and S.F. Fischer, *Theoretical Molecular Biophysics*,
Biological and Medical Physics, Biomedical Engineering,
DOI 10.1007/978-3-662-55671-9_3

where we define a reduced probability distribution for the protein

$$\widetilde{P}(X) = \int dY \quad P(X, Y) \tag{3.4}$$

which is represented by introducing the potential of mean force

$$\widetilde{P}(X) = \frac{\mathrm{e}^{-W(X)/k_B T}}{\int dX \quad \mathrm{e}^{-W(X)/k_B T}} \tag{3.5}$$

$$\begin{aligned} \mathrm{e}^{-W(X)/k_B T} &= \mathrm{e}^{-U_{prot}(X)/k_B T} \int dY \quad \mathrm{e}^{-(U_{solv}(Y)+U_{prot,solv}(X,Y))/k_B T} \\ &= \mathrm{e}^{-(U_{prot}(X)+\Delta W(X))/k_B T} \end{aligned} \tag{3.6}$$

where ΔW accounts implicitly but exactly for the solvents effect on the protein.

3.2 Dielectric Continuum Model

In the following we discuss implicit solvent models, which treat the solvent as a dielectric continuum. In response to the partial charges of the protein q_i polarization of the medium produces an electrostatic reaction potential ϕ^R (Fig. 3.1).

If the medium behaves linearly (no dielectric saturation) the reaction potential is proportional to the charges

$$\phi_i^R = \sum_j f_{ij} q_j . \tag{3.7}$$

Let us now switch on the charges adiabatically by introducing a factor

$$q_i \to q_i \lambda \qquad 0 < \lambda < 1. \tag{3.8}$$

The change of the free energy is

$$dF = \sum_i \phi_i q_i d\lambda = \sum_{i \neq j} \frac{q_i q_j \lambda}{4\pi\varepsilon r_{ij}} d\lambda + \sum_{ij} f_{ij} q_j q_i \lambda d\lambda \tag{3.9}$$

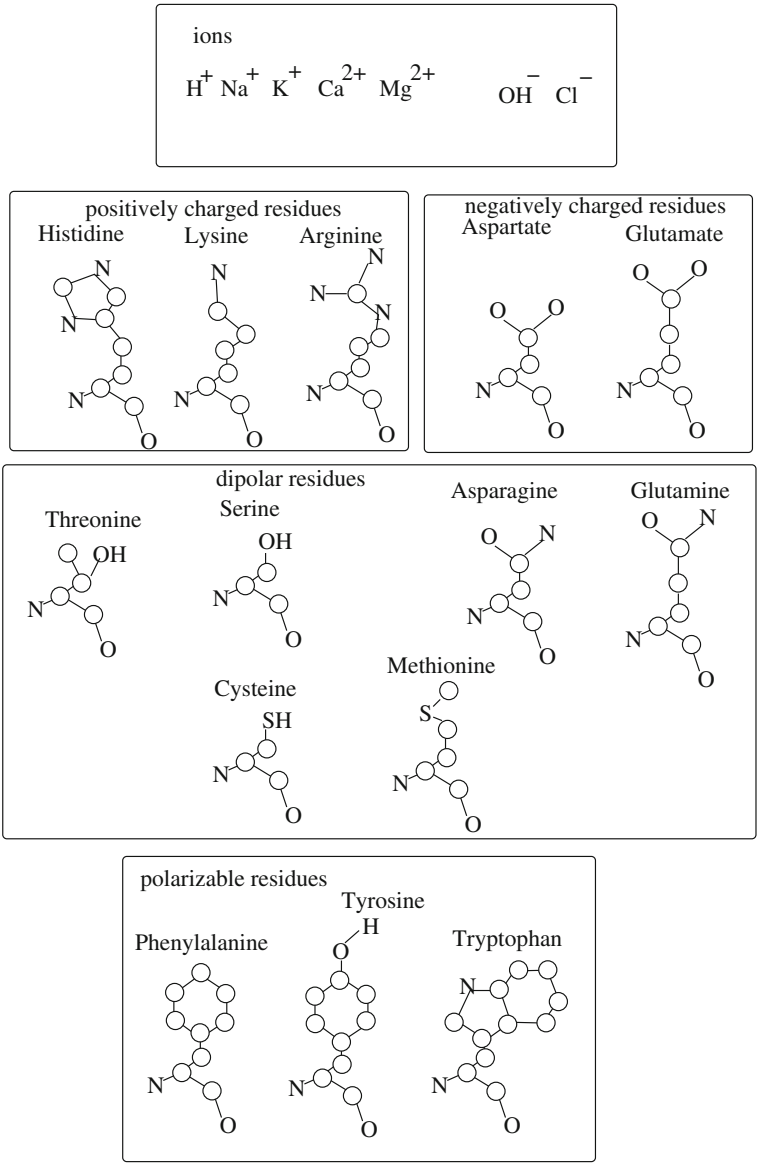

Fig. 3.1 Charged, polar, and polarizable groups in proteins. Biological macromolecules contain chemical compounds with certain electrostatic properties. These are often modeled using localized electric multipoles (partial charges, dipoles ...) and polarizabilities

and thermodynamic integration gives the change of free energy due to Coulombic interactions

$$\Delta F_{elec} = \int_0^1 \lambda d\lambda \left(\sum_{i \neq j} \frac{q_i q_j}{4\pi\varepsilon r_{ij}} + \sum_{ij} f_{ij} q_j q_i \right)$$
$$= \frac{1}{2} \sum_{i \neq j} \frac{q_i q_j}{4\pi\varepsilon r_{ij}} + \frac{1}{2} \sum_{ij} f_{ij} q_j q_i . \tag{3.10}$$

The first part is a property of the protein and hence included in U_{prot}. The second part is the mean force potential

$$\Delta W_{elec} = \frac{1}{2} \sum_{ij} f_{ij} q_i q_j . \tag{3.11}$$

3.3 Born Model

The Born model [11] is a simple continuum model to calculate the solvation free energy of an ion. Consider a point charge q in the center of a cavity with radius a (the so called Born radius of the ion). The dielectric constant is ε_1 inside the sphere and ε_2 outside (Fig. 3.2).

The electrostatic potential is given outside the sphere by

$$\Phi = \frac{q}{4\pi\varepsilon_2 r} \tag{3.12}$$

and inside by

$$\Phi = \Phi_0 + \frac{q}{4\pi\varepsilon_1 r} . \tag{3.13}$$

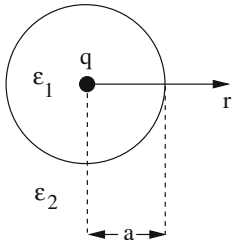

Fig. 3.2 Born model for Ion solvation

From the continuity of the potential at the cavity surface we find the reaction potential

$$\Phi_0 = \frac{q}{4\pi a}\left(\frac{1}{\varepsilon_2} - \frac{1}{\varepsilon_1}\right). \tag{3.14}$$

Since there is only one charge we have

$$f_{1,1} = \frac{1}{4\pi a}\left(\frac{1}{\varepsilon_2} - \frac{1}{\varepsilon_1}\right) \tag{3.15}$$

and the solvation energy is given by the famous Born formula

$$\Delta W_{elec} = \frac{q^2}{8\pi a}\left(\frac{1}{\varepsilon_2} - \frac{1}{\varepsilon_1}\right). \tag{3.16}$$

3.4 Charges in a Protein

The continuum model can be applied to a more general charge distribution in a protein. An important example is an ion pair within a protein ($\varepsilon_r = 2$) surrounded by water ($\varepsilon_r = 80$). We study an idealized model where the protein is represented by a sphere (Fig. 3.3).

We will first treat a single charge within the sphere. A system of charges can then be treated by superposition of the individual contributions.

Using polar coordinates (r, θ, φ) the potential of a system with axial symmetry (no dependence on φ) can be written with the help of Legendre polynomials as

$$\phi = \sum_{n=0}^{\infty} (A_n r^n + B_n r^{-(n+1)}) P_n(\cos\theta). \tag{3.17}$$

The general solution can be written as the sum of a special solution and a harmonic function. The special solution is given by the multipole expansion

Fig. 3.3 Ion pair in a protein

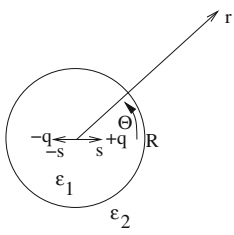

$$\frac{q}{4\pi\varepsilon_1|\mathbf{r}-\mathbf{s}_+|} = \frac{q}{4\pi\varepsilon_1}\frac{1}{r}\sum_{n=0}^{\infty}\left(\frac{s}{r}\right)^n P_n(\cos\theta). \tag{3.18}$$

Since the potential has to be finite at large distances, outside it has the form

$$\phi_2 = \sum_{n=0}^{\infty} B_n r^{-(n+1)} P_n(\cos\theta) \tag{3.19}$$

and inside the potential is given by

$$\phi_1 = \sum_{n=0}^{\infty}\left(A_n r^n + \frac{qs^n}{4\pi\varepsilon_1} r^{-(n+1)}\right) P_n(\cos\theta). \tag{3.20}$$

At the boundary we have two conditions

$$\phi_1(R) = \phi_2(R) \rightarrow B_n R^{-(n+1)} = A_n R^n + \frac{qs^n}{4\pi\varepsilon_1} R^{-(n+1)} \tag{3.21}$$

$$\varepsilon_1 \frac{\partial}{\partial r}\phi_1(R) = \varepsilon_2 \frac{\partial}{\partial r}\phi_2(R) = 0 \tag{3.22}$$

$$\rightarrow -\frac{\varepsilon_2}{\varepsilon_1}(n+1) B_n R^{-(n+2)} = n A_n R^{n-1} - (n+1)\frac{qs^n}{4\pi\varepsilon_1} R^{-(n+2)} \tag{3.23}$$

from which the coefficients can be easily determined

$$\begin{aligned} A_n &= \frac{qs^n}{4\pi\varepsilon_1} R^{-1-2n}\frac{(\varepsilon_1-\varepsilon_2)(n+1)}{n\varepsilon_1+(n+1)\varepsilon_2} \\ B_n &= \frac{qs^n}{4\pi\varepsilon_1}\frac{(2n+1)\varepsilon_1}{n\varepsilon_1+(n+1)\varepsilon_2}. \end{aligned} \tag{3.24}$$

The potential inside the sphere is

$$\phi_1 = \frac{q}{4\pi\varepsilon_1|\mathbf{r}-\mathbf{s}_+|} + \phi^R \tag{3.25}$$

with the reaction potential

$$\phi^R = \sum_{n=0}^{\infty}\frac{qs^n}{4\pi\varepsilon_1} R^{-1-2n}\frac{(\varepsilon_1-\varepsilon_2)(n+1)}{n\varepsilon_1+(n+1)\varepsilon_2} r^n P_n(\cos\theta) \tag{3.26}$$

and the electrostatic energy is given (without the infinite self energy) by

$$\frac{1}{2}q\phi(s,\cos\theta=1)=\frac{q}{2}\sum_{n=1}^{\infty}\frac{qs^n}{4\pi\varepsilon_1}R^{-1-2n}\frac{(\varepsilon_1-\varepsilon_2)(n+1)}{n\varepsilon_1+(n+1)\varepsilon_2}s^n \tag{3.27}$$

which for $\varepsilon_2 >> \varepsilon_1$ is approximately

$$\frac{q^2}{2}\frac{1}{4\pi R}\left(\frac{1}{\varepsilon_2}-\frac{1}{\varepsilon_1}\right)\sum\left(\frac{s}{R}\right)^{2n}=-\frac{q^2}{2}\frac{1}{4\pi R}\left(\frac{1}{\varepsilon_1}-\frac{1}{\varepsilon_2}\right)\frac{1}{1-s^2/R^2}. \tag{3.28}$$

Consider now two charges $\pm q$ at symmetric positions $\pm s$. The reaction potentials of the two charges add up to

$$\phi^R=\phi_+^R+\phi_-^R \tag{3.29}$$

and the electrostatic free energy is given by

$$\frac{-q^2}{4\pi\varepsilon_1(2s)}+\frac{1}{2}q\phi_+^R(s)+\frac{1}{2}q\phi_-^R(s)+\frac{1}{2}(-q)\phi_+^R(-s)+\frac{1}{2}(-q)\phi_-^R(-s). \tag{3.30}$$

By comparison we find

$$\frac{q^2}{2}f_{++}=\frac{1}{2}q\phi_+^R(s)=-\frac{q^2}{2}\frac{1}{4\pi R}\left(\frac{1}{\varepsilon_1}-\frac{1}{\varepsilon_2}\right)\frac{1}{1-s^2/R^2} \tag{3.31}$$

$$\frac{(-q)^2}{2}f_{--}=\frac{1}{2}(-q)\phi_-^R(-s)=-\frac{q^2}{2}\frac{1}{4\pi R}\left(\frac{1}{\varepsilon_1}-\frac{1}{\varepsilon_2}\right)\frac{1}{1-s^2/R^2} \tag{3.32}$$

$$\frac{(-q)q}{2}f_{-+}=\frac{1}{2}(-q)\phi_+^R(-s)=\frac{(-q)}{2}\sum_{n=1}^{\infty}\frac{qs^n}{4\pi\varepsilon_1}R^{-1-2n}\frac{(\varepsilon_1-\varepsilon_2)(n+1)}{n\varepsilon_1+(n+1)\varepsilon_2}(-s)^n \tag{3.33}$$

$$\approx\frac{-q^2}{2}\frac{1}{4\pi R}\left(\frac{1}{\varepsilon_2}-\frac{1}{\varepsilon_1}\right)\sum_{n=0}^{\infty}(-)^n\left(\frac{s}{R}\right)^{2n}=-\frac{(-q^2)}{2}\frac{1}{4\pi R}\left(\frac{1}{\varepsilon_1}-\frac{1}{\varepsilon_2}\right)\frac{1}{s^2/R^2+1} \tag{3.34}$$

$$\frac{q(-q)}{2}f_{+-}=\frac{1}{2}q\phi_-^R(s)=\frac{(-q)q}{2}f_{-+} \tag{3.35}$$

and finally the solvation energy is

$$W_{elec} = \sum_{n=1}^{\infty} \frac{q^2 s^n}{4\pi\varepsilon_1} R^{-1-2n} \frac{(\varepsilon_1 - \varepsilon_2)(n+1)}{n\varepsilon_1 + (n+1)\varepsilon_2} (s^n - (-s)^n) \tag{3.36}$$

$$\begin{aligned} W_{elec} &\approx -q^2 \frac{1}{4\pi R} \left(\frac{1}{\varepsilon_1} - \frac{1}{\varepsilon_2} \right) \frac{1}{1 - s^2/R^2} - (-q^2) \frac{1}{4\pi R} \left(\frac{1}{\varepsilon_1} - \frac{1}{\varepsilon_2} \right) \frac{1}{s^2/R^2 + 1} \\ &= -\frac{(2qs)^2}{8\pi R} \left(\frac{1}{\varepsilon_1} - \frac{1}{\varepsilon_2} \right) \frac{1}{1 - s^4/R^4}. \end{aligned} \tag{3.37}$$

If the extension of the system of charges in the protein is small compared to the radius $s << R$ the multipole expansion of the reaction potential converges rapidly. Since the total charge of the ion pair is zero the monopole contribution (n = 0)

$$W_{elec}^{(1)} = \frac{Q^2}{8\pi R} \left(\frac{1}{\varepsilon_2} - \frac{1}{\varepsilon_1} \right) \tag{3.38}$$

(which is nothing but the Born energy (3.16)) vanishes and the leading term is the dipole contribution[1] ($n = 1, \quad p = 2qs$)

$$W_{elec}^{(2)} = \frac{p^2}{4\pi\varepsilon_1 R^3} \frac{(\varepsilon_1 - \varepsilon_2)}{\varepsilon_1 + 2\varepsilon_2}. \tag{3.39}$$

3.5 Time Dependent Reaction Field

We consider now a solute which changes its dipole moment very fast at time $t = 0$ due to an optical excitation [12]. For $t < 0$ the charge distribution is in equilibrium with the reaction field given by (3.26), (3.29). After the change, the reaction field relaxes toward its new equilibrium value. We consider a continuum with frequency dependent dielectric constant, which is in the simplest case described by Debye's model with one relaxation time

$$\varepsilon_2 = \varepsilon(\omega) = \varepsilon_\infty + \frac{\varepsilon_0 - \varepsilon_\infty}{1 + \mathrm{i}\omega\tau_D}. \tag{3.40}$$

More complicated solvents can be described by a sum of such terms with several relaxation times.

We concentrate on the dipolar interactions, assuming that the multipole expansion converges fast. Then, the time dependent solvation energy is

[1] This has been associated with several names (Bell, Onsager, Kirkwood).

$$W_{elec}(t) = -p(t)\Phi^R_{dip}(t) \tag{3.41}$$

with the dipole reaction field

$$\Phi^R_{dip}(t) = \frac{1}{4\pi\varepsilon_1 R^3} f(t) \tag{3.42}$$

which is assumed to be a linear functional of the perturbation

$$f(t) = F[p(t)]. \tag{3.43}$$

The response to a monochromatic perturbation is

$$F\left[\mathrm{e}^{\mathrm{i}\omega t}\right] = g(\omega)\mathrm{e}^{\mathrm{i}\omega t} = \frac{(\varepsilon_1 - \varepsilon(\omega))}{\varepsilon_1 + 2\varepsilon(\omega)} \tag{3.44}$$

hence the impulse response is given by the Fourier transform

$$F\left[\delta(t)\right] = \frac{1}{2\pi} F\left[\int d\omega \mathrm{e}^{\mathrm{i}\omega t}\right] = \frac{1}{2\pi}\int d\omega\, g(\omega)\mathrm{e}^{\mathrm{i}\omega t} = \tilde{g}(t) \tag{3.45}$$

which for the Debye model becomes

$$\tilde{g}(t) = \frac{3\varepsilon_1(\varepsilon_0 - \varepsilon_\infty)}{\tau_D(2\varepsilon_\infty + \varepsilon_1)^2}\Theta(t)\mathrm{e}^{-t/\tau_L} + \frac{\varepsilon_\infty - \varepsilon_1}{2\varepsilon_\infty + \varepsilon_1}\delta(t) \tag{3.46}$$

with the longitudinal relaxation time

$$\tau_L = \tau_D \frac{2\varepsilon_\infty + \varepsilon_1}{2\varepsilon_0 + \varepsilon_1}. \tag{3.47}$$

The response to a time dependent dipole moment then is

$$F[p(t)] = F[\int_{-\infty}^{\infty} p(t')\delta(t - t')dt'] = \int_{-\infty}^{\infty} p(t')\tilde{g}(t - t')dt' \tag{3.48}$$

where, in fact the upper limit of the integral is t, due to causality ($\tilde{g}(t - t') = 0$ for $t' > t$).

The response to a sudden change is

$$f(t) = F\left[p_0 + \Delta p\, \Theta(t)\right] = p_0 \int_{-\infty}^{\infty} \tilde{g}(t')dt' + \Delta p\Theta(t) \int_0^t \tilde{g}(t')dt'$$

$$= p_0 \frac{\varepsilon_0 - \varepsilon_1}{2\varepsilon_0 + \varepsilon_1} \quad \text{for } t < 0$$

$$= p_0 \frac{\varepsilon_0 - \varepsilon_1}{2\varepsilon_0 + \varepsilon_1} + \Delta p \left[\frac{\varepsilon_\infty - \varepsilon_1}{2\varepsilon_\infty + \varepsilon_1} + \frac{3\varepsilon_1(\varepsilon_0 - \varepsilon_\infty)}{(2\varepsilon_\infty + \varepsilon_1)(2\varepsilon_0 + \varepsilon_1)} \left(1 - \mathrm{e}^{-t/\tau_L}\right) \right] \quad \text{for } t \geq 0.$$

Immediately after the excitation

$$f(t = 0^+) = p_0 \frac{\varepsilon_0 - \varepsilon_1}{2\varepsilon_0 + \varepsilon_1} + \Delta p \frac{\varepsilon_\infty - \varepsilon_1}{2\varepsilon_\infty + \varepsilon_1} \tag{3.49}$$

whereas at long times the slow degrees of freedom become effective and

$$f(t \gg \tau_L) = (p_0 + \Delta p) \frac{\varepsilon_0 - \varepsilon_1}{2\varepsilon_0 + \varepsilon_1}. \tag{3.50}$$

3.6 Generalized Born Models

The Generalized Born model approximates the protein as a sphere with a dielectric constant different from that of the solvent [13, 14].

Still and coworkers [14] proposed an approximate expression for the solvation free energy of an arbitrary distribution of N charges:

$$W_{elec} = \frac{1}{8\pi} \left(\frac{1}{\varepsilon_2} - \frac{1}{\varepsilon_1} \right) \sum_{i,j=1}^{N} \frac{q_i q_j}{f_{GB}(r_{ij}, a_{ij})} \tag{3.51}$$

with the smooth function

$$f_{GB} = \sqrt{r_{ij}^2 + a_i a_j \exp\left\{ -\frac{r_{ij}^2}{2a_i a_j} \right\}} \tag{3.52}$$

where the effective Born radius a_i accounts for the effect of neighboring solute atoms. Several methods have been developed to calculate appropriate values of the a_i [14–17].

Expression (3.51) interpolates between the Born energy of a total charge Nq at short distances

$$W_{elec} \to \frac{1}{8\pi} \left(\frac{1}{\varepsilon_2} - \frac{1}{\varepsilon_1} \right) \frac{N^2 q^2}{a} \text{ for } r_{ij} \to 0 \tag{3.53}$$

and the sum of the individual Born energies plus the change in Coulombic energy

$$W_{elec} \rightarrow \frac{1}{8\pi}\left(\frac{1}{\varepsilon_2}-\frac{1}{\varepsilon_1}\right)\left(\sum_i \frac{q_i^2}{a_i}+\sum_{i\neq j}\frac{q_i q_j}{r_{ij}}\right) \text{ for } r_{ij} \gg \sqrt{a_i a_j} \tag{3.54}$$

for a set of well separated charges. It gives a reasonable description in many cases without the computational needs of a full electrostatics calculation.

Chapter 4
Debye–Hückel Theory

Mobile charges like Na^+ or Cl^- ions are very important for the functioning of biomolecules. In a stationary state their concentration depends on the local electrostatic field which is produced by the charge distribution of the biomolecule which in turn depends for instance on the protonation state and on the conformation. In this chapter we present continuum models to describe the interaction between a biomolecule and surrounding mobile charges [18–21]. We derive the Poisson–Boltzmann equation and study its solutions for simple geometries like a charged sphere and cylinder and the Gouy–Chapman double layer including Stern's modification for finite ion radius.

4.1 Electrostatic Shielding by Mobile Charges

We consider a fully dissociated (strong) electrolyte containing N_i mobile ions of the sort $i = 1 \cdots$ with charges $Z_i e$ per unit volume. The charge density of the mobile charges is given by the average numbers of ions per volume

$$\varrho_{mob}(\mathbf{r}) = \sum_i Z_i e \overline{N}_i(\mathbf{r}). \tag{4.1}$$

The electrostatic potential is given by the Poisson equation

$$\varepsilon \Delta \phi(\mathbf{r}) = -\varrho(\mathbf{r}) = -\varrho_{mob}(\mathbf{r}) - \varrho_{fix}(\mathbf{r}). \tag{4.2}$$

Debye and Hückel [22] used Boltzmann's theorem to determine the mobile charge density. Without the presence of fixed charges the system is neutral

P.O.J. Scherer and S.F. Fischer, *Theoretical Molecular Biophysics*,
Biological and Medical Physics, Biomedical Engineering,
DOI 10.1007/978-3-662-55671-9_4

$$0 = \varrho^0_{mob} = \sum_i Z_i e N_i^0 \tag{4.3}$$

and the constant value of the potential can be chosen as zero.

$$\phi^0 = 0. \tag{4.4}$$

The fixed charges produce a change of the potential. The electrostatic energy of an ions of sort is

$$W_i = Z_i e \phi(\mathbf{r}) \tag{4.5}$$

and the density of such ions is given by a Boltzmann distribution

$$\frac{N_i(\mathbf{r})}{N_i^0} = \frac{\mathrm{e}^{-Z_i e\phi(\mathbf{r})/k_B T}}{\mathrm{e}^{-Z_i e\phi^0/k_B T}} \tag{4.6}$$

or

$$N_i(\mathbf{r}) = N_i^0 \mathrm{e}^{-Z_i e\phi(\mathbf{r})/k_B T}. \tag{4.7}$$

The total mobile charge density is

$$\varrho_{mob}(\mathbf{r}) = \sum_i Z_i e N_i^0 \mathrm{e}^{-Z_i e\phi(\mathbf{r})/k_B T} \tag{4.8}$$

and we obtain the Poisson–Boltzmann equation

$$\varepsilon \Delta\phi(\mathbf{r}) = -\sum_i Z_i e N_i^0 \mathrm{e}^{-Z_i e\phi(\mathbf{r})/k_B T} - \varrho_{fix}(\mathbf{r}). \tag{4.9}$$

If the solution is very dilute we can expect that the ion–ion interaction is much smaller than thermal energy

$$Z_i e\phi \ll k_B T \tag{4.10}$$

and linearize the Poisson–Boltzmann equation

$$\varepsilon \Delta\phi(\mathbf{r}) = -\varrho_{fix}(\mathbf{r}) - \sum_i Z_i e N_i^0 \left(1 - \frac{Z_i e}{k_B T}\phi(\mathbf{r}) + \cdots\right). \tag{4.11}$$

The first summand vanishes due to electroneutrality and we find finally

$$\Delta\phi(\mathbf{r}) - \kappa^2\phi(\mathbf{r}) = -\frac{1}{\varepsilon}\varrho_{fix}(\mathbf{r}) \tag{4.12}$$

with the inverse Debye length

$$\lambda_{Debye}^{-1} = \kappa = \sqrt{\frac{e^2}{\varepsilon k_B T}\sum_i N_i^0 Z_i^2}\,. \tag{4.13}$$

4.2 1-1 Electrolytes

If there are only two types of ions with charges $Z_{1,2} = \pm 1$ (also in semiconductor physics) the Poisson–Boltzmann equation can be written as

$$\frac{e}{k_B T}\Delta\phi(\mathbf{r}) + \frac{e^2}{\varepsilon k_B T}N^0(\mathrm{e}^{-e\phi(\mathbf{r})/k_B T} - \mathrm{e}^{e\phi(\mathbf{r})/k_B T}) = -\frac{e}{\varepsilon k_B T}\varrho_{fix}(\mathbf{r}) \tag{4.14}$$

which after substitution

$$\widetilde{\phi}(\mathbf{r}) = \frac{e}{k_B T}\phi(\mathbf{r}) \tag{4.15}$$

takes the form

$$\Delta\widetilde{\phi}(\mathbf{r}) - \kappa^2\sinh(\widetilde{\phi}(\mathbf{r})) = -\frac{e}{\varepsilon k_B T}\varrho_{fix}(\mathbf{r}) \tag{4.16}$$

and with the scaled radius vector $\mathbf{r}' = \kappa\mathbf{r} \rightarrow \widetilde{\phi}(\mathbf{r}) = f(\mathbf{r}') = f(\kappa\mathbf{r})$

$$\Delta f(\mathbf{r}') - \sinh(f(\mathbf{r}')) = -\frac{e}{\kappa^2\varepsilon k_B T}\varrho_{fix}(\kappa^{-1}\mathbf{r}'). \tag{4.17}$$

4.3 Charged Sphere

We consider a spherical protein (radius R) with a charged sphere (radius a) in its center (Fig. 4.1).

For a spherical problem we only have to consider the radial part of the Laplacian and the linearized Poisson–Boltzmann equation becomes outside the protein

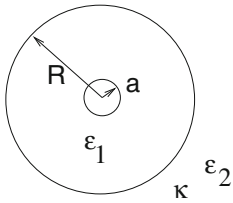

Fig. 4.1 Simple model of a charged protein

$$\frac{1}{r}\frac{\mathrm{d}^2}{\mathrm{d}r^2}\left(r\phi(r)\right) - \kappa^2\phi(r) = 0 \tag{4.18}$$

which has the solution

$$\phi_2(r) = \frac{c_1\mathrm{e}^{-\kappa r} + c_2\mathrm{e}^{\kappa r}}{r}\,. \tag{4.19}$$

Since the potential should vanish at large distances we have $c_2 = 0$. Inside the protein ($a < r < R$) solution of the Poisson equation gives

$$\phi_1(r) = c_3 + \frac{Q}{4\pi\varepsilon_1 r}. \tag{4.20}$$

At the boundary we have the conditions

$$\phi_1(R) = \phi_2(R) \rightarrow c_3 = \frac{c_1\mathrm{e}^{-\kappa R}}{R} - \frac{Q}{4\pi\varepsilon_1 R} \tag{4.21}$$

$$\varepsilon_1\frac{\partial}{\partial r}\phi_1(R) = \varepsilon_2\frac{\partial}{\partial r}\phi_2(R) \rightarrow -\frac{Q}{4\pi R^2} = c_1\varepsilon_2\left(-\frac{\mathrm{e}^{-\kappa R}}{R^2} - \kappa\frac{\mathrm{e}^{-\kappa R}}{R}\right) \tag{4.22}$$

which gives the constants

$$c_1 = \frac{Q\mathrm{e}^{\kappa R}}{4\pi\varepsilon_2(1+\kappa R)} \tag{4.23}$$

and

$$c_3 = -\frac{Q}{4\pi\varepsilon_1 R} + \frac{Q}{4\pi\varepsilon_2 R(1+\kappa R)}\,. \tag{4.24}$$

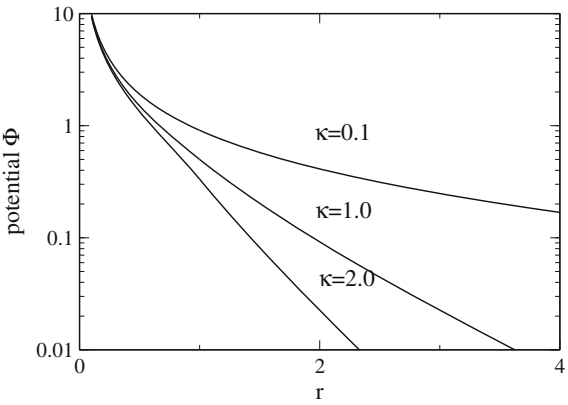

Fig. 4.2 Charged sphere in an electrolyte. The potential $\phi(r)$ is shown for $a = 0.1,\ R = 1.0$

Together we find the potential inside the sphere

$$\phi_1(r) = \frac{Q}{4\pi\varepsilon_1}\left(\frac{1}{r} - \frac{1}{R}\right) + \frac{Q}{4\pi\varepsilon_2 R(1+\kappa R)} \tag{4.25}$$

and outside (Fig. 4.2)

$$\phi_2(r) = \frac{Q}{4\pi\varepsilon_2(1+\kappa R)}\frac{\mathrm{e}^{-\kappa(r-R)}}{r}\,. \tag{4.26}$$

The ion charge density is given by

$$\varrho_{mob}(r) = \varepsilon_2 \Delta\phi_2 = \varepsilon_2\kappa^2\phi_2 \tag{4.27}$$

hence the ion charge at distances between r and $r + dr$ is given by

$$\kappa\frac{Q}{(1+\kappa R)} r\mathrm{e}^{-\kappa(r-R)}dr. \tag{4.28}$$

This function has a maximum at $r_{max} = 1/\kappa$ and decays exponentially at larger distances (Fig. 4.3).

Let the charge be concentrated on the surface of the inner sphere. Then we have

$$\phi_1(a) = \frac{Q}{4\pi\varepsilon_1}\left(\frac{1}{a} - \frac{1}{R}\right) + \frac{Q}{4\pi\varepsilon_2 R(1+\kappa R)}\,. \tag{4.29}$$

Without the medium ($\varepsilon_2 = \varepsilon_1$, $\kappa = 0$) the potential would be

$$\phi_1^0(a) = \frac{Q}{4\pi\varepsilon_1 a} \tag{4.30}$$

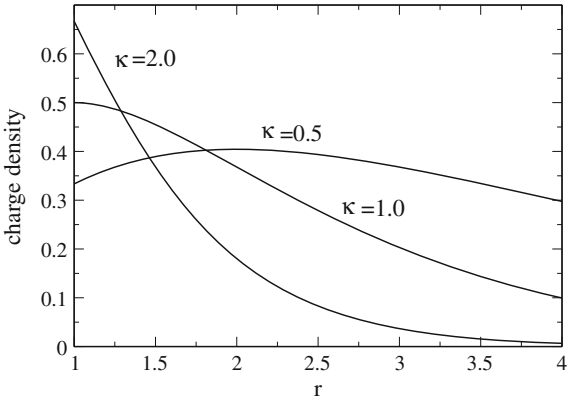

Fig. 4.3 Charge density around the charged sphere for $a = 0.1$, $R = 1.0$

hence the solvation energy is

$$W = \frac{1}{2} Q\phi^R = \frac{1}{2} Q(\phi_1(a) - \phi_1^0(a)) = \frac{Q^2}{8\pi R}\left(\frac{1}{\varepsilon_2(1+\kappa R)} - \frac{1}{\varepsilon_1}\right) \tag{4.31}$$

which for $\kappa = 0$ is given by the well-known Born formula

$$W = -\frac{Q^2}{8\pi R}\left(\frac{1}{\varepsilon_1} - \frac{1}{\varepsilon_2}\right) \tag{4.32}$$

and for $a \to R$, $\varepsilon_1 = \varepsilon_2$ gives the solvation energy of an ion in solution

$$\Delta G_{sol} = W = -\frac{Q^2}{8\pi\varepsilon}\frac{\kappa}{(1+\kappa R)}\,. \tag{4.33}$$

4.4 Charged Cylinder

Next we discuss a cylinder of radius a and length $l \ll a$ carrying the net charge Ne uniformly distributed on its surface (Fig. 4.4).

$$\sigma = \frac{Ne}{2\pi a l}\,. \tag{4.34}$$

Outside the cylinder this charge distribution is equivalent to a linear distribution of charges along the axis of the cylinder with a 1-d density

$$\frac{Ne}{l} = 2\pi a\sigma = \frac{e}{b}\,. \tag{4.35}$$

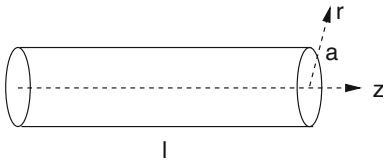

Fig. 4.4 Charged cylinder model

For the general case of a charged cylinder in an ionic solution we have to restrict the discussion to the linearized PBE which becomes outside the cylinder

$$\frac{1}{r}\frac{\mathrm{d}}{\mathrm{d}r}\left(r\frac{\mathrm{d}}{\mathrm{d}r}\right)\phi(r) = \kappa^2\phi(r). \tag{4.36}$$

Substitution $r \to x = \kappa r$ gives the equation

$$\frac{\mathrm{d}^2}{\mathrm{d}x^2}\phi(x) + \frac{1}{x}\frac{\mathrm{d}}{\mathrm{d}x}\phi(x) - \phi(x) = 0. \tag{4.37}$$

The solution of this equation are the modified Bessel functions of order zero denoted as $I_0(x)$ and $K_0(x)$. For large values of x

$$\lim_{x\to\infty} I_0(x) = \infty \qquad \lim_{x\to\infty} K_0(x) = 0 \tag{4.38}$$

and hence the potential in the outer region has the form

$$\phi(r) = C_1 K_0(\kappa r). \tag{4.39}$$

Inside the cylinder surface the electric field is given by Gauss' theorem

$$2\pi r l \varepsilon_1 E(r) = Ne \tag{4.40}$$

$$E(r) = -\frac{\mathrm{d}\phi(r)}{\mathrm{d}r} = \frac{Ne}{2\pi\varepsilon_1 r l} \tag{4.41}$$

and hence the potential inside is

$$\phi(r) = C_2 - \frac{Ne}{2\pi\varepsilon_1 l}\ln r. \tag{4.42}$$

The boundary conditions are

$$\phi(a) = C_1 K_0(\kappa a) = C_2 - \frac{Ne}{2\pi\varepsilon_1 l}\ln a \tag{4.43}$$

$$\varepsilon_1 \frac{\mathrm{d}\phi(a)}{\mathrm{d}r} = -\frac{Ne}{2\pi a l} = \varepsilon_2 \frac{\mathrm{d}\phi(a)}{\mathrm{d}r} = \varepsilon_2 C_1(-\kappa K_1(\kappa a)) \tag{4.44}$$

from which we find

$$C_1 = \frac{Ne}{2\pi a l \varepsilon_2 \kappa K_1(\kappa a)} \tag{4.45}$$

and

$$C_2 = \frac{Ne}{2\pi a l \varepsilon_2 \kappa} \frac{K_0(\kappa a)}{K_1(\kappa a)} + \frac{Ne}{2\pi \varepsilon_1 l} \ln a. \tag{4.46}$$

The potential is then outside

$$\phi(r) = \frac{Ne}{2\pi a l \varepsilon_2 \kappa} \frac{K_0(\kappa r)}{K_1(\kappa a)} \tag{4.47}$$

and inside

$$\phi(r) = \frac{Ne}{2\pi a l \varepsilon_2 \kappa} \frac{K_0(\kappa a)}{K_1(\kappa a)} + \frac{Ne}{2\pi \varepsilon_1 l} \ln a - \frac{Ne}{2\pi \varepsilon_1 l} \ln r. \tag{4.48}$$

For small $\kappa a \to 0$ we can use the asymptotic behavior of the Bessel functions

$$\begin{aligned} K_0(x) &\to \ln \frac{2}{x} - \gamma + \cdots \qquad \gamma = 0.577\cdots \\ K_1(x) &\to \frac{1}{x} + \cdots \end{aligned} \tag{4.49}$$

to have approximately

$$\begin{aligned} C_1 &\approx \frac{Ne}{2\pi a l \varepsilon_2 \kappa} \kappa a = \frac{Ne}{2\pi l \varepsilon_2} \\ C_2 &\approx \frac{Ne}{2\pi l \varepsilon_2} \left(\ln \frac{2}{\kappa a} - \gamma \right) + \frac{Ne}{2\pi \varepsilon_1 l} \ln a. \end{aligned} \tag{4.50}$$

The potential outside is

$$\phi(r) = -\frac{Ne}{2\pi l \varepsilon_2} \left(\gamma + \ln \frac{\kappa}{2} + \ln r \right) \tag{4.51}$$

and inside

$$\begin{aligned} \phi(r) &= \frac{Ne}{2\pi l \varepsilon_2} \left(\ln \frac{2}{\kappa a} - \gamma \right) + \frac{Ne}{2\pi \varepsilon_1 l} \ln a - \frac{Ne}{2\pi \varepsilon_1 l} \ln r \\ &= \frac{Ne}{2\pi l} \left(-\frac{\gamma}{\varepsilon_2} - \frac{1}{\varepsilon_2} \ln \frac{\kappa}{2} + \left(\frac{1}{\varepsilon_1} - \frac{1}{\varepsilon_2} \right) \ln a - \frac{1}{\varepsilon_1} \ln r \right). \end{aligned} \tag{4.52}$$

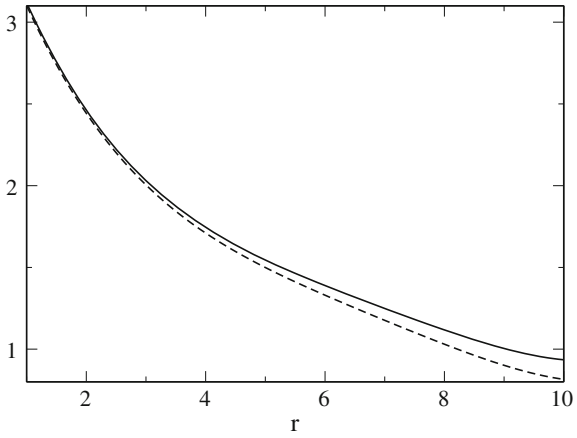

Fig. 4.5 Potential of a charged cylinder with unit radius $a = 1$ for $\kappa = 0.05$. *Solid curve*: $K_0(\kappa r)/(\kappa K_1(\kappa))$. *Dashed curve*: approximation by $-\ln\frac{\kappa}{2} - \ln r - \gamma$

Outside the potential consists of the potential of the charged line ($\ln r$) and an additional contribution from the screening of the ions (Fig. 4.5).

4.5 Charged Membrane (Goüy–Chapman Double Layer)

We approximate the surface charge of a membrane by a thin layer charged with a homogeneous charge distribution (Fig. 4.6).

Gouy [23, 24] and Chapman [25] derived the potential similar to Debye–Hückel theory. For a 1-1 electrolyte (NaCl for example) the one-dimensional Poisson–Boltzmann equation has the form (with transformed variables as above)

$$\frac{\mathrm{d}^2}{\mathrm{d}x^2} f(x) - \sinh(f(x)) = g(x) \tag{4.53}$$

where the source term $g(x) = -\frac{e}{\kappa^2 \varepsilon k_B T}\varrho(x/\kappa)$ has the character of a Delta-function centered at $x = 0$. Consider an area A of the membrane and integrate along the x-axis:

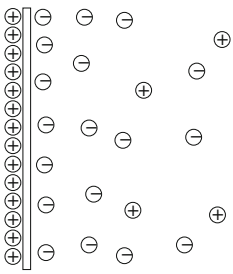

Fig. 4.6 Gouy–Chapman double layer

$$\int dA \int_{-0}^{+0} \varrho(x)dx = \sigma_0 A \tag{4.54}$$

$$\begin{aligned}\int dA \int_{-0}^{+0} dx \quad g(x) &= -\frac{e}{\kappa^2 \varepsilon k_B T} \int dA \int_{-0}^{+0} \kappa dx' \varrho(x') \\ &= -\frac{e}{\kappa \varepsilon k_B T} \sigma_0 A. \end{aligned} \tag{4.55}$$

Hence we identify

$$\varrho(x) = \sigma_0 \delta(x) \qquad g(x) = -\frac{e\sigma_0}{\kappa \varepsilon k_B T} \delta(x). \tag{4.56}$$

The Poisson–Boltzmann equation can be solved analytically in this simple case. But first we study the linearized homogeneous equation

$$\frac{\mathrm{d}^2}{\mathrm{d}x^2} f(x) - f(x) = 0 \tag{4.57}$$

with the solution

$$f(x) = f_0 \mathrm{e}^{\pm x} \tag{4.58}$$

or going back to the potential

$$\phi(x) = \frac{k_B T}{e} f_0 \mathrm{e}^{\pm \kappa x} = \phi_0 \mathrm{e}^{\pm \kappa x}. \tag{4.59}$$

The membrane potential is related to the surface charge density. Let us assume that on the left side (x<0) the medium has a dielectric constant of ε_1 and on the right side ε. Since in one dimension the field in a dielectric medium does not decay we introduce a shielding constant κ_1 on the left side and take the limit $\kappa_1 \to 0$ to remove contributions not related to the membrane charge. The potential then is given by

$$\phi(x) = \begin{cases} \phi_0 \mathrm{e}^{-\kappa x} & \text{x>0} \\ \phi_0 \mathrm{e}^{\kappa_1 x} & \text{x<0} \end{cases} \tag{4.60}$$

and ϕ_0 is determined from the b.c.

$$\varepsilon \frac{\mathrm{d}\phi}{\mathrm{d}x}(+0) - \varepsilon_1 \frac{\mathrm{d}\phi}{\mathrm{d}x}(-0) = -\sigma_0 \tag{4.61}$$

which gives

$$-\varepsilon \kappa \phi_0 - \varepsilon_1 \kappa_1 \phi_0 = -\sigma_0. \tag{4.62}$$

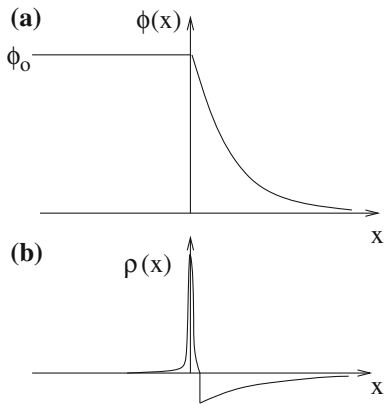

Fig. 4.7 Electrolytic double layer

In the limit $\kappa_1 \to 0$ we find

$$\phi_0 = \frac{\sigma_0}{\varepsilon\kappa}\,. \tag{4.63}$$

For $x < 0$ the potential is constant and for $x > 0$ the charge density is (Figs. 4.7, 4.8)

$$\varrho(x) = -\varepsilon\frac{\mathrm{d}^2\phi(x)}{\mathrm{d}x^2} = -\sigma_0\kappa \mathrm{e}^{-\kappa x} \tag{4.64}$$

which adds up to a total net charge per unit area of

$$\int_0^\infty \varrho(x)dx = -\sigma_0 \tag{4.65}$$

hence the system is neutral and behaves like a capacity of

$$\frac{\sigma_0 A}{\phi_0} = \varepsilon\kappa A = \varepsilon\frac{A}{L_{Debye}}\,. \tag{4.66}$$

The solution of the nonlinear homogeneous equation can be found multiplying the equation with $\frac{\mathrm{d}f(x)}{\mathrm{d}x}$

$$\frac{\mathrm{d}f}{\mathrm{d}x}\frac{\mathrm{d}^2 f}{\mathrm{d}x^2} = \sinh(f)\frac{\mathrm{d}f}{\mathrm{d}x} \tag{4.67}$$

and rewriting this as

$$\frac{1}{2}\frac{\mathrm{d}}{\mathrm{d}x}\left(\frac{\mathrm{d}f}{\mathrm{d}x}\right)^2 = \frac{\mathrm{d}}{\mathrm{d}x}\cosh(f) \tag{4.68}$$

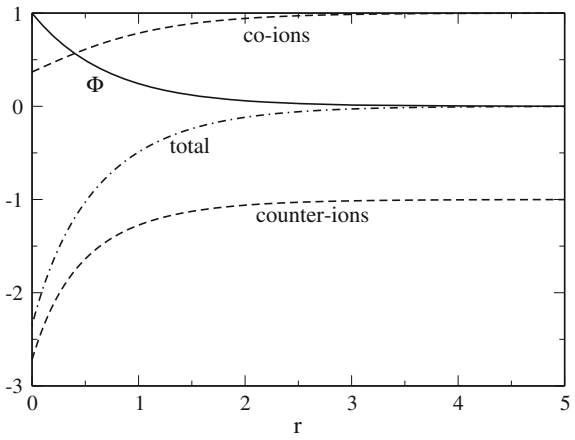

Fig. 4.8 Charge density of counter- and co-ions. For an exponentially decaying potential $\Phi(r)$ (*full curve*) the density of counter- and co-ions (*dashed curves*) and the total charge density (*dash-dotted curve*) are shown

which can be integrated

$$\left(\frac{\mathrm{d}f}{\mathrm{d}x}\right)^2 = 2\left[\cosh(f) + C\right]. \tag{4.69}$$

The constant C is determined by the asymptotic behavior[1]

$$\lim_{x\to\infty} f(x) = \lim_{x\to\infty} \frac{\mathrm{d}f}{\mathrm{d}x} = 0 \tag{4.70}$$

and obviously has the value $C = -1$. Making use of the relation

$$\cosh(f) - 1 = 2\sinh\left(\frac{f}{2}\right)^2 \tag{4.71}$$

we find

$$\frac{\mathrm{d}}{\mathrm{d}x} f(x) = \left(\pm 2\sinh\left(\frac{f(x)}{2}\right)\right). \tag{4.72}$$

Separation of variables then gives

$$\frac{\mathrm{d}f}{2\sinh(f/2)} = \pm \mathrm{d}x \tag{4.73}$$

[1] We consider only solutions for the region $x > 0$ in the following.

with the solution

$$f(x) = 2\ln\left(\pm\tanh\left(\frac{x}{2}+\frac{C}{2}\right)\right). \tag{4.74}$$

For $x > 0$ only the plus sign gives a physically meaningful expression. The constant C is generally complex valued. It can be related to the potential at the membrane surface

$$C = 2\,\mathrm{arctanh}\left(\mathrm{e}^{f(0)/2}\right) = \ln\left(\frac{1+\mathrm{e}^{f(0)/2}}{1-\mathrm{e}^{f(0)/2}}\right). \tag{4.75}$$

For $f(0) > 0$ the argument of the logarithm becomes negative. Hence we replace in (4.74) C by $C + \mathrm{i}\pi$ to have (Fig. 4.9)

$$f(x) = 2\ln\left(\tanh\left(\frac{x}{2}+\frac{C}{2}+\frac{\mathrm{i}\pi}{2}\right)\right) = -2\ln\left(\tanh\left(\frac{x}{2}+\frac{C}{2}\right)\right) \tag{4.76}$$

where C is now given by

$$C = 2\,\mathrm{arctanh}\left(\mathrm{e}^{-f(0)/2}\right) = \ln\left(\frac{1+\mathrm{e}^{-f(0)/2}}{1-\mathrm{e}^{-f(0)/2}}\right). \tag{4.77}$$

The integration constant C is again connected to the surface charge density by

$$\frac{\mathrm{d}\phi}{\mathrm{d}x}(0) = -\frac{\sigma_o}{\varepsilon} \tag{4.78}$$

and from

$$\frac{\mathrm{d}}{\mathrm{d}x}\phi(x) = \frac{k_B T}{e}\frac{\mathrm{d}}{\mathrm{d}x}f(\kappa x) = \frac{k_B T}{e}\kappa f'(\kappa x) \tag{4.79}$$

we find

$$\frac{\sigma_0}{\varepsilon} = -\frac{k_B T}{e}\kappa f'(0). \tag{4.80}$$

Now the derivative is in the case $f(0) > 0$ given by

$$f'(x) = \tanh\left(\frac{x}{2}+\frac{C}{2}\right) - \frac{1}{\tanh(\frac{x}{2}+\frac{C}{2})} \tag{4.81}$$

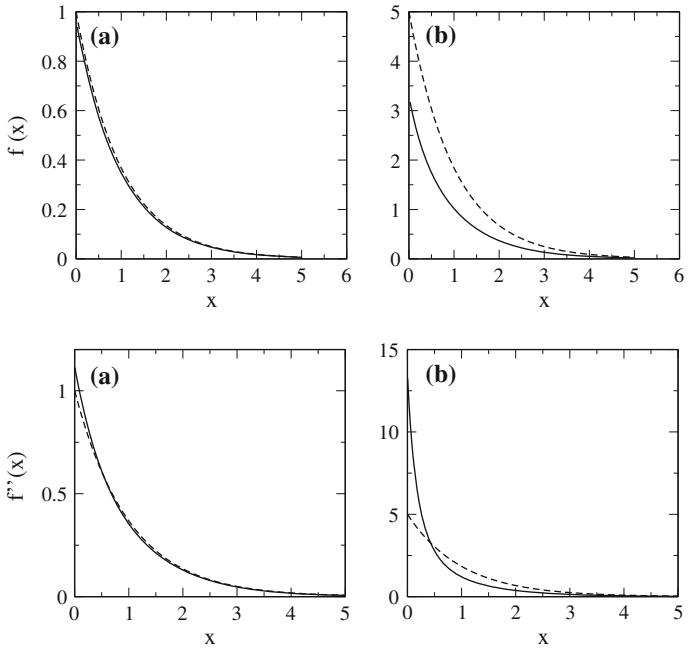

Fig. 4.9 One-dimensional Poisson–Boltzman equation. The solutions of the full (*full curves*) and the linearized equation (*broken curves*) are compared for (**a**) $B = -1$ and (**b**) $B = -5$

and especially

$$f'(0) = \tanh\left(\frac{C}{2}\right) - \frac{1}{\tanh(\frac{C}{2})} \tag{4.82}$$

and we have to solve the equation

$$t - \frac{1}{t} = -\frac{e\sigma_0}{k_B T \kappa \varepsilon} = B \tag{4.83}$$

which yields[2]

$$t = \frac{B}{2} + \frac{\sqrt{B^2+4}}{2} \tag{4.84}$$

$$C = 2\text{arctanh}\left(\frac{B}{2} + \frac{\sqrt{B^2+4}}{2}\right). \tag{4.85}$$

[2]The second root leads to imaginary values.

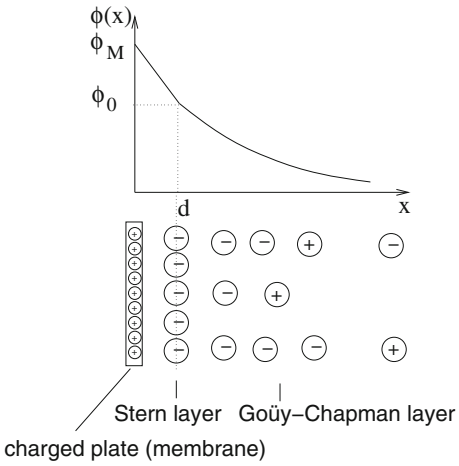

Fig. 4.10 Stern modification of the double layer

4.6 Stern Modification of the Double Layer

Real ions have a finite radius R. Therefore, they cannot approach the membrane closer than R and the ion density has a maximum possible value, which is reached when the membrane is occupied by an ion layer. To account for this, Stern [26] extended the Goüy–Chapman model by an additional ion layer between the membrane and the diffusive ion layer (Fig. 4.10).

Within the Stern layer of thickness d there are no charges and the potential drops linearly from the membrane potential ϕ_M to a value ϕ_0

$$\phi(x) = \phi_M - \frac{\phi_M - \phi_0}{d} x \qquad 0 < x < d \tag{4.86}$$

In the diffusive Goüy–Chapman layer the potential decays exponentially

$$\phi(x) = \phi_0 \mathrm{e}^{-\kappa(x-d)}. \tag{4.87}$$

Assuming the same dielectric constant for both layers we have to fulfill the boundary conditions

$$\frac{\mathrm{d}\phi}{\mathrm{d}x}(d) = -\frac{\phi_M - \phi_0}{d} = -\kappa\phi_0 \tag{4.88}$$

and hence

$$\phi_0 = \frac{\phi_M}{1 + \kappa d}\,. \tag{4.89}$$

The total ion charge in the diffusive layer now is

$$q_{dif} = \int_d^\infty \varrho(x)dx = -A\varepsilon\kappa^2\phi_0 \int_d^\infty \mathrm{e}^{-\kappa(x-a)}dx = -A\varepsilon\kappa\phi_0$$
$$= -A\frac{\varepsilon\kappa}{1+\kappa d}\phi_M \tag{4.90}$$

and the capacity is

$$C = \frac{-q_{dif}}{\phi_M} = \frac{A\varepsilon}{d+\kappa^{-1}} \tag{4.91}$$

which are just the capacities of the two layers in series

$$\frac{1}{C} = \frac{Ad}{\varepsilon} + \frac{A\lambda_{Debye}}{\varepsilon} = \frac{1}{C_{Stern}} + \frac{1}{C_{diff}}\,. \tag{4.92}$$

Problems

4.1 Membrane Potential

Consider a dielectric membrane in an electrolyte with an applied voltage V.

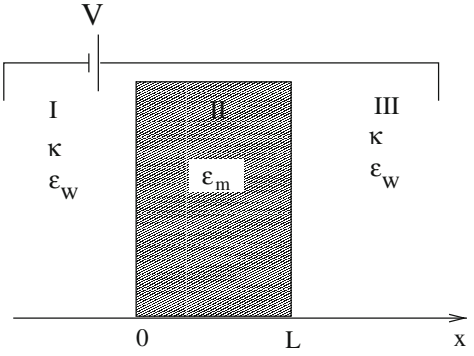

Solve the linearized Poisson–Boltzmann equation

$$\frac{\mathrm{d}^2}{\mathrm{d}x^2}\phi(x) = \kappa^2(\phi(x) - \phi^{(0)})$$

with boundary conditions

$$\phi^{(0)}(I) = \phi(-\infty) = 0$$
$$\phi^{(0)}(III) = \phi(\infty) = V$$

and determine the voltage difference

$$\Delta V = \phi(L) - \phi(0).$$

Calculate the charge density $\varrho_{mob}(x)$ and the integrated charge on both sides of the membrane. What is the capacity of the membrane?

4.2 Ionic Activity

The chemical potential of an ion with charge Ze is given in terms of the activity a by $\mu = \mu^0 + k_B T \ln a$. Assume that the deviation from the ideal behaviour $\mu^{id} = \mu^0 + k_B T \ln c$ is due to electrostatic interactions only. Then for an ion with radius R Debye–Hückel theory gives

$$\mu - \mu^{ideal} = k_B T \ln a - k_B T \ln c = \Delta(\mu_\alpha - \mu_\alpha^0) G_{solv} = -\frac{Z^2 e^2}{8\pi\varepsilon} \frac{\kappa}{(1+\kappa R)}.$$

For a 1–1 electrolyte calculate the mean activity coefficient

$$\gamma_\pm^c = \sqrt{\gamma_+^c \gamma_-^c} = \sqrt{\frac{a_+}{c_+}\frac{a_-}{c_-}}$$

and discuss the limit of extremely dilute solutions (Debye–Hückel limiting law).

Chapter 5
Protonation Equilibria

Some of the aminoacid residues building a protein can be in different protonation states and therefore differently charged states (Fig. 5.1).

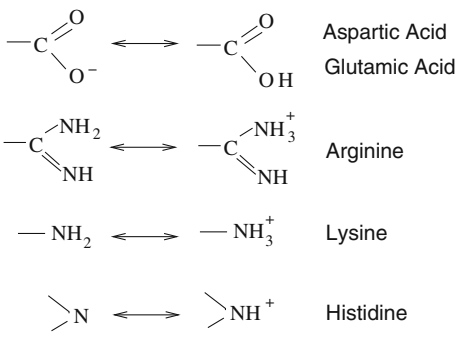

Fig. 5.1 Functional groups which can be in different protonation states

In this chapter, we discuss the dependence of the free energy of a protein on the electrostatic interactions of its charged residues. We investigate the chemical equilibrium between a large number of different protein conformations and the dependence on the pH value [27]. The partition function is evaluated and the results are applied to explain abnormal titration curves of coupled residues.

5.1 Protonation Equilibria in Solution

We consider a dilute aqueous solution (Fig. 5.2) containing N titrable molecules (i.e. which can be in two different protonation states 0 = deprotonated, 1 = protonated). For one molecule we have for fixed protonation state

$$G_0 = F_0 + pV_0 = -k_B T \ln z_0 + pV_0 \tag{5.1}$$

P.O.J. Scherer and S.F. Fischer, *Theoretical Molecular Biophysics*,
Biological and Medical Physics, Biomedical Engineering,
DOI 10.1007/978-3-662-55671-9_5

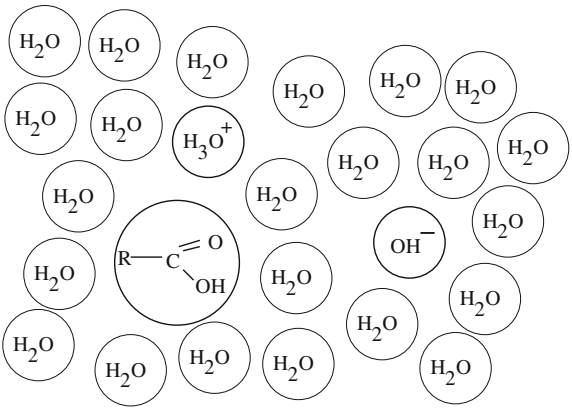

Fig. 5.2 Titration in solution

$$G_1 = F_1 + pV_1 = -k_B T \ln z_1 + pV_1 \tag{5.2}$$

and the free enthalpy difference between protonated and deprotonated form of the molecule is

$$G_1 - G_0 = -k_B T \ln \frac{z_1}{z_0} + p\Delta V. \tag{5.3}$$

In the following the volume change will be neglected[1]. If we now put N such molecules into the solution the number of protonated molecules can fluctuate by exchanging protons with the solvent. Removal of one proton from the solvent costs a free enthalpy of

$$\Delta G = -\mu_{H+} \tag{5.4}$$

where μ_{H+} is the chemical potential of the proton in solution[2]. Hence we come to the grand canonical partition function

$$\Xi = \sum_M Z_M \mathrm{e}^{\mu M / k_B T} \tag{5.5}$$

[1] At atmospheric pressure the mechanic work term $p\Delta V$ is very small. We prefer to discuss the free enthalpy G in the following since experimentally usually temperature and pressure are constant.

[2] We omit the index H+ in the following.

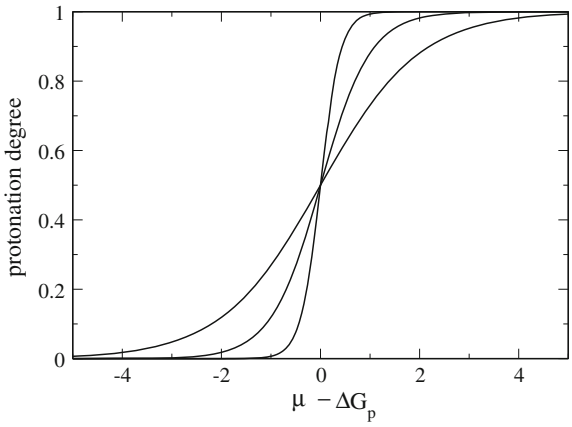

Fig. 5.3 Henderson–Hasselbalch titration curve. The protonation degree (5.9) is shown for $k_BT = 1, 2, 5$

where the partition function for fixed number M of protonated molecules is given by

$$Z_M = \frac{N!}{M!(N-M)!} z_1^M z_0^{N-M} \tag{5.6}$$

if the N molecules cannot be distinguished. Hence we find

$$\Xi = \sum_M \frac{N!}{M!(N-M)!} (z_1 \mathrm{e}^{\mu/k_BT})^M z_0^{N-M} = (z_0 + z_1 \mathrm{e}^{\mu/k_BT})^N. \tag{5.7}$$

The average number of protonated molecules can be found from

$$\overline{M} = \frac{\partial}{\partial(\mu/k_BT)} \ln \Xi = N \frac{z_1 \mathrm{e}^{\mu/k_BT}}{z_0 + z_1 \mathrm{e}^{\mu/k_BT}} \tag{5.8}$$

and the protonation degree, i.e. the fraction of protonated molecules is (Fig. 5.3)

$$\frac{\overline{M}}{N} = \frac{1}{1 + \frac{z_0}{z_1} \mathrm{e}^{-\mu/k_BT}} = \frac{1}{1 + \mathrm{e}^{(G_1 - G_0 - \mu)/k_BT}}. \tag{5.9}$$

In physical chemistry the following quantities are usually introduced:
The *activity* of a species a_i is defined by

$$\mu_i = \mu_i^0 + k_BT \ln a_i \tag{5.10}$$

in analogy to $\mu_i = \mu_i^0 + k_BT \ln p_i/p_i^0$ for the ideal gas. For very dilute solutions it can be approximated by

$$\mu_i = k_B T \ln N_i - k_B T \ln z_i = \mu_i^0 + k_B T \ln \frac{c_i}{c_0} \tag{5.11}$$

where (0) indicates the standard state (usually $p_0 = 1\text{atm}$, $c_0 = 1\text{mol/l}$).
The concentration of protons is measured by the pH-value[3]

$$pH = -\log_{10} a_{H+} = -\frac{\mu_{H+}}{k_B T \ln(10)} \approx -\log_{10}\left(\frac{c(H^+)}{c_0}\right). \tag{5.12}$$

The standard reaction enthalpy of an acid-base equilibrium

$$\mathrm{AH} \rightleftharpoons \mathrm{A}^- + \mathrm{H}^+ \tag{5.13}$$

where

$$0 = \sum \nu_i \mu_i = \Delta G_r^0 + k_B T \sum \nu_i \ln a_i \qquad K_a = \mathrm{e}^{-\Delta G_r^0 / k_B T} = \frac{a(A^-)a(H^+)}{a(AH)} \tag{5.14}$$

is measured by the *pK_a-value*

$$\begin{aligned} pK_a &= -\log_{10}(K_a) = \frac{1}{\ln(10)} \frac{\Delta G_r^0}{k_B T} = -\log_{10}\left(\frac{a(A^-)a(H^+)}{a(AH)}\right) \\ &\approx -\log_{10}\left(\frac{\frac{c(A^-)}{c_0}\frac{c(H^+)}{c_0}}{\frac{c(AH)}{c_0}}\right) \end{aligned} \tag{5.15}$$

which is usually simply written as[4]

$$pK_a = -\log_{10}\left(\frac{c(A^-)c(H^{+)})}{c(AH)}\right) \tag{5.16}$$

which together with (5.12) gives the Henderson–Hasselbalch equation

$$pH - pK_a = \log_{10}\left(\frac{c(A^-)}{c(AH)}\right). \tag{5.17}$$

The standard reaction enthalpy of the acid-base equilibrium is (with the approximation (5.11))

[3] The standard enthalpy of formation for a proton is zero per definition.

[4] But you have to be aware that all concentrations have to be taken in units of the standard concentration c_0. The argument of a logarithm should be dimensionless.

$$\begin{aligned}\Delta G_r^0 &= \mu_{HA}^0 + \mu_{M^-}^0 + \mu_{H^+}^0 \\ &= -(k_B T \ln L - k_B T \ln z_1) + (k_B T \ln L - k_B T \ln z_0) \\ &= -k_B T \ln \frac{z_0}{z_1} = -(G_1 - G_0). \end{aligned} \tag{5.18}$$

In the language of physical chemistry the protonation degree (5.9) is given by

$$\frac{c(AH)}{c(AH) + c(A^-)} = \frac{1}{1 + 10^{(pH - pK_a)}}. \tag{5.19}$$

5.2 Protonation Equilibria in Proteins

In the protein there are additional steric and electrostatic interactions with other groups of the protein, which contribute to the energies of the titrable site (Fig. 5.4).

5.2.1 Apparent pK_a Values

The pK_a of a titrable group depends on the interaction with background charges, with all the other residues and with the solvent which contains dipolar molecules and free moving ions.

As a consequence ΔG as well as pK_a values are different from that of a model compound containing the titrable group in solution (Fig. 5.5).
The difference of protonation enthalpies

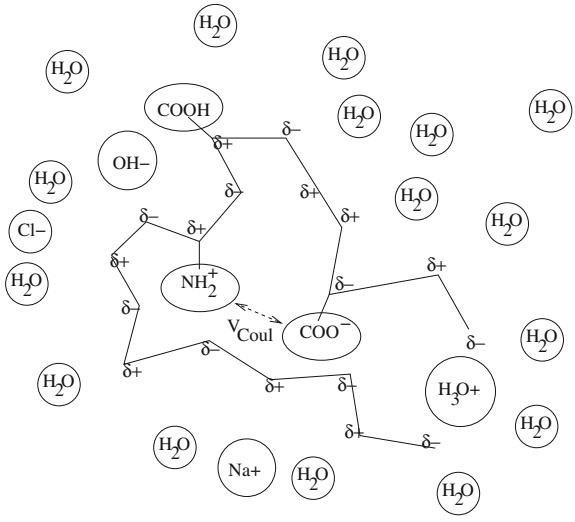

Fig. 5.4 Titration in a protein. Electrostatic interactions with fixed charges (charged residues and background charges) and mobile charges (ions) have to be taken into account

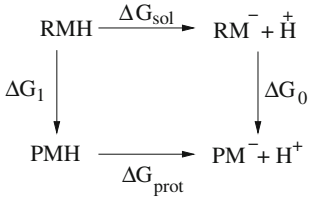

Fig. 5.5 Thermodynamic cycle. The protonation enthalpy of a titrable group in the protein (PMH) differs from that of a model compound in solution (RMH) [28]

$$\Delta\Delta G = \Delta G_{prot} - \Delta G_{solv} = \Delta G_0 - \Delta G_1 \tag{5.20}$$

can be divided into three parts

$$\Delta\Delta G = \Delta\Delta E + p\Delta\Delta V - T\Delta\Delta S. \tag{5.21}$$

In the following the volume change will be neglected. The pK_a value of a group in the protein

$$\begin{aligned} pK_a^{prot} &= \frac{1}{k_B T \ln(10)} \Delta G_{prot} = \frac{1}{k_B T \ln(10)} (\Delta G_{solv} + \Delta\Delta G) \\ &= pK_a^{model} + \frac{\Delta\Delta G}{k_B T \ln(10)} \end{aligned} \tag{5.22}$$

is called the apparent pK_a of the group in the protein. It depends on the mutual interactions of the titrable groups and hence on the pH-value. Therefore titration of groups in a protein cannot be described by a simple Henderson–Hasselbalch equation.

5.2.2 Protonation Enthalpy

The amino acids forming a protein can be enumerated by their appearance in the primary structure and are therefore distinguishable. The protonation state of a protein with a number of N titrable sites will be described by the protonation vector

$$\mathbf{s} = (s_1, s_2, \cdots s_N) \quad \text{with} \quad s_i = \begin{cases} 1 & \text{if group i is protonated} \\ 0 & \text{if group i is deprotonated} \end{cases} \tag{5.23}$$

The number of protonation states

$$N_{pstates} = 2^N$$

can be very big for real proteins[5]. Proteins are very flexible and have a large number of configurations. These will be denoted by the symbol γ which summarizes all the orientational angles between neighbouring residues of the protein. The apparent

[5] We do not take into account that some residues can be in more than two protonation states.

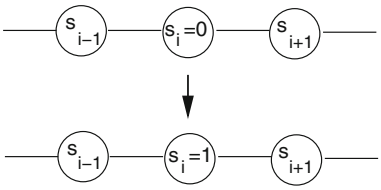

Fig. 5.6 Protonation of one Residue. The protonation state of the i-th residue changes together with its charge. Electrostatic interactions are divided into an intrinsic part and the interactions with all other residues

pK_a values will in general depend on this configuration vector, since for instance distances between the residues depend on the configuration.

The enthalpy change by protonating the i-th residue is denoted as

$$\begin{aligned} &G(s_1, \cdots s_{i-1} 1_i s_{i+1} \cdots s_N, \gamma) - G(s_1 \cdots s_{i-1} 0_i, s_{i+1} \cdots s_N, \gamma) \\ &= \Delta G_{i,intr} + \sum_{j \neq i} (E_{i,j}^{1,s_j} - E_{i,j}^{0,s_j}) \end{aligned} \tag{5.24}$$

with the Coulombic interaction between two residues i, j in the protonation states s_i, s_j (Fig. 5.6)

$$E_{i,j}^{s_i,s_j}(\gamma). \tag{5.25}$$

The so called intrinsic protonation energy $\Delta G_{i,intr}$ is the protonation energy of residue i if there are no Coulombic interactions with other residues, i.e. if all other residues are in their neutral state. It can be estimated from the model energy (5.3, 5.18) taking into account all remaining interactions with background charges[6] and the different solvation energies, which can be calculated using Born models (3.16, 3.51) or by solving the Poisson–Boltzman equation (4.9, 4.12)

$$\Delta G_{i,intr} \approx \Delta G_{i,solv} + \Delta E_{i,bg} + \Delta E_{i,Born}. \tag{5.26}$$

Let us now calculate the protonation enthalpy of a protein with S of its N titrable residues protonated. The contributions from the intrinsic enthalpy changes can be written as

$$\sum_i s_i \Delta G_{i,intr}. \tag{5.27}$$

The Coulombic interactions are divided into pairs of protonated residues

$$\sum_{i<j} s_i s_j E_{i,j}^{1,1} \tag{5.28}$$

[6] i.e. the charge distribution of the protein backbone and the non titrable residues

pairs of unprotonated residues

$$\sum_{i<j}(1-s_i)(1-s_j)E^{0,0}_{i,j} = \sum_{i<j}E^{0,0}_{i,j} + \sum_{i<j}s_i s_j E^{0,0}_{i,j} - \sum_{i\neq j}s_i E^{0,0}_{i,j} \tag{5.29}$$

and interactions between one protonated and one unprotonated residue

$$\sum_{i<j}\left(s_i(1-s_j)E^{1,0}_{i,j} + (1-s_i)s_j E^{0,1}_{i,j}\right) = -\sum_{i<j}s_i s_j\left(E^{1,0}_{i,j} + E^{0,1}_{i,j}\right) + \sum_{i\neq j}s_i E^{1,0}_{i,j}. \tag{5.30}$$

Summing up these contributions and subtracting the Coulombic interactions of the fully deprotonated protein we find the enthalpy change

$$\Delta G(\mathbf{s}) = \sum_i s_i\left(\Delta G_{i,intr} + \sum_{j\neq i}\left(E^{1,0}_{i,j} - E^{0,0}_{i,j}\right)\right) + \sum_{i<j}s_i s_j W_{i,j} \tag{5.31}$$

with the interaction parameter

$$W_{ij} = E_{ij}(1,1) - E_{ij}(1,0) - E_{ij}(0,1) + E_{ij}(0,0). \tag{5.32}$$

In fact for each pair i, j only one of the summands is non zero.

5.2.3 *Protonation Enthalpy Relative to the Uncharged State*

In the literature the enthalpy is often taken relative to a reference state (s^0_i) where all titrable residues are in their uncharged state. As is illustrated in Fig. 5.7, the formal dimensionless charge of a residue is given by

$$q_i = s_i - s^0_i. \tag{5.33}$$

Fig. 5.7 Protonation states. The correlation of protonation state s_i, protonation of the neutral state s^0_i, charge q_i and charge of the non neutral state q^c_i are shown

	$AH \rightleftharpoons A^- + H^+$		$BH^+ \rightleftharpoons B + H^+$	
s	1	0	1	0
s^0	1	1	0	0
$q=s-s^0$	0	−1	+1	0
$q^c=1-2s^0$	−1	−1	1	1

The enthalpy change relative to the uncharged reference state is

$$\Delta G(\mathbf{s}) - \Delta G(\mathbf{s}^0) = \sum_{i=1}^{N}(s_i - s_i^0)\Delta G_{i,intr} + \sum_{i=1}^{N}(s_i - s_i^0)\sum_{j\neq i,j=1}^{N}(E_{i,j}^{1,0} - E_{i,j}^{0,0}) + \frac{1}{2}\sum_i\sum_{j\neq i} W_{i,j}\left((s_i - s_i^0)(s_j - s_j^0) + s_i^0 s_j + s_i s_j^0 - 2s_i^0 s_j^0\right). \tag{5.34}$$

Note that $W_{ij} = W_{ji}$ and therefore the last sum can be simplified

$$\frac{1}{2}\sum_i\sum_{j\neq i} W_{i,j}\left((s_i - s_i^0)(s_j - s_j^0) + s_i^0 s_j + s_i s_j^0 - 2s_i^0 s_j^0\right) = \frac{1}{2}\sum_i\sum_{j\neq i} W_{i,j}(q_i q_j + 2(s_i - s_i^0)s_j^0). \tag{5.35}$$

Consider now the expression

$$\triangle W = \sum_{i=1}^{N} q_i \sum_{j\neq i,j=1}^{N}(E_{i,j}^{1,0} - E_{i,j}^{0,0} + s_j^0 W_{i,j}).$$

For each residue $j \neq i$ there are only the two alternatives[7]

$$s_j^0 = 0 \rightarrow E_{i,j}^{1,0} - E_{i,j}^{0,0} = 0 \tag{5.36}$$

$$s_j^0 = 1 \rightarrow E_{i,j}^{1,0} - E_{i,j}^{0,0} + W_{i,j} = E_{i,j}^{1,1} - E_{i,j}^{0,1} = 0 \tag{5.37}$$

and hence we have

$$\triangle W = 0 \tag{5.38}$$

$$\Delta G(\mathbf{s}) - \Delta G(\mathbf{s}^0) = \sum_{s_i\neq s_i^0}^{N} q_i \Delta G_{i,int} + \frac{1}{2}\sum_{i\neq j} W_{i,j} q_i q_j. \tag{5.39}$$

5.2.4 *Statistical Mechanics of Protonation*

The partition function for a specific total charge

$$Q = \sum_i q_i = \sum_i (s_i - s_i^0)$$

[7] The Coulomb interaction vanishes if one of the residues is in the neutral state.

is given by

$$Z(Q) = \sum_{\{\mathbf{s}, \sum q_i = Q\}} \sum_{\gamma} \mathrm{e}^{-\Delta G / k_B T}$$
$$= \sum_{\{\mathbf{s}, \sum q_i = Q\}} \sum_{\gamma} \mathrm{e}^{-[\sum (s_i - s_i^0) \Delta G_{i,int} + \frac{1}{2} \sum' W_{i,j} q_i q_j]/k_B T}. \tag{5.40}$$

We come to the grand canonical partition function by introducing the factor

$$\mathrm{e}^{\mu Q / k_B T} = \mathrm{e}^{\mu \sum (s_i - s_i^0)/k_B T} \tag{5.41}$$

and summing over all possible charge states of the protein

$$\Xi = \sum_{Q} Z(Q) e^{\mu Q / k_B T} = \sum_{\gamma, \mathbf{s}} \mathrm{e}^{-[\sum (s_i - s_i^0)(\Delta G_{i,int}(\gamma) - \mu) + \frac{1}{2} \sum' W_{i,j}(\gamma) q_i q_j]/k_B T}. \tag{5.42}$$

With the approximation (5.26) and (5.3) the partition function

$$Z(Q) \approx \sum_{\{\mathbf{s}, \sum q_i = Q\}} \left(\frac{z_1^{(i)}}{z_0^{(i)}} \right)^{q_i} Z_{conf}$$

becomes the product of one factor which relates to the internal degrees of freedom which are usually assumed to be configuration independent[8] and a second factor which depends only on the configurational degress of freedom

$$Z_{conf}(\mathbf{s}) = \sum_{\gamma} \mathrm{e}^{-[\sum (s_i - s_i^0)(\Delta E_{i,bg} + \Delta E_{i,Born}) + \frac{1}{2} \sum' W_{i,j} q_i q_j]/k_B T}.$$

5.3 Abnormal Titration Curves of Coupled Residues

Let us consider a simple example of a model protein with only two titrable sites of the same type. The free enthalpies of the four possible states are

$$\begin{aligned}
\Delta G(AH, AH) &= \Delta G_{1,intr} + \Delta G_{2,intr} + E_{1,2}^{1,1} - E_{1,2}^{0,0} \\
\Delta G(A-, AH) - \Delta G(AH, AH) &= -\Delta G_{1,intr} \\
\Delta G(AH, A-) - \Delta G(AH, AH) &= -\Delta G_{2,intr} \\
\Delta G(A-, A-) - \Delta G(AH, AH) &= -\Delta G_{1,intr} - \Delta G_{2,intr} + W_{12} \\
&= -\Delta G_{2,intr} - \Delta G_{1,intr} + E_{1,2}^{0,0}.
\end{aligned} \tag{5.43}$$

The grand partition function is

$$\Xi = 1 + \mathrm{e}^{-(-\Delta G_{1,intr} + \mu)/k_B T} + \mathrm{e}^{-(-\Delta G_{2,intr} + \mu)/k_B T}$$
$$+ \mathrm{e}^{-(-\Delta G_{2,intr} - \Delta G_{1,intr} + 2\mu + W)/k_B T}. \tag{5.44}$$

[8] Protonation–dependent degrees of freedom can be important in certain cases [29].

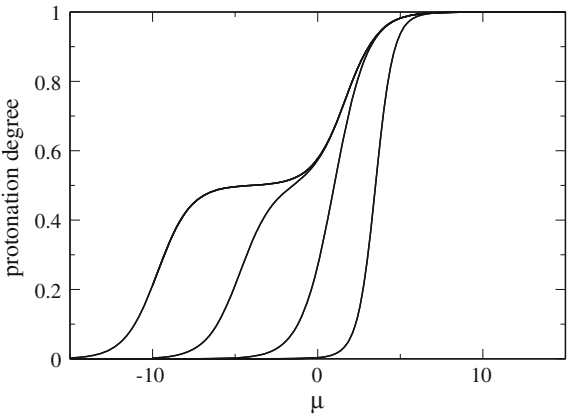

Fig. 5.8 Abnormal titration curves. Two interacting residues with neutral protonated states (AH), $\Delta G_{1,intr} = \Delta G_{2,intr} = 1.0$, $W = -5, 0, 5, 10$

The average protonation values are (Fig. 5.8)

$$\overline{s_1} = \frac{1 + \mathrm{e}^{-(-\Delta G_{2,intr} + \mu)/k_B T}}{\Xi} \tag{5.45}$$

$$\overline{s_2} = \frac{1 + \mathrm{e}^{-(-\Delta G_{1,intr} + \mu)/k_B T}}{\Xi}. \tag{5.46}$$

Problems

5.1 Abnormal Titration Curves

Consider a simple example of a model protein with only two titrable sites of the same type. Determine the relative free enthalpies of the four possible states

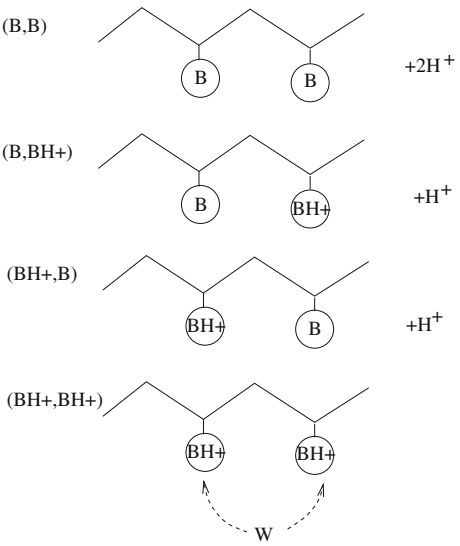

From the grand canonical partition function (the number of protons is not fixed) calculate the protonation degree for both sites and discuss them as a function of the interaction energy W.

Part III
Reaction Kinetics

Chapter 6
Formal Kinetics

In this chapter, we discuss the phenomenological description of elementary chemical reactions and photophysical processes with the help of rate equations. We explain the concept of reaction variable and reaction order, derive the Michaelis–Menten equation for enzymatic catalysis and discuss the importance of diffusion for reactions in solution.

6.1 Elementary Chemical Reactions

The basic steps of chemical reactions can be divided into several classes of elementary reactions. They can be photoinduced or thermally activated, may involve the transfer of an electron or proton and are accompanied by structural changes, like breaking and forming bonds (Fig. 6.2) or at least a reorganization of bond lengths and angles (Fig. 6.1).

All elementary reactions are reversible. There is a dynamical equilibrium between forward and backward reaction, which are independent, for instance

$$H_2 + J_2 \rightleftharpoons 2HJ. \tag{6.1}$$

6.2 Reaction Variable and Reaction Rate

We consider a general stoichiometric equation for the reaction of several species[1]

[1]The stochiometric coefficients ν_i are positive for products and negative for educts. This is the conventional definition. Products and educts can be exchanged at least in principle, since the backreaction is always possible.

P.O.J. Scherer and S.F. Fischer, *Theoretical Molecular Biophysics*,
Biological and Medical Physics, Biomedical Engineering,
DOI 10.1007/978-3-662-55671-9_6

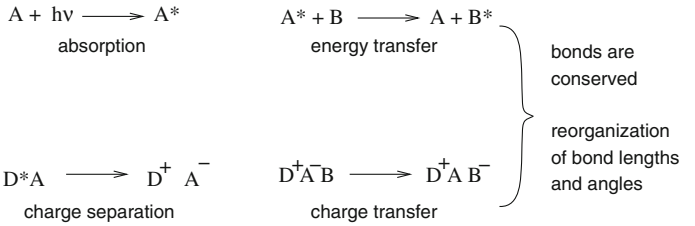

Fig. 6.1 Elementary reactions without bond reformation

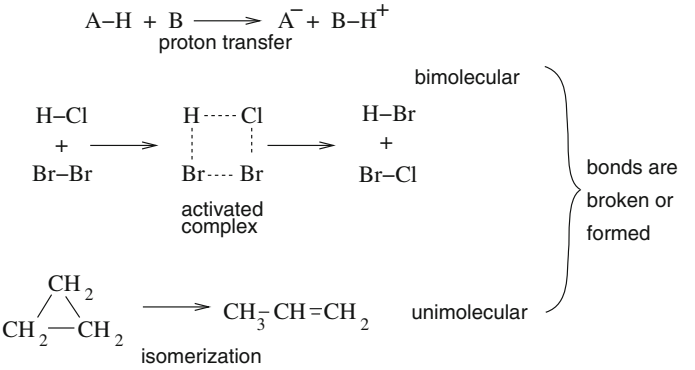

Fig. 6.2 Elementary reactions with bond reformation

$$\sum_i \nu_i A_i = 0 \tag{6.2}$$

and define a reaction variable x based on the concentration of the species A_i by

$$c_i = c_{i,0} + \nu_i x \tag{6.3}$$

as

$$x = \frac{c_i - c_{i,0}}{\nu_i} \tag{6.4}$$

and the reaction rate as its time derivative

$$r = \frac{\mathrm{d}x}{\mathrm{d}t} = \frac{1}{\nu_i}\frac{\mathrm{d}c_i}{\mathrm{d}t}\,. \tag{6.5}$$

6.3 Reaction Order

The progress of a chemical reaction can be frequently described by a simple rate expression such as

$$r = kc_1^{n_1} c_2^{n_2} \cdots = k \prod_{i \in educts} c_i^{n_i} \tag{6.6}$$

with the rate constant k. For such a system the exponent[2] of the i-th term is called the order of the reaction with respect to this substance and the sum of all the exponents is called the overall reaction order.

6.3.1 Zero-Order Reactions

Zero-order reactions proceed at the same rate regardless of concentration. The rate expression for a reaction of this type is

$$\frac{\mathrm{d}c}{\mathrm{d}t} = k_0 \tag{6.7}$$

which can be integrated

$$c = c_0 + k_0 t. \tag{6.8}$$

Zero-order reactions appear when the determining factor is an outside source of energy (light) or when the reaction occurs on the surface of a catalyst.

6.3.2 First-Order Reactions

First-order reactions describe the decay of an excited state, for instance a radioactive decay

$$\mathrm{A}^* \rightarrow \mathrm{A}\,. \tag{6.9}$$

The rate expression is

$$\frac{\mathrm{d}c_{A*}}{\mathrm{d}t} = -\frac{\mathrm{d}c_A}{\mathrm{d}t} = -kc_{A*} \tag{6.10}$$

[2]For more complicated reactions the exponents need not be integers. For simple reactions they are given by the stochiometric coefficients $n_i = |\nu_i|$ of the educts (the products for the backreaction).

which gives an exponential decay

$$c_{A*} = c_{A*}(0)\mathrm{e}^{-kt} \tag{6.11}$$

with a constant half-period

$$\tau_{1/2} = \frac{\ln(2)}{k}\,. \tag{6.12}$$

6.3.3 Second-Order Reactions

A second-order reaction between two different substances obeys the equations

$$\mathrm{A} + \mathrm{B} \rightarrow \cdots \tag{6.13}$$

$$\frac{\mathrm{d}c_A}{\mathrm{d}t} = \frac{\mathrm{d}c_B}{\mathrm{d}t} = -k_2 c_A c_B \tag{6.14}$$

which can be written down using the reaction variable x and the initial concentrations a,b as

$$c_A = a - x \qquad c_B = b - x \tag{6.15}$$

$$\frac{\mathrm{d}x}{\mathrm{d}t} = k_2(a - x)(b - x). \tag{6.16}$$

This can be integrated to give

$$\frac{1}{a - b} \ln \frac{b(a - x)}{a(b - x)} = k_2 t. \tag{6.17}$$

If two molecules of the same type react with each other we have instead

$$-\frac{\mathrm{d}c_A}{\mathrm{d}t} = -k_2 c_A^2 \tag{6.18}$$

which gives an algebraic decay

$$c_A(t) = \frac{1}{k_2 t + \frac{1}{a}} \tag{6.19}$$

where the half-period now depends on the initial concentration

$$\tau_{1/2} = \frac{1}{k_2 a}\,. \tag{6.20}$$

An example is exciton-exciton annihilation in the light-harvesting complex of photosynthesis

$$\mathrm{A}^* + \mathrm{A}^* \rightarrow \mathrm{A} + \mathrm{A}\,. \tag{6.21}$$

6.4 Dynamical Equilibrium

We consider a first-order reaction together with the back reaction

$$\mathrm{A} \underset{k_{-1}}{\overset{k_1}{\rightleftarrows}} \mathrm{B}\,. \tag{6.22}$$

The reaction variable of the backward reaction will be denoted by y. The concentrations are

$$c_A(t) = a - x + y \tag{6.23}$$

$$c_B(t) = b + x - y \tag{6.24}$$

and the reaction rates are

$$\frac{\mathrm{d}x}{\mathrm{d}t} = k_1 c_A = k_1(a - x + y) \tag{6.25}$$

$$\frac{\mathrm{d}y}{\mathrm{d}t} = k_{-1} c_B = k_{-1}(b + x - y) \tag{6.26}$$

Introducing an overall reaction variable

$$z = x - y \tag{6.27}$$

and the equilibrium value

$$s = \frac{k_1 a - k_{-1} b}{k_1 + k_{-1}} \tag{6.28}$$

we have

$$\frac{\mathrm{d}z}{\mathrm{d}t} = k_1 a - k_{-1} b - (k_1 - k_{-1}) z = (k_1 + k_{-1})(s - z) \tag{6.29}$$

which for $z(0) = 0$ has the solution

$$z = s(1 - \mathrm{e}^{-(k_1 + k_{-1})t}). \tag{6.30}$$

The reaction approaches the equilibrium with a rate constant $k_1 + k_{-1}$. In equilibrium $z = s$ and $\frac{\mathrm{d}z}{\mathrm{d}t} = 0$. The equilibrium concentrations are

$$c_A = a - s = (a + b)\frac{k_{-1}}{k_1 + k_{-1}} \tag{6.31}$$

$$c_B = b + s = (a + b)\frac{k_1}{k_1 + k_{-1}} \tag{6.32}$$

and the equilibrium constant is

$$K = \frac{c_A}{c_B} = \frac{k_{-1}}{k_1}\,. \tag{6.33}$$

6.5 Competing Reactions

If one species decays via seperate independent channels (fluorescence, electron transfer, radiationless transitions $\cdots$) the rates are additive

$$\frac{\mathrm{d}c_A}{\mathrm{d}t} = -(k_1 + k_2 + \cdots)c_A. \tag{6.34}$$

6.6 Consecutive Reactions

We consider a chain consisting of two first-order reactions[3]

$$\mathrm{A} \xrightarrow{k_1} \mathrm{B} \xrightarrow{k_2} \mathrm{C}. \tag{6.35}$$

The reaction variables are denoted by x and y, the initial concentrations by a,b,c. The concentrations are

$$c_A = a - x \tag{6.36}$$

$$c_B = b + x - y \tag{6.37}$$

$$c_C = c + y \tag{6.38}$$

and their time derivatives are

$$\frac{\mathrm{d}c_A}{\mathrm{d}t} = -\frac{\mathrm{d}x}{\mathrm{d}t} = -k_1 c_A = -k_1(a - x) \tag{6.39}$$

$$\frac{\mathrm{d}c_B}{\mathrm{d}t} = \frac{\mathrm{d}x}{\mathrm{d}t} - \frac{\mathrm{d}y}{\mathrm{d}t} = k_1 c_A - k_2 c_B = k_1 a - k_2 b + (k_2 - k_1)x - k_2 y \tag{6.40}$$

[3] with negligible back reactions.

$$\frac{\mathrm{d}c_C}{\mathrm{d}t} = \frac{\mathrm{d}y}{\mathrm{d}t} = k_2 c_B = k_2(b + x - y). \tag{6.41}$$

The first equation gives an exponential decay

$$c_A = a\mathrm{e}^{-k_1 t}. \tag{6.42}$$

Integration of

$$\frac{\mathrm{d}c_B}{\mathrm{d}t} + k_2 c_B = k_1 a\mathrm{e}^{-k_1 t} \tag{6.43}$$

gives the concentration of the intermediate state

$$c_B = \frac{k_1 a}{k_2 - k_1}\mathrm{e}^{-k_1 t} + \left(b - \frac{k_1 a}{k_2 - k_1}\right)\mathrm{e}^{-k_2 t}. \tag{6.44}$$

If at time zero only the species A is present the concentration of B has a maximum at

$$t_{max} = \frac{1}{k_1 - k_2}\ln\frac{k_1}{k_2} \tag{6.45}$$

with the value

$$c_{B,max} = a\left(\frac{k_1}{k_1 - k_2}\right)\left(\exp\left(\frac{k_2}{k_1 - k_2}\ln\frac{k_2}{k_1}\right) - \exp\left(\frac{k_1}{k_1 - k_2}\ln\frac{k_2}{k_1}\right)\right). \tag{6.46}$$

6.7 Enzymatic Catalysis

Enzymatic catalysis is very important for biochemical reactions. It can be described schematically by formation of an enzyme-substrate complex followed by decomposition into enzyme and product

$$\mathrm{E} + \mathrm{S} \underset{k_{-1}}{\overset{k_1}{\rightleftharpoons}} \mathrm{ES} \rightleftharpoons \mathrm{E} + \mathrm{P}. \tag{6.47}$$

We consider the limiting case of negligible $k_{-2} \ll k_2$ and large concentration of substrate $c_S \gg c_E$. Then we have to solve the equations

$$\frac{\mathrm{d}c_S}{\mathrm{d}t} \approx -k_1 c_E c_S^0 + k_{-1} c_{ES}$$
$$\frac{\mathrm{d}c_E}{\mathrm{d}t} \approx -k_1 c_E c_S^0 + (k_{-1} + k_2) c_{ES}$$

$$\frac{\mathrm{d}c_{ES}}{\mathrm{d}t} \approx k_1 c_E c_S^0 - (k_{-1} + k_2) c_{ES}$$
$$\frac{\mathrm{d}c_P}{\mathrm{d}t} = k_2 c_{ES}. \tag{6.48}$$

First we solve the equations for $\frac{\mathrm{d}c_E}{\mathrm{d}t}$ and $\frac{\mathrm{d}c_{ES}}{\mathrm{d}t}$:

$$\frac{\mathrm{d}}{\mathrm{d}t}\begin{pmatrix} c_{ES} \\ c_E \end{pmatrix} = \begin{pmatrix} -k_{-1} - k_2 & k_1 c_S^0 \\ k_{-1} + k_2 & -k_1 c_S^0 \end{pmatrix}\begin{pmatrix} c_{ES} \\ c_E \end{pmatrix}. \tag{6.49}$$

The matrix has one Eigenvalue $\lambda = 0$ corresponding to a stationary solution

$$\begin{pmatrix} -k_{-1} - k_2 & k_1 c_S^0 \\ k_{-1} + k_2 & -k_1 c_S^0 \end{pmatrix}\begin{pmatrix} \frac{k_1 c_S^0}{k_{-1}+k_2} \\ 1 \end{pmatrix} = \begin{pmatrix} 0 \\ 0 \end{pmatrix}. \tag{6.50}$$

The stationary concentration of the ES complex is

$$c_{ES}^{stat} = \frac{k_1}{k_{-1} + k_2} c_S c_E = \frac{c_S c_E}{K_M} \tag{6.51}$$

with the Michaelis constant

$$K_M = \frac{k_{-1} + k_2}{k_1}. \tag{6.52}$$

The second eigenvalue relates to the time constant for reaching the stationary state:

$$\begin{pmatrix} -k_{-1} - k_2 & k_1 c_S^0 \\ k_{-1} + k_2 & -k_1 c_S^0 \end{pmatrix}\begin{pmatrix} 1 \\ -1 \end{pmatrix} = -(k_1 c_S^0 + k_{-1} + k_2)\begin{pmatrix} 1 \\ -1 \end{pmatrix} \tag{6.53}$$

For the initial conditions

$$c_{ES}(0) = c_P(0) = 0 \tag{6.54}$$

we find

$$c_{ES}(t) = \frac{c_E^0}{1 + \frac{K_M}{c_S^0}}(1 - \mathrm{e}^{-(k_1 + k_{-1} + k_2)t})$$
$$c_E(t) = \frac{c_E^0}{1 + \frac{c_S^0}{K_M}}(1 + \frac{c_S^0}{K_M}\mathrm{e}^{-(k_1 + k_{-1} + k_2)t}). \tag{6.55}$$

The stationary state is stable, since any deviation will decrease exponentially. The overall rate of the enzyme catalyzed reaction is given by the rate of product formation

$$r = \frac{\mathrm{d}c_P}{\mathrm{d}t} = -\frac{\mathrm{d}c_S}{\mathrm{d}t} = k_2 c_{ES} \tag{6.56}$$

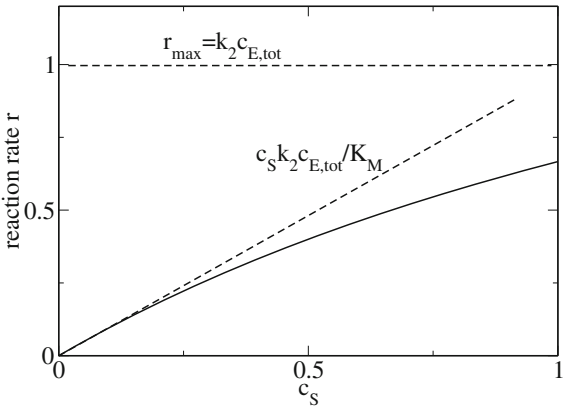

Fig. 6.3 Michaelis–Menten kinetics

and with the total concentration of enzyme

$$c_{E,tot} = c_E + c_{ES} \tag{6.57}$$

we have

$$c_{ES} = \frac{c_E c_S}{K_M} = \frac{(c_{E,tot} - c_{ES})c_S}{K_M} \tag{6.58}$$

and hence

$$c_{ES} = \frac{c_{E,tot} c_S}{c_S + K_M}\,. \tag{6.59}$$

The overall reaction rate is given by the Michaelis–Menten equation (Fig. 6.3)

$$r = \frac{k_2 c_{E,tot} c_S}{K_M + c_S} \tag{6.60}$$

$$\frac{r}{r_{max}} = \frac{c_S}{c_S + K_M} \qquad r_{max} = k_2 c_{E,tot}\,. \tag{6.61}$$

6.8 Reactions in Solutions

In solutions the reacting molecules approach each other by diffusive motion forming a reactive complex within a solvent cage which has a lifetime of typically 100 ps (Fig. 6.4). Formally, this can be described by an equilibrium between the free reactants A and B and a reactive complex {AB}

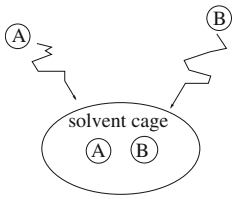

Fig. 6.4 Formation of a reactive complex

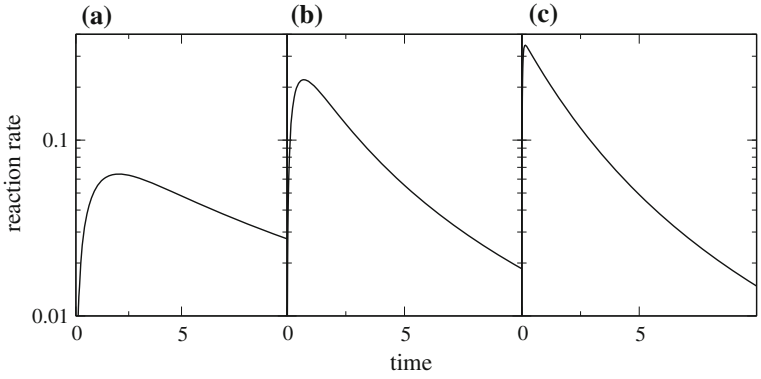

Fig. 6.5 Transition from the diffusion controlled to the reaction controlled limit. $r = k_2 c_{\{AB\}}$ is calculated numerically for $c_A(0) = c_B(0) = 1$, $k_2 = 1$. (**a**) $k_1 = k_{-1} = 0.1$, (**b**) $k_1 = k_{-1} = 1.0$, (**c**) $k_1 = k_{-1} = 10$

$$\mathrm{A} + \mathrm{B} \underset{k_{-1}}{\overset{k_1}{\rightleftharpoons}} \{\mathrm{A\,B}\} \overset{k_2}{\rightarrow} \mathrm{C}. \tag{6.62}$$

The concentrations obey the equations (Fig. 6.5)

$$\begin{aligned} \frac{\mathrm{d}c_A}{\mathrm{d}t} &= \frac{\mathrm{d}c_B}{\mathrm{d}t} = -k_1 c_A c_B + k_{-1} c_{\{AB\}} \\ \frac{\mathrm{d}c_C}{\mathrm{d}t} &= k_2 c_{\{AB\}} \\ \frac{\mathrm{d}c_{\{AB\}}}{\mathrm{d}t} &= k_1 c_A c_B - (k_{-1} + k_2) c_{\{AB\}}. \end{aligned} \tag{6.63}$$

Let us consider two limiting cases.

6.8.1 Diffusion Controlled Limit

If the reaction rate k_2 is large compared to $k_{\pm 1}$ we find for the stationary solution approximately

$$k_2 c_{\{AB\}} \approx k_1 c_A c_B \tag{6.64}$$

and hence for the overall reaction rate

$$\frac{\mathrm{d}c_C}{\mathrm{d}t} = k_2 c_{\{AB\}} \approx k_1 c_A c_B. \tag{6.65}$$

The reaction rate is determined by the formation of the reactive complex.

6.8.2 Reaction Controlled Limit

If on the other hand $k_2 \ll k_{\pm 1}$ an equilibrium between reactands and reactive complex will be established

$$\mathrm{A} + \mathrm{B} \rightleftharpoons \{\mathrm{A\,B}\} \qquad \frac{c_{\{AB\}}}{c_A c_B} = K = \frac{k_1}{k_{-1}}. \tag{6.66}$$

Now the overall reaction rate

$$\frac{\mathrm{d}c_C}{\mathrm{d}t} = k_2 c_{\{AB\}} = k_2 K c_A c_B \tag{6.67}$$

is determined by the reaction rate k_2 and the constant of the diffusion equilibrium.

Problems

6.1 pH-Dependence of Enzyme Activity

Consider an enzymatic reaction where the substrate can be in two protonation states

$$\mathrm{S^-} + \mathrm{H^+} \rightleftharpoons \mathrm{HS}$$

and the enzyme reacts only with the deprotonated form

$$\mathrm{E} + \mathrm{S^-} \rightleftharpoons \mathrm{ES^-} \rightarrow \mathrm{E} + \mathrm{P}.$$

Calculate the reaction rate as a function of the proton concentration c_{H+}.

6.2 Polymerization at the End of a Polymer

Consider the multiple equilibrium between the monomer M and the i-mer $i\,M$

$$\begin{aligned} c_{2M} &= K c_M^2 \\ c_{3M} &= K c_M c_{2M} \\ &\vdots \end{aligned}$$

$$c_{iM} = K c_M c_{(i-1)M}$$

where the equilibrium constant K is assumed to be independent of the degree of polymerization. Calculate the concentration of the i-mer c_{iM} and the mean degree of polymerization

$$< i >= \frac{\sum_i i c_{iM}}{\sum_i c_{iM}}.$$

6.3 Primary Salt Effect

Consider the reaction of two ionic species A and B with charges $Z_{A,B}\, e$ which are in equlibrium with an activated complex X (with charge $(Z_A + Z_B)\, e$) which decays into the products C and D:

$$\mathrm{A} + \mathrm{B} \rightleftharpoons \mathrm{X} \xrightarrow{k_1} \mathrm{C} + \mathrm{D}$$

The equlibrium constant is

$$K = \frac{a_X}{a_A a_B}$$

where the activities are given by the Debye-Hückel approximation

$$\mu_i = \mu_i^0 + k_B T \ln c_i - \frac{Z_i^2 e^2 \kappa}{8\pi\epsilon} \qquad \kappa^2 = \frac{e^2}{\epsilon k_B T} \sum_i N_i Z_i^2.$$

Calculate the reaction rate

$$r = \frac{\mathrm{d}c_C}{\mathrm{d}t}.$$

Chapter 7
Kinetic Theory – Fokker-Planck Equation

In this chapter we consider a model system (protein) interacting with a surrounding medium which is only taken implicitly into account. We are interested in the dynamics on a time scale slower than the medium fluctuations. The interaction with the medium is described approximately as the sum of an average force and a stochastic force [30]. We discuss the stochastic differential equation for 1-dimensional Brownian motion and derive the corresponding Fokker–Planck equation. We consider motion of a particle under the influence of an external force and derive the Klein–Kramers equation for diffusion in an external potential and the Smoluchowski equation as its large-friction limit. Finally we discuss the connection to the general Master equation for the probability density.

7.1 Stochastic Differential Equation for Brownian Motion

The simplest example describes 1-dimensional Brownian motion of a big particle in a sea of small particles. The average interaction leads to damping of the motion which is described in terms of a velocity dependent damping term

$$\frac{\mathrm{d}v(t)}{\mathrm{d}t} = -\gamma v(t). \tag{7.1}$$

This equation alone leads to exponential relaxation $v = v(0)\mathrm{e}^{-\gamma t}$ which is not compatible with thermodynamics, since the average kinetic energy should be $\frac{m}{2}v^2 = \frac{k_B T}{2}$ in equilibrium. Therefore, we add a randomly fluctuating force which represents the collisions with many solvent molecules during a finite time interval τ. The result is the Langevin equation

P.O.J. Scherer and S.F. Fischer, *Theoretical Molecular Biophysics*,
Biological and Medical Physics, Biomedical Engineering,
DOI 10.1007/978-3-662-55671-9_7

$$\frac{\mathrm{d}v(t)}{\mathrm{d}t} = -\gamma v(t) + F(t) \tag{7.2}$$

with the formal solution

$$v(t) = v_0 \mathrm{e}^{-\gamma t} + \int_0^t \mathrm{e}^{\gamma(t'-t)} F(t') dt'. \tag{7.3}$$

The average of the stochatic force has to be zero because the equation of motion for the average velocity should be

$$\frac{\mathrm{d} < v(t) >}{\mathrm{d}t} = -\gamma < v(t) > . \tag{7.4}$$

We assume that many collisions occur during τ and therefore forces at different times are not correlated

$$< F(t)F(t') >= C\delta(t - t'). \tag{7.5}$$

The velocity correlation function is

$$< v(t)v(t') >= \mathrm{e}^{-\gamma(t+t')} \left(v_0^2 + \int_0^t dt_1 \int_0^{t'} dt_2 \;\; \mathrm{e}^{\gamma(t_1+t_2)} < F(t_1)F(t_2) > \right). \tag{7.6}$$

Without losing generality we assume $t' > t$ and substitute $t_2 = t_1 + s$ to find

$$\begin{aligned} < v(t)v(t') > &= v_0^2 \mathrm{e}^{-\gamma(t+t')} \\ &\quad + \mathrm{e}^{-\gamma(t+t')} \int_0^t dt_1 \int_{-t_1}^{t'-t_1} ds\, \mathrm{e}^{\gamma(2t_1+s)} < F(t_1)F(t_1+s) > \\ &= v_0^2 \mathrm{e}^{-\gamma(t+t')} + \mathrm{e}^{-\gamma(t+t')} \int_0^t dt_1 \mathrm{e}^{2\gamma t_1} C \\ &= v_0^2 \mathrm{e}^{-\gamma(t+t')} + \mathrm{e}^{-\gamma(t+t')} \frac{\mathrm{e}^{2\gamma t} - 1}{2\gamma} C. \end{aligned} \tag{7.7}$$

The exponential terms vanish very quickly and we find

$$< v(t)v(t') > \to \mathrm{e}^{-\gamma|t'-t|} \frac{C}{2\gamma}. \tag{7.8}$$

Now C can be determined from the average kinetic energy as

$$\frac{m < v^2 >}{2} = \frac{k_B T}{2} = \frac{m}{2} \frac{C}{2\gamma} \to C = \frac{2\gamma k_B T}{m}. \tag{7.9}$$

The mean square displacement of a particle starting at x_0 with velocity v_0 is

$$< (x(t) - x(0))^2 > = < \left(\int_0^t dt_1 v(t_1) \right)^2 >= \int_0^t \int_0^t < v(t_1)v(t_2) > dt_1 dt_2$$
$$= \int_0^t \int_0^t \left(v_0^2 \mathrm{e}^{-\gamma(t_1+t_2)} + \frac{k_B T}{m} \mathrm{e}^{-\gamma|t_1-t_2|} \right) dt \tag{7.10}$$

and since

$$\int_0^t \int_0^t \mathrm{e}^{-\gamma(t_1+t_2)} dt_1 dt_2 = \left(\frac{1 - \mathrm{e}^{-\gamma t}}{\gamma} \right)^2 \tag{7.11}$$

and

$$\int_0^t \int_0^t \mathrm{e}^{-\gamma|t_1-t_2|} dt_1 dt_2 = 2 \int_0^t dt_1 \int_0^{t_1} \mathrm{e}^{-\gamma(t_1-t_2)} dt_2 = \frac{2}{\gamma} t - \frac{2}{\gamma^2}(1 - \mathrm{e}^{-\gamma t}) \tag{7.12}$$

we obtain

$$< (x(t) - x(0))^2 >= \left(v_0^2 - \frac{k_B T}{m} \right) \frac{\left(1 - \mathrm{e}^{-\gamma t}\right)^2}{\gamma^2} + \frac{2k_B T}{m\gamma} t - \frac{2k_B T}{m\gamma^2}(1 - \mathrm{e}^{-\gamma t}). \tag{7.13}$$

If we had started with an initial velocity distribution for the stationary state

$$< v_0^2 >= k_B T/m \tag{7.14}$$

then the first term in (7.12) would vanish. For very large times the leading term is[1]

$$< (x(t) - x(0))^2 >= 2Dt \tag{7.15}$$

with the diffusion coefficient

$$D = \frac{k_B T}{m\gamma}. \tag{7.16}$$

7.2 Probability Distribution

Now, we discuss the probability distribution $W(v)$. The time evolution can be described as

[1] This is the well known Einstein result for the diffusion constant D.

$$W(v,t+\tau)=\int P(v,t+\tau|v',t)W(v',t)dv'. \tag{7.17}$$

To derive an expression for the differential $\partial W(v,t)/\partial t$ we need the transition probability $P(v,t+\tau|v',t)$ for small τ. Introducing $\Delta = v - v'$ we expand the integrand in a Taylor series

$$P(v,t+\tau|v',t)W(v',t) = P(v,t+\tau|v-\Delta,t)W(v-\Delta,t) \tag{7.18}$$

$$=\sum_{n=0}^{\infty}\frac{(-1)^n}{n!}\Delta^n\left(\frac{\partial}{\partial v}\right)^n P(v+\Delta,t+\tau|v,t)W(v,t).$$

Inserting this into the integral gives

$$W(v,t+\tau)=\sum_{n=0}^{\infty}\frac{(-1)^n}{n!}\left(\frac{\partial}{\partial v}\right)^n\left(\int \Delta^n P(v+\Delta,t+\tau|v,t)d\Delta\right)W(v,t) \tag{7.19}$$

and assuming that the moments exist which are defined by

$$M_n(v',t,\tau) =< (v(t+\tau)-v(t))^n >_{|v(t)=v'} = \int (v-v')^n P(v,t+\tau|v',t)dv \tag{7.20}$$

we find

$$W(v,t+\tau)=\sum_{n=0}^{\infty}\frac{(-1)^n}{n!}\left(\frac{\partial}{\partial v}\right)^n M_n(v,t,\tau)W(v,t). \tag{7.21}$$

Expanding the moments into a Taylor series

$$\frac{1}{n!}M_n(v,t,\tau)=\frac{1}{n!}M_n(v,t,0)+D^{(n)}(v,t)\tau+\cdots \tag{7.22}$$

we have finally[2]

$$W(v,t+\tau)-W(v,t)=\sum_{1}^{\infty}\left(-\frac{\partial}{\partial v}\right)^n D^{(n)}(v,t)W(v,t)\tau+\cdots \tag{7.23}$$

which gives the equation of motion for the probability distribution[3]

[2] The zero order moment does not depend on τ.

[3] This is known as the Kramers–Moyal expansion.

$$\frac{\partial W(v,t)}{\partial t} = \sum_{1}^{\infty} \left(-\frac{\partial}{\partial v}\right)^n D^{(n)}(v,t) W(v,t). \tag{7.24}$$

If this expansion stops after the second term[4] the general form of the 1-dimensional Fokker–Planck equation results:

$$\frac{\partial W(v,t)}{\partial t} = \left(-\frac{\partial}{\partial v} D^{(1)}(v,t) + \frac{\partial^2}{\partial x^2} D^{(2)}(v,t)\right) W(v,t) \tag{7.25}$$

7.3 Diffusion

Consider a particle performing a random walk in one dimension due to collisions. We use the stochastic differential equation[5]

$$\frac{\mathrm{d}x}{\mathrm{d}t} = v_0 + f(t) \tag{7.26}$$

where the velocity has a drift component v_0 and a fluctuating part $f(t)$ with

$$< f(t) >= 0 \qquad < f(t) f(t') >= q\delta(t - t'). \tag{7.27}$$

The formal solution is simply

$$x(t) - x(0) = v_0 t + \int_0^t f(t')dt'. \tag{7.28}$$

The first moment

$$M_1(x_0, t, \tau) =< x(t+\tau) - x(t) >_{|x(t)=x_0} = v_0\tau + \int_0^\tau < f(t') > dt'$$

gives

$$D^{(1)} = v_0.$$

The second moment is

$$M_2(x_0, t, \tau) = v_0^2\tau^2 + v_0\tau \int_0^\tau < f(t') > dt' + \int_0^\tau \int_0^\tau < f(t_1) f(t_2) > dt_1 dt_2. \tag{7.29}$$

[4] It can be shown that this is the case for all Markov processes.

[5] This is a so called Wiener process.

The second term vanishes and the only linear term in τ comes from the double integral

$$\int_0^\tau \int_0^\tau < f(t_1) f(t_2) > dt_1 dt_2 = \int_0^\tau dt_1 \int_{-t_1}^{\tau - t_1} q\delta(t') dt' = q\tau. \tag{7.30}$$

Hence

$$D^{(2)} = \frac{q}{2} \tag{7.31}$$

and the corresponding Fokker–Planck equation is the diffusion equation

$$\frac{\partial W(x,t)}{\partial t} = -v_0 \frac{\partial W(x,t)}{\partial x} + D \frac{\partial^2 W(x,t)}{\partial x^2} \tag{7.32}$$

with the diffusion constant $D = D^{(2)}$.

7.3.1 Sharp Initial Distribution

We can easily find the solution for a sharp initial distribution $W(x,0) = \delta(x - x_0)$ by taking the Fourier transform

$$\widetilde{W}(k,t) = \int_{-\infty}^{\infty} dx\, W(x,t)\, \mathrm{e}^{-\mathrm{i}kx}. \tag{7.33}$$

We obtain the algebraic equation

$$\frac{\partial \widetilde{W}(k,t)}{\partial t} = (-Dk^2 + \mathrm{i}v_0 k)\widetilde{W}(k,t) \tag{7.34}$$

which is solved by

$$\widetilde{W}(k,t) = \widetilde{W}_0 \exp\left\{(-Dk^2 + \mathrm{i}v_0 k)t + \mathrm{i}kx_0\right\}. \tag{7.35}$$

Inverse Fourier transformation then gives[6]

$$W(x,t) = \frac{1}{\sqrt{4\pi Dt}} \exp\left\{-\frac{(x - x_0 - v_0 t)^2}{4Dt}\right\} \tag{7.36}$$

which is a Gaussian distribution centered at $x_c = x_0 + v_0 t$ with a variance of $< (x - x_c)^2 >= 4Dt$ (Fig. 7.1).

[6] With the proper normalization factor.

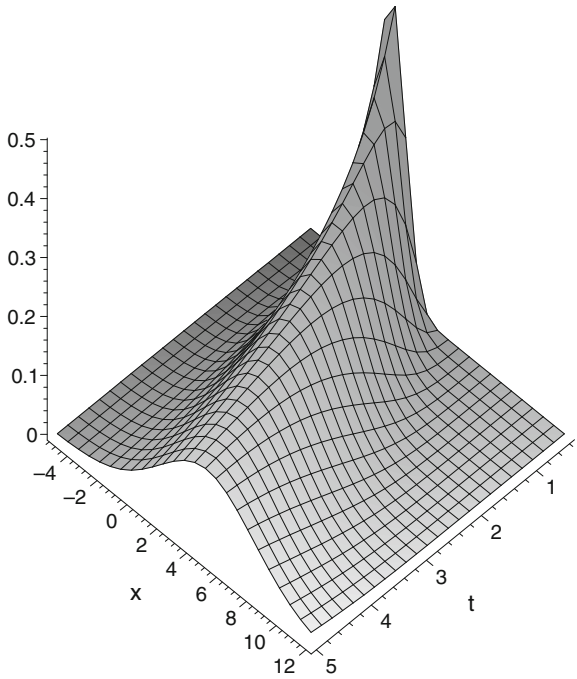

Fig. 7.1 Solution (7.36) of the diffusion equation for sharp initial conditions

7.3.2 Absorbing Boundary

Consider a particle from species A which can undergo a chemical reaction with a particle from species B at position $x_A = 0$

$$\text{A+B} \rightarrow \text{AB}. \tag{7.37}$$

If the reaction rate is very fast, then the concentration of A vanishes at $x = 0$ which gives an additional boundary condition

$$W(x = 0, t) = 0. \tag{7.38}$$

Starting again with a localized particle at time zero with

$$W(x, 0) = \delta(x - x_0) \quad v_0 = 0 \tag{7.39}$$

the probability distribution

$$W(x, t) = \frac{1}{\sqrt{4\pi D t}} \left(\mathrm{e}^{-\frac{(x - x_0)^2}{4Dt}} - \mathrm{e}^{-\frac{(x + x_0)^2}{4Dt}} \right) \tag{7.40}$$

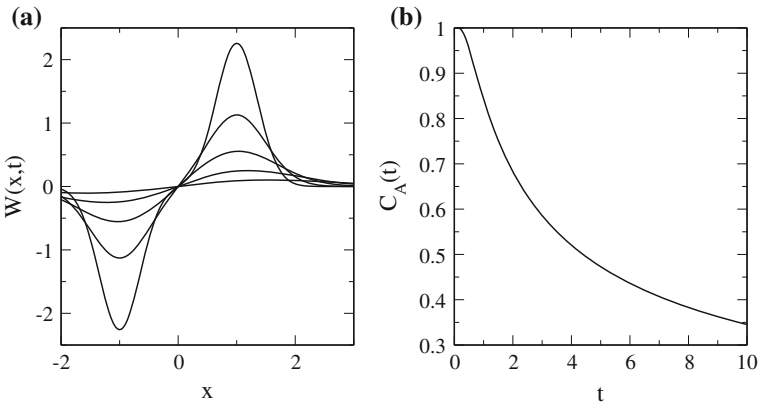

Fig. 7.2 Solution from the mirror principle. (**a**) The probability density distribution (7.40) at $t = 0.25,\ 0.5,\ 1,\ 2,\ 5$ and (**b**) the decay of the total concentration (7.41) are shown for $4D = 1$

is a solution which fullfills the boundary conditions. This solution is similar to the mirror principle known from electrostatics. The total concentration of species A in solution is then given by (Fig. 7.2)

$$C_A(t) = \int_0^\infty dx\ W(x,t) = erf\left(\frac{x_0}{\sqrt{4Dt}}\right). \tag{7.41}$$

7.4 Fokker–Planck Equation for Brownian Motion

For Brownian motion we have from the formal solution

$$v(\tau) = v_0(1 - \gamma\tau + \cdots) + \int_0^\tau (1 + \gamma(t_1 - \tau) + \cdots)F(t_1)dt_1. \tag{7.42}$$

The first moment[7]

$$M_1(v_0, t, \tau) =< v(\tau) - v(0) >= -\gamma\tau v_0 + \cdots \tag{7.43}$$

gives

$$D^{(1)}(v,t) = -\gamma v. \tag{7.44}$$

[7]Here and in the following we use $< F(t) >= 0$.

The second moment follows from

$$< (v(\tau) - v_0)^2 >= (v_0\gamma\tau)^2 + \int_0^\tau \int_0^\tau (1 + \gamma(t_1 + t_2 - 2\tau \cdots))F(t_1)F(t_2)dt_1dt_2. \tag{7.45}$$

The double integral gives

$$\int_0^\tau dt_1 \int_{-t_1}^{\tau - t_1} dt'(1 + \gamma(2t_1 + t' - 2\tau + \cdots)\frac{2\gamma k_B T}{m}\delta(t')$$

$$= \int_0^\tau dt_1 \frac{2\gamma k_B T}{m}(1 + \gamma(2t_1 - 2\tau + \cdots)$$
$$= \frac{2\gamma k_B T}{m}\tau + \cdots \tag{7.46}$$

and we have

$$D^{(2)} = \frac{\gamma k_B T}{m}. \tag{7.47}$$

The higher moments have no contributions linear in τ and the resulting Fokker–Planck equation is

$$\frac{\partial W(v,t)}{\partial t} = \gamma \frac{\partial}{\partial v}(vW(v,t)) + \frac{\gamma k_B T}{m}\frac{\partial^2}{\partial v^2}W(v,t). \tag{7.48}$$

7.5 Stationary Solution to the Fokker–Planck Equation

The Fokker–Planck equation can be written in the form of a continuity equation

$$\frac{\partial W(v,t)}{\partial t} = -\frac{\partial}{\partial v}S(v,t) \tag{7.49}$$

with the probability current

$$S(v,t) = -\frac{\gamma k_B T}{m}\left(\frac{mv}{k_B T}W(v,t) + \frac{\partial}{\partial v}W(v,t)\right). \tag{7.50}$$

The probability current has to vanish for a stationary solution (with open boundaries $-\infty < v < \infty$)

$$\frac{\partial}{\partial v}W(v,t) = -\frac{mv}{k_B T}W(v,t) \tag{7.51}$$

which has the Maxwell distribution as its solution

$$W_{stat}(v,t) = \sqrt{\frac{m}{2\pi k_B T}} \mathrm{e}^{-mv^2/2k_B T}. \tag{7.52}$$

Therefore we conclude, that the Fokker–Planck equation describes systems that reach thermal equilibrium, starting from a non equilibrium distribution. In the following we want to look at the relaxation process itself. We start with

$$\frac{\partial W(v,t)}{\partial t} = \gamma W(v,t) + \gamma v \frac{\partial W(v,t)}{\partial v} + D \frac{\partial^2 W(v,t)}{\partial v^2} \tag{7.53}$$

and introduce the new variables

$$\rho = v\mathrm{e}^{\gamma t} \qquad y(\rho,t) = W(\rho \mathrm{e}^{-\gamma t}, t) \tag{7.54}$$

which transform the differentials according to

$$\begin{aligned} \frac{\partial W}{\partial v} &= \frac{\partial y}{\partial \rho}\frac{\partial \rho}{\partial v} = \mathrm{e}^{\gamma t}\frac{\partial y}{\partial \rho} \\ \frac{\partial^2 W}{\partial v^2} &= \mathrm{e}^{2\gamma t}\frac{\partial^2 y}{\partial \rho^2} \\ \frac{\partial W}{\partial t} &= \frac{\partial y}{\partial t} + \frac{\partial y}{\partial \rho}\frac{\partial \rho}{\partial t} = \frac{\partial y}{\partial t} + \gamma\rho\frac{\partial y}{\partial \rho}. \end{aligned} \tag{7.55}$$

This leads to the new differential equation

$$\frac{\partial y}{\partial t} = \gamma y + D\mathrm{e}^{2\gamma t}\frac{\partial^2 y}{\partial \rho^2}. \tag{7.56}$$

To solve this equation we introduce new variables again

$$y = \chi \mathrm{e}^{\gamma t} \tag{7.57}$$

which results in

$$\frac{\partial \chi}{\partial t} = D\mathrm{e}^{2\gamma t}\frac{\partial^2 \chi}{\partial \rho^2}. \tag{7.58}$$

Now we introduce a new time scale

$$\theta = \frac{1}{2\gamma}(\mathrm{e}^{2\gamma t} - 1) \tag{7.59}$$

$$d\theta = \mathrm{e}^{2\gamma t} dt \tag{7.60}$$

satisfying the initial condition $\theta(t = 0) = 0$. Finally, we have to solve a diffusion equation

$$\frac{\partial \chi}{\partial \theta} = D \frac{\partial^2 \chi}{\partial \rho^2} \tag{7.61}$$

which gives

$$\chi(\rho, \theta, \rho_0) = \frac{1}{\sqrt{4\pi D\theta}} \exp\left(-\frac{(\rho - \rho_0)^2}{4\pi D\theta}\right). \tag{7.62}$$

After back substitution of all variables we find

$$W(v, t) = \sqrt{\frac{m}{2\pi k_B T(1 - \mathrm{e}^{-2\gamma t})}} \exp\left\{-\frac{m}{2k_B T} \frac{(v - v_0 \mathrm{e}^{-\gamma t})^2}{(1 - \mathrm{e}^{-2\gamma t})}\right\}. \tag{7.63}$$

This solution shows that the system behaves initially like

$$W(v, t) \approx \frac{1}{\sqrt{4\pi Dt}} \exp\left\{-\frac{(v - v_0)^2}{4Dt}\right\} \tag{7.64}$$

and relaxes to the Maxwell distribution with a time constant $\Delta t = 1/2\gamma$.

7.6 Diffusion in an External Potential

We consider motion of a particle under the influence of an external (mean) force $K(x) = -\frac{\mathrm{d}}{\mathrm{d}x} U(x)$. The stochastic differential equation for position and velocity is

$$\dot{x} = v \tag{7.65}$$

$$\dot{v} = -\gamma v + \frac{1}{m} K(x) + F(t). \tag{7.66}$$

We will calculate the moments for the Kramers–Moyal expansion. For small τ we have

$$\begin{aligned} M_x &= < x(\tau) - x(0) >= \int_0^\tau v(t)dt = v_0 \tau + \cdots \\ M_v &= < v(\tau) - v(0) >= \int_0^\tau \left(-\gamma v(t) + \frac{1}{m} K(x(t)) + < F(t) >\right) dt \\ &= \left(-\gamma v_0 + \frac{1}{m} K(x_0)\right) \tau + \cdots \end{aligned}$$

$$
\begin{aligned}
M_{xx} &= < (x(\tau) - x(0))^2 >= \int_0^\tau \int_0^\tau v(t_1)v(t_2)dt_1dt_2 = v_0^2\tau^2 + \cdots \\
M_{vv} &= < (v(\tau) - v(0))^2 > \\
&= \left(-\gamma v_0 + \frac{1}{m}K(x_0)\right)^2 \tau^2 + \int_0^\tau \int_0^\tau F(t_1)F(t_2)dt_1dt_2 \\
&= \frac{2\gamma k_B T}{m}\tau + \cdots
\end{aligned} \tag{7.67}
$$

The drift and diffusion coefficients are

$$D^{(x)} = v \tag{7.68}$$

$$D^{(v)} = -\gamma v + \frac{1}{m}K(x) \tag{7.69}$$

$$D^{(xx)} = 0 \tag{7.70}$$

$$D^{(vv)} = \frac{\gamma k_B T}{m} \tag{7.71}$$

which leads to the Klein–Kramers equation

$$
\begin{aligned}
\frac{\partial W(x,v,t)}{\partial t} &= \left[-\frac{\partial}{\partial x}D^{(x)} - \frac{\partial}{\partial v}D^{(v)} + \frac{\partial^2}{\partial v^2}D^{(vv)}\right] W(x,v,t) \\
&= \left[-\frac{\partial}{\partial x}v + \frac{\partial}{\partial v}(\gamma v - \frac{K(x)}{m}) + \frac{\gamma k_B T}{m}\frac{\partial^2}{\partial v^2}\right] W(x,v,t).
\end{aligned} \tag{7.72}
$$

This equation can be divided into a reversible and an irreversible part

$$\frac{\partial W}{\partial t} = (\mathfrak{L}_{rev} + \mathfrak{L}_{irrev})W \tag{7.73}$$

$$\mathfrak{L}_{rev} = \left[-v\frac{\partial}{\partial x} + \frac{1}{m}\frac{\partial U}{\partial x}\frac{\partial}{\partial v}\right] \qquad \mathfrak{L}_{irrev} = \left[\frac{\partial}{\partial v}\gamma v + \frac{\gamma k_B T}{m}\frac{\partial^2}{\partial v^2}\right]. \tag{7.74}$$

The reversible part corresponds to the Liouville operator for a particle moving in the potential without friction

$$\mathfrak{L} = \left[\frac{\partial \mathfrak{H}}{\partial x}\frac{\partial}{\partial p} - \frac{\partial \mathfrak{H}}{\partial p}\frac{\partial}{\partial x}\right] \qquad \mathfrak{H} = \frac{p^2}{2m} + U(x). \tag{7.75}$$

Obviously

$$\mathfrak{L}\mathfrak{H} = 0 \tag{7.76}$$

and

$$\mathfrak{L}_{irrev} \exp\left\{-\frac{\mathfrak{H}}{k_B T}\right\}$$
$$= \exp\left\{-\frac{\mathfrak{H}}{k_B T}\right\}\left[\gamma - \gamma v \frac{mv}{k_B T} + \frac{\gamma k_B T}{m}((\frac{mv}{k_B T})^2 - \frac{m}{k_B T})\right] = 0. \tag{7.77}$$

Therefore the Klein–Kramers equation has the stationary solution

$$W_{stat}(x, v, t) = Z^{-1} \mathrm{e}^{-(mv^2/2 + U(x))/k_B T} \tag{7.78}$$

$$Z = \int\int dv dx \, \mathrm{e}^{-(mv^2/2 + U(x))/k_B T}. \tag{7.79}$$

The Klein–Kramers equation can be written in the form of a continuity equation

$$\frac{\partial}{\partial t} W = -\frac{\partial}{\partial x} S_x - \frac{\partial}{\partial v} S_v \tag{7.80}$$

with the probability current

$$S_x = vW \tag{7.81}$$

$$S_v = -\left[\gamma v + \frac{1}{m}\frac{\partial U}{\partial x}\right] W - \frac{\gamma k_B T}{m}\frac{\partial W}{\partial v}. \tag{7.82}$$

7.7 Large Friction Limit – Smoluchowski Equation

For large friction constant γ we may neglect the second derivative with respect to time and obtain the stochastic differential equation

$$\dot{x} = \frac{1}{m\gamma} K(x) + \frac{1}{\gamma} F(t) \tag{7.83}$$

and the corresponding Fokker–Planck equation is the Smoluchowski equation,

$$\frac{\partial W(x,t)}{\partial t} = \left[-\frac{1}{m\gamma}\frac{\partial}{\partial x} K(x) + \frac{k_B T}{m\gamma}\frac{\partial^2}{\partial x^2}\right] W(x,t) \tag{7.84}$$

which can be written with the mean force potential $U(x)$ as

$$\frac{\partial W(x,t)}{\partial t} = \frac{1}{m\gamma}\frac{\partial}{\partial x}\left[k_B T \frac{\partial}{\partial x} + \frac{\partial U}{\partial x}\right] W(x,t). \tag{7.85}$$

7.8 Master Equation

The master equation is a very general linear equation for the probability density. If the variable x takes on only integer values, it has the form

$$\frac{\partial W_n}{\partial t} = \sum_m (w_{m\to n} W_m - w_{n\to m} W_n) \tag{7.86}$$

where W_n is the probability to find the integer value n and $w_{m\to n}$ is the transition probability. For continuous x the summation has to be replaced by an integration

$$\frac{\partial W(x,t)}{\partial t} = \int \left(w_{x'\to x} W(x',t) - w_{x\to x'} W(x,t)\right) dx'. \tag{7.87}$$

The Fokker–Planck equation is a special form of the master equation with

$$w_{x'\to x} = \left(-\frac{\partial}{\partial x} D^{(1)}(x) + \frac{\partial^2}{\partial x^2} D^{(2)}(x)\right) \delta(x - x'). \tag{7.88}$$

So far we have discussed only Markov processes where the change of probability at time t only depends on the probability at time t. If memory effects are included the generalized Master equation results.

Problems

7.1 Smoluchowski Equation

Consider a 1-dimensional random walk. At times $t_n = n\Delta t$ a particle at position $x_j = j\Delta x$ jumps either to the left side $j-1$ with probability w_j^- or to the right side $j+1$ with probability $w_j^+ = 1 - w_j^-$. The probability to find a particle at site j at the time $n+1$ is then given by

$$P_{n+1,j} = w_{j-1}^+ P_{n,j-1} + w_{j+1}^- P_{n,j+1}.$$

Show that in the limit of small Δx, Δt the probability distribution $P(t,x)$ obeys a Smoluchowski equation

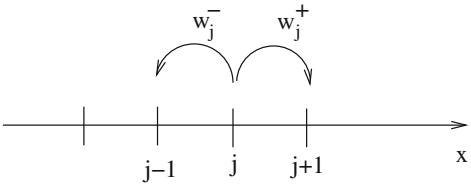

7.2 Eigenvalue Solution to the Smoluchowski Equation

Consider the 1-dimensional Smoluchowski equation

$$\frac{\partial W(x,t)}{\partial t} = \frac{1}{m\gamma}\frac{\partial}{\partial x}\left[k_B T\frac{\partial}{\partial x} + \frac{\partial U}{\partial x}\right] W(x,t) = -\frac{\partial}{\partial x}S(x)$$

for a harmonic potential

$$U(x) = \frac{m\omega^2}{2}x^2.$$

Show that the probability current can be written as

$$S(x,t) = -\frac{k_B T}{m\gamma}\mathrm{e}^{-U(x)/kT}\left(\frac{\partial}{\partial x}\mathrm{e}^{U(x)/k_B T}W(x,t)\right)$$

and that the Fokker–Planck operator can be written as

$$\mathfrak{L}_{FP} = \frac{1}{m\gamma}\frac{\partial}{\partial x}\left[k_B T\frac{\partial}{\partial x} + \frac{\partial U}{\partial x}\right] = \frac{k_B T}{m\gamma}\frac{\partial}{\partial x}\mathrm{e}^{-U(x)/k_B T}\frac{\partial}{\partial x}\mathrm{e}^{U(x)/k_B T}$$

and can be transformed into a hermitian operator by

$$\mathfrak{L} = \mathrm{e}^{U(x)/2k_B T}\mathfrak{L}_{FP}\mathrm{e}^{-U(x)/2k_B T}.$$

Solve the eigenvalue problem

$$\mathfrak{L}\psi_n(x) = \lambda_n\psi_n(x)$$

and use the function $\psi_0(x)$ to construct a special solution

$$W(x,t) = \mathrm{e}^{\lambda_0 t}\mathrm{e}^{-U(x)/2k_B T}\psi_0(x).$$

7.3 Diffusion Through a Membrane

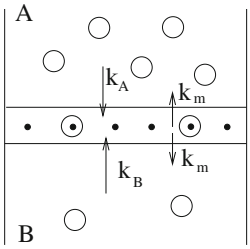

A membrane with M pore-proteins separates two half-spaces A and B. An ion X may diffuse through M pore proteins in the membrane from A to B or vice versa. The rate constants for the formation of the ion-pore complex are k_A and k_B respectively, while k_m is the constant for the decay of the ion-pore complex independent of the side to which the ion escapes. Let $P_N(t)$ denote the probability that there are N ion-pore complexes at time t. The master equation for the probability is

$$\frac{\mathrm{d}P_N(t)}{\mathrm{d}t} = -\left[(k_A + k_B)(M - N) + 2k_m N\right] P_N(t) +$$

$$+ (k_A + k_B)(M - N + 1) P_{N-1}(t) + 2k_m(N + 1) P_{N+1}(t).$$

Calculate mean and variance of the number of complexes

$$\overline{N} = \sum_N N P_N$$

$$\sigma^2 = \overline{N^2} - \overline{N}^2$$

and the mean diffusion current

$$J_{AB} = \frac{\mathrm{d}N_B}{\mathrm{d}t} - \frac{\mathrm{d}N_A}{\mathrm{d}t}$$

where $N_{A,B}$ is the number of ions in the upper or lower half-space.

Chapter 8
Kramers Theory

Kramers [31] used the concept of Brownian motion to describe motion of particles over a barrier as a model for chemical reactions in solution. The probability distribution of a particle moving in an external potential is described by the Klein–Kramers (7.68)

$$\frac{\partial W(x,v,t)}{\partial t} = \left[-\frac{\partial}{\partial x}v + \frac{\partial}{\partial v}\left(\gamma v - \frac{K(x)}{m}\right) + \frac{\gamma k_B T}{m}\frac{\partial^2}{\partial v^2}\right] W(x,v,t)$$
$$= -\frac{\partial}{\partial x}S_x - \frac{\partial}{\partial v}S_v$$

and the rate of the chemical reaction is related to the probability current S_x across the barrier. The famous Kramers relation describes the friction dependency of the reaction rate.

8.1 Kramers' Model

Particle A in the stable minimum has to reach the transition state by diffusive motion and then converts to the product C. The minimum well and the peak of the barrier are both approximated by parabolic functions (Fig. 8.1)

$$U_A = \frac{m}{2}\omega_a^2 (x - x_0)^2 \tag{8.1}$$

$$U^* = E_a - \frac{m}{2}\omega^{*2} x^2. \tag{8.2}$$

P.O.J. Scherer and S.F. Fischer, *Theoretical Molecular Biophysics*,
Biological and Medical Physics, Biomedical Engineering,
DOI 10.1007/978-3-662-55671-9_8

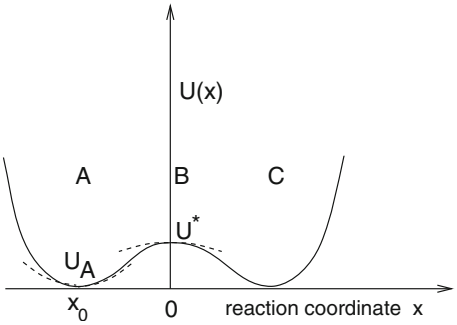

Fig. 8.1 Kramers model

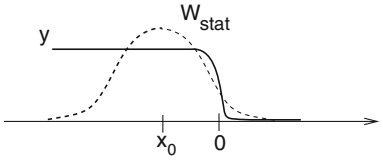

Fig. 8.2 Ansatz function. The stationary solution of a harmonic well is multiplied with the function $y(x, v)$ which switches from 1 to 0 at the saddlepoint

Without the chemical reaction the stationary solution is

$$W_{stat} = Z^{-1} \exp\{-\mathfrak{H}/k_B T\}. \tag{8.3}$$

We assume that the perturbation due to the reaction is small and make the following ansatz (Fig. 8.2)

$$W(x, v) = W_{stat}\, y(x, v) \tag{8.4}$$

where the partition function is approximated by the harmonic oscillator

$$Z = \frac{2\pi k_B T}{m\omega_a}. \tag{8.5}$$

The probability distribution should fullfill two boundary conditions.

(i) In the minimum of the A-well the particles should be in thermal equilibrium, and therefore

$$W(x, v) = Z^{-1} \exp\left\{-\frac{\mathfrak{H}}{k_B T}\right\} \to y = 1 \quad \text{if } x \approx x_0. \tag{8.6}$$

(ii) On the right side of the barrier ($x > 0$), all particles A are converted into C and there will be no particles of the A species here

$$W(x, v) = 0 \rightarrow y = 0 \quad \text{if } x > 0. \tag{8.7}$$

8.2 Kramers' Calculation of the Reaction Rate

Let us now insert the ansatz function into the Klein–Kramers equation For the reversible part, we have

$$\mathfrak{L}_{rev} \exp\left\{-\frac{\mathfrak{H}}{k_B T}\right\} y(x, v) = \exp\left\{-\frac{\mathfrak{H}}{k_B T}\right\} \mathfrak{L}_{rev} y(x, v) \tag{8.8}$$

and for the irreversible part

$$\left[\frac{\partial}{\partial v}\gamma v + \frac{\gamma k_B T}{m}\frac{\partial^2}{\partial v^2}\right] \exp\left\{-\frac{\mathfrak{H}}{k_B T}\right\} y(x, v) \tag{8.9}$$

$$= \left\{\exp\left\{-\frac{\mathfrak{H}}{k_B T}\right\}\left[-\gamma v\frac{\partial}{\partial v} + \frac{\gamma k_B T}{m}\frac{\partial^2}{\partial v^2}\right] y\right\}.$$

Note the subtle difference. The operator $\frac{\partial}{\partial v} v$ is replaced by $-v\frac{\partial}{\partial v}$. Together we have the following equation for y

$$0 = -v\frac{\partial y}{\partial x} + \frac{1}{m}\frac{\partial U}{\partial x}\frac{\partial y}{\partial v} - \gamma v\frac{\partial y}{\partial v} + \frac{\gamma k_B T}{m}\frac{\partial^2 y}{\partial v^2} \tag{8.10}$$

which becomes in the vicinity of the top

$$0 = -v\frac{\partial y}{\partial x} - \omega^{*2} x\frac{\partial y}{\partial v} - \gamma v\frac{\partial y}{\partial v} + \frac{\gamma k_B T}{m}\frac{\partial^2 y}{\partial v^2}. \tag{8.11}$$

Now we make a transformation of variables

$$(x, v) \rightarrow (\eta, \xi) = (x, v - \lambda x). \tag{8.12}$$

With

$$x = \eta \quad v = \xi + \lambda\eta \quad \frac{\partial}{\partial x} = \frac{\partial}{\partial \eta} - \lambda\frac{\partial}{\partial \xi} \quad \frac{\partial}{\partial v} = \frac{\partial}{\partial \xi} \tag{8.13}$$

equation (8.11) is transformed to

$$0 = (\xi+\lambda\eta)\frac{\partial}{\partial\eta}y+((\lambda-\gamma)\xi+(\lambda^2-\lambda\gamma-\omega^2)\eta)\frac{\partial}{\partial\xi}y+\frac{\gamma k_B T}{m}\frac{\partial^2}{\partial\xi^2}y. \tag{8.14}$$

Now choose

$$\lambda = \frac{\gamma}{2}+\sqrt{\frac{\gamma^2}{4}+\omega^{*2}} \tag{8.15}$$

to have the simplified equation

$$0 = (\xi+\lambda\eta)\frac{\partial}{\partial\eta}y+((\lambda-\gamma)\xi)\frac{\partial}{\partial\xi}y+\frac{\gamma k_B T}{m}\frac{\partial^2}{\partial\xi^2}y \tag{8.16}$$

which obviously has solutions which depend only on ξ and obey

$$\xi\frac{\partial}{\partial\xi}\Phi(\xi) = -\frac{\gamma k_B T}{m(\lambda-\gamma)}\frac{\partial^2}{\partial\xi^2}\Phi(\xi). \tag{8.17}$$

The general solution of this equation is[1]

$$\Phi(\xi) = C_1 + C_2\mathrm{erf}\left(\xi\sqrt{\frac{m(\lambda-\gamma)}{2\gamma k_B T}}\right). \tag{8.18}$$

Now we impose the boundary condition $\Phi \to 0$ for $x \to \infty$ which means $\xi \to -\infty$. From this we find

$$C_1 = -C_2\mathrm{erf}(-\infty) = C_2. \tag{8.19}$$

Together, we have for the probability density

$$W(x,v) = C_2\frac{m\omega_a}{2\pi k_B T}\exp\left\{-\frac{\frac{m}{2}v^2+U(x)}{k_B T}\right\}\left\{1+\mathrm{erf}\left(\sqrt{\frac{m(\lambda-\gamma)}{2\gamma k_B T}}(v-\lambda x)\right)\right\} \tag{8.20}$$

and the flux over the barrier is approximately

$$S = \int dv\ vW(0,v)$$

[1] Note that $\lambda-\gamma$ is always positive. This would not be true for the second root.

$$= C_2 \frac{m\omega_a}{2\pi k_B T} \mathrm{e}^{-U(x^*)/k_B T} \int dv\, v \mathrm{e}^{-mv^2/2k_B T} \left\{ 1 + \mathrm{erf}\left(\sqrt{\frac{m(\lambda - \gamma)}{2\gamma k_B T}} v \right) \right\}$$

$$= C_2 \frac{m\omega_a}{2\pi k_B T} \mathrm{e}^{-U(0)/k_B T} \frac{2k_B T}{m} \sqrt{1 - \frac{\gamma}{\lambda}}. \tag{8.21}$$

In the A-well, we have approximately

$$W(x, v) \approx 2C_2 \frac{m\omega_a}{2\pi k_B T} \exp\left\{ - \frac{\frac{mv^2}{2} + \frac{m\omega_a^2 (x - x_a)^2}{2}}{k_B T} \right\}. \tag{8.22}$$

The total concentration is approximately

$$[A] = \int dx \int dv W_A(x, v) = 2C_2. \tag{8.23}$$

Hence, we find

$$S = [A] \frac{\omega_a}{2\pi} \mathrm{e}^{-U(0)/k_B T} \sqrt{1 - \frac{\gamma}{\lambda}}. \tag{8.24}$$

The square root can be written as

$$\sqrt{1 - \frac{\gamma}{\frac{\gamma}{2} + \sqrt{\frac{\gamma^2}{4} + \omega^{*2}}}} = \sqrt{\frac{-\frac{\gamma}{2} + \sqrt{\frac{\gamma^2}{4} + \omega^{*2}}}{\frac{\gamma}{2} + \sqrt{\frac{\gamma^2}{4} + \omega^{*2}}}}$$

$$= \sqrt{\frac{\left(-\frac{\gamma}{2} + \sqrt{\frac{\gamma^2}{4} + \omega^{*2}} \right)^2}{-\frac{\gamma^2}{4} + \left(\frac{\gamma^2}{4} + \omega^{*2} \right)}}$$

$$= \frac{-\frac{\gamma}{2} + \sqrt{\frac{\gamma^2}{4} + \omega^{*2}}}{\omega^*} \tag{8.25}$$

and finally, we arrive at Kramers' famous result

$$k = \frac{S}{[A]} = \frac{\omega_a}{2\pi\omega^*} \mathrm{e}^{-U(0)/k_B T} \left(-\frac{\gamma}{2} + \sqrt{\frac{\gamma^2}{4} + \omega^{*2}} \right). \tag{8.26}$$

The bracket is Kramers correction to the escape rate. In the limit of high friction series expansion in γ^{-1} gives

$$k = \gamma^{-1} \frac{\omega_a \omega^*}{2\pi} \mathrm{e}^{-U(0)/k_B T}. \tag{8.27}$$

In the limit of low friction, the result is

$$k = \frac{\omega_a}{2\pi} \mathrm{e}^{-U(0)/k_B T}. \tag{8.28}$$

Chapter 9
Dispersive Kinetics

In this chapter we consider the decay of an optically excited state of a donor molecule in a fluctuating medium. The fluctuations are modelled by time-dependent decay rates k (electron transfer), k_{-1} (backreaction), k_{da} (deactivation by fluorescence or radiationless transitions) and k_{cr} (charge recombination to the groundstate) (Fig. 9.1).

The time evolution is described by the system of rate equations

$$\begin{aligned} \frac{\mathrm{d}}{\mathrm{d}t} W(D^*) &= -k(t) W(D^*) + k_{-1}(t) W(D^+A^-) - k_{da} W(D^*) \\ \frac{\mathrm{d}}{\mathrm{d}t} W(D^+A^-) &= k(t) W(D^*) - k_{-1}(t) W(D^+A^-) - k_{cr} W(D^+A^-) \end{aligned} \tag{9.1}$$

which has to be combined with suitable equations describing the dynamics of the environment. First we discuss a simple dichotomous model [32] where the fluctuations of the rates are modeled by a random process switching between two values representing two different configurations of the environment. We solve the master equation and discuss the limits of fast and slow solvent fluctuations. In the second part, we apply continuous time random walk processes to model the diffusive motion. For an uncorrelated Markovian process, the coupled equations are solved with the help of the Laplace transformation. The results are generalized to describe the powertime law as observed for CO rebinding in myoglobin at low temperatures.

P.O.J. Scherer and S.F. Fischer, *Theoretical Molecular Biophysics*,
Biological and Medical Physics, Biomedical Engineering,
DOI 10.1007/978-3-662-55671-9_9

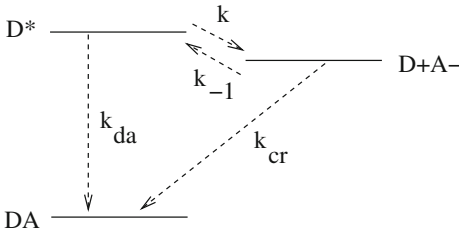

Fig. 9.1 Electron transfer in a fluctuating medium. The rates are time dependent

9.1 Dichotomous Model

The fluctuations of the rates are modeled by random jumps between two different configurations ($\pm$) of the environment which modulates the values of the rates. The probabilities of the two states are determined by the master equation

$$\frac{\mathrm{d}}{\mathrm{d}t}\begin{pmatrix} W(+) \\ W(-) \end{pmatrix} = \begin{pmatrix} -\alpha & \beta \\ \alpha & -\beta \end{pmatrix}\begin{pmatrix} W(+) \\ W(-) \end{pmatrix} \tag{9.2}$$

which has the general solution

$$\begin{aligned} W(+) &= C_1 + C_2\mathrm{e}^{-(\alpha+\beta)t} \\ W(-) &= C_1\frac{\alpha}{\beta} - C_2\mathrm{e}^{-(\alpha+\beta)t}. \end{aligned} \tag{9.3}$$

Obviously the equilibrium values are

$$W_{eq}(+) = \frac{\beta}{\alpha+\beta} \quad W_{eq}(-) = \frac{\alpha}{\alpha+\beta} \tag{9.4}$$

and the correlation function is (with $Q_\pm = \pm 1$)

$$\begin{aligned} < Q(t)Q(0) > &= W_{eq}(+)(P(+,t|+,0) - P(-,t|+,0)) \\ &+ W_{eq}(-)(P(-,t|-,0) - P(+,t|-,0)) \\ &= (W_{eq}(+) - W_{eq}(-))^2 + 4W_{eq}(+)W_{eq}(-)\mathrm{e}^{-(\alpha+\beta)t} \\ &= < Q >^2 + (< Q^2 > - < Q >^2)\mathrm{e}^{-(\alpha+\beta)t}. \end{aligned} \tag{9.5}$$

Combination of the two systems of equations (9.1, 9.2) gives the equation of motion

$$\frac{\mathrm{d}}{\mathrm{d}t}\mathbf{W} = A\mathbf{W} \tag{9.6}$$

for the four-component state vector

$$\mathbf{W} = \begin{pmatrix} W(D^*, +) \\ W(D^*, -) \\ W(D^+A^-, +) \\ W(D^+A^-, -) \end{pmatrix} \tag{9.7}$$

with the rate matrix

$$A = \begin{pmatrix} -\alpha - k^+ - k_{da} & \beta & k_{-1}^+ & 0 \\ \alpha & -\beta - k^- - k_{da} & 0 & k_{-1}^- \\ k^+ & 0 & -\alpha - k_{-1}^+ - k_{cr} & \beta \\ 0 & k^- & \alpha & -\beta - k_{-1}^- - k_{cr} \end{pmatrix}. \tag{9.8}$$

Generally, the solution of this equation can be expressed by using the left- and right eigenvectors and the eigenvalues λ of the rate matrix which obey

$$A\mathbf{R}_\nu = \lambda_\nu \mathbf{R}_\nu \tag{9.9}$$

$$\mathbf{L}_\nu A = \lambda_\nu \mathbf{L}_\nu. \tag{9.10}$$

For the initial values $\mathbf{W}(0)$ the solution is given by[1]

$$\mathbf{W}(t) = \sum_{\nu=1}^{4} \frac{(\mathbf{L}_\nu \bullet \mathbf{W}(0))}{(\mathbf{L}_\nu \bullet \mathbf{R}_\nu)} \mathbf{R}_\nu \mathrm{e}^{\lambda_\nu t}. \tag{9.11}$$

In the following we consider a simplified case of gated transfer with $k_{da} = k_{cr} = k_{-1}^{\pm} = k^- = 0$ (Fig. 9.2). Then the rate matrix becomes

$$\begin{pmatrix} -\alpha - k^+ & \beta & 0 & 0 \\ \alpha & -\beta & 0 & 0 \\ k^+ & 0 & -\alpha & \beta \\ 0 & 0 & \alpha & -\beta \end{pmatrix}. \tag{9.12}$$

[1] In the case of degenerate eigenvalues, linear combinations of the corresponding vectors can be found such that $\mathbf{L}_\nu \bullet \mathbf{L}_{\nu'} = 0$ for $\nu \neq \nu'$.

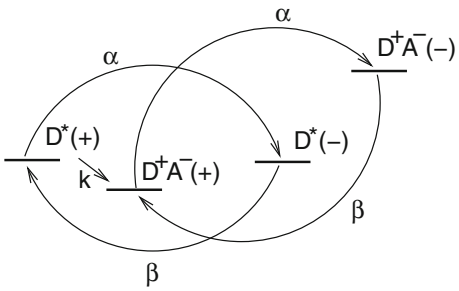

Fig. 9.2 Gated electron transfer

As initial values we chose

$$W_0 = \begin{pmatrix} W_{eq}(+) \\ W_{eq}(-) \\ 0 \\ 0 \end{pmatrix} = \begin{pmatrix} \frac{\beta}{\alpha+\beta} \\ \frac{\alpha}{\alpha+\beta} \\ 0 \\ 0 \end{pmatrix}. \tag{9.13}$$

There is one eigenvalue $\lambda_1 = 0$ corresponding to the eigenvectors

$$R_1 = \begin{pmatrix} 0 \\ 0 \\ \beta \\ \alpha \end{pmatrix} \quad L_1 = \begin{pmatrix} 1 & 1 & 1 & 1 \end{pmatrix}. \tag{9.14}$$

This reflects simply conservation of $\sum_{\nu=1}^{4} W_\nu$ in this special case. The contribution of the zero eigenvector is

$$\frac{\mathbf{L}_1 \bullet \mathbf{W}(0)}{\mathbf{L}_1 \bullet \mathbf{R}_1}\mathbf{R}_1 = \frac{1}{\alpha+\beta}\begin{pmatrix} 0 \\ 0 \\ \beta \\ \alpha \end{pmatrix} = \begin{pmatrix} 0 \\ 0 \\ W_{eq}(+) \\ W_{eq}(-) \end{pmatrix}. \tag{9.15}$$

A second eigenvalue $\lambda_2 = -(\alpha+\beta)$ corresponds to the equilibrium in the final state D^+A^- where no further reactions take place

$$\mathbf{R}_2 = \begin{pmatrix} 0 \\ 0 \\ 1 \\ -1 \end{pmatrix} \quad \mathbf{L}_2 = \begin{pmatrix} \alpha & -\beta & \alpha & -\beta \end{pmatrix}. \tag{9.16}$$

The contribution of this eigenvalue is

$$\frac{L_2 \bullet P_0}{L_2 \bullet R_2} R_2 = 0 \tag{9.17}$$

since we assumed equilibrium in the initial state. The remaining two eigenvalues are

$$\lambda_{3,4} = -\frac{\alpha + \beta + k}{2} \pm \frac{1}{2}\sqrt{(\alpha + \beta + k)^2 - 4\beta k} \tag{9.18}$$

and the resulting decay will be in general biexponential. We consider two limits:

9.1.1 Fast Solvent Fluctuations

In the limit of small k we expand the square root to find

$$\lambda_{3,4} = -\frac{\alpha + \beta}{2} \pm \frac{\alpha + \beta}{2} - \frac{k}{2} \pm \frac{\alpha - \beta}{\alpha + \beta}\frac{k}{2} + \cdots \tag{9.19}$$

One of the eigenvalues is

$$\lambda_3 = -(\alpha + \beta) - \frac{\alpha}{\alpha + \beta} k + \cdots \tag{9.20}$$

In the limit of $k \to 0$ the corresponding eigenvectors are

$$\mathbf{R}_3 = \begin{pmatrix} 1 \\ -1 \\ -1 \\ 1 \end{pmatrix} \quad \mathbf{L}_3 = \begin{pmatrix} \alpha & -\beta & 0 & 0 \end{pmatrix} \tag{9.21}$$

and will not contribute significantly. The second eigenvalue

$$\lambda_4 = -\frac{\beta}{\alpha + \beta} k + \cdots = -W_{eq}(+)k \tag{9.22}$$

is given by the average rate. The eigenvectors are

$$\mathbf{R}_4 = \begin{pmatrix} \beta \\ \alpha \\ -\beta \\ -\alpha \end{pmatrix} \quad \mathbf{L}_4 = \begin{pmatrix} 1 & 1 & 0 & 0 \end{pmatrix} \tag{9.23}$$

and the contribution to the dynamics is

$$\frac{(\mathbf{L}_4 \cdot \mathbf{W}_0)}{(\mathbf{L}_4 \cdot \mathbf{R}_4)} \mathbf{R}_4 \mathrm{e}^{\lambda_4 t} = \frac{1}{\alpha + \beta} \begin{pmatrix} \beta \\ \alpha \\ -\beta \\ -\alpha \end{pmatrix} \mathrm{e}^{\lambda_4 t}. \tag{9.24}$$

The total time dependence is approximately given by

$$W = \begin{pmatrix} W_{eq}(+)\mathrm{e}^{\lambda_4 t} \\ W_{eq}(-)\mathrm{e}^{\lambda_4 t} \\ W_{eq}(+)(1 - \mathrm{e}^{\lambda_4 t}) \\ W_{eq}(-)(1 - \mathrm{e}^{\lambda_4 t}) \end{pmatrix}. \tag{9.25}$$

9.1.2 Slow Solvent Fluctuations

In the opposite limit we expand the square root for small k^{-1} to find

$$\lambda_{3,4} = -\frac{\alpha + \beta}{2} - \frac{k}{2} \pm \frac{1}{2} \left(k + (\alpha - \beta) + 2\alpha\beta k^{-1} + \cdots \right) \tag{9.26}$$

$$\lambda_3 = -\beta + \frac{\alpha\beta}{k} + \cdots \tag{9.27}$$

$$\mathbf{R}_3 = \begin{pmatrix} 0 \\ 1 \\ 0 \\ -1 \end{pmatrix} \quad \mathbf{L}_3 = \begin{pmatrix} \alpha & k & 0 & 0 \end{pmatrix} \tag{9.28}$$

$$\lambda_4 = -k - \alpha + \cdots \tag{9.29}$$

$$\mathbf{R}_4 = \begin{pmatrix} k \\ -\alpha \\ -k \\ \alpha \end{pmatrix} \quad \mathbf{L}_4 = \begin{pmatrix} 1 & 0 & 0 & 0 \end{pmatrix} \tag{9.30}$$

and the time evolution is approximately

$$W(t) = \begin{pmatrix} \frac{\beta}{\alpha+\beta} e^{-kt} \\ \frac{\alpha}{\alpha+\beta}(e^{-\beta t} - \frac{\beta}{k} e^{-kt}) \\ \frac{\beta}{\alpha+\beta}(1 - e^{-kt}) \\ \frac{\alpha}{\alpha+\beta}(1 - e^{-\beta t} + \frac{\beta}{k} e^{-kt}) \end{pmatrix}. \tag{9.31}$$

This corresponds to an inhomogeneous situation. One part of the ensemble is in a favorable environment and decays with the fast rate k. The rest has to wait for a suitable fluctuation which appears with a rate of β.

9.1.3 Numerical Example

Figure 9.3 shows the transition from fast to slow solvent fluctuations.

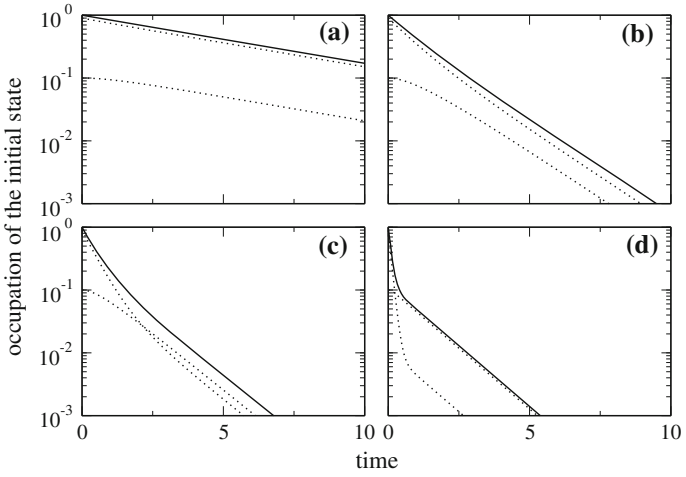

Fig. 9.3 Nonexponential decay. Numerical solutions of (9.12) are shown for $\alpha = 0.1$, $\beta = 0.9$, (**a**) $k = 0.2$, (**b**) $k = 2$, (**c**) $k = 5$, (**d**) $k = 10$. *Dotted curves* show the two components of the initial state, *solid curves* show the total occupation of the initial state

9.2 Continuous Time Random Walk Processes

Diffusive motion can be modeled by random walk processes along a one dimensional coordinate.

9.2.1 Formulation of the Model

The fluctuations of the coordinate X(t) are described as random jumps [33, 34]. The time intervals between the jumps (waiting time) and the coordinate changes are random variables with independent distribution functions

$$\psi(t_{n+1} - t_n) \quad \text{and} \quad f(X_{n+1}, X_n). \tag{9.32}$$

The probability that no jump happened in the interval $0 \cdots t$ is given by the survival function

$$\Psi_0(t) = 1 - \int_0^t \psi(t')\mathrm{d}t' = \int_t^\infty \psi(t')\mathrm{d}t' \tag{9.33}$$

and the probability of finding the walker at position X at time t is given by (Fig. 9.4)

$$P(X,t) = P(X,0)\int_t^\infty \psi(t')dt' + \int_0^t dt' \int_{-\infty}^\infty dX'\psi(t-t')f(X,X')P(X',t'). \tag{9.34}$$

Two limiting cases are well known from the theory of collisions. The correlated process with

$$f(X,X') = f(X - X') \tag{9.35}$$

corresponds to weak collisions. It includes normal diffusion processes as a special case. For instance if we chose

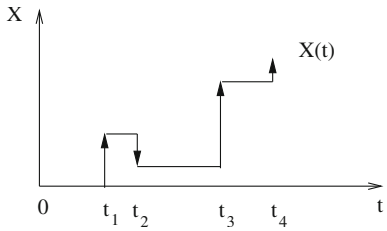

Fig. 9.4 Continuous time random walk

$$\psi(t_{n+1} - t_n) = \delta(t_{n+1} - t_n - \Delta t) \tag{9.36}$$

and

$$f(X - X') = p\delta(X - X' - \Delta X) + (1 - p)\delta(X - X' + \Delta X) \tag{9.37}$$

we have

$$P(X, t + \Delta t) = pP(X - \Delta X, t) + qP(X + \Delta X, t), \quad p + q = 1 \tag{9.38}$$

and in the limit $\Delta t \to 0$, $\Delta X \to 0$ Taylor expansion gives

$$P(X, t) + \frac{\partial P}{\partial t}\Delta t + \cdots = P(X, t) + \frac{\partial P}{\partial X}(q - p)\Delta X + \frac{\partial^2 P}{\partial X^2}\Delta X^2 + \cdots \tag{9.39}$$

The leading terms constitute a diffusion equation

$$\frac{\partial P}{\partial t}P = (q - p)\frac{\Delta X}{\Delta t}\frac{\partial P}{\partial X} + \frac{\Delta X^2}{\Delta t}\frac{\partial^2 P}{\partial X^2} \tag{9.40}$$

with drift velocity $(q - p)\frac{\Delta X}{\Delta t}$ and diffusion constant $\frac{\Delta X^2}{\Delta t}$.

The uncorrelated process, on the other hand with

$$f(X, X') = f(X) \tag{9.41}$$

corresponds to strong collisions. This kind of process can be analyzed analytically and will be applied in the following.

The (normalized) stationary distribution Φ_{eq} of the uncorrelated process obeys

$$\begin{aligned}\Phi_{eq}(X) &= \Phi_{eq}(X)\int_t^\infty \psi(t')dt' + f(X)\int_0^t dt'\psi(t - t')\int_{-\infty}^\infty dX'\phi_{eq}(X') \\ &= \Phi_{eq}(X)\int_t^\infty \psi(t')dt' + f(X)\int_0^t dt'\psi(t')\end{aligned} \tag{9.42}$$

which shows that

$$f(X) = \Phi_{eq}(X). \tag{9.43}$$

9.2.2 Exponential Waiting Time Distribution

Consider an exponential distribution of waiting times

$$\psi(t) = \tau^{-1}\mathrm{e}^{-t/\tau} \quad \Psi_0(t) = \int_t^\infty \tau^{-1}\mathrm{e}^{-t'/\tau}dt' = \mathrm{e}^{-t/\tau}. \tag{9.44}$$

It can be obtained from a Poisson process which corresponds to the master equation

$$\frac{\mathrm{d}P_n}{\mathrm{d}t} = -\tau^{-1}P_n + \tau^{-1}P_{n-1} \quad n = 0, 1, 2\ldots \tag{9.45}$$

with the solution

$$P_n(0) = \delta_{n,0}, \quad P_n(t) = \frac{(t/\tau)^n}{n!}\mathrm{e}^{-t/\tau} \tag{9.46}$$

if we identify the survival function with the probability to be in the initial state P_0

$$\Psi(t) = P_0(t) = \mathrm{e}^{-t/\tau}. \tag{9.47}$$

The general uncorrelated process (9.34) becomes for an exponential distribution

$$P(X,t) = P(X,0)\mathrm{e}^{-t/\tau} + \int_0^t dt'\tau^{-1}\mathrm{e}^{-(t-t')/\tau}\int dX' f(X,X')P(X',t'). \tag{9.48}$$

Laplace transformation gives

$$\tilde{P}(X,s) = P(X,0)\frac{1}{s+\tau^{-1}} + \frac{\tau^{-1}}{s+\tau^{-1}}\int dX' f(X,X')\tilde{P}(X',s) \tag{9.49}$$

which can be simplified

$$\left(s+\tau^{-1}\right)\tilde{P}(X,s) = P(X,0) + \tau^{-1}\int dX' f(X,X')\tilde{P}(X',s). \tag{9.50}$$

Back transformation gives

$$\left(\frac{\mathrm{d}}{\mathrm{d}t} + \tau^{-1}\right)P(X,t) = \tau^{-1}\int dX' f(X,X')P(X',t) \tag{9.51}$$

and finally

$$\frac{\partial}{\partial t}P(X,t) = -\frac{1}{\tau}P(X,t) + \frac{1}{\tau}\int dX' f(X,X')P(X',t) \tag{9.52}$$

which is obviously a Markovian process, since it involves only the time t. For the special case of an uncorrelated process with exponential waiting time distribution, the motion can be described by

$$\frac{\partial}{\partial t}P(X,t) = \mathcal{L}P(X,t) \tag{9.53}$$

$$\mathcal{L}P(X,t) = -\frac{1}{\tau}\left(P(X,t) - \phi_{eq}(X) < P(t) >\right). \tag{9.54}$$

9.2.3 Coupled Equations

Coupling of motion along the coordinate X with the reactions gives the following system of equations [35, 36]

$$\begin{aligned}\frac{\partial}{\partial t}P(X,t) &= \left(-k(X) + \mathcal{L}_1 - \tau_1^{-1}\right)P(X,t) + k_{-1}(X)C(X,t)\\ \frac{\partial}{\partial t}C(X,t) &= \left(-k_{-1}(X) + \mathcal{L}_2 - \tau_2^{-1}\right)C(X,t) + k(X)P(X,t)\end{aligned} \tag{9.55}$$

where $P(X,t)\Delta X$ and $C(X,t)\Delta X$ are the probabilities of finding the system in the electronic state D^* or D^+A^-, respectively, $\mathcal{L}_{1,2}$ are operators describing the motion in the two states and the rates $\tau_{1,2}^{-1}$ account for depopulation via additional channels. For the uncorrelated Markovian process (9.54) the rate equations take the form

$$\frac{\partial}{\partial t}\begin{pmatrix}P(X,t)\\ C(X,t)\end{pmatrix} = -\begin{pmatrix}k(X) + \tau_1^{-1} + \tau^{-1} & -k_{-1}(X)\\ -k(X) & k_{-1}(X) + \tau_2^{-1} + \tau^{-1}\end{pmatrix}\begin{pmatrix}P(X,t)\\ C(X,t)\end{pmatrix}$$

$$+\tau^{-1}\begin{pmatrix}\phi_1(X) & \\ & \phi_2(X)\end{pmatrix}\begin{pmatrix}< P(t) >\\ < C(t) >\end{pmatrix} \tag{9.56}$$

which can be written in matrix notation as

$$\frac{\partial}{\partial t}\mathbf{R}(X,t) = -A(X)\mathbf{R}(X,t) + \tau^{-1}B(X) < \mathbf{R}(t) > . \tag{9.57}$$

Substitution

$$\mathbf{R}(X,t) = \exp\{-A(X)\mathbf{U}(X,t)\} \tag{9.58}$$

gives

$$-A(X)\mathbf{R}(X,t) + \exp\left\{-A(X)\frac{\partial}{\partial t}\mathbf{U}(X,t)\right\}$$

$$= -A(X)\mathbf{R}(X,t) + \tau^{-1}B(X) < \mathbf{R}(t) > \tag{9.59}$$

$$\frac{\partial}{\partial t}\mathbf{U}(X,t) = \tau^{-1}\exp\{A(X)t\}\,B(X) < \mathbf{R}(t) > . \tag{9.60}$$

Integration gives

$$\mathbf{U}(X,t) = \mathbf{U}(X,0) + \tau^{-1}\int_0^t \exp\left\{A(X)t'\right\} B(X) < \mathbf{R}(t') > dt' \tag{9.61}$$

$$\mathbf{R}(X,t) = \exp(-A(X)t)\mathbf{R}(X,0) + \tau^{-1}\int_0^t \exp(A(X)(t'-t))B(X) < \mathbf{R}(t') > dt' \tag{9.62}$$

and the total populations obey the integral equation

$$< \mathbf{R}(t) > = < \exp(-At)\mathbf{R}(0) > + \tau^{-1}\int_0^t < \exp(A(t'-t))B >< \mathbf{R}(t') > dt' \tag{9.63}$$

which can be solved with the help of a Laplace transformation

$$\tilde{\mathbf{R}}(s) = \int_0^\infty \mathrm{e}^{-st} < \mathbf{R}(t) > dt \tag{9.64}$$

$$\int_0^\infty \mathrm{e}^{-st}\exp(-At)dt = (s+A)^{-1} \tag{9.65}$$

$$\int_0^\infty \mathrm{e}^{-st}\mathrm{d}t \int_0^t < \exp(A(t'-t))B >< \mathbf{R}(t') > dt' = < (s+A)^{-1}B > \tilde{\mathbf{R}}(s). \tag{9.66}$$

The Laplace transformed integral equation

$$\tilde{\mathbf{R}}(s) = < (s+A)^{-1}\mathbf{R}(0) > + \tau^{-1} < (s+A)^{-1}B > \tilde{\mathbf{R}}(s) \tag{9.67}$$

is solved by

$$\tilde{\mathbf{R}}(s) = \left[1 - \tau^{-1} < (s+A)^{-1}B >\right]^{-1} < (s+A)^{-1}\mathbf{R}(0) > . \tag{9.68}$$

We assume that initially the system is in the initial state D* and the motion is equilibrated

$$\mathbf{R}(X,0) = \begin{pmatrix} \phi_1(X) \\ 0 \end{pmatrix}. \tag{9.69}$$

For simplicity, we treat here only the case of $\tau_{12} \to \infty$. Then we have

$$A = \begin{pmatrix} k + \tau^{-1} & -k_{-1} \\ -k & k_{-1} + \tau^{-1} \end{pmatrix} \tag{9.70}$$

$$(s + A)^{-1} = \frac{1}{(s + \tau^{-1})(s + \tau^{-1} + k + k_{-1})} \begin{pmatrix} s + \tau^{-1} + k_{-1} & k_{-1} \\ k & s + \tau^{-1} + k \end{pmatrix} \tag{9.71}$$

and with the abbreviations

$$\alpha = \left(1 + \frac{1}{s + \tau^{-1}}(k + k_{-1})\right)^{-1} \tag{9.72}$$

and

$$< f(X) >_{1,2} = \int \phi_{1,2}(X) f(X) dX \tag{9.73}$$

we find

$$\begin{aligned} &< (s + A)^{-1} \mathbf{R}(0) > \\ &= \left\langle \frac{\phi_1 \alpha}{(s + \tau^{-1})^2} \begin{pmatrix} \alpha^{-1}(s + \tau^{-1}) - k \\ k \end{pmatrix} \right\rangle = \begin{pmatrix} \dfrac{1}{s + \tau^{-1}} - \dfrac{1}{(s + \tau^{-1})^2} < \alpha k >_1 \\ \dfrac{1}{(s + \tau^{-1})^2} < \alpha k >_1 \end{pmatrix} \end{aligned} \tag{9.74}$$

as well as

$$\begin{aligned} &< (s + A)^{-1} B > \\ &= \begin{pmatrix} \dfrac{1}{s + \tau^{-1}} - \dfrac{1}{(s + \tau^{-1})^2} < \alpha k >_1 & \dfrac{1}{(s + \tau^{-1})^2} < \alpha k_{-1} >_2 \\ \dfrac{1}{(s + \tau^{-1})^2} < \alpha k >_1 & \dfrac{1}{s + \tau^{-1}} - \dfrac{1}{(s + \tau^{-1})^2} < \alpha k_{-1} >_2 \end{pmatrix} \end{aligned} \tag{9.75}$$

and the final result becomes

$$\begin{aligned} \tilde{\mathbf{R}}(s) = &\frac{1}{s(s^2 + \tau^{-1}(s + < \alpha k >_1 + < \alpha k_{-1} >_2))} \\ &\times \begin{pmatrix} s(s + \tau^{-1}) - s < \alpha k >_1 + \tau^{-1} < \alpha k_{-1} >_2 \\ (s + \tau^{-1}) < \alpha k >_1 \end{pmatrix}. \end{aligned} \tag{9.76}$$

Let us discuss the special case of thermally activated electron transfer. Here

$$< \alpha k >_1, < \alpha k_{-1} >_2 \ll 1 \tag{9.77}$$

and the decay of the initial state is approximately given by

$$P(s) = \frac{(s+\tau^{-1}) + \tau^{-1}s^{-1} < \alpha k_{-1} >_2}{(s^2 + \tau^{-1}s^{-1}(1 + < \alpha k >_1 + < \alpha k_{-1} >_2)} = \frac{s + K_2}{s^2 + s(K_1 + K_2)} \tag{9.78}$$

with

$$K_2 = \tau^{-1}\left(1 + s^{-1}\int dX \phi_2(X) \frac{k_{-1}(X)}{1 + \frac{1}{s+\tau^{-1}}(k(X) + k_{-1}(X))}\right) \tag{9.79}$$

$$\approx \int dX \phi_2(X) \frac{k_{-1}(X)}{1 + \tau(k(X) + k_{-1}(X)} \tag{9.80}$$

$$K_1 = \int dX \phi_1(X) \frac{k(X)}{1 + \tau(k(X) + k_{-1}(X))}. \tag{9.81}$$

This can be visualized as the result of a simplified kinetic scheme

$$\frac{d}{dt} < P > = -K_1 < P > + K_2 < C > \tag{9.82}$$

$$\frac{d}{dt} < C > = K_1 < P > - K_2 < C > \tag{9.83}$$

with the Laplace transform

$$s\tilde{P} - P(0) = -K_1\tilde{P} + K_2\tilde{C} \tag{9.84}$$

$$s\tilde{C} - C(0) = K_1\tilde{P} + K_2\tilde{C} \tag{9.85}$$

which has the solution

$$P = \frac{sP_0 + K_2(P_0 + C_0)}{s(s + K_1 + K_2)} \quad C = \frac{sC_0 + K_1(C_0 + P_0)}{s(s + K_1 + K_2)}. \tag{9.86}$$

In the time domain we find

$$P(t) = \frac{K_2 + K_1 e^{-(K_1+K_2)t}}{K_1 + K_2} \quad C(t) = \frac{K_1}{K_1 + K_2}\left(1 - e^{-(K_1+K_2)t}\right). \tag{9.87}$$

Let us now consider the special case that the back reaction is negligible and $k(X) = k\Theta(X)$ (Fig. 9.5). Here, we have

$$\tilde{P}(s) = \frac{s(s + \tau^{-1}) - s < \alpha k >_1}{s(s^2 + \tau^{-1}(s + < \alpha k >_1))} \tag{9.88}$$

Fig. 9.5 Slow solvent limit

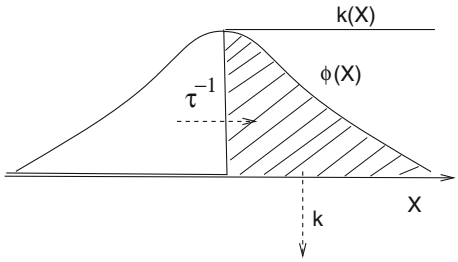

$$< \alpha k >_1 = \int dX \phi_1(X) \frac{k(X)}{1 + \frac{k(X)}{s+\tau^{-1}}} = \int_0^\infty \phi_1(X) \frac{k}{1 + \frac{k}{s+\tau^{-1}}} dX$$

$$= bk \frac{s + \tau^{-1}}{k + s + \tau^{-1}} \quad b = \int_0^\infty \phi_1(X) dX \quad a = 1 - b = \int_{-\infty}^0 \phi_1(X) dX \tag{9.89}$$

$$\tilde{P}(s) = \frac{\left(s + \tau^{-1} - bk \frac{s + \tau^{-1}}{k + s + \tau^{-1}}\right)}{\left(s^2 + \tau^{-1}(s + bk \frac{s + \tau^{-1}}{k + s + \tau^{-1}})\right)} = \frac{s + \tau^{-1} + k(1 - b)}{s^2 + s(\tau^{-1} + k) + bk\tau^{-1}}. \tag{9.90}$$

Inverse Laplace transformation gives a biexponential behaviour

$$P(t) = \frac{(\mu_+ + k(1-2b))\mathrm{e}^{-t(k+\mu_-)/2} - (\mu_- + k(1-2b))\mathrm{e}^{-t(k+\mu_+)/2}}{\mu_+ - \mu_-} \tag{9.91}$$

with

$$\mu_\pm = \tau^{-1} \pm \sqrt{k^2 + \tau^{-2} + 2k\tau^{-1}(1-2b)}. \tag{9.92}$$

If the fluctuations are slow $\tau^{-1} \ll k$ then

$$\sqrt{k^2 + \tau^{-2} + 2k\tau^{-1}(1-2b)} = k + (1-2b)\tau^{-1} + \cdots \tag{9.93}$$

$$\mu_+ = k + 2(1-b)\tau^{-1} + \cdots \quad \mu_- = -k + 2b\tau^{-1} + \cdots \tag{9.94}$$

and the two time constants are approximately

$$\frac{k + \mu_+}{2} = k + \cdots \quad \frac{k + \mu_-}{2} = b\tau^{-1} + \cdots \tag{9.95}$$

9.3 Powertime Law Kinetics

The last example can be generalized to describe the powertime law as observed for CO rebinding in myoglobin at low temperatures. The protein motion is now modeled by a more general uncorrelated process.[2]

We assume that the rate k is negligible for $X < 0$ and very large for $X > 0$. Consequently only jumps $X < 0 \to X > 0$ are considered. Then the probability obeys the equation

$$\begin{aligned} P(X,t)_{|X<0} &= P(X,0)\int_t^\infty \psi(t')dt' + \int_{-\infty}^0 dX' \int_0^t dt'\psi(t-t')f(X)P(X',t') \\ &= \phi_{eq}(X)\Psi_0(t) + \phi_{eq}(X)\int_0^t dt'\psi(t-t')\int_{-\infty}^0 dX' P(X',t') \end{aligned} \tag{9.96}$$

$$\Psi_0(t) = \int_t^\infty \psi(t')dt' \quad \tilde{\Psi}_0(s) = \frac{1-\tilde{\psi}(s)}{s} \tag{9.97}$$

and the total occupation of inactive configurations is

$$\begin{aligned} P_<(t) &= \int_{-\infty}^0 dX\phi_{eq}(X)\left(\Psi_0(t) + \int_0^t dt'\psi(t-t')P_<(t')\right) \\ &= a\left(\Psi_0(t) + \int_0^t dt'\psi(t-t')P_<(t')\right). \end{aligned} \tag{9.98}$$

Laplace transformation gives

$$\tilde{P}_<(s) = a\left(\tilde{\Psi}_0(s) + \tilde{\psi}(s)\tilde{P}_<(s)\right) \tag{9.99}$$

with

$$a = \int_{-\infty 0}^0 dX\phi_{eq}(X) \tag{9.100}$$

and the decay of the initial state is given by

$$\tilde{P}_<(s) = \frac{a\tilde{\Psi}_0(s)}{1-a\tilde{\psi}(s)} = \frac{1}{s+\frac{1-a}{a\tilde{\Psi_0}(s)}}. \tag{9.101}$$

[2] A much more detailed discussion is given in: [36].

For a simple Poisson process (9.44) with

$$\tilde{\Psi}_0 = \frac{1}{s + \tau^{-1}} \tag{9.102}$$

this gives

$$\tilde{P}_<(s) = \frac{a}{s + (1-a)\tau^{-1}} \tag{9.103}$$

which reproduces the exponential decay found earlier in the slow solvent limit (9.95)

$$P_<(t) = a\mathrm{e}^{-t\,(1-a)/\tau}. \tag{9.104}$$

The long time behaviour is given by the asymptotic behavior for $s \to 0$. As $P_<(t) \to 0$ for $t \to \infty$ this is also the case for $\tilde{P}_<(s)$ in the limit $s \to 0$. Hence the asymptotic behaviour must be

$$\tilde{P}_<(s) \approx \frac{a\tilde{\Psi_0}(s)}{1-a} \to 0 \quad s \to 0 \tag{9.105}$$

$$P_<(t) \to \frac{a}{1-a}\Psi_0(t) \quad t \to \infty. \tag{9.106}$$

In order to describe a powertime law at long times

$$P_<(t) \to t^{-\beta} \quad t \to \infty \tag{9.107}$$

$$\tilde{P}_<(s) \to s^{\beta-1} \quad s \to 0 \tag{9.108}$$

the waiting time distribution has to be chosen as

$$\Psi_0(t) \sim \frac{1}{(zt)^\beta} \quad t \to \infty. \tag{9.109}$$

which implies

$$\tilde{\Psi}_0(s) \sim z^{-\beta}s^{\beta-1} \tag{9.110}$$

where z^{-1} is the characteristic time for reaching the asymptotics. Finally, we find

$$\tilde{P}_<(s) \sim \frac{1}{s + \frac{1-a}{a}z^\beta s^{1-\beta}} = \frac{1}{s(1 + (\tilde{z}/s)^\beta)}. \tag{9.111}$$

In the time domain this corresponds to the Mittag–Leffler function[3]

$$P_<(t) = \sum_{l=0}^{\infty} \frac{(-1)^l (\tilde{z}t)^{\beta l}}{\Gamma(\beta l + 1)} = E_\beta(-(\tilde{z}t)^\beta) \tag{9.112}$$

which can be approximated by the simpler function

$$\frac{1}{1 + (t/\tau)^\beta}. \tag{9.113}$$

Problems

9.1 Dichotomous Model for Dispersive Kinetics

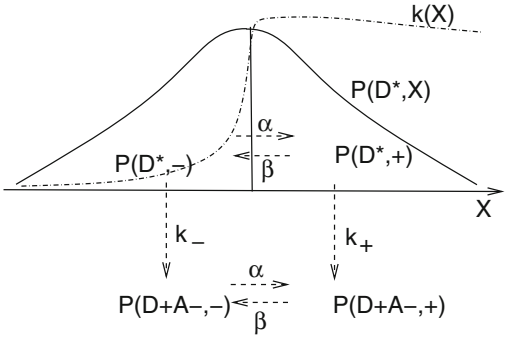

Consider the following system of rate equations

$$\frac{d}{dt}\begin{pmatrix} P(D*,+) \\ P(D*,-) \\ P(D+A-,+) \\ P(D+A-,-) \end{pmatrix} = \begin{pmatrix} -k_+ - \alpha & \beta & 0 & 0 \\ \alpha & -k_- - \beta & 0 & 0 \\ k_+ & 0 & -\alpha & \beta \\ 0 & k_- & \alpha & -\beta \end{pmatrix} \begin{pmatrix} P(D*,+) \\ P(D*,-) \\ P(D+A-,+) \\ P(D+A-,-) \end{pmatrix}$$

Determine the eigenvalues of the rate matrix M. Calculate the left- and right eigenvectors approximately for the two limiting cases:

(a) fast fluctuations $k_\pm \ll \alpha, \beta$. Show that the initial state decays with an average rate.
(b) slow fluctuations $k_\pm \gg \alpha, \beta$. Show that the decay is nonexponential.

[3] Which has also been discussed for nonexponential relaxation in inelastic solids and dipole relaxation processes corresponding to Cole-Cole spectra.

Part IV
Transport Processes

Chapter 10
Non-equilibrium Thermodynamics

Biological systems are far from thermodynamic equilibrium. Concentration gradients and electrostatic potential differences are the driving forces for diffusive currents and chemical reactions (Fig. 10.1).

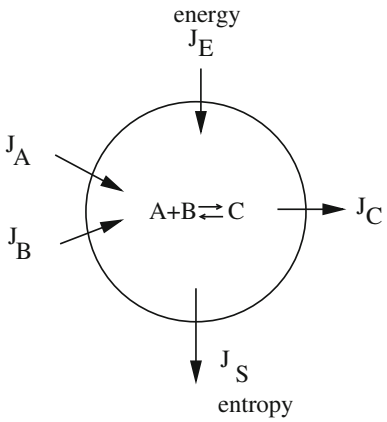

Fig. 10.1 Nonequilibrium processes

In this chapter, we present the basic ingredients of nonequilibrium thermodynamics. We derive continuity equations for mass and energy. Entropy production is a bilinear function of the thermodynamic forces which vanish at equilibrium. Close to equilibrium, the fluxes can be approximated as linear functions of the forces and the entropy production as a positive definite symmetric quadratic form. Finally, we discuss stationary states which are characterized by a minimum of entropy production, which is compatible with certain external conditions.

P.O.J. Scherer and S.F. Fischer, *Theoretical Molecular Biophysics*,
Biological and Medical Physics, Biomedical Engineering,
DOI 10.1007/978-3-662-55671-9_10

10.1 Continuity Equation for the Mass Density

We consider a system composed of n different species labeled by $k = 1 \ldots n$ which can undergo a number of r chemical reactions labeled by $j = 1 \ldots r$. We assume that the system is locally in equilibrium and that all thermodynamic quantities are locally well defined.

We introduce the partial mass densities

$$\varrho_k = \frac{m_k}{V} N_k = c_k m_k \tag{10.1}$$

the total density

$$\varrho = \sum_k \varrho_k = \frac{1}{V} \sum_k m_k N_k = \frac{M}{V} \tag{10.2}$$

and the mass fraction

$$x_k = \frac{m_k}{M} N_k = \frac{m_k N_k}{\sum_k m_k N_k} = \frac{\varrho_k}{\varrho} \,. \tag{10.3}$$

From the conservation of mass we have

$$\frac{d}{dt} M_k = m_k \frac{d}{dt} N_k = \int_V \frac{\partial}{\partial t} \varrho_k dV = -\int_{\partial V} \varrho_k \mathbf{v}_k d\mathbf{A} + \sum_{j=1}^{r} \int_V m_k \nu_{kj} r_j dV \tag{10.4}$$

which can also be expressed in the form of a continuity equation

$$\begin{aligned} \frac{\partial}{\partial t} \varrho_k &= -\mathrm{div}(\varrho_k \mathbf{v}_k) + \sum_{j=1}^{r} m_k \nu_{kj} r_j \\ &= -\mathrm{div}(m_k \mathbf{J}_k) + \sum_{j=1}^{r} m_k \nu_{kj} r_j \end{aligned} \tag{10.5}$$

with the diffusion fluxes $\mathbf{J}_k$. For the total mass density

$$\varrho = \sum_k \varrho_k \tag{10.6}$$

we have

$$\frac{\partial}{\partial t} \varrho = -\mathrm{div}\left(\sum_k \varrho_k \mathbf{v}_k \right) + \sum_k \sum_{j=1}^{r} m_k \nu_{kj} r_j \,. \tag{10.7}$$

Due to conservation of mass for each reaction, the last term vanishes

$$\sum_k m_k \nu_{kj} = 0 \tag{10.8}$$

and with the center of mass velocity

$$\mathbf{v} = \frac{1}{\varrho} \sum_k \varrho_k \mathbf{v}_k \tag{10.9}$$

we have

$$\frac{\partial}{\partial t} \varrho = -\mathrm{div}(\varrho \mathbf{v}). \tag{10.10}$$

10.2 Energy Conservation

We define the specific values of enthalpy, entropy and volume h, s, ϱ^{-1} by

$$\begin{aligned} H &= h\, \varrho\, V \\ S &= s\, \varrho\, V \\ V &= \varrho^{-1}\, \varrho\, V. \end{aligned} \tag{10.11}$$

The differential of the enthalpy is

$$\mathrm{d}H = T\mathrm{d}S + V\mathrm{d}p + \sum_k \mu_k \mathrm{d}N_k \tag{10.12}$$

where μ_k is a generalized chemical potential, which also includes the potential energy of electrostatic or gravitational fields which are assumed to be time-independent. For the specific quantities we find

$$\begin{aligned} V(h\mathrm{d}\varrho + \varrho \mathrm{d}h) = {} & TV(s\mathrm{d}\varrho + \varrho \mathrm{d}s) + V\mathrm{d}p \\ & + \sum_k \mu_k \frac{V}{m_k}(x_k \mathrm{d}\varrho + \varrho \mathrm{d}x_k) \end{aligned} \tag{10.13}$$

and if we combine all terms with $\mathrm{d}\varrho$

$$\varrho \mathrm{d}h - T\varrho \mathrm{d}s - \mathrm{d}p - \sum_k \frac{\mu_k}{m_k} \varrho \mathrm{d}x_k = \left(Ts + \sum_k \mu_k \frac{x_k}{m_k} - h \right) \mathrm{d}\varrho. \tag{10.14}$$

The right-hand side can be written as

$$\frac{1}{\varrho V}\left(TS+\sum_k \mu_k N_k - H\right)\mathrm{d}\varrho \tag{10.15}$$

which vanishes in equilibrium. Hence we have for the specific quantities

$$\mathrm{d}h = T\,\mathrm{d}s + \varrho^{-1}\mathrm{d}p + \sum_k \mu_k \frac{1}{m_k}\mathrm{d}x_k. \tag{10.16}$$

In the following, we consider a resting solvent without convection. We neglect the center of mass motion and its contribution to the total energy. The diffusion currents are taken relative to the solvent.[1] For constant pressure we have

$$\frac{\partial(\varrho h)}{\partial t} = T\frac{\partial(\varrho s)}{\partial t} + \sum_k \frac{\mu_k}{m_k}\frac{\partial \varrho_k}{\partial t} \tag{10.17}$$

and the enthalpy obeys the continuity equation

$$\frac{\partial(\varrho h)}{\partial t} = -\mathrm{div}(\mathbf{J}_h) \tag{10.18}$$

with the enthalpy flux $\mathbf{J}_h$.

10.3 Entropy Production

The entropy change

$$\mathrm{d}S = \mathrm{d}\left(\int_V \varrho s dV\right) \tag{10.19}$$

has contributions from the local entropy production dS_i and from exchange with the surroundings dS_e

$$dS = dS_i + dS_e. \tag{10.20}$$

The local entropy production can only be positive,

$$dS_i \geq 0 \tag{10.21}$$

whereas entropy exchange with the surroundings can be positive or negative (Fig. 10.2).

[1] A more general discussion can be found in [37].

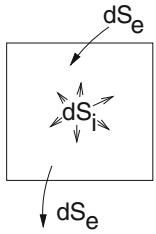

Fig. 10.2 Local entropy change

We denote by σ the entropy production per volume

$$\frac{\mathrm{d}S_i}{\mathrm{d}t} = \int_V \sigma \, dV \tag{10.22}$$

The entropy exchange is connected with the total entropy flux

$$\frac{\mathrm{d}S_e}{\mathrm{d}t} = -\int_{\partial V} \mathbf{J}_s d\mathbf{A}. \tag{10.23}$$

Together we have

$$\frac{\partial(\varrho s)}{\partial t} = -\mathrm{div}(\mathbf{J}_s) + \sigma \tag{10.24}$$

with

$$\sigma \geq 0. \tag{10.25}$$

From (10.17) the time derivative of the entropy per volume is

$$\frac{\partial(\varrho s)}{\partial t} = \frac{1}{T}\frac{\partial(\varrho h)}{\partial t} - \frac{1}{T}\sum_k \frac{\mu_k}{m_k}\frac{\partial \varrho_k}{\partial t} \tag{10.26}$$

and inserting ((10.5), (10.26))

$$\frac{\partial(\varrho s)}{\partial t} = -\frac{1}{T}\mathrm{div}(\mathbf{J}_h) - \frac{1}{T}\sum_k \frac{\mu_k}{m_k}\left(-\mathrm{div}(m_k\mathbf{J}_k) + \sum_{j=1}^{r} m_k \nu_{kj} r_j\right) \tag{10.27}$$

which can be written as

$$\begin{aligned}\frac{\partial(\varrho s)}{\partial t} = &-\mathrm{div}\left(\frac{1}{T}\mathbf{J}_h + \sum_k \frac{\mu_k}{T}\mathbf{J}_k\right) \\ &+ \mathbf{J}_h \mathrm{grad}\left(\frac{1}{T}\right) - \sum_k \mathbf{J}_k \mathrm{grad}\left(\frac{\mu_k}{T}\right) + \frac{1}{T}\sum_j A_j r_j\end{aligned} \tag{10.28}$$

with the chemical affinities

$$A_j = -\sum_k \mu_k \nu_{kj}. \tag{10.29}$$

From comparison of (10.28) and (10.24) we find the entropy flux

$$\mathbf{J}_s = \frac{1}{T}\left(\mathbf{J}_h - \sum_k \mu_k \mathbf{J}_k\right) \tag{10.30}$$

and the entropy production

$$\begin{aligned}\sigma &= \mathbf{J}_h \text{grad}\left(\frac{1}{T}\right) - \sum_k \mathbf{J}_k \text{grad}\left(\frac{\mu_k}{T}\right) + \frac{1}{T}\sum_j A_j r_j \\ &= \left(\mathbf{J}_h - \sum_k \mu_k \mathbf{J}_k\right)\text{grad}\left(\frac{1}{T}\right) - \sum_k \frac{1}{T}\mathbf{J}_k \text{grad}\,(\mu_k) + \frac{1}{T}\sum_j A_j r_j. \end{aligned} \tag{10.31}$$

We define the heat flux as[2]

$$\mathbf{J}_q = T\mathbf{J}_s. \tag{10.32}$$

The entropy production is a bilinear form

$$\sigma = \mathbf{K_q}\mathbf{J}_q + \sum_k \mathbf{K}_k \mathbf{J}_k + \sum_j K_j r_j \tag{10.33}$$

of the fluxes

$$\mathbf{J}_q, \mathbf{J}_k, r_j \tag{10.34}$$

and the thermodynamic forces

$$\begin{aligned}\mathbf{K}_q &= \text{grad}\left(\frac{1}{T}\right) \\ \mathbf{K}_k &= -\frac{1}{T}\text{grad}\,(\mu_k) \\ K_j &= \frac{1}{T}A_j \end{aligned} \tag{10.35}$$

[2]The definition of the heat flux is not unique in the case of simultaneous diffusion and heat transport. Our definition is in analogy to the relation $T\,\mathrm{d}S = \mathrm{d}H - V\,\mathrm{d}p - \sum_k \mu_k \mathrm{d}N_k$ for an isobaric system. With this convention the diffusion flux does not depend on the temperature gradient explicitly.

Instead of entropy production, alternatively the rate of energy dissipation can be considered which follows from multiplication of (10.31) with T

$$T\sigma = -\frac{1}{T}\mathbf{J}_q \text{grad}\,(T) - \sum_k \mathbf{J}_k \text{grad}\,(\mu_k) + \sum_j A_j r_j. \tag{10.36}$$

10.4 Phenomenological Relations

In equilibrium all fluxes and thermodynamic forces vanish

$$T = \text{const}, \quad \mu_k = \text{const}, \quad A_j = 0. \tag{10.37}$$

The entropy production is also zero and entropy has its maximum value. If the deviation from equilibrium is small the fluxes[3] can be approximated as linear functions of the forces

$$J_\alpha = \sum_\beta L_{\alpha,\beta} K_\beta \tag{10.38}$$

where the so-called Onsager coefficients $L_{\alpha,\beta}$ are material constants.[4] As Onsager has shown, the matrix of coefficients is symmetric $L_{\alpha,\beta} = L_{\beta,\alpha}$. The entropy production has the approximate form

$$\sigma = \sum_\alpha J_\alpha K_\alpha = \sum_{\alpha,\beta} L_{\alpha,\beta} K_\alpha K_\beta. \tag{10.39}$$

According to the second law of thermodynamics $\sigma \geq 0$, and therefore the matrix of Onsager coefficients is positive definite.

10.5 Stationary States

Under certain circumstances,[5] stationary states are characterized by a minimum of entropy production, which is compatible with certain external conditions. Consider a system with n independent fluxes and thermodynamic forces. If the forces $K_1 \ldots K_m$

[3] only a set of independent fluxes should be used here.

[4] Fluxes with different tensorial character are not coupled.

[5] Especially the Onsager coefficients have to be constants.

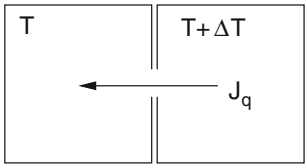

Fig. 10.3 Combined diffusion and heat transport

are kept fixed and a stationary state is reached then the fluxes corresponding to the remaining forces vanish

$$J_\alpha = 0 \quad \alpha = m+1 \ldots n \tag{10.40}$$

and the entropy production is minimal since

$$\frac{\partial \sigma}{\partial K_\alpha}_{|K_1 \ldots K_m} = J_\alpha \quad \alpha = m+1 \ldots n. \tag{10.41}$$

A simple example is the coupling of diffusion and heat transport between two reservoirs with fixed temperatures T and $T + \Delta T$ (Fig. 10.3).

In a stationary state the diffusion current must vanish $\mathbf{J}_d = 0$ since any diffusion would lead to time-dependent concentrations. The entropy production is

$$\sigma = \mathbf{J}_q \mathbf{K}_q + \mathbf{J}_d \mathbf{K}_d. \tag{10.42}$$

If the force

$$\mathbf{K}_q = \text{grad}\left(\frac{1}{T}\right) \approx -\frac{\Delta T}{T^2} \tag{10.43}$$

is fixed by keeping the temperature distribution fixed, then in the stationary state there is only transport of heat but not of mass. The entropy production is

$$\begin{aligned} \sigma &= L_{qq} K_q^2 + L_{dd} K_d^2 + 2 L_{qd} K_q K_d \\ &= \frac{L_{qq} L_{dd} - L_{qd}^2}{L_{dd}} K_q^2 + L_{dd} \left(K_d + \frac{L_{qd}}{L_{dd}} K_q \right)^2 \end{aligned} \tag{10.44}$$

where due to the positive definiteness of L_{ij}

$$L_{dd} > 0, L_{qq} > 0, L_{dd} L_{qq} - L_{qd}^2 > 0. \tag{10.45}$$

As a function of K_d the entropy production is minimal for

$$0 = K_d + \frac{L_{qd}}{L_{dd}} K_q = \frac{1}{L_{dd}} J_d \tag{10.46}$$

hence in the stationary state. Obviously, the chemical potential adjusts such that

$$K_d = -\frac{1}{T}\Delta\mu = \frac{L_{qd}}{L_{dd}}\frac{\Delta T}{T^2} \tag{10.47}$$

which leads to a concentration gradient.[6]

$$\frac{\Delta c}{c} \approx -\frac{L_{qd}}{L_{dd}}\frac{\Delta T}{k_B T^2}\,. \tag{10.48}$$

Problems

10.1 Entropy Production by Chemical Reactions

Consider an isolated homogeneous system with $T = \text{const}$ and $\mu_k = \text{const}$ but nonzero chemical affinities

$$A_j = -\sum_k \mu_k \nu_{kj}$$

and determine the rate of entropy increase.

[6] This is connected to the Seebeck effect.

Chapter 11
Simple Transport Processes

In this chapter, we discuss simple transport processes like heat transport and diffusion in an external electric field. We discuss the fluxes of mass, energy, and entropy and their dependence on the gradients of temperature, concentration, and electrostatic potential. We derive the Nernst–Planck equation for the diffusion flux and a generalized diffusion equation for the concentration.

11.1 Heat Transport

Consider a system without chemical reactions and diffusion and with constant chemical potentials.[1] The thermodynamic force is

$$\mathbf{K}_q = \text{grad}\left(\frac{1}{T}\right) \approx -\frac{1}{T^2}\,\text{grad}\,T \tag{11.1}$$

and the phenomenological relation is known as Fourier's law

$$\mathbf{J}_q = -\kappa\,\text{grad}\,T \tag{11.2}$$

The entropy flux is

$$\mathbf{J}_s = \frac{1}{T}\mathbf{J}_q = \frac{1}{T}\mathbf{J}_H \tag{11.3}$$

[1] We neglect the temperature dependence of the chemical potential here.

P.O.J. Scherer and S.F. Fischer, *Theoretical Molecular Biophysics*,
Biological and Medical Physics, Biomedical Engineering,
DOI 10.1007/978-3-662-55671-9_11

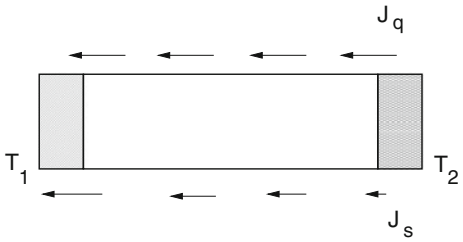

Fig. 11.1 Heat transport

and the energy dissipation is

$$T\sigma = -\frac{1}{T} J_q \text{ grad } T = \frac{\kappa}{T} (\text{grad } T)^2 . \tag{11.4}$$

From the continuity equation for the enthalpy we find

$$\frac{\partial(\varrho h)}{\partial t} = c_p \frac{\partial T}{\partial t} = \kappa \triangle T \tag{11.5}$$

and hence the diffusion equation for heat transport

$$\frac{\partial T}{\partial t} = \frac{\kappa}{c_p} \triangle T. \tag{11.6}$$

For stationary heat transport in one dimension, the temperature gradient is constant, hence also the heat flux. The entropy flux, however, is coordinate dependent due to the local entropy production (Fig. 11.1).

$$\text{div } \mathbf{J}_S = -\mathbf{J}_q \frac{1}{T^2} \text{ grad } (T) = \frac{\kappa}{T^2} (\text{grad } T)^2 = \sigma. \tag{11.7}$$

11.2 Diffusion in an External Electric Field

Consider an ionic solution at constant temperature without chemical reactions. The thermodynamic force is

$$\mathbf{K}_k = -\frac{1}{T} \text{ grad } (\mu_k). \tag{11.8}$$

For a dilute solution we have[2]

$$\mu_k = \mu_k^0 + k_B T \ln(c_k) + Z_k e \Phi \tag{11.9}$$

and hence the thermodynamic force

$$\mathbf{K}_k = -\frac{k_B}{c_k} \text{ grad } (c_k) - \frac{1}{T} \text{ grad } (Z_k e \Phi) . \tag{11.10}$$

The entropy production is given by

$$T\sigma = \sum_k \mathbf{J}_k \left(-\frac{k_B T}{c_k} \text{ grad } c_k - Z_k \, e \text{ grad } \Phi \right) . \tag{11.11}$$

The phenomenological relations have the general form

$$\mathbf{J}_k = \sum_{k'} L_{k,k'} \mathbf{K}_k \tag{11.12}$$

where the interaction mobilities $L_{k,k'}$ vanish for very small ion concentrations, whereas the direct mobilities $L_{k,k}$ are only weakly concentration dependent [38, 39]. Inserting the forces we find

$$\mathbf{J}_k = -\sum_{k'} L_{k,k'} \frac{k_B}{c_k} \text{ grad } c_{k'} - \frac{1}{T} \text{ grad } (\Phi) \sum_{k'} L_{k,k'} Z_{k'} e \tag{11.13}$$

which for small ion concentrations can be written more simply by introducing the diffusion constant as

$$\mathbf{J}_k = -D_k \text{ grad } c_k - \frac{c_k Z_k e D_k}{k_B T} \text{ grad } \Phi \tag{11.14}$$

which is known as the Nernst–Planck equation. This equation can be understood in terms of motion in a viscous medium (7.1). For the motion of a mass point we have

$$m\dot{\mathbf{v}} = \mathbf{F} - m\gamma\mathbf{v}. \tag{11.15}$$

In a stationary state the velocity is

$$\mathbf{v} = \frac{1}{m\gamma}\mathbf{F} \tag{11.16}$$

[2]The concentration (particles per volume) is $c_k = \varrho_k / m_k = \varrho x_k / m_k$.

and the particle current

$$\mathbf{J} = c\mathbf{v} = \frac{c}{m\gamma}\mathbf{F} = \frac{cD}{k_B T}\mathbf{F} \tag{11.17}$$

where we used the Einstein relation

$$D = \frac{k_B T}{m\gamma}. \tag{11.18}$$

From comparison with the Nernst–Planck equation we find

$$\mathbf{F} = -\frac{k_B T}{cD}\left(D \text{ grad } c + \frac{cZeD}{k_B T} \text{ grad } \Phi\right) = -\frac{k_B T}{c} \text{ grad}\, c - \text{grad } Ze\Phi. \tag{11.19}$$

The charge current is

$$\begin{aligned}\mathbf{J}_{el} &= Z_k e \mathbf{J}_k = -\frac{Z_k e c_k D_k}{k_B T}\left(\frac{k_B T}{c_k} \text{ grad } c_k + \text{grad} Z_k e\Phi\right) \\ &= -Z_k e D_k \text{ grad } c_k - \frac{(Z_k e)^2 c_k D_k}{k_B T} \text{ grad } \Phi.\end{aligned} \tag{11.20}$$

The prefactor of the potential gradient is connected to the electrical conductivity

$$G_k = \frac{(Z_k e)^2 c_k D_k}{k_B T}. \tag{11.21}$$

Together with the continuity equation

$$\frac{\partial c_k}{\partial t} = -\text{ div } \mathbf{J}_k \tag{11.22}$$

we arrive at a Smoluchowski type equation

$$\frac{\partial c_k}{\partial t} = \text{ div } \left(D_k \text{ grad } c_k + \frac{c_k Z_k e D}{k_B T} \text{ grad } \Phi\right). \tag{11.23}$$

In equilibrium we have

$$\mu_k = const \tag{11.24}$$

and hence

$$k_B T \ln c_k + Z_k e\Phi = const \tag{11.25}$$

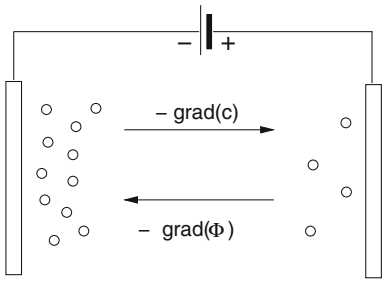

Fig. 11.2 Diffusion in an electric field

or

$$c_k = c_k^0 \mathrm{e}^{-Z_k e\Phi/k_B T}. \tag{11.26}$$

This is sometimes described as an equilibrium of the currents due to concentration gradient on the one side and to the electrical field on the other side (Fig. 11.2).

The Nernst–Planck equation has to be solved together with the Poisson–Boltzmann equation for the potential

$$\text{div}\ (\varepsilon\ \text{grad}\ \Phi) = -\sum_k Z_k e c_k$$

In one dimension the Poisson–Nernst–Planck equations are

$$J = -D\frac{\mathrm{d}c}{\mathrm{d}x} - \frac{ZecD}{k_B T}\frac{\mathrm{d}\Phi}{\mathrm{d}x} \tag{11.27}$$

$$\frac{\mathrm{d}}{\mathrm{d}x}\epsilon\frac{\mathrm{d}}{\mathrm{d}x}\Phi = -\sum_k Z_k e c_k. \tag{11.28}$$

Problems

11.1 Synthesis of ATP from ADP

In mitochondrial membranes, ATP is synthesized according to

$$\mathrm{ADP} + \mathrm{POH} + 2\mathrm{H}^+_{out} \rightleftharpoons \mathrm{ATP} + \mathrm{H_2O} + 2\mathrm{H}^+_{in}$$

where (in) and (out) refer to inside and outside of the mitochondrial membrane.

Express the equilibrium constant K as a function of the potential difference

$\Phi_{in} - \Phi_{out}$

and the proton concentration ratio

$c(H^+_{in})/c(H^+_{out})$.

Chapter 12
Ion Transport Through a Membrane

In this chapter, we study simple models related to ion transport through a membrane. We draw a close analogy to electronic circuit theory and describe the ion transport similar to a simple RC-network. We study the Goldman–Hodgkin–Katz model for a steady state with more than one ionic species present. The membrane potential is calculated as a function of the ion concentrations inside and outside the membrane. We discuss the famous Hodgkin–Huxley model for the quantitative description of the squid giant axon dynamics, which received the Nobel prize. Finally, we study models for ion channel cooperativity with a two-state model in analogy to ligand binding. We derive the master equations for ligand-gated channels within the MWC and KNF models and calculate the ratio of active channels as a function of ligand concentration to show the cooperative effect.

12.1 Diffusive Transport

We can draw a close analogy between diffusion and reaction on the one side and electronic circuit theory on the other side. We regard the membrane as a resistance for the current of diffusion and the difference in chemical potential as the driving force (Fig. 12.1):

$$\mu = \mu^0 + k_B T \ln c \tag{12.1}$$

$$c = \exp \frac{\mu - \mu^0}{k_B T}. \tag{12.2}$$

P.O.J. Scherer and S.F. Fischer, *Theoretical Molecular Biophysics*,
Biological and Medical Physics, Biomedical Engineering,
DOI 10.1007/978-3-662-55671-9_12

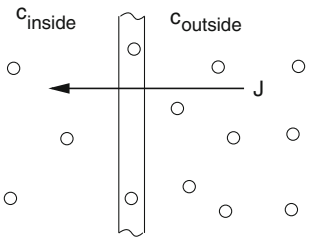

Fig. 12.1 Transport across a membrane

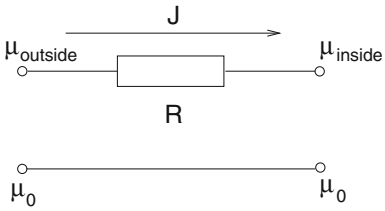

Fig. 12.2 Equivalent circuit for the diffusion through a membrane

Assuming linear variation of the chemical potential over the thickness a of the membrane we have

$$\mu(x) = \mu_{inside} + \frac{x}{a}\Delta\mu. \tag{12.3}$$

The diffusion current is

$$J = -C\frac{\partial\mu}{\partial x} = -C\frac{\Delta\mu}{a} \tag{12.4}$$

and the constant is determined from the diffusion equation in the center of the membrane

$$0 = \frac{\partial c}{\partial t} = -\frac{\partial}{\partial x}(J) = -\frac{\partial}{\partial x}(-C\frac{k_BT}{c}\frac{\partial c}{\partial x}) = \frac{\partial}{\partial x}\left(D(x)\frac{\partial}{\partial x}c\right) \rightarrow C = \frac{\overline{D}}{k_BT}\overline{c} \tag{12.5}$$

with

$$\overline{c} = \exp\frac{\mu_{inside} + \frac{\Delta\mu}{2}}{k_BT} = \exp\frac{\mu_{outside} + \mu_{inside}}{2k_BT} = \sqrt{c_{inside}c_{outside}}. \tag{12.6}$$

Finally, we have (Fig. 12.2)

$$J = -\frac{\overline{D}\overline{c}\Delta\mu}{ak_BT} = -\frac{\Delta\mu}{R}. \tag{12.7}$$

If we include a gradient of the electrostatic potential then the equations become

$$\mu = \mu^0 + k_B T \ln c + Ze\Phi \tag{12.8}$$

$$c = \exp \frac{\mu - \mu^0 - Ze\Phi}{k_B T} \tag{12.9}$$

$$J = -C\frac{\partial \mu}{\partial x} = -C\frac{\Delta \mu}{a} = -C\frac{k_B T \Delta \ln c + Ze\Delta\Phi}{a} \tag{12.10}$$

and the electric current is

$$\begin{aligned} I = ZeJ &= -\frac{(Ze)^2}{R}\left(\Delta \frac{k_B T \ln c}{Ze} + \Delta\phi\right) \\ &= -g(V_{Nernst} - V) \end{aligned} \tag{12.11}$$

with the Nernst potential

$$V_{Nernst} = \frac{k_B T}{Ze} \ln \frac{c_{outside}}{c_{inside}} \tag{12.12}$$

and the membrane potential (Fig. 12.3)

$$V = \Phi_{inside} - \Phi_{outside}. \tag{12.13}$$

The transport through biological membranes occurs often via the formation of pore–ligand complexes. The number of these complexes depends on the chemical potential of the ligands and needs time to build up. It may therefore be more realistic to associate also a capacity C_m with the membrane, which we define in analogy to the electronic capacity via the change of the potential (Fig. 12.4):

$$J_m = C_m \frac{d\mu_m}{dt}. \tag{12.14}$$

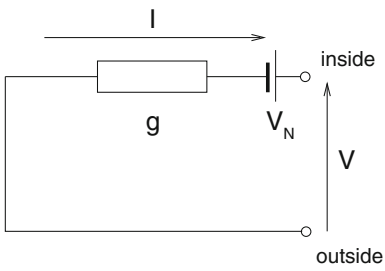

Fig. 12.3 Equivalent circuit for the electric current

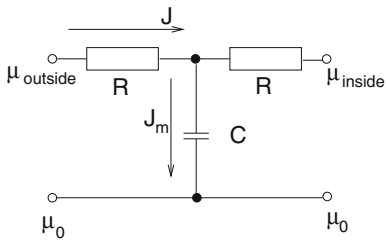

Fig. 12.4 Equivalent circuit with capacity

the change of the potential is

$$\frac{d\mu_m}{dt} = \frac{k_B T}{c}\frac{dc}{dt} \tag{12.15}$$

and the current is from the continuity equation

$$-\text{div } J = \frac{J_m}{a} = \frac{dc}{dt} \tag{12.16}$$

hence

$$C_m = \frac{ac}{k_B T}. \tag{12.17}$$

12.2 Goldman–Hodgkin–Katz Model

In the rest state of a neuron the potassium concentration is higher in the interior, whereas there are more sodium and chlorine ions outside. The concentration gradients have to be produced by (energy consuming) ion pumps.

Let us first consider only one type of ions and constant temperature. From (11.25) we have

$$\Phi + \frac{k_B T}{Z_k e} \ln c_k = \text{const}\,. \tag{12.18}$$

Usually, the potential is defined as zero on the outer side and

$$V_k = \Phi_{inside} - \Phi_{outside} = \frac{k_B T}{Z_k e} \ln \frac{c_{k,outside}}{c_{k,inside}} \tag{12.19}$$

is the Nernst potential (12.12) of the ion species k.

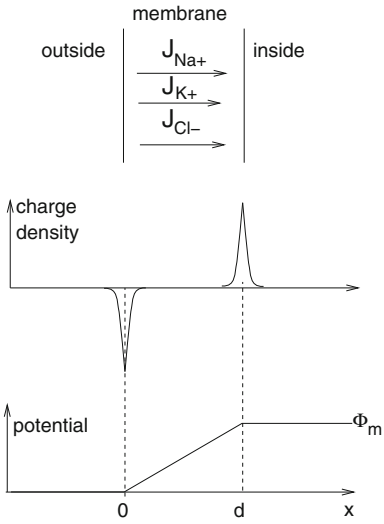

Fig. 12.5 Coupled ionic fluxes

We now want to calculate the potential for a steady state with more than one ionic species present. We take the ionic species Na^+, K^+, Cl^- which are most important in nerve excitation that will define the so-called Goldman–Hodgkin–Katz model [40] (Fig. 12.5).

We want to calculate the dependence of the fluxes J_k on the concentrations $c_{k,in}$ and $c_{k,out}$. To that end we multiply the Nernst–Planck (11.27) equation by e^{y_k} where

$$y_k = Z_k e \frac{\Phi}{k_B T} \tag{12.20}$$

to get

$$J_k e^{y_k} = -D_k e^{y_k} \left(\frac{dc_k}{dx} + c_k \frac{dy_k}{dx} \right) = -D_k \frac{d}{dx}(c_k e^{y_k}). \tag{12.21}$$

This can be integrated over the thickness d of the membrane

$$\int_0^d J_k e^{y_k} dx = -D \int_0^d \frac{d}{dx}(c_k e^{y_k}) dx = -D \left(c_{k,in} e^{Z_k e \Phi_m / k_B T} - c_{k,out} \right). \tag{12.22}$$

We assume a linear variation of the potential across the membrane

$$\Phi(x) = \frac{x}{d} \Phi_m. \tag{12.23}$$

This is an approximation which is consistent with the condition of electroneutrality. On the boundary between liquid and membrane the first derivative of Φ will be discontinuous corresponding to a surface charge distribution.[1] Assuming a stationary state with $\partial J/\partial x = 0$ we can evaluate the left-hand side of (12.22)

$$J_k \frac{k_B T d}{Z_k e \Phi_m} \left(\mathrm{e}^{Z_k e \Phi_m / k_B T} - 1\right) = -D \left(c_k(d) \mathrm{e}^{Z_k e \Phi_m / k_B T} - c_k(0)\right) \tag{12.24}$$

which gives the current

$$J_k = -\frac{D}{d} \frac{Z_k e \Phi_m}{k_B T} \frac{c_{k,in} \mathrm{e}^{Z_k e \Phi_m / k_B T} - c_{k,out}}{\mathrm{e}^{Z_k e \Phi_m / k_B T} - 1}. \tag{12.25}$$

In a stationary state the total charge current has to vanish

$$I = \sum_k Z_k e J_k = 0 \tag{12.26}$$

and we find

$$\frac{\mathrm{e}^2 \Phi_m}{k_B T d} \sum D_k Z_k^2 \frac{c_{k,in} \mathrm{e}^{Z_k e \Phi_m / k_B T} - c_{k,out}}{\mathrm{e}^{Z_k e \Phi_m / k_B T} - 1} = 0. \tag{12.27}$$

With $Z_{Na+} = Z_{K+} = 1$, $Z_{Cl-} = -1$ and

$$y_m = \frac{e \Phi_m}{k_B T} \quad b_m = \mathrm{e}^{y_m} \tag{12.28}$$

we have

$$\begin{aligned} &D_{Na+} \frac{c_{Na+,in} b_m - c_{Na+,out}}{b_m - 1} + D_{K+} \frac{c_{K+,in} b_m - c_{K+,out}}{b_m - 1} \\ &+ D_{Cl-} \frac{c_{Cl-,in} b_m^{-1} - c_{Cl-,out}}{b_m^{-1} - 1} = 0. \end{aligned} \tag{12.29}$$

Multiplication with $(b_m - 1)$ gives

$$\begin{aligned} &D_{Na+}(c_{Na+,in} b_m - c_{Na+,out}) + D_{K+}(c_{K+,in} b_m - c_{K+,out}) \\ &- b_m D_{Cl-}(C_{Cl-,in} b_m^{-1} - c_{Cl-,out}) = 0 \end{aligned} \tag{12.30}$$

[1] We do not consider a possible variation of ϵ here.

and we find

$$b_m = \frac{D_{Na+}c_{Na+,out} + D_{K+}c_{K+,out} + D_{Cl-}c_{Cl-,in}}{D_{Na+}c_{Na+,in} + D_{K+}c_{K+,in} + D_{Cl-}c_{Cl-,out}} \tag{12.31}$$

and finally

$$\Phi_m = \frac{k_B T}{e} \ln \frac{D_{Na+}c_{Na+,out} + D_{K+}c_{K+,out} + D_{Cl-}c_{Cl-,in}}{D_{Na+}c_{Na+,in} + D_{K+}c_{K+,in} + D_{Cl-}c_{Cl-,out}}. \tag{12.32}$$

This formula should be compared with the Nernst equation

$$V_k = \Phi_{inside} - \Phi_{outside} = \frac{k_B T}{Z_k e} \ln \frac{c_{k,outside}}{c_{k,inside}}. \tag{12.33}$$

The ionic contributions appear weighted with their mobilities. The Nernst equation is obtained if the membrane is permeable for only one ionic species.

12.3 Hodgkin–Huxley Model

In 1952, Hodgkin and Huxley won the Nobel prize for their quantitative description of the squid giant axon dynamics [41].

They thought of the axon membrane as an electrical circuit. They assumed independent currents of sodium and potassium, a capacitive current, and a catch-all leak current. The total current is the sum of these (Fig. 12.6):

$$I_{ext} = I_C + I_{Na} + I_K + I_L. \tag{12.34}$$

The capacitive current is

$$I_C = C_m \frac{\mathrm{d}V}{\mathrm{d}t}. \tag{12.35}$$

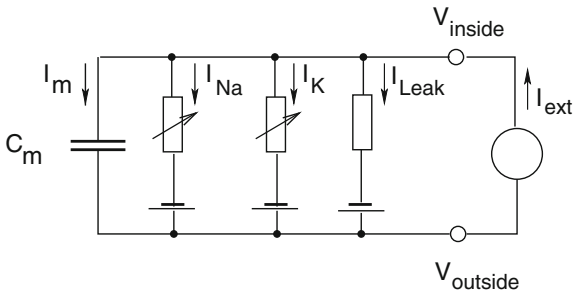

Fig. 12.6 Hodgkin–Huxley model

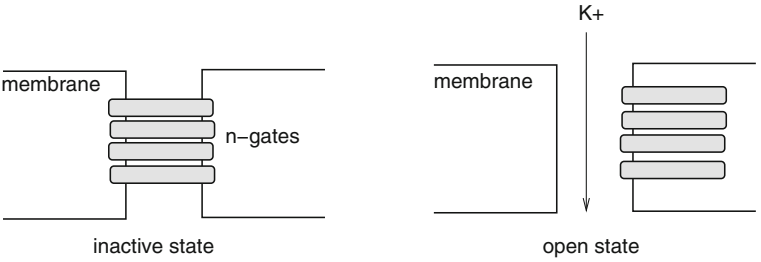

Fig. 12.7 Potassium gates

For the ionic currents we have (12.11)

$$I_k = g_k(V - V_k), \tag{12.36}$$

where g_k is the channel conductance which depends on the membrane potential and on time and V_k is the specific Nernst potential (12.19). The macroscopic current relates to a large number of ion channels which are controlled by gates which can be in either permissive or nonpermissive state. Hodgkin and Huxley considered a simple rate process for the transition between the two states with voltage-dependent rate constants

$$\text{closed} \underset{\beta(V)}{\overset{\alpha(V)}{\rightleftharpoons}} \text{open}. \tag{12.37}$$

The variable p which denotes the number of open gates obeys a first-order kinetics

$$\frac{\mathrm{d}p}{\mathrm{d}t} = \alpha(1 - p) - \beta p. \tag{12.38}$$

Hodgkin and Huxley introduced a gating particle n describing the potassium conductance (Fig. 12.7) and two gating particles for sodium (m being activating and h being inactivating). They used the specific equations

$$g_K = \overline{g}_k p_n^4 \tag{12.39}$$

$$g_{Na} = \overline{g}_{Na} p_m^3 p_h \tag{12.40}$$

which gives finally a highly nonlinear differential equation

$$I_{ext}(t) = C_m \frac{\mathrm{d}V}{\mathrm{d}t} + \overline{g}_k p_n^4 (V - V_K) + \overline{g}_{Na} p_m^3 p_h (V - V_{Na}) + \overline{g}_L (V - V_L). \tag{12.41}$$

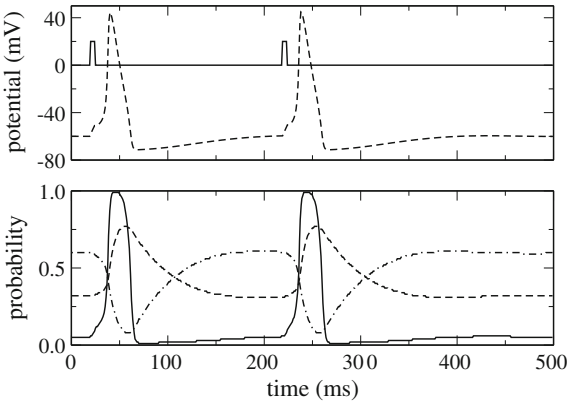

Fig. 12.8 Hodgkin–Huxley model. Equation (12.41) is solved numerically [42]. *Top* Excitation by two short rectangular pulses $I_{ext}(t)$ (*solid curve*) and membrane potential $V(t)$ (*dashed*). *Bottom* fraction of open gates p_m (*full*), p_n(*dashed*), p_h(*dash-dotted*)

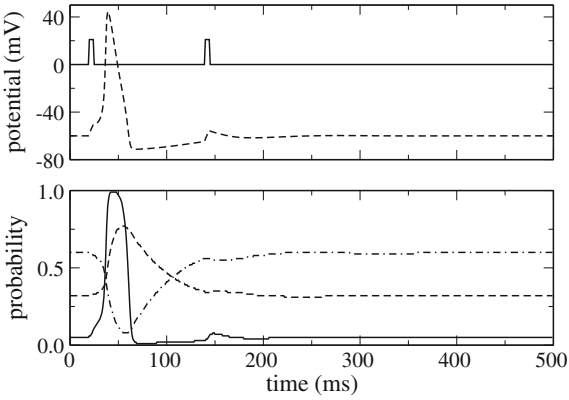

Fig. 12.9 Refractoriness of the Hodgkin–Huxley model. A second pulse cannot excite the system during the refractory period. Details as in Fig. 12.8

This equation has to be solved numerically. It describes many electrical properties of the neuron-like threshold and refractory behavior, repetitive spiking and temperature dependence (Figs. 12.8 and 12.9). Later, we will discuss a simplified model with similar properties in more detail (Sect. 13.3).

12.4 Cooperativity in Ion Channel Kinetics

Ion channel cooperativity can be described similar to ligand binding with a two-state model [43–45]. We consider an oligomeric protein consisting of a number n_T of subunits which can be in two configurations, R and T. In the presence of the ligand, the equilibrium between the two configurations is shifted to R, which has the greater affinity for the ligand. The kinetics can be described in terms of the number n of bound subunits in the T and R conformations. In case of the ion channel, R and T denote the open (or active) and closed (or inactive) state of the subunits (Fig. 12.10).

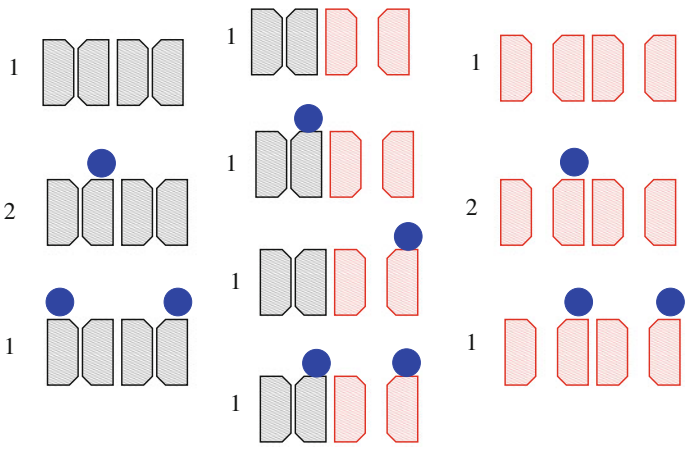

Fig. 12.10 Cooperative ion channels. The possible states of two ion channels are shown, each of which can bind to one ligand and is either in the open (R, *red*) or closed (T, *grey*) state. *Numbers* show the degeneracy

12.4.1 MWC Model

The traditional MWC [46] model assumes that all segments are in the same state. It is equivalent to a model with one channel and n_T binding sites. The following transitions are possible (Fig. 12.11):

- binding, proportional to number of unbound units:

$$-\Delta P_R(n) = \Delta P_R(n+1) \propto (n_T - n) P_R(n) k_R^+ \tag{12.42}$$

$$-\Delta P_T(n) = \Delta P_T(n+1) \propto (n_T - n) P_T(n) k_T^+ \tag{12.43}$$

- unbinding, proportional to number of bound units:

$$-\Delta P_R(n) = \Delta P_R(n-1) \propto n P_R(n) k_R^- \tag{12.44}$$

$$-\Delta P_T(n) = \Delta P_T(n-1) \propto n P_T(n) k_T^- \tag{12.45}$$

- configuration change

$$-\Delta P_R(n) = \Delta P_T(n) \propto P_R(n) v_R(n) \tag{12.46}$$

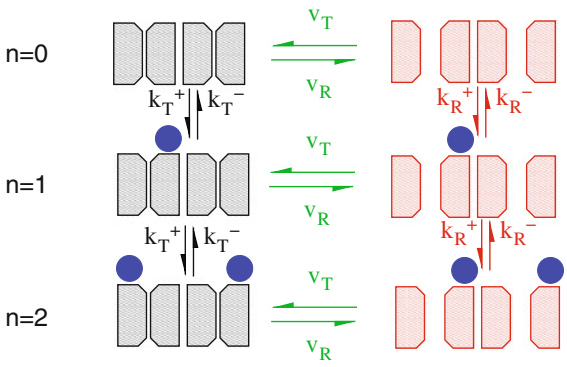

Fig. 12.11 MWC model for ion channels. The protein is characterized by the state of the segments (R or T) and the number of bound ligands n. Equilibrium between the two conformations is established by the transition rates $v_{R,T}(n)$. Rates of binding ($k^+_{R,T}$)and unbinding ($k^-_{R,T}$) depend on the state

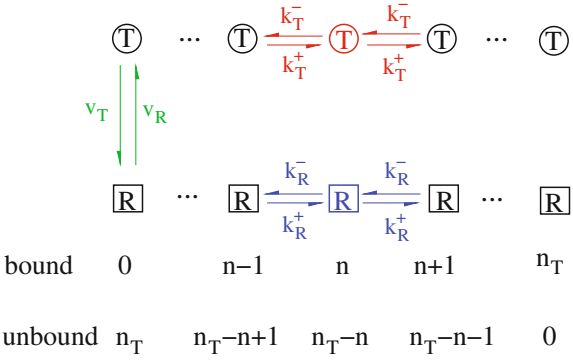

Fig. 12.12 MWC model for cooperative ion channels. Each of the n_T subunits is in either one of the two states R or T. The number of bound subunits is n, which can change according to *forward* and *backward* transition rates $k^\pm_{R,T}$. The equilibrium between the two configurations in the unbound state $n = 0$ depends on the transition rates $v_{R,T}$

$$-\Delta P_T(n) = \Delta P_R(n) \propto P_T(n) v_T(n). \tag{12.47}$$

In a simplified MWC model [43, 44] (Fig. 12.12), we assume that the configuration change only appears in the unbound (n=0) state.

The dynamic evolution is described by the rate equations for $n = 0$:

$$\frac{\partial P_R(0,t)}{\partial t} = k_R^- P_R(1,t) - k_R^+ n_T P_R(0,t) - v_R P_R(0,t) + v_T P_T(0,t) \tag{12.48}$$

$$\frac{\partial P_T(0,t)}{\partial t} = k_T^- P_T(1,t) - k_T^+ n_T P_T(0,t) + v_R P_R(0,t) - v_T P_T(0,t) \tag{12.49}$$

and for $n > 0$:

$$\frac{\partial P_R(n,t)}{\partial t} = k_R^+(n_T - n + 1)P_R(n-1,t) + k_R^-(n+1)P_R(n+1,t)$$
$$- k_R^+(n_T - n)P_R(n,t) - k_R^- n P_R(n,t) \tag{12.50}$$

$$\frac{\partial P_T(n,t)}{\partial t} = k_T^+(n_T - n + 1)P_T(n-1,t) + k_T^-(n+1)P_T(n+1,t)$$
$$- k_T^+(n_T - n)P_T(n,t) - k_T^- n P_T(n,t). \tag{12.51}$$

The following ansatz

$$P_R(n) = \frac{1}{z}\binom{n_T}{n} K_R^n \quad P_T(n) = \frac{1}{z}\binom{n_T}{n} K_T^n L \tag{12.52}$$

allows to find the stationary state by solving the following equations:

$$0 = k_R^- n_T K_R - k_R^+ n_T - v_R + v_T L \tag{12.53}$$

$$0 = k_T^- n_T K_T - k_T^+ n_T - v_T + v_R L^{-1} \tag{12.54}$$

$$0 = k_R^+ \frac{n_T!}{(n-1)!(n_T - n)!} K_R^{n-1} + k_R^- \frac{n_T!}{(n_T - n - 1)!n!} K_R^{n+1}$$
$$- k_R^+ \frac{n_T!}{n!(n_T - n - 1)!} K_R^n - k_R^- \frac{n_T!}{(n_T - n)!(n-1)!} K_R^n \tag{12.55}$$

$$0 = k_T^+ \frac{n_T!}{(n-1)!(n_T - n)!} K_T^{n-1} + k_T^- \frac{n_T!}{(n_T - n - 1)!n!} K_T^{n+1} -$$
$$0 - k_T^+ \frac{n_T!}{n!(n_T - n - 1)!} K_T^n - k_T^- \frac{n_T!}{(n_T - n)!(n-1)!} K_T^n \tag{12.56}$$

which simplify to

$$(k_R^+ - K_R k_R^-)\left(\frac{1}{n_T - n} - \frac{K_R}{n}\right) + \frac{K_R}{n_T - n}(L v_T K_T^n K_R^{-n} - v_R) = 0 \tag{12.57}$$

$$(k_T^+ - K_T k_T^-)\left(\frac{1}{n_T - n} - \frac{K_T}{n}\right) + \frac{K_T}{n_T - n}(L^{-1} v_R K_R^n K_T^{-n} - v_T) = 0 \tag{12.58}$$

with the solution

$$K_R = \frac{k_R^+}{k_R^-} \quad K_T = \frac{k_T^+}{k_T-}$$

and

$$L = -\frac{1}{v_T}(k_R^- n_T K_R - k_R^+ n_T - v_R) = \frac{v_R}{v_T} \tag{12.59}$$

$$L^{-1} = -\frac{1}{v_R}(k_T^- n_T K_T - k_T^+ n_T - v_R) = \frac{v_T}{v_R}. \tag{12.60}$$

Finally, the normalization factor is

$$z = \sum_{n=0}^{n_T} \binom{n_T}{n} (K_R^n + L K_T^n) = (1 + K_R)^{n_T} + L(1 + K_T)^{n_T}. \tag{12.61}$$

The probability of the active state R is

$$P_R = \frac{(1 + K_R)^{n_T}}{(1 + K_R)^{n_T} + L(1 + K_T)^{n_T}} \tag{12.62}$$

which in the absence of cooperativity (i.e., $K_R = K_T$) becomes

$$P_{R,nc} = \frac{1}{1 + L}. \tag{12.63}$$

For increasing number of binding sites n_T the dependency on the ligand concentration (to which K_R and K_T are assumed to be proportional) becomes steeper and more pronounced (Figs. 12.13, 12.14).

12.4.2 KNF Model

The KNF [47] model assumes a sequential mechanism where all bound segments are in the open state (Fig. 12.15).

If n ligands are already bound, binding of another one is possible for $n_T - n$ segments. Hence, the rate equations of the KNF model are

$$\frac{\partial P_n}{\partial t} = -n P_n k_n^- - (n_T - n) P_n k_n^+ + (n_T - n + 1) P_{n-1} k_{n-1}^+ + (n + 1) P_{n+1} k_{n+1}^-. \tag{12.64}$$

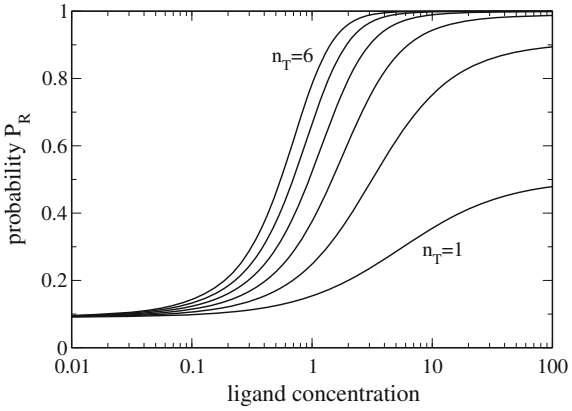

Fig. 12.13 Cooperativity of ligand-gated channels in the MWC model. The probability of the active state (12.62) is shown as a function of ligand concentration (calculated for $K_R/K_T = 10$, $L = 10$) and number of active sites n_T from 1 to 6

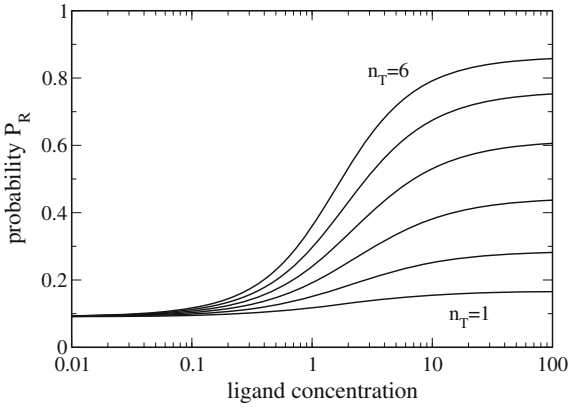

Fig. 12.14 Cooperativity of ligand-gated channels in the MWC model. The probability of the active state (12.62) is shown as a function of ligand concentration (calculated for $K_R/K_T = 2$, $L = 10$) and number of active sites n_T from 1 to 6

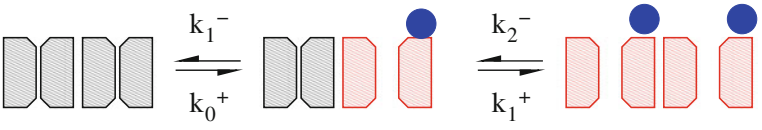

Fig. 12.15 KNF model. The KNF model assumes a sequential mechanism

To find the steady state, we use again an ansatz with a binomial degeneracy factor

$$P_n = \binom{n_T}{n} W_n \tag{12.65}$$

and obtain

$$\begin{aligned} 0 &= -k_n^- \frac{n_T!}{(n_T-n)!(n-1)!} W_n - k_n^+ \frac{n_T!}{n!(n_T-n-1)!} W_n \\ &+ k_{n-1}^+ \frac{n_T!}{(n-1)!(n_T-n)!} W_{n-1} + k_{n+1}^- \frac{n_T!}{n!(n_T-n-1)!} W_{n+1} \\ &= -k_n^- n W_n - k_n^+ (n_T-n) W_n + k_{n-1}^+ n W_{n-1} + k_{n+1}^- (n_T-n) W_{n+1} \end{aligned} \tag{12.66}$$

which gives the recursion

$$n = 0: \quad -k_0^+ n_T W_0 + k_1^- n_T W_1 = 0 \tag{12.67}$$

$$0 < n < n_T: \quad W_{n+1} = \frac{1}{k_{n+1}^-(n_T-n)} \left[(n k_n^- + (n_T-n) k_n^+) W_n - n k_{n-1}^+ W_{n-1} \right] \tag{12.68}$$

$$n = n_T: \quad -k_{n_T}^- n_T W_{n_T} + k_{n_T-1}^+ n_T W_{n_T-1} = 0 \tag{12.69}$$

which is solved by

$$W_1 = \frac{k_0^+}{k_1^-} W_0 \tag{12.70}$$

$$\begin{aligned} W_2 &= \frac{1}{k_2^-(n_T-1)} \left[(k_1^- + (n_T-1) k_1^+) \frac{k_0^+}{k_1^-} - k_0^+ \right] W_0 \\ &= \frac{1}{k_2^-(n_T-1)} \left[(k_0^+ + (n_T-1) k_1^+ \frac{k_0^+}{k_1^-}) - k_0^+ \right] W_0 \\ &= \frac{k_1^+}{k_2^-} \frac{k_0^+}{k_1^-} W_0 \end{aligned} \tag{12.71}$$

$$\vdots$$

$$W_{n_T-1} = \frac{k_{n_T-2}^+}{k_{n_T-1}^-} \cdots \frac{k_0^+}{k_1^-} W_0 \tag{12.72}$$

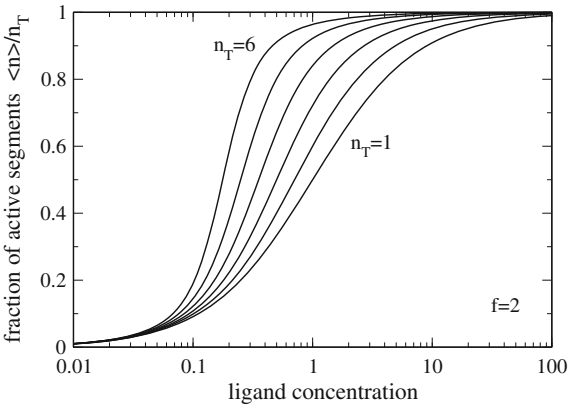

Fig. 12.16 Cooperativity in the KNF model. The average fraction of active sites (12.78) is shown as a function of ligand concentration for $f = 2$ and n_T from 1 to 6

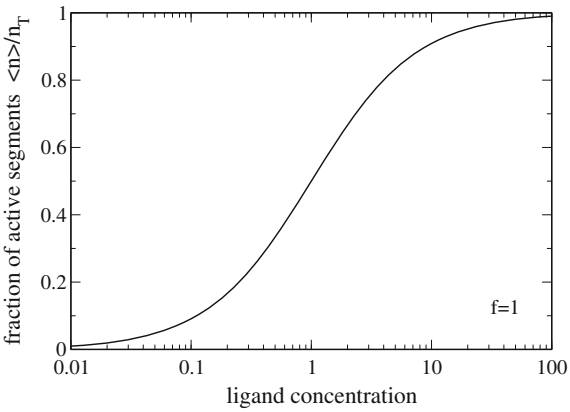

Fig. 12.17 KNF model in the uncooperative limit. For $f = 1$ all partial equilibria have the same equilibrium constant $K_n = K_0$ and the average fraction of active sites does not depend on the number of segments n_T

$$W_{n_T} = \frac{k^+_{n_T-1}}{k^-_{n_T}} W_{n_r-1}. \tag{12.73}$$

This can be summarized as

$$P_n = \frac{1}{z}\binom{n_T}{n} K_n K_{n-1} \ldots K_2 K_1 \tag{12.74}$$

with the equilibrium constants

$$K_n = \frac{k^+_{n-1}}{k^-_n}. \tag{12.75}$$

Now, assume a geometric series dependence [43] of the form

$$K_n = K_0 f^n, \tag{12.76}$$

where the parameter f is a measure of cooperativity and K_0 is proportional to the ligand concentration. Then,

$$P_n = \frac{1}{z}\binom{n_T}{n} K_0^n f^{n(n-1)/2} \tag{12.77}$$

and the average

$$< n >= \sum_{n=0}^{n_T} n P_n = \frac{n_T}{z} \sum_{n=0}^{n_T-1} \binom{n_T - 1}{n} K_0^{n+1} f^{n(n+1)/2}. \tag{12.78}$$

For $f = 1$, the system is uncooperative with

$$P_{n,nc} = \frac{1}{z}\binom{n_T}{n} K_0^n = \frac{1}{(1+K_0)^{n_T}}\binom{n_T}{n} K_0^n \tag{12.79}$$

and the average number of active segments

$$< n >_{nc}= \sum_{n=0}^{n_T} n P_{n,nc} = \sum_{n=1}^{n_T} \frac{1}{(1+K_0)^{n_T}} n_T \binom{n_T - 1}{n-1} K_0^n = \frac{n_T K_0}{1+K_0}. \tag{12.80}$$

Again, the dependency on ligand concentration becomes sharper for larger n_T (Figs. 12.16 and 12.17).

Chapter 13
Reaction–Diffusion Systems

Reaction–diffusion systems are described by nonlinear equations and show the formation of structures. Static as well as dynamic patterns found in biology can be very realistically simulated [48]. We derive the equations for a coupled diffusion–reaction system and classify possible instabilities. The Fitzhugh–Nagumo model as a simplification of the Hodgkin Huxley model is analyzed in detail.

13.1 Derivation

We consider now a coupling of diffusive motion and chemical reactions. For constant temperature and total density we have the continuity equation

$$\frac{\partial}{\partial t} c_k = -\text{div}\, \mathbf{J}_k + \sum_j \nu_{kj} r_j \tag{13.1}$$

together with the phenomenological equation

$$\mathbf{J}_k = -\sum_j L_{kj} \text{grad}\, k \ln c_j = -\sum_j D_{kj} \text{grad}\, c_j \tag{13.2}$$

which we combine to get

$$\frac{\partial}{\partial t} c_k = \sum_j D_{kj} \triangle c_j + \sum_j \nu_{kj} r_j, \tag{13.3}$$

where the reaction rates are nonlinear functions of the concentrations:

P.O.J. Scherer and S.F. Fischer, *Theoretical Molecular Biophysics*,
Biological and Medical Physics, Biomedical Engineering,
DOI 10.1007/978-3-662-55671-9_13

$$\sum_j \nu_{kj} r_j = F_k(\{c_i\}). \tag{13.4}$$

We assume for the diffusion coefficients the simplest case that the different species diffuse independently (but possibly with different diffusion constants) and that the diffusion fluxes are parallel to the corresponding concentration gradients. We write the diffusion–reaction equation in matrix form

$$\frac{\partial}{\partial t}\begin{pmatrix} c_1 \\ \vdots \\ c_N \end{pmatrix} = \begin{pmatrix} D_1 & & \\ & \ddots & \\ & & D_N \end{pmatrix} \triangle \begin{pmatrix} c_1 \\ \vdots \\ c_N \end{pmatrix} + \begin{pmatrix} F_1(\{c\}) \\ \vdots \\ F_N(\{c\}) \end{pmatrix} \tag{13.5}$$

or briefly

$$\frac{\partial}{\partial t}\mathbf{c} = D \triangle \mathbf{c} + \mathbf{F}(\mathbf{c}). \tag{13.6}$$

13.2 Linearization

Since a solution of the nonlinear equations is generally possible only numerically we investigate small deviations from an equilibrium solution $\mathbf{c_0}$[1] with

$$\frac{\partial}{\partial t}\mathbf{c}_0 = 0 \tag{13.7}$$

$$\triangle \mathbf{c}_0 = 0. \tag{13.8}$$

Obviously, the equilibrium corresponds to a root

$$\mathbf{F}(\mathbf{c}_0) = 0. \tag{13.9}$$

We linearize the equations by setting

$$\mathbf{c} = \mathbf{c}_0 + \boldsymbol{\xi} \tag{13.10}$$

and expanding around the equilibrium

$$\frac{\partial}{\partial t}\boldsymbol{\xi} = D \triangle \boldsymbol{\xi} + \mathbf{F}(\mathbf{c}_0 + \boldsymbol{\xi}) = D \triangle \boldsymbol{\xi} + \frac{\partial \mathbf{F}}{\partial \mathbf{c}}_{|\mathbf{c}_0} \boldsymbol{\xi}. \tag{13.11}$$

Denoting the matrix of derivatives by M_0 we can discuss several types of instabilities:

[1] We assume tacitly that such a solution exists.

- spatially constant solutions

For a spatially constant solution we have

$$\frac{\partial}{\partial t}\boldsymbol{\xi} = M_0\boldsymbol{\xi} \tag{13.12}$$

with the formal solution

$$\boldsymbol{\xi} = \boldsymbol{\xi}_0 \exp(M_0 t). \tag{13.13}$$

Depending on the eigenvalues of M there can be exponentially growing or decaying solutions, oscillating solutions, and exponentially growing or decaying solutions.

- plane waves

Plane waves are solutions of the linearized problem. Using the Ansatz

$$\boldsymbol{\xi} = \boldsymbol{\xi}_0 \mathrm{e}^{\mathrm{i}(\omega t - \mathbf{kx})} \tag{13.14}$$

gives

$$i\omega\boldsymbol{\xi} = -k^2 D\boldsymbol{\xi} + M_0\boldsymbol{\xi} = M_k\boldsymbol{\xi}. \tag{13.15}$$

For a stable plane wave solution $\lambda = i\omega$ is an eigenvalue of

$$M_k = M_0 - k^2 D \tag{13.16}$$

with

$$\Re(\lambda) \leq 0. \tag{13.17}$$

If there are purely imaginary eigenvalues for some $\mathbf{k}$, they correspond to stable solutions which are spatially inhomogeneous and lead to formation of certain patterns.

13.3 Fitzhugh–Nagumo Model

The Hodgkin-Huxley model (12.40) describes characteristic properties like the threshold behavior and the refractory period where the membrane is not excitable. Since the system of equations is rather complicated, a simpler model was developed by Fitzhugh (1961) and Nagumo (1962) which involves only two variables u, v (membrane potential and recovery variable):

$$\dot{u} = u - \frac{u^3}{3} - v + I(t) \tag{13.18}$$

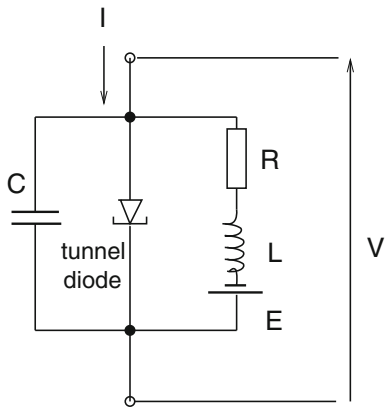

Fig. 13.1 Nagumo circuit

$$\dot{v} = \epsilon(u + a - bv). \tag{13.19}$$

The standard parameter values are

$$a = 0.7 \quad b = 0.8 \quad \epsilon = 0.08. \tag{13.20}$$

Nagumo studied an electronic circuit with a tunnel diode (Fig. 13.1) which is described by rather similar equations

$$I = C\dot{V} + I_{diode}(V) + I_{LR} \tag{13.21}$$

$$V = RI_{LR} + L\dot{I}_{LR} + E \rightarrow \dot{I}_{LR} = \frac{V - E - RI_{LR}}{L}. \tag{13.22}$$

The Fitzhugh Nagumo model can be used to describe the excitation propagation along the membrane. After rescaling the original equations and adding diffusive terms we obtain the reaction–diffusion equations

$$\frac{\partial}{\partial t}\begin{pmatrix} u \\ v \end{pmatrix} = \begin{pmatrix} u - \frac{u^3}{3} - v + I(t) \\ \epsilon(u - bv + a) \end{pmatrix} + \begin{pmatrix} 1 & \\ & \delta \end{pmatrix} \triangle \begin{pmatrix} u \\ v \end{pmatrix}. \tag{13.23}$$

The evolution of the FN model can be easily represented in a two-dimensional uv-plot. The u-nullcline and the v-nullcline are defined by

$$\dot{u} = 0 \rightarrow v = u - \frac{u^3}{3} + I_0 \tag{13.24}$$

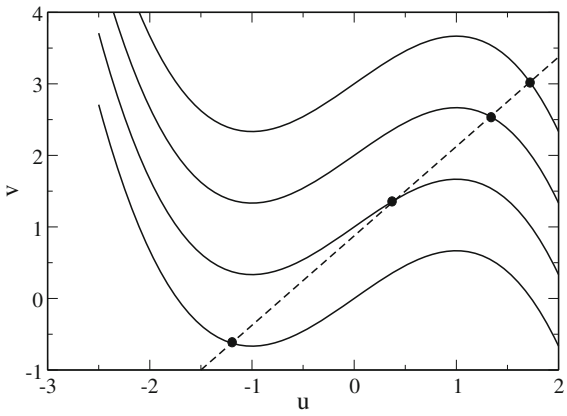

Fig. 13.2 Nullclines of the Fitzhugh Nagumo equations. The solutions of ((13.24), (13.25)) are shown for different values of the current $I = 0, 1, 2, 3$

$$\dot{v} = 0 \rightarrow v = \frac{a+u}{b}. \tag{13.25}$$

The intersection of the nullclines is an equilibrium since here $\dot{u} = \dot{v} = 0$ (Fig. 13.2).

Consider small deviations from the equilibrium values

$$u = u_{eq} + \mu \quad v = v_{eq} + \eta. \tag{13.26}$$

The linearized equations are

$$\dot{\mu} = (1 - u_{eq}^2)\mu - \eta \tag{13.27}$$

$$\dot{\eta} = \epsilon(\mu - b\eta). \tag{13.28}$$

Obviously instability has to be expected for $u_{eq}^2 < 1$.

The matrix of derivatives

$$M_0 = \begin{pmatrix} 1 - u_{eq}^2 & -1 \\ \epsilon & -\epsilon b \end{pmatrix} \tag{13.29}$$

has the eigenvalues

$$\lambda = \frac{1}{2}\left(1 - u_{eq}^2 - \epsilon b \pm \sqrt{(1 - u_{eq}^2 + \epsilon b)^2 - 4\epsilon}\right). \tag{13.30}$$

The square root is zero for

$$u_{eq} = \pm\sqrt{1 + \epsilon b \pm 2\sqrt{\epsilon}}. \tag{13.31}$$

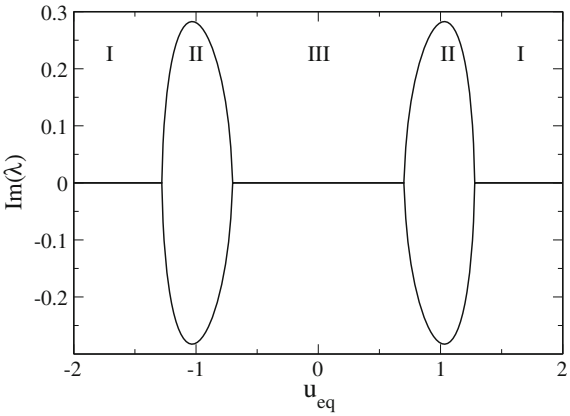

Fig. 13.3 Imaginary part of the eigenvalues

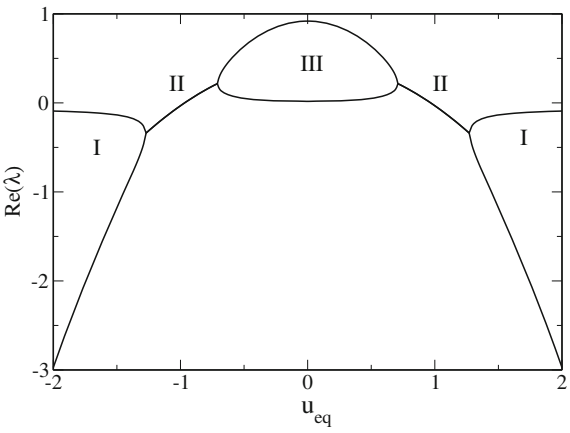

Fig. 13.4 Real part of the eigenvalues

This defines a region around $u_{eq} = \pm 1$ where the eigenvalues have a nonzero imaginary part (Fig. 13.3).

For standard parameters we distinguish the regions

$$\begin{aligned} I &: |u_{eq}| > \sqrt{1 + \epsilon b + 2\sqrt{M\epsilon}} = 1.277 \\ II &: \quad 0.706 < |u_{eq}| < 1.277 \\ III &: |u_{eq}| < \sqrt{1 + \epsilon b - 2\sqrt{\epsilon}} = 0.706. \end{aligned} \tag{13.32}$$

Within region II the real part of both eigenvalues is (Fig. 13.4)

$$\Re\lambda = \frac{1}{2}(1 - u_{eq}^2 - \epsilon b) \tag{13.33}$$

and since

$$1 + \epsilon b - 2\sqrt{\epsilon} < u_{eq}^2 < 1 + \epsilon b + 2\sqrt{\epsilon} \tag{13.34}$$

we have

$$1 - u_{eq}^2 - \epsilon b - 2\sqrt{\epsilon} + 2\epsilon b < 0 < 1 - u_{eq}^2 - \epsilon b + 2\sqrt{\epsilon} + 2\epsilon b \tag{13.35}$$

$$\Re\lambda + \epsilon b - \sqrt{\epsilon} < 0 < \Re\lambda + \epsilon b + \sqrt{\epsilon} \tag{13.36}$$

$$|\Re\lambda + \epsilon b| < \sqrt{\epsilon}. \tag{13.37}$$

For standard parameters

$$-0.35 < \Re\lambda < 0.22. \tag{13.38}$$

Oscillating instabilities appear in region II if

$$\sqrt{\epsilon} < \epsilon b \rightarrow \epsilon < b \tag{13.39}$$

which is the case for standard parameters. Outside region II instabilities appear if at least the larger of the two real eigenvalues is positive or

$$\sqrt{(1 - u_{eq}^2 + \epsilon b)^2 - 4\epsilon} > u_{eq}^2 - 1 + \epsilon b. \tag{13.40}$$

This is the case if the right-hand side is negative or

$$u_{eq}^2 < 1 - \epsilon b \tag{13.41}$$

hence in the center of region III if $\epsilon b < 1$. For standard parameters $1 - \epsilon b = 0.936$ and according to (13.32) the whole region III is unstable. If the right-hand side of (13.40) is positive we can take the square

$$(1 - u_{eq}^2 + \epsilon b)^2 - 4\epsilon > (u_{eq}^2 - 1 + \epsilon b)^2 \tag{13.42}$$

which simplifies to

$$u_{eq}^2 < 1 - \frac{1}{b}. \tag{13.43}$$

This is false for $b < 1$ and hence for standard parameters the whole region I is stable.

Part V
Reaction Rate Theory

Chapter 14
Equilibrium Reactions

In this chapter we study chemical equilibrium reactions. In thermal equilibrium of forward and backward reactions, the overall reaction rate vanishes and the ratio of the rate constants gives the equilibrium constant which usually shows an exponential dependence on the inverse temperature.[1] We derive the van't Hoff relation for the equilibrium constant and discuss its statistical interpretation.

14.1 Arrhenius Law

Reaction rate theory goes back to Arrhenius who in 1889 investigated the temperature-dependent rates of inversion of sugar in the presence of acids. Empirically, a temperature dependence is often observed of the form

$$k(T) = A\mathrm{e}^{-E_a/k_BT} \tag{14.1}$$

with the activation energy E_a. Considering a chemical equilibrium (Fig. 14.1)

$$\mathrm{A} \underset{k'}{\overset{k}{\rightleftharpoons}} \mathrm{B}. \tag{14.2}$$

This gives for the equilibrium constant

$$K = \frac{k}{k'} \tag{14.3}$$

[1] An overview over the development of rate theory during the past century is given by [49].

P.O.J. Scherer and S.F. Fischer, *Theoretical Molecular Biophysics*,
Biological and Medical Physics, Biomedical Engineering,
DOI 10.1007/978-3-662-55671-9_14

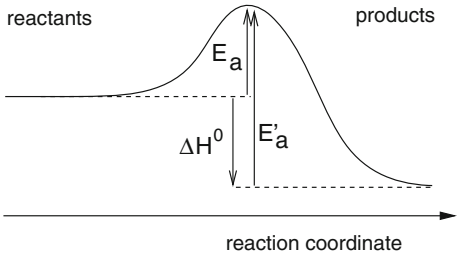

Fig. 14.1 Arrhenius law

and

$$\ln K = \ln k - \ln k' = \ln A - \ln A' - \frac{E_a - E'_a}{k_B T}. \tag{14.4}$$

In equilibrium the thermodynamic forces vanish

$$T = const \tag{14.5}$$

$$A = \sum_k \mu_k \nu_k = 0. \tag{14.6}$$

For dilute solutions with

$$\mu_k = \mu_k^0 + k_B T \ln c_k \tag{14.7}$$

we have

$$\sum_k \mu_k^0 \nu_k + k_B T \sum_k \nu_k \ln c_k = 0 \tag{14.8}$$

which gives the van't Hoff relation for the equilibrium constant

$$\ln(K_c) = \sum_k \nu_k \ln c_k = -\frac{\sum_k \mu_k^0 \nu_k}{k_B T} - \frac{\Delta G^0}{k_B T}. \tag{14.9}$$

The standard reaction free energy can be divided into an entropic and an energetic part

$$-\frac{\Delta G^0}{k_B T} = \frac{-\Delta H^0}{k_B T} + \frac{\Delta S^0}{k}. \tag{14.10}$$

Since volume changes are not important at atmospheric pressure, the free reaction enthalpy gives the activation energy difference

$$E_a - E_a' = \Delta H^0. \tag{14.11}$$

A catalyst can only change the activation energies but never the difference ΔH^0.

14.2 Statistical Interpretation of the Equilibrium Constant

The chemical potential can be obtained as

$$\mu_k = \left(\frac{\partial F}{\partial N_k}\right)_{T,V,N_k'} = -k_B T \left(\frac{\partial \ln Z}{\partial N_k}\right)_{T,V,N_k'}. \tag{14.12}$$

Using the approximation of the ideal gas we have

$$Z = \prod \frac{z_k^{N_k}}{N_k!} \tag{14.13}$$

and

$$\ln Z \approx \sum_k N_k \ln z_k - N_k \ln N_k + N_k \tag{14.14}$$

which gives the chemical potential

$$\mu_k = -k_B T \ln \frac{z_k}{N_k}. \tag{14.15}$$

Let us consider a simple isomerization reaction

$$\mathrm{A} \rightleftharpoons \mathrm{B}.$$

The partition functions for the two species are (Fig. 14.2)

$$z_A = \sum_{n=0,1\ldots} \mathrm{e}^{-\epsilon_n(A)/k_B T} \qquad z_B = \sum_{n=0,1,\ldots} \mathrm{e}^{-\epsilon_n(B)/k_B T}. \tag{14.16}$$

In equilibrium

$$\mu_B - \mu_A = 0 \tag{14.17}$$

$$-k_B T \ln \frac{z_B}{N_B} = -k_B T \ln \frac{z_A}{N_A} \tag{14.18}$$

$$\frac{z_B}{z_A} = \frac{N_B}{N_A} = (N_B/V)(N_A/V)^{-1} = K_c \tag{14.19}$$

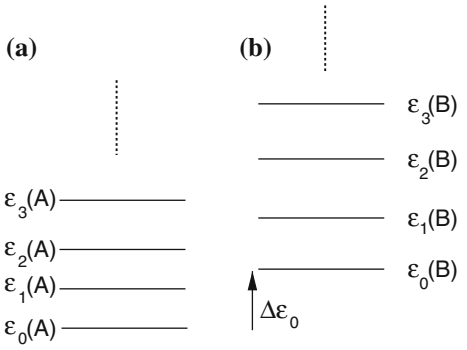

Fig. 14.2 Statistical interpretation of the equilibrium constant

$$K_c = \frac{\sum_{n=0,1,\ldots} \mathrm{e}^{-\epsilon_n(B)/k_BT}}{\sum_{n=0,1\ldots} \mathrm{e}^{-\epsilon_n(A)/k_BT}} = \frac{\sum_{n=0,1,\ldots} \mathrm{e}^{-(\epsilon_n(B)-\epsilon_0(B))/k_BT}}{\sum_{n=0,1\ldots} \mathrm{e}^{-(\epsilon_n(A)-\epsilon_0(A))/k_BT}} \mathrm{e}^{-\Delta\epsilon/k_BT}. \qquad (14.20)$$

This is the thermal distribution over all energy states of the system.

Chapter 15
Calculation of Reaction Rates

The activated behavior of the reaction rate can be understood from a simple model of two colliding atoms (Fig. 15.1). In this chapter, we discuss the connection to transition state theory, which takes into account the internal degrees of freedom of larger molecules and explains not only the activation energy, but also the prefactor of the Arrhenius law [50–52]. We formulate transition state theory in a thermodynamic context and discuss kinetic isotope effects. Finally, we present quite general rate expressions based on the flux over a saddle point.

15.1 Collision Theory

The Arrhenius expression consists of two factors. The exponential gives the number of reaction partners with enough energy and the prefactor gives the collision frequency times the efficiency.

We consider the collision of two spherical particles A and B in a coordinate system where B is fixed and A is moving with the relative velocity

$$\mathbf{v}_r = \mathbf{v}_A - \mathbf{v}_B. \tag{15.1}$$

The two particles collide if the distance between their centers is smaller than the sum of the radii

$$d = r_A + r_B. \tag{15.2}$$

During a time interval dt the number of possible collision partners is

$$c_B \pi d^2 v_r dt \tag{15.3}$$

P.O.J. Scherer and S.F. Fischer, *Theoretical Molecular Biophysics*,
Biological and Medical Physics, Biomedical Engineering,
DOI 10.1007/978-3-662-55671-9_15

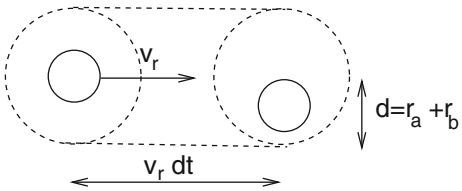

Fig. 15.1 Collision of two particles

and the number of collisions within a volume V is

$$N_{coll}/V = c_A c_B \pi (r_A + r_B)^2 v_r dt. \tag{15.4}$$

Assuming independent Maxwell distributions for the velocities

$$f(\mathbf{v}_a \mathbf{v}_b) d^3 v_a d^3 v_b = \left(\frac{m}{2\pi k_B T}\right)^3 \exp\left\{-\frac{m_a v_a^2}{2k_B T} - \frac{m_b v_b^2}{2k_B T}\right\} d^3 v_a d^3 v_b, \tag{15.5}$$

we have a Maxwell distribution also for the relative velocities

$$f(\mathbf{v}_r) d^3 v_r = \left(\frac{\mu}{2\pi k_B T}\right)^{3/2} \exp\left\{-\frac{\mu v_r^2}{2k_B T}\right\} d^3 v_r \tag{15.6}$$

with the reduced mass

$$\mu = \frac{M_A M_B}{M_A + M_B}. \tag{15.7}$$

The average relative velocity then is

$$\overline{v_r} = \sqrt{\frac{8k_B T}{\pi \mu}} \tag{15.8}$$

and the collision frequency is

$$\frac{\mathrm{d}N_{coll}}{V \mathrm{d}t} = c_a c_b \pi d^2 \sqrt{\frac{8k_B T}{\pi \mu}}. \tag{15.9}$$

If both particles are of the same species we have instead

$$\frac{\mathrm{d}N_{coll}}{V \mathrm{d}t} = \frac{1}{2} c_a^2 \pi d^2 \sqrt{\frac{16k_B T}{\pi M}} \tag{15.10}$$

since each collision involves two molecules. Since not each of the collisions will lead to a chemical reaction we introduce the reaction cross section $\sigma(E)$ which depends

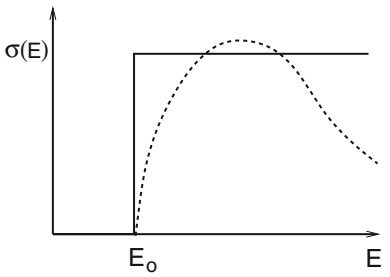

Fig. 15.2 Hard sphere approximation to the reaction cross section

on the kinetic energy of the relative velocity. As a simple approximation we use the reaction cross section of hard spheres

$$\sigma(E) = \begin{cases} 0 \text{ if } E < E_0 \\ \pi(r_a + r_b)^2 \text{ if } E > E_0 \end{cases}, \tag{15.11}$$

where E_0 is the minimum energy necessary for a reaction to occur (Fig. 15.2).

The distribution of relative kinetic energy can be determined as follows. From the one-dimensional Maxwell distribution

$$f(v)dv = \sqrt{\frac{m}{2\pi k_B T}} \mathrm{e}^{-mv^2/2k_B T} dv, \tag{15.12}$$

we find the distribution of relative kinetic energy for one particle as[1]

$$f(E_a)dE_a = 2\sqrt{\frac{m_a}{2\pi k_B T}} \mathrm{e}^{-E_a/k_B T} \frac{dE_a}{\sqrt{2mE_a}} = \frac{1}{\sqrt{\pi k_B T E_a}} \mathrm{e}^{-E_a/k_B T} dE_a. \tag{15.13}$$

The joint distribution for the two particles is

$$f(E_a, E_b)dE_a dE_b = \left(\frac{1}{\sqrt{\pi k_B T E_a}} \mathrm{e}^{-E_a/k_B T} dE_a\right)\left(\frac{1}{\sqrt{\pi k_B T E_b}} \mathrm{e}^{-E_b/k_B T} dE_b\right) \tag{15.14}$$

and the distribution of the total kinetic energy is given by

$$\begin{aligned} f(E) &= \int_0^E f(E_a, E - E_a)dE_a \\ &= \frac{1}{\pi k_B T} \int_0^E \frac{1}{\sqrt{E_a(E - E_a)}} \mathrm{e}^{-E_a/k_B T - (E-E_a)/k_B T} dE_a \end{aligned}$$

[1] There is a factor of two since $v^2 = (-v)^2$.

$$= \frac{1}{\pi k_B T} \mathrm{e}^{-E/k_B T} \int_0^E \frac{dE_a}{\sqrt{E_a(E - E_a)}}. \tag{15.15}$$

This integral can be evaluated by substitution

$$E_a = E \sin^2 \theta \quad dE_a = 2E \sin\theta \cos\theta d\theta$$

$$\int_0^E \frac{dE_a}{\sqrt{E_a(E - E_a)}} = \int_0^{\pi/2} \frac{2E \sin\theta \cos\theta d\theta}{\sqrt{E \sin^2\theta E \cos^2\theta}} = \int_0^{\pi/2} 2d\theta = \pi \tag{15.16}$$

and we find

$$f(E) = \frac{1}{k_B T} \mathrm{e}^{-E/k_B T}. \tag{15.17}$$

Now

$$\int_0^\infty f(E)\sigma(E)dE = \int_{E_0}^\infty f(E)\pi d^2 dE = \pi d^2 \mathrm{e}^{-E_0/k_B T} \tag{15.18}$$

and we have finally

$$r = c_a c_b \pi d^2 \sqrt{\frac{8k_B T}{\pi\mu}} \mathrm{e}^{-E_0/k_B T}. \tag{15.19}$$

For nonspherical molecules the reaction rate depends on the relative orientation. Therefore, a so-called steric factor p is introduced:

$$r = c_a c_b p \pi d^2 \sqrt{\frac{8k_B T}{\pi\mu}} \mathrm{e}^{-E_0/k_B T}. \tag{15.20}$$

There is no general way to calculate p and often it has to be estimated. Together p and d^2 give an effective molecular diameter[2]

$$d_{eff}^2 = pd^2. \tag{15.21}$$

15.2 Transition State Theory

According to transition state theory [53, 54] the reactants form an equilibrium amount of an activated complex which decomposes to yield the products (Fig. 15.3). The reaction path [55] leads over a saddle point called the transition state. As a simple

[2]The quantity $\pi d^2/4$ is equivalent to the collision cross section used in connection with nuclear reactions.

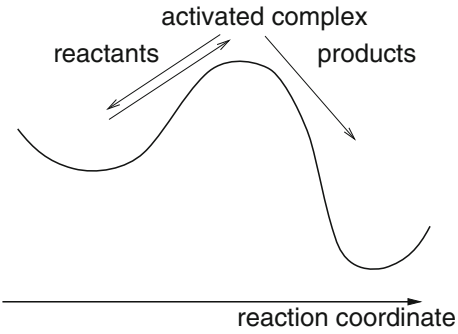

Fig. 15.3 Transition state theory. The reactants are in chemical equilibrium with the activated complex which can decompose into the products

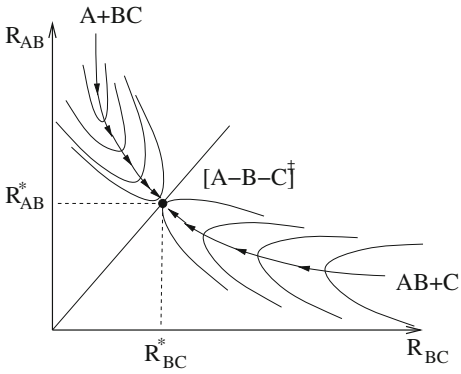

Fig. 15.4 Potential energy contour diagram. The potential energy for the reaction A+BC → $[A-B-C]^{\ddagger}$ → AB+C is shown schematically as a function of the distances R_{AB} and R_{BC}. *Arrows* indicate the reaction coordinate. The activated complex corresponds to a saddle point of the potential energy surface

example we consider the interaction of three atoms A, B, and C (Fig. 15.4). In general, three coordinates are needed to give the relative positions of the nuclei, but if atom A approaches the molecule BC, the direction of minimum potential energy is along the line of centers for the reaction.

According to TST, the reaction of two substances A and B is written as

$$\underset{\text{reactants}}{\text{A+B}} \overset{K}{\rightleftharpoons} \underset{\text{activated complex}}{[\text{A-B}]^{\ddagger}} \overset{k_1}{\rightarrow} \underset{\text{products.}}{\text{C+D}} \tag{15.22}$$

If all molecules behave like ideal gases, the equilibrium constant K may be calculated as

$$K_c = \frac{c_{[A-B]^{\ddagger}}}{c_A c_B} = \frac{z_{[A-B]^{\ddagger}}}{z_A z_B} \mathrm{e}^{-\Delta E_0 / k_B T}, \tag{15.23}$$

where ΔE_0 is the difference in zero point energies of the reactants and the activated complex. The activated complex may be considered a normal molecule, except that one of its vibrational modes is so loose that it allows immediate decomposition into the products. The corresponding contribution to the partition function is

$$z_{\omega\to 0} = \frac{1}{1 - \mathrm{e}^{-\hbar\omega/k_B T}} \to \frac{k_B T}{\hbar\omega}. \tag{15.24}$$

Thus the equilibrium constant becomes

$$K = \frac{k_B T}{\hbar\omega} \frac{z^{\ddagger}}{z_A z_B} \mathrm{e}^{-\Delta E_0/k_B T}, \tag{15.25}$$

where $z^{\ddagger}$ differs from $z_{[A-B]^{\ddagger}}$ by the contribution of the unique vibrational mode.

If $\omega/2\pi$ is considered the decomposition frequency, then the rate of decomposition is

$$r = \frac{\mathrm{d}c_C}{\mathrm{d}t} = \frac{\omega}{2\pi} c_{[A-B]^{\ddagger}} = \frac{k_B T}{2\pi\hbar} \frac{z^{\ddagger}}{z_A z_B} \mathrm{e}^{-\Delta E_0/k_B T} c_A c_B. \tag{15.26}$$

If not every activated complex decays into products, the expression for the rate constant has to be modified by a transmission coefficient κ

$$k_2 = \kappa \frac{k_B T}{2\pi\hbar} \frac{z^{\ddagger}}{z_A z_B} \mathrm{e}^{-\Delta E_0/k_B T}. \tag{15.27}$$

In most cases κ is close to 1. Important exceptions are the formation of a diatomic molecule, since the excess energy can only be eliminated by third-body collisions or radiation and reactions that involve changes from one type of electronic state to another—for instance, in certain cis–trans isomerizations.

15.3 Comparison Between Collision Theory and Transition State Theory

For comparison we apply transition state theory to the reaction of two spherical particles. For the reactants only translational degrees of freedom are relevant giving the partition function

$$z_T = \frac{(2\pi m k_B T)^{3/2}}{h^3}. \tag{15.28}$$

For the activated complex we consider the rotation around the center of mass. The moment of inertia is

$$I = (r_A + r_B)^2 \frac{m_A m_B}{m_A + m_B} \tag{15.29}$$

and the partition function is

$$z_R = \frac{8\pi^2 I k_B T}{h^2}. \tag{15.30}$$

The rate expression from TST is

$$\begin{aligned} k &= \frac{k_B T}{h} \frac{(2\pi(m_A + m_B)k_B T)^{3/2} h^3}{(2\pi k_B T)^3 m_A^{3/2} m_B^{3/2}} 8\pi^2 k_B T \frac{(r_A + r_B)^2}{h^2} \frac{m_A m_B}{m_A + m_B} \mathrm{e}^{-\Delta E_0/k_B T} \\ &= \sqrt{8\pi k_B T} \sqrt{\frac{m_A + m_B}{m_A m_B}} (r_A + r_B)^2 \mathrm{e}^{-\Delta E_0/k_B T} \end{aligned} \tag{15.31}$$

which is the same result obtained from collision theory.

We consider now a bimolecular reaction. Each reactant has three translational, three rotational, and 3N-6 vibrational[3] degrees of freedom. The partition functions are

$$\begin{aligned} z_A &= z_T^3 z_R^3 z_V^{3N_A - 6} \\ z_B &= z_T^3 z_R^3 z_V^{3N_B - 6} \\ z^\ddagger &= z_T^3 z_R^3 z_V^{3N_A + 3N_B - 7}. \end{aligned} \tag{15.32}$$

The reaction rate from TST is

$$k_{TST} = \frac{k_B T}{h} \frac{z^\ddagger}{z_A z_B} \mathrm{e}^{-E_0/k_B T} \approx \frac{k_B T}{h} \frac{z_V^5}{z_T^3 z_R^3} \mathrm{e}^{-E_0/k_B T}. \tag{15.33}$$

For the rigid sphere model

$$z_A = z_B = z_T^3 \qquad z^\ddagger = z_T^3 z_R^2 \tag{15.34}$$

hence the rate constant

$$k_{rigid} = \frac{k_B T}{h} \frac{z_R^2}{z_T^3} \mathrm{e}^{-E_0/k_B T}. \tag{15.35}$$

From comparison we see that the steric factor

$$p \approx \left(\frac{z_V}{z_R} \right)^5 \tag{15.36}$$

which is typically in the order of 10^{-5}.

[3] 3N-5 for a collinear molecule.

15.4 Thermodynamical Formulation of TST

Consider again the reaction

$$\mathrm{A+B} \rightleftharpoons [\mathrm{A-B}]^{\ddagger} \rightarrow \text{products} \tag{15.37}$$

with the equilibrium constant

$$K_c = \frac{c_{AB^{\ddagger}}}{c_A c_B}. \tag{15.38}$$

The TST rate expression (15.25) gives[4]

$$k_2 = \frac{k_B T}{h} K_c \tag{15.39}$$

and with (14.9) we have for an ideal solution

$$k_2 = \frac{k_B T}{h} \mathrm{e}^{-\Delta G^{0\ddagger}/k_B T} = \frac{k_B T}{h} \mathrm{e}^{-\Delta H^{0\ddagger}/k_B T} \mathrm{e}^{\Delta S^{0\ddagger}/k_B}. \tag{15.40}$$

The temperature dependence of the rate constant is

$$\frac{\mathrm{d} \ln k_2}{\mathrm{d}T} = \frac{1}{T} - \frac{\partial}{\partial T} \frac{\Delta G^{0\ddagger}}{k_B T}. \tag{15.41}$$

Now for ideal gases or solutions the chemical potential has the form

$$\mu = k_B T \ln c - k_B T \ln \frac{z}{V}, \tag{15.42}$$

and hence

$$\Delta G^{0\ddagger} = -k_B T \sum_i \nu_i \ln \frac{z_i}{V} \tag{15.43}$$

and

$$\frac{\partial}{\partial T} \frac{\Delta G^{0\ddagger}}{k_B T} = -\sum_i \nu_i \frac{\partial}{\partial T} \ln z_i = \sum_i \nu_i \frac{U_i}{k_B T^2} = \Delta U^{0\ddagger}. \tag{15.44}$$

Comparison with the Arrhenius law

$$\frac{\mathrm{d}}{\mathrm{d}T} \left(\ln A - \frac{E_a}{k_B T} \right) = \frac{E_a}{k_B T^2} \tag{15.45}$$

[4]The activated complex is treated as a normal molecule with the exception of the special mode.

shows that the activation energy is

$$E_a = k_B T + \Delta U^{0\ddagger} \approx k_B T + \Delta H^{0\ddagger} \quad \text{(ideal solutions)}. \tag{15.46}$$

For a bimolecular reaction in solution we find from

$$r_{TST} = \frac{k_B T}{h} e^{\Delta S^{0\ddagger}/k} e^{-\Delta H^{0\ddagger}/k_B T} = \frac{k_B T}{h} e^{\Delta S^{0\ddagger}/k} e^{-(E_a - k_B T)/k_B T} \tag{15.47}$$

that the steric factor is determined by the entropy of formation of the activated complex.

15.5 Kinetic Isotope Effects

There are two origins of the kinetic isotope effect. The first is quantum mechanical tunneling through the potential barrier.

It is only important at very low temperatures and for reactions involving very light atoms. For the simplest model case of a square barrier the tunneling probability is approximately

$$P = \exp\left\{-2\sqrt{\frac{2m(V_0 - E)}{\hbar^2}}a\right\}. \tag{15.48}$$

The tunneling probability depends on the mass m but is independent on temperature (Fig. 15.5).

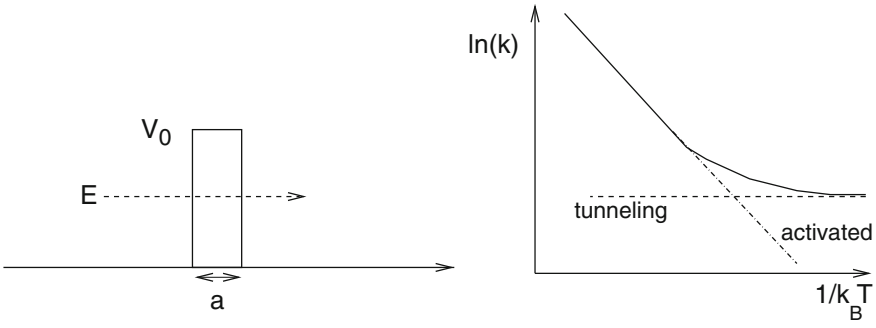

Fig. 15.5 Tunneling through a rectangular barrier. *Left* the tunneling probability depends on the height and width of the barrier. *Right* at low temperatures, tunneling dominates (*dashed*). At higher temperatures, activated behavior is observed (*dash-dotted*)

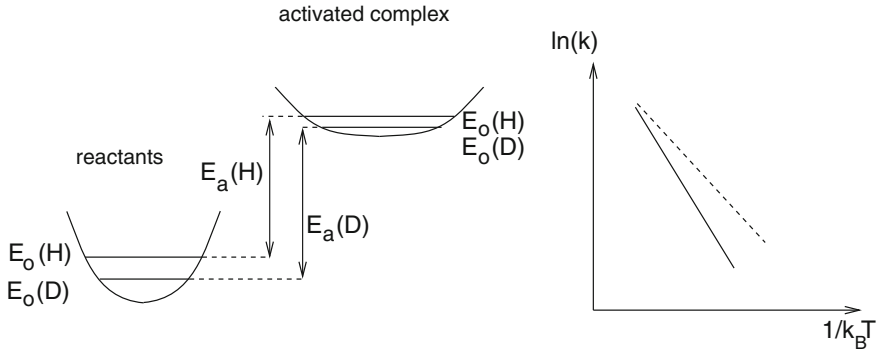

Fig. 15.6 Isotope dependence of the activation energy

The second origin of isotope effects is the difference in activation energy for reactions involving different isotopes. Vibrational frequencies and therefore vibrational zero point energies depend on the reduced mass μ of the vibrating system

$$\hbar\omega = \frac{\hbar}{2\pi}\sqrt{\frac{f}{\mu}}. \tag{15.49}$$

Since the transition state is usually more loosely bound than the reactants, the vibrational levels are more closely spaced. Therefore, the activation energy is higher for the heavier isotopomer (a normal isotope effect). The maximum isotope effect is obtained when the bond involving the isotope is completely broken in the transition state. Then the difference in activation energies is simply the difference in zero point energies of the reactants (Fig. 15.6).

15.6 General Rate Expressions

The potential energy surface has a saddle point in the transition state region. The surface S^*, passing through that saddle point along the direction of steepest ascent, defines the border separating the reactants from the products in quite a natural way. We introduce the so-called intrinsic reaction coordinate (IRC) q_r as the path of steepest descent from the cole connecting reactants and products. We set $q_r = 0$ for the points on the surface S^*. The instantaneous rate $r(t)$ is given by the flux of systems that cross the surface S^* at time t and are on the product side at $t \to \infty$. This definition allows for multiple crossings of the surface S^*. In general, however, it will depend on how exactly the surface S^* is chosen. Only if the fluxes become stationary, this dependence vanishes.

15.6.1 The Flux Operator

Classically, the flux is the product of the number of systems passing through the surface S^* and their velocity v_r normal to that surface. As we defined the reaction coordinate q_r to be normal to the surface S^*, the velocity is

$$v_r = \frac{dq_r}{dt} \tag{15.50}$$

and the classical flux is

$$< F >= \int d^{n-1}q \int d^n p \, v_r W(q, p, t) = \int d^n q \int d^n p \, \delta(q_r) \frac{p_r}{m_r} W(q, p, t). \tag{15.51}$$

Here $W(q, p, t)$ is the phase space distribution and m_r is the reduced mass corresponding to the coordinate q_r. We may therefore define the classical flux operator

$$F(q, p) = \delta(q_r) \frac{p_r}{m_r}. \tag{15.52}$$

In the quantum mechanical case we have to modify this definition since p and q do not commute. It can be shown that we have to use the symmetrized product

$$F = \frac{1}{2m_r}(p_r \delta(q_r) + \delta(q_r) p_r) = \frac{1}{2m_r}\{p_r, \delta(q_r)\} \tag{15.53}$$

with

$$p_r = \frac{\hbar}{\mathrm{i}} \frac{\partial}{\partial q_r}. \tag{15.54}$$

The projection operator on to the systems on the product side is simply given by

$$P = \theta(q_r). \tag{15.55}$$

However, we need the projector $P(t)$ on that states that at some time t in the future are on the product side. If H is the system Hamiltonian then

$$P(t) = \mathrm{e}^{\mathrm{i}Ht/\hbar} \quad \theta(q_r) \quad \mathrm{e}^{\mathrm{i}Ht/\hbar} \tag{15.56}$$

and that part of the density matrix $\rho(t)$ that will end in the product side in the far future is

$$\lim_{t' \to \infty} P(t' - t) \rho(t) P(t' - t). \tag{15.57}$$

The rate is given by

$$r(t) = \lim_{t' \to \infty} tr\left(P(t'-t)\rho(t)P(t'-t)F\right). \tag{15.58}$$

The time dependence of the density matrix is given by the van Neumann equation

$$i\hbar \frac{\mathrm{d}\rho(t)}{\mathrm{d}t} = [H, \rho(t)]. \tag{15.59}$$

In thermal equilibrium

$$\rho_{eq} = Q^{-1} \exp(-\beta H) \qquad Q = tr\,(\exp(-\beta H)) \tag{15.60}$$

is time independent as $[\exp(-\beta H), H] = 0$. It can be shown that for $t' \to \infty$ the density matrix ρ_{eq} and the projector $P(t)$ commute.[5]

$$\lim_{t' \to \infty} P(t'-t)\rho_{eq}P(t'-t) = \lim_{t' \to \infty} P(t')\rho_{eq}. \tag{15.61}$$

The rate will then be also independent of t

$$r = Q^{-1} \lim_{t' \to \infty} tr\left(\mathrm{e}^{-\beta H}\mathrm{e}^{\mathrm{i}Ht'/\hbar}\,\theta(q_r)\,\mathrm{e}^{-\mathrm{i}Ht'/\hbar}\,F\right). \tag{15.62}$$

This expression can be modified such that the limit operation does not appear explicitly any more. To that end, we note that the trace vanishes for $t' = 0$[6] and

$$\begin{aligned} r &= Q^{-1} tr\left(\mathrm{e}^{-\beta H}\mathrm{e}^{\mathrm{i}Ht'/\hbar}\,\theta(q_r)\,\mathrm{e}^{-\mathrm{i}Ht'/\hbar}\,F\right)\Big|_{t'=0}^{t'=\infty} \\ &= Q^{-1}\int_0^\infty \frac{d}{dt'}\left(\mathrm{e}^{-\beta H}\mathrm{e}^{\mathrm{i}Ht'/\hbar}\,\theta(q_r)\,\mathrm{e}^{-\mathrm{i}Ht'/\hbar}\,F\right)dt'. \end{aligned} \tag{15.63}$$

For the derivative we find

$$\frac{d}{dt}\mathrm{e}^{\mathrm{i}Ht'/\hbar}\,\theta(q_r)\,\mathrm{e}^{-\mathrm{i}Ht'/\hbar} = \frac{\mathrm{i}}{\hbar}\mathrm{e}^{\mathrm{i}Ht'/\hbar}\,[H, \theta(q_r)]\,\mathrm{e}^{-\mathrm{i}Ht'/\hbar}. \tag{15.64}$$

[5] Asymptotically, the states on the product side will leave the reaction zone with positive momentum p_r, so that we may replace $\theta(q_r)$ with $\theta(p_r)$. Again asymptotically these states are eigenfunctions of the Hamiltonian, so that $P(t = \infty)$ and $\exp(-\beta H)$ commute.

[6] This follows from time inversion symmetry: The trace has to be symmetric with respect to that operation. Time inversion changes $p_r \to -p_r$. The operators ρ and q_r are not affected. So the trace has to be symmetric and antisymmetric at the same time.

Since only the kinetic energy $p_r^2/2m_r$ does not commute with $\theta(q_r)$ the commutator is

$$[H, \theta(q_r)] = \left[\frac{p_r^2}{2m_r}, \theta(q_r)\right] = \frac{\hbar}{\mathrm{i}}\left(\frac{\partial}{\partial q_r}\frac{p_r}{2m_r}\theta(q_r) - \theta(q_r)\frac{\partial}{\partial q_r}\frac{p_r}{2m_r}\right)$$
$$= \frac{\hbar}{\mathrm{i}}\left(\frac{p_r}{2m_r}\delta(q_r) + \frac{p_r}{2m_r}\theta(q_r)\frac{\partial}{\partial q_r} - \theta(q_r)\frac{\partial}{\partial q_r}\frac{p_r}{2m_r}\right)$$
$$= \frac{\hbar}{\mathrm{i}}\left(\frac{p_r}{2m_r}\delta(q_r) + \delta(q_r)\frac{p_r}{2m_r}\right) = \frac{\hbar}{\mathrm{i}}F. \tag{15.65}$$

Therefore, we can express the reaction rate as an integral over the flux–flux correlation function

$$r = Q^{-1}\int_0^\infty tr\left(\mathrm{e}^{-\beta H}F(t)F(0)\right)dt = \int_0^\infty < F(t)F(0) > dt. \tag{15.66}$$

Ultimately, this expression for the reaction rate has been used a lot in numerical computations. It is quite general and may easily be extended to nonadiabatic reactions.

Problems

15.1 Transition State Theory

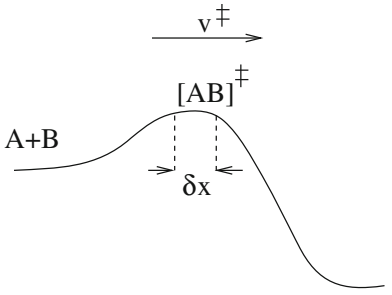

Instead of using a vibrational partition function to describe the motion of the activated complex over the reaction barrier, we can also use a translational partition function. We consider all complexes lying within a distance δx of the barrier to be activated complexes. Use the translational partition function for a particle of mass m in a box of length δx to obtain the TST rate constant. Assume that the average velocity of the particles moving over the barrier is[7]

$$v^\ddagger = \frac{1}{2}\sqrt{\frac{2k_BT}{\pi m^\ddagger}}.$$

[7]The particle moves to the left or right side with equal probability.

15.2 Harmonic Transition State Theory

For systems such as solids, which are well described as harmonic oscillators around stationary points, the harmonic form of TST is often a good approximation, which can be used to evaluate the TST rate constant, which can then be written as the product of the probability of finding the system in the transition state and the average velocity at the transition state.

$$k_{TST} = < v\delta(x - x^{\ddagger}) > .$$

For a one-dimensional model assume that the transition state is an exit point from the parabola at some position $x = x^{\ddagger}$ with energy $\Delta E = m\omega^2 x^{\ddagger 2}/2$ and evaluate the TST rate constant.

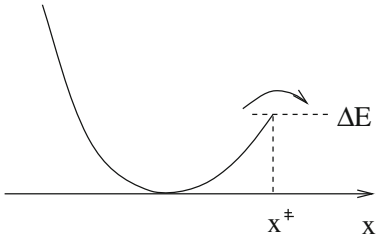

Chapter 16
Marcus Theory of Electron Transfer

In 1992, Rudolph Marcus received the Nobel Prize for chemistry. His theory is currently the dominant theory of electron transfer in chemistry. Originally Marcus explained outer sphere electron transfer, introducing reorganization energy and electronic coupling to relate the thermodynamic transition state to nonequilibrium fluctuations of the medium polarization [56–58]. We begin with a phenomenological description including diffusional motion of the reactands. Then, we apply a simplified model with one reaction coordinate to calculate the reaction rate as a function of reorganization energy and reaction free enthalpy. Next, we apply a continuum model for the dielectric medium and derive the free energy contribution of the nonequilibrium polarization quite generally. Reorganization energy and activation energy are calculated and transition state theory is applied to calculate the rate constant. We consider a model system consisting of two spherical reactants to calculate the reorganization energy explicitly and discuss charge separation and charge shift processes. We introduce the energy gap as a reaction coordinate and include inner shell reorganization. Finally, the mutual dependency of the electronic wavefunction and the polarization are discussed within a simple model for charge delocalization and self-trapping.

16.1 Phenomenological Description of ET

We want to describe the rate of electron transfer (ET) between two species, D and A, in solution. If D and A are neutral, this is an charge separation process

$$\mathrm{D} + \mathrm{A} \rightarrow \mathrm{D}^{+} + \mathrm{A}^{-}. \tag{16.1}$$

If the charge is transferred from one molecule to the other this is a charge resonance process

$$\mathrm{D}^{-} + \mathrm{A} \rightarrow \mathrm{D} + \mathrm{A}^{-} \tag{16.2}$$

P.O.J. Scherer and S.F. Fischer, *Theoretical Molecular Biophysics*,
Biological and Medical Physics, Biomedical Engineering,
DOI 10.1007/978-3-662-55671-9_16

or

$$\mathrm{D} + \mathrm{A}^{+} \rightarrow \mathrm{D}^{+} + \mathrm{A}. \tag{16.3}$$

In the following, we want to treat all these kinds of processes together. Therefore, from now on the symbols D and A implicitly have the meaning D^{Z_D} and A^{Z_A} and the general reaction scheme

$$\mathrm{D}^{Z_D} + \mathrm{A}^{Z_A} \rightarrow \mathrm{D}^{Z_D+1} + \mathrm{A}^{Z_A-1} \tag{16.4}$$

will be simply denoted as

$$\mathrm{D} + \mathrm{A} \rightarrow \mathrm{D}^{+} + \mathrm{A}^{-}. \tag{16.5}$$

Marcus theory is a phenomenological theory, in which the assumption is made, that ET proceeds in the following three steps:

(i) The two species approach each other by diffusive motion and form the so-called encounter complex

$$\mathrm{D} + \mathrm{A} \underset{k_{-dif}}{\overset{k_{dif}}{\rightleftharpoons}} [\mathrm{D} - \mathrm{A}]^{\ddagger}. \tag{16.6}$$

(ii) In the activated complex ET takes place

$$[\mathrm{D} - \mathrm{A}]^{\ddagger} \underset{k_{-et}}{\overset{k_{et}}{\rightleftharpoons}} [\mathrm{D}^{+}\mathrm{A}^{-}]^{\ddagger}. \tag{16.7}$$

The actual ET is much faster than the motion of the nuclei. The nuclear conformation of the activated complex and the solvent polarization do not change. According to the Franck–Condon principle, the two states $[D - A]^{\ddagger}$ and $[D^{+}A^{-}]^{\ddagger}$ have to be isoenergetic.

(iii) After the transfer, the polarization returns to a new equilibrium and the products separate

$$[\mathrm{D}^{+}\mathrm{A}^{-}]^{\ddagger} \overset{k_{sep}}{\rightarrow} \mathrm{D}^{+} + \mathrm{A}^{-}. \tag{16.8}$$

The overall reaction rate is

$$r = \frac{\mathrm{d}}{\mathrm{d}t} c_{A^-} = k_{sep} c_{[D^+A^-]^{\ddagger}}. \tag{16.9}$$

We want to calculate the observed quenching rate

$$r = -\frac{\mathrm{d}}{\mathrm{d}t}c_D = k_q c_D c_A. \tag{16.10}$$

We consider the stationary state

$$0 = \frac{\mathrm{d}}{\mathrm{d}t}c_{[D-A]^\ddagger} = \frac{\mathrm{d}}{\mathrm{d}t}c_{[D^+A^-]^\ddagger}. \tag{16.11}$$

We deduce that

$$0 = k_{dif} c_D c_A + k_{-et} c_{[D^+A^-]^\ddagger} - (k_{-dif} + k_{et}) c_{[D-A]^\ddagger} \tag{16.12}$$

$$0 = k_{et} c_{[D-A]^\ddagger} - (k_{-et} + k_{sep}) c_{[D^+A^-]^\ddagger}. \tag{16.13}$$

Eliminating the concentration of the encounter complex from these two equations, we find

$$c_{[D^+A^-]^\ddagger} = \frac{k_{et}}{k_{-et} + k_{sep}} c_{[D-A]^\ddagger} = \frac{k_{et} k_{dif}}{k_{-dif} k_{-et} + k_{-dif} k_{sep} + k_{et} k_{sep}} c_D c_A \tag{16.14}$$

and the observed quenching rate is

$$k_q = \frac{k_{dif}}{1 + \frac{k_{-dif}}{k_{et}} + \frac{k_{-dif} k_{-et}}{k_{et} k_{sep}}}. \tag{16.15}$$

The reciprocal quenching rate can be written as

$$\frac{1}{k_q} = \frac{1}{k_{dif}} + \frac{k_{-dif}}{k_{dif} k_{et}} + \frac{k_{-dif} k_{-et}}{k_{dif} k_{et} k_{sep}}. \tag{16.16}$$

There are some interesting limiting cases:

- If $k_{et} \gg k_{-dif}$ and $k_{sep} \gg k_{-et}$, then the observed quenching rate is given by the diffusion rate $k_q = k_{dif}$ and the ET rate is limited by the formation of the activated complex.
- If the probability of ET is very small $k_{et} \ll k_{-dif}$ and $k_{-et} \ll k_{dif}$, then the quenching rate is given by $k_q = k_{et} k_{dif} / k_{-dif} = k_{et} K_{dif}$.
- If diffusion is not important as in solids or proteins and in the absence of further decay channels, the quenching rate is given by $k_q^{-1} \approx k_{et}^{-1}$.

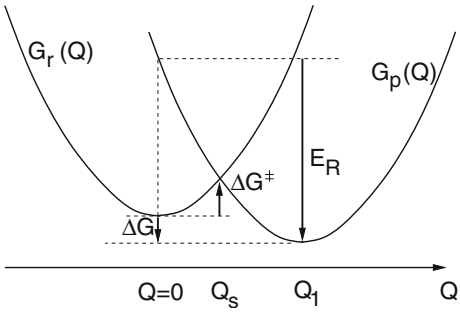

Fig. 16.1 Displaced oscillator model

16.2 Simple Explanation of Marcus Theory

The TST expression for the ET rate is

$$k_{et} = \frac{\omega_N}{2\pi}\kappa_{el}\mathrm{e}^{-\Delta G^{\ddagger}/k_B T} \tag{16.17}$$

where κ_{et} describes the probability of a transition between the two electronic states DA and D^+A^- and ω_N is the effective frequency of the nuclear motion. We consider a collective reaction coordinate Q, which summarizes the polarization coordinates of the system (Fig. 16.1).

Initially, the polarization is in equilibrium with the reactants and for small polarization fluctuations, series expansion of the Gibbs free energy gives

$$G_r(Q) = G_r^{(0)} + \frac{a}{2}Q^2. \tag{16.18}$$

If the polarization change induced by the ET is not too large (no dielectric saturation), the potential curve for the final state will have the same curvature but is shifted to a new equilibrium value Q_1

$$G_p(Q) = G_p^{(0)} + \frac{a}{2}(Q - Q_1)^2 = G_r^{(0)} + \Delta G + \frac{a}{2}(Q - Q_1)^2. \tag{16.19}$$

In the new equilibrium, the final state is stabilized by the reorganization energy[1]

$$E_R = -(G_p(Q_1) - G_p(0)) = \frac{a}{2}Q_1^2. \tag{16.20}$$

The transition between the two states is only possible if due to some thermal fluctuations the crossing point is reached which is at

[1] Sometimes the reorganization energy is defined as the negative quantity $G_P(Q_1) - G_P(0)$.

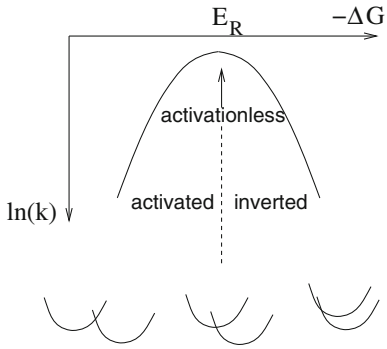

Fig. 16.2 Marcus parabola

$$Q_s = \frac{\frac{a}{2}Q_1^2 + \Delta G}{aQ_1} = \frac{E_R + \Delta G}{\sqrt{2aE_R}}. \tag{16.21}$$

The corresponding activation energy is

$$\Delta G^{\ddagger} = \frac{a}{2}Q_s^2 = \frac{(\Delta G + E_R)^2}{4E_R} \tag{16.22}$$

hence the rate expression becomes

$$k_{et} = \frac{\omega_N}{2\pi}\kappa_{et}\exp\left(-\frac{(\Delta G + E_R)^2}{4E_R k_B T}\right). \tag{16.23}$$

If we plot the logarithm of the rate as a function of the driving force ΔG, we obtain the famous Marcus parabola which has a maximum at $\Delta G = -E_R$ (Fig. 16.2).

16.3 Free Energy Contribution of the Nonequilibrium Polarization

In Marcus theory, the solvent is treated in a continuum approximation. The medium is characterized by its static dielectric constant ε_{st} and its optical dielectric constant $\varepsilon_{op} = \varepsilon_0 n^2$. The displacement $\mathbf{D}$ is generated by the charge distribution ϱ

$$\text{div}\,\mathbf{D} = \varrho. \tag{16.24}$$

In equilibrium it is related to the electric field by

$$\mathbf{D} = \varepsilon_0\mathbf{E} + \mathbf{P} = \varepsilon\mathbf{E}. \tag{16.25}$$

Here $\mathbf{P}$ is the polarization, which is nothing else but the induced dipole density. It consists of two parts:[59]

(i) The optical or electronical polarization $\mathbf{P}_{op}$. It is due to the induced dipole moments due to the response of the molecular electrons to the applied field. At optical frequencies, the electrons still move fast enough to follow the electric field adiabatically.
(ii) The inertial polarization $\mathbf{P}_{in}$ which is due to the reorganization of the solvent molecules (reorientation of the dipoles, changes of molecular geometry). This part of the polarization corresponds to the static dielectric constant. The nuclear motion of the solvent molecules cannot follow the rapid oscillations at optical frequencies.

The total frequency-dependent polarization is

$$\mathbf{P}(\omega) = \mathbf{P}_{op}(\omega) + \mathbf{P}_{in}(\omega) = \mathbf{D}(\omega) - \varepsilon_0 \mathbf{E}(\omega) = (\varepsilon(\omega) - \varepsilon_0)\mathbf{E}(\omega). \tag{16.26}$$

In the static limit this becomes

$$\mathbf{P}_{op} + \mathbf{P}_{in} = (\varepsilon_{st} - \varepsilon_0)\mathbf{E} \tag{16.27}$$

and at optical frequencies

$$\mathbf{P}_{op} = (\varepsilon_{op} - \varepsilon_0)\mathbf{E}. \tag{16.28}$$

Hence the contribution of the inertial polarization is in the static limit

$$\mathbf{P}_{in} = (\varepsilon_{st} - \varepsilon_{op})\mathbf{E}. \tag{16.29}$$

In general $\operatorname{rot}\mathbf{D} \neq 0$ and the calculation of the field for given charge distribution is difficult. Therefore, we use a model of spherical ions behaving as ideal conductors with the charge distributed over the surface. Then in our case, the displacement is normal to the surface and $\operatorname{rot}\mathbf{D} = 0$ and the displacement is the same as it would be generated by the charge distribution ϱ in vacuum. The corresponding electric field in vacuum would be $\varepsilon_0^{-1}\mathbf{D}$ and the field in the medium can be expressed as

$$\begin{aligned}\mathbf{E} &= \frac{1}{\varepsilon_0}(\mathbf{D} - \mathbf{P}) = \frac{1}{\varepsilon_0}\mathbf{D} - \frac{1}{\varepsilon_0}(\mathbf{P}_{op} + \mathbf{P}_{in}) \\ &= \frac{1}{\varepsilon_0}(\mathbf{D} - \mathbf{P}_{in}) - \frac{1}{\varepsilon_0}(\varepsilon_{op} - \varepsilon_0)\mathbf{E} \\ \mathbf{E} &= \frac{1}{\varepsilon_{op}}(\mathbf{D} - \mathbf{P}_{in})\end{aligned} \tag{16.30}$$

where we assumed that the optical polarization reacts instantaneously to changes of the charge distribution or to fluctuations of the inertial polarization. In equilibrium (16.29) gives

$$\mathbf{E} = \frac{1}{\varepsilon_{op}}(\mathbf{D} - (\varepsilon_{st} - \varepsilon_{op})\mathbf{E})$$
$$\mathbf{E} = \frac{1}{\varepsilon_{st}}\mathbf{D}. \tag{16.31}$$

If the polarization is in equilibrium with the field $\frac{1}{\varepsilon_0}\mathbf{D}$ produced by the charge distribution of either AB or A^+B^- the free energy G of the two configurations will, in general, not be the same. We designate these two configurations as I and II respectively. Marcus calculated the free energy of a nonequilibrium polarization for which the free energies of the reaction complexes $[AB]^\ddagger$ and $[A^+B^-]^\ddagger$ become equal. The contribution to the free energy is

$$G_{el} = \int d^3r \int \mathbf{E} d\mathbf{D} = \frac{1}{\varepsilon_{op}} \int d^3r \int (\mathbf{D} - \mathbf{P}_{in}) d\mathbf{D} \tag{16.32}$$

which can be divided into two contributions:

(i) The energy without inertial polarization:

$$G_{el,0} = \frac{1}{\varepsilon_{op}} \int d^3r \frac{D^2}{2} \tag{16.33}$$

(ii) The contribution of the inertial polarization:

$$-\frac{1}{\varepsilon_{op}} \int d^3r \mathbf{P}_{in} d\mathbf{D} \tag{16.34}$$

In equilibrium, we have

$$\mathbf{P}_{in} = (\varepsilon_{st} - \varepsilon_{op})\mathbf{E} = (\varepsilon_{st} - \varepsilon_{op})\frac{1}{\varepsilon_{st}}\mathbf{D} = \varepsilon_{op}\left(\frac{1}{\varepsilon_{op}} - \frac{1}{\varepsilon_{st}}\right)\mathbf{D} \tag{16.35}$$

and we can express the free energy as a function of P_{in}

$$G_{el}^{eq} = G_{el,0} - \frac{1}{\frac{1}{\varepsilon_{op}} - \frac{1}{\varepsilon_{st}}} \int d^3r \frac{1}{2}\left(\frac{\mathbf{P}_{in}}{\varepsilon_{op}}\right)^2. \tag{16.36}$$

Now, we have to calculate the free energies of the activated complexes. Consider a thermal fluctuation of the inertial polarization. We will do this in two steps (Fig. 16.3).

In the first step it is assumed that the polarization is always in equilibrium with the charge distribution. However, this charge density will be chosen such that the nonequilibrium polarization $\mathbf{P}_{in}^\ddagger$ of the activated complex is generated. The electric displacement is D^*, given by

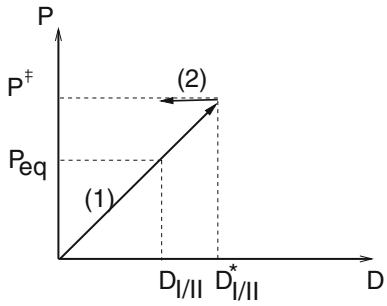

Fig. 16.3 Calculation of the free energy change

$$\frac{1}{\varepsilon_{op}}\mathbf{P}_{in}^{\ddagger} = \left(\frac{1}{\varepsilon_{op}} - \frac{1}{\varepsilon_{st}}\right)\mathbf{D}^{*}. \tag{16.37}$$

The corresponding free energy is

$$\begin{aligned}\Delta G_{el}^{1} &= \frac{1}{\varepsilon_{op}}\int d^3r \int_{D}^{D^*} \mathbf{D}d\mathbf{D} - \frac{1}{\varepsilon_{op}}\int d^3r \int_{D}^{D^*} \mathbf{P}_{in}d\mathbf{D} \\ &= G_{el,0}^{*} - G_{el,0} - \frac{1}{\frac{1}{\varepsilon_{op}} - \frac{1}{\varepsilon_{st}}}\int d^3r \frac{\mathbf{P}_{in}^{\ddagger 2} - \mathbf{P}_{in}^{2}}{2\varepsilon_{op}^{2}}.\end{aligned} \tag{16.38}$$

In the second step, the electric field of the charge distribution will be reduced to the equilibrium value while keeping the nonequilibrium polarization fixed.[2] Then this fixed polarization acts as an additional displacement

$$\mathbf{E} = \frac{1}{\varepsilon_0}(\mathbf{D} - \mathbf{P}_{in}^{\ddagger}) - \frac{1}{\varepsilon_0}\mathbf{P}_{op} \tag{16.39}$$

where the optical polarization depends on the electric field according to (16.28)

$$\mathbf{E} = \frac{1}{\varepsilon_0}(\mathbf{D} - \mathbf{P}_{in}^{\ddagger}) - \left(\frac{\varepsilon_{op}}{\varepsilon_0} - 1\right)\mathbf{E}. \tag{16.40}$$

Hence, if we treat the optical polarization as following the slow fluctuations of the inertial polarization instantaneously

$$\mathbf{E} = \frac{1}{\varepsilon_{op}}(\mathbf{D} - \mathbf{P}_{in}^{\ddagger}) \tag{16.41}$$

[2] We tacitly assume that this is possible. In general, the polarization $P_{in}^{\ddagger}$ will also modify the charge distribution on the reactants. If however, the distance between the two ions is large in comparison with the radii, these changes can be neglected. Marcus calls this the point-charge approximation.

which means, the inertial polarization is shielded by the optical polarization it creates. We may now calculate the change in free energy as

$$\begin{aligned}\Delta G^2_{el} &= \frac{1}{\varepsilon_{op}} \int d^3r \int_{D^*}^{D} (\mathbf{D} - \mathbf{P}^{\ddagger}_{in}) d\mathbf{D} \\ &= G_{el,0} - G^*_{el,0} - \int d^3r \frac{1}{\varepsilon_{op}} \mathbf{P}^{\ddagger}_{in} (\mathbf{D} - \mathbf{D}^*). \end{aligned} \tag{16.42}$$

If we substitute $\mathbf{D}*$ from (16.37) we get

$$\frac{1}{\varepsilon_{op}} \mathbf{P}^{\ddagger}_{in} (\mathbf{D} - \mathbf{D}^*) = \frac{1}{\frac{1}{\varepsilon_{op}} - \frac{1}{\varepsilon_{st}}} \frac{\mathbf{P}^{\ddagger}_{in}}{\varepsilon_{op}} \left(\frac{\mathbf{P}_{in} - \mathbf{P}^{\ddagger}_{in}}{\varepsilon_{op}} \right) \tag{16.43}$$

and the total free energy change due to the polarization fluctuation is

$$\begin{aligned} G^{\ddagger}_{el} - G^{eq}_{el} &= \Delta G^1_{el} + \Delta G^2_{el} \\ &= -\frac{1}{\frac{1}{\varepsilon_{op}} - \frac{1}{\varepsilon_{st}}} \int d^3r \frac{\mathbf{P}^{\ddagger 2}_{in} - \mathbf{P}^2_{in}}{2\varepsilon^2_{op}} \\ &\quad -\frac{1}{\frac{1}{\varepsilon_{op}} - \frac{1}{\varepsilon_{st}}} \int d^3r \frac{1}{\varepsilon^2_{op}} \mathbf{P}^{\ddagger}_{in} (\mathbf{P}_{in,eq} - \mathbf{P}^{\ddagger}_{in}) \\ &= \frac{1}{\frac{1}{\varepsilon_{op}} - \frac{1}{\varepsilon_{st}}} \int d^3r \frac{1}{2} \left(\frac{\mathbf{P}^{\ddagger}_{in} - \mathbf{P}_{in,eq}}{\varepsilon_{op}} \right)^2 . \end{aligned} \tag{16.44}$$

16.4 Activation Energy

The free energy $G^{\ddagger}_{el}$ is a functional of the polarization fluctuation

$$\delta\mathbf{P} = \mathbf{P}^{\ddagger}_{in} - \mathbf{P}_{in}. \tag{16.45}$$

If we minimize the free energy

$$\delta G^{\ddagger}_{el} = 0 \tag{16.46}$$

we find that

$$\delta\mathbf{P} = 0 \qquad G^{\ddagger}_{el} = G^{eq}_{el}. \tag{16.47}$$

Marcus asks now, for which polarizations $\mathbf{P}^{\ddagger}_{in}$ the two states I and II become isoenergetic,i.e.

$$\Delta U^{\ddagger} = U_{II}^{\ddagger} - U_{I}^{\ddagger} = 0. \tag{16.48}$$

We want to rephrase the last condition in terms of the free energy

$$G = U - TS + pV \approx U - TS. \tag{16.49}$$

We conclude that

$$\Delta G^{\ddagger} = G_{II}^{\ddagger} - G_{I}^{\ddagger} = -T\Delta S^{\ddagger}. \tag{16.50}$$

Here (Fig. 16.4)

$$\begin{aligned} G_{I}^{\ddagger} &= \frac{1}{\frac{1}{\varepsilon_{op}} - \frac{1}{\varepsilon_{st}}} \frac{1}{2} \int d^3r \left(\frac{\delta \mathbf{P}_I}{\varepsilon_{op}} \right)^2 + G_{el,I}^{eq}(R) - G_{el,I}^{eq}(\infty) + G_{I}^{\infty} \\ G_{II}^{\ddagger} &= \frac{1}{\frac{1}{\varepsilon_{op}} - \frac{1}{\varepsilon_{st}}} \frac{1}{2} \int d^3r \left(\frac{\delta \mathbf{P}_{II}}{\varepsilon_{op}} \right)^2 + G_{el,II}^{eq}(R) - G_{el,II}^{eq}(\infty) + G_{II}^{\infty}. \end{aligned} \tag{16.51}$$

The quantity

$$\Delta G_{\infty} = G_{II}^{\infty} - G_{I}^{\infty} = \Delta G_{vac} + \Delta G_{solv,\infty} \tag{16.52}$$

is the difference of free energies for an ideal solution of A and B on the one side and A^+ and B^- on the other side at infinite distance $R \to \infty$. Usually it is determined experimentally. It contains all the information on the internal structure of the ions. The entropy difference is the difference of internal entropies of the reactants, since the contribution from the polarization drops out due to $\mathbf{P}_{in,I}^{\ddagger} = \mathbf{P}_{in,II}^{\ddagger}$. Usually this entropy difference is small. The electrostatic energies $G_{el,I/II}^{eq}$ a are composed of the polarization contribution (the solvation free energy) and the mutual interaction of the reactants which will be considered later. The reaction free energy is

$$\Delta G_{eq} = \Delta G_{\infty} + \Delta G_{el}^{eq}(R) - \Delta G_{el}^{eq}(\infty). \tag{16.53}$$

It can be easily seen that the condition $\Delta G^{\ddagger} = 0$ will be fulfilled for infinitely many polarizations $\mathbf{P}_{in}^{\ddagger}$. We will, therefore, look for that one which minimizes simultaneously the free energy of the transition state $G_{I,II}^{\ddagger}$. We introduce a Lagrange parameter m to impose the isoenergeticity condition

$$\delta \left[G_{I}^{\ddagger}(\mathbf{P}_{in}^{\ddagger}) + m(G_{II}^{\ddagger}(\mathbf{P}_{in}^{\ddagger}) - G_{I}^{\ddagger}(\mathbf{P}_{in}^{\ddagger})) \right] = 0. \tag{16.54}$$

The variation is with respect to $\mathbf{P}_{in}^{\ddagger}$ or, equivalently with respect to $\delta \mathbf{P}_I$ for fixed change of the inertial polarization

$$\Delta \mathbf{P}_{in} = \delta \mathbf{P}_I - \delta \mathbf{P}_{II} = (\mathbf{P}_{in}^{\ddagger} - \mathbf{P}_{I,in}) - (\mathbf{P}_{in}^{\ddagger} - \mathbf{P}_{II,in}) = \mathbf{P}_{II,in} - \mathbf{P}_{I,in} \tag{16.55}$$

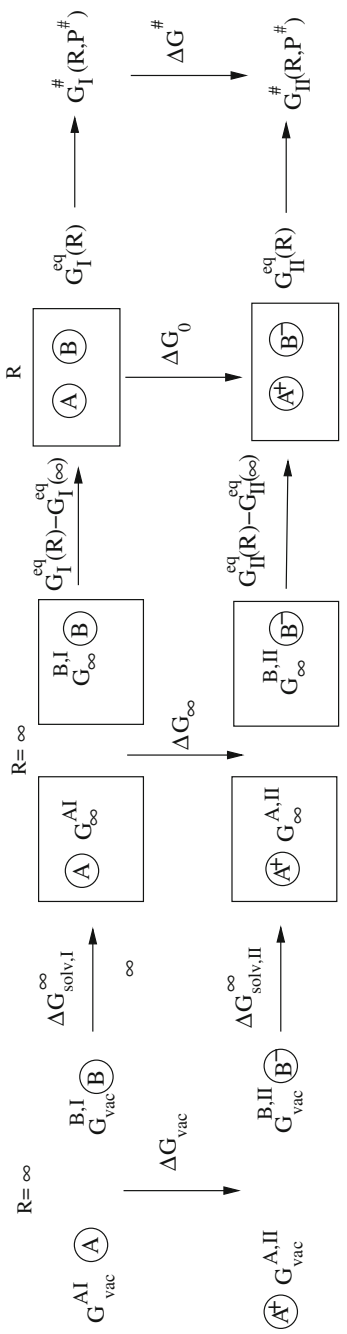

Fig. 16.4 Free energy differences

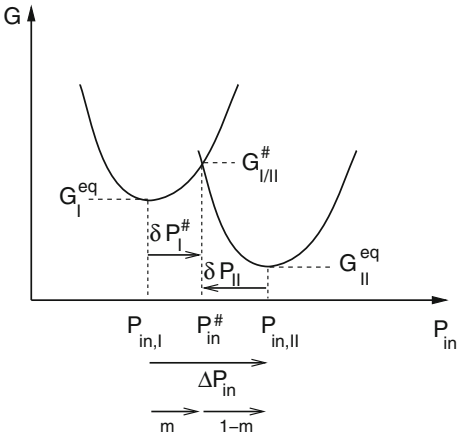

Fig. 16.5 Variation of the nonequilibrium polarization

We have to solve

$$\delta\Big[(1-m)G_I^{\ddagger}(\mathbf{P}_{I,in}+\delta\mathbf{P}_I)+mG_{II}^{\ddagger}(\mathbf{P}_{II,in}-\Delta\mathbf{P}_{in}+\delta\mathbf{P}_{I,in})\Big]. \tag{16.56}$$

Due to the quadratic dependence of the free energies, we find the condition

$$[(1-m)\delta\mathbf{P}_I+m(\delta\mathbf{P}_I-\Delta\mathbf{P}_{in})]=0 \tag{16.57}$$

and hence the solution (Fig. 16.5)

$$\delta\mathbf{P}_I^{\ddagger}=m\Delta\mathbf{P}_{in}. \tag{16.58}$$

The Lagrange parameter m is determined by inserting this solution into the isoenergicity condition,

$$\begin{aligned}-T\Delta S&=\Delta G^{\ddagger}(\mathbf{P}_{in}^{\ddagger})\\&=G_{II}^{\ddagger}(\mathbf{P}_{in,II}+(m-1)\Delta P_{in})-G_I^{\ddagger}(\mathbf{P}_{in,I}+m\Delta\mathbf{P}_{in})\\&=\Delta G_{eq}+((m-1)^2-m^2)\frac{1}{\frac{1}{\varepsilon_{op}}-\frac{1}{\varepsilon_{st}}}\frac{1}{2}\int d^3r\left(\frac{\Delta\mathbf{P}_{in}}{\varepsilon_{op}}\right)^2\\&=\Delta G_{eq}+(1-2m)\lambda\end{aligned} \tag{16.59}$$

where

$$\begin{aligned}\lambda&=G_{II}(\mathbf{P}_{in,II}-\Delta\mathbf{P}_{in})-G_{II}(\mathbf{P}_{in,II})\\&=\frac{1}{\frac{1}{\varepsilon_{op}}-\frac{1}{\varepsilon_{st}}}\frac{1}{2}\int d^3r\left(\frac{\Delta\mathbf{P}_{in}}{\varepsilon_{op}}\right)^2=\left(\frac{1}{\varepsilon_{op}}-\frac{1}{\varepsilon_{st}}\right)\frac{1}{2}\int d^3r\,(\Delta\mathbf{D})^2\end{aligned} \tag{16.60}$$

is the reorganization energy. Solving for m we find

$$m = \frac{\Delta G_{eq} + T\Delta S^{\ddagger} + \lambda}{2\lambda}. \tag{16.61}$$

The free energy of activation is given by

$$\begin{aligned}\Delta G_a = G_I^{\ddagger} - G_I^{eq} &= m^2 \frac{1}{\frac{1}{\varepsilon_{op}} - \frac{1}{\varepsilon_{st}}} \frac{1}{2} \int d^3r \left(\frac{\Delta \mathbf{P}_{in}}{\varepsilon_{op}}\right)^2 \\ &= m^2\lambda = \frac{(\Delta G_{eq} + T\Delta S^{\ddagger} + \lambda)^2}{4\lambda}.\end{aligned} \tag{16.62}$$

Finally, we insert this into the TST rate expression to find

$$k \sim \mathrm{e}^{-\Delta G_a/k_B T} \sim \exp\left\{-\frac{(\Delta G_{eq} + T\Delta S^{\ddagger} + \lambda)^2}{4\lambda k_B T}\right\}. \tag{16.63}$$

16.5 Simple Model Systems

We will now calculate reorganization energy and free energy differences explicitly for a model system consisting of two spherically reactants. We assume that the charge distribution of the reactants is not influenced by mutual Coulomb interaction or changes of the medium polarization (we apply the point charge approximation again) (Fig. 16.6).

We have already calculated the solvation energy at large distances (page 48)

$$\left(-\frac{Q_A^2}{8\pi a_A} - \frac{Q_B^2}{8\pi a_B}\right)\left(\frac{1}{\varepsilon_0} - \frac{1}{\varepsilon_{st}}\right) \tag{16.64}$$

from which we find the polarization energy at large distances

$$G_{el}^{eq}(R = \infty) = \frac{1}{8\pi\varepsilon_{st}}\left(\frac{Q_A^2}{a_A} + \frac{Q_B^2}{a_B}\right). \tag{16.65}$$

We now consider a finite distance R. If we take the origin of the coordinate system to coincide with the center of the reactant A, then the dielectric displacement is

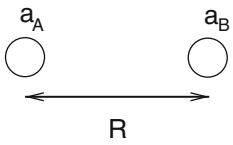

Fig. 16.6 Simple donor–acceptor geometry

$$\mathbf{D}_{I/II}(\mathbf{r}) = \frac{1}{4\pi}\left(Q_{A,I/II}\frac{\mathbf{r}}{r^3} + Q_{B,I/II}\frac{\mathbf{r}-\mathbf{R}}{|\mathbf{r}-\mathbf{R}|^3}\right) \tag{16.66}$$

and the polarization free energy

$$G^{eq}_{el,I/II} = \int d^3r \frac{D^2}{2\varepsilon_{st}} \tag{16.67}$$

contains two types of integrals. The first is

$$I_1 = \int \frac{d^3r}{r^4}. \tag{16.68}$$

The range of this integral is outside the spheres A and B. As the integrand falls off rapidly with distance, we may extend the integral over the volume of the other sphere. Introducing polar coordinates we find

$$I_1 \approx \int_a^\infty 4\pi \frac{dr}{r^2} = \frac{4\pi}{a}. \tag{16.69}$$

The second kind of integral is

$$I_2 = \int d^3r \frac{\mathbf{r}(\mathbf{r}-\mathbf{R})}{r^3|\mathbf{r}-\mathbf{R}|^3}. \tag{16.70}$$

Again, we extend the integration range and use polar coordinates

$$I_2 \approx 2\pi \int_0^\pi \sin\theta\, d\theta \int_0^\infty r^2 dr \frac{r^2 - rR\cos\theta}{r^3(r^2+R^2-2rR\cos\theta)^{3/2}}. \tag{16.71}$$

The integral over r gives

$$\int_0^\infty \frac{r - R\cos\theta}{(r^2+R^2-2rR\cos\theta)^{3/2}} dr = -\frac{1}{\sqrt{r^2+R^2-2rR\cos\theta}}\Big|_0^\infty = \frac{1}{R} \tag{16.72}$$

and the integral over θ then gives

$$I_2 = \int_0^\pi \frac{2\pi\sin\theta}{R} d\theta = \frac{4\pi}{R}. \tag{16.73}$$

Together, we have the polarization free energy

$$\begin{aligned} G^{eq}_{el} &= \frac{1}{2\varepsilon_{st}}\int d^3r\, D^2_\varrho = \frac{1}{8\pi\varepsilon_{st}}\left(\frac{Q_A^2}{a_A} + \frac{Q_B^2}{a_B}\right) + \frac{1}{8\pi\varepsilon_{st}}\frac{2Q_AQ_B}{R} \\ &= G^{eq}(\infty) + \frac{Q_AQ_B}{4\pi\varepsilon_{st}R} \end{aligned} \tag{16.74}$$

and the difference

$$G^{eq}_{el,II} - G^{eq}_{el,I} = \frac{e^2}{8\pi\varepsilon_{st}} \left(\frac{1+2Z_A}{a_A} + \frac{1-2Z_B}{a_B} + 2\frac{Z_B - Z_A - 1}{R} \right). \tag{16.75}$$

Similarly, the reorganization energy is

$$\begin{aligned} \lambda &= \frac{1}{2} \left(\frac{1}{\varepsilon_{op}} - \frac{1}{\varepsilon_{st}} \right) \int d^3r \, (\Delta \mathbf{D})^2 \\ &= \frac{1}{8\pi} \left(\frac{1}{\varepsilon_{op}} - \frac{1}{\varepsilon_{st}} \right) \left(\frac{\Delta Q_A^2}{a_A} + \frac{\Delta Q_B^2}{a_B} + \frac{2\Delta Q_A \Delta Q_B}{R} \right). \end{aligned} \tag{16.76}$$

Now since $\Delta Q_A = -\Delta Q_B = e$ we can write this as

$$\lambda = \frac{e^2}{8\pi} \left(\frac{1}{\varepsilon_{op}} - \frac{1}{\varepsilon_{st}} \right) \left(\frac{1}{a_A} + \frac{1}{a_B} - \frac{2}{R} \right). \tag{16.77}$$

We consider here the most important special cases:

16.5.1 Charge Separation

If an ion pair is created during the ET reaction ($Q_{A,I} = Q_{B,I} = 0$, $Q_{A,II} = e$, $Q_{B,II} = -e$) we have

$$\frac{Q_A^2}{a_A} + \frac{Q_B^2}{a_B} + \frac{2Q_A Q_B}{R} = \begin{cases} 0 & (I) \\ \frac{1}{a_A} + \frac{1}{a_B} - \frac{2}{R} & (II) \end{cases}. \tag{16.78}$$

The free energy is

$$\begin{aligned} G^{eq}_{el,I} &= 0 \\ G^{eq}_{el,II} &= \frac{e^2}{8\pi\varepsilon_{st}} \left(\frac{1}{a_A} + \frac{1}{a_B} - \frac{2}{R} \right) = G^{eq}_{el,II}(\infty) - \frac{e^2}{4\pi\varepsilon_{st} R} \end{aligned} \tag{16.79}$$

and the activation energy becomes

$$\Delta G_a = \frac{(\Delta G_\infty + T\Delta S^\ddagger + \lambda - \frac{e^2}{4\pi\varepsilon_{st} R})^2}{4\lambda}. \tag{16.80}$$

If the process is photoinduced, the free energy at large distance can be expressed in terms of the ionization potential of the donor, the electron affinity of the acceptor, and the energy of the optical transition (Fig. 16.7)

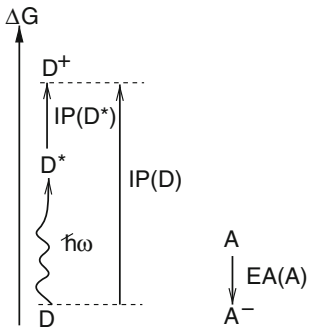

Fig. 16.7 Photoinduced charge separation

$$\Delta G_\infty = EA(A) - (IP(D) - \hbar\omega). \tag{16.81}$$

16.5.2 Charge Shift

For a charge shift reaction of the type $Q_{A,I} = Q_{B,II} = -e$, $Q_{B,I} = Q_{A,II} = 0$

$$G_I^{eq} = \frac{e^2}{8\pi\varepsilon_{st} a_A} \qquad G_{II}^{eq} = \frac{e^2}{8\pi\varepsilon_{st} a_B} \tag{16.82}$$

and for the second type $Q_{A,I} = Q_{B,II} = 0$, $Q_{B,I} = Q_{A,II} = e$

$$G_I^{eq} = \frac{e^2}{8\pi\varepsilon_{st} a_B} \qquad G_{II}^{eq} = \frac{e^2}{8\pi\varepsilon_{st} a_A}. \tag{16.83}$$

The activation energy now does not contain a Coulomb term

$$\Delta G_a = \frac{(\Delta G_\infty + T\Delta S^\ddagger + \lambda)^2}{4\lambda}. \tag{16.84}$$

16.6 The Energy Gap as the Reaction Coordinate

We want to construct one single reaction coordinate, which summarizes the polarization fluctuations. To that end we consider the energy gap

$$
\begin{aligned}
\Delta U^{\ddagger} &= \Delta G^{\ddagger} + T\Delta S^{\ddagger} \approx G_{II}^{\ddagger}(\mathbf{P}_{in}^{\ddagger}) - G_{I}^{\ddagger}(\mathbf{P}_{in}^{\ddagger}) \\
&= G_{II}^{\ddagger}(\mathbf{P}_{II,in} - \Delta\mathbf{P}_{in} + \delta\mathbf{P}_{I,in}) - G_{I}^{\ddagger}(\mathbf{P}_{I,in} + \delta\mathbf{P}_{I,in}) \\
&= \Delta G_{eq} + \frac{1}{\frac{1}{\varepsilon_{op}} - \frac{1}{\varepsilon_{st}}} \frac{1}{2} \int d^3r \left(\frac{(\delta\mathbf{P}_{I,in} - \Delta\mathbf{P}_{in})}{\varepsilon_{op}} \right)^2 \\
&\quad - \frac{1}{\frac{1}{\varepsilon_{op}} - \frac{1}{\varepsilon_{st}}} \frac{1}{2} \int d^3r \left(\frac{\delta\mathbf{P}_{I,in}}{\varepsilon_{op}} \right)^2 \\
&= \Delta G_{eq} + \frac{1}{\frac{1}{\varepsilon_{op}} - \frac{1}{\varepsilon_{st}}} \frac{1}{2} \int d^3r \frac{\Delta\mathbf{P}_{in}^2 - 2\delta\mathbf{P}_{I,in}\Delta\mathbf{P}_{in}}{\varepsilon_{op}^2} \\
&= \Delta G_{eq} + \lambda - \delta U(t)
\end{aligned}
\tag{16.85}
$$

with the thermally fluctuating energy

$$
\delta U(t) = \frac{1}{\frac{1}{\varepsilon_{op}} - \frac{1}{\varepsilon_{st}}} \int d^3r \frac{\delta\mathbf{P}_{I,in}\Delta\mathbf{P}_{in}}{\varepsilon_{op}^2}. \tag{16.86}
$$

In the equilibrium of the reactants

$$
\delta U = 0 \qquad \Delta U = \Delta G_{eq} + \lambda \quad \text{(I)} \tag{16.87}
$$

and in the equilibrium of the products (Fig. 16.8)

$$
\delta U = 2\lambda \qquad \Delta U = \Delta G_{eq} - \lambda \quad \text{(II)}. \tag{16.88}
$$

The free energies now take the form

$$
G_I = G_I^{eq} + \frac{1}{4\lambda}(\delta U)^2 \tag{16.89}
$$

$$
G_{II} = G_{II}^{eq} + \frac{1}{4\lambda}(\delta U - 2\lambda)^2. \tag{16.90}
$$

The free energy fluctuations in the reactant state are given by

$$
< (G_I - G_I^{eq} > = \frac{1}{4\lambda} < \delta U^2 > . \tag{16.91}
$$

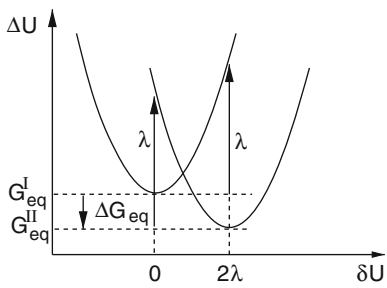

Fig. 16.8 Energy gap as reaction coordinate

If we identify this with the thermal average $k_B T/2$ of a one-dimensional harmonic motion, we have

$$< \delta U^2 > = 2k_B T\lambda. \tag{16.92}$$

The fluctuations of the energy gap can for instance be investigated with molecular dynamics methods. They can be modeled by diffusive motion in a harmonic potential $U(Q) = Q^2/4\lambda$ which leads to the equation

$$\frac{\partial}{\partial t}W(Q,t) = -D_E\left\{\frac{\partial^2}{\partial Q^2}W + \frac{1}{k_B T}\frac{\partial}{\partial Q}\left(\frac{\partial U}{\partial Q}W\right)\right\} - \kappa\delta(Q-\lambda)W \tag{16.93}$$

where the diffusion constant is

$$D_E = \frac{2k_B T\lambda}{\tau_L} \tag{16.94}$$

and τ_L is the longitudinal relaxation time of the medium.

16.7 Inner Shell Reorganization

Intramolecular modes can also contribute to the reorganization. Low-frequency modes ($\hbar\omega < k_B T$) which can be treated classically, can be taken into account by adding an inner shell contribution to the reorganization energies

$$\lambda = \lambda_{outer} + \lambda_{inner}. \tag{16.95}$$

Often C-C stretching modes at $\hbar\omega \approx 1400\,\mathrm{cm}^{-1}$ change their equilibrium positions during the ET process. They must be treated quantum mechanically.[3] Often the Franck–Condon progression of one dominant mode $\hbar\omega_v$ is used to analyze experimental data in the inverted region. Since $\hbar\omega_v \gg k_B T$ thermal occupation is negligible. In the inverted region, the vibration can accept the excess energy and reduce the activation energy (Figs. 16.9 and 16.10). Summation over all $0 \to n$ transitions leads to the rate expression

$$k = \frac{\omega}{2\pi}\kappa_{el}\sum_{n=0}^{\infty}\mathrm{e}^{-g^2}\frac{g^{2n}}{n!}\exp\left(-\frac{(\Delta G + E_R + n\hbar\omega_v)^2}{4E_R k_B T}\right) \tag{16.96}$$

where $g^2\hbar\omega_v$ is the partial reorganization energy of the stretching mode.

[3] A more general discussion follows later.

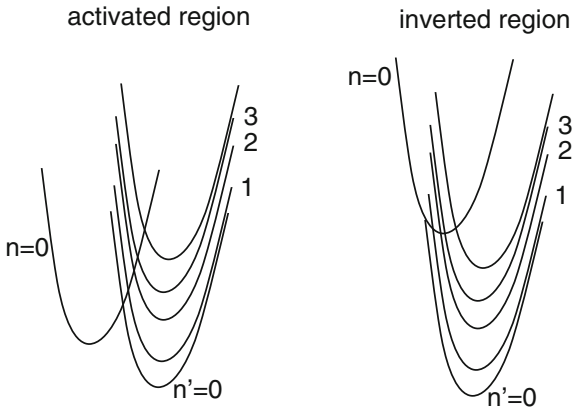

Fig. 16.9 Accepting mode. In the inverted region, vibrations can accept the excess energy

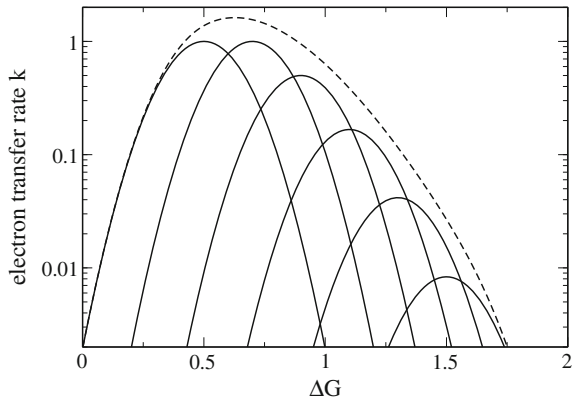

Fig. 16.10 Inclusion of a high-frequency mode progression. Equation (16.96) is evaluated for typical values of $\hbar\omega_V = 0.2eV$, $g = 1, \lambda = 0.5\,\text{eV}$ (broken *curve*). The full *curves* show the contributions of different $0 \to n$ transitions

16.8 The Transmission Coefficient for Nonadiabatic Electron Transfer

The transmission coefficient κ will be considered later in more detail. For adiabatic electron transfer it approaches unity. For nonadiabatic transfer (small crossing probability), it depends on the electronic coupling matrix element V_{et}. The quantum mechanical rate expression for nonadiabatic transfer becomes in the high temperature limit ($\hbar\omega \ll k_B T$ for all coupling modes)

$$k = \frac{2\pi V_{et}^2}{\hbar} \frac{\mathrm{e}^{-(\Delta G+\lambda)^2/4\lambda k_B T}}{\sqrt{4\pi\lambda k_B T}}.$$

16.9 Charge Delocalization and Self-Trapping

The electronic charge can be delocalized over donor and acceptor, if the electronic coupling V is sufficiently large. In the following we discuss the mutual dependency of the electronic wavefunction and the medium polarization within a simple model.

We consider the transition between two states ψ_1 and ψ_2 representing an electron localized at the donor (1) or acceptor (2) molecule, respectively, which are identical molecules (we consider a charge shift reaction). A nuclear coordinate Q is linearly coupled to this transition which represents the medium polarization (Fig. 16.11). In the semiclassical approximation, the nuclear motion is described by one wavepacket for both states

$$\psi = (c(Q)\psi_1 + s(Q)\psi_2)\Phi(Q) \quad c^2 + s^2 = 1 \tag{16.97}$$

and the classical position is identified as the expectation value of Q

$$Q(t) = \int Q|\Phi(Q)|^2 dQ. \tag{16.98}$$

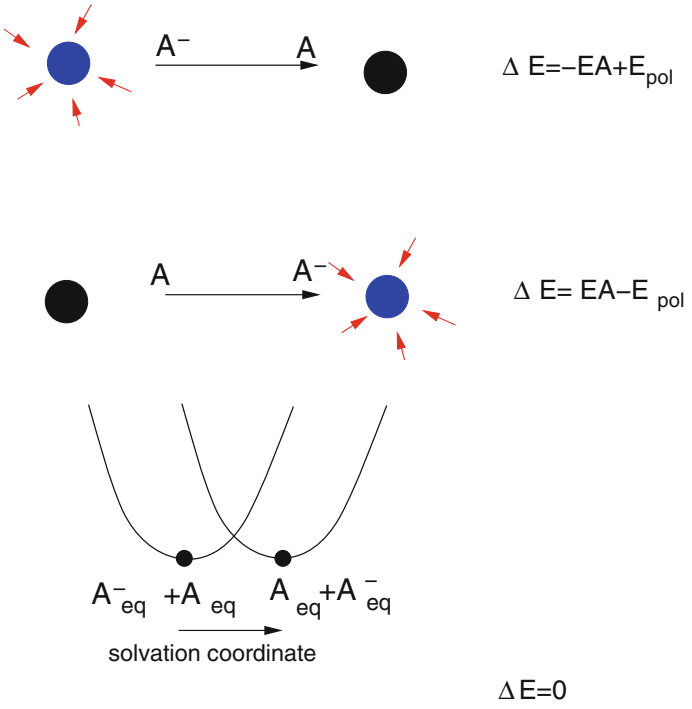

Fig. 16.11 Symmetric charge shift reaction

We apply the displaced harmonic oscillator model. The potential energies of the two states are parabolas

$$E_1 = \frac{k}{2}(Q - \delta Q)^2 \tag{16.99}$$

$$E_2 = \frac{k}{2}(Q + \delta Q)^2 \tag{16.100}$$

which are shifted relative to the equilibrium of the neutral state by $\pm\delta Q$. The model Hamiltonian is

$$H = H_{el} + H_{vib} + H_{el,vib} = \frac{\hat{P}^2}{2M} + \begin{pmatrix} \frac{k}{2}(\hat{Q} - \delta Q)^2 & V \\ V & \Delta E + \frac{k}{2}(\hat{Q} + \delta Q)^2 \end{pmatrix}. \tag{16.101}$$

The average over the electronic part of the wavefunction gives the potential energy

$$\begin{aligned} E(Q,s) &= <\psi| \begin{pmatrix} \frac{k}{2}(\hat{Q} - \delta Q)^2 & V \\ V & \frac{k}{2}(\hat{Q} + \delta Q)^2 \end{pmatrix} |\psi> \\ &= 2csV + c^2\left[\frac{k}{2}(Q - \delta Q)^2\right] + s^2\left[\frac{k}{2}(Q + \delta Q)^2\right] \\ &= 2csV + \frac{k}{2}Q^2 + \frac{k}{2}\delta Q^2 - (c^2 - s^2)kQ\delta Q. \end{aligned} \tag{16.102}$$

The equilibrium of the mixed state follows from minimizing the potential energy

$$0 = \frac{\partial}{\partial Q}E(Q) = \frac{\partial}{\partial Q}\left[\frac{k}{2}Q^2 - kQ\delta Q\left(c^2 - s^2\right)\right] = k\left[Q - \delta Q(c^2 - s^2)\right]. \tag{16.103}$$

It is given by the average

$$\delta Q^{(m)} = (c^2 - s^2)\delta Q = c_2\delta Q. \tag{16.104}$$

With the reorganization energy

$$\Lambda = \frac{k}{2}\delta Q^2 \tag{16.105}$$

we have

$$E_1(\delta Q^{(m)}) = \Lambda(c^2 - s^2 - 1)^2 = \Lambda(-2s^2)^2 = 4\Lambda s^4 \tag{16.106}$$

$$E_2(\delta Q^{(m)}) = 4\Lambda c^4. \tag{16.107}$$

According to the variational principle, the energy functional

$$\begin{aligned} E(\delta Q^{(m)}) &= 2csV + c^2 E_1(\delta Q^{(m)}) + s^2 E_2(\delta Q^{(m)}) \\ &= 2csV + 4\Lambda c^2 s^2 \\ &= s_2 V + s_2^2 \Lambda \end{aligned} \tag{16.108}$$

has to be minimized. With

$$d(\sin 2\chi) = 2(\cos 2\chi) d\chi \tag{16.109}$$

we have to solve

$$0 = V ds_2 + \Lambda \quad 2s_2 ds_2 = (V + 2\Lambda s_2) 2c_2 d\chi. \tag{16.110}$$

One pair of solutions is given by

$$\cos(2\chi) = 0, \sin(2\chi) = \pm 1 \quad \cos^2\chi = \sin^2\chi = \frac{1}{2} \tag{16.111}$$

$$\begin{pmatrix} \cos\chi \\ \sin\chi \end{pmatrix} = \begin{pmatrix} \frac{1}{\sqrt{2}} \\ \pm\frac{1}{\sqrt{2}} \end{pmatrix} \quad E = \Lambda \pm V. \tag{16.112}$$

If $V^2 < 4\Lambda^2$, there is a second pair with degenerate energies

$$\sin(2\chi) = -\frac{V}{2\Lambda}, \cos(2\chi) = \pm\sqrt{1 - \frac{V^2}{4\Lambda^2}} \quad \sin^2\chi = \frac{1 \mp \sqrt{1 - \frac{V^2}{4\Lambda^2}}}{2} \tag{16.113}$$

$$\begin{pmatrix} \cos\chi \\ \sin\chi \end{pmatrix} = \begin{pmatrix} c_{1,2} \\ s_{1,2} \end{pmatrix} = \begin{pmatrix} -\text{sign}(V)\sqrt{\frac{1 \pm \sqrt{1 - \frac{V^2}{4\Lambda^2}}}{2}} \\ \sqrt{\frac{1 \mp \sqrt{1 - \frac{V^2}{4\Lambda^2}}}{2}} \end{pmatrix} \quad E = -\frac{V^2}{4\Lambda} \tag{16.114}$$

which provides two localized minima, whereas for $|V| > 2\Lambda$ there is only one delocalized minimum (Fig. 16.12)

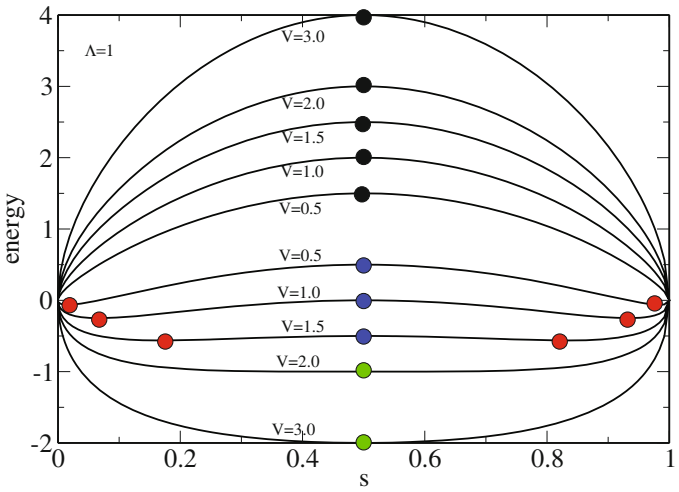

Fig. 16.12 Energy functional. One delocalized solution always represents a maximum (*black dots*). For small coupling $|V| < 2\Lambda$ there are two localized minima (*red dots*) and a second delocalized maximum (*blue dots*). For large coupling the localized extrema disappear and a second delocalized minimum (*green dots*) is found

Problems

16.1 Marcus Cross Relation

(a) Calculate the activation energy for the self-exchange reaction

$$\mathrm{A}^- + \mathrm{A} \overset{k_{AA}}{\rightarrow} \mathrm{A} + \mathrm{A}^-$$

in the harmonic model

$$G_R(Q) = \frac{a}{2}Q^2 \qquad G_P(Q) = \frac{a}{2}(Q - Q_1)^2.$$

(b) Show that for the cross reaction

$$\mathrm{A{+}D} \overset{k}{\rightarrow} \mathrm{A}^- + \mathrm{D}^+$$

the reorganization energy is given by the average of the reorganization energies for the two self-exchange reactions

$$\lambda = \frac{\lambda_{AA} + \lambda_{DD}}{2}$$

and the rate k can be expressed as

$$k = \sqrt{k_{AA} k_{DD} K_{eq} f}$$

where k_{AA} and k_{DD} are the rate constants of the self-exchange reactions, K_{eq} is the equilibrium constant of the cross reaction and f is a factor, which is usually close to unity.

Part VI
Elementary Photophysics

Chapter 17
Molecular States

Bio-molecules have a large number of vibrational degrees of freedom, which are more or less strongly coupled to transitions between different electronic states. In this chapter, we discuss the vibronic states on the basis of the Born–Oppenheimer separation and the remaining nonadiabatic coupling of the adiabatic states. The nuclear motion is approximated by independent harmonic normal modes. Matrix elements of the nuclear gradient operator are evaluated in the model of parallel displaced harmonic oscillators. Finally, we discuss mixing of the Born–Oppenheimer states due to nonadiabatical coupling and the damping approximation for finite lifetimes.

17.1 Born–Oppenheimer Separation

In molecular physics usually the Born–Oppenheimer separation of electronic ($\mathbf{r}_i$) and nuclear motion ($\mathbf{R}_\alpha$) is used.

The molecular Hamiltonian (without considering spin[1] or relativistic effects) can be written as

$$H = T_N(\mathbf{R}_\alpha) + T_{el}(\mathbf{r}_i) + V_N(\mathbf{R}_\alpha) + V_{eN}(\mathbf{R}_\alpha, \mathbf{r}_i) + V_{ee}(\mathbf{r}_i) \tag{17.1}$$

with the kinetic energy operators

$$T_N = \sum_\alpha -\frac{\hbar^2}{2m_\alpha}\nabla^2_{\mathbf{R}_\alpha} \qquad T_{el} = \sum_i -\frac{\hbar^2}{2m_e}\nabla^2_{\mathbf{r}_i} \tag{17.2}$$

[1] Even if spin does not appear explicitly we will have to take care of the proper symmetry properties.

P.O.J. Scherer and S.F. Fischer, *Theoretical Molecular Biophysics*,
Biological and Medical Physics, Biomedical Engineering,
DOI 10.1007/978-3-662-55671-9_17

and the Coulomb interaction

$$U(\mathbf{R}_\alpha, \mathbf{r}_i) = V_N(\mathbf{R}_\alpha) + V_{eN}(\mathbf{R}_\alpha, \mathbf{r}_i) + V_{ee}(\mathbf{r}_i)$$
$$= \sum_{\alpha<\alpha'} \frac{Z_\alpha Z_{\alpha'} e^2}{4\pi\varepsilon|\mathbf{R}_\alpha - \mathbf{R}_{\alpha'}|} - \sum_{\alpha,i} \frac{Z_\alpha e^2}{4\pi\varepsilon|\mathbf{R}_\alpha - \mathbf{r}_i|} + \sum_{i<k} \frac{e^2}{4\pi\varepsilon|\mathbf{r}_i - \mathbf{r}_k|}. \tag{17.3}$$

The Born–Oppenheimer wave function is a product

$$\psi(\mathbf{R}_\alpha, \mathbf{r}_i)\chi(\mathbf{R}_\alpha) \tag{17.4}$$

where the electronic part depends parametrically on the nuclear coordinates. The nuclear masses are much larger than the electronic mass

$$m_\alpha \gg m_e. \tag{17.5}$$

Therefore the kinetic energy of the nuclei is neglected for the electronic motion. The electronic wave function is obtained approximately from the eigenvalue problem,

$$H_{BO}\psi_s(\mathbf{R}_\alpha, \mathbf{r}_i) = E_s(\mathbf{R}_\alpha)\psi_s(\mathbf{R}_\alpha, \mathbf{r}_i) \tag{17.6}$$

with the simplified Hamiltonian

$$H_{BO} = \sum_i -\frac{\hbar^2}{2m_e}\nabla^2_{\mathbf{r}_i} + U(\mathbf{R}_\alpha, \mathbf{r}_i). \tag{17.7}$$

This eigenvalue problem has to be solved separately for each set of nuclear coordinates. Using the Born–Oppenheimer product ansatz for the electronic state s we have

$$H\psi_s(\mathbf{R}_\alpha, \mathbf{r}_i)\chi_s(\mathbf{R}_\alpha) = (T_N + H_{BO})\psi_s(\mathbf{R}_\alpha, \mathbf{r}_i)\chi_s(\mathbf{R}_\alpha)$$
$$= T_N\psi_s(\mathbf{R}_\alpha, \mathbf{r}_i)\chi_s(\mathbf{R}_\alpha) + E_s\psi_s(\mathbf{R}_\alpha, \mathbf{r}_i)\chi(\mathbf{R}_\alpha)$$
$$= \psi_s(\mathbf{R}_\alpha, \mathbf{r}_i)(T_N + E_s(\mathbf{R}_\alpha))\chi_s(\mathbf{R}_\alpha)$$
$$- \sum_\alpha \frac{\hbar^2}{2m_\alpha}\left(\chi_s(\mathbf{R}_\alpha)\nabla^2_{\mathbf{R}_\alpha}\psi_s(\mathbf{R}_\alpha, \mathbf{r}_i) + \left(\nabla_{\mathbf{R}_\alpha}\chi_s(\mathbf{R}_\alpha)\right)\left(\nabla_{\mathbf{R}_\alpha}\psi_s(\mathbf{R}_\alpha, \mathbf{r}_i)\right)\right). \tag{17.8}$$

The sum constitutes the so called non-adiabatic interaction V_{nad}. If it is neglected in lowest order the nuclear wave function is a solution of the eigenvalue problem

$$(T_N + E_s(\mathbf{R}_\alpha))\chi_s(\mathbf{R}_\alpha) = E\chi_s(\mathbf{R}_\alpha). \tag{17.9}$$

17.2 Harmonic Approximation to the Nuclear Motion

We consider a molecule which has a stable equilibrium configuration.[2] We assume that in the equilibrium configuration all nuclei are at rest $\dot{\mathbf{R}}_\alpha = 0$, hence there is no translational or rotational motion.[3]

Under these assumptions, the harmonic approximation allows a simplified description of small amplitude motion around the equilibrium configuration. In the following we collect the Cartesian coordinates of the N nuclei into a vector with $3N$ coordinates[4]

$$Q_1 = R_{1,x} \ldots Q_{3N} = R_{N,z}. \tag{17.10}$$

The potential energy $E_s(Q)$ is expanded around the equilibrium configuration Q_{0s}[5]

$$E_s(Q) = E_s^{min} + \frac{1}{2}\sum_{j,j'}(Q_j - Q_{j0s})(Q_{j'} - Q_{j'0s})\frac{\partial^2}{\partial Q_j \partial Q_{j'}}E_s + \cdots \tag{17.11}$$

Within the harmonic approximation the matrix of mass weighted second derivatives

$$D_{jj'} = \frac{1}{\sqrt{m_j m_{j'}}}\frac{\partial^2}{\partial Q_j \partial Q_{j'}} \tag{17.12}$$

is diagonalized by solving

$$\sum_{j'} D_{jj'} u^r_{j'} = \omega_r^2 u^r_j \tag{17.13}$$

and the nuclear motion becomes a superposition of independent normal mode vibrations with amplitudes q_r and frequencies ω_r[6]

$$Q_j - Q_{j0s} = \frac{1}{\sqrt{m_j}}\sum_r q_r u^r_j. \tag{17.14}$$

---

[2] We do not consider special cases like internal rotations or large amplitude motions with very low frequency.

[3] Strictly speaking, there is still an infinite number of equivalent equilibria unless the orientation of the molecule is uniquely defined.

[4] Strictly speaking, there are only $3N - 6$ independent coordinates and 6 normal modes with zero frequency, corresponding to translation and rotation of the molecule, have to be eliminated.

[5] Which will be different for different electronic states s in general.

[6] These quantities will be different for different electronic states s of course.

After transformation to normal mode coordinates the eigenvalue problem (17.9) decouples according to

$$E_s + T_N = E_s^{min} + \sum_r \left(\frac{\omega_r^2}{2} q_r^2 - \frac{\hbar^2}{2} \frac{\partial^2}{\partial q_r^2} \right) \tag{17.15}$$

or, introducing the ladder operators

$$b = \frac{1}{\sqrt{2}} \left(\sqrt{\frac{\omega}{\hbar}} x + \sqrt{\frac{\hbar}{\omega}} \frac{\partial}{\partial x} \right) \tag{17.16}$$

$$b^\dagger = \frac{1}{\sqrt{2}} \left(\sqrt{\frac{\omega}{\hbar}} x - \sqrt{\frac{\hbar}{\omega}} \frac{\partial}{\partial x} \right) \tag{17.17}$$

to

$$E_s + T_N = E_s^{min} + \sum_r \hbar\omega_r \left(b_r^\dagger b_r + \frac{1}{2} \right). \tag{17.18}$$

The nuclear eigenfunctions factorize

$$\chi_s = \prod_r \chi_{s,r,n_r}(q_r) \tag{17.19}$$

and the total energy of a molecular state is the sum

$$E_s(\{n_r\}) = E_s^{min} + \sum_r \hbar\omega_r^{(s)} \left(n_r + \frac{1}{2} \right). \tag{17.20}$$

Often the zero point energy of the vibrations is added to the electronic energy and the vibrational energies are taken relative to the lowest state

$$E_s(\{n_r\}) = E_s^0 + \sum_r \hbar\omega_r^{(s)} n_r. \tag{17.21}$$

The vibrations form a very dense manifold of states for biological molecules. This is schematically represented in a Jablonsky-diagram (Fig. 17.1).[7]

Model calculations for Bacteriopheophytine (Fig. 17.2) are shown in Fig. 17.3.

[7] Which usually also shows electronic states of higher multiplicity.

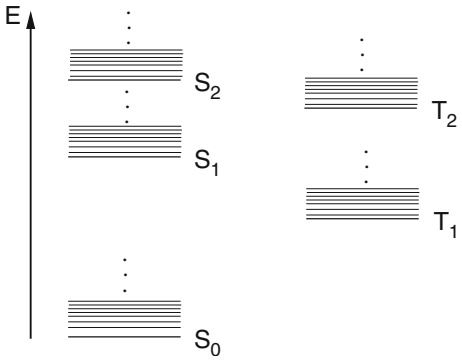

Fig. 17.1 Jablonsky diagram

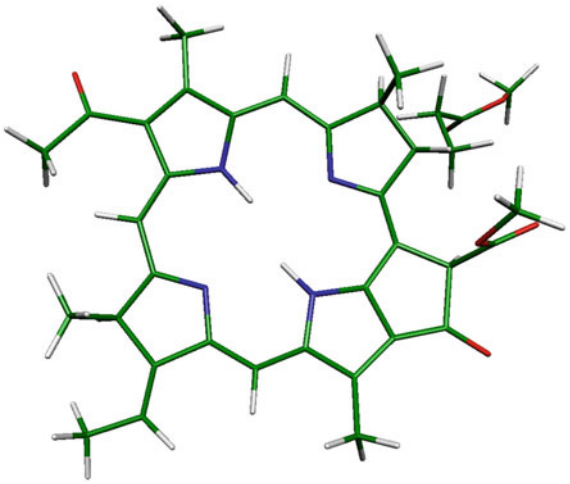

Fig. 17.2 Model for Bacteriopheophytine. Coordinates from the reaction center of rps.viridis [61–64] are shown with Molekel graphics [65]. The Phytyl tail was cut off

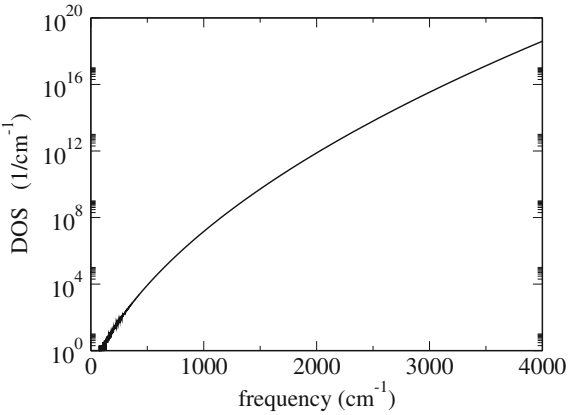

Fig. 17.3 Density of vibrational states. Normal modes for the Bacteriopheophytine model were calculated quantum chemically. The density of vibrational states was evaluated with a simple counting algorithm

17.3 Nonadiabatic Interaction

If two or more electronic states (s) are close in energy and V_{nad} cannot be neglected, a more general ansatz for the wave function is given by the linear combination (known as Born expansion [60])[8]

$$\Psi(r, Q) = \sum_s \psi_s(r, Q)\chi_s(Q) \tag{17.22}$$

which will also be written in matrix notation

$$\Psi = \sum_s \psi_s(r, Q)\chi_s(Q) = \left(\psi_1 \ldots\right)\begin{pmatrix}\chi_1\\ \vdots\end{pmatrix} = \boldsymbol{\psi}^\dagger\boldsymbol{\chi} \tag{17.23}$$

In the absence of nonadiabatic coupling, the Born–Oppenheimer wave functions of the electronic states s

$$\psi_s(r, Q)\chi_s(Q) \tag{17.24}$$

obey the eigenvalue equations

$$[T_N(Q) + E_s(Q)]\,\chi_s(Q) = \hbar\omega_{sn}\chi_s(Q) \tag{17.25}$$

$$[T_{el}(r) + U(r, Q)]\,\psi_s(r, Q) = E_s(Q)\psi_s(r, Q) \tag{17.26}$$

where the electronic functions $\psi_s(r, Q)$ form a complete basis for each configuration Q. The time dependent Schrödinger equation reads in matrix notation

$$\boldsymbol{\psi}^\dagger \mathrm{i}\hbar\frac{\partial}{\partial t}\boldsymbol{\chi} = \boldsymbol{\psi}^\dagger \mathrm{diag}(E_s + T_N)\boldsymbol{\chi} + \hat{V}_{nad}\boldsymbol{\psi}^\dagger\boldsymbol{\chi} \tag{17.27}$$

For a fixed configuration, the ψ_s are a complete and orthonormalized system. After taking the scalar product with $\boldsymbol{\psi}$ from left and integration over all electronic coordinates[9] we obtain a system of coupled equations for the nuclear motion

$$\mathrm{i}\hbar\frac{\partial}{\partial t}\boldsymbol{\chi} = \mathrm{diag}(E_s + T_N)\boldsymbol{\chi} + < \boldsymbol{\psi}\hat{V}_{nad}\boldsymbol{\psi}^\dagger > \boldsymbol{\chi} \tag{17.28}$$

[8] In the following r denotes the set of all electron coordinates whereas Q are the nuclear coordinates as in (17.10).

[9] Which in the following will be denoted by brackets $<>$.

or component wise

$$i\hbar\dot{\chi}_s = \left[E_s(Q_j) + T_N(Q_j)\right]\chi_s + \sum_{s'} < \psi_s \hat{V}_{nad}\psi_{s'} > \chi_{s'}. \tag{17.29}$$

The nonadiabatic interaction couples the adiabatic electronic states.[10] We consider the matrix elements (NACM)[11]

$$\begin{aligned} V^{nad}_{s,s'} &= < \chi_{s'}(Q)\psi_{s'}(r,Q)\,\hat{V}_{nad}\,\psi_s(r,Q)\chi_s(Q) > \\ &= -\sum_j \frac{\hbar^2}{2M_j} < \chi_{s'}(Q)\,\chi_s(Q) >< \psi_{s'}(r,Q)\left(\frac{\partial^2}{\partial Q_j^2}\psi_s(r,Q)\right) > \\ &\quad -\sum \frac{\hbar^2}{2M_j} < \chi_{s'}(Q)\left(\frac{\partial}{\partial Q_j}\chi_s(Q)\right) >< \psi_{s'}(r,Q)\,\left(\frac{\partial}{\partial Q_j}\psi_s(r,Q)\right) > . \end{aligned} \tag{17.30}$$

The matrix element of the nuclear gradient can be evaluated for $s \neq s'$ from

$$< \psi_{s'}\frac{\partial}{\partial Q_k}\left[T_e(r) + U(r,Q)\right]\psi_s >=< \psi_{s'}|\frac{\partial}{\partial Q_k}E_s(Q)|\psi_s > \tag{17.31}$$

$$\begin{aligned} &< \psi_{s'}\left\{\frac{\partial U(r,Q)}{\partial Q_k} + \left[T_e(r) + U(r,Q)\right]\frac{\partial}{\partial Q_k}\right\}\psi_s > \\ &=< \psi_{s'}\left\{\frac{\partial E_s(Q)}{\partial Q_k} + E_s(Q)\frac{\partial}{\partial Q_k}\right\}\psi_s > \end{aligned} \tag{17.32}$$

$$\begin{aligned} &E_{s'}(Q) < \psi_{s'}\frac{\partial}{\partial Q_k}\psi_s > + < \psi_{s'}\frac{\partial U(r,Q)}{\partial Q_k}\psi_s > \\ &= \frac{\partial E_s(Q)}{\partial Q_k}\delta_{s's} + E_s(Q) < \psi_{s'}\frac{\partial}{\partial Q_k}\psi_s > \end{aligned} \tag{17.33}$$

$$< \psi_{s'}\frac{\partial}{\partial Q_k}\psi_s >= \frac{< \psi_{s'}\frac{\partial U(r,Q)}{\partial Q_k}\psi_s >}{E_s(Q) - E_{s'}(Q)} \tag{17.34}$$

which becomes large if the energy gap between two electronic states is small. The second derivative follows from

$$\frac{\partial}{\partial Q_k} < \psi_{s'}\frac{\partial}{\partial Q_k}\psi_s >=< \psi_{s'}\frac{\partial^2}{\partial Q_k^2}\psi_s > + < \left(\frac{\partial}{\partial Q_k}\psi_{s'}\right)|\left(\frac{\partial}{\partial Q_k}\psi_s\right) > \tag{17.35}$$

[10] Sometimes called channels.

[11] Without a magnetic field the molecular wave functions can be chosen real valued.

after inserting a sum over the complete set of electronic states

$$< \psi_{s'} \frac{\partial^2}{\partial Q_k^2} \psi_s >= \frac{\partial}{\partial Q_k} < \psi_{s'} \frac{\partial}{\partial Q_k} \psi_s > + \sum_l < \psi_{s'} \frac{\partial}{\partial Q_k} \psi_l >< \psi_l \frac{\partial}{\partial Q_k} \psi_s > . \tag{17.36}$$

The first term in (17.30) is generally small. If we evaluate the second term at an equilibrium configuration $Q^{(0)}$ of the state s and neglect the dependence on Q[12] we have

$$< \psi_{s'}(r, Q) \left(\frac{\partial}{\partial Q_j} \psi_s(r, Q) \right) >= V_{s',s}^{nad,el} + \ldots \tag{17.37}$$

$$V_{s,s'}^{nad} \approx -V_{s,s'}^{nad,el} \sum \frac{\hbar^2}{2m_j} < \chi(Q) \left(\frac{\partial}{\partial Q_j} \chi_s(Q) \right) > . \tag{17.38}$$

Within the harmonic approximation the gradient operator can be expressed as

$$\frac{1}{\sqrt{m_j}} \frac{\partial}{\partial Q_j} = \sum_r u_j^r \frac{\partial}{\partial q_r} = \sum_r u_j^r \sqrt{\frac{\omega_r}{2\hbar}} (b_r^\dagger - b_r) \tag{17.39}$$

and the nonadiabatic matrix element becomes

$$V_{s',n(r'),s,n(r)}^{nad} = -V_{s,s'}^{nad,el} \sum \frac{\hbar^2}{2} \sqrt{\frac{\omega_r}{2\hbar}} \int dq_1 dq_2 \cdots \left(\prod_{r'} \chi_{s'r'n(r')} \right)$$
$$\times \left(\prod_{r'' \neq r} \chi_{s,r'',n(r'')} \right) \left(\sqrt{n(r)+1} \chi_{s,r,n(r)+1} + \sqrt{n(r)} \chi_{s,r,n(r)-1} \right) . \tag{17.40}$$

This expression simplifies considerably if the mixing of normal modes in the state s' can be neglected (the so called parallel mode approximation). Then the overlap integral factorizes into a product of Franck–Condon factors.

$$V_{s',n(r'),s,n'(r)}^{nad} = -V_{s,s'}^{nad,el} \sum \frac{\hbar^2}{2} \sqrt{\frac{\omega_r}{2\hbar}}$$
$$\times \left(\prod_{r' \neq r} FC_{r'}^{s's}(n', n) \right) \left(\sqrt{n_r + 1} FC_r^{s's}(n'_r, n_r + 1) + \sqrt{n_r} FC_r^{s's}(n'_r n_r - 1) \right) \tag{17.41}$$

[12] This is known as the Condon approximation.

with

$$FC_r^{s's}(n'_r n_r) = \int dq_r \, \chi_{s'r,n'(r)}(q_r) \, \chi_{s,r,n(r)}(q_r). \tag{17.42}$$

17.4 "True" Molecular Eigenstates

Whereas the adiabatic approximation is quite accurate in the electronic groundstate, it breaks down if the molecule is excited to higher electronic states where highly excited vibronic levels of a lower electronic state are isoenergetic and form a quasi-continuum. In a popular model [66] one optically accessible state $|s>$ is in resonance with a manifold of dark states $|l>$ (Fig. 17.4).

The molecular eigenstates $|\nu>$ are mixtures of $|s>$ and $|l>$

$$|\nu> = a_{\nu s}|s> + \sum_l b_{\nu l}|l> \tag{17.43}$$

and the transition dipole of the bright state is distributed over the eigenstates according to the mixing coefficient

$$\boldsymbol{\mu}_\nu = a_{\nu s}\boldsymbol{\mu}_s \tag{17.44}$$

All excited states have finite lifetimes and decay, for instance due to their coupling to the electromagnetic radiation field, molecular collisions etc. For a dipole allowed transition (i.e. the $|s>$ state) the radiative lifetime is given by

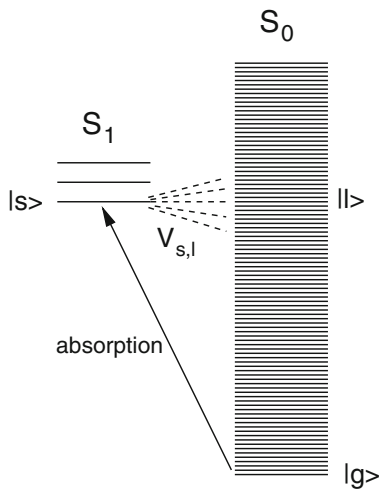

Fig. 17.4 Optical excitation. After optical excitation from the bottom of the S_0-manifold an electronically excited Born–Oppenheimer state $|s> = |\psi_e\chi_e>$ is populated (*bright state*) which is coupled by the nonadiabatic interaction to a manifold $|l> = |\psi_g\chi_{gl}>$ of resonant S_0-states which can not be optically excited (*dark states*) and form a quasi-continuum

$$\tau_r^{-1} = \Gamma_r = \frac{\omega^3 n |\mu|^2}{3\pi\varepsilon_0 \hbar c_0^3}. \tag{17.45}$$

As a result the corresponding transition has a finite width which can be calculated from the lifetime as

$$\mathrm{FWHH/cm^{-1}} = \frac{10.6}{\tau/\mathrm{psec}}. \tag{17.46}$$

For instance, a lifetime of 10 nsec corresponds to a FWHH of $0.001\mathrm{cm}^{-1}$. The coupling of the dark manifold $|l>$ to the radiation field is much weaker but since the density of rovibrational states increases very rapidly with the energy gap, in larger molecules the linewidth can become larger than the spacing of the states. Neglecting interferences the finite lifetimes can be described by introducing complex energies

$$\tilde{E}_m = E_m - i\frac{\Gamma_m}{2} \tag{17.47}$$

and a non-Hermitian effective Hamiltonian

$$\tilde{H} = \sum_m |m> \left(E_m - i\frac{\Gamma_m}{2}\right) < m| \tag{17.48}$$

where the stationary states are replaced by exponentially decaying states

$$\psi_m = e^{-\Gamma_m t/2} e^{-iE_m t/\hbar} |m> \tag{17.49}$$

which are solutions of

$$i\hbar\frac{\partial}{\partial t}\psi = \left(H - \frac{i}{2}\Gamma\right)\psi \tag{17.50}$$

(Interference effects lead to non diagonal elements of the damping matrix Γ).

Chapter 18
Intramolecular Electronic Transitions

In this chapter, we discuss the coupling to the electromagnetic radiation field semiclassically and derive the transition rates for absorption and induced emission in the dipole approximation. We compare with the fully quantized treatment and derive the rate of spontaneous fluorescence. We introduce the Condon approximation for optical transitions. The Franck–Condon-weighted density of states is formulated with the time-correlation function formalism. We discuss the generation of pure Born–Oppenheimer states with very short excitation pulses. Finally, we consider radiationless transitions.

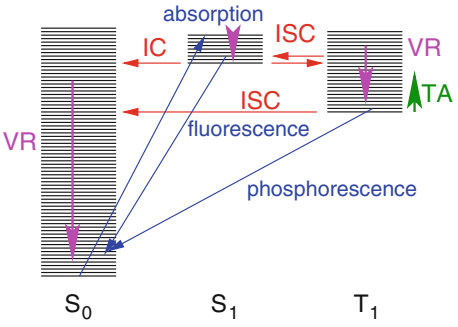

Fig. 18.1 Intramolecular electronic transitions. Transitions between different electronic states (singlet groundstate S_0 and excited state S_1, triplet state T_1) are shown including radiative transitions (absorption, fluorescence, phosphorescence), radiationless processes (internal conversion and intersystem crossing) and energy exchange with the environment (vibrational relaxation and thermal activation)

P.O.J. Scherer and S.F. Fischer, *Theoretical Molecular Biophysics*,
Biological and Medical Physics, Biomedical Engineering,
DOI 10.1007/978-3-662-55671-9_18

The total energy of an isolated system is conserved. Coupling to the electromagnetic radiation field, however, is always present and the total energy of a molecule can be changed by radiative transitions with absorption or emission of a photon.[1] Radiationless intramolecular transitions occur between isoenergetic states and conservation of energy makes it necessary that highly excited vibrational states are involved and take up the excess energy. Transitions between states of the same multiplicity (mostly singlet–singlet or triplet–triplet transitions) are known as internal conversion processes. Intersystem crossing processes change multiplicity (mostly between singlet and triplet) and require, e.g., spin-orbit coupling as do radiative transitions between triplet and singlet (phosphorescence). If energy can be exchanged with the environment, vibrational relaxation and thermal activation also have to be considered (Fig. 18.1).

18.1 Coupling to the Radiation Field

In semiclassical approximation, the electromagnetic field is a function of space and time. The vector potential of a monochromatic plane wave is

$$\mathbf{A} = A_0 \mathbf{e}_k (\mathrm{e}^{\mathrm{i}(\mathbf{kr}-\omega t)} + \mathrm{e}^{-\mathrm{i}(\mathbf{kr}-\omega t)}) \tag{18.1}$$

from which the electric field follows (radiation gauge, $\Phi = 0,\ \mathrm{div}\mathbf{A} = 0$)

$$\mathbf{E} = -\frac{\partial \mathbf{A}}{\partial t} = -\mathrm{i} E_0 \mathbf{e}_k (\mathrm{e}^{\mathrm{i}(\mathbf{kr}-\omega t)} - \mathrm{e}^{-\mathrm{i}(\mathbf{kr}-\omega t)}) \tag{18.2}$$

$$E_0 = \omega A_0. \tag{18.3}$$

The time-averaged energy density is

$$u = \left\langle \varepsilon_0 E^2 \right\rangle = 2\varepsilon_0 A_0^2 \omega^2 = 2\varepsilon_0 E_0^2. \tag{18.4}$$

The interaction of a charged particle with mass m and charge q with the radiation field has the standard form (for a molecule the sum over all electrons and nuclei has to be taken)

$$\hat{H}_{int} = -\frac{q}{m} \mathbf{A}\hat{\mathbf{p}} = \hat{V}_{int} \mathrm{e}^{-\mathrm{i}\omega t} + \hat{V}_{int}^{\dagger} \mathrm{e}^{\mathrm{i}\omega t} \tag{18.5}$$

where

$$\hat{V}_{int}(\mathbf{r}, \omega) = -\frac{q}{m} A_0(\omega) \mathbf{e}_k \hat{\mathbf{p}}\, \mathrm{e}^{\mathrm{i}\mathbf{kr}}. \tag{18.6}$$

[1] The total energy of molecule plus radiation field is conserved.

If the wavelength is larger than the extension of the molecule, the electric dipole approximation is valid which approximates

$$e^{\mathbf{ikr}} \approx 1. \tag{18.7}$$

The matrix element of the momentum operator can be expressed by the matrix element of the position operator. From the commutator

$$[\hat{H}, \mathbf{r}] = [\frac{\hat{\mathbf{p}}^2}{2m} + U(\mathbf{r}), \mathbf{r}] = -\frac{i\hbar}{m}\hat{\mathbf{p}} \tag{18.8}$$

we obtain

$$< f|\frac{q}{m}\mathbf{e}_k\hat{\mathbf{p}}|i >= \frac{i}{\hbar}(E_f - E_i)\mathbf{e}_k < f|q\mathbf{r}|i >= i\omega_{fi}\mathbf{e}_k\boldsymbol{\mu}_{fi} \tag{18.9}$$

with the transition dipole moment vector $\boldsymbol{\mu}$. The golden rule then gives the transition rates for absorption

$$\begin{aligned} \Gamma_{i\to f} &= \frac{2\pi}{\hbar^2}|V_{if}|^2\delta(\omega_{fi} - \omega) = \frac{2\pi}{\hbar^2}A_0^2(\omega_{fi})\omega_{fi}^2|\mathbf{e}\boldsymbol{\mu}_{fi}|^2\delta(\omega_{fi} - \omega) \\ &= \frac{2\pi}{\hbar^2}|\mathbf{E}_0(\omega_{fi})\boldsymbol{\mu}_{fi}|^2\delta(\omega_{fi} - \omega) \end{aligned} \tag{18.10}$$

and induced fluorescence

$$\Gamma_{i\to f} = \frac{2\pi}{\hbar^2}|\mathbf{E}_0(\omega_{fi})\boldsymbol{\mu}_{fi}|^2\delta(\omega_{fi} + \omega). \tag{18.11}$$

For incoherent radiation, the rates of all waves have to be summed up ($\rho(\omega)$ is the number of modes in the interval $\omega \ldots \omega + d\omega$).

$$\begin{aligned} \Gamma_{i\to f} &= \frac{2\pi}{\hbar^2}\int |V_{if}|^2\delta(\omega_{fi} - \omega)\rho(\omega)d\omega \\ &= \frac{2\pi}{\hbar^2}|V_{if}(\omega_{fi})|^2\rho(\omega_{fi}). \end{aligned} \tag{18.12}$$

The total energy density is

$$u(\omega) = 2\varepsilon_0 A_0^2(\omega)\omega^2\rho(\omega) = 2\varepsilon_0 E_0^2(\omega)\rho(\omega) \tag{18.13}$$

and finally the transition rate in dipole approximation is

$$\Gamma_{i\to f} = \frac{\pi}{\hbar^2}\frac{u(\omega_{fi})}{\varepsilon_0}|\mathbf{e}_k\boldsymbol{\mu}_{fi}|^2. \tag{18.14}$$

The semiclassical treatment cannot explain spontaneous emission since without an electromagnetic field there is no perturbation. If the radiation field is treated quantum mechanically, the fields become operators. The vector potential is a superposition of its Fourier components (within the volume V)

$$\mathbf{A} = \sum_{\mathbf{k},\lambda} \sqrt{\frac{\hbar\omega_k}{2\varepsilon_0 V}} \frac{1}{\omega_k} \left(\hat{a}_{k,\lambda} \mathbf{e}_{k,\lambda} \mathrm{e}^{\mathrm{i}\mathbf{kr}} + \hat{a}^{\dagger}_{k,\lambda} \mathbf{e}^{*}_{\mathbf{k},\lambda} \mathrm{e}^{-\mathrm{i}\mathbf{kr}} \right) \tag{18.15}$$

where $\hat{a}^{\dagger}_{\mathbf{k}\lambda}$ creates a photon with energy $\hbar\omega_k = \hbar ck$ and polarization vector $\mathbf{e}_{k\lambda}$ and the Hamiltonian of the radiation field is

$$\hat{H}_{rad} = \sum_{\mathbf{k}\lambda} \hbar\omega_k \hat{a}^{\dagger}_{k\lambda} \hat{a}_{k\lambda}. \tag{18.16}$$

Now, consider transitions between eigenstates of the total Hamiltonian

$$\hat{H}_0 + \hat{H}_{rad} \tag{18.17}$$

due to the interaction

$$\hat{H}_{int} = -\frac{q}{m} \mathbf{A}\hat{\mathbf{p}} = \hat{V} + \hat{V}^{\dagger} \tag{18.18}$$

where in dipole approximation

$$\hat{V}(\omega) \approx \mathrm{i}\omega_{fi} \mathbf{e}_{k\lambda} \boldsymbol{\mu} \sqrt{\frac{\hbar}{2\varepsilon_0 V \omega_k}}\, \hat{a}_{k,\lambda}. \tag{18.19}$$

For an absorptive transition one photon disappears

$$|i, n_{k\lambda} > \rightarrow |f, n_{k\lambda} - 1 > \quad \Delta E = E_f - E_i - \hbar\omega_k \tag{18.20}$$

and since

$$\hat{a}|n> = \sqrt{n}|n-1> \tag{18.21}$$

the transition rate is

$$\Gamma_{i,n\rightarrow f,n-1} = \frac{2\pi}{\hbar^2} \delta(\omega_{fi} - \omega_k) \frac{n_{k\lambda}\hbar\omega_{fi}}{2\varepsilon_0 V} |\mathbf{e}_k \boldsymbol{\mu}_{fi}|^2. \tag{18.22}$$

An emissive transition creates one photon

$$|i, n_{k\lambda} > \rightarrow |f, n_{k\lambda} + 1 > \tag{18.23}$$

but now

$$\hat{a}^{\dagger}|n>=\sqrt{n+1}|n+1> \tag{18.24}$$

and the rate

$$\Gamma_{i,n\to f,n+1}=\frac{2\pi}{\hbar^2}\delta(\omega_{fi}-\omega_k)\frac{[n_{k\lambda}+1]\hbar\omega_{fi}}{2\varepsilon_0 V}|\mathbf{e}_k\boldsymbol{\mu}_{fi}|^2 \tag{18.25}$$

includes both stimulated and spontaneous emission. In the classical limit, the operators behave like (see Appendix B)

$$a_{k\lambda}\approx \mathrm{e}^{-\mathrm{i}\omega_k t}\sqrt{n_{k\lambda}} \tag{18.26}$$

$$\hat{A}(\omega_k,\mathbf{k})=\sqrt{\frac{u(\omega_k,\mathbf{k})}{2\varepsilon_0\omega_k^2}}\left(\mathbf{e}_{k,\lambda}\mathrm{e}^{\mathrm{i}(\mathbf{kr}-\omega_k t)}+\mathbf{e}^{*}_{\mathbf{k},\lambda}\mathrm{e}^{-\mathrm{i}(\mathbf{kr}-\omega_k t)}\right). \tag{18.27}$$

The energy density is

$$u_{k\lambda}=\frac{n_{k\lambda}\hbar\omega_{k\lambda}}{V} \tag{18.28}$$

and both rates (18.22) and (18.25) are given by the semiclassical expression (18.10)

$$\Gamma_{i,n\to f,n+1}=\frac{2\pi}{\hbar^2}\delta(\omega_{fi}-\omega_k)\frac{u_{k\lambda}}{2\varepsilon_0}|\mathbf{e}_k\boldsymbol{\mu}_{fi}|^2.$$

To obtain the total rate of spontaneous emission, we have to sum over all k-vectors and polarizations (Fig. 18.2).

$$\begin{aligned}
&\sum_{\mathbf{k}}\to\frac{V}{(2\pi)^3}\int d^3k=\frac{V}{(2\pi)^3}\int k^2dk\,d\Omega\\
&\Gamma_{sp}=\sum_{\lambda}\int\frac{2\pi}{\hbar^2}\frac{1}{c}\delta(\frac{1}{c}\omega_{fi}-k)\frac{\hbar\omega_{fi}}{2\varepsilon_0}|\mathbf{e}_k\boldsymbol{\mu}_{fi}|^2\frac{V}{(2\pi)^3}k^2dk\,d\Omega\\
&=\frac{1}{\hbar^2c}\frac{\hbar\omega_{fi}}{2\varepsilon_0(2\pi)^2}\frac{\omega_{fi}^2}{c^2}\sum_{\lambda}\int|\mathbf{e}_k\boldsymbol{\mu}_{fi}|^2d\Omega\\
&=\frac{1}{3\pi}\mu_{fi}^2\frac{\omega_{fi}^3}{\varepsilon_0\hbar c^3}
\end{aligned} \tag{18.29}$$

The unit length vectors $\frac{\mathbf{k}}{k},\mathbf{e}_{k1},\mathbf{e}_{k2}$ form an orthogonal basis. Therefore

$$|\mathbf{e}_{k1}\boldsymbol{\mu}|^2+|\mathbf{e}_{k2}\boldsymbol{\mu}|^2+|\frac{\mathbf{k}}{k}\mu|^2=\mu^2$$

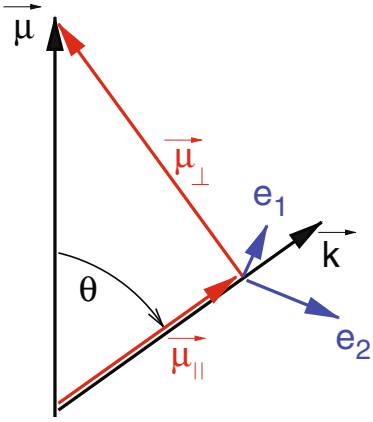

Fig. 18.2 Summation over directions and polarization

$$|\mathbf{e}_{k1}\boldsymbol{\mu}|^2 + |\mathbf{e}_{k2}\boldsymbol{\mu}|^2 = \mu^2 - \mu_\parallel^2$$

We chose the z-axis along $\boldsymbol{\mu}$. Then $\mu_\parallel = \mu\cos\theta$ and

$$\sum_\lambda \int |\mathbf{e}_k \boldsymbol{\mu}_{fi}|^2 d\Omega = \mu_{fi}^2 \int (1-\cos^2\theta) d\cos\theta d\phi$$
$$= 2\pi\mu_{fi}^2 \left[\cos\theta - \frac{\cos^3\theta}{3}\right]_{-1}^{1} = \frac{8\pi}{3}\mu_{fi}^2$$

18.2 Optical Transitions

We consider allowed optical transitions between two electronic states of a molecule, for instance the ground state (g) and an excited singlet state (e). Within the adiabatic approximation (17.19) we take into account transitions between the manifolds of Born–Oppenheimer vibronic states

$$\psi_g(r, Q)\chi_g(Q) \to \psi_e(r, Q)\chi_e(Q). \tag{18.30}$$

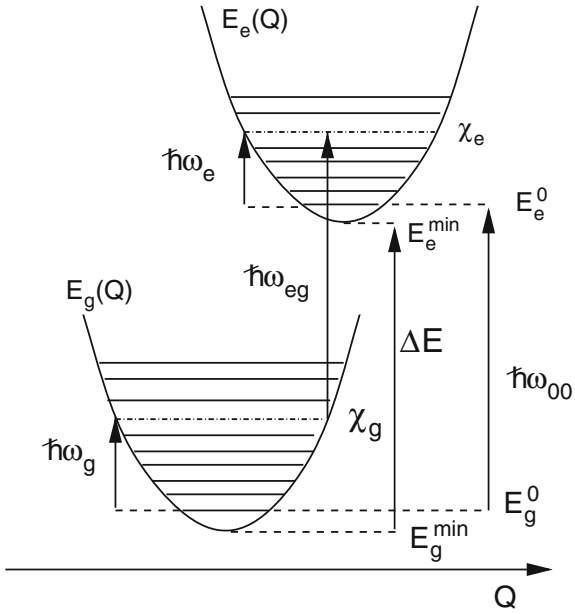

Fig. 18.3 Optical transition

The molecular Hamiltonian is

$$H_0 = |\psi_e > (E_e^0 + H_e) < \psi_e| + |\psi_g > (E_g^0 + H_g) < \psi_g| \tag{18.31}$$

where we introduced Hamiltonians (18.40) for the nuclear motion in the two states

$$H_{g(e)} = T_N + E_{g(e)}(Q) - E_{g(e)}^0. \tag{18.32}$$

We count vibrational energies relative to the lowest vibrational state of the manifold, which is E_g^0 in the electronic groundstate and E_e^0 in the excited state. The quantity $\hbar\omega_{00} = E_e^0 - E_g^0$ denotes the so-called $0-0$ transition energy, which differs from the purely electronic transition energy $\Delta E = E_e^{min} - E_g^{min}$ by the difference of the zero-point energies. (Fig. 18.3)
The nuclear wavefunctions obey

$$H_{g(e)}\chi_{g(e)} = \hbar\omega_{g(e)}\chi_{g(e)}. \tag{18.33}$$

The energy difference corresponding to the transition

$$|\psi_g\chi_g > \rightarrow |\psi_e\chi_e > \tag{18.34}$$

is given by

$$\hbar\omega_{eg} = \hbar\omega_{00} + \hbar\omega_e - \hbar\omega_g. \tag{18.35}$$

Assuming that the occupation of initial states is given by a canonical distribution $P(\chi_g)$ the golden rule (18.10) gives the transition rate for absorption of photons with energy $\hbar\omega$

$$k = \frac{2\pi}{\hbar} \sum_{\chi_g \chi_e} P(\chi_g) \left| < \psi_g(r, Q)\chi_g(Q) \left| \mathbf{E_0} e\mathbf{r} \right| \psi_e(r, Q)\chi_e(Q) > \right|^2 \delta(\hbar\omega_{eg} - \hbar\omega). \tag{18.36}$$

18.3 Dipole Transitions in the Condon Approximation

The matrix element of the dipole operator $e\mathbf{r}$ can be simplified by performing the integration over the electronic coordinates

$$\begin{aligned} &\int dQ \chi_g^*(Q)\chi_e(Q) \int dr \psi_g^*(r, Q) e\mathbf{r} \psi_e(r, Q) \\ &= \int dQ \chi_g^*(Q)\chi_e(Q) \, \mathbf{M}_{ge}(Q). \end{aligned} \tag{18.37}$$

The dipole moment function $\mathbf{M}_{eg}(Q)$ is expanded as a series with respect to the nuclear coordinates around the equilibrium configuration

$$\mathbf{M}_{eg}(Q) = \mathbf{M}_{eg}(Q_{eq}) + \frac{\partial \mathbf{M}_{eg}}{\partial Q}(Q - Q_{eq}) + \cdots \tag{18.38}$$

If its equilibrium value does not vanish for symmetry reasons, the dipole moment can be approximated by neglecting all higher order terms (this is known as Condon approximation)

$$\mathbf{M}_{eg}(Q) \approx \boldsymbol{\mu}_{eg} = \mathbf{M}_{eg}(Q_{eq}). \tag{18.39}$$

The transition rate becomes a product of an electronic factor and an overlap integral of the nuclear wavefunctions which is known as Franck–Condon factor (in fact the Franck– Condon-weighted density of states) or lineshape function. Since each transition consumes an energy amount of $\hbar\omega_{eg}$ the rate for energy absorption is

$$\begin{aligned} k_{abso} &= \frac{2\pi}{\hbar} |\mathbf{E}_0 \boldsymbol{\mu}_{eg}|^2 \sum_{\chi_g, \chi_e} P(\chi_g) \left| < \chi_g(Q) | \chi_e(Q) > \right|^2 \hbar\omega \delta(\hbar\omega - \hbar\omega_{00} - (\hbar\omega_e - \hbar\omega_g)) \\ &= 2\pi\omega |\mathbf{E_0} \boldsymbol{\mu}_{eg}|^2 \, FCD(\hbar\omega - \hbar\omega_{00}) \end{aligned} \tag{18.40}$$

The transition rate for fluorescence behaves very similar. If we assume thermal distribution of excited states

$$k_{fluo} = \frac{|\mu_{eg}|^2}{3\pi\varepsilon_0\hbar c^3} \sum_{\chi_g,\chi_e} P(\chi_e) \left| < \chi_e(Q)|\chi_g(Q) > \right|^2 \omega^3 \delta(\hbar\omega - \hbar\omega_{00} + (\hbar\omega_g - \hbar\omega_e))$$
$$= \frac{|\mu_{eg}|^2\omega^3}{3\pi\varepsilon_0\hbar c^3} FCD_{fluo}(\hbar\omega - \hbar\omega_{00}) \tag{18.41}$$

18.4 Time-Correlation Function (TCF) Formalism

The transition rate can be written in an alternative way, which is quite suitable for practical calculations writing the delta function in (18.40) as a Fourier integral

$$\delta(\hbar\omega) = \frac{1}{2\pi\hbar} \int_{-\infty}^{\infty} \mathrm{e}^{-\mathrm{i}\omega t} dt \tag{18.42}$$

$$k = \frac{|\mathbf{E}_0\boldsymbol{\mu}_{eg}|^2}{\hbar^2} \int dt \sum_{\chi_g\chi_e} P(\chi_g)| < \chi_g|\chi_e > |^2 \mathrm{e}^{\mathrm{i}(\omega_e - \omega_g + \omega_{00} - \omega)t} \tag{18.43}$$

which can be written as a thermal average over the vibrations of the ground state

$$k = \frac{|\mathbf{E}_0\boldsymbol{\mu}_{eg}|^2}{\hbar^2} \int dt \sum_{\chi_g\chi_e} < \chi_g \frac{\mathrm{e}^{-\beta H_g}}{Q_g} \mathrm{e}^{-\mathrm{i}\omega_g t}|\chi_e > \mathrm{e}^{\mathrm{i}\omega_e t} < \chi_e|\chi_g > \mathrm{e}^{\mathrm{i}(\omega_{00}-\omega)t}$$
$$= \frac{|\mathbf{E}_0\boldsymbol{\mu}_{eg}|^2}{\hbar^2} \int dt\, \mathrm{e}^{-\mathrm{i}(\omega-\omega_{00})t} \left\langle \mathrm{e}^{-\mathrm{i}tH_g/\hbar} \mathrm{e}^{\mathrm{i}tH_e/\hbar} \right\rangle_g . \tag{18.44}$$

The coupling square can be written as the expectation value

$$|\mathbf{E}_0\boldsymbol{\mu}_{eg}|^2 = < \psi_g|V|\psi_e >< \psi_e|V|\psi_g > = < \psi_g|V^2|\psi_g > . \tag{18.45}$$

Here, it was assumed that the excitation frequency is large and the excited state is not occupied thermally. The rate can be formulated as a thermal average over nuclear and electronic states as

$$k = \frac{1}{\hbar^2} \sum \int dt\, \mathrm{e}^{-\mathrm{i}(\omega-\omega_{00})t} < \psi_g\chi_g| \frac{\mathrm{e}^{-\beta H_g}}{Q_g} |\psi_g > (-\boldsymbol{\mu}_{eg}\mathbf{E}_0) < \psi_e|\mathrm{e}^{\mathrm{i}tH_e/\hbar}$$
$$\times |\psi_e > (-\boldsymbol{\mu}_{eg}\mathbf{E}_0) < \psi_g|\mathrm{e}^{-\mathrm{i}tH_g/\hbar}\chi_g\psi_g >$$
$$= \frac{1}{\hbar^2} \int dt\, \mathrm{e}^{-\mathrm{i}(\omega-\omega_{00})t} \left\langle\!\left\langle V \mathrm{e}^{\mathrm{i}tH_0/\hbar} V \mathrm{e}^{-\mathrm{i}tH_0/\hbar} \right\rangle\!\right\rangle_g \tag{18.46}$$

which involves the time- correlation function of the coupling operator (hence the dipole moment operator)

$$\langle V(0)V(t)\rangle = \left\langle\!\left\langle V \mathrm{e}^{\mathrm{i}tH_0/\hbar} V \mathrm{e}^{-\mathrm{i}tH_0/\hbar} \right\rangle\!\right\rangle_g = |\mathbf{E}_0\boldsymbol{\mu}_{eg}|^2 F(t) \tag{18.47}$$

with[2] the time-correlation function of the nuclear motion

$$F(t) = \left\langle e^{itH_e/\hbar} e^{-itH_g/\hbar} \right\rangle_g = \left\langle e^{-itH_g/\hbar} e^{itH_e/\hbar} \right\rangle_g \tag{18.48}$$

which is related to the lineshape function (18.40) by a Fourier transformation

$$FCD(\hbar\omega) = \frac{1}{2\pi\hbar} \int_{-\infty}^{\infty} dt\, e^{-i\omega t} F(t). \tag{18.49}$$

We will evaluate the correlation function for some simple models in the following chapter.

18.5 Excitation by a Short Pulse

The rate expression (18.40) holds for continuous excitation. In the following, we study excitation by a very short light pulse.

In Condon's approximation, the matrix element of the perturbation operator factorizes

$$< \psi_e(r,q)\chi_e(q) \left| \hat{V}_{int} \right| \psi_g(r,q)\chi_g(q) > \approx -\mathbf{E}_0 \boldsymbol{\mu}_{eg} < \chi_e(q) | \chi_g(q) > \tag{18.50}$$

and $\hat{V}_{int}$ changes only the electronic part of the wavefunction

$$\hat{V}_{int} |\psi_g \chi_g >= \sum_{\chi_e} |\psi_e \chi_e >< \psi_e \chi_e | \hat{V}_{int} | \psi_g \chi_g >=$$

$$= -\mathbf{E}_0 \boldsymbol{\mu}_{eg} \sum_{\chi_e} |\psi_e \chi_e >< \chi_e | \chi_g > \tag{18.51}$$

Let us consider a model (Sect. 17.4) where the state $|s >= |\psi_e \chi_{es} >$carries intensity and is coupled to a manifold of dark states $|l >= |\psi_g \chi_l >$ which form a quasi-continuum. The true molecular eigenstates are mixtures

$$|\nu >= a_{\nu s} |s > + \sum_l b_{\nu l} |l >= a_{\nu s} |\psi_e \chi_{es} > + \sum_l b_{\nu l} |\psi_g \chi_{gl} > \tag{18.52}$$

and carry transition dipoles

$$\boldsymbol{\mu}_{\nu g} = a_{\nu s} \boldsymbol{\mu}_s. \tag{18.53}$$

[2]The trace is invariant to a cyclic permutation.

The coupling to the molecular eigenstates is

$$< \psi_g \chi_g | \hat{V}_{int} | \nu >= a_{\nu s} < \psi_g \chi_g | \hat{V}_{int} | s > \tag{18.54}$$

hence

$$\hat{V}_{int} | \psi_g \chi_g >= \sum_{\nu} | \nu >< \nu | \hat{V}_{int} | \psi_g \chi_g >= \sum_{\nu} a^*_{\nu s} | \nu > . \tag{18.55}$$

But due to the orthonormality of the eigenstates,

$$\sum_{\nu} a^*_{\nu s} | \nu >= \sum_{\nu} a^*_{\nu s} \left(a_{\nu s} | s > + \sum_{l} b_{\nu l} | l > \right) = | s > \tag{18.56}$$

i.e., a very short pulse excites the pure Born–Oppenheimer state

18.6 Radiationless Transitions

We consider a molecule which is in an eigenstate $|\psi_i \chi_{is} >$ of the Born–Oppenheimer Hamiltonian H_0 at time t_0. For $t > t_0$ nonadiabatic and spin-orbit coupling are effective. The perturbation operator

$$\hat{H}' = \hat{V}_{nad} + H_{SO} \tag{18.57}$$

induces transitions to other Born–Oppenheimer states $|\psi_f \chi_{fl} >$ (Fig. 18.4)

$$|\psi_i(r, q)\chi_{i,s}(q) > \rightarrow |\psi_f(r, q)\chi_{f,l}(q) > . \tag{18.58}$$

In lowest order, the decay rate is the sum over all final states [67, 68]

$$k_s = \sum_{l} k_{s,l} = \frac{2\pi}{\hbar} \sum_{l} |V_{s,l}|^2 \delta(E_f - E_i) \tag{18.59}$$

with the matrix element

$$V_{s,l} =< \psi_f(r, q)\chi_{f,l}(q) | \hat{H}' | \psi_i(r, q)\chi_{i,s}(q) > . \tag{18.60}$$

If the lowest order vanishes, e.g., if it is forbidden by symmetry, higher orders also have to be considered and the matrix element $V_{s,l}$ of the interaction has to be replaced by the corresponding element of the T-matrix [69] to obtain the generalized golden rule

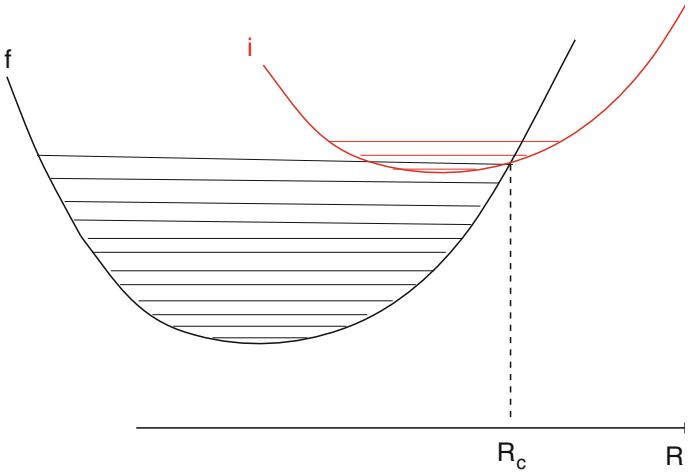

Fig. 18.4 Radiationless transitions. Transition from a higher electronic state (i) to a lower one (f). Energy conservation is possible if vibrational excitations in the final state are created. The multidimensional nuclear coordinates are represented schematically by the coordinate R

$$k_s = \sum_l k_{s,l} = \frac{2\pi}{\hbar} \sum_l |V_{s,l} + \sum_j \frac{V_{s,j} V_{j,l}}{E_s - E_j} + \ldots|^2 \delta(E_f - E_i). \tag{18.61}$$

18.6.1 Internal Conversion

For transitions between states of the same multiplicity only the nonadiabatic interaction Sect. 17.3 is relevant. Neglecting the second derivative, its matrix elements are

$$V_{s,l} = -\frac{\hbar^2}{2} \int \left[\psi_f^*(r,q) \chi_{f,l}^*(q) \sum_r \left(\frac{\partial}{\partial q_r} \chi_{i,s}(q) \right) \left(\frac{\partial}{\partial q_r} \psi_{i,s}(\mathbf{r},q) \right) + \ldots \right] dr\, dq. \tag{18.62}$$

If the dependency of the nonadiabatic coupling on the nuclear coordinates is weak, the Condon approximation may be applied to factorize the nonadiabatic coupling into an electronic and a nuclear part

$$V_{s,l} \approx -\frac{\hbar^2}{2} \sum_r \frac{< \psi_f(\mathbf{r}, 0) \frac{\partial U}{\partial q_r} \psi_i(\mathbf{r}, 0) >}{E_f(0) - E_i(0)} \int \chi^*_{f,l}(q) \frac{\partial}{\partial q_r} \chi_{i,s}(q) dq. \tag{18.63}$$

Non-Condon effects can be taken into account by treating the potential energy difference $U(q) - U(0)$ as a perturbation and expanding the adiabatic wavefunctions [70] in a crude diabatic basis

$$\psi_j(r, q) = \psi_j(r, 0) + \sum_{j' \neq j} \frac{< \psi_j(r, 0)(U(q) - U(0))\psi_{j'}(r, 0) >}{E_j(0) - E_{j'}(0)} \psi_{s'}(r, 0) + \ldots \tag{18.64}$$

In general, however, the Born–Oppenheimer approximation breaks down near configurations where the potential energy surfaces cross. Then the transformation to a nonadiabatic basis can remove the divergence of the gradient coupling [71]. Ultimately, the transition has to be discussed in the framework of conical intersections [72].

18.6.2 Intersystem Crossing

The Coulomb interaction does not depend on spin, therefore the nonadiabatic interaction couples only states of the same multiplicity. Transitions between singlet and triplet states involve the spin-orbit coupling H_{SO} which together with the nonadiabatic coupling has to be treated as a perturbation [73–75]. If spin-orbit coupling is large enough, the dominant mechanism involves direct spin-orbit coupling

$$\begin{aligned} V^{(1)}_{sl} &= <^1 \psi_f \chi_{f,l} | H_{SO} |^3 \psi_i \chi_{i,s} > \\ &\approx <^1 \psi_f(r, 0) | H_{SO} |^3 \psi_i(r, 0) > \int dr \chi^*_{fl} \chi_{is} \end{aligned} \tag{18.65}$$

where again the Condon approximation has been applied. If direct spin-orbit coupling is forbidden, higher order terms involving H_{SO} and $\hat{V}_{nad}$ as well non-Condon effects have to be considered leading to vibronic spin-orbit coupling [76].

Problems

18.1 Absorption Spectrum

Within the Born–Oppenheimer approximation, the rate for optical transitions of a molecule from its ground state to an electronically excited state is proportional to

$$\alpha(\hbar\omega) = \sum_{i,f} P_i | < i|\mu|f > |^2 \delta(\hbar\omega_f - \hbar\omega_i - \hbar\omega)$$

Show that this Golden rule expression can be formulated as the Fourier integral of the dipole moment correlation function

$$\frac{1}{2\pi\hbar} \int dt \, \mathrm{e}^{\mathrm{i}\omega t} < \mu(0)\mu(t) >$$

and that within the Condon approximation this reduces to the correlation function of the nuclear motion.

Chapter 19
The Displaced Harmonic Oscillator

In this chapter, we discuss a more specific model for the transition between the vibrational manifolds using parallel displaced harmonic normal modes, for which the time-correlation function can be evaluated explicitly. We consider the limit of high frequency modes (or low temperature) where vibrational progressions appear and the limit of low frequencies (or high temperature) where the lineshape becomes Gaussian where position and width only depend on the total reorganization energy.

19.1 The Time-Correlation Function in the Displaced Harmonic Oscillator Approximation

We apply the harmonic approximation (17.11) for the nuclear motion to the zero-order Hamiltonian (18.31)

$$H_0 = |\psi_e > \left(E_e^0 + \sum_r \hbar\omega_r^e b_r^{e\dagger} b_r^e\right) < \psi_e| + |\psi_g > \left(E_g^0 + \sum_r \hbar\omega_r^g b_r^{g\dagger} b_r^g\right) < \psi_g|. \tag{19.1}$$

In a simplified but popular model, we neglect mixing of the normal modes (parallel mode approximation, the eigenvectors (u_j^r in 17.13) are the same) and frequency changes ($\omega_r^g = \omega_r^e = \omega_r$) in the excited state but allow for a shift of the equilibrium

P.O.J. Scherer and S.F. Fischer, *Theoretical Molecular Biophysics*,
Biological and Medical Physics, Biomedical Engineering,
DOI 10.1007/978-3-662-55671-9_19

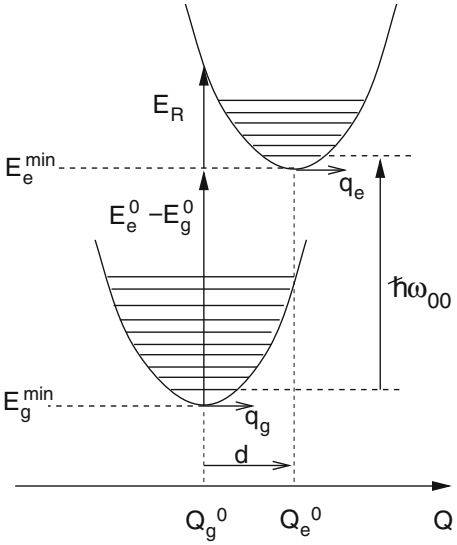

Fig. 19.1 Displaced oscillator model. The displaced oscillator model assumes that the normal mode eigenvectors are the same in both electronic states involved. Then the different modes are still independent. The figure shows the potential energy along one such normal mode Q. The minima at Q_g^0 and Q_e^0 are shifted relative to each other by a distance $d = Q_e^0 - Q_g^0$. The elongation of the normal mode is denoted as $q_{g(e)} = Q - Q_{g(e)}^0$. The curvature of the two parabolas is the same. Thus neglecting frequency changes in the excited state, the vibrationless transition energy $\hbar\omega_{00}$ equals the pure electronic transition energy $E_e^{min} - E_g^{min}$. The reorganization energy $E_R = \frac{1}{2}\omega^2 d^2$ is the amount of energy which can be released in the excited state after a vertical transition from the vibronic groundstate

position ($q_r^e = q_r^g + d_r$).[1] The potential energy for the two states then is approximated by (Fig. 19.1)

$$E_g = E_g^{min} + \frac{1}{2}\sum_r \omega_r^2 q_r^2 \tag{19.2}$$

$$E_e = E_e^{min} + \frac{1}{2}\sum_r \omega_r^2 (q_r^e)^2 = E_e^{min} + \frac{1}{2}\sum_r \omega_r^2 (q_r + d_r)^2. \tag{19.3}$$

The vertical excitation energy is[2]

$$E_e(q_r = 0) - E_g(q_r = 0) = E_e^{min} + \frac{1}{2}\sum_r \omega_r^2 {d_r}^2 - E_g^{min} = \hbar\omega_{00} + E_R \tag{19.4}$$

[1] We retain only the lowest order of the potential difference.

[2] Without frequency changes the zero point energies are the same and $E_e^{min} - E_g^{min} = E_e^0 - E_g^0 = \hbar\omega_{00}$.

with the reorganization energy

$$E_R = \frac{1}{2}\sum_r \omega_r^2 d_r^2. \tag{19.5}$$

We introduce the ladder operators by substituting

$$q_r = \sqrt{\frac{\hbar}{2\omega_r}}\left(b_r^g + b_r^{g\dagger}\right) \tag{19.6}$$

$$q_r^e = \sqrt{\frac{\hbar}{2\omega_r}}\left(b_r^e + b_r^{e\dagger}\right) = \sqrt{\frac{\hbar}{2\omega_r}}\left(b_r^g + b_r^{g\dagger}\right) + d_r. \tag{19.7}$$

Since d_r is real valued we find

$$b_r^e = b_r^g + \frac{1}{2}\sqrt{\frac{2\omega_r}{\hbar}}d_r = b_r^g + \sqrt{\frac{\omega_r}{2\hbar}}d_r = b_r^g + g_r$$

with the vibronic coupling parameter

$$g_r = \sqrt{\frac{\omega_r}{2\hbar}}d_r.$$

From

$$\begin{aligned}\hbar\omega_r\left(b_r^{e\dagger}b_r^e + \frac{1}{2}\right) &= \hbar\omega_r\left((b_r^{g\dagger} + g_r)(b_r^g + g_r) + \frac{1}{2}\right)\\ &= \hbar\omega_r\left(b_r^{g\dagger}b_r^g + \frac{1}{2}\right) + \hbar\omega_r g_r\left(b_r^g + b_r^{g\dagger}\right) + \hbar\omega_r g_r^2\end{aligned}$$

we obtain the "displaced harmonic oscillator" model (DHO)

$$H_g = \sum_r \hbar\omega_r b_r^+ b_r \tag{19.8}$$

$$\begin{aligned}H_e &= \sum_r \hbar\omega_r b_r^{e\dagger}b_r^e\\ &= H_g + \sum_r g_r\hbar\omega_r(b_r^\dagger + b_r) + \sum_r g_r^2\hbar\omega_r\end{aligned} \tag{19.9}$$

where the superscript g is omitted from now and the last term is the reorganization energy

$$E_R = \sum_r g_r^2 \hbar\omega_r . \tag{19.10}$$

The correlation function (18.50)

$$F(t) = \left\langle \mathrm{e}^{-\frac{\mathrm{i}t}{\hbar}H_g} \mathrm{e}^{\frac{\mathrm{i}t}{\hbar}H_e} \right\rangle_g = Q^{-1} \mathrm{tr}\left(\mathrm{e}^{-H_g/k_BT} \mathrm{e}^{-\frac{\mathrm{i}t}{\hbar}H_g} \mathrm{e}^{\frac{\mathrm{i}t}{\hbar}H_e} \right) \tag{19.11}$$

with

$$Q = \mathrm{tr}(\mathrm{e}^{-H_g/k_BT}) \tag{19.12}$$

factorizes in the parallel mode approximation

$$F(t) = \prod_r F_r(t) \tag{19.13}$$

$$\begin{aligned} F_r(t) &= Q_r^{-1} \mathrm{tr}\left(\mathrm{e}^{-\hbar\omega_r b_r^\dagger b_r/k_BT} \mathrm{e}^{-\mathrm{i}t\omega_r b_r^\dagger b_r} \mathrm{e}^{\mathrm{i}t\omega_r (b_r^\dagger + g_r)(b_r + g_r)} \right) \\ &= \left\langle \mathrm{e}^{-\mathrm{i}t\omega_r b_r^\dagger b_r} \mathrm{e}^{\mathrm{i}t\omega_r (b_r^\dagger + g_r)(b_r + g_r)} \right\rangle . \end{aligned} \tag{19.14}$$

As shown in the appendix this can be evaluated as

$$\begin{aligned} F_r(t) &= \exp\left(g_r^2 \left[(\mathrm{e}^{\mathrm{i}\omega_r t} - 1)(\overline{n_r} + 1) + (\mathrm{e}^{-\mathrm{i}\omega_r t} - 1)\overline{n_r} \right] \right) \\ &= \exp\left(g_r^2 (2\overline{n}_r + 1)(\cos\omega_r t - 1) + \mathrm{i} g_r^2 \sin\omega_r t \right) \end{aligned} \tag{19.15}$$

with the average phonon numbers

$$\overline{n_r} = \frac{1}{\mathrm{e}^{\hbar\omega_r/k_BT} - 1} . \tag{19.16}$$

Expression (19.14) contains phonon absorption (positive frequencies) and emission processes (negative frequencies). We discuss two important limiting cases.

19.2 High Frequency Modes

In the limit $\hbar\omega_r \gg k_BT$ the average phonon number

$$\overline{n_r} = \frac{1}{\mathrm{e}^{\hbar\omega/k_BT} - 1} \tag{19.17}$$

is small and the correlation function becomes

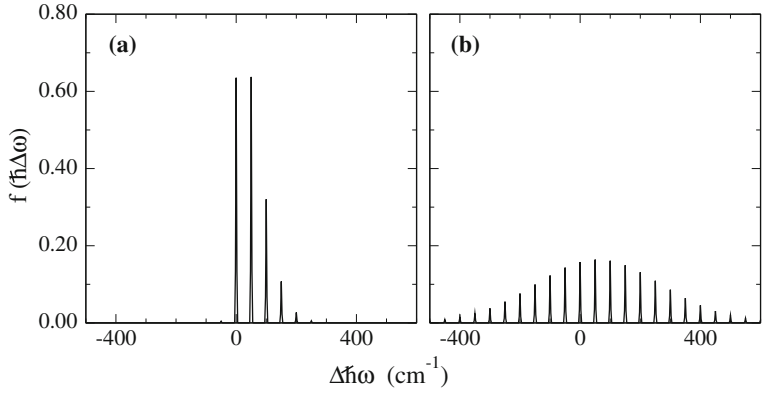

Fig. 19.2 Progression of a low frequency mode. The Fourier transform of (19.15) is shown for typical values of $\hbar\omega = 50\,\mathrm{cm}^{-1}$, 1, $E_r = 50\,\mathrm{cm}^{-1}$ and **(a)** $kT = 10\,\mathrm{cm}^{-1}$ **(b)** $kT = 200\,\mathrm{cm}^{-1}$. A small damping was introduced to obtain finite linewidths

$$F_r(t) \to \exp\left(g_r^2(\mathrm{e}^{\mathrm{i}\omega t} - 1)\right). \tag{19.18}$$

Expansion of $F_r(t)$ as a power series of g_r^2 gives

$$F_r(t) = \sum_j \frac{g_r^{2j}}{j!}\mathrm{e}^{-g_r^2}\mathrm{e}^{\mathrm{i}(j\omega_r)t} \tag{19.19}$$

which corresponds to a progression of transitions $0 \to j\,\omega_r$ with Franck–Condon factors (Fig. 19.2)

$$FC(0, j) = \frac{g_r^{2j}}{j!}\mathrm{e}^{-g_r^2}. \tag{19.20}$$

19.3 Low Frequency Modes

In the high temperature limit ($\hbar\omega_r \ll k_B T$) the time-correlation function of one oscillator (19.15) has peaks at $t = 0, \pm\frac{2\pi}{\omega_r}, \ldots$ which become very sharp for large $\overline{n}_r \approx k_B T/\hbar\omega_r$[3] (Fig. 19.3). The product correlation function of many oscillators is non vanishing only around $t = 0$, i.e. the correlation function decays rapidly and can be approximated by the Taylor series (in this context also known as short time approximation)

$$F(t) \approx \exp\left\{-t^2\sum_r(\overline{n}_r + \frac{1}{2})g_r^2\omega_r^2 + it\sum_r g_r^2\omega_r\right\} \approx \exp\left\{-t^2\frac{E_R k_B T}{\hbar^2} + \frac{it}{\hbar}E_R\right\}. \tag{19.21}$$

[3] Also for very strong vibronic coupling g_r.

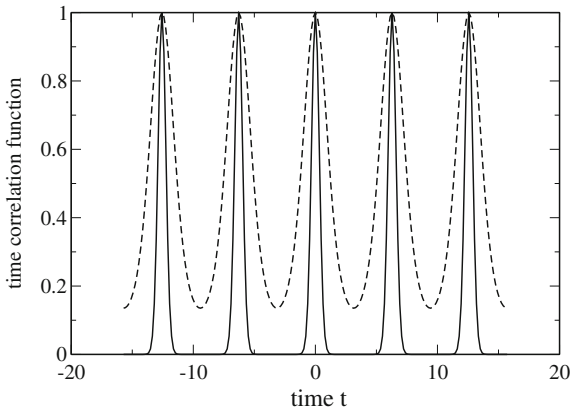

Fig. 19.3 Time-correlation function. $|F_r(t)| = \exp\left\{g_r^2(2\overline{n}_r + 1)(\cos(t) - 1)\right\}$ is shown for $g_r^2(2\overline{n}_r + 1) = 1$(*broken curve*) and $g_r^2(2\overline{n}_r + 1) = 10$(*full curve*)

Fig. 19.4 Gaussian envelope

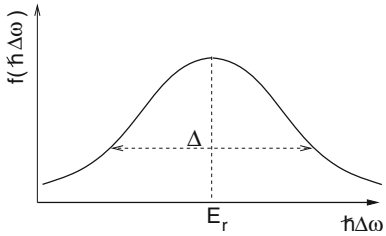

The lineshape is approximately given by a Gaussian (Fig. 19.4)

$$\begin{aligned} FCD(\hbar\omega) &= \frac{1}{2\pi\hbar}\int_{-\infty}^{\infty} dt\, e^{-i\omega_0 t}\exp\left\{-t^2\frac{E_R k_B T}{\hbar^2} + \frac{it}{\hbar}E_R\right\} \\ &= \frac{1}{2\pi\hbar}\sqrt{\frac{\pi\hbar^2}{E_R k_B T}}\exp\left\{-\frac{(\hbar\omega - E_R)^2}{4E_R k_B T}\right\} \\ &= \sqrt{\frac{1}{4\pi E_R k_B T}}\exp\left\{-\frac{(\hbar\omega - E_R)^2}{4E_R k_B T}\right\} \end{aligned} \tag{19.22}$$

with the reorganization energy

$$E_r = \sum_r g_r^2\hbar\omega_r \tag{19.23}$$

and the variance

$$\Delta^2 = 2E_R k_B T. \tag{19.24}$$

Chapter 20
Spectral Diffusion

Electronic excitation energies of a chromophore within a protein environment are not static quantities but fluctuate in time. This can be directly observed with the methods of single molecule spectroscopy. If instead an ensemble average is measured, then the relative timescales of measurement and fluctuations determine if an inhomogeneous distribution is observed or if the fluctuations lead to a homogeneous broadening. In this chapter we discuss simple models [77–79], which are capable of describing the transition between these two limiting cases. First we derive the transition rate semiclassically for fluctuating transition energy which depends on the Fourier transform of the dephasing function. For Gaussian fluctuations (e.g., for the model of a Brownian oscillator) the second-order cumulant expansion becomes exact. We apply Kubo's model of exponentially decaying frequency correlations and discuss the limits of long and short correlation time.

20.1 Dephasing

We study a semiclassical model of a two-state system. Due to interaction with the environment the energies of the two states are fluctuating quantities. The system is described by a time-dependent Hamiltonian

$$H_0 = \begin{pmatrix} E_1(t) & 0 \\ 0 & E_2(t) \end{pmatrix} \tag{20.1}$$

where the time evolution can be described by the propagator

$$\psi(t) = \exp\left\{\frac{1}{\mathrm{i}\hbar}\int_0^t H_0 dt\right\}\psi(0) = U_0(t)\psi(0) \tag{20.2}$$

P.O.J. Scherer and S.F. Fischer, *Theoretical Molecular Biophysics*,
Biological and Medical Physics, Biomedical Engineering,
DOI 10.1007/978-3-662-55671-9_20

$$U_0(t) = \exp\left\{\frac{1}{\mathrm{i}\hbar}\int_0^t H_0 dt\right\} = \begin{pmatrix} \mathrm{e}^{\frac{1}{\mathrm{i}\hbar}\int^t E_1(t)dt} & \\ & \mathrm{e}^{\frac{1}{\mathrm{i}\hbar}\int^t E_2(t)} \end{pmatrix}. \tag{20.3}$$

Optical transitions are induced by the perturbation operator

$$H' = \begin{pmatrix} 0 & \mu\mathrm{e}^{\mathrm{i}\omega t} \\ \mu\mathrm{e}^{-\mathrm{i}\omega t} & 0 \end{pmatrix}. \tag{20.4}$$

We make the following ansatz

$$\psi(t) = U_0(t)\phi(t) \tag{20.5}$$

and find

$$(H_0 + V)\psi = \mathrm{i}\hbar\frac{\mathrm{d}}{\mathrm{d}t}\psi = H_0 U_0(t)\phi + \mathrm{i}\hbar U_0(t)\frac{\mathrm{d}}{\mathrm{d}t}\phi \tag{20.6}$$

hence

$$\mathrm{i}\hbar\frac{\mathrm{d}}{\mathrm{d}t}\phi = U_0(-t)VU_0(t)\phi. \tag{20.7}$$

Now the operator product is

$$U_0(-t)VU_0(t) = \begin{pmatrix} 0 & \mu\mathrm{e}^{\mathrm{i}\omega t - \frac{\mathrm{i}}{\hbar}\int_0^t (E_2 - E_1)dt} \\ \mu\mathrm{e}^{-\mathrm{i}\omega t + \frac{\mathrm{i}}{\hbar}\int_0^t (E_2 - E_1)dt} & 0 \end{pmatrix} \tag{20.8}$$

which can be written with a time-dependent dipole moment

$$\mathrm{i}\hbar\frac{\mathrm{d}}{\mathrm{d}t}\phi = \begin{pmatrix} 0 & \mu(t)\mathrm{e}^{\mathrm{i}\omega t} \\ \mu(t)^*\mathrm{e}^{-\mathrm{i}\omega t} & 0 \end{pmatrix}\phi \tag{20.9}$$

$$\frac{\mathrm{d}}{\mathrm{d}t}\mu(t) = \frac{1}{\mathrm{i}\hbar}(E_2(t) - E_1(t))\mu(t) = -\mathrm{i}\omega_{21}(t)\mu(t) = -\mathrm{i}(<\omega_{21}> + \delta\omega(t))\mu(t). \tag{20.10}$$

Starting from the initial condition

$$\phi(t=0) = \begin{pmatrix} 1 \\ 0 \end{pmatrix} \tag{20.11}$$

we find in lowest order

$$\phi(t) = \begin{pmatrix} 1 \\ \frac{1}{\mathrm{i}\hbar}\int_0^t dt\, \mathrm{e}^{-\mathrm{i}\omega t}\mu^*(t) \end{pmatrix} \tag{20.12}$$

and the transition probability is given by

$$\begin{aligned} P(t) &= \frac{1}{\hbar^2}\int_0^t dt'' \int_0^t dt' \mathrm{e}^{\mathrm{i}\omega(t''-t')}\mu(t'')\mu^*(t') \\ &= \frac{|\mu_0|^2}{\hbar^2}\int_0^t dt'' \int_0^t dt' \mathrm{e}^{\mathrm{i}\omega(t''-t')}\mathrm{e}^{-\mathrm{i}<\omega_{21}>(t''-t')}\mathrm{e}^{-\mathrm{i}\int_{t'}^{t''}\delta\omega(t''')dt'''}. \end{aligned} \tag{20.13}$$

The ensemble average gives for stationary fluctuations

$$P(t) = \frac{|\mu_0|^2}{\hbar^2}\int_0^t \int_0^t dt''\, dt'\, \mathrm{e}^{\mathrm{i}\omega(t''-t')}\mathrm{e}^{-\mathrm{i}<\omega_{21}>(t''-t')}F(t''-t') \tag{20.14}$$

with the dephasing function

$$F(t) = <\exp(-\mathrm{i}\int_0^t \delta\omega(t')dt')> . \tag{20.15}$$

With the help of the Fourier transformation

$$F(t) = \frac{1}{2\pi}\int_{-\infty}^{\infty} \mathrm{e}^{-\mathrm{i}\omega' t}\hat{F}(\omega')d\omega'$$

the transition probability becomes

$$\begin{aligned} P(t) &= \frac{|\mu_0|^2}{2\pi\hbar^2}\int_{-\infty}^{\infty} d\omega' \int_0^t \int_0^t dt''\, dt'\, \mathrm{e}^{\mathrm{i}(\omega-\omega')(t''-t')}\mathrm{e}^{-\mathrm{i}<\omega_{21}>(t''-t')}\hat{F}(\omega') \\ &= \frac{|\mu_0|^2}{2\pi\hbar^2}\int_{-\infty}^{\infty} d\omega' \hat{F}(\omega')\frac{2(1-\cos((\omega-\omega'-<\omega_{21}>)t)}{(\omega-\omega'-<\omega_{21}>)^2} \end{aligned} \tag{20.16}$$

where the quotient approximates a delta function for longer times

$$\frac{2(1-\cos((\omega-\omega'-<\omega_{21}>)t)}{(\omega-\omega'-<\omega_{21}>)^2} \to 2\pi t\delta(\omega-\omega'-<\omega_{21}>) \tag{20.17}$$

and hence the golden rule expression is obtained in the form

$$\frac{P(t)}{t} \to \frac{|\mu_0|^2}{\hbar^2}\hat{F}(\omega-<\omega_{21}>) \tag{20.18}$$

20.2 Gaussian Fluctuations

We consider the dephasing function

$$F(t) = < \mathrm{e}^{\mathrm{i} \int_0^t \delta\omega(\tau) d\tau} > = < \mathrm{e}^{\mathrm{i} X_t} > \tag{20.19}$$

and assume that (for fixed integration time t) the random variable

$$X_t = \int_0^t \delta\omega(\tau) d\tau \tag{20.20}$$

has a Gaussian probability distribution

$$W_t(X) = \frac{1}{\Delta_t \sqrt{2\pi}} \mathrm{e}^{-X_t^2/2\Delta_t^2} \tag{20.21}$$

with zero mean

$$< X_t > = 0 \tag{20.22}$$

and variance

$$< X_t^2 > = \Delta_t^2. \tag{20.23}$$

This is for instance applicable if the frequency fluctuations are described by diffusive motion in a harmonic potential. Then

$$F(t) = < \mathrm{e}^{\mathrm{i} X_t} > = \int_{-\infty}^{\infty} \mathrm{e}^{\mathrm{i} X_t} W_t(X) dX = \mathrm{e}^{-\Delta_t/2} \tag{20.24}$$

where the width can be expressed by the second moment

$$\Delta_t^2 = < X_t^2 > = < \left(\int_0^t \delta\omega(t') dt' \right)^2 > = < \int_0^t dt' \int_0^t dt'' \delta\omega(t') \delta\omega(t'') > . \tag{20.25}$$

For more general processes, a cumulant expansion can be applied. Fourier transformation of the probability distribution (for fixed integration time t) gives the characteristic function

$$\Phi_t(\lambda) = < e^{i\lambda X_t} > = \int dX \, e^{i\lambda X_t} W_t(X) \tag{20.26}$$

with

$$F(t) = \Phi_t(\lambda = 1). \tag{20.27}$$

We expand the logarithm of Φ

$$\ln \Phi = \ln \Phi(0) + \lambda \frac{\Phi'(0)}{\Phi(0)} + \frac{\lambda^2}{2} \frac{\Phi''\Phi - \Phi'^2}{\Phi^2} + \frac{\lambda^3}{6} \frac{\Phi'''\Phi^2 - 3\Phi''\Phi'\Phi + 2\Phi'^3}{\Phi^3} \cdots \tag{20.28}$$

where the derivatives are

$$\Phi^{(n)} = \int dX \, (\mathrm{i}X)^n \, e^{\mathrm{i}\lambda X} W(X) \tag{20.29}$$

with

$$\Phi^{(n)}(0) = < (\mathrm{i}X)^n > \tag{20.30}$$

from which we obtain the series expansion

$$\ln \Phi = \lambda < \mathrm{i}X > + \frac{\lambda^2}{2} \left(< -X^2 > - < iX >^2 \right) + \cdots \tag{20.31}$$

Setting now $\lambda = 1$ gives the cumulant expansion

$$\begin{aligned} \ln(< \mathrm{e}^{\mathrm{i}x} >) = & < \mathrm{i}X > - \frac{1}{2}(< X^2 > - < X >^2) \\ & + \frac{1}{6}(< -\mathrm{i}X^3 > -3 < -X^2 >< \mathrm{i}X > +2 < \mathrm{i}X >^3) \cdots \end{aligned} \tag{20.32}$$

which for a distribution with zero mean simplifies to

$$-\frac{1}{2} < X^2 > - \frac{\mathrm{i}}{6} < X^3 > \cdots \tag{20.33}$$

For the special case of a Gaussian distribution all cumulants except the first and second order vanish.

For the simplest model of exponentially decaying frequency correlations

$$< \delta\omega(t)\delta\omega(0) > = \Delta^2 \mathrm{e}^{-t/\tau_c} \tag{20.34}$$

integration gives

$$F(t) = \exp\left(-\Delta^2 \tau_c^2 (\mathrm{e}^{-|t|/\tau_c} - 1 + |t|/\tau_c) \right). \tag{20.35}$$

Let us look at the limiting cases.

20.2.1 Long Correlation Time

This corresponds to the inhomogeneous case where $< \delta\omega(t)\delta\omega(0) > = \Delta^2$ is constant. We expand the exponential for $t << \tau_c$:

$$\mathrm{e}^{-t/\tau_c} - 1 + t/\tau_c = \frac{t^2}{2\tau_c^2} + \cdots \tag{20.36}$$

$$F(t) = \mathrm{e}^{-\Delta^2 t^2/2}. \tag{20.37}$$

The transition probability is

$$P(t) = \frac{|\mu_0|^2}{\hbar^2} \int_0^t dt' \int_0^t dt'' \mathrm{e}^{\mathrm{i}(t''-t')(\omega - <\omega_{21}>)} \mathrm{e}^{-\Delta^2 (t''-t')^2/2}. \tag{20.38}$$

Since F(t) is symmetric

$$\begin{aligned} P(t) &= \frac{|\mu_0|^2}{4\hbar^2} \int_{-t}^t dt' \int_{-t}^t dt'' \mathrm{e}^{\mathrm{i}(t''-t')(\omega - <\omega_{21}>)} \mathrm{e}^{-\Delta^2 (t''-t')^2/2} \\ &\approx \frac{|\mu_0|^2}{2\hbar^2}\, t \int_{-\infty}^{\infty} dt \mathrm{e}^{\mathrm{i}t(\omega - <\omega_{21}>)} \mathrm{e}^{-\Delta^2 t^2/2} \end{aligned} \tag{20.39}$$

and the lineshape has the form of a Gaussian (Fig. 20.1)

$$\lim \frac{P(t)}{t} \sim \exp\left(-\frac{(\omega - < \omega_{21} >)^2}{2\Delta^2}\right). \tag{20.40}$$

20.2.2 Short Correlation Time

For very short correlation time $\tau_c \ll t$ we approximate

$$F(t) = \exp\left(-\Delta^2 \tau_c |t|\right) = \exp\left(-|t|/T_2\right) \tag{20.41}$$

with the dephasing time

$$T_2 = (\Delta^2 \tau_c)^{-1}. \tag{20.42}$$

The lineshape has now the form of a Lorentzian

$$\int_{-\infty}^{\infty} dt\, \mathrm{e}^{\mathrm{i}t(\omega - <\omega_{21}>)} \mathrm{e}^{-|t|/T_2} = \frac{2T_2^{-1}}{T_2^{-2} + (\omega - < \omega_{21} >)^2}. \tag{20.43}$$

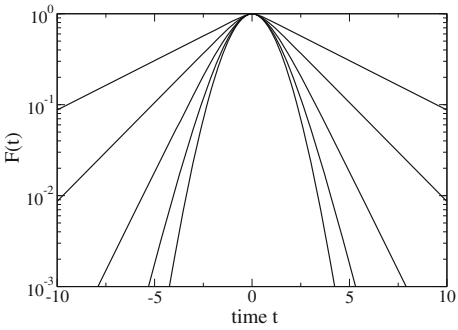

Fig. 20.1 Time correlation function of the Kubo model. F(t) from (20.35) is shown for $\Delta = 1$ and several values of τ_c. For large correlation times the Gaussian $\exp(-\Delta^2 t^2/2)$ is approximated whereas for short correlation times the correlation function becomes approximately exponential and the width increases with τ^{-1}. Correspondingly, the Fourier transform becomes sharp in this case (motional narrowing)

This result shows the motional narrowing effect when the correlation time is short or the motion very fast.

20.3 Markovian Modulation

Another model which can be analytically investigated describes the frequency fluctuations by a Markovian random walk. We discuss the simplest case of a dichotomous process (9.2), i.e., the oscillator frequency switches randomly between two values $\omega_\pm$. This is, for instance relevant for NMR spectra of a species which undergoes a chemical reaction

$$\text{A+B} \rightleftharpoons \text{AB} \tag{20.44}$$

where the NMR resonance frequencies depend on the chemical environment. For a dichotomous Markovian process switching between two states $X = \pm$ we have for the conditional transition probability

$$P(X, t+\tau|X_0 t_0) = P(X, t+\tau|+, t)P(+, t|X_0 t_0) + P(X, t+\tau|-, t)P(-, t|X_0 t_0). \tag{20.45}$$

For small time increment τ linearization gives

$$
\begin{aligned}
P(+,t+\tau|+,t) &= 1-\alpha\tau \\
P(-,t+\tau|-,t) &= 1-\beta\tau \\
P(-,t+\tau|+,t) &= \alpha\tau \\
P(+,t+\tau|-,t) &= \beta\tau
\end{aligned}
\tag{20.46}
$$

and hence

$$
\begin{aligned}
P(+,t+\tau|+t_0) &= P(+,t+\tau|+,t)P(+,t|+t_0) + P(+,t+\tau|-,t)P(-,t|+t_0) \\
&= (1-\alpha\tau)P(+,t|+,t_0) + \beta\tau P(-,t|+,t_0)
\end{aligned}
\tag{20.47}
$$

and we obtain the differential equation

$$
\frac{\partial}{\partial t}P(+,t|+,t_0) = -\alpha P(+,t|+,t_0) + \beta P(-,t|+,t_0)
$$

and similarly

$$
\begin{aligned}
\frac{\partial}{\partial t}P(-,t|-,t_0) &= -\beta P(-,t|-,t_0) + \alpha P(+,t|-,t_0) \\
\frac{\partial}{\partial t}P(-,t|+,t_0) &= -\beta P(-,t|+,t_0) + \alpha P(+,t|+,t_0) \\
\frac{\partial}{\partial t}P(+,t|-,t_0) &= -\alpha P(+,t|-,t_0) + \beta P(-,t|-,t_0).
\end{aligned}
\tag{20.48}
$$

In a stationary system the probabilities depend only on $t - t_0$ and the differential equations can be written as a matrix equation

$$
\frac{\partial}{\partial t}P(t) = A\,P(t) \tag{20.49}
$$

with

$$
P(t) = \begin{pmatrix} P(+,t|+,0) & P(+,t|-,0) \\ P(-,t|+,0) & P(-,t|-,0) \end{pmatrix} \tag{20.50}
$$

and the rate matrix

$$
A = \begin{pmatrix} -\alpha & \beta \\ \alpha & -\beta \end{pmatrix}. \tag{20.51}
$$

Let us define the quantity

$$
Q(X,t|X',0) = \left\langle \mathrm{e}^{-\mathrm{i}\int_0^t \omega(t')dt'} \right\rangle_{X,X'} \tag{20.52}
$$

where the average is taken under the conditions that the system is in state X at time t and in state X' at time 0. Then we find

$$Q(X,t+\tau|X',0) = \left\langle \mathrm{e}^{-\mathrm{i}\int_0^t \omega(t')dt'} \mathrm{e}^{\mathrm{i}\omega(t)\tau} \right\rangle_{X,X'}$$
$$= Q(X,t+\tau|+,t)Q(+,t|X',0) + Q(X,t+\tau|-,t)Q(-,t|X',0). \tag{20.53}$$

Expansion for small τ gives

$$\begin{aligned} Q(+,t+\tau|+,t) &= \left\langle \mathrm{e}^{-\mathrm{i}\omega_+\tau} \right\rangle_{+,+} = 1 - (\mathrm{i}\omega_+ + \alpha)\tau \\ Q(-,t+\tau|-,t) &= \left\langle \mathrm{e}^{-\mathrm{i}\omega_-\tau} \right\rangle_{-,-} = 1 - (\mathrm{i}\omega_- + \beta)\tau \\ Q(-,t+\tau|+,t) &= \left\langle \mathrm{e}^{-\mathrm{i}\omega_+\tau} \right\rangle_{-,+} = \alpha\tau \\ Q(+,t+\tau|-,t) &= \left\langle \mathrm{e}^{-\mathrm{i}\omega_-\tau} \right\rangle_{+,-} = \beta\tau \end{aligned} \tag{20.54}$$

and for the time derivatives

$$\begin{aligned} \frac{\partial}{\partial t} Q(+,t|+,0) &= \lim_{\tau\to 0} \frac{1}{\tau} \left[(-\mathrm{i}\omega_+ - \alpha)\tau Q(+,t|+,0) + \beta\tau Q(-,t|+,0) \right] \\ &= -(\mathrm{i}\omega_+ + \alpha) Q(+,t|+,0) + \beta Q(-,t|+,0) \\ \frac{\partial}{\partial t} Q(-,t|-,0) &= -(\mathrm{i}\omega_- - + \beta) Q(-,t|-,0) + \alpha Q(+,t|-,0) \\ \frac{\partial}{\partial t} Q(+,t|-,0) &= \lim_{\tau\to 0} \frac{1}{\tau} \left[(-\mathrm{i}\omega_+ - \alpha)\tau Q(+,t|-,0) + \beta\tau Q(-,t|-,0) \right] \\ &= -(\mathrm{i}\omega_+ + \alpha) Q(+,t|-,0) + \beta Q(-,t|-,0) \\ \frac{\partial}{\partial t} Q(-,t|+,0) &= -(\mathrm{i}\omega_- + \beta) Q(-,t|+,0) + \alpha Q(+,t|+,0) \end{aligned} \tag{20.55}$$

or in matrix notation

$$\frac{\partial}{\partial t} Q = (-\mathrm{i}\Omega + A) Q \tag{20.56}$$

with

$$Q = \begin{pmatrix} Q(+,t|+,0) & Q(+,t|-,0) \\ Q(-,t|+,0) & Q(-,t|-,0) \end{pmatrix} \tag{20.57}$$

and

$$\Omega = \begin{pmatrix} \omega_+ & \\ & \omega_- \end{pmatrix}. \tag{20.58}$$

Equation (20.56) is formally solved by

$$Q(t) = \exp\{(-\mathrm{i}\Omega + A)t\}. \tag{20.59}$$

For a steady-state system, we have to average over the initial state and to sum over the final states to obtain the dephasing function. This can be expressed as

$$F(t) = (1,1)Q(t)\begin{pmatrix} \frac{\beta}{\alpha+\beta} \\ \frac{\alpha}{\alpha+\beta} \end{pmatrix} = (1,1)\exp\{(-\mathrm{i}\Omega + A)t\}\begin{pmatrix} \frac{\beta}{\alpha+\beta} \\ \frac{\alpha}{\alpha+\beta} \end{pmatrix}. \tag{20.60}$$

Laplace transformation gives

$$\widetilde{F}(s) = \int_0^\infty \mathrm{e}^{-st} F(t) = (1,1)(s + \mathrm{i}\Omega - A)^{-1}\begin{pmatrix} \frac{\beta}{\alpha+\beta} \\ \frac{\alpha}{\alpha+\beta} \end{pmatrix} \tag{20.61}$$

which can be easily evaluated to give

$$\begin{aligned} \widetilde{F}(s) &= \frac{1}{(s+\mathrm{i}\omega_1)(s+\mathrm{i}\omega_2) + (\alpha+\beta)s + \mathrm{i}(\alpha\omega_2 + \beta\omega_1)} \\ &\quad \times (1,1)\begin{pmatrix} s+\mathrm{i}\omega_2 - \beta & -\beta \\ -\alpha & s+\mathrm{i}\omega_1 - \alpha \end{pmatrix}\begin{pmatrix} \frac{\beta}{\alpha+\beta} \\ \frac{\alpha}{\alpha+\beta} \end{pmatrix} \\ &= \frac{s + (\alpha+\beta) + \mathrm{i}\frac{\beta\omega_2+\alpha\omega_1}{\alpha+\beta}}{(s+\mathrm{i}\omega_1)(s+\mathrm{i}\omega_2) + (\alpha+\beta)s + \mathrm{i}(\alpha\omega_2+\beta\omega_1)}. \end{aligned} \tag{20.62}$$

Since the dephasing function generally obeys the symmetry $F(-t) = F(t)^*$, the lineshape is obtained from the real part

$$2\pi\hat{F}(\omega) = \int_{-\infty}^{\infty} \mathrm{e}^{\mathrm{i}\omega t} F(t)dt = \left(\int_0^\infty \mathrm{e}^{\mathrm{i}\omega t} F(t)dt + \int_0^\infty \mathrm{e}^{-\mathrm{i}\omega t} F^*(t)dt\right)$$

$$= 2\Re\left(\widetilde{F}(-\mathrm{i}\omega)\right) = 2\frac{\alpha\beta}{\alpha+\beta}\frac{(\omega_1-\omega_2)^2}{(\omega-\omega_1)^2(\omega-\omega_2)^2 + (\alpha+\beta)^2(\omega - \frac{\alpha\omega_2+\beta\omega_1}{\alpha+\beta})^2}. \tag{20.63}$$

Let us introduce the average frequency

$$\overline{\omega} = \frac{\alpha\omega_2 + \beta\omega_1}{\alpha+\beta} \tag{20.64}$$

and the correlation time of the dichotomous process

$$\tau_c = \omega_c^{-1} = (\alpha+\beta)^{-1}.$$

In the limit of slow fluctuations ($\omega_c \to 0$) two sharp resonances appear at $\omega = \omega_{1,2}$ with relative weights given by the equilibrium probabilities $P(+) = \beta/(\alpha+\beta)$ and $P(-) = \alpha/(\alpha+\beta)$. With increasing ω_c the two resonances become broader and finally merge into one line. For further increasing ω_c the resonance, which is now centered at $\overline{\omega}$ becomes very narrow (this is known as the motional narrowing effect) (Fig. 20.2).

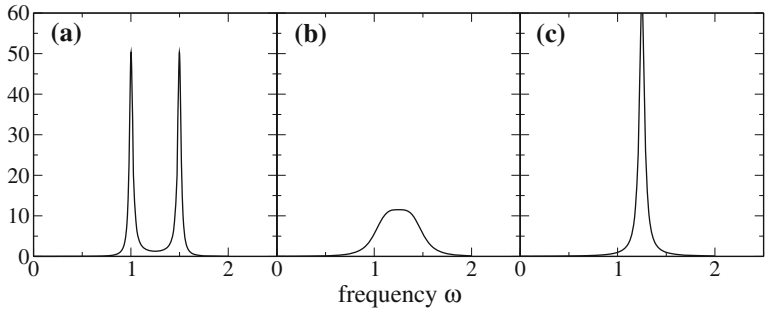

Fig. 20.2 Motional narrowing. The lineshape (20.63) is evaluated for $\omega_1 = 1.0, \omega_2 = 1.5$ and $\alpha = \beta =$ (**a**) 0.02 (**b**) 0.18 (**c**) 1.0

Problems

20.1 Motional Narrowing

Discuss the poles of the lineshape function and the motional narrowing effect (20.63) for the symmetrical case $\alpha = \beta = (2\tau_c)^{-1}$,$\omega_{1,2} = \overline{\omega} \pm \Delta\omega/2$.

Chapter 21
Crossing of Two Electronic States

In this chapter, we discuss crossing between two or more Born–Oppenheimer states. We begin with wave packet motion which allows to introduce the classical limit for nuclear motion. The matrix elements of the nonadiabatic coupling can become very large or even divergent, whenever two electronic states come close. The "adiabatic to diabatic" transformation eliminates at least the singular parts of the derivative coupling. We derive the so-called diabatic Schrödinger equation and discuss the simplest case of a crossing between two states. For a Hamiltonian depending on only one nuclear coordinate, the transformation to a diabatic basis is possible and yields a diabatic coupling which is given by half the splitting of the adiabatic states. The semiclassical approximation makes use of narrow localized wavepackets and describes nuclear motion as a classical trajectory defined as the time-dependent average position. The famous Landau Zener model uses a linear approximation of the trajectory in the vicinity of the crossing point and obtains an explicit solution for the transition probability. If more coordinates are involved, conical intersections appear which are very important for ultrafast transitions. We discuss the linear vibronic coupling model for the dynamics in the vicinity of a conical intersection.

21.1 Wavepacket Motion

A particle (e.g., one of the nuclei of a molecule) moving in the potential $V(\mathbf{R})$ is described by the time dependent Schrödinger equation

$$i\hbar\frac{\partial}{\partial t}\psi = \left[-\frac{\hbar^2}{2M}\nabla^2 + V(\mathbf{R})\right]\psi = H\psi. \tag{21.1}$$

P.O.J. Scherer and S.F. Fischer, *Theoretical Molecular Biophysics*,
Biological and Medical Physics, Biomedical Engineering,
DOI 10.1007/978-3-662-55671-9_21

The expectation values of position and momentum

$$< \mathbf{R} >= \int \psi^*(\mathbf{R}, t)\mathbf{R}\psi(\mathbf{R}, t)d^3R \quad < \mathbf{P} >= \int \psi^*(\mathbf{R}, t)\frac{\hbar}{\mathrm{i}}\nabla\psi(\mathbf{R}, t)d^3R \tag{21.2}$$

obey equations of motion quite similar to Newton's equations

$$\frac{\mathrm{d}}{\mathrm{d}t} < \mathbf{R} >= \frac{1}{M} < \mathbf{P} > \tag{21.3}$$

$$\frac{\mathrm{d}}{\mathrm{d}t} < \mathbf{P} >=< -\nabla V(\mathbf{R}) > . \tag{21.4}$$

In order to assign values of "position" and "momentum" the wavefunction should be a localized wavepacket in real space and momentum space. Due to the laws of quantum mechanics both values cannot be simultaneously sharp but are subject to a probability distribution with eventually growing width due to dispersion. Simple cases allow description by Gaussian wave packets, especially a free particle and the harmonic oscillator.

21.1.1 Free Particle Motion

For a free particle ($V = 0$) in one dimension a special solution of (21.1) is given by

$$\psi(x, t) = \left(\frac{2a}{\pi}\right)^{1/4} \frac{1}{\sqrt{a + 2\frac{\mathrm{i}\hbar}{m}t}} \exp\left\{-\frac{\left(x - \mathrm{i}\frac{ak_0}{2}\right)^2 + \frac{ak_0^2}{4}\left(a + 2\frac{\mathrm{i}\hbar}{m}t\right)}{a + 2\frac{\mathrm{i}\hbar}{m}t}\right\} \tag{21.5}$$

which is initially a Gaussian wave packet with constant momentum

$$\psi(x, 0) = \left(\frac{2a}{\pi}\right)^{1/4} \frac{1}{\sqrt{a}} e^{-x^2/a} e^{\mathrm{i}k_0 x} \tag{21.6}$$

$$\begin{aligned} &< p(0) >= \frac{\hbar}{\mathrm{i}} < \frac{\partial}{\partial x} > \\ &= \frac{\hbar}{\mathrm{i}}\sqrt{\frac{2a}{\pi}}\frac{1}{a}\int dx\, e^{-x^2/a} e^{-\mathrm{i}k_0 x}\left(-\frac{2x}{a} + \mathrm{i}k\right) e^{-x^2/a} e^{\mathrm{i}k_0 x} = \hbar k_0. \end{aligned} \tag{21.7}$$

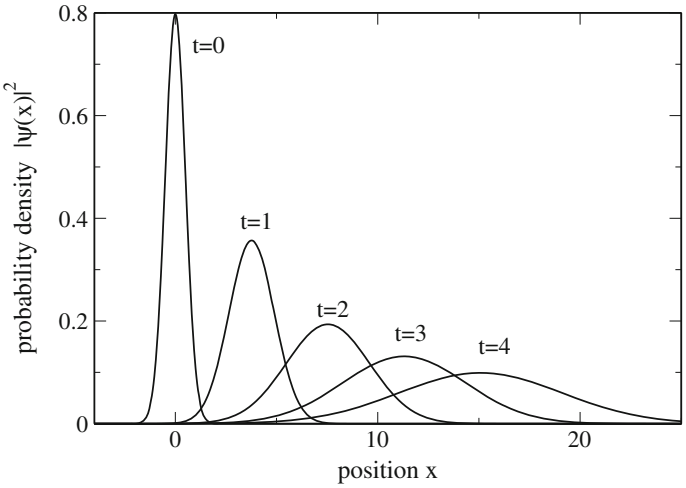

Fig. 21.1 Free particle motion. The Gaussian wave packet (21.5) moves with constant velocity and shows dispersion according to (21.10). Time in units of $m/\hbar$

The probability density stays Gaussian

$$|\psi(x,t)|^2 = \sqrt{\frac{2a}{\pi}}\frac{1}{\sqrt{a^2+\left(2\frac{\hbar}{m}t\right)^2}}\exp\left\{-\frac{2a}{a^2+\left(2\frac{\hbar}{m}t\right)^2}\left(x-\frac{\hbar k_0}{m}t\right)^2\right\}. \quad (21.8)$$

The wavepacket moves with constant velocity (Fig. 21.1)

$$< x >= \frac{\hbar k_0}{m}t = v_0 t \quad (21.9)$$

and its standard deviation increases with time

$$\sigma_x = \sqrt{\frac{a}{4}+\frac{\frac{\hbar^2}{m^2}t^2}{a}}. \quad (21.10)$$

Fourier transformation gives a Gaussian probability density again which is time independent

$$|\tilde{\psi}(k,t)|^2 = \sqrt{\frac{a}{2\pi}}\exp\left\{-\frac{a}{2}(k-k_0)^2\right\} \quad (21.11)$$

with standard deviation

$$\sigma_k = \frac{1}{\sqrt{a}} \tag{21.12}$$

from which the uncertainty relation is obtained

$$\sigma_x \sigma_p = \hbar \sqrt{\frac{1}{4} + \frac{\hbar^2}{a^2 m^2} t^2} \geq \frac{\hbar}{2}. \tag{21.13}$$

21.1.2 Harmonic Oscillator

Wavepackets for a particle in a harmonic potential are provided by the coherent oscillator states (also known as Glauber states) which are linear combinations of stationary oscillator states, and therefore solutions of the time dependent Schrödinger equation (Appendix B)

$$\varphi_\alpha(x,t) = e^{-|\alpha|^2/2} \sum_{n=0}^{\infty} \frac{\alpha^n}{\sqrt{n!}} e^{-i(n+1/2)\omega t} \psi_n(x). \tag{21.14}$$

Coherent states describe dispersionless wavepackets with probability density (Fig. 21.2)

$$\begin{aligned} |\varphi_\alpha(x,t)|^2 &= \left| \psi_0 \left(x - \sqrt{2} \Re(\alpha e^{i\omega t}) x_0 \right) \right|^2 \\ &= \frac{1}{\sqrt{\pi} x_0} \exp \left\{ - \frac{\left(x - x_0 \sqrt{2} |\alpha| \cos\left(\omega t - \arg(\alpha)\right) \right)^2}{x_0^2} \right\}. \end{aligned} \tag{21.15}$$

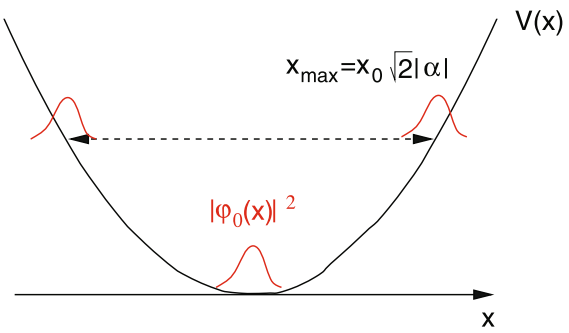

Fig. 21.2 Probability density of a coherent oscillator state

The expectation values of coordinate and momentum oscillate like for a classical oscillator and the standard deviations are

$$\sigma_x = \frac{x_0}{\sqrt{2}} \quad \sigma_p = \frac{\hbar}{x_0\sqrt{2}}. \tag{21.16}$$

The uncertainty product has the minimum possible value

$$\sigma_x \sigma_p = \frac{\hbar}{2}. \tag{21.17}$$

For large amplitudes

$$x_{max} = x_0\sqrt{2}|\alpha| \quad p_{max} = \frac{\hbar}{x_0}\sqrt{2}|\alpha| \tag{21.18}$$

the relative uncertainties become small

$$\frac{\sigma_x}{x_{max}} = \frac{\sigma_p}{p_{max}} = \frac{1}{2|\alpha|} \tag{21.19}$$

and the oscillator behaves classically with energy

$$< E >= m\omega^2 \frac{x_{max}^2}{2} \quad \frac{\sigma_E}{< E >} = \frac{1}{|\alpha|}. \tag{21.20}$$

21.2 The Adiabatic to Diabatic Transformation

The Schrödinger equation for the nuclear motion (17.28) can be written as [80–84][1]

$$\begin{aligned} \mathrm{i}\hbar\frac{\partial}{\partial t}\boldsymbol{\chi} &= \left[\mathrm{diag}(E_s) + T_N + < \boldsymbol{\psi}\hat{V}_{nad}\boldsymbol{\psi}^\dagger >\right]\boldsymbol{\chi} \\ &= \left[\mathrm{diag}(E_s) - \sum_j \frac{\hbar^2}{2M_j}\left(\frac{\partial}{\partial Q_j} + T_j\right)^2\right]\boldsymbol{\chi} \end{aligned} \tag{21.21}$$

with

$$T_j = < \boldsymbol{\psi}\frac{\partial \boldsymbol{\psi}^\dagger}{\partial Q_j} > . \tag{21.22}$$

[1] Without a magnetic field the electronic wavefunctions can be assumed to be real valued.

Equation (21.21) looks much like an ordinary Schrödinger equation where the gradient has been replaced by

$$\frac{\partial}{\partial Q_j} \to \frac{\partial}{\partial Q_j} + T_j \tag{21.23}$$

a substitution which is well known in the field of gauge theories [85].

Equation (21.21) follows from

$$\left[\frac{\partial}{\partial Q_j} + < \psi \frac{\partial \psi^\dagger}{\partial Q_j} >\right]^2 = \frac{\partial^2}{\partial Q_j^2} + < \psi(r) \frac{\partial \psi^\dagger(r)}{\partial Q_j} >< \psi(r') \frac{\partial \psi^\dagger(r')}{\partial Q_j} > + 2 < \psi \frac{\partial \psi^\dagger}{\partial Q_j} > \frac{\partial}{\partial Q_j} + < \frac{\partial \psi}{\partial Q_j} \frac{\partial \psi^\dagger}{\partial Q_j} > + < \psi \frac{\partial^2 \psi^\dagger}{\partial Q_j^2} > \tag{21.24}$$

where due to orthonormality

$$< \psi \psi^\dagger >= \begin{pmatrix} 1 & & \\ & 1 & \\ & & \ddots \end{pmatrix} \tag{21.25}$$

$$0 = \frac{\partial}{\partial Q_j} < \psi \psi^\dagger >=< \frac{\partial \psi}{\partial Q_j} \psi^\dagger > + < \psi \frac{\partial \psi^\dagger}{\partial Q_j} > . \tag{21.26}$$

Therefore

$$< \psi \frac{\partial \psi^\dagger}{\partial Q_j} >< \psi \frac{\partial \psi^\dagger}{\partial Q_j} >= - < \frac{\partial \psi}{\partial Q_j} \psi^\dagger > < \psi \frac{\partial \psi^\dagger}{\partial Q_j} > \tag{21.27}$$

and from completeness of the basis

$$\psi^\dagger(r)\psi(r') = \sum_s \psi_s(r)\psi_s(r') = \delta(r - r') \tag{21.28}$$

$$< \psi \frac{\partial \psi^\dagger}{\partial Q_j} >< \psi \frac{\partial \psi^\dagger}{\partial Q_j} >= - < \frac{\partial \psi(r)}{\partial Q_j} \frac{\partial \psi^\dagger(r)}{\partial Q_j} > . \tag{21.29}$$

The matrix elements of the nonadiabatic coupling can become very large whenever two electronic states come close (17.34). They even diverge at conical intersections [86]. Therefore we look for a unitary transformation $U(Q)$ which eliminates the

derivative coupling or at least its singular parts. Electronic and nuclear parts of the wavefunction are transformed according to[2]

$$\tilde{\chi} = U^{-1}\chi \quad \tilde{\psi}^{\dagger} = \psi^{\dagger}U \tag{21.30}$$

which does not change the total wavefunction

$$\tilde{\psi}^{\dagger}\tilde{\chi} = (\psi^{\dagger}U)(U^{-1}\chi) = \psi^{\dagger}\chi. \tag{21.31}$$

The gradient and the nonadiabatic coupling matrix transform according to

$$\frac{\partial}{\partial Q_j}\tilde{\chi} = \frac{\partial U^{-1}}{\partial Q_j}\chi + U^{-1}\frac{\partial}{\partial Q_j}\chi \tag{21.32}$$

$$\tilde{T}_j = <\tilde{\psi}\frac{\partial}{\partial Q_j}\tilde{\psi}^{\dagger}> = <U^{-1}\psi\frac{\partial}{\partial Q_j}\psi^{\dagger}U> = U^{-1}T_jU + U^{-1}\frac{\partial U}{\partial Q_j}$$

$$= U^{-1}T_jU - \frac{\partial U^{-1}}{\partial Q_j}U. \tag{21.33}$$

Both involve an inhomogeneous term, whereas their combination transforms simply like χ itself[3]

$$\begin{aligned}\frac{\partial}{\partial Q_j}\tilde{\chi} + \tilde{T}_j\tilde{\chi} &= \left(\frac{\partial U^{-1}}{\partial Q_j} + U^{-1}\frac{\partial}{\partial Q_j} + U^{-1}T_jU + U^{-1}\frac{\partial U}{\partial Q_j}\right)U^{-1}\chi \\ &= \left(\frac{\partial U^{-1}}{\partial Q_j} + U^{-1}\frac{\partial}{\partial Q_j} + U^{-1}T_j - \frac{\partial U^{-1}}{\partial Q_j}\right)\chi \\ &= U^{-1}\left(\frac{\partial}{\partial Q_j} + T_j\right)\chi = U^{-1}\left(\frac{\partial}{\partial Q_j} + T_j\right)U\,\tilde{\chi}.\end{aligned} \tag{21.34}$$

Finally the time dependent Schrödinger equation transforms into

$$\mathrm{i}\hbar\frac{\partial}{\partial t}\tilde{\chi} = \left[U^{-1}\mathrm{diag}(E_s)U - U^{-1}\sum_j \frac{\hbar^2}{2M_j}\left(\frac{\partial}{\partial Q_j} + T_j\right)^2 U\right]\tilde{\chi}. \tag{21.35}$$

[2] In the following we make use of $0 = \frac{\partial}{\partial Q}UU^{-1} = \frac{\partial U}{\partial Q}U^{-1} + U\frac{\partial U^{-1}}{\partial Q}$ and $0 = \frac{\partial}{\partial Q}U^{-1}U = \frac{\partial U^{-1}}{\partial Q}U + U^{-1}\frac{\partial U}{\partial Q}$.

[3] In the language of gauge theories the substitution (21.23) is known as covariant gradient.

The transformed energy matrix

$$E^d = U^{-1}\mathrm{diag}(E_s)U \tag{21.36}$$

is generally not diagonal and contains coordinate dependent couplings between the states. Let us assume, the transformation eliminates the gradient coupling. Then from (21.33)

$$0 = \tilde{T}_j = U^{-1}T_jU + U^{-1}\frac{\partial U}{\partial Q_j} \tag{21.37}$$

and the transformation has to satisfy

$$\frac{\partial U}{\partial Q_j} + T_jU = 0. \tag{21.38}$$

Then,

$$U^{-1}\left(\frac{\partial}{\partial Q_j} + T_j\right)U = \frac{\partial}{\partial Q_j} \tag{21.39}$$

and (21.35) simplifies to the so-called diabatic [87] Schrödinger equation

$$\mathrm{i}\hbar\frac{\partial}{\partial t}\chi^d = \left[E^d - \sum_j \frac{\hbar^2}{2M_j}\frac{\partial^2}{\partial Q_j^2}\right]\chi^d. \tag{21.40}$$

Since the basis of adiabatic electronic wavefunctions is complete for any configuration Q, the gradient can be expanded as

$$\frac{\partial\psi^{d\dagger}}{\partial Q_j} = \psi^{d\dagger} < \psi^d\frac{\partial}{\partial Q_j}\psi^{d\dagger} >= \psi^d T_j^d = 0 \tag{21.41}$$

hence ψ^d is independent of the nuclear coordinates. This corresponds to a crude diabatic basis [88–90]. In order for (21.38) to have a single-valued solution, T_jU must be the gradient of a function of Q_j. This leads to the generalized curl condition which also guarantees that the second derivatives of U do not depend on their order

$$\begin{aligned} 0 &= \frac{\partial^2 U}{\partial Q_j\partial Q_i} - \frac{\partial^2 U}{\partial Q_i\partial Q_j} = \mathrm{curl}(T_jU)_i \\ &= \frac{\partial(T_jU)}{\partial Q_i} - \frac{\partial(T_iU)}{\partial Q_j} = \left(\frac{\partial T_j}{\partial Q_i} - \frac{\partial T_i}{\partial Q_j}\right)U + T_j\frac{\partial U}{\partial Q_i} - T_i\frac{\partial U}{\partial Q_j} \\ &= \frac{\partial T_j}{\partial Q_i}U - \frac{\partial T_i}{\partial Q_j}U - T_jT_iU + T_iT_jU \end{aligned} \tag{21.42}$$

or simpler

$$0 = F_{ij} = \frac{\partial T_j}{\partial Q_i} - \frac{\partial T_i}{\partial Q_j} - (T_j T_i - T_i T_j). \tag{21.43}$$

This equation is satisfied trivially, if there is only one nuclear coordinate, i.e., for diatomic molecules if rotation is neglected.

Now, the gradient of the NACM is

$$\frac{\partial}{\partial Q_j} T_i = \frac{\partial}{\partial Q_j} < \psi_s \frac{\partial}{\partial Q_i} \psi_{s'} > = < \frac{\partial}{\partial Q_j} \psi_s \frac{\partial}{\partial Q_i} \psi_{s'} > + < \psi_s \frac{\partial^2}{\partial Q_i \partial Q_j} \psi_{s'} > \tag{21.44}$$

from which

$$\frac{\partial}{\partial Q_j} T_i - \frac{\partial}{\partial Q_i} T_j = < \frac{\partial}{\partial Q_j} \psi_s \frac{\partial}{\partial Q_i} \psi_{s'} > - < \frac{\partial}{\partial Q_i} \psi_s \frac{\partial}{\partial Q_j} \psi_{s'} > . \tag{21.45}$$

Furthermore, inserting the complete basis

$$T_i T_j = -\sum_{s'} < \frac{\partial \psi_s}{\partial Q_i} \psi_{s'} > < \psi_{s'} \frac{\partial}{\partial Q_j} \psi_{s''} > = - < \frac{\partial \psi_s}{\partial Q_i} \frac{\partial}{\partial Q_j} \psi_{s''} > \tag{21.46}$$

$$T_j T_i - T_i T_j = < \frac{\partial \psi_s}{\partial Q_i} \frac{\partial}{\partial Q_j} \psi_{s''} > - < \frac{\partial \psi_s}{\partial Q_j} \frac{\partial}{\partial Q_i} \psi_{s''} > . \tag{21.47}$$

Hence the curl condition (21.43) is satisfied if the basis is complete. Such a basis, however, is not useful for practical calculations, as convergence is very slow and a large number of basis states would have to be included.

Now we consider a general unitary transformation of the curl (21.43)

$$\tilde{F}_{ij} = \frac{\partial \tilde{T}_j}{\partial Q_i} - \frac{\partial \tilde{T}_i}{\partial Q_j} - (\tilde{T}_j \tilde{T}_i - \tilde{T}_i \tilde{T}_j) \tag{21.48}$$

$$\tilde{T}_j = U^{-1} T_j U + U^{-1} \frac{\partial U}{\partial Q_j}.$$

From (21.33) we obtain

$$\tilde{T}_j \tilde{T}_i = U^{-1} T_j T_i U + U^{-1} T_j \frac{\partial U}{\partial Q_i} - \frac{\partial U^{-1}}{\partial Q_j} T_i U - \frac{\partial U^{-1}}{\partial Q_j} \frac{\partial U}{\partial Q_i} \tag{21.49}$$

and the commutator

$$\tilde{T}_j\tilde{T}_i - \tilde{T}_i\tilde{T}_j = U^{-1}(T_jT_i - T_iT_j)U + \frac{\partial U^{-1}}{\partial Q_i}\frac{\partial U}{\partial Q_j} - \frac{\partial U^{-1}}{\partial Q_j}\frac{\partial U}{\partial Q_i}$$
$$+ U^{-1}\left(T_j\frac{\partial U}{\partial Q_i} - T_i\frac{\partial U}{\partial Q_j}\right) - \left(\frac{\partial U^{-1}}{\partial Q_i}T_j - \frac{\partial U^{-1}}{\partial Q_j}T_i\right)U. \tag{21.50}$$

The gradient

$$\frac{\partial\tilde{T}_j}{\partial Q_i} = \frac{\partial U^{-1}}{\partial Q_i}\left(T_jU + \frac{\partial U}{\partial Q_j}\right) + U^{-1}\left(\frac{\partial T_j}{\partial Q_i}U + T_j\frac{\partial U}{\partial Q_i} + \frac{\partial^2 U}{\partial Q_i\partial Q_j}\right) \tag{21.51}$$

gives the curl of $\tilde{T}$

$$\frac{\partial\tilde{T}_j}{\partial Q_i} - \frac{\partial\tilde{T}_i}{\partial Q_j} = \left(\frac{\partial U^{-1}}{\partial Q_i}T_j - \frac{\partial U^{-1}}{\partial Q_j}T_i\right)U$$
$$+ U^{-1}\left(\frac{\partial T_j}{\partial Q_i} - \frac{\partial T_i}{\partial Q_j}\right)U + U^{-1}\left(T_j\frac{\partial U}{\partial Q_i} - T_i\frac{\partial U}{\partial Q_j}\right)$$
$$+ \frac{\partial U^{-1}}{\partial Q_i}\frac{\partial U}{\partial Q_j} - \frac{\partial U^{-1}}{\partial Q_j}\frac{\partial U}{\partial Q_i} + U^{-1}\left(\frac{\partial^2 U}{\partial Q_i\partial Q_j} - \frac{\partial^2 U}{\partial Q_j\partial Q_i}\right). \tag{21.52}$$

Assuming that the second derivatives do not depend on the order, we have finally

$$\tilde{F}_{ij} = \frac{\partial\tilde{T}_j}{\partial Q_i} - \frac{\partial\tilde{T}_i}{\partial Q_j} - (\tilde{T}_j\tilde{T}_i - \tilde{T}_i\tilde{T}_j)$$
$$= U^{-1}\left(\frac{\partial T_j}{\partial Q_i} - \frac{\partial T_i}{\partial Q_j} - (T_jT_i - T_iT_j)\right)U = U^{-1}F_{ij}U. \tag{21.53}$$

which shows that the curl condition $F_{ij} = 0$ is invariant to unitary transformations.

21.3 Quasidiabatic States

We would like to reduce the sum in (17.22) to a small group of relevant basis states which interact strongly, whereas interaction with states outside the group is small [84]. We denote the group of states by g and its complement by o and use a block matrix notation where the projectors onto the group and its complement are

$$P = \begin{pmatrix} 1^g & 0 \\ 0 & 0 \end{pmatrix} \quad Q = 1 - P = \begin{pmatrix} 0 & 0 \\ 0 & 1^o \end{pmatrix}. \tag{21.54}$$

We define the group Hamiltonian by restricting (21.21)

$$H^g = P\left[\mathrm{diag}(E_s) - \sum_j \frac{\hbar^2}{2M_j}\left(\frac{\partial}{\partial Q_j} + T_j\right)^2\right]P. \tag{21.55}$$

The full matrix of NACMs is

$$T_i = \begin{pmatrix} T_i^g & T_i^{go} \\ T_i^{og} & T_i^o \end{pmatrix} \tag{21.56}$$

and the restriction of its square is not identical with the square of the restriction since

$$(T_j^2)^g = (T_j^g)^2 + T_j^{go}T_j^{og}. \tag{21.57}$$

The restricted covariant gradient is

$$\left(\frac{\partial}{\partial Q_j} + T_j\right)^g = \frac{\partial}{\partial Q_j} + T_j^g \tag{21.58}$$

and the restriction of its square is

$$\left(\left[\frac{\partial}{\partial Q_j} + T_j\right]^2\right)^g = \left(\frac{\partial^2}{\partial Q_j^2} + T_j^2 + 2T_j\frac{\partial}{\partial Q_j} + \frac{\partial T_j}{\partial Q_j}\right)^g = \left(\frac{\partial}{\partial Q_j} + T_j^g\right)^2 + T_j^{go}T_j^{og} \tag{21.59}$$

hence the group Hamiltonian involves coupling to states outside the group[4]

$$H^g = \mathrm{diag}(E_s)^g - \sum_j \frac{\hbar^2}{2M_j}\left(\frac{\partial}{\partial Q_j} + T_j^g\right)^2 - \sum_j \frac{\hbar^2}{2M_j}T_j^{go}T_j^{og}. \tag{21.60}$$

Now, with

$$(T_iT_j - T_jT_i)^g = (T_i^gT_j^g - T_j^gT_i^g) + (T_i^{go}T_j^{og} - T_j^{go}T_i^{og}) \tag{21.61}$$

the curl condition gives

$$\begin{aligned} 0 = F_{ij}^g &= \frac{\partial T_j^g}{\partial Q_i} - \frac{\partial T_i^g}{\partial Q_j} - (T_jT_i - T_iT_j)^g \\ &= \frac{\partial T_j^g}{\partial Q_i} - \frac{\partial T_i^g}{\partial Q_j} - (T_i^gT_j^g - T_j^gT_i^g) - (T_i^{go}T_j^{og} - T_j^{go}T_i^{og}). \end{aligned} \tag{21.62}$$

[4]This is in principle also the case for the Born–Oppenheimer approximation with only one term.

Hence the curl condition cannot be satisfied within the reduced space of group states unless coupling to states outside the group is neglected. Therefore derivative couplings within the group generally cannot be eliminated totally by unitary transformations within the group. Several methods have been proposed to remove at least the divergent terms and to find a basis of *quasidiabatic* states.

21.4 Crossing Between Two States

In the following, we consider the simplest case of two crossing states. A unitary transformation among these can be described by a rotation matrix

$$U^g = \begin{pmatrix} \cos\alpha & \sin\alpha \\ -\sin\alpha & \cos\alpha \end{pmatrix} \tag{21.63}$$

with the derivative

$$\frac{\partial U^g}{\partial Q_i} = \begin{pmatrix} -\sin\alpha & \cos\alpha \\ -\cos\alpha & -\sin\alpha \end{pmatrix} \frac{\partial\alpha}{\partial Q_i} \tag{21.64}$$

and

$$\frac{\partial U^g}{\partial Q_i} U^{g\dagger} = \frac{\partial\alpha}{\partial Q_i} \begin{pmatrix} -\sin\alpha & \cos\alpha \\ -\cos\alpha & -\sin\alpha \end{pmatrix} \begin{pmatrix} \cos\alpha & -\sin\alpha \\ \sin\alpha & \cos\alpha \end{pmatrix} = \frac{\partial\alpha}{\partial Q_i} \begin{pmatrix} 0 & 1 \\ -1 & 0 \end{pmatrix}. \tag{21.65}$$

The antisymmetric matrix of derivative couplings has the form

$$T_i^g = \begin{pmatrix} 0 & \tau_i \\ -\tau_i & 0 \end{pmatrix} \tag{21.66}$$

with[5]

$$\tau_i = \frac{\partial\alpha}{\partial Q_i}. \tag{21.67}$$

The transformed kinetic energy has diagonal and off-diagonal contributions

$$-\sum \frac{\hbar^2}{2M_i} \left(\frac{\partial}{\partial Q_i} + T_i^g \right)^2 = -\sum \frac{\hbar^2}{2M_i} \left[\frac{\partial^2}{\partial Q_i^2} - \tau_i^2 + \left(2\tau_i \frac{\partial}{\partial Q_i} + \frac{\partial\tau_i}{\partial Q_i} \right) \begin{pmatrix} 0 & 1 \\ -1 & 0 \end{pmatrix} \right]. \tag{21.68}$$

[5]The integrability condition (21.73) for the inverse rotation is fulfilled by construction.

From

$$\frac{\partial \tau_i}{\partial Q_j} = < \psi_1 \frac{\partial^2 \psi_2}{\partial Q_j \partial Q_i} > + < \frac{\partial \psi_1}{\partial Q_j} \frac{\partial \psi_2}{\partial Q_i} > \tag{21.69}$$

we obtain

$$T_i^g T_j^g - T_j^g T_i^g = (\tau_i \tau_j - \tau_j \tau_i) \begin{pmatrix} -1 & \\ & -1 \end{pmatrix} = 0 \tag{21.70}$$

and

$$\frac{\partial T_i^g}{\partial Q_j} - \frac{\partial T_j^g}{\partial Q_i} = \left(\frac{\partial \tau_i}{\partial Q_j} - \frac{\partial \tau_j}{\partial Q_i} \right) \begin{pmatrix} 0 & 1 \\ -1 & 0 \end{pmatrix} \tag{21.71}$$

with

$$\begin{aligned} \frac{\partial \tau_i}{\partial Q_j} - \frac{\partial \tau_j}{\partial Q_i} &= < \frac{\partial \psi_1}{\partial Q_j} \frac{\partial \psi_2}{\partial Q_i} > - < \frac{\partial \psi_1}{\partial Q_i} \frac{\partial \psi_2}{\partial Q_j} > \\ &= \sum_{s>2} T_j^{(1,s)} T_i^{(s,2)} - T_i^{(1,s)} T_j^{(s,2)}. \end{aligned} \tag{21.72}$$

The integrability condition demands

$$\frac{\partial \alpha}{\partial Q_i} + \tau_i = 0 \tag{21.73}$$

which cannot be fulfilled in general unless the coupling to states outside the group is neglected. Now, τ_i is a vector in coordinate space and Helmhotz' theorem is applicable which states that it can be written as the sum of a curl free (or longitudinal) and a purely rotational (or transversal) part. Obviously only the longitudinal part can be removed by a unitary transformation. According to (21.72) the remaining rotational part does not involve the divergent terms $\propto (E_1(Q) - E_2(Q))^{-1}$. It might, however, involve other divergences if three or more states happen to cross at the same point.

21.5 Avoided Crossing Along One Coordinate

The diabatic energy matrix has the form

$$E^d = \begin{pmatrix} E_1^d(Q) & V(Q) \\ V(Q) & E_2^d(Q) \end{pmatrix} \tag{21.74}$$

and the adiabatic energies are the eigenvalues of E^d

$$E^a_{1,2} = \frac{E^d_2 + E^d_1}{2} \pm \frac{1}{2}\sqrt{(E^d_2 - E^d_1)^2 + 4V^2}. \tag{21.75}$$

Let us now discuss a one-dimensional model with one reaction coordinate Q [91]. Here, crossing of the adiabatic curves is very unlikely, since it occurs only if the two conditions

$$E^d_1(Q) - E^d_d(Q) = V(Q) = 0 \tag{21.76}$$

are fulfilled simultaneously.[6] We consider an avoided crossing where the gap between the two adiabatic curves has a minimum.

Equation (21.73) becomes

$$\frac{\partial U}{\partial Q} = -\tau(Q)U \tag{21.77}$$

which can be formally solved by

$$U = \exp\left\{\int_Q^\infty \tau(Q)dQ\right\}. \tag{21.78}$$

For antisymmetric T, the exponential function can be easily evaluated[7] to give

$$U = \begin{pmatrix} \cos\zeta(Q) & \sin\zeta(Q) \\ -\sin\zeta(Q) & \cos\zeta(Q) \end{pmatrix} \qquad \zeta(Q) = \int_Q^\infty \tau(Q)dQ. \tag{21.79}$$

The diabatic energy matrix now is

$$\begin{aligned} E^d &= U^{-1}\begin{pmatrix} E^a_1 & \\ & E^a_2 \end{pmatrix} U \\ &= \begin{pmatrix} \cos^2\zeta E^a_1 + \sin^2\zeta E^a_2 & \sin\zeta\cos\zeta(E^a_1 - E^a_2) \\ \sin\zeta\cos\zeta(E^a_1 - E^a_2) & \cos^2\zeta E^a_2 + \sin^2\zeta E^a_1 \end{pmatrix}. \end{aligned} \tag{21.80}$$

At the crossing point

$$(\cos^2\zeta_0 - \sin^2\zeta_0)(E^{ad}_1 - E^{ad}_2) = 0, \tag{21.81}$$

[6] If the two states are of different symmetry then $V = 0$ and crossing is possible in one dimension.

[7] For instance by a series expansion.

which implies

$$\cos^2\zeta_0 = \sin^2\zeta_0 = \frac{1}{2}. \tag{21.82}$$

Expanding the sine and cosine functions around the crossing point, we have

$$E^d \approx \begin{pmatrix} \frac{E_1^a+E_2^a}{2} + (E_2^a - E_1^a)(\zeta-\zeta_0) + \cdots & (E_1^a - E_2^a)(\frac{1}{2} + (\zeta-\zeta_0)^2 + \cdots) \\ (E_1^a - E_2^a)(\frac{1}{2} + (\zeta-\zeta_0)^2 + \cdots) & \frac{E_1^a+E_2^a}{2} - (E_2^a - E_1^a)(\zeta-\zeta_0) + \cdots \end{pmatrix}. \tag{21.83}$$

Expanding furthermore the matrix elements

$$E_1^{ad} = \bar{E} + \frac{\Delta}{2} + g_1(Q-Q_0) + \cdots \tag{21.84}$$

$$E_2^{ad} = \overline{E} - \frac{\Delta}{2} + g_2(Q-Q_0) + \cdots \tag{21.85}$$

$$\zeta - \zeta_0 = -(Q-Q_0)T_{12}(Q_0) \tag{21.86}$$

where Δ is the splitting of the adiabatic energies at the crossing point, the interaction matrix becomes

$$E^d = \overline{E} + \frac{g_1+g_2}{2}Q + \begin{pmatrix} -(Q-Q_0)\tau(Q_0)\Delta & \frac{\Delta}{2} + \frac{g_1-g_2}{2}(Q-Q_0) \\ \frac{\Delta}{2} + \frac{g_1-g_2}{2}(Q-Q_0) & (Q-Q_0)\tau(Q_0)\Delta \end{pmatrix} + \cdots. \tag{21.87}$$

We see that in the diabatic basis the interaction is given by half the splitting of the adiabatic energies at the crossing point (Fig. 21.3).

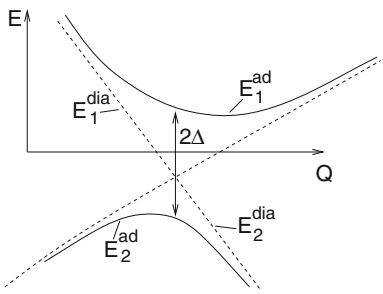

Fig. 21.3 Curve crossing

21.6 Semiclassical Approximation

We want to describe the nuclear motion classically. Therefore we approximate both nuclear wavefunctions

$$\chi_1 = \chi_2 = \phi \tag{21.88}$$

as a narrow wave packet centered at $Q(t)$ moving in an effective potential $V^{eff}(Q)$ with velocity $v(t) = \dot{Q}(t)$

$$i\hbar\dot{\phi} = -\frac{\hbar^2}{2M}\frac{\partial^2\phi}{\partial Q^2} + V^{eff}(Q)\phi. \tag{21.89}$$

The wavefunction has the form

$$\Psi = \begin{pmatrix} a(t) \\ b(t) \end{pmatrix} \phi(Q). \tag{21.90}$$

From the time-dependent Schrödinger equation

$$i\hbar\dot{\Psi} = i\hbar\begin{pmatrix} \dot{a}(t) \\ \dot{b}(t) \end{pmatrix}\phi(Q) + \begin{pmatrix} a(t) \\ b(t) \end{pmatrix} i\hbar\dot{\phi}(Q) = \left[-\frac{\hbar^2}{2M}\frac{\partial^2}{\partial Q^2} + \begin{pmatrix} E_1^0 & V \\ V & E_2^0 \end{pmatrix}\right]\begin{pmatrix} a(t) \\ b(t) \end{pmatrix}\phi(Q) \tag{21.91}$$

we obtain

$$i\hbar\begin{pmatrix} \dot{a}(t) \\ \dot{b}(t) \end{pmatrix}\phi(Q) = \begin{pmatrix} a(t) \\ b(t) \end{pmatrix}\left[-i\hbar\frac{\partial}{\partial t} - \frac{\hbar^2}{2M}\frac{\partial^2}{\partial Q^2}\right]\phi + \begin{pmatrix} E_1^0 & V \\ V & E_2^0 \end{pmatrix}\begin{pmatrix} a(t) \\ b(t) \end{pmatrix}\phi(Q) \tag{21.92}$$

$$i\hbar\begin{pmatrix} \dot{a}(t) \\ \dot{b}(t) \end{pmatrix}\phi(Q) = \begin{pmatrix} E_1^0 - V_{eff} & V \\ V & E_2^0 - V_{eff} \end{pmatrix}\begin{pmatrix} a(t) \\ b(t) \end{pmatrix}\phi(Q). \tag{21.93}$$

We take the average over Q

$$\begin{aligned} & i\hbar\int dQ\,\phi^*(Q)\begin{pmatrix} \dot{a}(t) \\ \dot{b}(t) \end{pmatrix}\phi(Q) = i\hbar\begin{pmatrix} \dot{a}(t) \\ \dot{b}(t) \end{pmatrix} \\ & = \int \phi^*(Q)\begin{pmatrix} E_1^0 - V_{eff} & V \\ V & E_2^0 - V_{eff} \end{pmatrix}\begin{pmatrix} a(t) \\ b(t) \end{pmatrix}\phi(Q) \\ & = \begin{pmatrix} E_1^0(Q(t)) - V_{eff}(Q(t)) & V(Q(t)) \\ V(Q(t)) & E_2^0(Q(t)) - V_{eff}(Q(t)) \end{pmatrix}\begin{pmatrix} a(t) \\ b(t) \end{pmatrix}. \end{aligned} \tag{21.94}$$

Since we are only interested in occupation probabilities we neglect the phase shift due to $V_{eff}(Q)$ and obtain the semiclassical approximation

$$i\hbar\begin{pmatrix}\dot{a}(t)\\ \dot{b}(t)\end{pmatrix}=\begin{pmatrix}E_1^0(Q(t)) & V(Q(t))\\ V(Q(t)) & E_2^0(Q(t))\end{pmatrix}\begin{pmatrix}a(t)\\ b(t)\end{pmatrix}. \tag{21.95}$$

The position of the wavepacket obeys the equation of motion

$$\begin{aligned}\frac{\partial}{\partial t}<Q>&=\int dQ\,Q\,|\chi_1(Q)|^2+\int dQ\,Q\,|\chi_2(Q)|^2\\ &=\frac{1}{i\hbar}\int dQ\left(\chi_1^{d*}\;\chi_2^{d*}\right)\left[Q,-\frac{\hbar^2}{2M}\frac{\partial^2}{\partial Q^2}+H_d(Q)\right]_-\begin{pmatrix}\chi_1^d\\ \chi_2^d\end{pmatrix}.\end{aligned} \tag{21.96}$$

Since the second derivative and H_d are self-adjoint and the commutator

$$\left[-\frac{\hbar^2}{2M}\frac{\partial^2}{\partial Q^2}+H_d(Q),\,Q\right]_-=-\frac{\hbar^2}{M}\frac{\partial}{\partial Q} \tag{21.97}$$

we have

$$\frac{\partial}{\partial t}<Q>=<\frac{i\hbar}{M}\frac{\partial}{\partial Q}> \tag{21.98}$$

and similarly

$$\begin{aligned}\frac{\partial}{\partial t}<\frac{i\hbar}{M}\frac{\partial}{\partial Q}>&=\frac{1}{M}\int dQ\left(\chi_1^{d*}\;\chi_2^{d*}\right)\left[\frac{\partial}{\partial Q},-\frac{\hbar^2}{2M}\frac{\partial^2}{\partial Q^2}+H_d(Q)\right]_-\begin{pmatrix}\chi_1^d\\ \chi_2^d\end{pmatrix}\\ &=\frac{1}{M}<\frac{\partial}{\partial Q}H_d(Q)>.\end{aligned} \tag{21.99}$$

Consistency then requires

$$V_{eff}(Q(t))=<H_d(Q)>+\text{const.} \tag{21.100}$$

but calculation of the average implies knowledge of the exact solution! However, if the initial velocity of the wavepacket is large enough and the acceleration due to the average force can be neglected, we may approximate the classical trajectory as a motion with constant velocity. This leads to the famous Landau–Zener model.

21.7 Landau–Zener Model

Landau and Zener [92, 93] investigated the curve crossing process treating the nuclear motion classically by introducing a trajectory

$$Q(t)=Q_0+vt \tag{21.101}$$

where they assumed a constant velocity in the vicinity of the crossing point. They investigated the time-dependent model Hamiltonian with constant diabatic coupling

$$H(t) = \begin{pmatrix} E_1(Q(t)) & V \\ V & E_2(Q(t)) \end{pmatrix} = \begin{pmatrix} -\frac{1}{2}\frac{\partial \Delta E}{\partial t} t & V \\ V & \frac{1}{2}\frac{\partial \Delta E}{\partial t} t \end{pmatrix} \tag{21.102}$$

and solved the time dependent Schrödinger equation

$$\mathrm{i}\hbar \frac{\partial}{\partial t} \begin{pmatrix} c_1 \\ c_2 \end{pmatrix} = H(t) \begin{pmatrix} c_1 \\ c_2 \end{pmatrix} \tag{21.103}$$

which reads explicitly

$$\begin{aligned} \mathrm{i}\hbar \frac{\partial c_1}{\partial t} &= E_1(t) c_1 + V c_2 \\ \mathrm{i}\hbar \frac{\partial c_2}{\partial t} &= E_2(t) + V c_1. \end{aligned} \tag{21.104}$$

Substituting

$$\begin{aligned} c_1 &= a_1 \mathrm{e}^{\frac{1}{\mathrm{i}\hbar}\int E_1(t)dt} \\ c_2 &= a_2 \mathrm{e}^{\frac{1}{\mathrm{i}\hbar}\int E_2(t)dt} \end{aligned} \tag{21.105}$$

the equations simplify

$$\begin{aligned} \mathrm{i}\hbar \frac{\partial a_1}{\partial t} &= V \mathrm{e}^{\frac{1}{\mathrm{i}\hbar}\int (E_2(t)-E_1(t)dt} a_2 \\ \mathrm{i}\hbar \frac{\partial a_2}{\partial t} &= V \mathrm{e}^{-\frac{1}{\mathrm{i}\hbar}\int (E_2(t)-E_1(t)dt} a_1. \end{aligned} \tag{21.106}$$

Let us consider the limit of small V and calculate the transition probability in lowest order. From the initial condition $a_1(-\infty) = 1$, $a_2(-\infty) = 0$ we get

$$\int_0^t (E_2(t') - E_1(t'))dt' = \frac{\partial \Delta E}{\partial t}\frac{t^2}{2} \tag{21.107}$$

$$a_2(\infty) \approx \frac{1}{\mathrm{i}\hbar} V \int_{-\infty}^{\infty} \mathrm{e}^{-\frac{1}{\mathrm{i}\hbar}\frac{\partial \Delta E}{\partial t}\frac{t^2}{2}} dt = \frac{V}{\mathrm{i}\hbar}\sqrt{\frac{2\pi\hbar}{-\mathrm{i}\frac{\partial \Delta E}{\partial t}}} \tag{21.108}$$

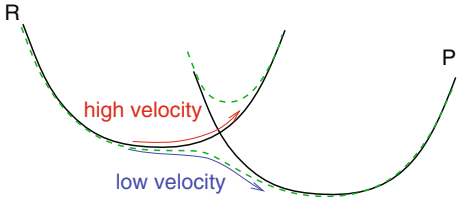

Fig. 21.4 Velocity dependence of the transition. At *low velocities* the electronic wavefunction follows the nuclear motion adiabatically corresponding to a transition between the diabatic states. At *high velocities* the probability for this transition (21.110) becomes slow. *Full* diabatic states, *dashed* adiabatic states

and the transition probability is

$$P_{12} = |a_2(\infty)|^2 = \frac{2\pi V^2}{\hbar|\frac{\partial \Delta E}{\partial t}|}. \tag{21.109}$$

Landau and Zener calculated the transition probability for arbitrary coupling strength (Fig. 21.4)

$$P_{12}^{LZ} = 1 - \exp\left(-\frac{2\pi V^2}{\hbar|\frac{\partial \Delta E}{\partial t}|}\right). \tag{21.110}$$

21.8 Application to Diabatic ET

If we describe the diabatic potentials as displaced harmonic oscillators

$$E_1(Q) = \frac{m\omega^2}{2}Q^2 \qquad E_2(Q) = \Delta G + \frac{m\omega^2}{2}(Q - Q_1)^2 \tag{21.111}$$

the energy gap is with

$$Q_1 = \sqrt{\frac{2\lambda}{m\omega^2}} \tag{21.112}$$

$$E_2 - E_1 = \Delta G + \frac{m\omega^2}{2}(Q_1^2 - 2Q_1 Q) = \Delta G + \lambda - \omega\sqrt{2m\lambda}Q. \tag{21.113}$$

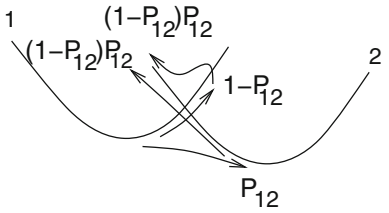

Fig. 21.5 Multiple crossing

The time derivative of the energy gap is

$$\frac{\partial(E_2(Q) - E_1(Q))}{\partial t} = -\omega\sqrt{2m\lambda}\frac{\partial Q}{\partial t} \tag{21.114}$$

and the average velocity is

$$< \frac{\partial Q}{\partial t} >= \frac{\int_{-\infty}^{\infty} |v| \mathrm{e}^{-mv^2/2kT} \mathrm{d}v}{\int_{-\infty}^{\infty} \mathrm{e}^{-mv^2/2kT} \mathrm{d}v} = \sqrt{\frac{2kT}{m\pi}}. \tag{21.115}$$

The probability of curve crossing during one period of the oscillation is given by $2P_{12}$ (see Fig. 21.5).

Together, this gives a transmission coefficient

$$\kappa_{el} = 2\frac{2\pi V^2}{\hbar|\omega\sqrt{2\lambda}\sqrt{\frac{2kT}{\pi}}|} = \frac{2\pi V^2}{\hbar}\frac{2\pi}{\omega}\frac{1}{\sqrt{4\pi\lambda kT}} \tag{21.116}$$

and a rate of

$$k = \frac{2\pi V^2}{\hbar}\frac{1}{\sqrt{4\pi\lambda kT}}\mathrm{e}^{-\Delta G_a/kT}. \tag{21.117}$$

21.9 Conical Intersections

In a diabatic representation, the potential energy of a two-state system has the general form

$$V = \begin{pmatrix} E_1^d(\mathbf{Q}) & V_{12}(\mathbf{Q}) \\ V_{12}(\mathbf{Q})^\dagger & E_2^d(\mathbf{Q}) \end{pmatrix}. \tag{21.118}$$

At a point of degeneracy $\mathbf{Q}^0$ two conditions have to be fulfilled simultaneously

$$V_{12}(\mathbf{Q}^0) = E_1^d(\mathbf{Q}^0) - E_2^d(\mathbf{Q}^0) = 0 \tag{21.119}$$

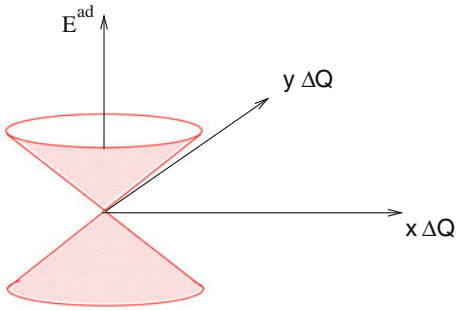

Fig. 21.6 Conical intersection

which is in general only possible if at least two different coordinates are involved. In two dimensions degeneracy is found at a single point, a so-called conical intersection (Fig. 21.6). This type of curve crossing is very important for ultrafast transitions. In more than two dimensions crossings appear at higher dimensional surfaces. The terminology of conical intersections is also used here.

We expand the potential energy matrix around the point of degeneracy [84][8]

$$V = \begin{pmatrix} E(\mathbf{Q^0}) & 0 \\ 0 & E(\mathbf{Q}^0) \end{pmatrix} + \Delta\mathbf{Q} \begin{pmatrix} \nabla E_1^d & \nabla V_{12} \\ \nabla V_{12}^\dagger & \nabla E_2^d \end{pmatrix} + \cdots$$
$$= E(Q_i^0) + \frac{\Delta\mathbf{Q}}{2}\nabla(E_1 + E_2) + \Delta\mathbf{Q} \begin{pmatrix} \mathbf{x} & \mathbf{y} \\ \mathbf{y}^* & -\mathbf{x} \end{pmatrix} + \cdots \tag{21.120}$$

The degeneracy is lifted in the two-dimensional space spanned by the vectors

$$\mathbf{x} = \frac{1}{2}\nabla(E_1^d - E_2^d) \tag{21.121}$$

$$\mathbf{y} = \nabla V_{12} \tag{21.122}$$

the so-called branching space. Orthogonal to it is the intersection space in which degeneracy is not lifted. For a number of N internal coordinates it forms a (N-2) dimensional seam. The topology of the adiabatic energy surfaces

$$E_{1,2}^a = E(\mathbf{Q}^0) + \frac{\Delta\mathbf{Q}}{2}\nabla(E_1 + E_2) \pm \sqrt{|\mathbf{x}\Delta\mathbf{Q}|^2 + |\mathbf{y}\Delta\mathbf{Q}|^2} \tag{21.123}$$

is a double cone with the two surfaces meeting at the intersection point (Fig. 21.6). If the two electronic states are of different symmetry, the modulation of the diabatic energies H_{11}, H_{22} is due to totally symmetric modes whereas the interaction

[8]The energy at the intersection point is $E(\mathbf{Q}^0) = E^a(\mathbf{Q}^0) = E^d(\mathbf{Q}^0)$. Furthermore the sum of the diagonal elements (the trace) is invariant $E_1^a + E_2^a = E_1^d + E_2^d = E_1 + E_2$.

H_{12} is induced by non-totally symmetric modes. (The product of the symmetries of the two states and the vibration must include the totally symmetric representation.) This kind of conical intersection is called symmetry induced, whereas intersections between states of the same or no symmetry are called accidental. A special case is the interaction of two states which are degenerate by symmetry, e.g., belong to an E representation. This case relates to the Jan-Teller effect [94].

21.10 Linear Vibronic Coupling Model

The simplest model to study the dynamics in the vicinity of a conical intersection is the LVC model which is obtained by combining the harmonic oscillator model (Chap. 19) with the expansion (21.120) for two harmonic modes [94] with elongations $x_{1,2}$ relative to the intersection point. The diabatic model Hamiltonian reads [84]

$$H = T_N + \frac{\omega_1^2}{2}x_1^2 + \frac{\omega_2^2}{2}x_2^2 + \sigma x_1 + \begin{pmatrix} -\delta x_1 & \lambda x_2 \\ \lambda x_2 & \delta x_1 \end{pmatrix} \tag{21.124}$$

and the corresponding adiabatic energy surfaces are

$$E_{1,2}^{ad} = \frac{\omega_1^2}{2}x_1^2 + \frac{\omega_2^2}{2}x_2^2 + \sigma x_1 \pm \sqrt{(\delta x_1)^2 + (\lambda x_2)^2}. \tag{21.125}$$

Depending on the parameters, two different types of geometry can be distinguished [95]. For $|\sigma| < |\delta|$ the slopes of the two diabatic energies have different sign and the intersection point is at the minimum of the upper energy surface (peaked intersection). In the opposite case $|\sigma| > |\delta|$ the signs are the same and the intersection is of the sloped type (Fig. 21.7).

The potential energy matrix (21.124) is diagonalized by a rotation (21.63)

$$\begin{aligned} \begin{pmatrix} E_1^{ad} & \\ & E_2^{ad} \end{pmatrix} &= \begin{pmatrix} \cos\alpha & -\sin\alpha \\ \sin\alpha & \cos\alpha \end{pmatrix} \begin{pmatrix} E_1 & V \\ V & E_2 \end{pmatrix} \begin{pmatrix} \cos\alpha & \sin\alpha \\ -\sin\alpha & \cos\alpha \end{pmatrix} \\ &= \begin{pmatrix} E_1 + \frac{1-\cos(2\alpha)}{2}(E_2 - E_1) - \sin(2\alpha)V & \cos(2\alpha)V - \frac{1}{2}\sin(2\alpha)(E_2 - E_1) \\ \cos(2\alpha)V + \frac{1}{2}\sin(2\alpha)(E_2 - E_1) & E_2 - \frac{1-\cos(2\alpha)}{2}(E_2 - E_1) + \sin(2\alpha)V \end{pmatrix} \end{aligned} \tag{21.126}$$

where the rotation angle satisfies

$$\tan(2\alpha) = \frac{2V}{E_2 - E_1} = \frac{\lambda x_2}{\delta x_1}. \tag{21.127}$$

Now, let us follow a circle in the $x_1 - x_2$ plane around the intersection point. The polar angle γ in the $x_1 - x_2$ plane is related to α by

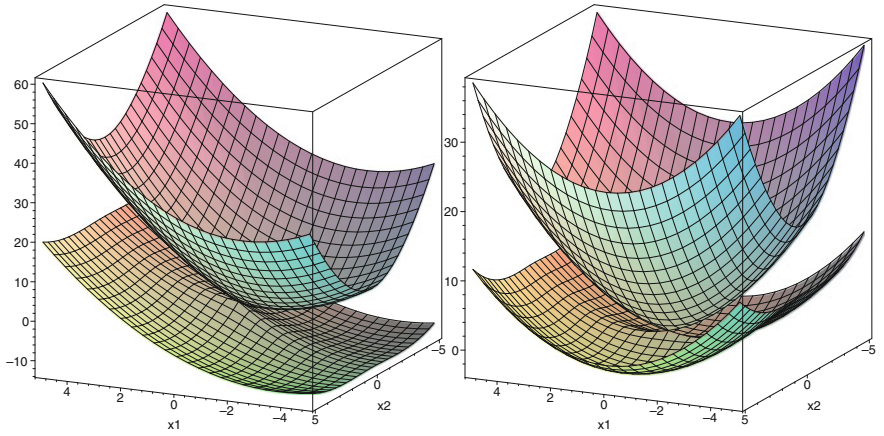

Fig. 21.7 Linear vibronic coupling model. *Left* If the slopes of the diabatic energies have the same sign, a sloped intersection results. *Right* If the slopes of the diabatic energies have different sign, the intersection peaks at the minimum of the upper adiabatic surface

$$\tan\gamma = \frac{x_2}{x_1} = \frac{\delta}{\lambda}\tan(2\alpha). \tag{21.128}$$

Following a closed loop around the intersection changes γ by 2π and α by π and therefore produces a sign change [96] of the two adiabatic electronic wavefunctions

$$\psi_1^{ad} = \psi_1^d \cos\alpha - \psi_2^d \sin\alpha \tag{21.129}$$

$$\psi_2^{ad} = \psi_1^d \sin\alpha + \psi_2^d \cos\alpha. \tag{21.130}$$

This phenomenon is well known as geometric phase [97] or Berry phase [98]. Since the total wavefunction must be single-valued, the sign change must appear both for its electronic and the nuclear part which has to be taken into account for simulations of the nuclear dynamics by special boundary conditions at a cut in the $x_1 - x_2$ plane or an extra phase factor which makes the electronic wavefunction complex valued [99].

The nuclear derivatives transform according to

$$\begin{pmatrix} \cos\alpha & -\sin\alpha \\ \sin\alpha & \cos\alpha \end{pmatrix} \frac{\partial}{\partial x_i} \begin{pmatrix} \cos\alpha & \sin\alpha \\ -\sin\alpha & \cos\alpha \end{pmatrix} = \frac{\partial}{\partial x_i} + \begin{pmatrix} 0 & \tau_i \\ -\tau_i & 0 \end{pmatrix} \tag{21.131}$$

where now explicitly

$$\tau_{x_1} = \frac{\partial\alpha}{\partial x_1} = \frac{-\lambda\delta}{2(\delta^2 x_1^2 + \lambda^2 x_2^2)} x_2 \tag{21.132}$$

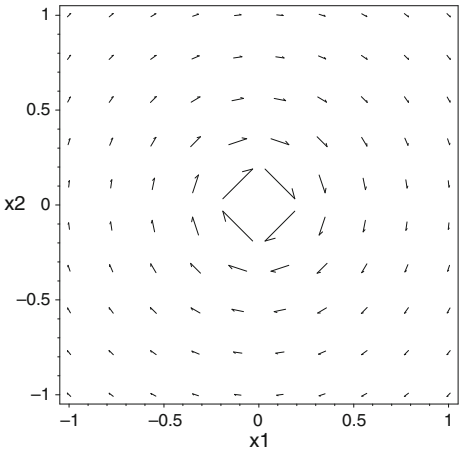

Fig. 21.8 Nuclear gradient of the LVC model

$$\tau_{x_2} = \frac{\partial \alpha}{\partial x_2} = \frac{\lambda\delta}{2(\delta^2 x_1^2 + \lambda^2 x_2^2)} x_1. \tag{21.133}$$

This gradient field looks like that of a curl around the intersection point (Fig. 21.8) where it diverges as

$$|\tau| = \frac{|\lambda\delta|\sqrt{x_1^2 + x_2^2}}{2(\delta^2 x_1^2 + \lambda^2 x_2^2)} \sim \frac{1}{r}. \tag{21.134}$$

The kinetic energy is

$$-\frac{\hbar^2}{2}\sum\left[\frac{\partial}{\partial x_i} + \begin{pmatrix} 0 & 1 \\ -1 & 0 \end{pmatrix}\tau_i\right]_i^2 = -\frac{\hbar^2}{2}\sum_i\left[\frac{\partial^2}{\partial x_i^2} - \tau_i^2 + \begin{pmatrix} 0 & 1 \\ -1 & 0 \end{pmatrix}\left(\frac{\partial \tau_i}{\partial x_i} + 2\tau_i\frac{\partial}{\partial x_i}\right)\right]. \tag{21.135}$$

The diagonal element of the vibronic coupling is

$$V_{1,1}^{nad} = V_{2,2}^{nad} = \frac{\hbar^2}{2}(\tau_{x_1}^2 + \tau_{x_2}^2) = \frac{\hbar^2}{8}\frac{\lambda^2\delta^2(x_1^2 + x_2^2)}{(\delta^2 x_1^2 + \lambda^2 x_2^2)^2} \tag{21.136}$$

and the nondiagonal element

$$\begin{aligned} V_{1,2}^{nad} &= -\frac{\hbar^2}{2}\sum_i\left(\frac{\partial \tau_i}{\partial x_i} + 2\tau_i\frac{\partial}{\partial x_i}\right) \\ &= -\frac{\hbar^2}{2}\left[\frac{\lambda\delta(\delta^2 - \lambda^2)x_1 x_2}{(\delta^2 x_1^2 + \lambda^2 x_2^2)^2} + \frac{\lambda\delta}{(\delta^2 x_1^2 + \lambda^2 x_2^2)}\left(x_1\frac{\partial}{\partial x_2} - x_2\frac{\partial}{\partial x_1}\right)\right] \end{aligned} \tag{21.137}$$

which can be rewritten with

$$\hat{L} = -i\hbar\left(x_1\frac{\partial}{\partial x_2} - x_2\frac{\partial}{\partial x_1}\right)$$

and the commutator

$$\left[\hat{L}, \frac{1}{(\delta^2 x_1^2 + \lambda^2 x_2^2)}\right] = -i\hbar\frac{2x_1x_2(\delta^2 - \lambda^2)}{(\delta^2 x_1^2 + \lambda^2 x_2^2)^2}$$

as

$$\begin{aligned} &-\frac{\hbar^2\lambda\delta}{2}\left\{\frac{1}{(\delta^2 x_1^2 + \lambda^2 x_2^2)}\frac{i}{\hbar}\hat{L} + \frac{i}{2\hbar}\left[\hat{L}, \frac{1}{(\delta^2 x_1^2 + \lambda^2 x_2^2)}\right]\right\} \\ &= -\frac{i\hbar\lambda\delta}{4}\left\{\frac{1}{(\delta^2 x_1^2 + \lambda^2 x_2^2)}\hat{L} + \hat{L}\frac{1}{(\delta^2 x_1^2 + \lambda^2 x_2^2)}\right\}. \end{aligned} \tag{21.138}$$

Problems

21.1 Crude Adiabatic Model

Consider the crossing of two electronic states along a coordinate Q. As basis functions we use two coordinate independent electronic wavefunctions which diagonalize the Born–Oppenheimer Hamiltonian at the crossing point Q_0

$$(T_{el} + V(Q_0))\varphi^{1,2} = E^{1,2}\varphi^{1,2}.$$

Use the following ansatz functions

$$\Psi_1(r, Q) = (\cos\zeta(Q)\varphi^1(r) - \sin\zeta(Q)\varphi^2(r))\chi^1(Q)$$

$$\Psi_2(r, Q) = (\sin\zeta(Q)\varphi^1(r) + \cos\zeta(Q)\varphi^2(r))\chi^2(Q)$$

which can be written in more compact form

$$(\Psi_1, \Psi_2) = (\varphi^1, \varphi^2)\begin{pmatrix} c & s \\ -s & c \end{pmatrix}\begin{pmatrix} \chi_1 \\ \chi_2 \end{pmatrix}.$$

The Hamiltonian is partitioned as

$$H = T_N + T_{el} + V(r, Q_0) + \Delta V(r, Q).$$

Calculate the matrix elements of the Hamiltonian

$$\begin{pmatrix} H_{11} & H_{12} \\ H_{21} & H_{22} \end{pmatrix} = \\ = \begin{pmatrix} c & -s \\ s & c \end{pmatrix} \begin{pmatrix} \varphi_1^\dagger \\ \varphi_2^\dagger \end{pmatrix} \left(-\frac{\hbar^2}{2m} \frac{\partial^2}{\partial Q^2} + T_{el} + V(Q_0) + \Delta V \right) (\varphi^1, \varphi^2) \begin{pmatrix} c & s \\ -s & c \end{pmatrix} \tag{21.139}$$

where $\chi(Q)$ and $\zeta(Q)$ depend on the coordinate Q whereas the basis functions $\varphi^{1,2}$ do not. Chose $\zeta(Q)$ such that $T_{el} + V$ is diagonalized. Evaluate the nonadiabatic interaction terms at the crossing point Q_0.

Chapter 22
Dynamics of an Excited State

In this chapter, we discuss the decay of an initially excited state into a quasi-continuum of final states. We introduce the Green's formalism to calculate the propagator and apply it to the ladder model, which can be solved analytically. In the statistical limit which is applicable to larger, especially bio-molecules, an exponential decay results. We use the saddle point method to treat a more realistic model with a distribution of coupling matrix elements and energies. Applying the displaced oscillator model, we obtain the Marcus expression in the classical limit. Finally, we discuss the energy gap law for intramolecular radiationless transitions.

22.1 Coupling to a Quasi-continuum

In the following, we would like to describe the dynamics of an excited state $|s>$ which is prepared, e.g., by electronic excitation, due to absorption of radiation. This state is an eigenstate of the diabatic Hamiltonian with energy E_s^0. Close in energy to $|s>$ is a manifold of other states $\{|l>\}$, which is not populated during the short time excitation, since from the ground state only the transition $|0> \rightarrow |s>$ is optically allowed. The l-states are weakly coupled to a continuum of bath states[1] and therefore have a finite lifetime (Fig. 22.1).

[1] For instance the field of electromagnetic radiation.

P.O.J. Scherer and S.F. Fischer, *Theoretical Molecular Biophysics*,
Biological and Medical Physics, Biomedical Engineering,
DOI 10.1007/978-3-662-55671-9_22

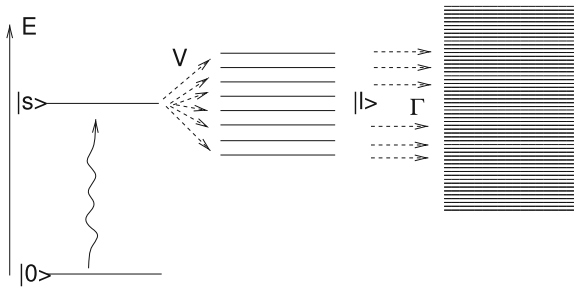

Fig. 22.1 Dynamics of an excited state. The excited state $|s>$ decays into a manifold of states $|l>$ which are weakly coupled to a continuum

The bath states will not be considered explicitly. Instead, we use a non Hermitian Hamiltonian for the subspace spanned by $|s>$ and $\{|l>\}$. We assume that the Hamiltonian is already diagonal[2] with respect to the manifold $\{|l>\}$, which has complex energies[3]

$$E_l^0 = \epsilon_l - \mathrm{i}\frac{\Gamma_l}{2}. \tag{22.1}$$

This describes the exponential decay $\sim \mathrm{e}^{-\Gamma_l t}$ of the l-states into the continuum states.

Thus, the model Hamiltonian takes the form

$$H = H^0 + V = \begin{pmatrix} E_s^0 & V_{s1} & \cdots & V_{sL} \\ V_{1s} & E_1^0 & & \\ \vdots & & \ddots & \\ V_{Ls} & & & E_L \end{pmatrix}. \tag{22.2}$$

22.2 Green's Formalism

For a Hamiltonian $\hat{H}$ with a complete set of eigenstates $|n>$ obeying

$$\hat{H}|n> = E_n|n> \tag{22.3}$$

the corresponding Green's operator or resolvent [69] is defined as

$$\hat{G}(E) = (E - \hat{H})^{-1} = \sum_n |n> \frac{1}{E - E_n} <n|. \tag{22.4}$$

[2]For non Hermitian operators we have to distinguish left eigenvectors and right eigenvectors.

[3]This is also known as the damping approximation.

The Green's operator is very useful for perturbation theory. For a Hamiltonian which can be divided into a zero order part with known eigenstates and a perturbation $\hat{V}$

$$\hat{H} = \hat{H}^0 + \hat{V}. \tag{22.5}$$

An eigenstate Ψ of $\hat{H}$ with energy E obeys

$$0 = (E - \hat{H})\Psi = (E - \hat{H}^0)\Psi - \hat{V}\Psi \tag{22.6}$$

from which

$$(E - \hat{H}^0)\Psi = \hat{V}\Psi \tag{22.7}$$

which can be formally solved by

$$\Psi = G^0(E)\hat{V}\Psi. \tag{22.8}$$

This equation serves as the basis for an iterative improvement of an approximate eigenstate.

22.2.1 Resolvent and Propagator

For a Hermitian Hamiltonian, the poles of the Green's operator are on the real axis and the time evolution operator (the so-called propagator) is defined by (Fig. 22.2)

$$\widetilde{G}(t) = G_+(t) - G_-(t) \tag{22.9}$$

$$G_\pm(t) = \frac{-1}{2\pi \mathrm{i}} \int_{-\infty \pm \mathrm{i}\epsilon}^{\infty \pm \mathrm{i}\epsilon} \mathrm{e}^{-\frac{\mathrm{i}E}{\hbar}t} G(E)\, dE. \tag{22.10}$$

$\widetilde{G}(t)$ is given by an integral, which encloses all the poles E_n. Integration between two poles does not contribute, since the integration path can be taken to be on the real axis and the two contributions vanish. Clockwise integration along a small circle around a pole gives $-2\pi\mathrm{i}$ times the residual value which is (Fig. 22.3)

$$\lim_{E \to E_n} e^{-\frac{\mathrm{i}E}{\hbar}t} G(E)(E - E_n) = |n > e^{-\mathrm{i}E_n t/\hbar} < n|. \tag{22.11}$$

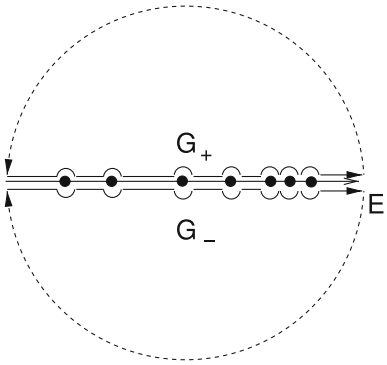

Fig. 22.2 Integration contour for $G_{\pm}(t)$

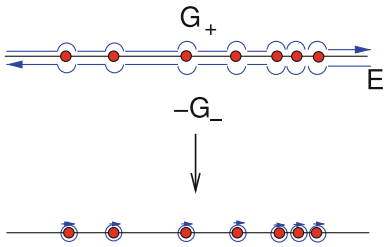

Fig. 22.3 Integration contour for $\widetilde{G}(t) = G_{+}(t) - G_{-}(t)$

Hence, we find

$$\widetilde{G}(t) = \sum |n> \mathrm{e}^{-\frac{\mathrm{i}E}{\hbar}t} <n| = \exp\left(\frac{t}{\mathrm{i}\hbar}H\right). \tag{22.12}$$

For times $t < 0$, the integration path for G_{+} can be closed in the upper half of the complex plane where the integrand

$$\mathrm{e}^{-\frac{\mathrm{i}E}{\hbar}t}G(E) = \mathrm{e}^{-|t|\Im(E)/\hbar}\mathrm{e}^{-\mathrm{i}t\Re(E)/\hbar}G(E) \tag{22.13}$$

vanishes exponentially for large $|E|$ (Fig. 22.4).

Hence

$$G_{+}(t) = 0 \quad \text{for} \quad t < 0. \tag{22.14}$$

We shift the integration path for times $t > 0$ into the lower half of the complex plane, where again the integrand

$$\mathrm{e}^{-\frac{\mathrm{i}E}{\hbar}t}G(E) = \mathrm{e}^{|t|(-|\Im(E)|)/\hbar}\mathrm{e}^{-\mathrm{i}t\Re(E)/\hbar}G(E) \tag{22.15}$$

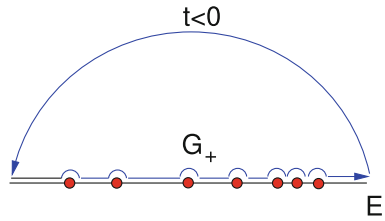

Fig. 22.4 Deformation of the integration contour for $G_+(t)$

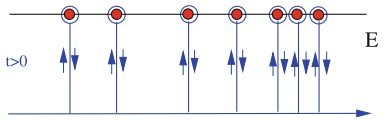

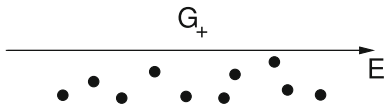

Fig. 22.5 Integration contour for a non-Hermitian Hamiltonian

vanishes exponentially and we sum over all residuals to find

$$G_+(t) = \widetilde{G}(t) \text{ for } t > 0. \tag{22.16}$$

Hence $G_+(t) = \Theta(t)\widetilde{G}(t)$ is the time evolution operator for $t > 0$.[4] There are additional interactions for times $t < 0$ which prepare the initial state

$$\psi(t = 0) = |s > . \tag{22.17}$$

The integration contour for a non-Hermitian Hamiltonian can be chosen as the real axis for $G_+(t)$, which now becomes the Fourier transform of the resolvent

$$G_+(t) = \frac{-1}{2\pi \mathrm{i}} \int_{-\infty}^{\infty} dE\, \mathrm{e}^{-\frac{\mathrm{i}E}{\hbar}t} G(E) \tag{22.18}$$

(Fig. 22.5).

On the real axis, each pole corresponds to a Lorentzian

$$\frac{1}{E - E_n \pm \mathrm{i}\epsilon} = \frac{(E - E_n)}{(E - E_n)^2 + \epsilon^2} \mp \mathrm{i}\frac{\epsilon}{(E - E_n)^2 + \epsilon^2}$$

[4] Similarly we find $G_-(t) = \Theta(-t)\widetilde{G}(t)$ is the time evolution operator for negative times.

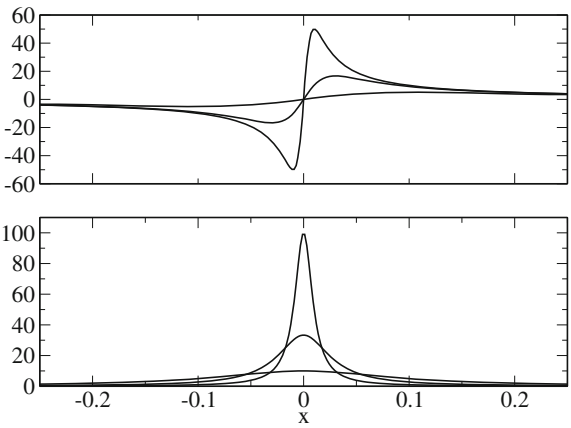

Fig. 22.6 Lorentzian. Real (*top*) and imaginary (*bottom*) part of $1/(x - \mathrm{i}\epsilon)$ are shown for $\epsilon = 0.1, 0.3, 0.01$

which in the limit of small ϵ becomes a distribution (generalized function) (Fig. 22.6)[5]

$$\lim_{\epsilon \to 0} \frac{1}{E - E_n \pm \mathrm{i}\epsilon} = (P.V.) \frac{1}{E - E_n} \mp \pi \mathrm{i} \delta(E - E_n). \tag{22.19}$$

22.2.2 Dyson Equation

Dividing the Hamiltonian in the diagonal part H^0 and the interaction V we have

$$(G^0)^{-1} = E - H^0 \tag{22.20}$$

$$G^{-1} = E - H = (G^0)^{-1} - V. \tag{22.21}$$

Multiplication from the left with G^0 and from the right with G gives the Dyson equation

$$G = G^0 + G^0 V G \tag{22.22}$$

which can be iterated

$$G = G^0 + G^0 V (G^0 + G^0 V G) = G^0 + G^0 V G^0 + G^0 V G^0 V G \tag{22.23}$$

[5] P.V. denotes the Cauchy principal value for which $\int_{-\infty}^{\infty} (P.V.) \frac{1}{x} f(x) dx = \lim_{\epsilon \to 0} \int_{-\infty}^{-\epsilon} \frac{1}{x} f(x) dx + \int_{\epsilon}^{\infty} \frac{1}{x} f(x) dx$ and δ the delta-distribution, for which $\int_{-\infty}^{\infty} \delta(x) f(x) dx = f(0)$.

$$G = G^0 + G^0 V(G^0 + G^0 V(G^0 + G^0 V G) = G^0 + G^0 V G^0 + G^0 V G^0 V G^0 + \cdots \tag{22.24}$$

22.2.3 Transition Operator

The transition operator or T-matrix is defined as

$$T = V + VGV = V + VG^0 V + VG^0 VG^0 V + \cdots \tag{22.25}$$

From

$$G^0 T G^0 = G^0 V G^0 + G^0 V G^0 V G^0 + \cdots \tag{22.26}$$

we find an expansion similar to (22.23)

$$G = G^0 + G^0 T G^0 \tag{22.27}$$

which is quite useful for higher order perturbation theory. The transition rate between two eigenstates of H_0, which are induced by the interaction V, is given in arbitrary order by the generalized golden rule expression [69]

$$\Gamma_{n\to m} = \frac{2\pi}{\hbar} | < m|T(E_n + \mathrm{i}\varepsilon)|n > |^2 \delta(E_n - E_m) \tag{22.28}$$

with the matrix element

$$< m|T(E_n + \mathrm{i}\varepsilon)|n > = < m|V|n > + \sum_{k\neq m} \frac{< m|V|k >< k|V|n >}{E_m - E_k} + \cdots \tag{22.29}$$

22.2.4 Level Shift

We consider now a state $|s>$which is initially populated and decays into a weakly coupled manifold of bath states $|l>$. At times $t > 0$ the wavefunction can be written as a superposition of stationary states

$$\psi(t) = G_+(t)|s > = \sum_n |n > e^{-\mathrm{i}E_n t/\hbar} < n|s > \tag{22.30}$$

and the survival probability is

$$P_s(t) = |< s|\psi >|^2 = |< s|G_+(t)|s >|^2 = |\tilde{G}_{ss}(t)|^2. \tag{22.31}$$

We project the iterated Dyson equation (22.23) on the initial state

$$|s >= \begin{pmatrix} 1 \\ 0 \\ \vdots \\ 0 \end{pmatrix} \tag{22.32}$$

$$G_{ss} =< s|G|s >=< s|G^0|s > + < s|G^0VG^0|s > + < s|G^0VG^0VG|s > . \tag{22.33}$$

Now

$$G^0(E) = \begin{pmatrix} (E - E_s^0)^{-1} & & & \\ & (E - E_1^0)^{-1} & & \\ & & \ddots & \\ & & & (E - E_L^0)^{-1} \end{pmatrix} \tag{22.34}$$

is diagonal and

$$V = \begin{pmatrix} 0 & V_{s1} & \cdots & V_{sL} \\ V_{1s} & 0 & & \\ \vdots & & \ddots & \\ V_{Ls} & & & 0 \end{pmatrix} \tag{22.35}$$

has only off diagonal zero elements. Therefore

$$< s|G^0VG^0|s >=< s|G^0|s >< s|V|s >< s|G^0|s >= 0 \tag{22.36}$$

and

$$< s|G^0VG^0VG|s >=< s|G^0|s >< s|V|l >< l|G^0|l >< l|V|s >< s|G|s > \tag{22.37}$$

$$G_{ss} = G_{ss}^0 + \sum_l G_{ss}^0 V_{sl} G_{ll}^0 V_{ls} G_{ss} \tag{22.38}$$

$$\left(1 - G_{ss}^0 \sum_l V_{sl} G_{ll}^0 V_{ls}\right) G_{ss} = G_{ss}^0 \tag{22.39}$$

$$G_{ss} = \frac{G^0_{ss}}{1 - G^0_{ss}\sum_l V_{sl} G^0_{ll} V_{ls}} = \frac{\frac{1}{E-E^0_s}}{1 - \frac{1}{E-E^0_s}\sum_l \frac{|V_{sl}|^2}{E-E^0_l}} = \frac{1}{E - E^0_s - R_s(E)} \tag{22.40}$$

with the level shift operator [100]

$$R_s(E) = \sum_l \frac{|V_{sl}|^2}{E - \epsilon_l + \mathrm{i}\frac{\Gamma_l}{2}}. \tag{22.41}$$

The poles of the Green's function G_{ss} are given by the implicit equation

$$E_p = E^0_s + R_s(E_p) = E^0_s + \sum_l \frac{|V_{sl}|^2}{E_p - E^0_l}. \tag{22.42}$$

Generally, the Green's function is meromorphic and can be represented as

$$G_{ss}(E) = \sum_p \frac{A_p}{E - E_p} \tag{22.43}$$

where the residuals are defined by

$$A_p = \lim_{E \to E_p} G_{ss}(E)(E - E_p). \tag{22.44}$$

The probability of finding the system still in the state $|s>$ at time $t > 0$ is

$$P_s(t) = | < s|\widetilde{G}(t)|s > |^2 = |\widetilde{G}_{ss}(t)|^2, \tag{22.45}$$

where the propagator is the Fourier transform of the Green's function

$$\widetilde{G}_{+ss}(t) = \frac{1}{2\pi\mathrm{i}} \int_{-\infty}^{\infty} e^{\frac{E}{\mathrm{i}\hbar}t} G_{ss}(E) dE = \theta(t) \sum_p A_p e^{\frac{E_p}{\mathrm{i}\hbar}t}. \tag{22.46}$$

22.3 Ladder Model

We now want to study a simplified model which can be solved analytically. The energy of $|s>$ is set to zero. The manifold $\{|l>\}$ consists of infinitely equally spaced states with equal width

$$E^0_l = \alpha + l\Delta\epsilon - \mathrm{i}\frac{\Gamma}{2} \tag{22.47}$$

and the interaction $V_{sl} = V$ is taken independent on l. With this simplification the poles are solutions of

$$E_p = \sum_{l=-\infty}^{l=\infty} \frac{V^2}{E_p - \alpha - l\Delta\epsilon + \mathrm{i}\frac{\Gamma}{2}} \tag{22.48}$$

which can be written using the identity[6]

$$\cot(z) = \sum_{l=-\infty}^{\infty} \frac{1}{z - l\pi} \tag{22.49}$$

as

$$E_p = \frac{V^2\pi}{\Delta\epsilon} \cot\left(\frac{\pi}{\Delta\epsilon}\left(E_p - \alpha + \mathrm{i}\frac{\Gamma}{2}\right)\right). \tag{22.50}$$

For the following discussion, it is convenient to measure all energy quantities in units of $\pi/\Delta\epsilon$ and define

$$\widetilde{\alpha} = \alpha\pi/\Delta\epsilon \quad \widetilde{\Gamma} = \Gamma\pi/\Delta\epsilon \tag{22.51}$$

$$\widetilde{E}_p = E_p\pi/\Delta\epsilon \quad \widetilde{V} = V\pi/\Delta\epsilon \tag{22.52}$$

to have

$$\widetilde{E}_p = \widetilde{E}_p^r - \frac{\mathrm{i}\widetilde{\Gamma}_p}{2} = \widetilde{V}^2 \cot\left\{\widetilde{E}_p - \widetilde{\alpha} + \mathrm{i}\frac{\widetilde{\Gamma}}{2}\right\} \tag{22.53}$$

which can be split into real and imaginary part

$$\frac{\widetilde{E}_p^r}{\widetilde{V}^2} = \frac{\sin(2(\widetilde{E}_p^r - \widetilde{\alpha}))}{\cosh(\widetilde{\Gamma_p} - \widetilde{\Gamma}) - \cos(2(\widetilde{E}_p^r - \widetilde{\alpha}))} \tag{22.54}$$

$$-\frac{\widetilde{\Gamma}_p}{2\widetilde{V}^2} = \frac{\sinh(\widetilde{\Gamma}_p - \widetilde{\Gamma})}{\cosh(\widetilde{\Gamma_p} - \widetilde{\Gamma}) - \cos(2(\widetilde{E}_p^r - \widetilde{\alpha}))}. \tag{22.55}$$

We now have to distinguish two limiting cases.

[6] $\cot(z)$ has single poles at $z = l\pi$ with residues $\lim_{z\to l\pi} \cot(z)(z - l\pi) = 1$.

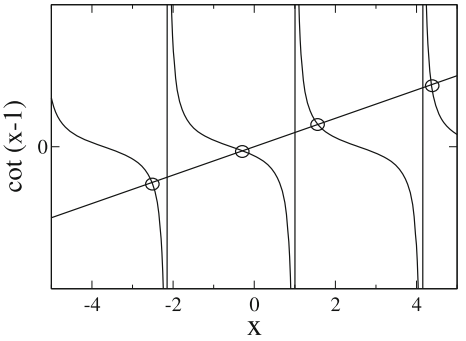

Fig. 22.7 Small molecule limit. The figure shows the graphical solution of $x = \cot(x-1)$

The Small Molecule Limit

For small molecules the density of states $1/\Delta\epsilon$ is small. If we keep the lifetime of the l-states fixed then $\widetilde{\Gamma}$ is small in this limit and the poles are close to the real axis.[7]

We consider first the solution which is closest to zero

$$\tilde{E}_p = \tilde{E}_p^0 - \mathrm{i}\frac{\tilde{\Gamma}_p}{2}. \tag{22.56}$$

The complex cotangent can be expanded for small imaginary part of its argument

$$\cot(x + \mathrm{i}y) \approx \cot x - \mathrm{i}y(1 + \cot^2 x) \tag{22.57}$$

For $0 < \alpha < \Delta\epsilon$ we approximate

$$\tilde{E}_p^0 - \mathrm{i}\frac{\tilde{\Gamma}_p}{2} \approx \tilde{V}^2 \cot\left(\tilde{E}_p^0 - \tilde{\alpha}\right) - \left[1 + \cot^2\left(\tilde{E}_p^0 - \tilde{\alpha}\right)\right]\mathrm{i}\tilde{V}^2\frac{\tilde{\Gamma} - \tilde{\Gamma}_p}{2}. \tag{22.58}$$

The real part is the solution of the real equation (Fig. 22.7)

$$\tilde{E}_p^0 \approx \tilde{V}^2 \cot\left(\tilde{E}_p^0 - \tilde{\alpha}\right) \tag{22.59}$$

and the imaginary part

$$\begin{aligned}\tilde{\Gamma}_p &\approx \tilde{V}^2\left[1 + \cot^2\left(\tilde{E}_p^0 - \tilde{\alpha}\right)\right](\tilde{\Gamma} - \tilde{\Gamma}_p) \\ &\approx (\tilde{\Gamma} - \tilde{\Gamma}_p)\left(\tilde{V}^2 + \left(\frac{\tilde{E}_p^0}{\tilde{V}}\right)^2\right)\end{aligned} \tag{22.60}$$

[7] We assume that $\alpha \neq 0$.

$$\Gamma_p \approx \frac{\left(\tilde{V}^2 + \left(\frac{\tilde{E}_p^0}{\tilde{V}}\right)^2\right)}{1 + \left(\tilde{V}^2 + \left(\frac{\tilde{E}_p^0}{\tilde{V}}\right)^2\right)} \Gamma \tag{22.61}$$

which in the case $\tilde{V}$ small but $\tilde{V} > \tilde{E}_p^0$ gives

$$\tilde{\Gamma}_p \approx \tilde{V}^2 \tilde{\Gamma}, \quad \Gamma_p \approx \pi^2 \frac{V^2}{\Delta\epsilon^2} \Gamma \tag{22.62}$$

and in the case of large $\tilde{V}$

$$\tilde{\Gamma}_p \approx \tilde{\Gamma}. \tag{22.63}$$

All other poles are only weakly disturbed. The residual of the Green's function follows from

$$E = E_p + z \tag{22.64}$$

$$\begin{aligned} \frac{1}{E - R_s(E)} &= \frac{1}{E_p + z - R_s(E_p + z)} \\ &= \frac{1}{E_p + z - R_s(E_p) - z\frac{dR_s}{dE_p}} = \frac{1}{z(1 - \frac{dR_s}{dE}(E_p))} \end{aligned} \tag{22.65}$$

$$\begin{aligned} A_p &= \frac{1}{1 - \frac{dR_s}{dE}(E_p)} = \frac{1}{1 + V^2\left[1 + \cot^2\left(\frac{\pi}{\Delta\epsilon}(E_p - \alpha + \mathrm{i}\frac{\Gamma}{2})\right)\right]} = \frac{1}{1 + V^2\frac{\pi^2}{\Delta\epsilon^2} + E_p^2/V^2} \\ &= \frac{V^2}{E_p^2 + (1 + V^2\frac{\pi^2}{\Delta\epsilon^2})V^2}. \end{aligned} \tag{22.66}$$

As a function of E_p, it has the form of a Lorentzian with a width of $V\sqrt{1 + V^2\frac{\pi^2}{\Delta\epsilon^2}}$. Since the poles are between the l-states, the density of poles is also given by $1/\Delta\epsilon$. Hence contributions from poles close to zero are the most important and for small V one pole is dominant.

The Statistical Limit

Consider now the limit of very dense states with $\tilde{\Gamma} > 1$. This condition is usually fulfilled in larger, especially bio-molecules. To calculate the propagator we need the Green's function G_{ss} on the real axis. For real valued E, the level shift becomes approximately (Fig. 22.8)

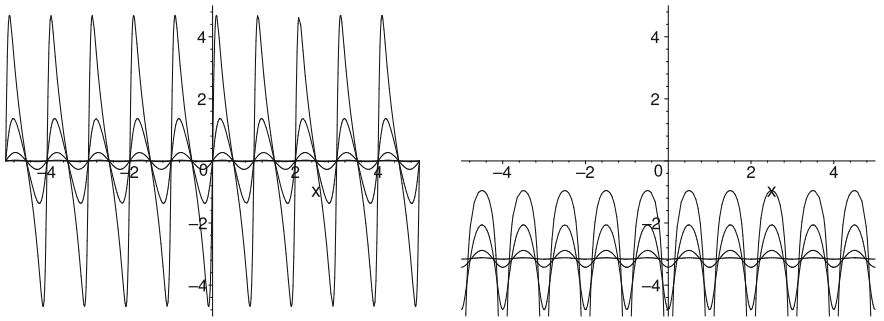

Fig. 22.8 Statistical Limit. Real (*left*) and imaginary (*right*) parts of $\sum_n \frac{1}{E-n\Delta\epsilon+\mathrm{i}\Gamma/2} = \frac{\pi}{\Delta\epsilon}\cot\left(\frac{\pi}{\Delta\epsilon}(E+\mathrm{i}\frac{\Gamma}{2})\right)$ are shown for $\Delta\epsilon = 1,\ \Gamma = 0.2, 0.5, 1.0, 2.0$ on the real E-axis. For large damping Γ the real part approaches 0 and the imaginary part -1

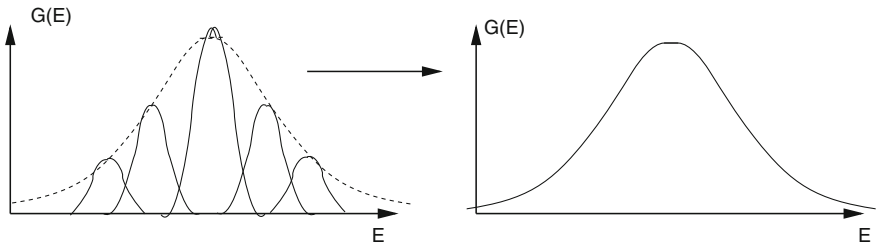

Fig. 22.9 On the real energy axis, a large number of poles is replaced by one effective pole

$$R_s(E) = V^2\pi\rho\cot\left(\frac{\pi}{\Delta\epsilon}\left(E-\alpha+\mathrm{i}\frac{\Gamma}{2}\right)\right) \approx -\mathrm{i}V^2\frac{\pi}{\Delta\epsilon} \tag{22.67}$$

and the Green's function G_{ss} becomes a smooth function on the real axis

$$G_{ss} \approx \frac{1}{E+\mathrm{i}V^2\frac{\pi}{\Delta\epsilon}}. \tag{22.68}$$

The large number of poles is replaced by one effective imaginary pole (Fig. 22.9)

$$E_p = -\mathrm{i}V^2\frac{\pi}{\Delta\epsilon} \tag{22.69}$$

and the initial state decays as

$$P(t) = |e^{\frac{-\mathrm{i}V^2\pi\rho}{\hbar}t}|^2 = e^{-kt} \tag{22.70}$$

with the rate

$$k = \frac{2\pi V^2}{\hbar}\rho \tag{22.71}$$

where

$$\rho = \frac{1}{\Delta\epsilon} \tag{22.72}$$

is the density of states.

22.4 Description Within the Saddle Point Method

In the following we use the saddle point method (Appendix E)[8] which is an asymptotic method to calculate integrals of the type

$$\int_{-\infty}^{\infty} e^{\phi(x)} dx \approx e^{\phi(z_0)} \sqrt{\frac{2\pi}{|\phi''(z_0)|}} \tag{22.73}$$

where the complex valued saddle point z_0 is determined by the equation

$$\phi'(z_0) = 0. \tag{22.74}$$

This method is useful also for more general cases in the statistical limit, i.e., provided the width of the states is large compared to the energy spacing.

Application to the Ladder Model

We consider a more realistic ladder model where the energy of the states is bounded from below (Fig. 22.10). The initial state is at $E_s = \Delta E$ and the ladder states have energies

$$E_l = l\Delta\epsilon, \quad l = 0, 1, 2, \ldots \tag{22.75}$$

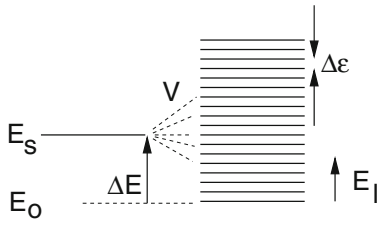

Fig. 22.10 Decay into a quasi-continuum

[8] Also known as method of steepest descent or Laplace method.

We start from the Golden rule expression

$$k = \sum_{l=0}^{\infty} \frac{2\pi V^2}{\hbar} \delta(E_s - E_l) = \sum_{l=0}^{\infty} \frac{2\pi V^2}{\hbar} \delta(\Delta E - \epsilon_l) \tag{22.76}$$

and represent the delta function by a Fourier integral

$$\delta(E) = \frac{1}{2\pi\hbar} \int_{-\infty}^{\infty} \mathrm{e}^{-\mathrm{i}\frac{E}{\hbar}t} dt. \tag{22.77}$$

The rate is

$$k = \sum_{l=0}^{\infty} \frac{V^2}{\hbar^2} \int_{-\infty}^{\infty} \mathrm{e}^{-\mathrm{i}\frac{\Delta E - \epsilon_l}{\hbar}t} dt \tag{22.78}$$

and exchanging integration and summation

$$k = \int dt \sum_{l=0}^{\infty} \frac{V^2}{\hbar^2} \mathrm{e}^{-\mathrm{i}t(\Delta E - l\Delta\epsilon)/\hbar}. \tag{22.79}$$

With the definition

$$z(t) = \sum_{l=0}^{\infty} \frac{V^2}{\hbar^2} \mathrm{e}^{\mathrm{i}t\, l\Delta\epsilon/\hbar} \tag{22.80}$$

we have

$$\phi = -\mathrm{i}t\, \Delta E/\hbar + \ln(z) \tag{22.81}$$

$$k = \int e^{\phi} dt = \int dt\, \mathrm{e}^{-\mathrm{i}t\, \Delta E/\hbar} e^{\ln(z)}. \tag{22.82}$$

The saddle point equation is

$$0 = \frac{\mathrm{d}\phi}{\mathrm{d}t} = -\frac{\mathrm{i}\Delta E}{\hbar} + \frac{1}{z}\frac{\mathrm{d}z}{\mathrm{d}t} \tag{22.83}$$

from which

$$\Delta E = -\mathrm{i}\hbar \frac{\sum_{l=0}^{\infty} \frac{\mathrm{i}l\Delta\epsilon}{\hbar} \mathrm{e}^{\mathrm{i}t\, l\Delta\epsilon/\hbar}}{\sum_{l=0}^{\infty} \mathrm{e}^{\mathrm{i}t\, l\Delta\epsilon/\hbar}} = \frac{\sum_{l=0}^{\infty} l\Delta\epsilon \mathrm{e}^{\mathrm{i}t\, l\Delta\epsilon/\hbar}}{\sum_{l=0}^{\infty} \mathrm{e}^{\mathrm{i}t\, l\Delta\epsilon/\hbar}}. \tag{22.84}$$

Since ΔE is real valued, we look for a saddle point on the positive imaginary axis and substitute

$$\mathrm{i}t_s/\hbar = -\beta \tag{22.85}$$

$$\begin{aligned} \Delta E &= \frac{\sum_{l=0}^{\infty} l\Delta\epsilon\, \mathrm{e}^{-l\beta\Delta\epsilon}}{\sum_{l=0}^{\infty} \mathrm{e}^{-l\beta\Delta\epsilon}} = -\frac{\partial}{\partial\beta} \ln\left[\sum_{l=0}^{\infty} \mathrm{e}^{-l\beta\Delta\epsilon}\right] = -\frac{\partial}{\partial\beta} \ln\left[\frac{1}{1-\mathrm{e}^{-\beta\Delta\epsilon}}\right] \\ &= \frac{\partial}{\partial\beta} \ln\left[1-\mathrm{e}^{-\beta\Delta\epsilon}\right] = \frac{\Delta\epsilon}{\mathrm{e}^{-\beta\Delta\epsilon}-1} \end{aligned} \tag{22.86}$$

which determines

$$\beta = \frac{1}{\Delta\epsilon} \ln\left[1 + \frac{\Delta\epsilon}{\Delta E}\right]. \tag{22.87}$$

The saddle point equation now has a quasi-thermodynamic meaning

$$\Delta E = \frac{1}{z} \sum_{l=0}^{\infty} \frac{V^2}{\hbar^2} l\Delta\epsilon \mathrm{e}^{-l\beta\Delta\epsilon} = < l\Delta\epsilon > \tag{22.88}$$

where β plays the role of $1/k_B T$. The second derivative relates to the width of the energy distribution

$$\begin{aligned} \frac{\mathrm{d}^2 \ln z}{\mathrm{d}t^2} &= \frac{\mathrm{d}}{\mathrm{d}t}\left(\frac{\frac{\mathrm{d}z}{\mathrm{d}t}}{z}\right) = \frac{\frac{\mathrm{d}^2 z}{\mathrm{d}t^2}}{z} - \left(\frac{\frac{\mathrm{d}z}{\mathrm{d}t}}{z}\right)^2 \\ &= \frac{1}{z} \sum_l \frac{V^2}{\hbar^2} \frac{-(l\Delta\epsilon)^2}{\hbar^2} \mathrm{e}^{-\beta l\Delta\epsilon} - \frac{1}{z^2}\left(\sum_l \frac{V^2}{\hbar^2} \frac{\mathrm{i}l\Delta\epsilon}{\hbar} \mathrm{e}^{-\beta l\Delta\epsilon}\right)^2 \\ &= - < \frac{(l\Delta\epsilon)^2}{\hbar^2} > + < \frac{l\Delta\epsilon}{\hbar} >^2 . \end{aligned} \tag{22.89}$$

For small energy spacing $\Delta\epsilon \ll \Delta E$ we find

$$\beta \approx \frac{1}{\Delta E} \tag{22.90}$$

$$z = \sum_{l=0}^{\infty} \frac{V^2}{\hbar^2} \mathrm{e}^{-l\beta\Delta\epsilon} \approx \frac{V^2}{\hbar^2} \frac{1}{1-\mathrm{e}^{-\beta\Delta\epsilon}} \approx \frac{V^2}{\hbar^2} \frac{\Delta E}{\Delta\epsilon} \tag{22.91}$$

$$\phi(t_s) = \beta\Delta E + \ln(z) \approx 1 + \ln\left[\frac{V^2}{\hbar^2}\frac{\Delta E}{\Delta\epsilon}\right] \tag{22.92}$$

$$\mathrm{e}^{\phi(t_s)} = z\mathrm{e}^1 = \frac{V^2}{\hbar^2}\frac{\Delta E}{\Delta\epsilon}\mathrm{e}^1 \tag{22.93}$$

$$\begin{aligned}
&\frac{\partial^2}{\partial t^2}\phi = \frac{\partial^2}{\partial t^2}\ln z = -\frac{1}{\hbar^2}\frac{\partial^2}{\partial\beta^2}\ln\left[1-\mathrm{e}^{-\beta\Delta\epsilon}\right] \\
&= -\frac{1}{\hbar^2}\frac{\partial}{\partial\beta}\left[\frac{-\Delta\epsilon\,\mathrm{e}^{-\beta\Delta\epsilon}}{1-\mathrm{e}^{-\beta\Delta\epsilon}}\right] \approx \frac{1}{\hbar^2}\frac{\partial}{\partial\beta}\left[\frac{\mathrm{e}^{-\beta\Delta\epsilon}}{\beta}\right] \\
&\approx \frac{1}{\hbar^2}\left[-\frac{\mathrm{e}^{-\beta\Delta\epsilon}\Delta\epsilon}{\beta} - \frac{\mathrm{e}^{-\beta\Delta\epsilon}}{\beta^2}\right] \approx -\frac{(\Delta E)^2}{\hbar^2}
\end{aligned} \tag{22.94}$$

$$e^{\phi(t_s)}\sqrt{\frac{2\pi}{|\phi''(t_s)|}} = \frac{V^2}{\hbar^2}\frac{\Delta E}{\Delta\epsilon}\mathrm{e}^1\sqrt{\frac{2\pi}{(\Delta E)^2}\hbar^2} = \frac{2\pi V^2}{\hbar}\mathrm{e}^1\sqrt{\frac{1}{2\pi}}\frac{1}{\Delta\epsilon} \tag{22.95}$$

where the factor

$$\mathrm{e}^1\sqrt{\frac{1}{2\pi}} \approx 1.08. \tag{22.96}$$

Now let us consider a more general model with a distribution of matrix elements V_{sl} and energies ϵ_l [101].

All energies are taken relative to the lowest state of the continuum E_0 (Fig. 22.11)

$$E_s = E_0 + \Delta E \quad E_l = E_0 + \epsilon_l. \tag{22.97}$$

The rate (22.79) becomes

$$k = \int_{-\infty}^{\infty} dt \sum_{l=0}^{\infty} \frac{V_{sl}^2}{\hbar^2} \mathrm{e}^{\frac{\Delta E-\epsilon_l}{\mathrm{i}\hbar}t} = \int_{-\infty}^{\infty} dt\, \mathrm{e}^{-\frac{\mathrm{i}}{\hbar}\Delta E\, t + \ln(z)} \tag{22.98}$$

with

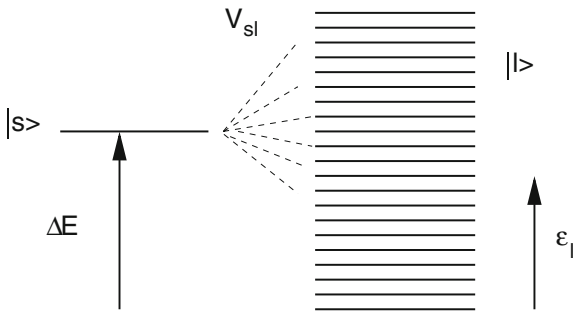

Fig. 22.11 General ladder model

$$z = \sum_{l=0}^{\infty} \frac{V_{sl}^2}{\hbar^2} \mathrm{e}^{\frac{\mathrm{i}\epsilon_l}{\hbar}t}. \tag{22.99}$$

The saddle point equation becomes

$$-\frac{\mathrm{i}}{\hbar}\Delta E + \frac{\mathrm{d}\ln z(t_s)}{\mathrm{d}t} = 0 \tag{22.100}$$

which after substitution

$$\frac{\mathrm{i}t_s}{\hbar} = -\beta \tag{22.101}$$

involves the quasi-thermodynamic average

$$\Delta E = \frac{1}{z}\sum_{l=0}^{\infty} \frac{V_{sl}^2}{\hbar^2}\epsilon_l \mathrm{e}^{-\beta\epsilon_l} = <\epsilon_l> \tag{22.102}$$

where the real variable β plays the role of $1/k_B T$ and $g_l = V_{sl}^2/\hbar^2$ that of a degeneracy factor. The second derivative again relates to the width of the energy distribution

$$\frac{\mathrm{d}^2\ln z}{\mathrm{d}t^2} = \frac{1}{z}\sum_{l=0}^{\infty} g_l \frac{-\epsilon_l^2}{\hbar^2}\mathrm{e}^{-\beta\epsilon_l} - \frac{1}{z^2}\left(\sum_{l=0}^{\infty} g_l \frac{\mathrm{i}\epsilon_l}{\hbar}\mathrm{e}^{-\beta\epsilon_l}\right)^2 \tag{22.103}$$

$$= -<\frac{\epsilon_l^2}{\hbar^2}> + <\frac{\epsilon_l}{\hbar}>^2 .$$

Finally, the saddle point approximation gives

$$k = \int_{-\infty}^{\infty} dt\, \mathrm{e}^{-\frac{\mathrm{i}}{\hbar}\Delta E\, t + \ln(z)} = z(t_s)\mathrm{e}^{\beta\Delta E}\sqrt{\frac{2\pi\hbar^2}{<\epsilon^2> - <\epsilon>^2}}$$
$$= \sum_l \frac{V_{sl}^2}{\hbar}\mathrm{e}^{-\beta(\epsilon_l - \Delta E)}\sqrt{\frac{2\pi}{<\epsilon^2> - <\epsilon>^2}}. \qquad (22.104)$$

22.5 The Energy Gap Law

We now want to apply the displaced harmonic oscillator model (Chap. 19) to the transition between the vibrational manifolds of two electronic states. We assume that the Condon approximation is applicable and the transition matrix element factorizes into an electronic factor V and a Franck–Condon factor $FC(i, f) = |<\chi_i|\chi_f>|^2$. This approximation is valid in many cases, e.g., for allowed optical transitions (18.3) and intramolecular radiationless transitions but also for intermolecular energy transfer processes. Energy conservation requires that the released electronic excitation energy is balanced by vibrational excitation (Fig. 22.12), hence

$$0 = E_f - E_i = \hbar\omega_f - (\Delta E + \hbar\omega_i) \qquad (22.105)$$

The transition rate for a radiationless process with constant V is (compare (18.40) for a radiative transition)

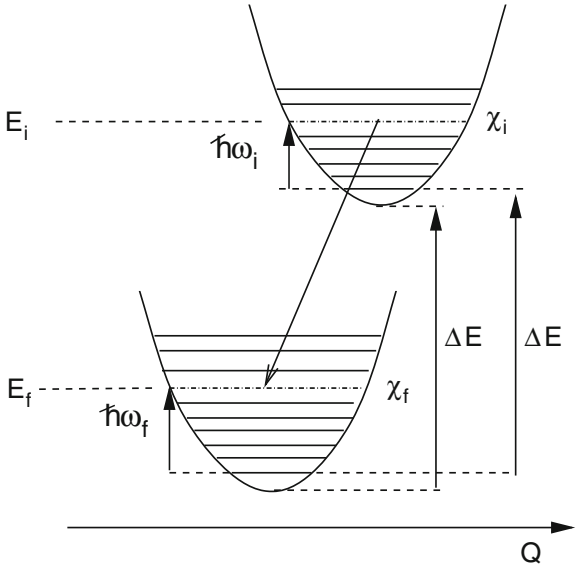

Fig. 22.12 Displaced oscillator model for radiationless transitions

$$
\begin{aligned}
k &= \frac{2\pi V^2}{\hbar} \sum_i P_i \, FC(i,f)\delta(\Delta E - \hbar\omega_f + \hbar\omega_i) \\
&= \frac{2\pi V^2}{\hbar} FCD(\Delta E) \\
&= \frac{V^2}{\hbar^2} \int_{-\infty}^{\infty} dt \, \mathrm{e}^{\frac{-\mathrm{i}t}{\hbar}\Delta E} < \mathrm{e}^{\frac{\mathrm{i}t}{\hbar}H_f} \mathrm{e}^{-\frac{\mathrm{i}t}{\hbar}H_i} > = \frac{V^2}{\hbar^2} \int_{-\infty}^{\infty} dt \, \mathrm{e}^{\frac{-\mathrm{i}t}{\hbar}\Delta E} F(t)
\end{aligned} \tag{22.106}
$$

where H_f (H_i) is the Hamiltonian of the nuclear vibrations (18.32) in the final (initial) state and the correlation function $F(t) = \exp(g(t))$ for independent displaced oscillators is derived in the appendix (C.11). The rate becomes

$$
k = \frac{V^2}{\hbar^2} \mathrm{e}^{-G} \int_{-\infty}^{\infty} dt \, \mathrm{e}^{\frac{-\mathrm{i}t}{\hbar}\Delta E} \exp\left\{ \sum_r g_r^2 \left[(\overline{n}_r + 1)\mathrm{e}^{\mathrm{i}\omega_r t} + \overline{n}_r \mathrm{e}^{-\mathrm{i}\omega_r t} \right] \right\} \tag{22.107}
$$

with the total coupling strength

$$
G = \sum_r g_r^2 (2\overline{n}_r + 1). \tag{22.108}
$$

The short time expansion of the correlation function gives

$$
\begin{aligned}
F(t) &= \exp\left\{ \sum_r g_r^2 \left[(\overline{n}_r + 1) \left(\mathrm{i}\omega_r t - \frac{\omega_r^2 t^2}{2} + \cdots \right) \right.\right. \\
&\qquad \left.\left. + \overline{n}_r \left(-\mathrm{i}\omega_r t - \frac{\omega_r^2 t^2}{2} + \cdots \right) \right] \right\} \\
&= \exp\left\{ \sum_r g_r^2 \left[\mathrm{i}\omega_r t - \frac{\omega_r^2 t^2}{2} (2\overline{n}_r + 1) + \cdots \right] \right\} \\
&= \exp\left\{ \frac{E_R}{\hbar} \mathrm{i}t - \frac{1}{2\hbar^2} \Delta^2 t^2 + \cdots \right\}
\end{aligned} \tag{22.109}
$$

with

$$
\Delta^2 = \sum_r g_r^2 (2\overline{n}_r + 1)(\hbar\omega)_r^2. \tag{22.110}
$$

The coefficient of the quadratic term is roughly

$$
\frac{\Delta^2}{\hbar^2} \approx G\tilde{\omega}^2 \tag{22.111}
$$

where the average frequency $\tilde{\omega}$ (major accepting modes) is defined as

$$\tilde{\omega} = \frac{\sum_r g_r^2(2\overline{n}_r + 1)\omega_r}{\sum_r g_r^2(2\overline{n}_r + 1)}. \tag{22.112}$$

In the strong coupling limit $G > 1$ the correlation decays rapidly $\left(\propto \exp\left(-G\tilde{\omega}^2 t^2/2\right)\right)$ before the quadratic approximation becomes invalid (which is roughly after $t \geq 1/\tilde{\omega}$). Then the rate is given by a Gaussian expression

$$k = \frac{V^2}{\hbar^2}\sqrt{\frac{2\pi\hbar^2}{\Delta^2}}\exp\left\{-\frac{(\Delta E - E_R)^2}{2\Delta^2}\right\}. \tag{22.113}$$

If all modes can be treated classically $\hbar\omega_r \ll k_B T$ the phonon number is $\bar{n}_r = k_B T/\hbar\omega_r$ and

$$\Delta^2 \approx 2k_B T\sum_r g_r^2\hbar\omega_r = 2k_B T E_R \tag{22.114}$$

which gives the Marcus expression in the classical limit (see also (19.22) and (16.23))

$$k = \frac{2\pi V^2}{\hbar}\sqrt{\frac{1}{4\pi k_B T E_R}}\exp\left\{-\frac{(\Delta E - E_R)^2}{4E_r k_B T}\right\}. \tag{22.115}$$

In the limit of weak vibronic coupling $G < 1$, we use the saddle point method. The saddle point equation reads

$$\begin{aligned}\frac{\mathrm{i}}{\hbar}\Delta E &= \sum_r g_r^2\left[\mathrm{i}\omega_r(\overline{n}_r + 1)\mathrm{e}^{\mathrm{i}\omega_r t} - \mathrm{i}\omega_r\overline{n}_r\mathrm{e}^{-\mathrm{i}\omega_r t}\right] \\ &= \mathrm{i}\sum_r g_r^2\omega_r\left[(\overline{n}_r + 1)\mathrm{e}^{-\mathrm{i}\omega_r t} - \overline{n}_r\mathrm{e}^{\mathrm{i}\omega_r t}\right].\end{aligned} \tag{22.116}$$

For intramolecular radiationless transitions and large energy gap the important accepting modes usually are at high frequencies $\hbar\omega_r \gg k_B T$. Here the saddle point equation simplifies to

$$\Delta E = \sum_r g_r^2\hbar\omega_r\mathrm{e}^{\mathrm{i}\omega_r t} \tag{22.117}$$

and the average frequency $\widetilde{\omega}$ becomes

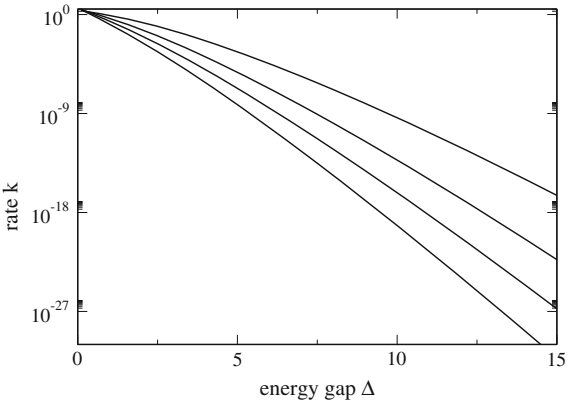

Fig. 22.13 Energy gap law. The relative rate (22.123) is shown as a function of the energy gap in units of the average frequency for S = 0.05, 0.1, 0.2, 0.5

$$\tilde{\omega} = \frac{\sum_r g_r^2 \omega_r}{\sum_r g_r^2} = \frac{E_R}{\hbar S} \tag{22.118}$$

with the Huang–Rhys factor

$$S = \sum_r g_r^2. \tag{22.119}$$

The saddle point equation is approximated as

$$\Delta E = S\hbar\tilde{\omega} \mathrm{e}^{\mathrm{i}t_s\tilde{\omega}} \tag{22.120}$$

with the solution

$$\mathrm{i}t_s = \frac{1}{\tilde{\omega}} \ln \frac{\Delta E}{S\hbar\tilde{\omega}}. \tag{22.121}$$

The second derivative is

$$-\sum_r g_r^2 \omega_r^2 \mathrm{e}^{\mathrm{i}\omega_r t_s} \approx -S\tilde{\omega}^2 \mathrm{e}^{\ln(\Delta E/S\hbar\tilde{\omega})} = -\frac{1}{\hbar}\Delta E\tilde{\omega} \tag{22.122}$$

and the rate is

$$\begin{aligned} k &= \frac{V^2}{\hbar^2}\sqrt{\frac{2\pi\hbar}{\Delta E\tilde{\omega}}} \exp\left\{-\frac{\Delta E}{\hbar}\frac{1}{\tilde{\omega}} \ln \frac{\Delta E}{S\hbar\tilde{\omega}} + S\frac{\Delta E}{S\hbar\tilde{\omega}} - S\right\} \\ &= \frac{V^2}{\hbar}\sqrt{\frac{2\pi}{\Delta E\hbar\tilde{\omega}}} \exp\left\{-S - \frac{\Delta E}{\hbar\tilde{\omega}}\left[\ln \frac{\Delta E}{S\hbar\tilde{\omega}} - 1\right]\right\}. \end{aligned} \tag{22.123}$$

The dependence on ΔE , which is close to exponential, is known as the energy gap law (Fig. 22.13).

Problems

22.1 Ladder model

Solve the time evolution for the ladder model approximately

$$H = \begin{pmatrix} 0 & V & \cdots & V \\ V & E_1 & & \\ \vdots & & \ddots & \\ V & & & E_n \end{pmatrix} \qquad E_j = \alpha + (j-1)\Delta\epsilon$$

First derive an integral equation for $C_0(t)$ only by substitution. Then replace the sum by integration over $\omega = j\frac{\Delta\epsilon}{\hbar}$ and extend the integration over the whole real axis. Replace the integral by a delta function and show that the initial state decays exponentially with a rate

$$k = \frac{2\pi V^2}{\hbar\Delta\epsilon}.$$

Part VII
Elementary Photoinduced Processes

Chapter 23
Photophysics of Chlorophylls and Carotenoids

Chlorophylls and Carotenoids (Figs. 23.1, 23.2) are very important light receptors. Both classes of molecules have a large π-electron system which is delocalized over many conjugated bonds and is responsible for strong absorption bands in the visible region. In this chapter, we introduce the molecular orbital method for the electronic wavefunction. We apply the free electron model and the Hückel MO method to linear and cyclic polyenes as model systems and discuss Gouterman's four orbital model for Porphyrins and Kohler's simplified CI model for polyenes. Finally, we comment on energy transfer processes involving Chlorophylls and Carotenoids in photosynthesis.

23.1 MO Model for the Electronic States

The electronic wavefunctions of larger molecules are usually described by introducing one-electron wavefunctions $\phi(r)$ and expanding the wavefunction in terms of one or more Slater determinants. Singlet ground states can be in most cases described quite sufficiently by one determinant representing a set of doubly occupied orbitals

$$|S_0> = |\phi_{1\uparrow}\phi_{1,\downarrow}\cdots\phi_{nocc,\uparrow}\phi_{nocc,\downarrow}|$$

$$= \frac{1}{\sqrt{(2N_{occ})!}} \begin{vmatrix} \phi_{1\uparrow}(r_1) & \phi_{1\downarrow}(r_1) & \cdots & \phi_{nocc,\downarrow}(r_1) \\ \phi_{1\uparrow}(r_2) & \phi_{1\downarrow}(r_2) & \cdots & \phi_{nocc,\downarrow}(r_2) \\ \vdots & \vdots & & \vdots \\ \phi_{1\uparrow}(r_{2N_{occ}}) & \phi_{1\downarrow}(r_{2N_{occ}}) & & \phi_{nocc,\downarrow}(r_{2N_{occ}}) \end{vmatrix}.$$

Excited states can be described as a linear combination of excited electronic configurations. The lowest excited state can often be reasonably approximated as the

P.O.J. Scherer and S.F. Fischer, *Theoretical Molecular Biophysics*,
Biological and Medical Physics, Biomedical Engineering,
DOI 10.1007/978-3-662-55671-9_23

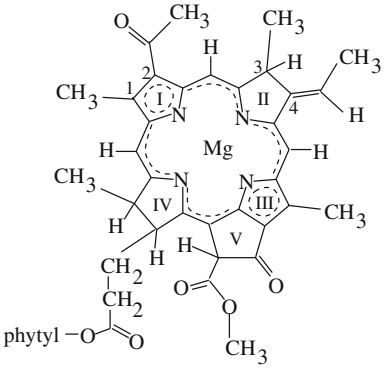

Fig. 23.1 Structure of Bacteriochlorophyll-b [102]. This is the principal green pigment of the photosynthetic bacterium *Rhodopseudomonas viridis*. *Dashed curves* indicate the delocalized π-electron system. Chlorophylls have an additional double bond between positions 3 and 4. Variants have different side-chains at positions 2 and 3

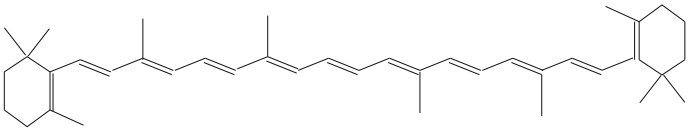

Fig. 23.2 Structure of β-Carotene. The basic structure of the carotenoids is a conjugated chain made up of isoprene units. Variants have different end groups

transition of one electron from the highest occupied orbital ϕ_{nocc} (HOMO) to the lowest unoccupied orbital ϕ_{nocc+1} (LUMO). We have already learnt that a singlet excitation is given by

$$|S_1 >= \frac{1}{\sqrt{2}}(|\phi_{1\uparrow}\phi_{1,\downarrow}\cdots\phi_{HOMO,\uparrow}\phi_{LUMO,\downarrow}|-|\phi_{1\uparrow}\phi_{1,\downarrow}\cdots\phi_{HOMO,\downarrow}\phi_{LUMO,\uparrow}|). \tag{23.1}$$

The molecular orbitals can be determined from a more or less sophisticated method.

23.2 The Free Electron Model for Polyenes

We approximate a polyene with a number of N double bonds by a 1-dimensional box of length $L = (2N + 1)d$.[1] The orbitals of the free electron model

$$H = -\frac{\hbar^2}{2m_e}\frac{\partial^2}{\partial x^2} + V(r) \tag{23.2}$$

[1]The end of the box is one bond length behind the last C-atom.

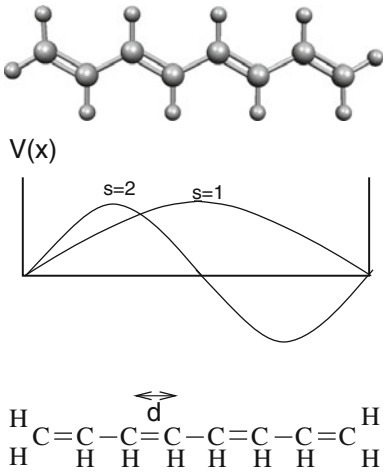

Fig. 23.3 Octatetraene. *Top* optimized structure. *Middle* potential energy and lowest two eigenfunctions of the free electron model. *Bottom* linear model with equal bond lengths *d*

have to fulfill the b.c. $\phi(0) = \phi(L) = 0$. Therefore, they are given by

$$\phi_s(x) = \sqrt{\frac{2}{L}} \sin \frac{\pi s x}{L} \tag{23.3}$$

with energies (Fig. 23.3)

$$E_s = \frac{2}{L} \int_0^L \frac{\hbar^2}{2m_e} \left(\frac{\pi s}{L}\right)^2 \left(\sin \frac{\pi s x}{L}\right)^2 dx = \frac{1}{2m_e} \left(\frac{\pi \hbar s}{L}\right)^2. \tag{23.4}$$

Since there are 2N π-electrons, the energy of the lowest excitation is estimated as

$$\Delta E = E_{n+1} - E_n = \frac{\pi^2 \hbar^2}{2m_e d^2 (2N+1)^2} \left((N+1)^2 - N^2\right) = \frac{\pi^2 \hbar^2}{2m_e d^2 (2N+1)}. \tag{23.5}$$

The transition dipole matrix element for the singlet–singlet transition is

$$\begin{aligned} \boldsymbol{\mu} &= < |\phi_{nocc\uparrow} \phi_{nocc\downarrow}| \sum (-e\mathbf{r}) | \frac{1}{\sqrt{2}} (|\phi_{nocc\uparrow} \phi_{nocc+1\downarrow}| - |\phi_{nocc\downarrow} \phi_{nocc+1\uparrow}|) > \\ &= -\sqrt{2} e \int dr \; \phi_{nocc}(r) \mathbf{r} \phi_{nocc+1}(r) \\ &= -\sqrt{2} e \frac{2}{L} \int_0^L \sin \frac{(N+1)\pi x}{L} \, x \, \sin \frac{N \pi x}{L} dx \\ &= \frac{2\sqrt{2} e}{L} \frac{4L^2 N(N+1)}{\pi^2 (2N+1)^2} = \frac{8\sqrt{2} e d}{\pi^2} \frac{N(N+1)}{2N+1} \end{aligned} \tag{23.6}$$

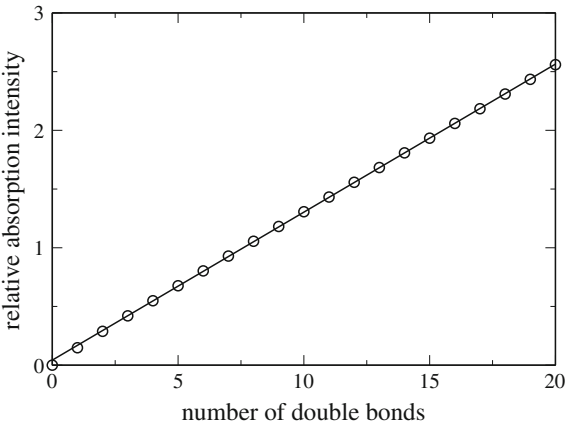

Fig. 23.4 Length dependence of the polyene absorption. The *circles* show the relative absorption from (23.7). The line is a linear fit

which grows with increasing length of the polyene. The absorption coefficient is proportional to

$$\alpha \sim \mu^2 \Delta E \sim \frac{N^2(N+1)^2}{(2N+1)^3} \tag{23.7}$$

which is nearly proportional to the number of double bonds N (Fig. 23.4).

23.3 The LCAO Approximation

The molecular orbitals are usually expanded in a basis of atomic orbitals

$$\phi(r) = \sum_s C_s \varphi_s(r) \tag{23.8}$$

where the atomic orbitals are centered on the nuclei and the coefficients are determined from diagonalization of a certain one-electron Hamiltonian (for instance, Hartree–Fock, Kohn–Sham, semiempirical approximations such as AM1)

$$H\psi = E\psi. \tag{23.9}$$

Inserting the LCAO wavefunction gives

$$\sum_s C_s H \varphi_s(r) = E \sum_s C_s \varphi_s(r) \tag{23.10}$$

and projection on one of the atomic orbitals $\varphi_{s'}$ gives a generalized eigenvalue problem

$$0 = \int d^3r\, \varphi_{s'}(r) \sum_s C_s (H - E)\varphi_s(r)$$
$$= \sum_s C_s (H_{s's} - E S_{s's}). \tag{23.11}$$

23.4 Hückel Approximation

The Hückel approximation [103] is a very simple LCAO model for the π-electrons. It makes the following approximations:

- The diagonal matrix elements $H_{ss} = \alpha$ have the same value (Coulomb integral) for all Carbon atoms.
- The overlap of different p_z-orbitals is neglected $S_{ss'} = \delta_{ss'}$.
- The interaction between bonded atoms is $H_{ss'} = \beta$ (resonance integral) and has the same value for all bonds.
- The interaction between nonbonded atoms is zero $H_{ss'} = 0$.

The Hückel matrix for a linear polyene has the form of a tridiagonal matrix (Fig. 23.5)

$$H = \begin{pmatrix} \alpha & \beta & & & \\ \beta & \alpha & \beta & & \\ & \ddots & \ddots & \ddots & \\ & & \beta & \alpha & \beta \\ & & & \beta & \alpha \end{pmatrix} \tag{23.12}$$

and can be easily diagonalized with the eigenvectors (Fig. 23.6)

$$\phi_r = \sqrt{\frac{2}{2N+1}} \sum_{s=1}^{2N} \sin \frac{rs\pi}{2N+1} \varphi_s \qquad r = 1, 2, \ldots 2N. \tag{23.13}$$

The eigenvalues are

$$E_r = \alpha + 2\beta \cos \frac{r\pi}{2N+1}. \tag{23.14}$$

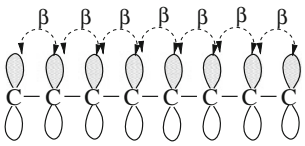

Fig. 23.5 Hückel model for polyenes

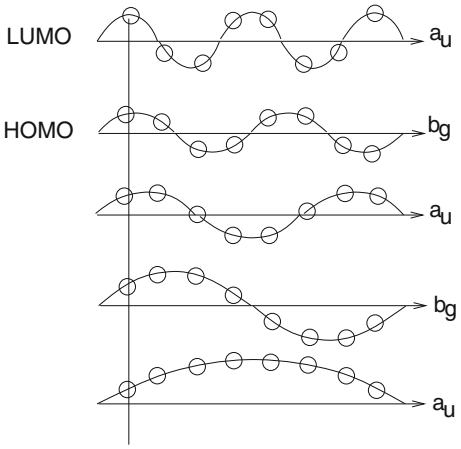

Fig. 23.6 Hückel orbitals for octatetraene

C_{2h}	E	C_2	σ	i
A_g	1	1	1	1
A_u	1	1	−1	−1
B_g	1	−1	−1	1
B_u	1	−1	1	−1

Fig. 23.7 Character table of the symmetry group C_{2h}. All π-orbitals are antisymmetric with respect to the reflection σ and are therefore of a_u or b_g symmetry

The symmetry of the molecule is C_{2h} (Fig. 23.7). All π-orbitals are antisymmetric with respect to the vertical reflection σ_h. With respect to the C_2 rotation they have alternating a or b symmetry. Since $\sigma_h \times C_2 = i$, the orbitals are of alternating a_u and b_g symmetry. The lowest transition energy is in the Hückel model

$$\Delta E = E_{N+1} - E_N = 2\beta \left(\cos \frac{(N+1)\pi}{2N+1} - \cos \frac{N\pi}{2N+1} \right) \tag{23.15}$$

which can be simplified with the help of $(x = \pi/(2N+1))$

$$\begin{aligned} &\cos(N+1)x - \cos Nx = \frac{1}{2}\left(\mathrm{e}^{\mathrm{i}(N+1)x} + \mathrm{e}^{-\mathrm{i}(N+1)x} - \mathrm{e}^{\mathrm{i}Nx} - \mathrm{e}^{-\mathrm{i}Nx}\right) \\ &= \frac{1}{2}\mathrm{e}^{\mathrm{i}(N+1/2)x}\left(\mathrm{e}^{\mathrm{i}x/2} - \mathrm{e}^{-\mathrm{i}x/2}\right) + \frac{1}{2}\mathrm{e}^{-\mathrm{i}(N+1/2)x}\left(\mathrm{e}^{-\mathrm{i}x/2} - \mathrm{e}^{\mathrm{i}x/2}\right) \\ &= -2\sin\left(\left(N+\frac{1}{2}\right)x\right)\sin\frac{x}{2} \end{aligned} \tag{23.16}$$

to give[2]

$$\Delta E = -4\beta \sin \frac{\pi}{4N+2} \sim \frac{1}{N} \quad \text{for large n.} \tag{23.17}$$

This approximation can be improved if the bond length alternation is taken into account, by using two alternating β-values [104]. The resulting energies are

$$E_k = \alpha \pm \sqrt{\beta^2 + \beta'^2 + 2\beta\beta' \cos k} \tag{23.18}$$

where the k-values are solutions of

$$\beta \sin(N+1)k + \beta' \sin Nk = 0. \tag{23.19}$$

In the Hückel model, the lowest excited state has the symmetry $a_u \times b_g = B_u$ and is strongly allowed. However, it is known that in reality for longer polyenes the lowest excited singlet is totally symmetric A_g and forbidden. This can be only understood if correlation effects are taken into account [105–108].

23.5 Simplified CI model for Polyenes

In a very simple model Kohler [109] treats only transitions from the b_g-HOMO into the a_u-LUMO and b_g-LUMO+1 orbitals. The HOMO-LUMO+1 transition as well as the double HOMO-LUMO transition are both of A_g symmetry and can therefore interact. If the interaction is strong enough, then the lowest excited state will be of A_g-symmetry and will be optically forbidden (Fig. 23.8).

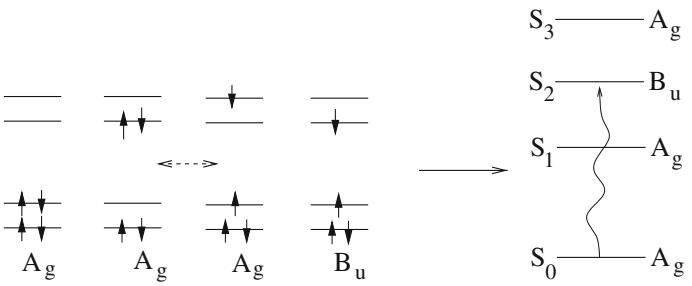

Fig. 23.8 Simplified CI model for linear polyenes

[2] β is a negative quantity.

23.6 Cyclic Polyene as a Model for Porphyrins

For a cyclic polyene with N carbon atoms the Hückel matrix has the form

$$H = \begin{pmatrix} \alpha & \beta & & & \beta \\ \beta & \alpha & \beta & & \\ & \ddots & \ddots & \ddots & \\ & & \beta & \alpha & \beta \\ \beta & & & \beta & \alpha \end{pmatrix} \tag{23.20}$$

with eigenvectors

$$\phi_k = \frac{1}{\sqrt{N}} \sum_{s=1}^{N} \mathrm{e}^{\mathrm{i}ks} \varphi_s \qquad k = 0, \frac{2\pi}{N}, 2\frac{2\pi}{N} \cdots (N-1)\frac{2\pi}{N} \tag{23.21}$$

and eigenvalues

$$E_k = \alpha + 2\beta \cos k. \tag{23.22}$$

This can be used as a model for the class of Porphyrin molecules [110, 111] (Fig. 23.9).

For the metal-porphyrin, there are in principle two possibilities for the assignment of the essential π-system, an inner ring with 16 atoms or an outer ring with 20 atoms, both reflecting the D_{4h}-symmetry of the molecule. Since it is not possible to draw a unique chemical structure, we have to count the π-electrons. The free base porphin is composed of 14 H atoms (of which the peripheral ones are not shown), 20 C atoms and 4 N atoms which provide a total of $14 + 4{*}20 + 5{*}4 = 114$ valence electrons. There are 42 σ-bonds (including those to the peripheral H atoms) and 2

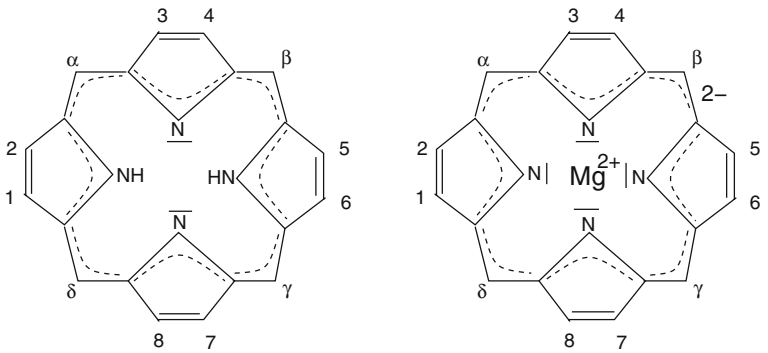

Fig. 23.9 Free base Porphin and Mg-Porphin. The bond character was assigned on the basis of the bond lengths from HF-optimized structures

lonely electron pairs involving a total of 88 electrons. Therefore the number of π-electrons is $114 - 88 = 26$. Usually, it is assumed that the outer double bonds are not so strongly coupled to the π-system and a model with 18 π-electrons distributed over the N = 16-ring is used. For the metal Porphin, the number of H atoms is only 12 but there are 4 lonely electron pairs instead of 2. Therefore, the number of non-π valence electrons is the same as for the free base porphin. The total number of valence electrons is again 114 since the Mg atom formally donates 2 electrons.

23.7 The Four Orbital Model for Porphyrins

Gouterman [112–114] introduced the four orbital model which considers only the doubly degenerate HOMO ($k = \pm 4 \times 2\pi/N$) and LUMO ($k = \pm 5 \times 2\pi/N$) orbitals. There are 4 HOMO-LUMO transitions (Fig. 23.10). Their transition dipoles are given by

$$\boldsymbol{\mu} = \frac{1}{N} \sum_{ss'} \mathrm{e}^{-\mathrm{i}k's'} \mathrm{e}^{\mathrm{i}ks} \int \varphi^*_{s'}(r)(-e\mathbf{r})\varphi_s(r) d^3r \tag{23.23}$$

which is approximately[3]

$$\boldsymbol{\mu} = \frac{1}{N} \sum_{ss'} \mathrm{e}^{-\mathrm{i}k's'} \mathrm{e}^{\mathrm{i}ks} \delta_{ss'}(-eR) \begin{pmatrix} \cos(s \times \frac{2\pi}{N}) \\ \sin(s \times \frac{\pi}{N}) \\ 0 \end{pmatrix} \tag{23.24}$$

where the z-component vanishes and the perpendicular components have circular polarization[4]

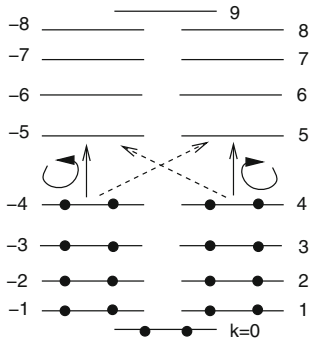

Fig. 23.10 Porphin orbitals

[3]Neglecting differential overlaps and assuming a perfect circular arrangement.

[4]For an average R=3Å this gives a total intensity of 207 Debye^2 which is comparable to the 290 Debye^2 from a HF/CI calculation.

$$\boldsymbol{\mu}\left(\frac{1}{\sqrt{2}}, \pm\frac{\mathrm{i}}{\sqrt{2}}, 0\right) = \frac{-eR}{\sqrt{2}N}\sum_s \mathrm{e}^{\mathrm{i}(k-k'\pm 2\pi/N)s} = \frac{-eR}{\sqrt{2}}\delta_{k-k',\pm 2\pi/N}. \tag{23.25}$$

The selection rule is

$$k - k' = \pm 2\pi/N. \tag{23.26}$$

Hence two of the HOMO-LUMO transitions are allowed and circularly polarized:

$$4\frac{2\pi}{N} \rightarrow 5\frac{2\pi}{N}$$

$$-4\frac{2\pi}{N} \rightarrow -5\frac{2\pi}{N}. \tag{23.27}$$

If configuration interaction is taken into account, these four transitions split into two degenerate excited states of E-symmetry. The higher one carries most of the intensity and corresponds to the Soret band in the UV. The lower one is very weak and corresponds to the Q band in the visible [115, 116]. As a result of ab initio

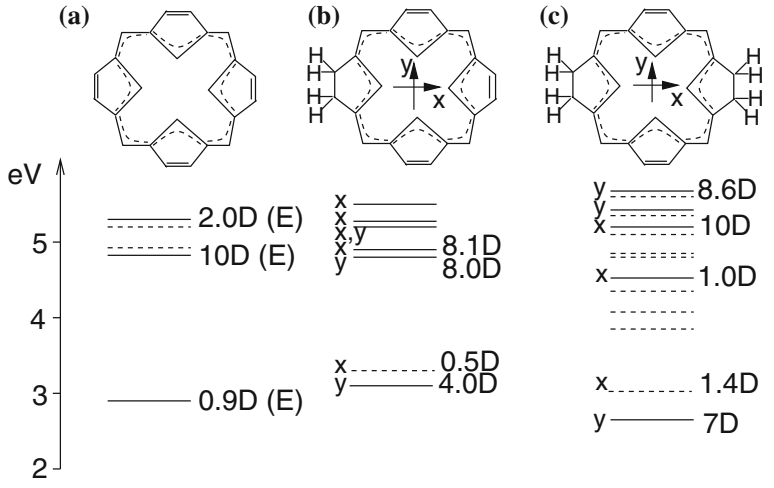

Fig. 23.11 Electronic structure of Porphins and Porphin derivatives. 631G-HF/CI calculations were performed with GAMESS [117]. *Numbers* give transition dipoles in Debyes. *Dashed lines* indicate very weak or dipole forbidden transitions. (**a**) Mg-Porphin has two allowed transitions of E-symmetry, corresponding to the weak Q band at lower and the strong B-band at higher energy. (**b**) In Mg-Chlorin (dihydroporphin) the double bond 1–2 is saturated similar to Chlorophylls. The Q band splits into the lower and stronger Q_y band and the weaker Q_x band (**c**) Tetrahydroporphin, double bonds 1–2 and 5–6 are saturated similar to Bacteriochlorphyll. The Q_y band is shifted to lower energies

calculations, the four orbitals of the Gouterman model stay approximately separated from the rest of the MO orbitals [116]. If the symmetry is disturbed as for Chlorin, the Q band splits into the lower Q_y band which gains large intensity and the higher weak Q_x band. Figure 23.11 shows calculated spectra for Mg-Porphin, Mg-Chlorin, and Mg-Tetrahydroporphin.

23.8 Energy Transfer Processes

Carotenoids and Chlorophylls are very important for photosynthetic systems [118]. Chlorophyll molecules with different absorption maxima are used to harvest light energy and to direct it to the reaction center where the special pair dimer has the lowest absorption band of the Chlorophylls (Fig. 23.12). Carotenoids can act as

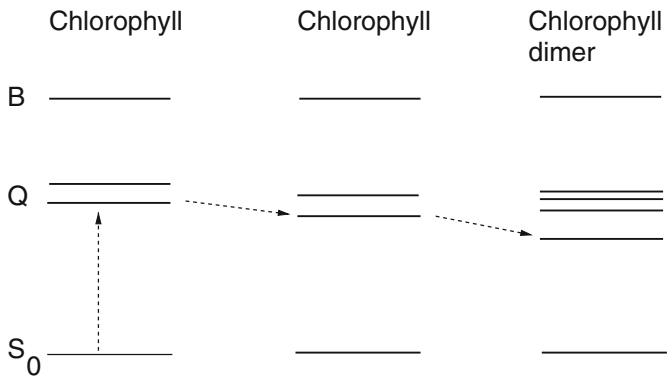

Fig. 23.12 Chl-Chl energy transfer. Energy is transferred via a sequence of chromophores with decreasing absorption energies

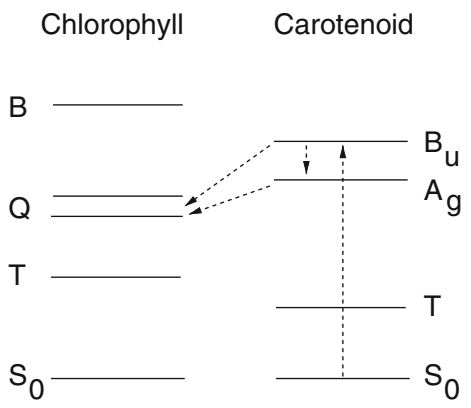

Fig. 23.13 Car-Chl energy transfer. Carotenoids absorb light in the blue region of the spectrum and transfer energy to chlorophylls which absorb at longer wavelengths

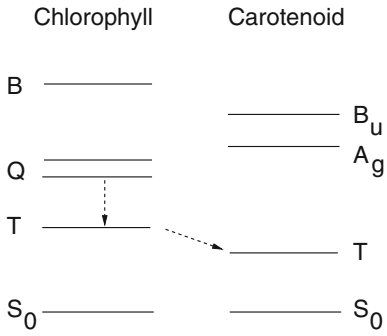

Fig. 23.14 Chl-Car triplet energy transfer. Carotenoid triplet states are below the lowest chlorophyll triplet and therefore important triplet quenchers

additional light-harvesting pigments in the blue region of the spectrum [119, 120] (Fig. 23.13) and transfer energy to chlorophylls which absorb at longer wavelengths. Carotenoids are also important as triplet quenchers to prevent the formation of triplet oxygen and for dissipation of excess energy (Fig. 23.14).

Problems

23.1 Polyene with bond length alternation

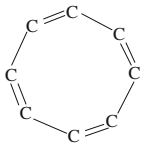

Consider a cyclic polyene with 2 N carbon atoms with alternating bond lengths.

The Hückel matrix has the form $H = \begin{pmatrix} \alpha & \beta & & & & \beta' \\ \beta & \alpha & \beta' & & & \\ & \beta' & \ddots & \ddots & & \\ & & \ddots & \alpha & \beta & \\ & & & \beta & \alpha & \\ \beta' & & & & & \end{pmatrix}$.

(a) Show that the eigenvectors can be written as

$$c_{2n} = \mathrm{e}^{\mathrm{i}kn} \quad c_{2n-1} = \mathrm{e}^{\mathrm{i}(kn+\chi)}.$$

(b) Determine the phase angle χ and the eigenvalues for $\beta \neq \beta'$.

(c) We want now to find the eigenvectors of a linear polyene. Therefore we use the real valued functions

$$c_{2n} = \sin kn \qquad c_{2n-1} = \sin(kn + \chi) \quad n = 1 \ldots N$$

with the phase angle as in (b).

We now add two further Carbon atoms with indices 0 and 2N+1. The first of these two obviously has no effect since $c_0 = \sin(0 \times k) = 0$. For the atom 2N+1, we demand that the wavefunction again vanishes which restricts the possible k-values:

$$0 = c_{2N+1} = \sin((N+1)k + \chi) = \Im\left(\mathrm{e}^{\mathrm{i}\chi + \mathrm{i}(N+1)k}\right).$$

For these k-values, the cyclic polyene with 2N+2 atoms is equivalent to the linear polyene with 2 N atoms as the off diagonal interaction becomes irrelevant. Show that the k-values obey the equation

$$\beta \sin((N+1)k) + \beta' \sin(Nk) = 0.$$

(d) Find a similar treatment for a linear polyene with odd number of C-atoms.

Chapter 24
Incoherent Energy Transfer

In this chapter, we study the transfer of energy from an excited donor molecule to an acceptor molecule. We discuss different mechanisms involving electron exchange, simultaneous radiationless deexcitation and excitation or photon emission followed by reabsorption. Using a simplified MO model, we calculate the coupling matrix element of the Coulomb interaction in dipole approximation and evaluate the famous Förster expression for the transition rate. Within the Condon approximation, the overlap of donor emission and acceptor absorption spectra becomes an essential factor. Finally, we comment on energy transfer in the triplet state.

24.1 Excited States

We consider the transfer of energy from an excited donor molecule D^* to an acceptor molecule A

$$D^* + A \rightarrow D + A^*. \tag{24.1}$$

We assume that the optical transitions of both molecules can be described by the transition between the highest occupied (HOMO) and lowest unoccupied (LUMO) molecular orbitals. The Hartree–Fock ground state of one molecule can be written as a Slater determinant of doubly occupied molecular orbitals (Fig. 24.1)

$$|HF> = |\phi_{1\uparrow}\phi_{1\downarrow}\cdots\phi_{HO\uparrow}\phi_{HO\downarrow}|. \tag{24.2}$$

Promotion of an electron from the HOMO to the LUMO creates a singlet or a triplet state both of which are linear combinations of the four determinants

P.O.J. Scherer and S.F. Fischer, *Theoretical Molecular Biophysics*,
Biological and Medical Physics, Biomedical Engineering,
DOI 10.1007/978-3-662-55671-9_24

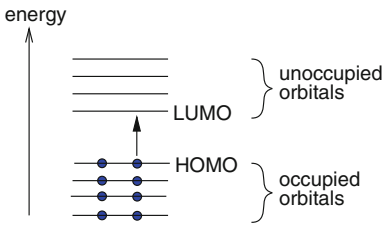

Fig. 24.1 HOMO-LUMO transition

$$
\begin{aligned}
|\uparrow\downarrow> &= |\phi_{1\uparrow}\phi_{1\downarrow}\cdots\phi_{HO\uparrow}\phi_{LU\downarrow}| \\
|\downarrow\uparrow> &= |\phi_{1\uparrow}\phi_{1\downarrow}\cdots\phi_{HO\downarrow}\phi_{LU\uparrow}| \\
|\uparrow\uparrow> &= |\phi_{1\uparrow}\phi_{1\downarrow}\cdots\phi_{HO\uparrow}\phi_{LU\uparrow}| \\
|\downarrow\downarrow> &= |\phi_{1\uparrow}\phi_{1\downarrow}\cdots\phi_{HO\downarrow}\phi_{LU\downarrow}|.
\end{aligned} \tag{24.3}
$$

Obviously, the last two determinants are the components of the triplet state with $S_z = \pm 1$

$$
\begin{aligned}
|1,+1> &= |\uparrow\uparrow> \\
|1,-1> &= |\downarrow\downarrow> .
\end{aligned} \tag{24.4}
$$

Linear combination of the first two determinants gives the triplet state with $S_z = 0$

$$
|1,0> = \frac{1}{\sqrt{2}}(|\uparrow\downarrow> + |\downarrow\uparrow>) \tag{24.5}
$$

and the singlet state

$$
|0,0> = \frac{1}{\sqrt{2}}(|\uparrow\downarrow> - |\downarrow\uparrow>). \tag{24.6}
$$

Let us now consider the states of the molecule pair DA. The singlet ground state is

$$
|\phi_{1\uparrow}\phi_{1\downarrow}\cdots\phi_{HO,D,\uparrow}\phi_{HO,D,\downarrow}\phi_{HO,A,\uparrow}\phi_{HO,A,\downarrow}| \tag{24.7}
$$

which will simply be denoted as

$$
|^1DA> = |D_\uparrow D_\downarrow A_\uparrow A_\downarrow|. \tag{24.8}
$$

The excited singlet state of the donor is

$$
|^1D^*A> = \frac{1}{\sqrt{2}}(|D^*_\uparrow D_\downarrow A_\uparrow A_\downarrow| - |D^*_\downarrow D_\uparrow A_\uparrow A_\downarrow|) \tag{24.9}
$$

and the excited state of the acceptor is

$$|^1 DA^* >= \frac{1}{\sqrt{2}}(|D_\uparrow D_\downarrow A^*_\uparrow A_\downarrow| - |D_\uparrow D_\downarrow A^*_\downarrow A_\uparrow|). \tag{24.10}$$

24.2 Energy Transfer Mechanism

Dexter Mechanism

At very short distances, the electronic wavefunctions of donor and acceptor overlap and electron exchange is possible (Fig. 24.2). This mechanism [123] is strongly distance dependent since the overlap integrals decay exponentially.

Förster Mechanism

This mechanism [121, 122] involves a coupled deexcitation of the donor and excitation of the acceptor (Fig. 24.2). At very short distances (as compared to the extension of the electronic orbitals), details of the electronic wavefunctions are important which can be taken into account by a full quantum calculation of the Coulomb interaction or an approximation on the basis of interacting transition densities. At not too large distances, both molecules undergo a simultaneous radiationless transition which can be described as emission and reabsorption of a virtual photon. If the optical transitions of donor and acceptor are dipole-allowed, the relevant coupling term is of the transition dipole—transition dipole type and the distance dependence follows a R^{-6} law. At larger distances, the emission of a real photon by the donor and later reabsorption by the acceptor is the dominant process. The efficiency shows a much weaker R^{-2}decay reflecting Lambert's law. In both cases, spectral overlap and transition intensities are important factors.

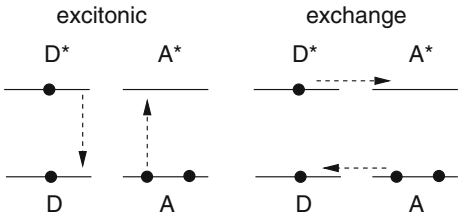

Fig. 24.2 Intramolecular energy transfer. *Left* the excitonic or Förster mechanism [121, 122] depends on transition intensities and spectral overlap. *Right* the exchange or Dexter mechanism [123] depends on the overlap of the wavefunctions.

Radiationless and radiative mechanism turn out to be limiting cases of the proper quantum electrodynamical treatment, which gives a transition rate of [124] (here, $\rho_m$is the density of molecular states and donor and acceptor have the same transition dipole moment μ)

$$\Gamma_{D^*A\to DA^*} = \frac{2\pi|\mu|^4}{9\hbar}\rho_m \frac{2}{(4\pi\varepsilon_0 R^3)^2}\left(3+\left(\frac{2\pi R}{\lambda}\right)^2+\left(\frac{2\pi R}{\lambda}\right)^4\right). \tag{24.11}$$

This expression switches from the R^{-6} to the R^{-2} behavior at a critical distance of

$$R_0' = \frac{3^{1/4}}{2\pi}\lambda \tag{24.12}$$

which, for visible light is in the range of 150 nm.

24.3 Interaction Matrix Element

The interaction responsible for energy transfer is the electron–electron interaction

$$V_C = \frac{e^2}{4\pi\varepsilon|r_1 - r_2|}. \tag{24.13}$$

With respect to the basis of molecular orbitals its matrix elements are denoted as

$$V(\phi_1\phi_{1'}\phi_2\phi_{2'}) = \int d^3r_1 d^3r_2 \phi^*_{1\sigma}(r_1)\phi^*_{2,\sigma'}(r_2)\frac{e^2}{4\pi\varepsilon|r_1-r_2|}\phi_{1'\sigma}(r_1)\phi_{2',\sigma'}(r_2). \tag{24.14}$$

The transfer interaction

$$\begin{aligned} V_{if} &= <^1 D^*A|V_C|^1 DA^* > \\ &= \frac{1}{2} < |D^*_\uparrow D_\downarrow A_\uparrow A_\downarrow|V_C|D_\uparrow D_\downarrow A^*_\uparrow A_\downarrow| > - \frac{1}{2} < |D^*_\uparrow D_\downarrow A_\uparrow A_\downarrow|V_C|D_\uparrow D_\downarrow A^*_\downarrow A_\uparrow > \\ &- \frac{1}{2} < |D^*_\downarrow D_\uparrow A_\uparrow A_\downarrow|V_C||D_\uparrow D_\downarrow A^*_\uparrow A_\downarrow| > + \frac{1}{2}|D^*_\downarrow D_\uparrow A_\uparrow A_\downarrow|V_C|D_\uparrow D_\downarrow A^*_\downarrow A_\uparrow| > \end{aligned} \tag{24.15}$$

consists of four summands. The first one gives two contributions

$$\frac{1}{2} < |D^*_\uparrow D_\downarrow A_\uparrow A_\downarrow |V| D_\uparrow D_\downarrow A^*_\uparrow A_\downarrow | >= \frac{1}{2} V(D^* D\ A\ A^*) - \frac{1}{2} V(D^* A^* A\ D), \tag{24.16}$$

where the first part is the excitonic interaction and the second part is the exchange interaction (Fig. 24.2).

The second summand

$$-\frac{1}{2} < |D^*_\uparrow D_\downarrow A_\uparrow A_\downarrow |V| D_\uparrow D_\downarrow A^*_\downarrow A_\uparrow | >= \frac{1}{2} V(D^* D\ A\ A^*) \tag{24.17}$$

has no exchange contribution due to the spin orientations. The two remaining summands are just mirror images of the first two. Altogether the interaction for singlet energy transfer is

$$<^1 D^* A|V_C|^1 DA^* >= 2V(D^* DAA^*) - V(D^* A^* AD). \tag{24.18}$$

In the triplet case

$$\begin{aligned} V_{if} &=<^3 D^* A|V_C|^3 DA^* > \\ &= \frac{1}{2} < |D^*_\uparrow D_\downarrow A_\uparrow A_\downarrow |V_C| D_\uparrow D_\downarrow A^*_\uparrow A_\downarrow | > + \frac{1}{2} < |D^*_\uparrow D_\downarrow A_\uparrow A_\downarrow |V_C| D_\uparrow D_\downarrow A^*_\downarrow A_\uparrow > \\ &+ \frac{1}{2} < |D^*_\downarrow D_\uparrow A_\uparrow A_\downarrow |V_C| |D_\uparrow D_\downarrow A^*_\uparrow A_\downarrow | > + \frac{1}{2} |D^*_\downarrow D_\uparrow A_\uparrow A_\downarrow |V_C| D_\uparrow D_\downarrow A^*_\downarrow A_\uparrow | > \\ &= -V(D^* A^* AD). \end{aligned} \tag{24.19}$$

Here energy can only be transferred by the exchange coupling (Dexter [123]). Since this involves the overlap of electronic wavefunctions it is important at small distances. In the singlet state, the excitonic interaction (Förster [121, 122]) allows for energy transfer also at larger distances.

24.4 Multipole Expansion of the Excitonic Interaction

We will now apply a multipole expansion to the excitonic matrix element

$$\begin{aligned} V_{exc} &= 2V(D^* DAA^*) \\ &= 2 \int d^3 r_1 d^3 r_2 \phi^*_{D*}(r_1) \phi^*_{A'}(r_2) \frac{e^2}{4\pi\varepsilon |r_1 - r_2|} \phi_D(r_1) \phi_{A*}(r_2). \end{aligned} \tag{24.20}$$

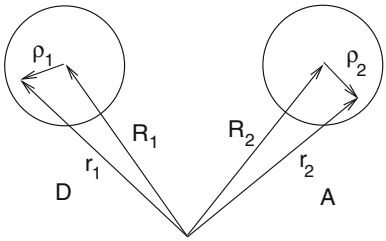

Fig. 24.3 Multipole expansion

We take the position of the electrons relative to the centers of the molecules (Fig. 24.3)

$$r_{1,2} = R_{1,2} + \varrho_{1,2} \tag{24.21}$$

and expand the Coulomb interaction

$$\frac{1}{|r_1 - r_2|} = \frac{1}{|R_1 - R_2 + \varrho_1 - \varrho_2|} \tag{24.22}$$

using the Taylor series

$$\frac{1}{|R+\varrho|} = \frac{1}{|R|} - \frac{1}{|R|^2}\frac{\varrho R}{|R|} + \frac{1}{2}\frac{3|R|(R\varrho)^2 - |R|^3\varrho^2}{|R|^6} + \cdots \tag{24.23}$$

for

$$R = R_1 - R_2 \quad \varrho = \varrho_1 - \varrho_2. \tag{24.24}$$

The zero-order term vanishes due to the orthogonality of the orbitals. The first-order term gives

$$-2\frac{e^2}{4\pi\varepsilon|R|^3} R \int d^3\varrho_1 d^3\varrho_2 \phi^*_{D*}(r_1)\phi_D(r_1)(\varrho_1 - \varrho_2)\phi^*_A(r_2)\phi_{A*}(r_2) \tag{24.25}$$

and also vanishes due to the orthogonality. The second-order term gives the leading contribution

$$\begin{aligned}&\frac{e^2}{4\pi\varepsilon|R|^6}\int d^3\varrho_1 d^3\varrho_2 \phi^*_{D*}(r_1)\phi_D(r_1)\\ &\times(3|R|(R\varrho_1 - R\varrho_2)^2 - |R|^3(\varrho_1-\varrho_2)^2)\phi^*_A(r_2)\phi_{A*}(r_2).\end{aligned} \tag{24.26}$$

Only the integrals over mixed products of ϱ_1 and ϱ_2 are not zero. They can be expressed with the help of the transition dipoles

$$\mu_D = <^1 D|e\mathbf{r}|^1 D^* > = \sqrt{2}\int d^3\varrho_1 \phi^*_{D*}(\varrho_1) e\varrho_1 \phi_D(\varrho_1)$$

$$\mu_A = <^1 A|e\mathbf{r}|^1 A^* > = \sqrt{2}\int d^3\varrho_2 \phi_A^*(\varrho_2) e\varrho_2 \phi_{A*}(\varrho_2). \tag{24.27}$$

Finally, the leading term of the excitonic interaction is the dipole–dipole term

$$V_{exc} = \frac{e^2}{4\pi\varepsilon|R|^5}\left(|R|^2\mu_D\mu_A - 3(R\mu_D)(R\mu_A)\right). \tag{24.28}$$

This is often written with an orientation dependent factor K as

$$V_{exc} = \frac{K}{|R|^3}|\mu_D||\mu_A|. \tag{24.29}$$

24.5 Energy Transfer Rate

We consider excitonic interaction of two molecules. The Hamilton operator is divided into the zero-order Hamiltonian

$$H_0 = |D^*A > H_{D*A} < D^*A| + |DA^* > H_{DA*} < DA^*| \tag{24.30}$$

and the interaction operator

$$H' = |D^*A > V_{exc} < DA^*| + |DA^* > V_{exc} < D^*A|. \tag{24.31}$$

We neglect electron exchange between the two molecules and apply the Condon approximation. Then taking energies relative to the electronic ground state $|DA >$ we have

$$\begin{aligned} H_{D*A} &= \hbar\omega_{D*} + H_{D*} + H_A \\ H_{DA*} &= \hbar\omega_{A*} + H_D + H_{A*} \end{aligned} \tag{24.32}$$

with electronic excitation energies $\hbar\omega_{D*(A*)}$ and nuclear Hamiltonians H_D, H_{D*}, H_A, H_{A*}. Now, consider once more Fermi's golden rule for the transition between vibronic states $|i > \rightarrow |f >$

$$\begin{aligned} k &= \frac{2\pi}{\hbar}\sum_{i,f} P_i| < i|H'|f > |^2\delta(\omega_f - \omega_i) \\ &= \frac{1}{\hbar^2}\int \sum_{if} P_i < i|H'|f >< f|H'|i > \mathrm{e}^{\mathrm{i}(\omega_f-\omega_i)t}dt \\ &= \frac{1}{\hbar^2}\int \sum_{if} P_i < i|H'|f > \mathrm{e}^{\mathrm{i}\omega_f t} < f|H'|\mathrm{e}^{\mathrm{i}\omega_i t} i > dt \end{aligned} \tag{24.33}$$

$$= \frac{1}{\hbar^2} \int \sum_i < i|Q^{-1} \mathrm{e}^{-H_0/k_B T} H' \mathrm{e}^{\mathrm{i}tH_0/\hbar} H' \mathrm{e}^{\mathrm{i}tH_0/\hbar}|i > dt$$

$$= \frac{1}{\hbar^2} \int dt \left\langle H'(0) H'(t) \right\rangle . \tag{24.34}$$

Initially, only the donor is excited. Then the average is restricted to the vibrational states of D^*A

$$k = \frac{1}{\hbar^2} \int dt \left\langle H'(0) H'(t) \right\rangle_{D*A} . \tag{24.35}$$

With the transition dipole operators

$$\begin{aligned} \hat{\mu}_D &= |D > \mu_D < D^*| + |D^* > \mu_D < D| \\ \hat{\mu}_A &= |A > \mu_A < A^*| + |A^* > \mu_A < A| \end{aligned} \tag{24.36}$$

the rate becomes

$$k = \frac{K^2}{\hbar^2 R^6} \int dt \left\langle \hat{\mu}_D(0) \hat{\mu}_A(0) \hat{\mu}_D(t) \hat{\mu}_A(t) \right\rangle_{D*A} .$$

Here, we assumed that the orientation does not change on the relevant time scale. Since each of the dipole operators acts only on one of the molecules we have

$$\begin{aligned} k &= \frac{1}{\hbar^2} \frac{K^2}{|R|^6} \int dt \left\langle \hat{\mu}_D(0) \hat{\mu}_D(t) \hat{\mu}_A(0) \hat{\mu}_A(t) \right\rangle_{D*A} \\ &= \frac{1}{\hbar^2} \frac{K^2}{|R|^6} \int dt \left\langle \hat{\mu}_D(0) \hat{\mu}_D(t) \right\rangle_{D*A} \left\langle \hat{\mu}_A(0) \hat{\mu}_A(t) \right\rangle_{D*A} \\ &= \frac{1}{\hbar^2} \frac{K^2}{|R|^6} \int dt \left\langle \hat{\mu}_D(0) \hat{\mu}_D(t) \right\rangle_{D*} \left\langle \hat{\mu}_A(0) \hat{\mu}_A(t) \right\rangle_{A} . \end{aligned} \tag{24.37}$$

24.6 Spectral Overlap

The two factors are related to the acceptor absorption and donor fluorescence spectra. Consider optical transitions between the singlet states $|^1D^* > \rightarrow |^1D >$ and $|^1A \rightarrow {}^1 A^* >$. The number of fluorescence photons per time is given by the Einstein coefficient for spontaneous emission[1]

$$A_{D*D} = \frac{2\omega_{D*D}^3}{3\varepsilon_0 hc^3} |\mu_D|^2 \tag{24.38}$$

[1] a detailed discussion of the relationships between absorption cross section and Einstein coefficients is found in [125].

with the donor transition dipole moment (24.27)

$$\mu_D = \sqrt{2} \int d^3r \, \phi_{D*}(e\mathbf{r})\phi_D. \tag{24.39}$$

The frequency resolved total fluorescence is then

$$I_e(\omega) = A_{D*D} g_e(\omega) = \frac{2\omega^3}{3\varepsilon_0 hc^3} |\mu_D|^2 g_e(\omega) \tag{24.40}$$

with the normalized lineshape function $g_e(\omega)$.

The absorption cross section can be expressed with the help of the Einstein coefficient for absorption B_{12}^{ω} as [125]

$$\sigma_a(\omega) = B_{AA*}^{\omega} \hbar\omega g_a(\omega)/c. \tag{24.41}$$

The Einstein coefficients for absorption and emission are related by

$$B_{AA*}^{\omega} = \frac{\pi^2 c^3}{\hbar\omega_{A*A}^3} A_{A*A} = \frac{1}{3}\frac{\pi}{\hbar^2\varepsilon_0}|\mu_A|^2$$

and therefore

$$\sigma_a(\omega) = \frac{1}{3}\frac{\pi}{\hbar c\varepsilon_0}|\mu_A|^2 \omega g_a(\omega).$$

In the following, we discuss absorption and emission in terms of the modified spectra (Fig. 24.4)

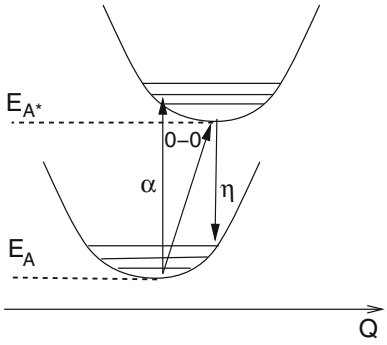

Fig. 24.4 Absorption and emission. Within the displaced oscillator model the $0 \rightarrow 0$ transition energy is located between the maxima of absorption (α) and emission (η)

$$\begin{aligned}\alpha(\omega) &= \frac{3\hbar c\varepsilon_0}{\pi}\frac{\sigma_a(\omega)}{\omega} = |\hat{\mu}_A|^2 g_a(\omega)\\ &= \sum_{i,f} P_i| < i|\hat{\mu}_A|f > |^2\delta(\omega_f - \omega_i - \omega)\\ &= \frac{1}{2\pi}\int dt \mathrm{e}^{-\mathrm{i}\omega t}\sum_i < i|\frac{\mathrm{e}^{-H/k_BT}}{Q}\hat{\mu}_A|f > \mathrm{e}^{\mathrm{i}\omega_f t} < f|\hat{\mu}_A\mathrm{e}^{-\mathrm{i}\omega_i t}|i >\\ &= \frac{1}{2\pi}\int dt\, \mathrm{e}^{-\mathrm{i}\omega t}\left\langle\hat{\mu}_A(0)\hat{\mu}_A(t)\right\rangle_A \end{aligned} \tag{24.42}$$

and[2]

$$\begin{aligned}\eta(\omega) &= \frac{3\varepsilon_0 hc^3 I_e(\omega)}{2\omega^3} = |\mu_D|^2 g_e(\omega)\\ &= \sum_{i,f} P_f| < f|\hat{\mu}_D|i > |^2\delta(\omega_f - \omega_i - \omega)\\ &= \frac{1}{2\pi}\int dt \mathrm{e}^{-\mathrm{i}\omega t}\sum_f < f|\frac{\mathrm{e}^{-H/k_BT}}{Q}\mathrm{e}^{\mathrm{i}\omega_f t}\hat{\mu}_D|i > \mathrm{e}^{-\mathrm{i}\omega_i t} < i|\hat{\mu}_D|f >\\ &= \frac{1}{2\pi}\int dt\, \mathrm{e}^{-\mathrm{i}\omega t}\left\langle\hat{\mu}_D(t)\hat{\mu}_D(0)\right\rangle_{D*}\\ &= \frac{1}{2\pi}\int dt\, \mathrm{e}^{\mathrm{i}\omega t}\left\langle\hat{\mu}_D(0)\hat{\mu}_D(t)\right\rangle_{D*}. \end{aligned} \tag{24.43}$$

Within the Condon approximation

$$\begin{aligned}\left\langle\hat{\mu_A}(0)\hat{\mu}_A(t)\right\rangle_A &= \mathrm{e}^{\mathrm{i}\omega_{A*}t}|\mu_A|^2\left\langle\mathrm{e}^{\mathrm{i}tH_{A*}/\hbar}\mathrm{e}^{-\mathrm{i}tH_A/\hbar}\right\rangle_A\\ &= \mathrm{e}^{\mathrm{i}\omega_{A*}t}|\mu_A|^2 F_A(t)\end{aligned} \tag{24.44}$$

and therefore the lineshape function is the Fourier transform of the correlation function

$$g_a(\omega) = \frac{1}{2\pi}\int dt\, \mathrm{e}^{\mathrm{i}(\omega-\omega_{A*})t}F_A(t). \tag{24.45}$$

Similarly,

$$\begin{aligned}\left\langle\hat{\mu_D}(0)\hat{\mu}_D(t)\right\rangle_{D*} &= \mathrm{e}^{-\mathrm{i}\omega_{D*}t}|\mu_D|^2\left\langle\mathrm{e}^{\mathrm{i}tH_D/\hbar}\mathrm{e}^{-\mathrm{i}tH_{D*}/\hbar}\right\rangle_{D*}\\ &= \mathrm{e}^{-\mathrm{i}\omega_{D*}t}|\mu_D|^2 F_{D*}(t)\end{aligned} \tag{24.46}$$

[2]Note the sign change which appears since we now have to average over the excited state vibrations.

and

$$g_e(\omega) = \frac{1}{2\pi} \int dt\, \mathrm{e}^{\mathrm{i}(\omega-\omega_{D*})t} F_{D*}(t). \tag{24.47}$$

With the inverse Fourier integrals

$$\begin{aligned} \left\langle \hat{\mu}_A(0)\hat{\mu}_A(t)\right\rangle_A &= \int d\omega \mathrm{e}^{\mathrm{i}\omega t}\alpha(\omega) \\ \left\langle \hat{\mu}_D(0)\hat{\mu}_D(t)\right\rangle_{D*} &= \int d\omega \mathrm{e}^{-\mathrm{i}\omega t}\eta(\omega) \end{aligned} \tag{24.48}$$

equation (24.37) becomes

$$\begin{aligned} k &= \frac{1}{\hbar^2}\frac{K^2}{|R|^6} \int dt \int d\omega \mathrm{e}^{\mathrm{i}\omega t}\eta(\omega) \int d\omega' \mathrm{e}^{-\mathrm{i}\omega' t}\alpha(\omega') \\ &= \frac{1}{\hbar^2}\frac{K^2}{|R|^6} \int d\omega d\omega' \eta(\omega)\alpha(\omega')\, 2\pi\delta(\omega-\omega') \\ &= \frac{2\pi}{\hbar^2}\frac{K^2}{|R|^6} \int d\omega \eta(\omega)\alpha(\omega) \\ &= \frac{2\pi}{\hbar^2}\frac{K^2}{|R|^6} |\mu_A|^2|\mu_D|^2 \int d\omega g_e(\omega) g_a(\omega). \end{aligned} \tag{24.49}$$

This is the famous rate expression for Förster [121] energy transfer which involves the spectral overlap of donor emission and acceptor absorption [126, 127]. For optimum efficiency of energy transfer, the maximum of the acceptor absorption should be at longer wavelength than the maximum of the donor emission (Fig. 24.5).

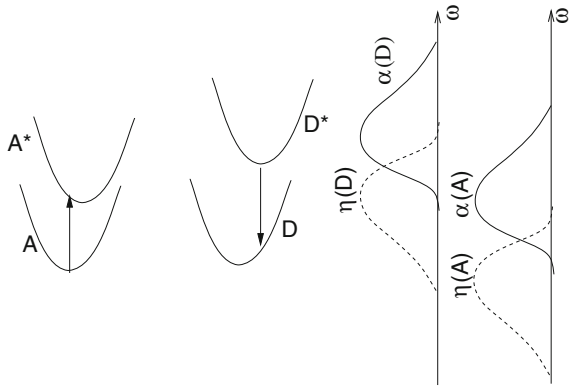

Fig. 24.5 Energy transfer and spectral overlap

24.7 Energy Transfer in the Triplet State

Consider now energy transfer in the triplet state. Here the transitions are optically not allowed. We consider a more general interaction operator which changes the electronic state of both molecules simultaneously and can be written as[3]

$$H' = |D^* > |A > V_{exch} < A^*| < D| + h.c. \tag{24.50}$$

We start from the rate expression (24.34)

$$k = \frac{1}{\hbar^2} \int dt \, \left\langle H'(0) H'(t) \right\rangle . \tag{24.51}$$

The thermal average has to be taken over the initially populated state $|D^* A >$

$$k = \frac{1}{\hbar^2} \int dt \, \left\langle H'(0) H'(t) \right\rangle_{D*A} .$$

In the static case ($V_{exc} = const$)

$$\begin{aligned} k &= \frac{1}{\hbar^2} \int dt \left\langle H' \mathrm{e}^{\mathrm{i}t H_{DA*}/\hbar} H' \mathrm{e}^{-\mathrm{i}t H_{D*A}/\hbar} \right\rangle_{D*A} \\ &= \frac{1}{\hbar^2} \int dt \mathrm{e}^{\mathrm{i}(\omega_{A*} - \omega_{D*})t} \left\langle H' \mathrm{e}^{\mathrm{i}t(H_D + H_{A*})/\hbar} H' \mathrm{e}^{-\mathrm{i}t(H_{D*} + H_A)/\hbar} \right\rangle_{D*A} \\ &= \frac{V_{exch}^2}{\hbar^2} \int dt \mathrm{e}^{\mathrm{i}(\omega_{A*} - \omega_{D*})t} \left\langle \mathrm{e}^{\mathrm{i}t H_D/\hbar} \mathrm{e}^{-\mathrm{i}t H_{D*}/\hbar} \right\rangle_{D*} \left\langle \mathrm{e}^{\mathrm{i}t H_{A*}/\hbar} \mathrm{e}^{-\mathrm{i}t H_A/\hbar} \right\rangle_A \\ &= \frac{V_{exch}^2}{\hbar^2} \int dt \, \mathrm{e}^{\mathrm{i}t(\omega_{A*} - \omega_{D*})} F_{D*}(t) F_A(t) \end{aligned} \tag{24.52}$$

with the correlation functions

$$F_A(t) = \left\langle \mathrm{e}^{\mathrm{i}t H_{A*}/\hbar} \mathrm{e}^{-\mathrm{i}t H_A/\hbar} \right\rangle_A \tag{24.53}$$

$$F_{D*}(t) = \left\langle \mathrm{e}^{\mathrm{i}t H_D/\hbar} \mathrm{e}^{-\mathrm{i}t H_{D*}/\hbar} \right\rangle_{D*} . \tag{24.54}$$

Introducing lineshape functions (24.45), (24.47) similar to the excitonic case the rate becomes

[3] we assume that the wavefunction of the pair can be factorized approximately.

$$
\begin{aligned}
k &= \frac{V_{exch}^2}{\hbar^2} \int dt\, \mathrm{e}^{\mathrm{i}t(\omega_{A*}-\omega_{D*})} \int d\omega' \mathrm{e}^{-\mathrm{i}(\omega'-\omega_{D*})t} g_e(\omega') \int d\omega \mathrm{e}^{\mathrm{i}(\omega-\omega_{A*})t} g_a(\omega) \\
&= \frac{V_{exch}^2}{\hbar^2} \int d\omega d\omega' g_e(\omega') g_a(\omega) 2\pi \delta(\omega - \omega') \\
&= \frac{2\pi V_{exch}^2}{\hbar} \int d\omega g_a(\omega) g_e(\omega) \qquad (24.55)
\end{aligned}
$$

which is very similar to the Förster expression (24.49). The excitonic interaction is replaced by the exchange coupling matrix element and the overlap of the optical spectra is replaced by the overlap of the Franck–Condon weighted densities of states.

Chapter 25
Coherent Excitations in Photosynthetic Systems

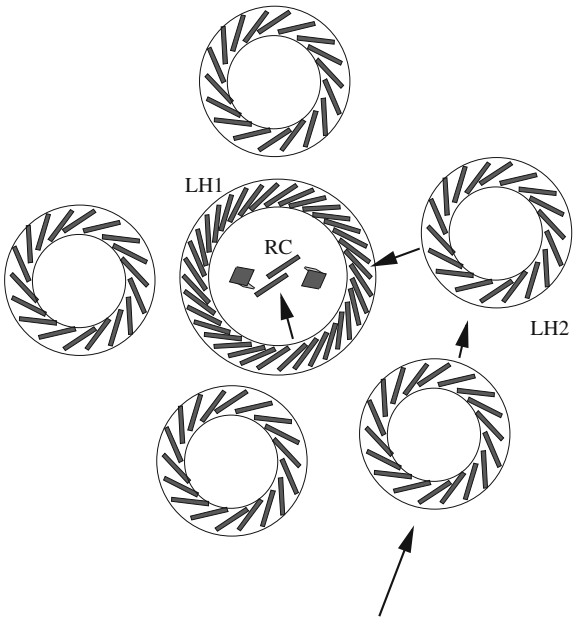

Fig. 25.1 Energy transfer in bacterial photosynthesis

Photosynthetic units of plants and bacteria consist of antenna complexes and reaction centers. Rings of closely coupled chlorophyll chromophores form the light harvesting complexes which transfer the incoming photons very efficiently and rapidly to the reaction center where the photon energy is used to create an ion pair (Fig. 25.1).

P.O.J. Scherer and S.F. Fischer, *Theoretical Molecular Biophysics*,
Biological and Medical Physics, Biomedical Engineering,
DOI 10.1007/978-3-662-55671-9_25

In this chapter, we concentrate on the properties of strongly coupled chromophore aggregates. We discuss an exciton model for a strongly coupled dimer including internal charge transfer states and apply it to the special pair of the photosynthetic reaction center. Next, we study circular molecular aggregates, as found in the light harvesting complexes of photosynthesis. We calculate the exciton spectrum including dimerization and apply it to the light harvesting complex LHII. The influence of disorder is discussed including symmetry breaking local perturbations and periodic modulations as well as general diagonal and off-diagonal disorder.

25.1 Coherent Excitations

If the excitonic coupling is large compared to fluctuations of the excitation energies, a coherent excitation of two or more molecules can be generated.

25.1.1 Strongly Coupled Dimers

Let us consider a dimer consisting of two strongly coupled molecules A and B as in the reaction center of photosynthesis (Fig. 25.2). The two excited states

$$|A^*B>, |AB^*> \tag{25.1}$$

are mixed due to the excitonic interaction. The eigenstates are given by the eigenvectors of the matrix

$$\begin{pmatrix} E_{A*B} & V \\ V & E_{AB*} \end{pmatrix}. \tag{25.2}$$

For a symmetric dimer, the diagonal energies have the same value and the eigenvectors can be characterized as symmetric or antisymmetric

$$\begin{pmatrix} \frac{1}{\sqrt{2}} & -\frac{1}{\sqrt{2}} \\ \frac{1}{\sqrt{2}} & \frac{1}{\sqrt{2}} \end{pmatrix} \begin{pmatrix} E_{A*B} & V \\ V & E_{A*B} \end{pmatrix} \begin{pmatrix} \frac{1}{\sqrt{2}} & \frac{1}{\sqrt{2}} \\ -\frac{1}{\sqrt{2}} & \frac{1}{\sqrt{2}} \end{pmatrix} = \begin{pmatrix} E_{A*B} - V & \\ & E_{A*B} + V \end{pmatrix}. \tag{25.3}$$

The two excitonic states are split by $2V$.[1] The transition dipoles of the two dimer bands are given by

$$\mu_{\pm} = \frac{1}{\sqrt{2}}(\mu_A \pm \mu_B) \tag{25.4}$$

and the intensities by

[1] Also known as Davydov splitting.

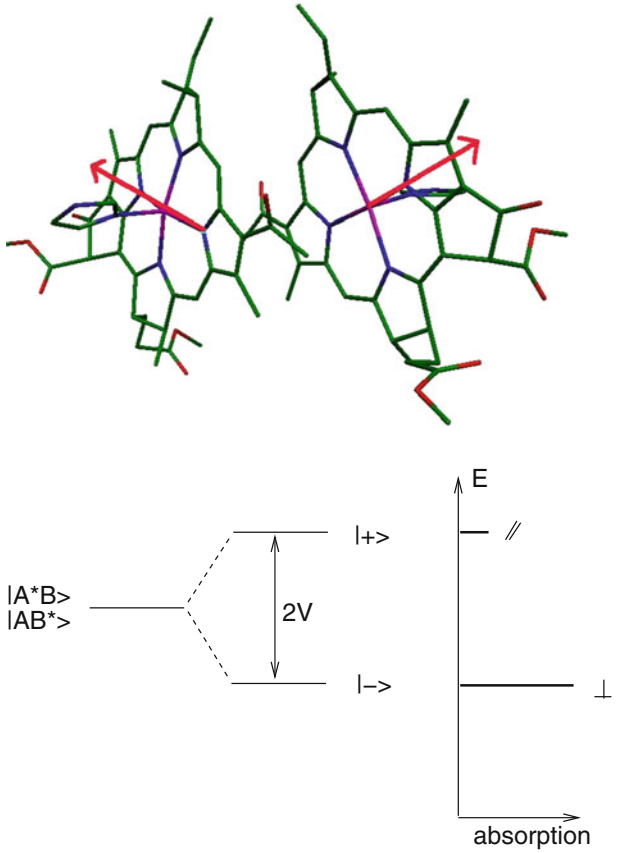

Fig. 25.2 The "special pair" dimer. *Top* The nearly C_2-symmetric molecular arrangement for the reaction center of Rps.viridis (molekel graphics [65]).The transition dipoles of the two molecules (*arrows*) are essentially antiparallel. *Bottom* The lower exciton component carries most of the oscillator strength

$$|\mu_{\pm}|^2 = \frac{1}{2}(\mu_A^2 + \mu_B^2 \pm 2\mu_A\mu_B). \tag{25.5}$$

For a symmetric dimer $\mu_A^2 = \mu_B^2 = \mu^2$ and

$$|\mu_{\pm}|^2 = \mu^2(1 \pm \cos\alpha), \tag{25.6}$$

where α denotes the angle between μ_A and μ_B. In case of an approximately C_2 symmetric structure, the components of μ_A and μ_B are furthermore related by symmetry operations.

If we choose the C_2 axis along the z-axis we have

$$\begin{pmatrix} \mu_{Bx} \\ \mu_{By} \\ \mu_{Bz} \end{pmatrix} = \begin{pmatrix} -\mu_{Ax} \\ -\mu_{Ay} \\ \mu_{Az} \end{pmatrix} \tag{25.7}$$

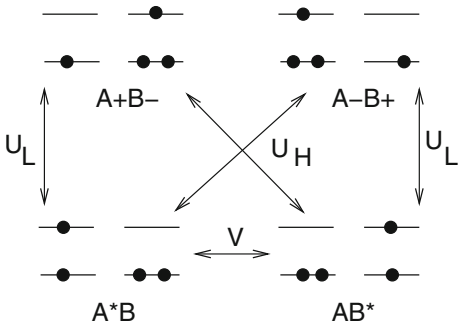

Fig. 25.3 Extended dimer model

and therefore

$$\frac{1}{\sqrt{2}}(\mu_A + \mu_B) = \frac{1}{\sqrt{2}} \begin{pmatrix} 0 \\ 0 \\ 2\mu_{Az} \end{pmatrix}$$
$$\frac{1}{\sqrt{2}}(\mu_A - \mu_B) = \frac{1}{\sqrt{2}} \begin{pmatrix} 2\mu_{Ax} \\ 2\mu_{Ay} \\ 0 \end{pmatrix} \tag{25.8}$$

which shows that the transition to the state $|+>$ is polarized along the symmetry axis whereas the transition to $|->$ is polarized perpendicularly. For the special pair, dimer interaction with internal charge transfer states $|A+B->$ and $|A-B+>$ has to be considered. In the simplest model, the following interaction matrix elements are important (Fig. 25.3).

The local excitation A^*B is coupled to the CT state A^+B^- by transferring an electron between the two LUMOS

$$< A^*B|H|A^+B^- >= \frac{1}{2} < (A^*_\uparrow A_\downarrow - A^*_\downarrow A_\uparrow)B_\uparrow B_\downarrow H(B^*_\uparrow A_\downarrow - B^*_\downarrow A_\uparrow)B_\uparrow B_\downarrow >$$
$$= H_{A^*,B^*} = U_L \tag{25.9}$$

and to the CT state A^-B^+ by transferring an electron between the HOMOs

$$< A^*B|H|A^-B^+ >= \frac{1}{2} < (A^*_\uparrow A_\downarrow - A^*_\downarrow A_\uparrow)B_\uparrow B_\downarrow H(A^*_\uparrow B_\downarrow - A^*_\downarrow B_\uparrow)A_\uparrow A_\downarrow >$$
$$= -H_{A,B} = U_H. \tag{25.10}$$

Similarly the second local excitation couples to the CT states by

$$< AB^*|H|A^+B^- >= \frac{1}{2} < (B^*_\uparrow B_\downarrow - B^*_\downarrow B_\uparrow)A_\uparrow A_\downarrow H(B^*_\uparrow A_\downarrow - B^*_\downarrow A_\uparrow)B_\uparrow B_\downarrow >$$
$$= -H_{A,B} = U_H \tag{25.11}$$

$$< AB^*|H|A^-B^+ >= \frac{1}{2} < (B^*_\uparrow B_\downarrow - B^*_\downarrow B_\uparrow)A_\uparrow A_\downarrow H(A^*_\uparrow B_\downarrow - A^*_\downarrow B_\uparrow)A_\uparrow A_\downarrow >$$
$$= H_{A^*,B^*} = U_L. \tag{25.12}$$

The interaction of the four states is summarized by the matrix

$$H = \begin{pmatrix} E_{A^*B} & V & U_L & U_H \\ V & E_{B^*A} & U_H & U_L \\ U_L & U_H & E_{A^+B^-} & \\ U_H & U_L & & E_{A^-B^+} \end{pmatrix}. \tag{25.13}$$

Again for a symmetric dimer $E_{B^*A} = E_{AB^*}$ and $E_{A^+B^-} = E_{A^-B^+}$ and the interaction matrix can be simplified by transforming to symmetrized basis functions with the transformation matrix

$$S = \begin{pmatrix} \frac{1}{\sqrt{2}} & \frac{1}{\sqrt{2}} & & \\ -\frac{1}{\sqrt{2}} & \frac{1}{\sqrt{2}} & & \\ & & \frac{1}{\sqrt{2}} & \frac{1}{\sqrt{2}} \\ & & -\frac{1}{\sqrt{2}} & \frac{1}{\sqrt{2}} \end{pmatrix}. \tag{25.14}$$

The transformation gives

$$S^{-1}H\,S = \begin{pmatrix} E_* - V & & U_L - U_H & \\ & E_* + V & & U_L + U_H \\ U_L - U_H & & E_{CT} & \\ & U_L + U_H & & E_{CT} \end{pmatrix} \tag{25.15}$$

where the states of different symmetry are decoupled (Fig. 25.4)

$$H_+ = \begin{pmatrix} E_* + V & U_L + U_H \\ U_L + U_H & E_{CT} \end{pmatrix} \quad H_- = \begin{pmatrix} E_* - V & U_L - U_H \\ U_L - U_H & E_{CT} \end{pmatrix}. \tag{25.16}$$

In an external electric field, the degeneracy of the internal CT states is readily lifted due to their large dipole moments. In this case, we symmetrize only the excitonic states by transforming with

$$S = \begin{pmatrix} \frac{1}{\sqrt{2}} & \frac{1}{\sqrt{2}} & & \\ -\frac{1}{\sqrt{2}} & \frac{1}{\sqrt{2}} & & \\ & & 1 & \\ & & & 1 \end{pmatrix} \tag{25.17}$$

Fig. 25.4 Dimer states

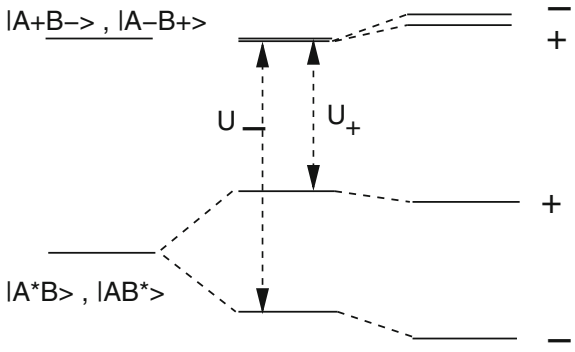

which yields

$$S^{-1}H\,S = \begin{pmatrix} E_* - V & & \frac{U_L-U_H}{\sqrt{2}} & -\frac{U_L-U_H}{\sqrt{2}} \\ & E_* + V & \frac{U_L+U_H}{\sqrt{2}} & \frac{U_L+U_H}{\sqrt{2}} \\ \frac{U_L-U_H}{\sqrt{2}} & \frac{U_L+U_H}{\sqrt{2}} & E_{CT} - \frac{\Delta_{CT}}{2} & \\ -\frac{U_L-U_H}{\sqrt{2}} & \frac{U_L+U_H}{\sqrt{2}} & & E_{CT} + \frac{\Delta_{CT}}{2} \end{pmatrix} \tag{25.18}$$

with the field-induced energy shift

$$\frac{\Delta_{CT}}{2} = -\mathbf{p}_{A^+B^-}\mathbf{E}. \tag{25.19}$$

Perturbation theory gives the correction to the lowest state

$$|P^*(-)> = \frac{1}{\sqrt{2}}(A^* - B^*) + \frac{\frac{U_L-U_H}{\sqrt{2}}}{E_* - V - E_{CT} - \frac{\Delta_{CT}}{2}}|A^+B^-> - \frac{\frac{U_L-U_H}{\sqrt{2}}}{E_* - V + E_{CT} - \frac{\Delta_{CT}}{2}}|A^-B^+> \tag{25.20}$$

with energy

$$\begin{aligned} E_{P*(-)} &= E_* - V - \frac{(U_L-U_H)^2}{2}\left[\frac{1}{E_{CT} - \frac{\Delta_{CT}}{2} - (E_* - V)} + \frac{1}{E_{CT} + \frac{\Delta_{CT}}{2} - (E_* - V)}\right] + \ldots \\ &= E_* - V - \frac{(U_L-U_H)^2}{2}\left[\frac{2}{E_{CT} - (E_* - V)} + \frac{\Delta_{CT}^2}{2(E_{CT} - (E_* - V)^3}\right] + \ldots \\ &= E_* - V - \frac{(U_L-U_H)^2}{E_{CT} - (E_* - V)} - \frac{(U_L-U_H)^2\Delta_{CT}^2}{4(E_{CT} - (E_* - V)^3} + \ldots \end{aligned} \tag{25.21}$$

and permanent dipole

$$\mathbf{p}(P^*(-)) = \left[\frac{(U_L - U_H)^2}{2(E_* - V - E_{CT} - \frac{\Delta_{CT}}{2})^2} - \frac{(U_L - U_H)^2}{2(E_* - V - E_{CT} + \frac{\Delta_{CT}}{2})^2}\right]\mathbf{p}_{A^+B^-}$$

$$= \frac{(U_L - U_H)^2}{(E_* - V - E_{CT})^3}\Delta_{CT}\mathbf{p}_{A^+B^-}. \tag{25.22}$$

Equations (25.21) and (25.22) explain that in a symmetry breaking field, the dimer band obtains large permanent dipole and polarizability which show up experimentally in the Stark effect (electrochromicity) spectra.

25.1.2 Excitonic Structure of the Reaction Center

The reaction center of bacterial photosynthesis consists of six chromophores. Two bacteriochlorophyll molecules (P_L, P_M) form the special pair dimer. Another bacteriochlorophyll (B_L) and a bacteriopheophytine (H_L) act as the acceptors during the first electron transfer steps. Both have symmetry-related counterparts (B_M, H_M) which are not directly involved in the charge separation process. Due to the short neighbor distances (11–13Å), delocalization of the optical excitation has to be considered to understand the optical spectra. Whereas the dipole–dipole approximation is not applicable to the strong coupling of the dimer chromophores, it has been used to estimate the remaining excitonic interactions in the reaction center. The strongest couplings are expected for the pairs $P_L B_L$, $B_L H_L$, $P_M B_M$, $B_M H_M$ due to favorable distances and orientational factors (Fig. 25.5 and Table 25.1).

Starting from a system with full C_2 symmetry, the excitations again can be classified as symmetric or antisymmetric. The lowest dimer band interacts with the antisymmetric combinations of B and H excitations. Due to the differences of excitation energies, this leads only to a small amount of state mixing. For the symmetric states, the situation is quite different as the upper dimer band is close to the B- excitation (Fig. 25.6).

If the symmetry is disturbed by structural differences or interactions with the protein, excitations of different symmetry character interact. Qualitatively, we expect

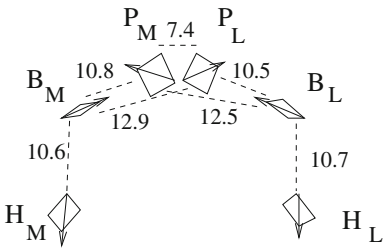

Fig. 25.5 Transition dipoles of the Reaction Center rps.Viridis. Arrows show the transition dipoles of the isolated chromophores. Center–center distances (as defined by the nitrogen atoms) are given in Å

Table 25.1 Excitonic couplings for the reaction center of rps.Viridis. The matrix elements were calculated within the dipole–dipole approximation for $\mu^2 = 45 Debye^2$ for bacteriochlorophyll and $30 Debye^2$ for bacteriopheophytine [128]. All values in cm^{-1}

	H_M	B_M	P_M	P_L	B_L	H_L
H_M		160	33	−9	−11	6
B_M	160		−168	−37	29	−11
P_M	33	−168		770	−42	−7
P_L	−9	−37	770		−189	35
B_L	−11	29	−42	−189		167
H_L	6	−11	−7	35	167	

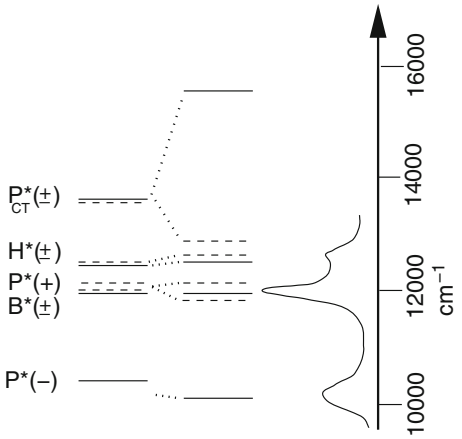

Fig. 25.6 Excitations of the reaction center. The absorption spectrum of rps.viridis in the Q_y region is assigned on the basis of symmetric excitonic excitations [129]. The charge transfer states P^*_{CT} are very broad and cannot be observed directly

that the lowest excitation is essentially the lower dimer band, the highest band [2] reflects absorption from the pheophytines and in the region of the B absorption we expect mixtures of the B* excitations and the upper dimer band (Fig. 25.6).

25.1.3 Circular Molecular Aggregates

We consider now a circular aggregate of N chromophores (Fig. 25.7) as it is found in the light harvesting complexes (Fig. 25.8) of photosynthesis [130–132].

We align the C_N symmetry axis along the z-axis. The position of the nth molecule is

[2] In the Q_y region.

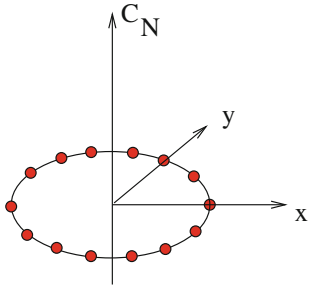

Fig. 25.7 Circular aggregate

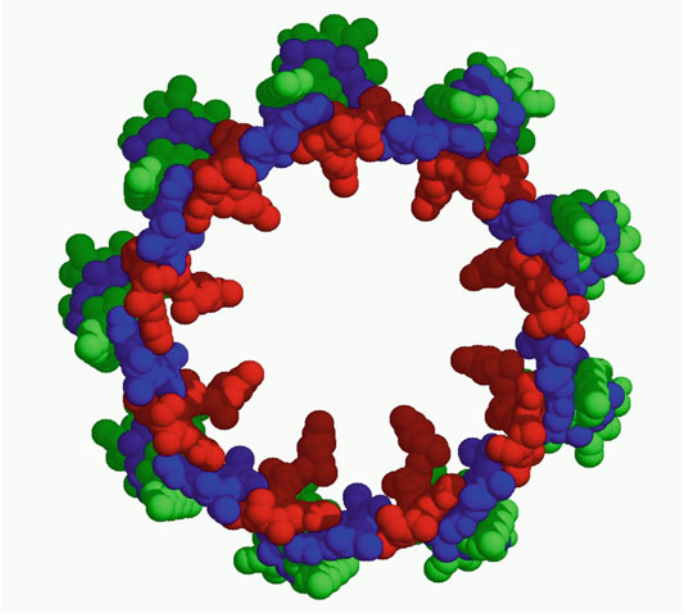

Fig. 25.8 Light harvesting complex. The light harvesting complex from Rps. acidophila (structure 1 kzu [133–137]from the protein data bank [138, 139] consists of a ring of 18 closely coupled (shown in *red* and *blue*) and another ring of 9 less strongly coupled bacteriochlorophyll molecules (*green*). Rasmol graphics [140]

$$\mathbf{R}_n = R \begin{pmatrix} \cos(2\pi\, n/N) \\ \sin(2\pi\, n/N) \\ 0 \end{pmatrix} \quad n = 0, 1 \cdots N-1 \tag{25.23}$$

which can also be written with the help of a rotation matrix

$$S_N = \begin{pmatrix} \cos(2\pi/N) & -\sin(2\pi/N) & \\ \sin(2\pi/N) & \cos(2\pi/N) & \\ & & 1 \end{pmatrix} \tag{25.24}$$

as

$$\mathbf{R}_n = S_N^n \mathbf{R}_0 \quad \mathbf{R}_0 = \begin{pmatrix} 1 \\ 0 \\ 0 \end{pmatrix}. \tag{25.25}$$

Similarly the transition dipoles are given by

$$\boldsymbol{\mu}_n = S_N^n \boldsymbol{\mu}_0. \tag{25.26}$$

The component parallel to the symmetry axis is the same for all monomers

$$\mu_{n,z} = \mu_{\parallel} \tag{25.27}$$

whereas for the component in the perpendicular plane

$$\begin{pmatrix} \mu_{n,x} \\ \mu_{n,y} \end{pmatrix} = \begin{pmatrix} \cos(n2\pi/N) & -\sin(n2\pi/N) \\ \sin(n2\pi/N) & \cos(n2\pi/N) \end{pmatrix} \begin{pmatrix} \mu_{0,x} \\ \mu_{0,y} \end{pmatrix}. \tag{25.28}$$

We describe the orientation of $\boldsymbol{\mu}_0$ in the x-y plane by the angle ϕ:

$$\begin{pmatrix} \mu_{0,x} \\ \mu_{0,y} \end{pmatrix} = \mu_{\perp} \begin{pmatrix} \cos(\phi) \\ \sin(\phi) \end{pmatrix}. \tag{25.29}$$

Then we have (Fig. 25.9)

$$\begin{pmatrix} \mu_{n,x} \\ \mu_{n,y} \\ \mu_{n,z} \end{pmatrix} = \begin{pmatrix} \mu_{\perp} \cos(\phi + n2\pi/N) \\ \mu_{\perp} \cos(\phi + n2\pi/N) \\ \mu_{\parallel} \end{pmatrix}. \tag{25.30}$$

We denote the local excitation of the nth molecule by

$$|n> = |A_0 A_2 \cdots A_n^* \cdots A_{N-1}> . \tag{25.31}$$

Due to the symmetry of the system, the excitonic interaction is invariant against the S_N rotation and therefore

$$< m|V|n > = < m-n|V|0 > = < 0|V|n-m> . \tag{25.32}$$

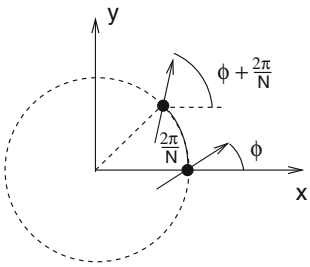

Fig. 25.9 Orientation of the transition dipoles

Table 25.2 Excitonic couplings. The matrix elements are calculated within the dipole–dipole approximation (25.33) for $R = 26.5\,\text{Å}\,\phi_0 = 66°$ and $\mu^2 = 37\text{Debye}^2$

$\lvert m-n\rvert$	$V_{\lvert m-n\rvert}(cm^{-1})$
1	−352.5
2	−43.4
3	−12.6
4	−5.1
5	−2.6
6	−1.5
7	−0.9
8	−0.7
9	−0.6

Without a magnetic field, the coupling matrix elements can be chosen real and depend only on $|m-n|$. Within the dipole–dipole approximation, we have furthermore[3]

$$V_{|m-n|} = < m|V|n > = \frac{e^2}{4\pi\varepsilon|R_{mn}|^5}\left(|R_{mn}|^2\boldsymbol{\mu}_m\boldsymbol{\mu}_n - 3(\mathbf{R}_{mn}\boldsymbol{\mu}_m)(\mathbf{R}_{mn}\boldsymbol{\mu}_n)\right). \tag{25.33}$$

The interaction matrix has the form (Table 25.2)

$$H = \begin{pmatrix} E_0 & V_1 & V_2 & \cdots & V_2 & V_1 \\ V_1 & E_1 & V_1 & \cdots & V_3 & V_2 \\ V_2 & V_1 & \ddots & & & \vdots \\ \vdots & \vdots & & & & V_2 \\ V_2 & V_3 & & & & V_1 \\ V_1 & V_2 & \cdots & V_2 & V_1 & E_{N-1} \end{pmatrix}. \tag{25.34}$$

The excitonic wavefunctions are easily constructed as

$$|k> = \frac{1}{\sqrt{N}}\sum_{n=0}^{N-1} e^{ikn}|n> \tag{25.35}$$

[3] A more realistic description based on a semiempirical INDO/S method is given by [141].

with

$$k = \frac{2\pi}{N} l \qquad l = 0, 1, \cdots N-1 \tag{25.36}$$

$$\begin{aligned} < k'|H|k > &= \frac{1}{N} \sum_{n'=0}^{N-1} \sum_{n=0}^{N-1} \mathrm{e}^{\mathrm{i}kn} \mathrm{e}^{-\mathrm{i}k'n'} < n'|H|n > \\ &= \frac{1}{N} \sum_{n'=0}^{N-1} \sum_{n=0}^{N-1} \mathrm{e}^{\mathrm{i}kn} \mathrm{e}^{-\mathrm{i}k'n'} H_{|n-n'|}. \end{aligned} \tag{25.37}$$

We substitute

$$m = n - n' \tag{25.38}$$

to get

$$\begin{aligned} < k'|H|k > &= \frac{1}{N} \sum_{n=0}^{N-1} \sum_{m=n}^{n-N+1} \mathrm{e}^{\mathrm{i}(k-k')n + \mathrm{i}k'm} H_{|m|} \\ &= \delta_{k,k'} \sum_{m=0}^{N-1} \mathrm{e}^{\mathrm{i}k'm} H_{|m|} \\ &= \delta_{k,k'} \left(E_0 + 2V_1 \cos k + 2V_2 \cos 2k + \cdots \right). \end{aligned} \tag{25.39}$$

For even N, the lowest and highest states are not degenerate whereas for all of the other states (Fig. 25.10)

$$E_k = E_{N-k} = E_{-k}. \tag{25.40}$$

The transition dipoles of the k-states are given by

$$\begin{aligned} \boldsymbol{\mu}_k &= \frac{1}{\sqrt{N}} \sum_{n=0}^{N-1} \mathrm{e}^{\mathrm{i}kn} \boldsymbol{\mu}_n = \frac{1}{\sqrt{N}} \sum_{n=0}^{N-1} \mathrm{e}^{\mathrm{i}kn} S_N^n \boldsymbol{\mu}_0 \\ &= \frac{1}{\sqrt{N}} \sum_{n=0}^{N-1} \mathrm{e}^{\mathrm{i}kn} \begin{pmatrix} \mu_x \cos(2\pi\, n/N) + \mu_y \sin(2\pi\, n/N) \\ \mu_y \cos(2\pi\, n/N) - \mu_x \sin(2\pi\, n/N) \\ \mu_z \end{pmatrix}. \end{aligned} \tag{25.41}$$

For the z-component, we have (Fig. 25.11)

$$\frac{1}{\sqrt{N}} \mu_z \sum_{n=0}^{N-1} \mathrm{e}^{\mathrm{i}kn} = \sqrt{N} \mu_z \delta_{k,0}. \tag{25.42}$$

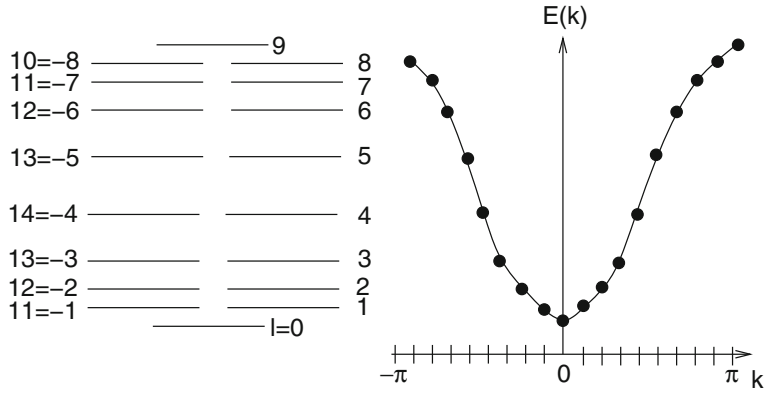

Fig. 25.10 Exciton dispersion relation. The figure shows the case of negative excitonic interaction where the k = 0 state is the lowest in energy

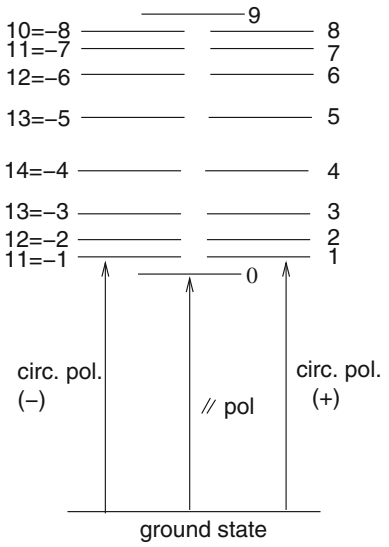

Fig. 25.11 Allowed optical transitions. The figure shows the case of negative excitonic interaction, where the lowest three exciton states carry intensity

For the component in the x,y plane, we introduce complex polarization vectors

$$\mu_{k,\pm} = \left(\tfrac{1}{\sqrt{2}} \ \tfrac{\pm \mathrm{i}}{\sqrt{2}} \ 0\right) \boldsymbol{\mu}_k$$
$$= \frac{1}{\sqrt{N}} \sum_{n=0}^{N-1} \mathrm{e}^{\mathrm{i}kn} \left(\tfrac{1}{\sqrt{2}} \ \pm\tfrac{\mathrm{i}}{\sqrt{2}} \ 0\right) \begin{pmatrix} \cos(\frac{2\pi n}{N}) & -\sin(\frac{2\pi n}{N}) & \\ \sin(\frac{2\pi n}{N}) & \cos(\frac{2\pi n}{N}) & \\ & & 1 \end{pmatrix} \begin{pmatrix} \mu_x \\ \mu_y \\ \mu_z \end{pmatrix}$$

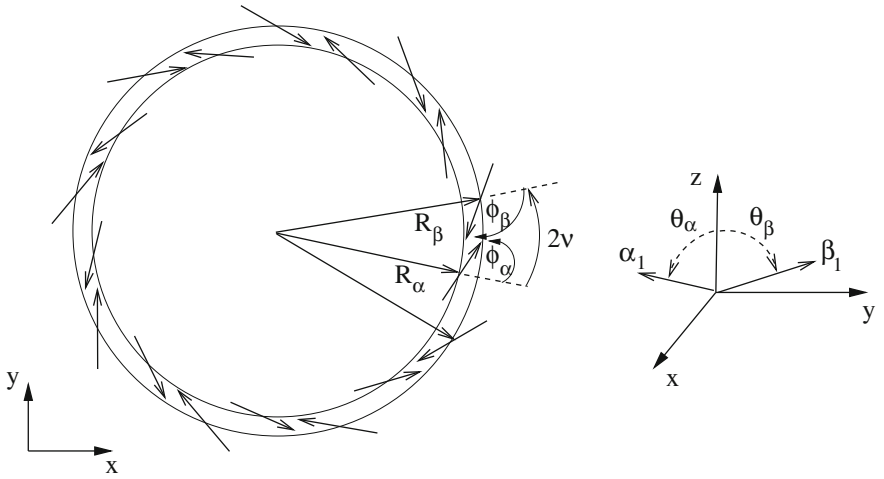

Fig. 25.12 BChl arrangement for the LH2 complex of *Rps.Acidophila* [133–137, 142]. *Arrows* represent the transition dipole moments of the BChl molecules as calculated on the 631G/HF-CI level. Distances are with respect to the center of the four nitrogen atoms. $R_\alpha = 26.1$Å, $R_\beta = 26.9$Å, $2\nu = 20.7°$, $\phi_\alpha = 70.5°$, $\phi_\beta = -117.7°$, $\theta_\alpha = 83.7°$, $\theta_\beta = 80.3°$

$$
\begin{aligned}
&= \frac{1}{\sqrt{N}} \sum_{n=0}^{N-1} \mathrm{e}^{\mathrm{i}kn} \left(\tfrac{1}{\sqrt{2}} \mathrm{e}^{\pm \mathrm{i}2n\pi/N} \pm \tfrac{\mathrm{i}}{\sqrt{2}} \mathrm{e}^{\pm \mathrm{i}2n\pi/N} \; 0 \right) \begin{pmatrix} \mu_x \\ \mu_y \\ \mu_z \end{pmatrix} \\
&= \frac{1}{\sqrt{N}} \sum_{n=0}^{N-1} \mathrm{e}^{\mathrm{i}(k \pm 2\pi/N)} \left(\tfrac{1}{\sqrt{2}} \; \tfrac{\pm \mathrm{i}}{\sqrt{2}} \right) \begin{pmatrix} \mu_x \\ \mu_y \end{pmatrix} \\
&= \sqrt{N} \delta_{k, \mp 2\pi/N} \mu_\pm \qquad \text{with } \mu_\pm = \frac{1}{\sqrt{2}} (\mu_x \pm \mathrm{i}\mu_y) = \frac{1}{\sqrt{2}} \mu_\perp \mathrm{e}^{\pm \mathrm{i}\phi}. \qquad (25.43)
\end{aligned}
$$

25.1.4 Dimerized Systems of LHII

The light harvesting complex LHII of *Rps.Acidophila* contains a ring of nine weakly coupled chlorophylls and another ring of nine stronger coupled chlorophyll dimers. The two units forming a dimer will be denoted as α, β, the number of dimers as N (Fig. 25.12).

The transition dipole moments are

$$
\boldsymbol{\mu}_{n,\alpha} = \mu \begin{pmatrix} \sin\theta_\alpha \cos(n\frac{2\pi}{N} - \nu + \phi_\alpha) \\ \sin\theta_\alpha \sin(n\frac{2\pi}{N} - \nu + \phi_\alpha) \\ \cos\theta_\alpha \end{pmatrix} = \mu S_N^n R_z(-\nu + \phi_\alpha) \begin{pmatrix} \sin\theta_\alpha \\ 0 \\ \cos\theta_\alpha \end{pmatrix}
$$

$$\boldsymbol{\mu}_{n,\beta} = \mu \begin{pmatrix} \sin\theta_\beta \cos(n\frac{2\pi}{N} + \nu + \phi_\beta) \\ \sin\theta_\beta \sin(n\frac{2\pi}{N} + \nu + \phi_\beta) \\ \cos\theta_\beta \end{pmatrix} = \mu S_N^n R_z(+\nu + \phi_\beta) \begin{pmatrix} \sin\theta_\beta \\ 0 \\ \cos\theta_\beta \end{pmatrix}. \tag{25.44}$$

For a circle with C_{2N}-symmetrical positions ($2\nu = \frac{\pi}{N}, \theta_\alpha = \theta_\beta$) and alternating transition dipole directions ($\phi_\beta = \pi + \phi_\alpha$), we find the relation

$$\boldsymbol{\mu}_{n,\beta} = R_z(2\nu + \phi_\beta - \phi_\alpha)\boldsymbol{\mu}_{n,\alpha} = R_z\left(\frac{\pi}{N} + \pi\right)\boldsymbol{\mu}_{n,\alpha}. \tag{25.45}$$

The experimental value of

$$2\nu + \phi_\beta - \phi_\alpha = 208.9^o \tag{25.46}$$

is in fact very close to the value of $180^o + 20^o$ (or $\pi + \frac{\pi}{N}$).

We have to distinguish the following interaction matrix elements between two monomers in different unit cells (Fig. 25.13, Table 25.3):

$$V_{\alpha,\alpha,|m|},\ V_{\alpha,\beta,m} = V_{\beta,\alpha,-m},\ V_{\alpha,\beta,-m} = V_{\beta,\alpha,m},\ V_{\beta,\beta,|m|} \tag{25.47}$$

The interaction matrix of one dimer is

$$\begin{pmatrix} E_\alpha & V_{dim} \\ V_{dim} & E_\beta \end{pmatrix}. \tag{25.48}$$

The wavefunction has to be generalized as

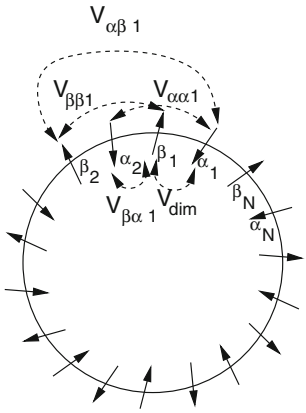

Fig. 25.13 Couplings in the dimerized ring

Table 25.3 Excitonic couplings for the LH2 complex of *Rps.Acidophila*. The matrix elements were calculated within the dipole–dipole approximation for the structure shown in Fig. 25.12 for $\mu^2 = 37 Debye^2$. All values in cm^{-1}

n	$V_{\alpha\beta n}$	$V_{\beta\alpha n}$	$V_{\alpha\alpha n}$	$V_{\beta\beta n}$
0	356.1	356.1		
1	13.3	324.5	−49.8	−35.0
2	2.8	11.8	−6.1	−4.0
3	1.0	2.4	−1.8	−1.0
4	0.7	0.9	−0.9	−0.4

$$|k, s >= \frac{1}{\sqrt{N}} \sum_{n=0}^{N-1} \mathrm{e}^{\mathrm{i}kn} (C_{s\alpha}|n\alpha > + C_{s\beta}|n\beta >) \tag{25.49}$$

$$< k's'|H|ks >= \frac{1}{N} \sum_{n=0}^{N-1} \sum_{n'=0}^{N-1} \mathrm{e}^{\mathrm{i}(kn-k'n')} \left(C_{s'\alpha} C_{s\alpha} H_{\alpha\alpha|n-n'|} \right.$$

$$\left. + C_{s'\beta} C_{s\beta} H_{\beta\beta|n-n'|} + C_{s'\alpha} C_{s\beta} H_{\alpha\beta(n-n')} + C_{s'\beta} C_{s\alpha} H_{\beta\alpha(n-n')} \right)$$

$$= \frac{1}{N} \begin{pmatrix} C_{s'\alpha} & C_{s'\beta} \end{pmatrix} \sum_{n=0}^{N-1} \sum_{m=0}^{N-1} \mathrm{e}^{\mathrm{i}(k-k')n + \mathrm{i}k'm} \begin{pmatrix} H_{\alpha\alpha|m|} & H_{\alpha\beta m} \\ H_{\beta\alpha m} & H_{\beta\beta|m|} \end{pmatrix} \begin{pmatrix} C_{s\alpha} \\ C_{s\beta} \end{pmatrix}$$

$$= \delta_{k,k'} \begin{pmatrix} C_{s'\alpha} & C_{s'\beta} \end{pmatrix} \begin{pmatrix} \sum_{m=0}^{N-1} \mathrm{e}^{\mathrm{i}km} H_{\alpha\alpha|m|} & \sum_{m=0}^{N-1} \mathrm{e}^{\mathrm{i}km} H_{\alpha\beta m} \\ \sum_{m=0}^{N-1} \mathrm{e}^{\mathrm{i}km} H_{\beta\alpha m} & \sum_{m=0}^{N-1} \mathrm{e}^{\mathrm{i}km} H_{\beta\beta m} \end{pmatrix} \begin{pmatrix} C_{s\alpha} \\ C_{s\beta} \end{pmatrix}. \tag{25.50}$$

The coefficients $C_{s\alpha}$and $C_{s\beta}$ are determined by diagonalization of the matrix

$$H_k = \\ = \begin{pmatrix} E_\alpha + 2V_{\alpha\alpha,1} \cos k + \cdots & V_{dim} + \mathrm{e}^{\mathrm{i}k} V_{\alpha\beta,1} + \mathrm{e}^{-\mathrm{i}k} V_{\alpha\beta,-1} + \cdots \\ V_{dim} + \mathrm{e}^{-\mathrm{i}k} V_{\alpha\beta,1} + \mathrm{e}^{\mathrm{i}k} V_{\alpha\beta,-1} + \cdots & E_\alpha + 2V_{\beta\beta,1} \cos k + \cdots \end{pmatrix}. \tag{25.51}$$

If we consider only interactions between nearest neighbors this simplifies to

$$H_k = \begin{pmatrix} E_\alpha & V_{dim} + \mathrm{e}^{-\mathrm{i}k} W \\ V_{dim} + \mathrm{e}^{\mathrm{i}k} W & E_\beta \end{pmatrix} \quad \text{with } W = V_{\alpha\beta,-1}. \tag{25.52}$$

In the following, we discuss the limit $E_\alpha = E_\beta$. The general case is discussed in the problems section. The eigenvectors of

$$H_k = \begin{pmatrix} E_\alpha & V_{dim} + \mathrm{e}^{-\mathrm{i}k} W \\ V_{dim} + \mathrm{e}^{\mathrm{i}k} W & E_\alpha \end{pmatrix}$$

are given by

$$\frac{1}{\sqrt{2}} \begin{pmatrix} 1 \\ \pm \mathrm{e}^{\mathrm{i}\chi} \end{pmatrix}, \tag{25.53}$$

where the angle χ is chosen such that

$$V + \mathrm{e}^{\mathrm{i}k} W = U(k) \mathrm{e}^{\mathrm{i}\chi} \tag{25.54}$$

with

$$U(k) = \mathrm{sign}(V) |V + \mathrm{e}^{\mathrm{i}k} W|$$

and the eigenvalues are

$$E_{k,\pm} = E_\alpha \pm U(k) = E_\alpha \pm \ \mathrm{sign}(V) \sqrt{V_{dim}^2 + W^2 + 2 V_{dim} W \cos k}. \tag{25.55}$$

The transition dipoles follow from

$$\boldsymbol{\mu}_{k,\pm} = \frac{1}{\sqrt{2N}} \sum_{n=0}^{N-1} \mathrm{e}^{\mathrm{i}kn} (\boldsymbol{\mu}_{n,\alpha} \pm \mathrm{e}^{\mathrm{i}\chi} \boldsymbol{\mu}_{n,\beta})$$

$$= \frac{\mu}{\sqrt{2N}} \sum_{n=0}^{N-1} \mathrm{e}^{\mathrm{i}kn} S_N^n \left(\begin{pmatrix} \sin\theta_\alpha \cos(-\nu + \phi_\alpha) \\ \sin\theta_\alpha \sin(-\nu + \phi_\alpha) \\ \cos\theta_\alpha \end{pmatrix} \pm \mathrm{e}^{\mathrm{i}\chi} \begin{pmatrix} \sin\theta_\beta \cos(\nu + \phi_\beta) \\ \sin\theta_\beta \sin(\nu + \phi_\beta) \\ \cos\theta_\beta \end{pmatrix} \right) \tag{25.56}$$

and similar selection rules as for the simple ring system follow for the first factor

$$\begin{aligned} \begin{pmatrix} 0 & 0 & 1 \end{pmatrix} \boldsymbol{\mu}_{k,\pm} &= \frac{\mu}{\sqrt{2N}} \sum_{n=0}^{N-1} \mathrm{e}^{\mathrm{i}kn} \left(\cos\theta_\alpha \pm \mathrm{e}^{\mathrm{i}\chi} \cos\theta_\beta \right) \\ &= \delta_{k,0} \, \mu \sqrt{\frac{N}{2}} \left(\cos\theta_\alpha \pm \cos\theta_\beta \right) \end{aligned} \tag{25.57}$$

$$\begin{aligned} \begin{pmatrix} \frac{1}{\sqrt{2}} & \frac{\mathrm{i}}{\sqrt{2}} & 0 \end{pmatrix} \boldsymbol{\mu}_{k,\pm} &= \frac{1}{\sqrt{2N}} \sum_{n=0}^{N-1} \mathrm{e}^{\mathrm{i}(k \pm 2\pi/N)n} \begin{pmatrix} 1 & i & 0 \end{pmatrix} (\boldsymbol{\mu}_{\alpha,1} \pm \mathrm{e}^{\mathrm{i}\chi} \boldsymbol{\mu}_{\beta,1}) \\ &= \sqrt{\frac{N}{2}} \delta_{k, \mp 2\pi/N} \mu \left(\sin\theta_\alpha \mathrm{e}^{\mathrm{i}(\phi_\alpha - \nu)} \pm \mathrm{e}^{\mathrm{i}\chi} \sin\theta_\beta \mathrm{e}^{\mathrm{i}(\phi, M_\beta + \nu)} \right) \end{aligned} \tag{25.58}$$

$$\left(\tfrac{1}{\sqrt{2}}\ \tfrac{-\mathrm{i}}{\sqrt{2}}\ 0\right)\boldsymbol{\mu}_{k,\pm} = \frac{1}{\sqrt{2N}}\sum_{n=0}^{N-1}\mathrm{e}^{\mathrm{i}(k\pm 2\pi/N)n}\left(1\ -i\ 0\right)\left(\boldsymbol{\mu}_{\alpha,1}\pm\mathrm{e}^{\mathrm{i}\chi}\boldsymbol{\mu}_{\beta,1}\right)$$
$$= \sqrt{\frac{N}{2}}\delta_{k,\mp 2\pi/N}\mu\left(\sin\theta_\alpha\mathrm{e}^{\mathrm{i}(\phi_\alpha-\nu)}\mp\mathrm{e}^{\mathrm{i}\chi}\sin\theta_\beta\mathrm{e}^{\mathrm{i}(\phi_\beta+\nu)}\right). \quad (25.59)$$

The second factor determines the distribution of intensity among the + and − states.

In the limit of $2N$ equivalent molecules $V = W$, $2\nu+\phi_\beta-\phi_\alpha = \pi+\frac{\pi}{N}$, $\theta_\alpha = \theta_\beta$ and we have

$$V + \mathrm{e}^{\mathrm{i}k}W = (1+\mathrm{e}^{\mathrm{i}k})V = \mathrm{e}^{\mathrm{i}k/2}(\mathrm{e}^{-\mathrm{i}k/2}+\mathrm{e}^{+\mathrm{i}k/2})V = \mathrm{e}^{\mathrm{i}k/2}2V\cos k/2 \quad (25.60)$$

and hence

$$\chi = k/2 \quad U(k) = 2V\cos k/2 \quad (25.61)$$

and (25.58) becomes

$$\left(\tfrac{1}{\sqrt{2}}\ \tfrac{\mathrm{i}}{\sqrt{2}}\ 0\right)\boldsymbol{\mu}_{k,\pm} = \sqrt{\frac{N}{2}}\delta_{k,\mp 2\pi/N}\mu\sin\theta\mathrm{e}^{\mathrm{i}(\phi_\alpha-\nu)}\left(1\mp\mathrm{e}^{\mathrm{i}(k/2+\pi/N)}\right)$$

which is zero for the upper case (+ states) and

$$\sqrt{2N}\delta_{k,2\pi/N}\mu\sin\theta\mathrm{e}^{\mathrm{i}(\phi_\alpha-\nu)} \quad (25.62)$$

for the (−) states. Similarly (25.59) becomes

$$\frac{1}{\sqrt{2}}(\mu_{k,x}-\mathrm{i}\mu_{k,y}) = \sqrt{2N}\delta_{k,+2\pi/N}\mu\sin\theta\mathrm{e}^{-\mathrm{i}(\phi_\alpha-\nu)} \quad (25.63)$$

for the - states and zero for the + states. (For positive V the + states are higher in energy than the - states.) For the z-component, the selection rule of k=0 implies (Fig. 25.14)

$$\mu_{z,+} = \sqrt{2N}\delta_{k,0}\mu\cos\theta, \quad \mu_{z,-} = 0. \quad (25.64)$$

In the LHC, the transition dipoles of the two dimer halves are nearly antiparallel. The oscillator strengths of the N molecules are concentrated in the degenerate next to lowest transitions $k = \pm 2\pi/N$. This means that the lifetime of the optically allowed states will be reduced compared to the radiative lifetime of a monomer. In the LHC, the transition dipoles have only a very small z-component. Therefore, in a perfectly symmetric structure, the lowest (k=0) state is almost forbidden and has a longer lifetime than the optically allowed $k = \pm 2\pi/N$ states. Due to the degeneracy of the $k = \pm 2\pi/N$ states, the absorption of photons coming along the symmetry axis does not depend on the polarization.

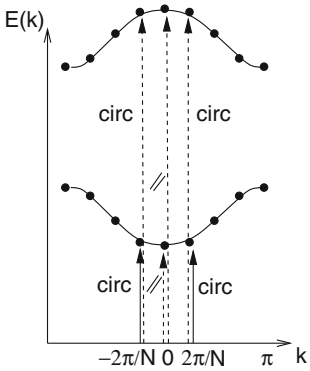

Fig. 25.14 Dispersion relation of the dimer ring

25.2 Influence of Disorder

So far we considered a perfectly symmetrical arrangement of the chromophores. In reality, there exist deviations due to the protein environment and low-frequency nuclear motion which leads to variations of the site energies, the coupling matrix elements, and the transition dipoles. In the following, we neglect the effects of dimerization and study a ring of N equivalent chromophores.

25.2.1 Symmetry Breaking Local Perturbation

We consider perturbation of the symmetry by a specific local interaction, for instance due to an additional hydrogen bond at one site. We assume that the excitation energy at the site $n_0 = 0$ is modified by a small amount δE. The Hamiltonian

$$H = \sum_{n=0}^{N-1} |n> E_0 < n| + |0> \delta E < 0| + \sum_{n=0}^{N-1} \sum_{n'=0, n' \neq n}^{N-1} |n> V_{nn'} < n'| \quad (25.65)$$

is transformed to the basis of k-states (25.35) to give

$$< k'|H|k > = \frac{1}{N} \sum_{n,n'} \mathrm{e}^{-\mathrm{i}k'n' + \mathrm{i}kn} < n'|H|n >$$

$$= \frac{1}{N} \sum_{n} \mathrm{e}^{\mathrm{i}(k-k')n} E_0 + \frac{\delta E}{N} + \frac{1}{N} \sum_{n} \sum_{n' \neq n} \mathrm{e}^{-\mathrm{i}k'n' + \mathrm{i}kn} V_{nn'}$$

$$= \delta_{k,k'} E_k + \frac{\delta E}{N}. \quad (25.66)$$

Obviously the energy of all k-states is shifted by the same amount

$$< k|H|k >= E_k + \frac{\delta E}{N}. \tag{25.67}$$

The degeneracy of the pairs $| \pm k >$ is removed due to the interaction

$$< k|H|-k >= \frac{\delta E}{N}. \tag{25.68}$$

The zero-order eigenstates are the linear combinations

$$|k_\pm >= \frac{1}{\sqrt{2}}(|k > \pm|-k >) \tag{25.69}$$

with zero-order energies (Fig. 25.15)

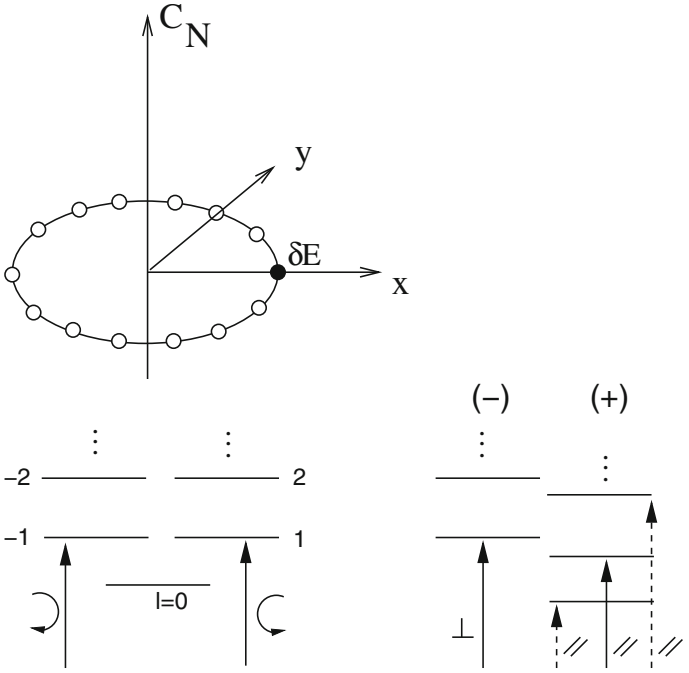

Fig. 25.15 Local perturbation of the symmetry

$$E(k) = E_k + \frac{\delta E}{N} \quad \text{(nondegenerate states)}$$
$$E(k_-) = E_k \quad E(k_+) = E_k + 2\frac{\delta E}{N} \quad \text{(degenerate states).} \tag{25.70}$$

Only the symmetric states are affected by the perturbation. The interaction between degenerate pairs is given by the matrix elements

$$\begin{aligned} &< k'_+|H|k_+ >= \delta_{k,k'} E_k + 2\frac{\delta E}{N} \\ &< k_-|H|k_- >= \delta_{k,k'} E_k \\ &< k_+|H|k_- >= 0 \end{aligned} \tag{25.71}$$

and the coupling to the nondegenerate $k = 0$ state is

$$\begin{aligned} &< 0|H|k_+ >= \frac{\sqrt{2}\delta E}{N} \\ &< 0|H|k_- >= 0. \end{aligned} \tag{25.72}$$

Optical transitions to the $|1_\pm >$ states are linearly polarized with respect to perpendicular axes. In first order, intensity is transferred from the $|1_+ >$ state to the $|0 >$ and the other $|k_+ >$ states and hence the $|1_- >$ state absorbs stronger than the $|1_+ >$ state which is approximately

$$|1_+ > + \frac{\sqrt{2}\delta E}{N(E_0 - E_1)}|0 > + \frac{2\delta E}{N(E_2 - E_1)}|2_+ > + \cdots \tag{25.73}$$

Its intensity is reduced by a factor of

$$\frac{1}{1 + \frac{\delta E^2}{N^2}\left(\frac{2}{(E_0 - E_1)^2} + \frac{4}{(E_2 - E_1)^2} + \cdots\right)}. \tag{25.74}$$

25.2.2 Periodic Modulation

The local perturbation (25.66) has Fourier components

$$H'(\Delta k) =< k|H'|k + \Delta k >= \frac{1}{N}\sum_n \mathrm{e}^{\mathrm{i}n\Delta k}\delta E_n \tag{25.75}$$

for all possible values of Δk. In this section, we discuss the most important Fourier components separately. These are the $\Delta k = \pm 4\pi/N$ components which mix the

$k = \pm 2\pi/N$ states and the $\Delta k = \pm 2\pi/N$ components which couple the $k = \pm 2\pi/N$ to the $k = 0, \pm 4\pi/N$ states and thus redistribute the intensity of the allowed states.

A general modulation of the diagonal energies with Fourier components $\Delta k = \pm 2\pi/N$ is given by

$$\delta E_n = \delta E \cos(\chi_0 + 2n\pi/N) \tag{25.76}$$

and its matrix elements are

$$H'(\Delta k) = \frac{e^{i\chi_0}\delta E}{2}\delta_{\Delta k,-2\pi/N} + \frac{e^{-i\chi_0}\delta E}{2}\delta_{\Delta k,2\pi/N}. \tag{25.77}$$

Transformation to linear combinations of the degenerate pairs

$$\begin{aligned} |k,+> &= \frac{1}{\sqrt{2}}\left(e^{i\chi_0}|-k> + e^{-i\chi_0}|k>\right) \quad k>0 \\ |k,-> &= \frac{1}{\sqrt{2}}\left(-e^{-i\chi_0}|-k> + e^{i\chi_0}|k>\right) \quad k>0 \end{aligned} \tag{25.78}$$

leads to two decoupled sets of states with (Fig. 25.16)

$$\begin{aligned} <0|H'|k,+> &= \frac{\delta E}{\sqrt{2}}\cos(2\chi_0)\delta_{k,2\pi/N} \\ <0|H'|k,-> &= 0 \\ <k,-|H'|k',+> &= 0 \\ <k,-|H'|k',-> &= \frac{\delta E}{2}\cos\chi_0(\delta_{k'-k,2\pi/N} + \delta_{k'-k,-2\pi/N}) \\ <k,+|H'|k',+> &= \frac{\delta E}{2}\cos(3\chi_0)(\delta_{k'-k,2\pi/N} + \delta_{k'-k,-2\pi/N}). \end{aligned}$$

The $|k = 2\pi/N, \pm>$ states are linearly polarized

$$\begin{aligned} \mu_{2\pi/N,+,\Theta} &= \frac{e^{i\chi_0}}{\sqrt{2}}\mu_{-2\pi/N,\Theta} + \frac{e^{i\chi_0}}{\sqrt{2}}\mu_{2\pi/N,\Theta} = \sqrt{N}\mu_\perp\cos(\Phi + \chi_0 - \Theta) \\ \mu_{2\pi/N,-,\Theta} &= -\frac{e^{-i\chi_0}}{\sqrt{2}}\mu_{-2\pi/N,\Theta} + \frac{e^{i\chi_0}}{\sqrt{2}}\mu_{2\pi/N,\Theta} = i\sqrt{N}\mu_\perp\sin(\Phi + \chi_0 - \Theta). \end{aligned} \tag{25.79}$$

Let us now consider a C_2 symmetric modulation [143]

$$\delta E_n = \delta E \cos(\chi_0 + 4\pi n/N) \tag{25.80}$$

with matrix elements

$$<k|H'|k'> = \frac{\delta E}{2}\left(e^{i\chi_0}\delta_{k'-k,-4\pi/N} + e^{-i\chi_0}\delta_{k'-k,4\pi/N}\right). \tag{25.81}$$

The $|k = \pm 2\pi/N>$ states are mixed to give the zero-order states

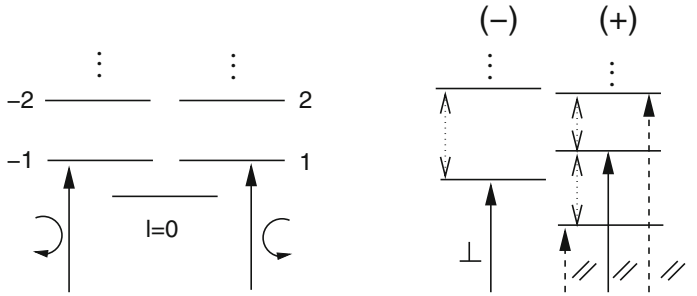

Fig. 25.16 C_1 symmetric perturbation. Modulation of the diagonal energies by the perturbation $\delta E_n = \delta E\ \cos(\chi_0 + 2\pi n/N)$ does not mix the $|k, + >$ and $|k, - >$ states. In first-order, the allowed $k = \pm 2\pi/N$ states split into two states $|k = 2\pi/N, \pm >$ with mutually perpendicular polarization and intensity is transferred to the $|k = 0 >$ and $|k = 4\pi/N, \pm >$ states

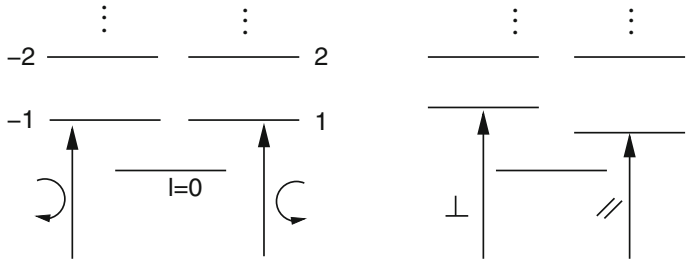

Fig. 25.17 C_2 symmetric perturbation. Modulation of the diagonal energies by the perturbation $\delta E_n = \delta E\ \cos(\chi_0 + 4\pi n/N)$ splits the $|k = \pm 2\pi/N>$ states in zero order into a pair with equal intensity and mutually perpendicular polarization

$$|2\pi/N, + > = \frac{1}{\sqrt{2}}\left(|-2\pi/N> + e^{i\chi_0}|2\pi/N>\right)$$
$$|2\pi/N, - > = \frac{1}{\sqrt{2}}\left(|-2\pi/N> - e^{i\chi_0}|2\pi/N>\right) \tag{25.82}$$

which are again linearly polarized (Fig. 25.17).

A perturbation of this kind could be due to an elliptical deformation of the ring [143], but also due to interaction with a static electric field, which is given up to second order by

$$\delta E_n = -\mathbf{p}_n\mathbf{E} + \frac{1}{2}\mathbf{E}^t\alpha_n\mathbf{E} \tag{25.83}$$

where the permanent dipole moments are given by an expression similar[4] to (25.26)

[4]The angle Φ is different for permanent and transition dipoles.

$$\mathbf{p}_n = S_N^n \mathbf{p}_0 = \begin{pmatrix} p_\perp \cos(\Phi + n2\pi/N) \\ p_\perp \sin(\Phi + n2\pi/N) \\ p_\parallel \end{pmatrix} \tag{25.84}$$

and the polarizabilities transform as

$$\alpha_n = S_N^n \alpha_0 S_N^{-n}. \tag{25.85}$$

With the field vector

$$\mathbf{E} = \begin{pmatrix} E_\perp \cos\xi \\ E_\perp \sin\xi \\ E_\parallel \end{pmatrix} \tag{25.86}$$

we find

$$-\mathbf{p}_n \mathbf{E} = -p_\perp E_\perp \cos(\Phi + n2\pi/N - \xi) \tag{25.87}$$

and

$$\begin{aligned} \frac{1}{2}\mathbf{E}^t \alpha_n \mathbf{E} &= \frac{1}{2}(\mathbf{E}^t S_N^n)\alpha_0 (S_N^{-n}\mathbf{E}) \\ &= \frac{E_\perp^2}{2}\left\{\alpha_{xx}\cos^2(n2\pi/N - \xi) + \alpha_{yy}\sin^2(n2\pi/N - \xi)\right. \\ &\quad \left. + 2\alpha_{xy}\sin(n2\pi/N - \xi)\cos(n2\pi/N - \xi)\right\} \\ &\quad + E_| E_\perp \left\{\alpha_{xz}\cos(n2\pi/N - \xi) + \alpha_{yz}\sin(n2\pi/N - \xi)\right\} \\ &\quad + \frac{E_\parallel^2}{2}\alpha_{zz}. \end{aligned} \tag{25.88}$$

The quadratic term has Fourier components $\Delta k = \pm 4\pi/N$ and can therefore act as an elliptic perturbation.

25.2.3 Diagonal Disorder

Let us consider a static distribution of site energies for a ring of N chromophores [144–146]. The Hamiltonian

$$H = \sum_{n=0}^{N-1} |n> (E_0 + \delta E_n) < n| + \sum_{n=0}^{N-1} \sum_{n'=0, n' \neq n}^{N-1} |n> V_{nn'} < n'| \tag{25.89}$$

contains energy shifts δE_n which are assumed to have a Gaussian distribution function.

$$P(\delta E_n) = \frac{1}{\Delta\sqrt{\pi}} \exp(-\delta E_n^2/\Delta^2). \tag{25.90}$$

Transforming to the delocalized states, the Hamiltonian becomes

$$\begin{aligned} &< k'|H|k >= \frac{1}{N} \sum_{n,n'} \mathrm{e}^{-\mathrm{i}k'n'+\mathrm{i}kn} < n'|H|n > \\ &= \frac{1}{N} \sum_{n} \mathrm{e}^{\mathrm{i}(k-k')n}(E_0 + \delta E_n) + \frac{1}{N} \sum_{n} \sum_{n' \neq n} \mathrm{e}^{-\mathrm{i}k'n'+\mathrm{i}kn} V_{nn'} \\ &= \delta_{k,k'} E_k + \frac{1}{N} \sum_{n} \mathrm{e}^{\mathrm{i}(k-k')n} \delta E_n \end{aligned} \tag{25.91}$$

and due to the disorder the k-states are mixed. The energy change of a nondegenerate state(for instance k = 0) is in lowest order perturbation theory given by the diagonal matrix element

$$\delta E_k = \frac{1}{N} \sum_{n} \delta E_n \tag{25.92}$$

as the average of the local energy fluctuations. Obviously the average is zero

$$< \delta E_k >=< \delta E_n >= 0 \tag{25.93}$$

and

$$< \delta E_k^2 >= \frac{1}{N^2} \sum_{n,n'} < \delta E_n \delta E_{n'} >. \tag{25.94}$$

If the fluctuations of different sites are uncorrelated

$$< \delta E_n \delta E_{n'} >= \delta_{n,n'} < \delta E^2 > \tag{25.95}$$

the width of the k-state

$$< \delta E_k^2 >= \frac{< \delta E^2 >}{N} \tag{25.96}$$

is smaller by a factor $1/\sqrt{N}$.[5] If the fluctuations are fully correlated, on the other hand, the k-states have the same width as the site energies.

For the pairs of degenerate states $\pm k$, we have to consider the secular matrix ($\Delta k = k - k' = 2k$)

[5]This is known as exchange or motional narrowing.

$$H_1 = \begin{pmatrix} \frac{1}{N}\sum_n \delta E_n & \frac{1}{N}\sum_n \mathrm{e}^{\mathrm{i}n\Delta k}\delta E_n \\ \frac{1}{N}\sum_n \mathrm{e}^{-\mathrm{i}n\Delta k}\delta E_n & \frac{1}{N}\sum_n \delta E_n \end{pmatrix} \tag{25.97}$$

which has the eigenvalues

$$\delta E_{\pm k} = \frac{1}{N}\sum_n \delta E_n \pm \frac{1}{N}\sqrt{\sum_n \mathrm{e}^{\mathrm{i}n\Delta k}\delta E_n \sum_{n'} \mathrm{e}^{-\mathrm{i}n'\Delta k}\delta E_{n'}}. \tag{25.98}$$

Obviously the average is not affected

$$< \frac{\delta E_{+k} + \delta E_{-k}}{2} >= 0 \tag{25.99}$$

and the width is given by

$$\begin{aligned} &< \frac{\delta E_{+k}^2 + \delta E_{-k}^2}{2} > \\ &= \frac{1}{N^2}\sum_{nn'} < \delta E_n \delta E_{n'} > + \frac{1}{N^2}\sum_{nn'} \mathrm{e}^{\mathrm{i}(n-n')\Delta k} < \delta E_n \delta E_{n'} > \\ &= 2\frac{< \delta E^2 >}{N}. \end{aligned} \tag{25.100}$$

25.2.4 Off-Diagonal Disorder

Consider now fluctuations also of the coupling matrix elements, for instance due to fluctuations of orientation and distances. The Hamiltonian contains an additional perturbation

$$H'_{kk'} = \frac{1}{N}\sum_{n'n} \mathrm{e}^{-\mathrm{i}k'n' + ikn}\delta V_{nn'}. \tag{25.101}$$

For uncorrelated fluctuations with the properties[6]

$$< \delta V_{nn'} >= 0 \tag{25.102}$$

$$< \delta V_{nn'}\delta V_{mm'} >= (\delta_{nm}\delta_{n'm'} + \delta_{nm'}\delta_{n'm} - \delta_{nm}\delta_{n'm'}\delta_{nn'}) < \delta V^2_{|n-n'|} > \tag{25.103}$$

[6]We assume here that the fluctuation amplitudes obey the $C_N - symmetry$.

it follows

$$
\begin{aligned}
&< H'_{kk'} >= 0 \\
&< |H'_{kk'}|^2 >= \frac{1}{N^2} \sum_{n'n} \sum_{m'm} \mathrm{e}^{\mathrm{i}k(n-m)+ik'(m'-n')} < \delta V_{nn'} \delta V_{mm'} > \\
&= \frac{1}{N^2} \sum_{n'n} < \delta V^2_{nn'} > + \frac{1}{N^2} \sum \mathrm{e}^{\mathrm{i}(k+k')(n-n')} < \delta V^2_{nn'} > \\
&= \frac{< \delta E^2 >}{N} + \frac{1}{N} \sum_{m \neq 0} < \delta V^2_{|m|} > \left[1 + \cos\left(m(k+k')\right)\right]. \qquad (25.104)
\end{aligned}
$$

If the dominant contributions come from the fluctuation of site energies and nearest neighbor couplings, this simplifies to

$$
< |H'_{kk'}|^2 >= \frac{1}{N} (< \delta E^2 > + 2 < \delta V^2_{\pm 1} > (1 + \cos(k + k')). \qquad (25.105)
$$

For the nondegenerate states, the width is

$$
< \delta E^2_k >= \frac{< \delta E^2 > + 4 < \delta V^2_{\pm 1} >}{N} \qquad (25.106)
$$

and for the degenerate pairs, the eigenvalues of the secular matrix become

$$
\delta E_{\pm k} = H_{kk} \pm \left| H_{k,-k} \right|. \qquad (25.107)
$$

Again the average of the two is not affected

$$
< \frac{\delta E_{+k} + \delta E_{-k}}{2} >= 0 \qquad (25.108)
$$

whereas the width now is given by

$$
\begin{aligned}
&< \frac{\delta E^2_{+k} + \delta E^2_{-k}}{2} >=< H^2_{kk} > + < H^2_{k,-k} > \\
&= \frac{2}{N} \left(< \delta E^2 > + < \delta V^2_{\pm 1} > (3 + \cos(2k)) \right). \qquad (25.109)
\end{aligned}
$$

Off-diagonal disorder has a similar effect as diagonal disorder, but it influences the optically allowed $k = \pm 1$ states stronger than the states in the center of the exciton band. More sophisticated investigations, including also partially correlated disorder and disorder of the transition dipoles, can be found in the literature [144–149].

Problems

25.1 Photosynthetic Reaction Center

The "special pair" in the photosynthetic reaction center of Rps.viridis is a dimer of two bacteriochlorophyll molecules whose centers of mass have a distance of 7Å. The transition dipoles of the two molecules include an angle of 139^o.

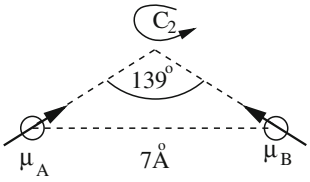

Calculate energies and intensities of the two dimer bands from a simple exciton model

$$\mathcal{H} = \begin{pmatrix} -\Delta/2 & V \\ V & \Delta/2 \end{pmatrix}$$

as a function of the energy difference Δ and the interaction V. The Hamiltonian is represented here in a basis spanned by the two localized excited states $|A^*B>$ and $|B^*A>$.

25.2 Light Harvesting Complex

The circular light harvesting complex of the bacterium *Rhodopseudomonas acidophila* consists of nine bacteriochlorophyll dimers in a C_9-symmetric arrangement. The two subunits of a dimer are denoted as α and β. The exciton Hamiltonian with nearest neighbor and next to nearest neighbor interactions only is (with the index n taken as modulo 9)

$$\mathcal{H} = \sum_{n=1}^{9} \Big\{ E_\alpha |n;\alpha><n;\alpha| + E_\beta |n;\beta><n;\beta|$$

$$+ V_{dim}(|n;\alpha><n;\beta| + |n;\beta><n;\alpha|)$$

$$+ V_{\beta\alpha,1}\,(|n;\alpha><n-1;\beta| + |n;\beta><n+1;\alpha|)$$

$$+ V_{\alpha\alpha,1}\,(|n;\alpha><n+1;\alpha| + |n;\alpha><n-1;\alpha|)$$

$$+ V_{\beta\beta,1}\,(|n;\beta><n+1;\beta| + |n;\beta><n-1;\beta|)\Big\}\,.$$

Transform the Hamiltonian to delocalized states

$$|k;\alpha>=\frac{1}{3}\sum_{n=1}^{9}\mathrm{e}^{\mathrm{i}kn}|n;\alpha> \quad |k;\beta>=\frac{1}{3}\sum_{n=1}^{9}\mathrm{e}^{\mathrm{i}kn}|n;\beta>$$

$$k=l\,2\pi/9 \qquad l=0,\pm1,\pm2,\pm3,\pm4.$$

(a) Show that states with different k-values do not interact

$$<k',\alpha(\beta)|\mathcal{H}|k,\alpha(\beta)>=0 \quad \text{if } k\neq k'.$$

(b) Find the matrix elements

$$H_{\alpha\alpha}(k)=<k;\alpha|\mathcal{H}|k;\alpha> \quad H_{\beta\beta}(k)=<k;\beta|\mathcal{H}|k;\beta>$$

$$H_{\alpha\beta}(k)=<k;\alpha|\mathcal{H}|k;\beta>.$$

(c) Solve the eigenvalue problem

$$\begin{pmatrix} H_{\alpha\alpha}(k) & H_{\alpha\beta}(k) \\ H^{*}_{\alpha\beta}(k) & H_{\beta\beta}(k) \end{pmatrix}\begin{pmatrix} C_\alpha \\ C_\beta \end{pmatrix}=E_{1,2}(k)\begin{pmatrix} C_\alpha \\ C_\beta \end{pmatrix}.$$

(d) The transition dipole moments are given by

$$\boldsymbol{\mu}_{n,\alpha}=\mu\begin{pmatrix} \sin\theta\,\cos(\phi_\alpha-\nu+n\phi) \\ \sin\theta\,\sin(\phi_\alpha-\nu+n\phi) \\ \cos\theta \end{pmatrix} \quad \boldsymbol{\mu}_{n,\beta}=\mu\begin{pmatrix} \sin\theta\,\cos(\phi_\beta+\nu+n\phi) \\ \sin\theta\,\sin(\phi_\beta+\nu+n\phi) \\ \cos\theta \end{pmatrix}$$

$\nu=10.3^o$, $\phi_\alpha=-112.5^o$, $\phi_\beta=63.2^o$, $\theta=84.9^o$.
Determine the optically allowed transitions from the ground state and calculate the relative intensities.

25.3 Exchange Narrowing

Consider excitons in a ring of chromophores with uncorrelated diagonal disorder. Show that in lowest order, the distribution function of E_k is Gaussian. Hint: write the distribution function as

$$P(\delta E_k=X)=\int d\delta E_1 d\delta E_2\cdots P(\delta E_1)P(\delta E_2)\cdots\delta(X-\frac{\sum\delta E_n}{N})$$

and replace the delta function with a Fourier integral.

Chapter 26
Charge Transfer in DNA

Photoinduced charge transfer in DNA [150, 151] occurs via two different hole transfer mechanisms (Fig. 26.1), diffusive hopping between sites with similar potential and tunneling over barriers with high potential (Fig. 26.2). We discuss a simple kinetic scheme for diffusive motion and determine the stationary solution of the corresponding master equation. A continuous treatment leads to the diffusion equation. Hole tunneling appears over one or more bridge states and has to be described by a higher order superexchange mechanism. In general, both mechanisms are effective, dependent on the DNA sequence.

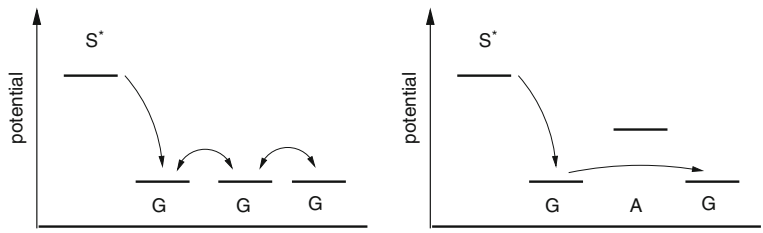

Fig. 26.1 Charge Transfer in DNA After hole injection from the excited photosensitizer S^*, charge transfer proceeds via two mechanisms. ***Left*** Between nucleic acids with similar oxidation potential, charge is transferred by diffusive hopping. ***Right*** nucleic acids with higher oxidation potential act as virtual intermediates during a tunneling process. Over longer distances, both mechanisms contribute

P.O.J. Scherer and S.F. Fischer, *Theoretical Molecular Biophysics*,
Biological and Medical Physics, Biomedical Engineering,
DOI 10.1007/978-3-662-55671-9_26

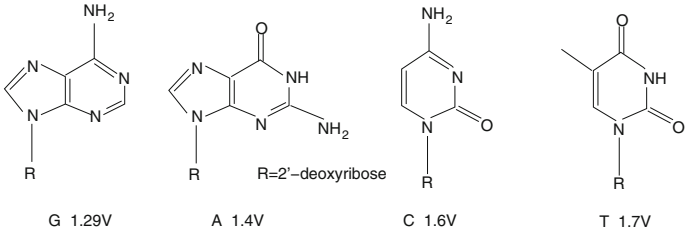

Fig. 26.2 Oxidation potentials of 2'-deoxynucleosides

26.1 Diffusive Hole Transfer

The hopping process among residues with the same potential is described by the kinetic scheme [152] (the loss channels are left out for simplicity)

$$\begin{array}{ccccccccc} S & & k & & k & & k & & k_T \\ \rightarrow & G_1 & \rightleftarrows & G_2 & \rightleftarrows & G_3 & \ldots & \rightleftarrows & G_N \rightarrow GGG \\ & & k & & k & & & & \end{array} \tag{26.1}$$

where S is the injection rate and trapping at the end of the chain is irreversible. The system of master equations reads

$$\frac{\partial P_1}{\partial t} = S + k(P_2 - P_1) \tag{26.2}$$

$$\frac{\partial}{\partial t} P_j = kP_{j-1} + kP_{j+1} - 2kP_j \quad 1 < j < N. \tag{26.3}$$

$$\frac{\partial}{\partial t} P_N = kP_{N-1} - (k + k_T)P_N. \tag{26.4}$$

Figures 26.3 and 26.4 show numerical results for an instantaneous charge injection $S = \delta(t)$ (i.e., initially only G_1 is charged). Experimentally, often the quantum yield is measured, which corresponds to a stationary state with $S = \text{const}$. The stationary solution of the master equation can be found recursively

$$P_{N-1} = (1 + \frac{k_T}{k})P_N \tag{26.5}$$

$$P_{N-2} = 2P_{N-1} - P_N = (1 + \frac{2k_T}{k})P_N \tag{26.6}$$

$$\vdots$$

$$P_2 = 2P_3 - P_4 = (1 + (N-2)\frac{k_T}{k})P_N \tag{26.7}$$

$$P_1 = 2P_2 - P_3 = (1 + (N-1)\frac{k_T}{k})P_N \tag{26.8}$$

$$P_1 = P_2 + \frac{S}{k}. \tag{26.9}$$

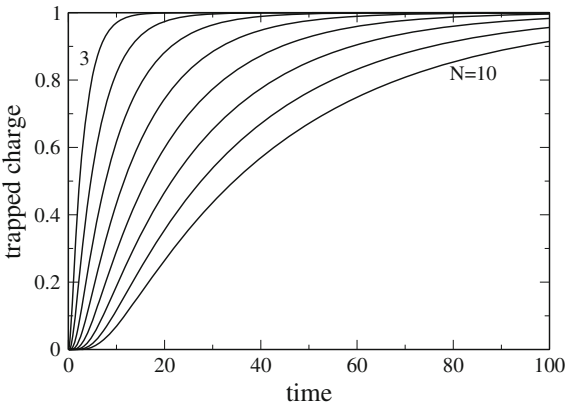

Fig. 26.3 Kinetics of the hopping process The master (26.3) is solved for $k = 1, \quad k_T = 20$ and N from 3 to 10. The *curves* show the charge arrived at the trap. The transfer time is approximately proportional to N^2

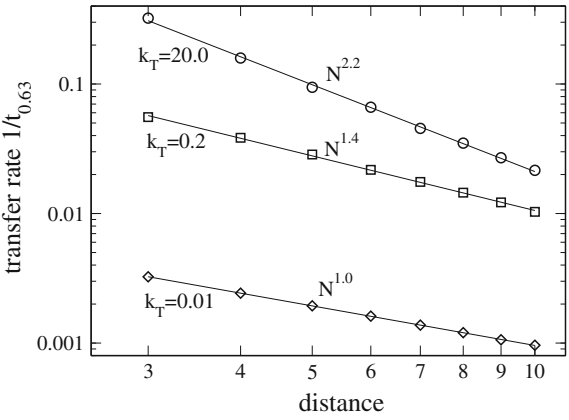

Fig. 26.4 Power law of the hopping process For fast trapping rate $k_T \gtrsim k$ the transfer rate is approximately proportional to N^{-2}. For small trapping rate a N^{-1}-behavior is approached

From combination of the last three equations, we obtain

$$P_N = \frac{S}{k_T} \tag{26.10}$$

and finally

$$P_j = \left(1 + (N - j)\frac{k_T}{k}\right)\frac{S}{k_T}\,. \tag{26.11}$$

Hence, the relative yield shows an algebraic length dependence in agreement with experimental data [152]

$$\frac{P_N}{P_1} = \frac{1}{1 + (N-1)\frac{k_T}{k}}\,. \tag{26.12}$$

Approximating the probabilities by a continuous function

$$P_j = P(j\Delta x) \tag{26.13}$$

and the second derivative by a difference quotient

$$\frac{\partial^2 P}{\partial x^2} = \frac{P(x+\Delta x) + P(x-\Delta x) - 2P(x)}{\Delta x^2} \tag{26.14}$$

we obtain a diffusion equation (Sect. 7.3)

$$\frac{\partial P}{\partial t} = D\frac{\partial P^2}{\partial x^2} \tag{26.15}$$

with the diffusion constant

$$D = k\Delta x^2. \tag{26.16}$$

For large trapping rate $k_T \gg k$, the trap at the end of the chain can be represented as a zero boundary condition. From the general behavior of the diffusion equation (7.36), we expect that the transfer time will be proportional to the square of the distance. A small trapping rate can be neglected for the kinetics. In this limit, the transfer time becomes (Figs. 26.3, 26.4) proportional to N [152].

26.2 Tunneling over Bridge States

Transfer through virtual states (Fig. 26.5) with large energy gap ($\Delta E \gg k_B T$) is described by higher order perturbation theory. In leading order, the matrix element of the transition operator becomes

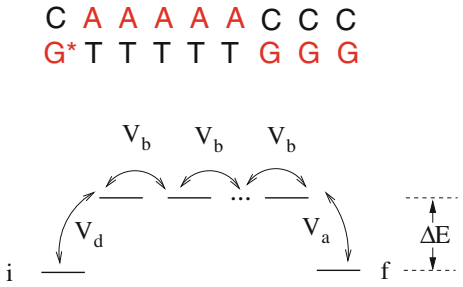

Fig. 26.5 Hole tunneling. States with energies above the initial and final states ($\Delta E \gg k_B T$) can not be real intermediates. Hole tunneling over one or more bridge states has to be described by higher order perturbation theory

$$V_{eff} =< i|T|f >=< i|VG_0(E_f)VG_0(E_f)\ldots VG_0(E_f)|f >= \frac{V_d V_a}{\Delta E}\left(\frac{V_b}{\Delta E}\right)^{n-1} \tag{26.17}$$

where n is the number of bridges and $\Delta E = E_b - E_f$ is the height of the potential barrier. For hole tunneling, this leads to an exponential distance dependence of the transfer rate

$$V_{eff}^2(N) = V_0^2 \mathrm{e}^{-\mathrm{fiN}} \tag{26.18}$$

$$k = \frac{2\pi}{\hbar}\,\mathrm{FCD}\,V_0^2 \mathrm{e}^{-\mathrm{fiN}}. \tag{26.19}$$

26.3 Combined Transfer Mechanism

In general, both mechanisms are effective (Fig. 26.6). The charge hops from one type-G nucleoside to the next one with a rate determined by the superexchange interaction

$$k_j = \frac{2\pi}{\hbar}\,\mathrm{FCD}V_j^2. \tag{26.20}$$

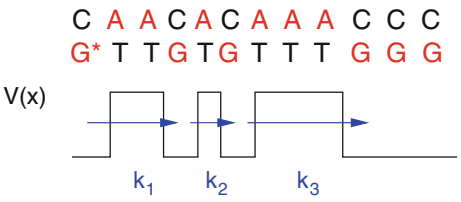

Fig. 26.6 Hole transfer by combined hopping and tunneling

Chapter 27
Proton Transfer in Biomolecules

Intra-protein proton transfer is perhaps the most fundamental flux in the biosphere [153]. It is essential for such important processes as photosynthesis, respiration, and ATP synthesis [154]. Within a protein, protons appear only in covalently bound states. Here proton transfer is essentially the motion along a hydrogen bond, for instance, peptide or DNA H-bonds (Fig. 27.1) or the more complicated pathways in proton-pumping proteins.

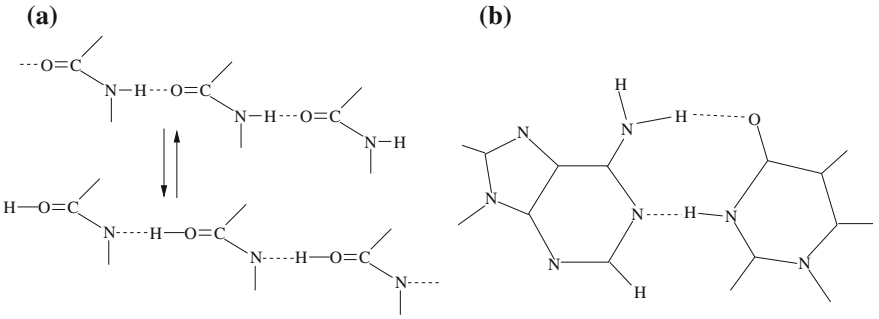

Fig. 27.1 Proton transfer in peptide H-bonds (**a**) and in DNA H-bonds (**b**)

The energy barrier for this reaction depends strongly on the conformation of the reaction complex, concerning as well its geometry as its protonation state. Due to the small mass of the proton, the description of the proton transfer process has to be discussed on the basis of quantum mechanics. This chapter begins with a discussion of the photocycle of the proton pump bacteriorhodopsin. We introduce the double Born–Oppenheimer separation for the different time scales of electrons, protons, and the heavier nuclei and discuss nonadiabatic proton transfer in analogy to Marcus' electron transfer theory. We present the model by Borgis and Hynes which includes non-Condon effects. Finally, we comment on adiabatic proton transfer.

P.O.J. Scherer and S.F. Fischer, *Theoretical Molecular Biophysics*,
Biological and Medical Physics, Biomedical Engineering,
DOI 10.1007/978-3-662-55671-9_27

27.1 The Proton Pump Bacteriorhodopsin

Rhodopsin proteins collect the photon energy in the process of vision. Since the end of the 1950s, it has been recognized that the photoreceptor molecule retinal undergoes a structural change, the so-called cis-trans isomerization (Fig. 27.4) upon photo-excitation (G. Wald, R. Granit, H.K. Hartline, Nobel prize for medicine 1961). Rhodopsin is not photostable and its spectroscopy remains difficult. Therefore, much more experimental work has been done on its bacterial analogue bacteriorhodopsin [155], which performs a closed photocycle (Figs. 27.2 and 27.3).

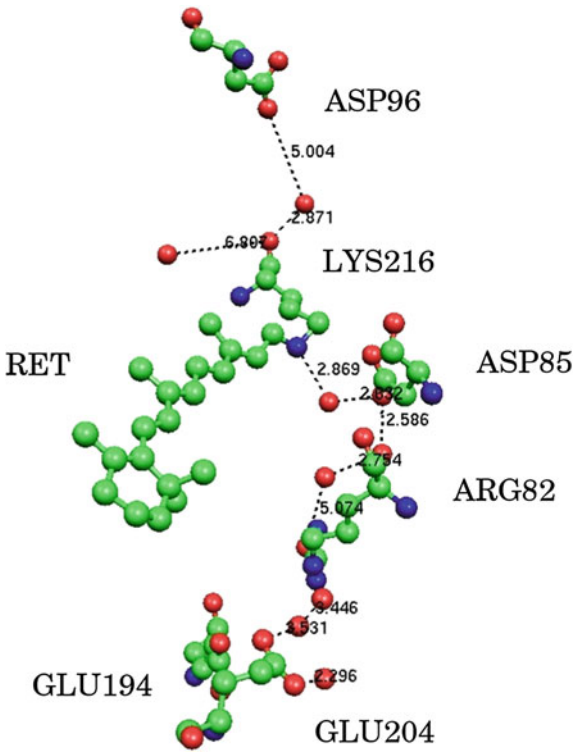

Fig. 27.2 X-ray structure of bR. The most important residues and structural waters are shown, together with possible pathways for proton transfer. Coordinates are from the structure 1kzu [133–137] in the protein data bank [138, 139]. Molekel graphics [65]

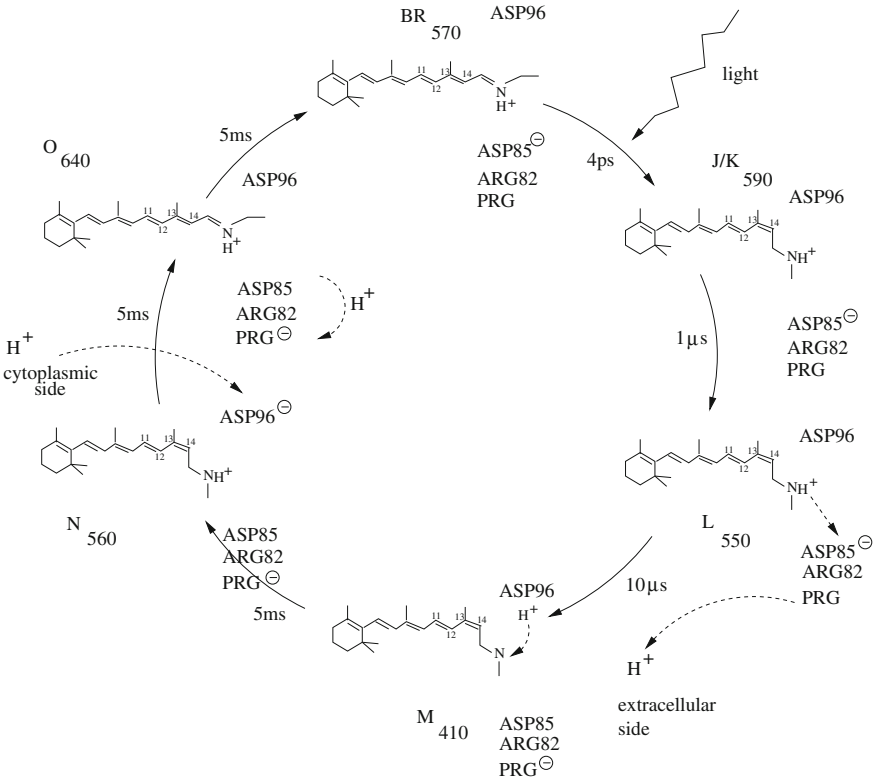

Fig. 27.3 The photocycle of bacteriorhodopsin [156]. Different states are labeled by the corresponding absorption maximum (nm)

Fig. 27.4 Photoisomerization of bR

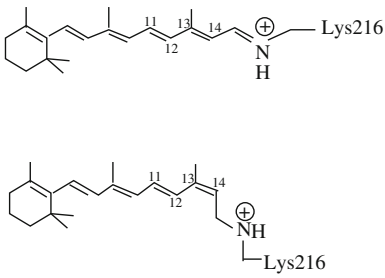

Bacteriorhodopsin is the simplest known natural photosynthetic system. Retinal is covalently bound to a lysine residue forming the so-called protonated Schiff base. This form of the protein absorbs sun light very efficiently over a large spectral range (480–360 nm).

After photoinduced isomerization a proton is transferred from the Schiff base to the negatively charged ASP85 ($L \rightarrow M$). This induces a large blue shift. In wild

type bR, under physiological conditions, a proton is released into the extracellular medium on the same timescale of 10 μs. The proton release group is believed to consist of GLU194, GLU204, and some structural waters. During the M state, a large rearrangement on the cytoplasmatic side appears, which is not seen spectroscopically and which induces the possibility to reprotonate the Schiff base from ASP96 subsequently ($M \rightarrow N$). ASP96 is then reprotonated from the cytoplasmatic side and the retinal reisomerizes thermally to the all trans configuration ($N \rightarrow O$). Finally, a proton is transferred from ASP85 via ARG82 to the release group and the ground state BR is recovered.

27.2 Born–Oppenheimer Separation

Protons move on a faster time scale than the heavy nuclei but are slower than the electrons. Therefore, we use a double BO approximation for the wavefunction[1]

$$\psi(r, R_P, Q)\chi(R_p, Q)\Phi(Q). \tag{27.1}$$

The protonic wavefunction χ depends parametrically on the coordinates Q of the heavy atoms and the electronic wavefunction ψ depends parametrically on all nuclear coordinates. The Hamiltonian consists of the kinetic energy contributions and a potential energy term

$$H = T_{el} + T_p + T_N + V. \tag{27.2}$$

The Born–Oppenheimer approximation leads to the following hierarchy of equations. First all nuclear coordinates (R_p, Q) are fixed and the electronic wavefunction of the state s is obtained from

$$(T_{el} + V(r, R_p, Q))\psi_s(r, R_p, Q) = E_{el,s}(R_p, Q)\psi_s(r, R_p, Q). \tag{27.3}$$

In the second step, only the heavy atoms (Q) are fixed but the action of the kinetic energy of the proton on the electronic wavefunction is neglected. Then the wavefunction of proton state n obeys

$$(T_p + E_{el,s}(R_p, Q))\chi_{s,n}(R_p, Q) = \varepsilon_{s,n}(Q)\chi_{s,n}(R_p, Q). \tag{27.4}$$

The electronic energy $E_{el}(R_p, Q)$ plays the role of a potential energy surface for the nuclear motion. It is shown schematically in Fig. 27.5 for one proton coordinate (for instance the O-H bond length) and one promoting mode of the heavy atoms which modulates the energy gap between the two minima.

[1] The Born-Oppenheimer approximation and the nonadiabatic corrections to it are discussed more systematically in Sect. 17.1.

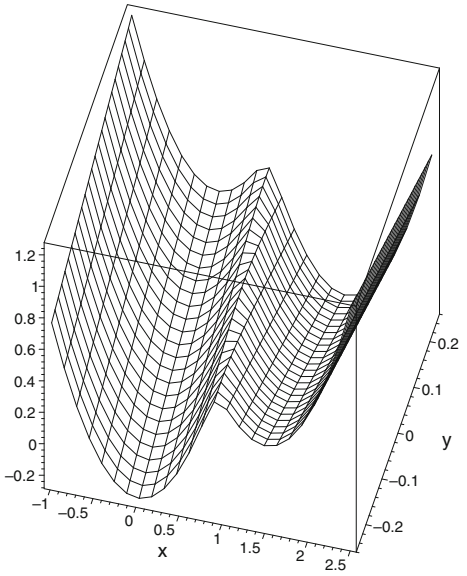

Fig. 27.5 Proton transfer potential. The figure shows schematically the potential which, as a function of the proton coordinate x, has two local minima corresponding to the structures $\cdots N - H \cdots O \cdots$ and $\cdots N \cdots H - O \cdots$ and which is modulated by a coordinate y representing the heavy atoms

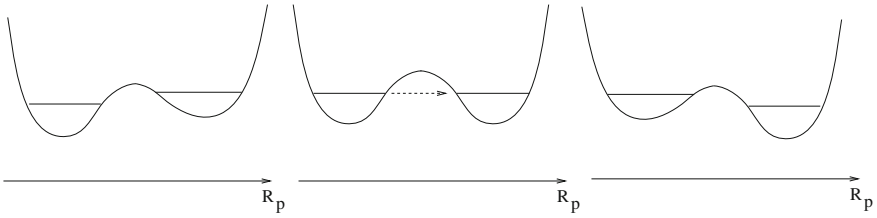

Fig. 27.6 Proton tunneling. The double well of the proton along the H-bond is shown schematically for different configurations of the reaction complex

For fixed positions Q of the heavy nuclei $E_{el}(R_p, Q)$ has a double well structure as shown in Fig. 27.6. The rate of proton tunneling depends on the configuration and is most efficient if the two localized states are in resonance.

Finally, the wavefunction of the heavy nuclei in state α is the approximate solution of

$$(T_N + \varepsilon_{s,n}(Q))\Phi_{s,n,\alpha}(Q) = E_{s,n,\alpha}\Phi_{s,n,\alpha}(Q). \tag{27.5}$$

27.3 Nonadiabatic Proton Transfer (Small Coupling)

Initial and final states (s, n) and (s', m) are stabilized by the reorganization of the heavy nuclei. The transfer occurs whenever fluctuations bring the two states in resonance.

We use the harmonic approximation (Fig. 27.7)

$$\varepsilon_{s,n}(Q) = \varepsilon_{s,n}^{(0)} + \frac{a}{2}(Q - Q_s^{(0)})^2 + \cdots = \varepsilon_{s,0}(Q) + (\varepsilon_{s,n} - \varepsilon_{s,0}) \tag{27.6}$$

similar to nonadiabatic electron transfer theory (Chap. 16). The activation free energy for the $(s, 0) \to (s', 0)$ transition is given by

$$\Delta G_{00}^{\ddagger} = \frac{(\Delta G_0 + E_R)^2}{4E_R} \tag{27.7}$$

and for the transition $(s, n) \to (s', m)$ we have approximately

$$\begin{aligned} \Delta G_{nm}^{\ddagger} &= \Delta G_0^{\ddagger} + (\varepsilon_{sm} - \varepsilon_{s0}) - (\varepsilon_{s'n} - \varepsilon_{s'0}) \\ &= \frac{(\Delta G_0 + E_R + \varepsilon_{sm} - \varepsilon_{s'n} - \varepsilon_{s0} + \varepsilon_{s'0})^2}{4E_R}. \end{aligned} \tag{27.8}$$

The partial rate k_{nm} is given in analogy to the ET rate (16.23) as

$$k_{nm} = \frac{\omega}{2\pi} \kappa_{nm}^{P} \exp\left\{ -\frac{\Delta G_{nm}^{\ddagger}}{kT} \right\}. \tag{27.9}$$

The interaction matrix element will be calculated using the BO approximation and treating the heavy nuclei classically

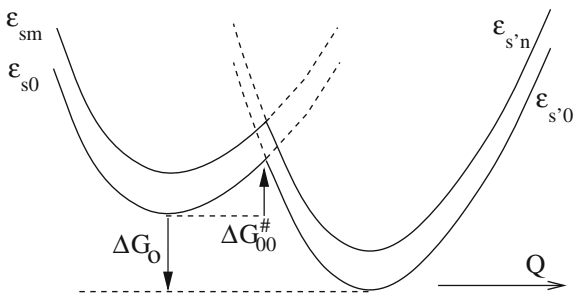

Fig. 27.7 Harmonic model for proton transfer

$$V_{sns'm} = \int dr\, dR_p\, \psi_s(r, R_P, Q)\chi_{sn}(R_p, Q) \quad V \quad \chi_{s'm}(R_p, Q)\psi_{s'}(r, R_P, Q)$$
$$= \int dR_p \left(\int dr\, \psi_s(r, R_P, Q) V \psi_{s'}(r, R_P, Q) \right) \chi_{sn}(R_p, Q)\chi_{s'm}(R_p, Q)$$
$$= \int dR_p V^{el}_{ss'}(R_p, Q)\, \chi_{sn}(R_p, Q)\chi_{s'm}(R_p, Q).$$

The electronic matrix element

$$V^{el}_{ss'} = \int \psi_s(r, R_p, Q) V \psi_{s'}(r, R_p, Q) dr \tag{27.10}$$

is expanded around the equilibrium position of the proton R^*_p

$$V^{el}_{ss'}(R_p, Q) \approx V^{el}_{ss'}(R^*_P, Q) + \cdots \tag{27.11}$$

and we have approximately

$$V_{sns'm} \approx V^{el}_{ss'}(R^*_P, Q) S^{nm}_{ss'}(Q) \tag{27.12}$$

with the overlap integral of the protonic wavefunctions (Franck–Condon factor)

$$S^{nm}_{ss'}(Q) = \int \chi_{sn}\chi_{s'm} dR_p. \tag{27.13}$$

27.4 Strongly Bound Protons

The frequencies of O-H or N-H bond vibrations are typically in the range of 3000 cm^{-1} which is much larger, than thermal energy. If on the other hand, the barrier for proton transfer is on the same order, only the transition between the vibrational ground states is involved. For small electronic matrix element V^{el}, the situation is very similar to electron transfer described by Marcus theory (Chap. 16) and the reaction rate is given by [157] for symmetrical proton transfer ($E_R \gg \Delta G_0$, $\Delta G^{\ddagger}_{00} = E_R/4$)

$$k = \frac{2\pi V_0^2}{\hbar} \sqrt{\frac{1}{4\pi k T E_R}} \exp\left(-\frac{E_R}{4kT} \right). \tag{27.14}$$

In the derivation of (27.14), the Condon approximation has been used which corresponds to application of (27.11) and approximation of the overlap integral (27.13) by a constant value. However, for certain modes (which influence the distance of the two potential minima), the modulation of the coupling matrix element can be much stronger than in the case of electron transfer processes due to the larger mass of the

proton. The dependence on the transfer distance $\delta Q = Q_{s'}^{(0)} - Q_s^{(0)}$ is approximately exponential

$$V_{s0s'0} \sim \mathrm{e}^{-\alpha \delta Q} \tag{27.15}$$

where typically $\alpha \approx 25 \cdots 35 A^{-1}$ whereas for electron transfer processes typical values are around $\alpha \approx 0.5 \cdots 1 A^{-1}$. Borgis and Hynes [157] found the following result for the rate when the low-frequency substrate mode with frequency Ω and reduced mass M is thermally excited

$$k = \frac{2\pi < V^2 >}{\hbar} \sqrt{\frac{1}{4\pi k T 4 \Delta G_{tot}}} \exp\left(-\frac{\Delta G_{tot}}{kT}\right) \chi_{SC} \tag{27.16}$$

where the average coupling square can be expanded as

$$< V^2 >= V_0^2 \exp\left(\frac{\hbar \alpha^2}{2M\Omega}\left\{\frac{4kT}{\hbar\Omega} + \frac{\hbar\Omega}{3kT} + O\left(\left(\frac{\hbar\Omega}{kT}\right)^2\right)\right\}\right) \tag{27.17}$$

the activation energy is

$$\Delta G_{tot} = \Delta G^{\ddagger} + \frac{\hbar^2 \alpha^2}{8M} \tag{27.18}$$

and the additional factor χ_{SC} is given by

$$\chi_{SC} = \exp\left(\gamma_{SC}\left(1 - \frac{\gamma_{SC} kT}{4\Delta G_{tot}}\right)\right) \tag{27.19}$$

$$\gamma_{SC} = \frac{\alpha < D >}{M\Omega^2} \tag{27.20}$$

where

$$D = \frac{\partial \Delta H}{\partial Q}(Q_0) \tag{27.21}$$

measures the modulation of the energy difference by the promoting mode Ω.

27.5 Adiabatic Proton Transfer

If V^{el} is large and the tunnel factor approaches unity (for s=s'), then the application of the low friction result (8.28) gives

$$k_{nm} = \frac{\omega}{2\pi} \exp\left\{-\frac{\Delta G^{\ddagger ad}_{nm}}{kT}\right\}$$

where the activation energy has to be corrected by the tunnel splitting

$$\Delta G^{\ddagger ad}_{nm} = \Delta G^{\ddagger}_{nm} - \frac{1}{2}\Delta \varepsilon^{p}_{nm}$$

Chapter 28
Proton Coupled Coherent Charge Transfer

Photosynthetic reaction centers perform light induced charge separation over a membrane with a high quantum yield of 95%. Since the structure of the membrane complex of the bacterial reaction center of Rps. viridis has been resolved, by Michel, Deisenhofer and Huber (Nobel prize 1985), it became a great challenge to resolve the observed dynamics on the basis of the structure information. The ongoing research in the field is motivated by the hope to learn from nature, how to improve the efficiency of artificial solar cells. We start with the so called step model, where the transfer to the primary stable acceptor proceeds via an intermediate in terms of two nonadiabatic electron transfer rate processes. In the second part we provide information on the involvement of reversible proton shifts, which modulates the electronic coupling via adiabatic delocalization of hole states. Finally we simulate coherence effects, which support the more complex model of coherently modulated superexchange.

28.1 The Nonadiabatic Electronic Incoherent Step Transfer Model

In Fig. 28.1 the prosthetic molecules are shown together with experimental transfer times. Most notable is the inverted ordering with the first transfer step between the excited special pair dimer P, consisting of the two bacteriochlorophylls P_L and P_M to the so named accessory bacteriochlorophyll monomer B_L, being about four times slower than the second step to the bacteriopheophytine H_L. This inverted-kinetics model explains many features of the time resolved spectra. In this section we want to test to what extent our knowledge of the spectral function is capable to simulate the observed temperature dependence and magnitude of the two postulated rate processes $P^* \rightarrow P^+ B_L^-$ and $B_L^- \rightarrow H_L^-$.

P.O.J. Scherer and S.F. Fischer, *Theoretical Molecular Biophysics*,
Biological and Medical Physics, Biomedical Engineering,
DOI 10.1007/978-3-662-55671-9_28

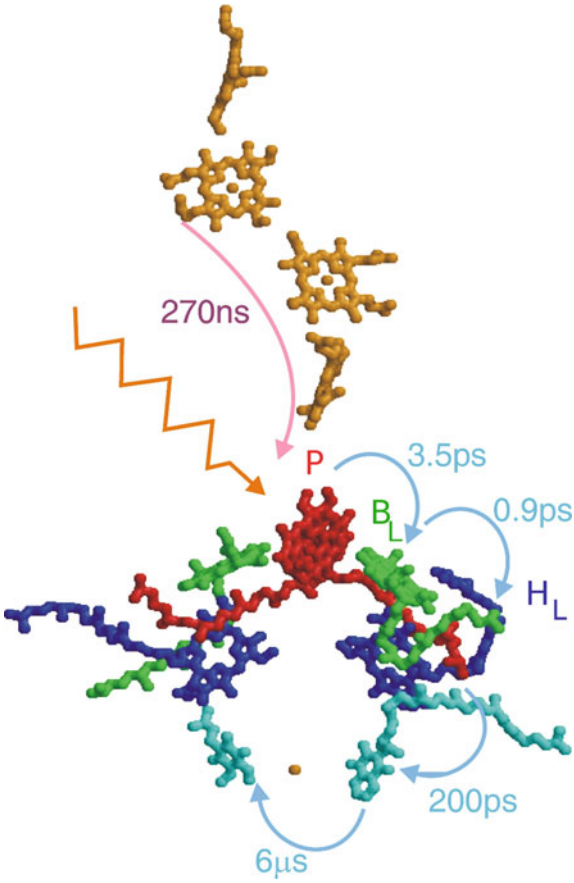

Fig. 28.1 Electron transfer processes in the reaction center of bacterial photosynthesis. After photo-excitation of the special pair dimer P an electron is transferred to bacteriopheophytine H_L in few picoseconds via bacteriochlorophyll B_L. The electron is then transferred on a longer time scale to quinone Q_A and finally to Q_B via a non-heme ferrous ion. The electron hole in the special pair is filled by an electron from the hemes of the cytochrome c (*orange*). After a second excitation of the dimer another electron is transferred via the same route to the semiquinone to form ubiquinone which then diffuses freely within the membrane. The figure was created with rasmol [140] based on the structure of rps.viridis [61–64] from the protein data bank [138, 139]

28.1.1 The Rate Expression

We discuss a model for biological systems where the density of vibrational states is very high. The vibrational modes which are coupled to the electronic transition[1] are treated within the model of displaced parallel harmonic oscillators (Chap. 19). This gives the following approximation to the diabatic potential surfaces

$$E_i = E_i^0 + \sum_r \frac{\omega_r^2}{2} q_r^2 \tag{28.1}$$

[1] which have different equilibrium positions in the two states |i> and |f>.

$$E_f = E_f^0 + \sum_r \frac{\omega_r^2}{2}(q_r - \Delta q_r)^2 \tag{28.2}$$

and the energy gap

$$E_f - E_i = \Delta E + \sum_r \frac{(\omega_r \Delta q_r)^2}{2} - \sum_r \omega_r^2 \Delta q_r q_r. \tag{28.3}$$

The total reorganization energy is the sum of all partial reorganization energies

$$E_R = \sum_r \frac{(\omega_r \Delta q_r)^2}{2} = \sum_r g_r^2 \hbar \omega_r \tag{28.4}$$

with the vibronic coupling strength

$$g_r = \sqrt{\frac{\omega_r}{2\hbar}} \Delta q_r. \tag{28.5}$$

The golden rule expression gives the rate for nonadiabatic electron transfer in analogy to (18.40)

$$\begin{aligned} k_{et} &= \frac{2\pi V^2}{\hbar} \sum_{n_r n_{r'}} P(\{n_r\}) \prod_r (FC_r(n_r, n_{r'}))^2 \delta\left(\Delta E + \sum_r \hbar\omega_r (n_{r'} - n_r)\right) \\ &= \frac{2\pi V^2}{\hbar} FCD(\Delta E) \end{aligned} \tag{28.6}$$

where the Franck Condon weighted density of states $FCD(\Delta E)$ can be expressed with the help of the time correlation formalism (Sect. 18.4) as

$$\begin{aligned} FCD(\Delta E) &= \frac{1}{2\pi\hbar} \int dt\, \mathrm{e}^{-\mathrm{i}t\Delta E/\hbar} F(t) \\ F(t) &= \prod_r \exp\left(g_r^2 (\mathrm{e}^{\mathrm{i}\omega_r t} - 1)(\overline{n_r} + 1) + (\mathrm{e}^{-\mathrm{i}\omega_r t} - 1)\overline{n_r}\right) \end{aligned} \tag{28.7}$$

with the average occupation numbers

$$\overline{n_r} = \frac{1}{\mathrm{e}^{\hbar\omega_r/k_B T} - 1}. \tag{28.8}$$

Quantum chemical calculations for the reaction center [158–161] put the electronic coupling in the range of $V = 5 \cdots 50\,\mathrm{cm}^{-1}$ for the first step $P^* \to P^+B^-$ and $V = 15 \cdots 120\,\mathrm{cm}^{-1}$ for the second step $P^+B^- \to P^+H^-$. For a rough estimate we take a reorganization energy of $2000\,\mathrm{cm}^{-1}$ and a maximum of the Franck Condon weighted density of states $FCD \approx 1/2000\,\mathrm{cm}^{-1}$ yielding an electronic coupling

of $V = 21\,\mathrm{cm}^{-1}$ for the first (3.5 psec) and $V = 42\,\mathrm{cm}^{-1}$ for the second (0.9 psec) step in quite good agreement with the calculations.

28.1.2 Application of the Saddle Point Method

The main contributions to the reorganization energy for forming the anions B_L^- and H_L^- originate from coupling to internal vibrations of the chromophores which show a peculiar behavior due to the quasi 2-dimensionality of the $\pi-$electron systems. We performed ab initio (631G/HF) calculations [117] to evaluate vibronic coupling parameters and partial reorganization energies. The density of normal modes is roughly constant $\rho(\hbar\omega) =< \sum_j \delta(\hbar\omega - \hbar\omega_j) >\approx \rho_0$ between $30 \ldots 2000\,\mathrm{cm}^{-1}$ (Fig. 17.3), as well as the distribution of partial reorganization energies $\lambda(\hbar\omega) =< \sum_j \lambda_j \delta(\hbar\omega - \hbar\omega_j) >\approx \lambda_0\rho_0$. Correspondingly, the distribution of $g^2(\hbar\omega) = \lambda(\hbar\omega)/\hbar\omega \propto \hbar\omega^{-1}$ and its integral can be fitted by a logarithmic dependence (Figs. 28.2, 28.3)

$$< \sum_j g_j^2 \theta(\hbar\omega - \hbar\omega_j) > \approx \int_{\hbar\omega_{min}}^{\hbar\omega} \frac{\lambda_0\rho_0}{\hbar\omega} d(\hbar\omega) = \lambda_0\rho_0 \ln \frac{\hbar\omega}{\hbar\omega_{min}}. \tag{28.9}$$

Since we are dealing with a multi mode system with intermediate strong couplings the application of the saddle point method is advisable [162]. However, we have to exclude those modes as energy acceptors, whose quanta exceed the free energy change. They must be factored out as 0–0 Franck Condon overlaps. That means, the reorganization energy involved in the dynamics becomes energy dependent due to the quantum effect of the high frequency modes. So we get for the case $kT < \Delta G < \hbar\omega_{max}$ with

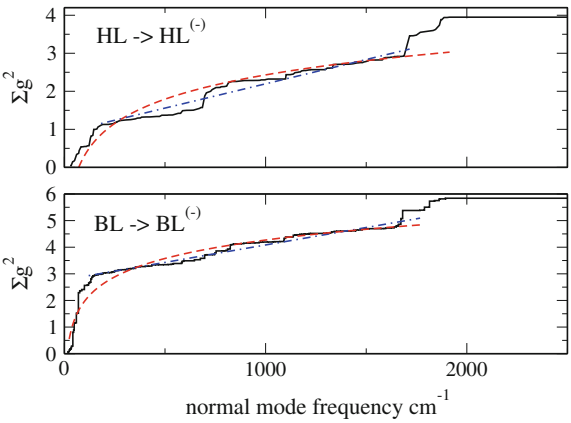

Fig. 28.2 Calculated distribution of vibronic couplings for BChl and BPh. The *dashed curve* shows a logarithmic fit of the cumulative distribution of g^2, the *dash dotted curve* shows a linear fit for comparison

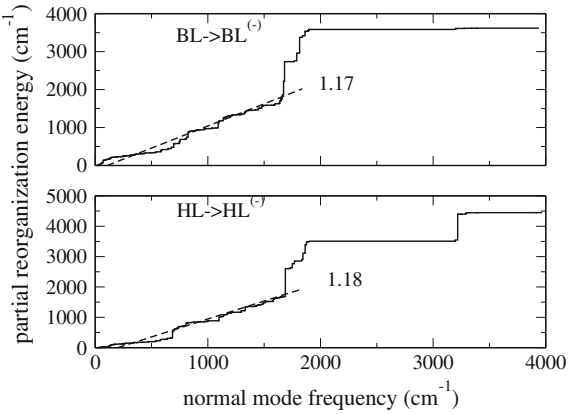

Fig. 28.3 Distribution of reorganization energies for BChl and BPh. The *dashed curve* shows a linear fit of the cumulative distribution of $\lambda = \hbar\omega g^2$

$$\Delta G = \Delta_0 + \sum_j \hbar\omega_j g_j^2 \tag{28.10}$$

and

$$g^2(\Delta G) = \sum_{\omega_j > \Delta G} g_j^2 = \int_{\Delta G}^{\hbar\omega_{max}} d(\hbar\omega)\, \frac{\rho_0 \lambda_0}{\hbar\omega} = \rho_0 \lambda_0 \ln \frac{\hbar\omega_{max}}{\Delta G} \tag{28.11}$$

corresponding to

$$\mathrm{e}^{-g^2(\Delta G)} = \left(\frac{\Delta G}{\hbar\omega_{max}}\right)^{\rho_0\lambda_0} \tag{28.12}$$

the following rate expression

$$\begin{aligned} k &= \frac{V^2}{\hbar^2}\left(\frac{\Delta G}{\hbar\omega_{max}}\right)^{\rho_0\lambda_0} \int_{-\infty}^{\infty} dt\, \exp\left\{-\mathrm{i}\frac{\Delta G t}{\hbar}\right. \\ &\quad \left. + \int_0^{\Delta G} dE\, \rho_0 \frac{\lambda_0}{E}\left[(n(E)+1)(\mathrm{e}^{\mathrm{i}\frac{E}{\hbar}t} - 1) + n(E)(\mathrm{e}^{-\mathrm{i}\frac{E}{\hbar}t} - 1)\right]\right\} \\ &= \frac{V^2}{\hbar^2}\left(\frac{\Delta G}{\hbar\omega_{max}}\right)^{\rho_0\lambda_0} \int_{-\infty}^{\infty} dt\, \exp\left\{-\mathrm{i}t\frac{\Delta G}{\hbar} + f(t)\right\}. \end{aligned} \tag{28.13}$$

The equation for the saddle point t_s reads

$$0 = -\frac{\mathrm{i}\Delta G}{\hbar} + \frac{\mathrm{d}f(t)}{\mathrm{d}t} = -\frac{\mathrm{i}\Delta G}{\hbar} + \int_0^{\Delta G} dE\, \rho_0 \frac{\lambda_0}{E}\left[(n(E)+1)\mathrm{i}\frac{E}{\hbar}\mathrm{e}^{\mathrm{i}\frac{E}{\hbar}t_s} - n(E)\mathrm{i}\frac{E}{\hbar}\mathrm{e}^{-\mathrm{i}\frac{E}{\hbar}t_s}\right] \tag{28.14}$$

which we can linearize in $E/\hbar t_s$ for $kT < \Delta G < \hbar\omega_m$ and $\rho_0\lambda_0$ to get

$$-\frac{\mathrm{i}\Delta G}{\hbar} + \frac{\mathrm{i}}{\hbar}\rho_0\lambda_0\Delta G + \frac{\mathrm{i}t_s}{2\hbar^2}\rho_0\lambda_0\Delta G^2 + 2\frac{\mathrm{i}t_s}{\hbar^2}\rho_0\lambda_0\int_0^{\Delta G} dE\ n(E) = 0. \tag{28.15}$$

With the solution for the saddle point

$$\frac{t_s}{\hbar} = \frac{2\Delta G(1-\rho_0\lambda_0)}{\rho_0\lambda_0\left(\Delta G^2 + 4\int_0^{\Delta G} dE\, E\, n(E)\right)} \tag{28.16}$$

the second derivative of f is

$$\begin{aligned}\frac{\mathrm{d}^2 f}{\mathrm{d}t^2} &= -\frac{\rho_0\lambda_0}{\hbar^2}\int_0^{\Delta G} dE\, E\left[\mathrm{e}^{\mathrm{i}\frac{E}{\hbar}t}(n(E)+1) + \mathrm{e}^{\mathrm{i}\frac{E}{\hbar}t}n(E)\right] \\ &\approx -\frac{\rho_0\lambda_0}{\hbar^2}\int_0^{\Delta G} dE\, E\,(2n(E)+1) = \frac{\rho_0\lambda_0}{\hbar^2}\left(\frac{\Delta G^2}{2} + 2\int_0^{\Delta G} dE\, n(E)\, E\right).\end{aligned} \tag{28.17}$$

The integral over $n(E)E$ can be approximated for $\Delta G > 2k_BT$ with an error not exceeding 10% by

$$\int_0^{\infty} dE\, n(E)E = (k_BT)^2\frac{\pi^2}{6}. \tag{28.18}$$

So we find

$$\frac{\mathrm{d}^2 f}{\mathrm{d}t^2} \approx -\frac{\rho_0\lambda_0}{\hbar^2}\left(\frac{\Delta G^2}{2} + \frac{\pi^2}{3}(k_BT)^2\right) \tag{28.19}$$

and

$$t_s/\hbar = -\frac{2\Delta G(1-\rho_0\lambda_0)}{\rho_0\lambda_0\left(\Delta G^2 + \frac{2}{3}\pi^2(k_BT)^2\right)}. \tag{28.20}$$

Performing the Gauss-integration around the saddle point t_s gives the result in algebraic form

$$\begin{aligned}k &= \frac{V^2}{\hbar^2}\left(\frac{\Delta G}{\hbar\omega_{max}}\right)^{\rho_0\lambda_0}\exp\left\{-\mathrm{i}t\frac{\Delta G}{\hbar} + f(t_s)\right\}\sqrt{\frac{2\pi}{|f''(t_s)|}} \\ &= \frac{V^2}{\hbar^2}\left(\frac{\Delta G}{\hbar\omega_{max}}\right)^{\rho_0\lambda_0}\sqrt{\frac{2\pi\hbar^2}{\rho_0\lambda_0\left(\frac{\Delta G^2}{2} + \frac{\pi^2}{3}(k_BT)^2\right)}}\exp\left\{-\frac{\Delta G^2(1-\rho_0\lambda_0)^2}{\rho_0\lambda_0\left(\frac{\Delta G^2}{2} + \frac{1}{3}\pi^2(k_BT)^2\right)}\right\}.\end{aligned} \tag{28.21}$$

It holds for $2k_BT < \Delta G < \hbar\omega_{max}$ and gives for the special case

$$\rho_0\lambda_0 = 1$$

$$k = \frac{V^2}{\hbar}\left(\frac{\Delta G}{\hbar\omega_{max}}\right)\sqrt{\frac{2\pi}{\left(\frac{\Delta G^2}{2} + \frac{\pi^2}{3}(k_BT)^2\right)}}. \tag{28.22}$$

For $\Delta E = 0$ corresponding to $\Delta G = \rho_0\lambda_0\hbar\omega_{max}$ and $\hbar\omega_{max} \gg k_BT$ the result has the simple form

$$k = \frac{2\sqrt{\pi}}{(\rho_0\,\lambda_0)^{3/2}}\frac{V^2}{\hbar^2\omega_{\max}}\exp\left\{-\frac{2(1-\rho_0\lambda_0)^2}{\rho_0\lambda_0}\right\}. \tag{28.23}$$

The expression (28.21) applies to non adiabatic electron transfer between large molecules with a coupling to a quasi dense set of vibrations reminiscent of a two dimensional solid. The constant density together with the equally distributed reorganization energies lead to a very specific dependence on the free energy change and on temperature. For low temperatures ($2k_BT < \Delta G$) and $\Delta G < \hbar\omega_{max}$, $\ln k$ shows a long plateau as a function of ΔG between $\Delta G = k_BT$ and $\hbar\omega_{\max}$ instead of the classical bell shape structure. The rate is almost temperature independent in this regime, with a tendency of weak temperature inversion. The inversion regime is most extended for the special coupling case $\rho_0\lambda_0 = 1$. For very large values $\Delta G \gg \hbar\omega_{\max} \gg k_BT$ the rate follows an energy gap law [163]

$$k = \frac{2\sqrt{\pi}}{(\rho_0\,\lambda_0)^{3/2}}\frac{V^2}{\hbar^2\,\omega_{\max}}\exp\left\{-\frac{\Delta G}{\hbar\omega_{\max}}\ln\left(\frac{\Delta G}{\hbar\,\omega_{\max}\,\rho_0\lambda_0}\right) - \frac{2(1-\rho_0\,\lambda_0)^2}{\rho_0\,\lambda_0}\right\}. \tag{28.24}$$

We can extend the algebraic expression (28.21) into the range $0 < \Delta G < 2k_BT$ approximately by replacing in (28.7) the lower cut-off energy ΔG by $\Delta G + 2k_BT$. This leads to the following rate equation for $0 < \Delta G < \hbar\omega_{\max} + 2k_BT$:

$$k = \frac{V^2}{\hbar^2}\left(\frac{\Delta G + 2k_BT}{\hbar\omega_{max}}\right)^{\rho_0\lambda_0}\sqrt{\frac{2\pi\hbar 2}{\rho_0\lambda_0\left(\frac{(\Delta G+2k_BT)^2}{2} + \frac{\pi^2}{3}(k_BT)^2\right)}}\times$$
$$\times\exp\left\{-\frac{(\Delta G(1-\rho_0\lambda_0) - 2k_BT\rho_0\lambda_0)^2}{\rho_0\lambda_0\left(\frac{(\Delta G+2k_BT)^2}{2} + \frac{1}{3}\pi^2(k_BT)^2\right)}\right\}. \tag{28.25}$$

The analytic approximation (28.25) can be used to simulate the rates for the step model on the basis of calculations for the partial reorganization energies and

calculated couplings. This approach has to be extended if one considers mutants. For instance, a weak dependence of the charge separation process on ΔG and on T has been found for mutants [164] which differ substantially in their redox potentials, but which are insensitive towards changes in their rates, contrary to predictions based on the energy gap law. This stability against changes in ΔG is certainly an evolutionary advantage to assure a robust functioning. Also the strong suppression of recombination and the universal activationless rates need better understanding.

28.2 Heterogeneous Superexchange Coupling

Heterogeneities are well documented by stimulated emission from P* [165]. Here we want to concentrate on their influence on the superexchange coupling. We consider electronic superexchange coupling V_s between the donor P* and the acceptor $P^+H_L^-$, bridged by the intermediate $P^+B_L^-$. We get for the coupling squared

$$V_s^2 = \varphi^2\, V'^2 = \frac{2V^2}{\Delta^2 + 4\,V^2 + \mid \Delta \mid \sqrt{\Delta^2 + 4\,V^2}}\; V'^2\,. \tag{28.26}$$

This expression results from the diagonalization of the 2×2 electronic Hamiltonian of the states P* and $P^+B_L^-$. With $V = V(P^+B_L, P^*)$ and $V' = V(P^+B_L, P^+H_L^-)$ and P^+H_L, Δ is the zero order energy difference between $P^+B_L^-$ and P^* prior to diagonalization, and φ is the $P^+B_L^-$ -component of that eigenstate which lies in energy closer to the initially excited donor. Implying a vibrational quasi-continuum of acceptor states we obtain the superexchange rate

$$k_\Delta = \frac{2\pi}{\hbar}\, V_s^2\, \mathrm{FCD}\,, \tag{28.27}$$

with the Franck-Condon weighted density FCD corresponding to the true energy release ΔG between P* and $P^+H_L^-$. Inserting here V_s^2 from (28.26) and introducing the rate

$$k = \frac{2\,\pi}{\hbar}\, V'^2\, \mathrm{FCD} \tag{28.28}$$

we get for Δ-dependent rate

$$k_\Delta = \frac{2V^2}{\Delta^2 + +4\,V^2 + \mid \Delta \mid \sqrt{\Delta^2 + 4\,V^2}}\; k\,. \tag{28.29}$$

This expression contains the common superexchange rate for large values of the energy spacing between $P^+B_L^-$ and P^*. If one neglects V in the denominator, k_Δ goes over into $(V^2/\Delta^2)k$ with Δ replaced by its average Δ_c.

So far we did not include vibrational degrees of freedom explicitly in the energy denominator for the heterogeneous components of our distribution. The slow vibrations with $\omega_j < k_\Delta$ contribute actually to our distribution, and the faster may be averaged by arguments given in [166], as long as the superexchange limit $\Delta > V$ is realized. For the near resonance components we still use the superexchange coupling expression, since we treat the interaction in a non perturbative way. This treatment differs in that respect from the resonance Raman model with slow vibrational relaxation of Sumi and Kakitani [167].

The width of CT states is around 0.1 eV [168]. It is mainly due to heterogeneous broadening. We will show how this modifies the transfer dynamics. The effect is particularly strong for near resonance superexchange processes, since small variations of near resonance intermediate energy gaps have a large effect on the transfer rate. Considering a Gaussian distribution $G(\Delta)$ with mean value Δ_c (the subscript 'c' stands for 'center') and with the rms deviation σ from Δ_c,

$$G(\Delta) = (2\pi\,\sigma^2)^{-1/2}\,\exp\left\{-\frac{(\Delta-\Delta_c)^2}{2\sigma^2}\right\} \tag{28.30}$$

we get the following expression for the dispersive decay of the initially excited state

$$P(t) = \int_{-\infty}^{\infty} G(\Delta)\mathrm{e}^{-k_\Delta t}\,d\Delta = (2\pi\,\sigma^2)^{-1/2}\int_{-\infty}^{\infty}\exp\left\{-\frac{(\Delta-\Delta_c)^2}{2\sigma^2}-k_\Delta t\right\}d\Delta\,. \tag{28.31}$$

If we introduce the dimensionless quantities

$$v = \frac{V}{\sigma},\quad \delta = \frac{\Delta}{\sigma} \tag{28.32}$$

and consider the typical ordering small $v\,(\lesssim 0.5)$ and $\delta \gtrsim v$, P(t) can be approximated within error less than 10% by

$$P(t) = \exp\left\{-\mathrm{e}^{-\delta^2/2}\,\frac{v\,kt}{1+\sqrt{kt}} - \frac{\delta\,v^2\,kt}{\delta^3+2\,v\,\sqrt{kt}}\right\}. \tag{28.33}$$

In the short time limit $kt < \min(1, \delta^6 v^{-2}/4)$ we find an exponential decay with the initial rate k_i

$$k_i = k_{\mathrm{nr}} + k_s = \mathrm{e}^{-\delta^2/2}\,v\,k + \frac{v^2}{\delta^2}\,k. \tag{28.34}$$

The first term, $k_{\rm nr}$, is the rate of a system which has the states P* and $P^+B_L^-$ in near resonance ($v/\delta \leq 1$), and the second term, k_s, is the superexchange rate for a large central gap ($v/\delta \ll 1$). In the long time limit $kt > \max(1, \delta^6 v^{-2}/4)$, we get from (28.33)

$$P(t) = \exp\left\{-\left(\mathrm{e}^{-\delta^2/2} + \frac{\delta}{2}\right) v\sqrt{kt}\right\}. \tag{28.35}$$

The first term in k_{nr} dominates for $kt < 1$, $k_{nr} > k_s$ and $v < \delta < 1$, which can be expressed in terms of the original quantities V, Δ and σ as

$$V < \mid \Delta_c \mid \lesssim \sigma. \tag{28.36}$$

The rate $k_{\rm nr}$ is proportional to $vk = (V/\sigma)k$. To understand this dependence, we consider the distribution $\tilde{G}(\tilde{\Delta})$ of the ('real') energy gap $\tilde{\Delta}$, which originates from the diagonalization of the electronic Hamiltonian of $P^+B_L^-$ and P^*,

$$\tilde{G}(\tilde{\Delta}) = G(\Delta) \mid \frac{\mathrm{d}\Delta}{\mathrm{d}\tilde{\Delta}} \mid \tag{28.37}$$

with

$$\tilde{\Delta} = \mathrm{sign}(\Delta)\sqrt{\Delta^2 + 4\,V^2}. \tag{28.38}$$

Distinguishing between cases, with the energy of the intermediate state lying above or below the energy of the donor state, respectively (subscripts '+' and '–'), we consider the restrictions of $\tilde{G}(\tilde{\Delta})$ on the positive and negative $\tilde{\Delta}$- half axes $\tilde{G}_+(\tilde{\Delta})$ and $\tilde{G}_-(\tilde{\Delta})$,

$$\tilde{G}(\tilde{\Delta}) = \begin{cases} \tilde{G}_+(\tilde{\Delta}) \text{ for } \tilde{\Delta} > 0 \\ \tilde{G}_-(\tilde{\Delta}) \text{ for } \tilde{\Delta} < 0 \end{cases}. \tag{28.39}$$

Using (28.37) and (28.30) together with the inversion of (28.38) for Δ,

$$\Delta = \mathrm{sign}\tilde{\Delta}\sqrt{\tilde{\Delta}^2 - 4\,V^2} \tag{28.40}$$

where $\mid \tilde{\Delta} \mid \geq 2\,\mathrm{V}$, we obtain the distributions of the signed energy gap $\tilde{\Delta}$,

$$\tilde{G}_\pm(\tilde{\Delta}) = \frac{1}{\sqrt{2\pi}\sigma} \frac{\mid \tilde{\Delta} \mid}{\sqrt{\tilde{\Delta}^2 - 4\,V^2}} \exp\left\{-\frac{(\pm\sqrt{\tilde{\Delta}^2 - 4V^2} - \Delta_c)^2}{2\sigma^2}\right\} \tag{28.41}$$

as well as the respective contributions $P_\pm(t)$ to the donor decay function

$$P(t) = P_+(t) + P_-(t) \tag{28.42}$$

$$P_{\pm}(t) = \int_{2V}^{\infty} \tilde{G}_{\pm}(\tilde{\Delta}) \exp\left\{-k_{\Delta}(\tilde{\Delta})\, t\right\} d\tilde{\Delta}. \tag{28.43}$$

The $\tilde{\Delta}$-dependence of k_{Δ} results by substituting Δ from (28.40) into (28.29),

$$k_{\Delta}(\tilde{\Delta}) = \frac{2\,V^2}{\tilde{\Delta}^2 + \mid \tilde{\Delta} \mid \sqrt{\tilde{\Delta}^2 - 4\,V^2}}\; k. \tag{28.44}$$

We can evaluate now the average superexchange rate $\bar{k}$ expressed in terms of the energy gap $\tilde{\Delta}$,

$$\bar{k} = \int_{2V}^{\infty} [k_{\Delta}(\tilde{\Delta})\, \tilde{G}_{+}(\tilde{\Delta}) + k_{\Delta}(\tilde{\Delta})\, \tilde{G}_{-}(\tilde{\Delta})]\, d\tilde{\Delta}. \tag{28.45}$$

Invoking (28.36) one finds that the main contribution of the integrand to the integral in (28.45) originates from the subrange of the integration variable $\tilde{\Delta}$ with a lower limit of 2 V and an upper limit of ≈3 V and that the Gaussian function $G(\Delta)$ varies only little across this range. Hence, after substituting (28.41) for $\tilde{G}_{+}(\tilde{\Delta})$ and $\tilde{G}_{-}(\tilde{\Delta})$ into (28.45), we can approximate this function by its value at the gap edges $\tilde{\Delta} = \pm V$, and obtain

$$\bar{k} = \frac{2}{\sqrt{2\pi}\sigma} \exp\left\{-\frac{\Delta_c^2}{2\sigma^2}\right\} \int_{2V}^{\infty} \frac{\tilde{\Delta}}{\sqrt{\tilde{\Delta}^2 - 4\,V^2}}\; k_{\Delta}(\tilde{\Delta})\; d\tilde{\Delta}, \tag{28.46}$$

and in terms of the new integration variable $x \equiv \tilde{\Delta} + \sqrt{\tilde{\Delta}^2 - 4\,V^2}$

$$\bar{k} = \frac{4\,k}{\sqrt{2\pi}\sigma} \exp\left\{-\frac{\Delta_c^2}{2\sigma^2}\right\} \int_{2V}^{\infty} \frac{V^2}{x^2}\, dx \;= \sqrt{\frac{2}{\pi}} \exp\left\{-\frac{\Delta_c^2}{2\sigma^2}\right\} \frac{V}{\Delta_c}\, k. \tag{28.47}$$

The average rate $\bar{k}$ thus differs from the near resonant rate k_{nr} only by the constant factor $\sqrt{2/\pi} \approx 0.8$ (28.34). The linear dependence in V of the prefactor to k in k_{nr} for fixed σ, compared to the quadratic of k_s, can thus be visualized as the linear decrease with V of the dashed areas below the integrand functions $k_{\Delta}(\tilde{\Delta})\, \tilde{G}_{\pm}(\tilde{\Delta})$, which enter the average rate expression via (28.45) (Fig. 28.4a, b). This decrease has its origin in the diminished participation of near resonance states for decreasing V and fixed σ. It is due to the state repulsion at near resonance conditions. The occurrence of the dip in the gap distribution with a width of 2 V (Fig. 28.4a, b) can also hamper the equilibration in the intermediate state. At the same time the electron delocalization at the dip edges reduces the coupling to the vibrations. Both effects diminish the formation of incoherent population of the intermediate $P^{+}B_L^{-}$ and that may reduce the recombination $P^{+}B_L^{-} \rightarrow P B_L$. The arguments hold also for the energetic low dip edge. Only at energetic distances below the dip center by more

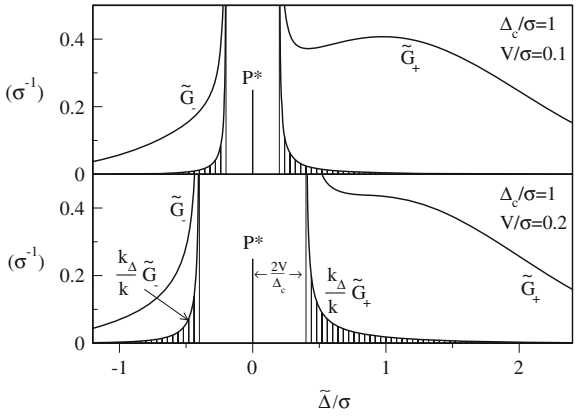

Fig. 28.4 Gap distribution. The gap distribution $G(\Delta)$ and the integrand of the average decay rate are shown for small V. The area below the integrand in the upper part of the picture is half as large as in the lower part. This reflects the linear V dependence of the decay rate in the small V limit due to level repulsion at gap edges

than 2 V the relaxation will destroy the coherent transfer and the two step mechanism can evolve in competition with the recombination. So we conclude, the loss from the near resonance coherent transfer will come from $P_-(t)$. A square root dependence for $P_+(t)$ dominates the kinetics for $\delta \lesssim 1$ and $kt > 1$ (Fig. 28.5). For $\delta \gtrsim 1$ the second term of (28.33) dominates. In this case the exponential drop off can be large. We see that a non-exponential decay pattern is a natural outcome of the dispersive character of the superexchange coupling.

To understand the inverted temperature dependence in more detail we like to point at the close similarity in the temperature dependence of the charge separation rate and the position and width of the absorption peak of P* [169]. In the latter case we have to consider the strong one-electron interaction of about 0.15 eV [170] between the state P^* and the internal CT- states of the dimer, $P_M^+ P_L^-$ and $P_L^+ P_M^-$. The energies of the internal CT states increase for increasing temperature and this causes the blue shift of P*. This conclusion is consistent with the observation of a strong broadening

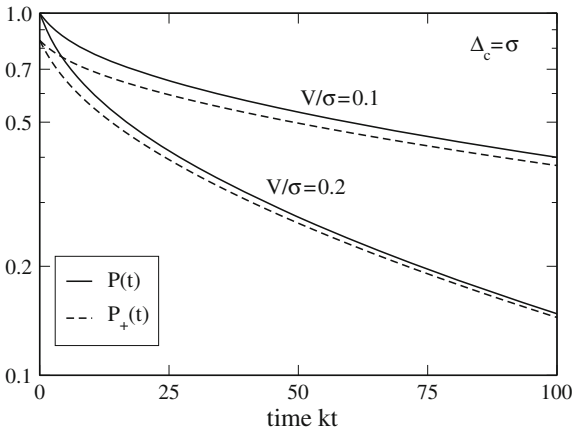

Fig. 28.5 Donor decay via heterogeneous superexchange. Parameters as in Fig. 28.4. The contribution P_+ is from states with energies above the donor energy

of the Stark spectrum only for the lower of the two split dimer bands of P [171]. The strength of the Stark spectrum provides information on the coherent admixture of the CT states into these exciton bands. To relate the temperature dependence of the energy shift and width of P^* to that of the transfer rate from P^* to H_L, we have to scale the admixed components of the corresponding CT states to P^*. In first order perturbation these are given by the ratio of the corresponding couplings to the related mean energy gap Δ_c. For the P^* spectrum this is a factor of about 0.2 [170]. A similar value for the superexchange coupling $V/\Delta_c = 0.2$ between P^* and $P^+B_L^-$ is larger than predicted by quantum calculations but can be reached by a relaxation preceding the transfer process (Sect. 28.5). Such a process provides the proper amplitude for the appearance of the $P^+B_L^-$ state in the simulated time resolved measurements (Sect. 28.5). So we can take the spectral data as empirical input for the determination of the parameters of our model. To quantify the temperature dependence of CT states, we like to refer to spectra of solvated electrons. Their absorption peak position decreases with increasing temperature [172]. The same holds for the solvation energy, which is responsible for the spectral shift [173]. We can approximate the temperature dependence of the shift by [172]

$$\frac{\Delta_c}{\Delta_c^0} = 1 + \frac{a}{T_r}\frac{T^2}{T+T_0} \equiv \alpha(T) \tag{28.48}$$

with $\Delta_c^0 = \Delta_c(T=0)$ and room temperature $T_r = 300\,\mathrm{K}$. The parameter a is given as $a = 0.5$ [172], and for the temperature T_0 we assume 50 K, a value at which structure fluctuations freeze out. To specify the temperature dependence of the width we use the observation of Kirmaier and Holten, that the relative shift and width dependencies are proportional to each other [174, 175]. From the expressions (28.32)–(28.35) and (28.48) we get the temperature dependence for the parameters v and δ as

$$v = \frac{V}{\sigma} = \frac{V}{\sigma_0}\,\alpha^{-1}(T) \tag{28.49}$$

$$\delta = \frac{\Delta_c}{\sigma} = \delta_0 \tag{28.50}$$

with $\sigma_0 = \sigma(T=0)$ and $\delta_0 = \delta_c(T=0)$. For P(t) we find a temperature dependence via $\alpha(T)$ as (see Fig. 28.6 for 30 and 300 K),

$$P(t) = \exp\left\{-\frac{\kappa_1(T)\,k\,t}{1+\sqrt{k\,t}} - \frac{2\,\kappa_2(T)\,k_s^0\,t}{\delta^2\alpha(T) + 2\sqrt{k_s^0\,t}}\right\} \tag{28.51}$$

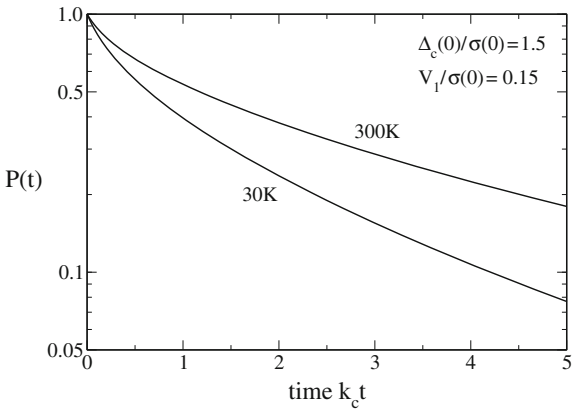

Fig. 28.6 Donor decay for heterogeneous superexchange. The decay of P^* is shown versus time in units of the superexchange lifetime for $T = 0K, 30K, 300K$

with

$$k_s^0 = \frac{V^2}{(\Delta_c^0)^2} \tag{28.52}$$

$$\kappa_1(T) = \frac{V}{\sigma_0} \exp\left(-\frac{\delta^2}{2}\right) \alpha^{-1}(T) \tag{28.53}$$

$$\kappa_2(T) = \frac{(\Delta_c^0)^2}{2\,\sigma_0^2}\, \alpha^{-1}(T)\,. \tag{28.54}$$

In Fig. (28.6a–c) the temperature dependence of the square root and exponential components

$$k_{\rm nr} = \kappa_1 k \quad \text{and} \quad k_s = k_s^0\, \alpha(T)^{-2} \tag{28.55}$$

are shown. Experimentally, the inversion effect on the temperature is found to be higher for the faster component [169, 176, 177]. This would imply in our model that the temperature dependence of the width σ might be stronger than that of Δ_c. Also destruction of the coherence by the temperature would point in this direction.

We should mention that the simulation of the initial charge separation by a stationary near resonance process can get in conflict with Stark effect measurements. They are well interpreted as resulting from the internal CT states of P [178]. A strong admixture of a near resonance states $P^+ B_L^-$ should show up in the orientational effects [179]. At the same time we need relatively small Δ_c-values in order to get an efficient transfer. The conflict can be resolved if we incorporate an initial relaxation of P^* on the sub-picosecond timescale, which lowers the $P^+ B_L^-$ into the energy range of the excited state B_L^*.

28.3 Proton Coupled Superexchange

Even though it is possible to simulate the time dependence of many reaction centers including mutants within the frame of the step models or the superexchange model, there are fundamental short-comings, which we shall address in this section. The suppression of recombination is in the step model related to the inverted transfer kinetics. It implies that the first step, the transition from P^* to the charge transfer state (CT-state) $P^+B_L^-$ is slower than the second from $P^+B_L^-$ to $P^+H_L^-$ [180]. The implicit assumption is that a rapid relaxation in $P^+B_L^-$precedes the nonadiabatic transition to $P^+B_L^-$. This assumption of equilibration on a 100 fs time scale is in conflict with the observation of coherent oscillations, observed with correlated phases by detecting stimulated emission from P^* as well as transient absorption of B_L^- [181]. Alternatively, we will consider now the adiabatic evolution of the state mixing driven by low frequency librational modes, which affect the hydrogen bonds over long distances. This approach incorporates specific structure properties of the dimer such as the C2-symmetry and its dynamic breakage. We make use of ab initio calculations of the TDHF type, which incorporate the electronic one-electron interactions. The analysis of the eigenstates provides evidence for hole transfer via the excitonically coupled P^* and B_L^* states. We simulate the dynamics in the P^* state by the application of an electric field, which shifts the $P^+B_L^-$ state in the energetic regime of the B_L^* state. The field mimics that way the high polarizability of the P^* state, which shows up in the Stark spectrum of the dimer [182]. Apart from a proper field modulation we search for a reaction coordinate by varying hydrogen positions involved in H-bonding (Fig. 28.7), capable to lower the energy of the $P^+B_L^-$ state in the presence of the P^* state. The participation in the proton dynamics is also documented by mutation and modifications of the structure.

For instance, rotation of HisL168, which can be induced by the excitation lowers its H-bond strength to the oxygen of the P_L acetyl. It reduces that way the electron affinity which increases the electron delocalization. Internal structure changes within the P^* state are due to a planarization of the acetyl with the pyrrole I ring, lowering the energy via extending that way the $\pi-$system of P_L. Such structure effects are supported by the structure of a mutant HisL168 replaced by tryptophane, the only mutant, which does not form a H-bond but enhances the charge separation. This structure can act as guidance to readjust the acetyl configuration for an internal P^* state which we denote as P^{**}. In Fig. 28.8 two examples are shown, which demonstrate how the absorption spectra change when the CT state $P^+B_L^-$ approaches B_L^* and P^* as a function proton shifts and electric field. The configuration with optimized coupling will act as the activationless "transition state" for the fast charge separation. It has been shown, that the time resolved transient spectra of P^* can also be reinterpreted in such a model. Sub-picosecond dynamics in P^* is also observed by transient vibrational spectroscopy, showing changes of the acetyl structure. In addition it is important to shift H-atoms of the water, bridging to HisM200 and the keto group of B_L stabilizing the $P^+B_L^-$ state. Most sensitive is the approach of the protonic hydrogen from TyrM208 towards B_L. From the intensities and the splittings

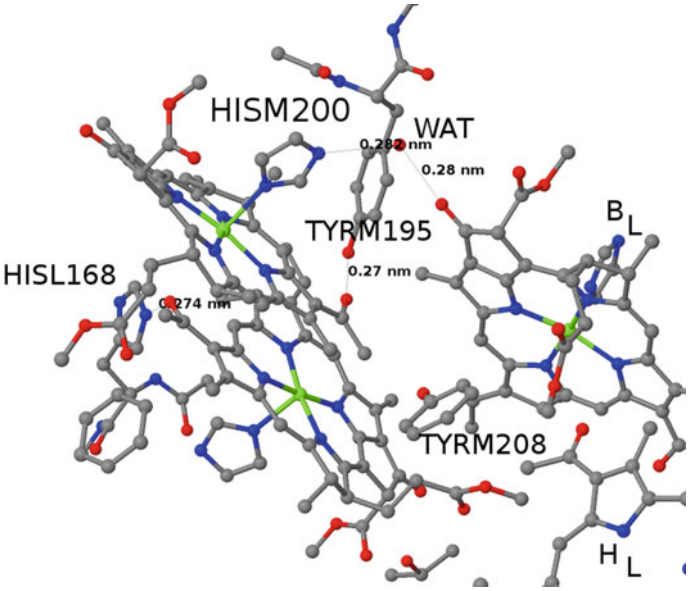

Fig. 28.7 Hydrogen bonds around the special pair. The acetyl oxygens of the special pair dimer P are hydrogen bonded to HISL168 and TYRM195. A water molecule bridges between HISM200 and Bacteriochlorophyll B_L. The proton of TYRM208 is not involved in a hydrogen bond and can move towards P or B_L

of the interacting states one can extract the one-electron coupling V and the excitonic interaction W. For increasing field strength and proton shifts the spacing between the LUMO and the HOMO of B_L reduces relative to those for P by about $1000\,\mathrm{cm}^{-1}$. Such shifts result in a redshift of the B_L^* absorption and an increase of the excitonic coupling between P^* and B_L^*. Continuous changes are strongly correlated and adiabatic. We tried to assure that the dynamic changes effect the spectra in an exothermic manner. We found out that the one-electron coupling between B_L^* and $P^+B_L^-$, which relates to the hole transfer from the HOMO of P to that of B is surprisingly strong (about $100\,\mathrm{cm}^{-1}$). This fact we take as main source for the coherent hole transfer model. Experimentally, it is supported by the observation of a very fast, sub-picosecond, charge separation after excitation of B_L^*. In an earlier publication [183], the possible involvement of B_L^* as virtual intermediate had been considered on the basis of semi empirical (PPP/CI) calculations. New is the involvement of hole transfer. It plays a major role in light induced biological processes, mostly in combination of excited state proton transfer. Its role in the primary step in photosynthesis is in the forefront of research.

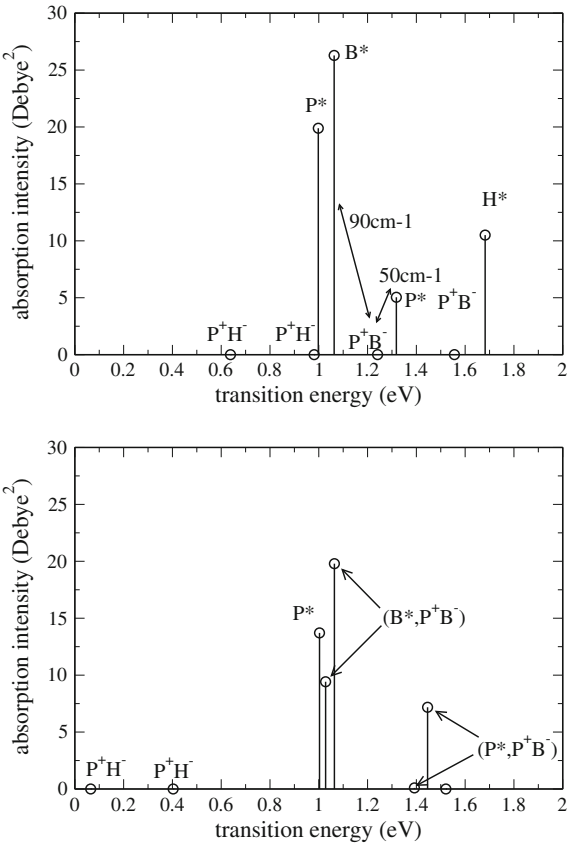

Fig. 28.8 TDHF model spectra. The absorption spectrum of a model system consisting of the special pair P, the Bacteriochlorophyll B_L and the Bacteriopheophytin H_L on the active branch and some selected residues (see Fig. 28.7) is calculated with the 631G/TDHF method [117]. The hydroxyl proton of TYRM208 is oriented to and shifted by 0.4 A towards B, HISL168 is rotated by 90^0, Further two protons are shifted by 0.4 A from the HISM200 towards the water and from the water towards B. The CT state $P^+B_L^-$ is brought into resonance with P* and B_L^* by a suitable electric field

28.4 Coherent Dynamics

Coherent oscillations result from the excitation of vibrational wave packets. They can be generated in the excited state, but also in the groundstate through stimulated Raman scattering. In the reaction center an impulsive reorientation of the acetyle of P_L is induced together with an orientation change of HISL169 , which reduces the strength of the hydrogen-bond between these molecules. This change initiates an oscillating modulation with the dominant frequency Ω of the charge distribution between the dimer halfs P_L and P_M by means of admixing a variable $P_L^+P_M^-$ component to the state P^*. This component is strongly coupled to the $P_L^+B_L^-$ charge transfer state. It can be occupied via the hole transfer, that is the electron transfer from the HOMO of P to the HOMO of B_L, if B_L is excited. We propose, that the excitonically admixed component of B_L^* into P^* is increased in the relaxed configuration P^{**} that the protonic wave packet follows the reaction coordinate for the enhancement of the $P^+B_L^-$ character of the P^{**} state.

To obtain the decay of the P^* state, we consider first the decay of B_L^*. In damping approximation (17.49), we have

$$e^{-iHt/\hbar}|B_L^*> = e^{-itE(B_L^*)/\hbar - kt/2}|B_L^*> . \tag{28.56}$$

The decay into the CT state $P^+H_L^-$ involves the electronic one-electron coupling between the LUMOs of B_L and H_L closely related to the second step in the incoherent step model. Finally we incorporate the excitonic coupling between P^{**} and B_L^* with their mixed orbitals. We treat the excitation induced relaxation of the CT state $P^+B_L^-$ semiclassically. When it gets in near resonance with the B_L^* state the two states undergo avoided crossing with a splitting of $2U_h$. For an heterogeneous energy distribution of the CT states, the split states denoted by + and − signs for the lower and upper components respectively, we get

$$k_\pm = a_\pm^2 k \tag{28.57}$$

with

$$a_\pm^2 = \frac{1}{2}\left(1 \pm \frac{\Delta}{\sqrt{\Delta^2 + 4U^2}}\right). \tag{28.58}$$

In lowest order perturbation the decay of the mixed $(P^+B_L^-, B_L^*)$ state is coupled to the decay of P^{**} state via the excitonic coupling $V(P^*, B_L^*)$ to yield the superexchange rate k_s for the electron transfer from P^* to $P^+H_L^-$ as

$$k_s = k_\pm \left(\frac{V(P^*, B_L^*)}{E(B_L^*) - E(P^*)}\right)^2 . \tag{28.59}$$

The decay of B_L^* is on the 100 fs time scale. In the estimate of the reduction factor due to coherent admixture between the B_L^* into the P^* state, it should be noted that the energy difference incorporates the Franck Condon overlaps with excited vibrational modes including C-C stretches in the energy regime of $1000\,cm^{-1}$. As a result the energy difference has to be weighted by the effect which reduced the effective energy difference seen in the ground state absorption. With this in mind a lifetime around 1ps becomes reasonable. The model avoids solvation of the not equilibrated relaxing intermediate $P^+B_L^-$. It helps to interpret the oscillatory features observed for the P^* decay and the same time the phase coupled oscillations in the detection of the B^-band at 1020 nm. We will interpret these oscillations now in more detail.

28.5 Coherent Oscillations

The anionic band $P^+B_L^-$ can be observed via transient absorption between 1020 and 1040 nm [184] Here we analyze the time evolution of the time dependent population

of the $P^+B_L^-$ state denoted as $P_\pm(t)$ as well as the oscillating contribution $P_{osc}(t)$ resulting from the short pulse excitation in the diabatic representation. It reads

$$P_\pm(t) = \frac{1}{\sqrt{2}\sigma}\int_{-\infty}^{\infty} d\Delta\, \frac{U^2}{\Delta^2+4U^2}\exp\left\{-\frac{(\Delta-\Delta_c)^2}{2\sigma^2} - \frac{1}{2}\left(1 \pm \frac{\Delta}{\sqrt{\Delta^2+4U^2}}\right)kt\right\} \tag{28.60}$$

$$P_{osc}(t) = \frac{1}{\sqrt{2}\sigma}\Re\left[2\int_{-\infty}^{\infty} d\Delta\, \frac{U^2}{\Delta^2+4U^2}\exp\left\{-\frac{(\Delta-\Delta_c)^2}{2\sigma^2} - \frac{k}{2}t + \mathrm{i}t\sqrt{\Delta^2+4U^2}\right\}\right]. \tag{28.61}$$

Here U is the one-electron hole interaction between BL* and $P^+B_L^-$, Δ is the energy difference between the diabatic states B_L* and $P^+B_L^-$, and Δ^2+4U^2 is the corresponding adiabatic energy difference. The integral over the Gauss-function accounts for the average over the heterogeneous distribution with the weighting factor $U^2/(\Delta^2+4U^2)$ representing the delocalization. The width of the distribution is given by σ. For $P_\pm$ the integral over Δ can be evaluated by the saddle point approximation. We get the saddle point Δ_s from the derivative of the two exponents, which must be zero. This condition yields for the oscillating term the implicit equation for the saddle point

$$\Delta_{s,\pm} = \Delta_c \pm \frac{2\sigma^2U^2kt}{(\Delta_s^2+4U^2)^{3/2}}. \tag{28.62}$$

Coherent vibrational oscillations are usually quickly damped out. However, we should remember, that the energy difference between two adiabatic states coupled by U has 2U as a lower limit. The probability to find this limit is shown in Fig. 28.4. It diverges at the boundaries splitting the distribution in two section $G_\pm$. Their relative weight depends on Δ_c. At this point we must remember that the excitation of P^* induces a protein dynamic. That means the distribution is not static. The inhomogeneity results from the disorder of polar groups or water molecules. The driving force reacts to the polarization induced dipole of the dimer. The response is gated by the protonic configuration changes. They drive the whole distribution. In first order we keep the Gaussian form and shift only $\Delta_c(t)$ towards B_L^*. Its energy will be red shifted as long as the charge transfer state $P^+B_L^-$ falls not below B_L^*. That implies that there will be a high probability to find $P^+B_L^-$ at the turning point $\Delta_c = 0$. With this in mind we expand Δ_s around this configuration, which characterizes also the P^{**} configuration. The solution of (28.62) is in first order in $\Delta_s/4U$ given by

$$\Delta_- = \Delta_c + \frac{2\sigma^2U^2kt}{\left(\Delta_c^2+4U^2+6U\sqrt{2kt}\right)^{3/2}}. \tag{28.63}$$

So we get in first order for small kt

$$P_{\pm}(t) = \frac{U^2}{\Delta_c^2 + 4U^2} \exp\left\{-U\sqrt{\frac{kt}{2\sigma^2}}\right\} \exp\left\{-\frac{1}{2}\left(1 \pm \frac{\Delta_c}{\sqrt{\Delta_c^2 + 4U^2}} kt\right)\right\}. \tag{28.64}$$

This probability has to be multiplied by the excitonic coupling factor to yield the probability for the real admixed portion of the $P^+B_L^-$ component in P^{**}

$$P_{\pm}^{**}(P^+B_L^-) = P_{\pm}(t) \frac{V^2}{\left(E(B_L^*) - E(P^{**})\right)^2}. \tag{28.65}$$

The predictions from this result are of special interest from the point of optimizing the primary charge separation process in photosynthesis. Heterogeneities cause non exponential quasi dispersive kinetics, but the efficiency for high yield remains extremely high due to the superexchange character of the decay. It avoids rapid localization followed by internal conversion of the $B^+B_L^-$ state. The coherent character of the process is manifested by the observations in the stimulated emission from P^{**} phase related to the observed admixed $P^+B_L^-$.

$$P_{osc}(t) = \frac{1}{\sqrt{2}} \left(\frac{V}{E(B_L^*) - E(P^{**})}\right)^2 \cos(2\Omega t) \mathrm{e}^{-kt/2}. \tag{28.66}$$

If $\Delta_c(t)$ is modulated by a frequency of $32\,\mathrm{cm}^{-1}$ and if the Gaussian integral is applied, the oscillations can be well simulated. In addition the theory predicts two separated kinetics corresponding to the $\pm$ components, which can be used to fit recent well resolved measurements with additional features such of the appearance of H_L^- with the fast time, even though the model avoids equilibration for the virtual intermediate $P^+B_L^-$.

Part VIII
Molecular Motor Models

Chapter 29
Continuous Ratchet Models

The molecular motor enzyme Kinesin can travel along a microtubule and transport various objects. This protein can move linearly along its designated track, against an external force, by using chemical energy provided by a high concentration of ATP (adenosine triphosphate) molecules in the environment. We derive a Smoluchowski-type Fokker–Planck equation for motion in a periodic potential and determine the stationary solution including an external force. We consider a simplified ratchet model with a sawtooth potential and discuss the force–velocity relation. For a ratchet with smooth potential, we find in the low temperature limit a behavior which can be interpreted in terms of Kramers–Smoluchowski escape rates from the potential minimum over the barriers on the right and left side. We combine the Smoluchowski equation with a simplified four-state model for the chemical reaction cycle of the kinesin molecule and end up with a system of four coupled equations, where the reaction rates depend on the concentrations of ATP, ADP (adenosine diphosphate), and P (inorganic phosphate). We discuss a further simplified 2-state model in larger detail. In the fast reaction limit, the system moves in an average potential, whereas in the fast diffusion limit, the model of a Brownian ratched is recovered. Close to thermal equilibrium, nonlinear thermodynamics yields a linear velocity–force relation. The analytical treatment of the ratchet model simplifies considerably, if it is assumed that the chemical transitions take place only at certain well-defined configurations giving piecewise constant fluxes in the stationary state.

The following discussion is mainly based on the work by Jülicher, Prost and Lipowski [185–191]. A detailed overview over Brownian ratchet models is given by Reimann [192].

P.O.J. Scherer and S.F. Fischer, *Theoretical Molecular Biophysics*,
Biological and Medical Physics, Biomedical Engineering,
DOI 10.1007/978-3-662-55671-9_29

29.1 Transport Equations

The movement of a single protein within a cell is subject to thermal agitation from its environment and is therefore a Brownian motion with drift, which is described by a stochastic differential equation (7.66)

$$m\dot{v} = -\eta v + K(x) + \xi(t) \tag{29.1}$$

where the deterministic part of the mechanical force has contributions from an effective potential and an external extra force

$$K(x) = -\frac{\partial U}{\partial x} + F_{ext}. \tag{29.2}$$

and the stochastic force obeys

$$< \xi(t)\xi(t') >= 2\eta k_B T\, \delta(t - t'). \tag{29.3}$$

On the small length scale of the molecular motor, inertial effects can be neglected [193], which leaves us with the first order equation (7.83)

$$\eta\dot{x} = -\frac{\partial U}{\partial x} + F_{ext} + \xi(t). \tag{29.4}$$

The ensemble average of the position $x(t)$ gives the probability distribution function[1]

$$W(x,t) =< \delta(x - x(t)) >. \tag{29.5}$$

The Fokker–Planck equation corresponding to (29.4) is a Smoluchowski equation (Sect. 7.7) for the probability

$$\begin{aligned}\frac{\partial}{\partial t}W(x,t) &= \frac{k_B T}{\eta}\frac{\partial^2}{\partial x^2}W(x,t) + \frac{1}{\eta}\frac{\partial}{\partial x}\left(\left[\frac{\partial U}{\partial x} - F_{ext}\right]W(x,t)\right) \\ &= \frac{k_B T}{\eta}\frac{\partial^2}{\partial x^2}W(x,t) - \frac{1}{\eta}\frac{\partial}{\partial x}\left(K(x)W(x,t)\right).\end{aligned} \tag{29.6}$$

In terms of the probability flux

$$S(x,t) = -\frac{k_B T}{\eta}\frac{\partial}{\partial x}W(x,t) + \frac{1}{\eta}K(x)W(x,t) \tag{29.7}$$

[1] Here $x(t)$ denotes the random variable whereas x is the argument of W.

we have

$$\frac{\partial}{\partial t}W(x,t) = -\frac{\partial}{\partial x}S(x,t). \tag{29.8}$$

By comparison with the continuity equation for the density

$$\frac{\partial}{\partial t}\rho = -\mathrm{div}(\rho v) \tag{29.9}$$

we find

$$\frac{\partial W}{\partial t} = -\frac{\partial}{\partial x}S = -\frac{\partial}{\partial x}(Wv) \tag{29.10}$$

hence, the drift velocity at position x is

$$v_d(x) = \frac{S(x)}{W(x)}. \tag{29.11}$$

In the following, we assume that the potential is periodic

$$U(x+L) = U(x) \tag{29.12}$$

and introduce the reduced probability density [192]

$$\tilde{W}(x) = \sum_{n=-\infty}^{\infty} W(x+nL) \tag{29.13}$$

which obviously is periodic

$$\tilde{W}(x+L) = \tilde{W}(x) \tag{29.14}$$

and solves the same Fokker–Planck equation (29.6) as $W(x,t)$

$$\begin{aligned}
\frac{\partial}{\partial t}\tilde{W} &= \sum_{n=-\infty}^{\infty}\frac{\partial}{\partial t}W(x+nL) \\
&= \frac{1}{\eta}\sum_{n=-\infty}^{\infty}\left\{k_BT\frac{\partial^2}{\partial x^2}W(x+nL,t) + \frac{\partial}{\partial x}\left(\left[U'(x+nL) - F_{ext}\right]W(x+nL,t)\right)\right\} \\
&= \frac{k_BT}{\eta}\frac{\partial^2}{\partial x^2}\sum_{n=-\infty}^{\infty}W(x+nL,t) + \frac{\partial}{\partial x}\left[\left(U'(x) - F_{ext}\right)\sum_{n=-\infty}^{\infty}W(x+nL,t)\right] \\
&= \frac{k_BT}{\eta}\frac{\partial^2}{\partial x^2}\tilde{W}(x,t) + \frac{\partial}{\partial x}\left[\left(U'(x) - F_{ext}\right)\tilde{W}(x,t)\right].
\end{aligned} \tag{29.15}$$

It is normalized according to

$$\int_0^L \tilde{W}(x)dx = \int_0^L \sum_{n=-\infty}^{\infty} W(x+nL)dx = \int_{-\infty}^{\infty} W(x)dx = 1. \tag{29.16}$$

The average velocity is

$$\begin{aligned} < v > &= \int_{-\infty}^{\infty} W(x)v_d(x)dx = \int_{-\infty}^{\infty} S(x)dx = \sum_{n=-\infty}^{\infty} \int_{nL}^{(n+1)L} S(x)dx \\ &= \sum_{n=-\infty}^{\infty} \int_0^L S(x+nL)dx = \int_0^L \tilde{S}(x)dx. \end{aligned} \tag{29.17}$$

Whereas this result is quite general, for the special case of the Smoluchowski equation (29.4)

$$\begin{aligned} < v > &= \frac{1}{\eta}\left[< -\frac{\partial U}{\partial x} > + F_{ext} \right] = \frac{1}{\eta}\left[F_{ext} - \int_{-\infty}^{\infty} W(x)U'(x)dx \right] \\ &= \frac{1}{\eta}\left[F_{ext} - \sum_{n=-\infty}^{\infty} \int_{nL}^{(n+1)L} W(x)U'(x)dx \right] \\ &= \frac{1}{\eta}\left[F_{ext} - \sum_{n=-\infty}^{\infty} \int_0^L W(x+nL)U'(x+nL)dx \right] \\ &= \frac{1}{\eta}\left[F_{ext} - \int_0^L U'(x)\tilde{W}(x)dx \right]. \end{aligned} \tag{29.18}$$

Equation (29.10) shows, that for a stationary solution ($\frac{\partial W}{\partial t} = \frac{\partial S}{\partial t} = 0$) the flux has to be constant. The stationary distribution is easily found by integration of

$$\frac{\partial}{\partial x}\tilde{W}_{st}(x) = \frac{1}{k_B T}K(x)\tilde{W}_{st}(x) - \frac{\eta}{k_B T}\tilde{S} \tag{29.19}$$

and has the form

$$\begin{aligned} \tilde{W}_{st}(x) &= \exp\left\{ \int_0^x \frac{K(x')}{k_B T}dx' \right\} \left[\tilde{W}_{st}(0) - \frac{\eta\tilde{S}}{k_B T}\int_0^x \exp\left\{ -\int_0^{x''} \frac{K(x')}{k_B T}dx' \right\} dx'' \right] \\ &= \mathrm{e}^{(xF_{ext}+U(0)-U(x))/k_B T}\left[\tilde{W}_{st}(0) - \frac{\eta\tilde{S}}{k_B T}\int_0^x dx'\mathrm{e}^{-(x'F_{ext}+U(0)-U(x'))/k_B T} \right] \\ &= \tilde{W}_{st}(0)\mathrm{e}^{(xF_{ext}+U(0)-U(x))/k_B T} - \frac{\eta\tilde{S}}{k_B T}\mathrm{e}^{(xF_{ext}-U(x))/k_B T}\int_0^x dx'\mathrm{e}^{-(x'F_{ext}-U(x'))/k_B T}. \end{aligned} \tag{29.20}$$

From the periodic boundary conditions

$$\tilde{W}_{st}(0) = \tilde{W}_{st}(L) = \tilde{W}_{st}(0)\mathrm{e}^{LF/k_BT} - \frac{\eta\tilde{S}}{k_BT}\mathrm{e}^{(LF_{ext}-U(0))/k_BT}\int_0^L dx'\mathrm{e}^{-(x'F_{ext}-U(x'))/k_BT} \tag{29.21}$$

we obtain

$$\begin{aligned}
\tilde{W}_{st}(0) &= \frac{\mathrm{e}^{-U(0)/k_BT}}{1-\mathrm{e}^{-LF_{ext}/k_BT}}\frac{\eta\tilde{S}}{k_BT}\int_0^L dx'\mathrm{e}^{-(x'F_{ext}-U(x'))/k_BT} \\
\tilde{W}_{st}(x) &= \frac{\mathrm{e}^{(xF_{ext}-U(x))/k_BT}}{1-\mathrm{e}^{-LF_{ext}/k_BT}}\frac{\eta\tilde{S}}{k_BT}\int_0^L dx'\mathrm{e}^{-(x'F_{ext}-U(x'))/k_BT} \\
&- \frac{\eta\tilde{S}}{k_BT}\mathrm{e}^{(xF_{ext}-U(x))/k_BT}\int_0^x dx'\mathrm{e}^{-(x'F_{ext}-U(x'))/k_BT} \\
&= \frac{\eta\tilde{S}}{k_BT}\mathrm{e}^{(xF_{ext}-U(x))/k_BT}\frac{\mathrm{e}^{-LF_{ext}/k_BT}}{(1-\mathrm{e}^{-LF_{ext}/k_BT})}\int_0^x dx'\mathrm{e}^{-(x'F_{ext}-U(x'))/k_BT} \\
&+ \frac{\eta\tilde{S}}{k_BT}\mathrm{e}^{(xF_{ext}-U(x))/k_BT}\frac{1}{(1-\mathrm{e}^{-LF_{ext}/k_BT})}\int_x^L dx'\mathrm{e}^{-(x'F_{ext}-U(x'))/k_BT}.
\end{aligned} \tag{29.22}$$

But, since

$$\begin{aligned}
&\int_0^x dx'\mathrm{e}^{-(x'F_{ext}-U(x'))/k_BT} = \int_L^{x+L} dx'\mathrm{e}^{-(x'F_{ext}-LF_{ext}-U(x'-L))/k_BT} \\
&= \mathrm{e}^{LF_{ext}/k_BT}\int_L^{x+L} dx'\mathrm{e}^{-(x'F_{ext}-U(x'))/k_BT}
\end{aligned} \tag{29.23}$$

we obtain the more compact expression [192]

$$\tilde{W}_{st}(x) = \frac{\eta\tilde{S}}{k_BT}\frac{\mathrm{e}^{(xF_{ext}-U(x))/k_BT}}{(1-\mathrm{e}^{-LF_{ext}/k_BT})}\int_x^{x+L} dx'\mathrm{e}^{-(x'F_{ext}-U(x'))/k_BT} \tag{29.24}$$

where the value of $\tilde{S}$ has to be determined from normalization of W_{st} as

$$\tilde{S} = \frac{k_BT}{\eta}(1-\mathrm{e}^{-LF_{ext}/k_BT})\left[\int_0^L dx\,\mathrm{e}^{(xF_{ext}-U(x))/k_BT}\int_x^{x+L} dx'\mathrm{e}^{-(x'F_{ext}-U(x'))/k_BT}\right]^{-1}. \tag{29.25}$$

Without an external force, we find from the periodic b.c.

$$\tilde{W}_{st}(L) = C\mathrm{e}^{-U(0)/k_BT} - \frac{\eta}{k_BT}\tilde{S}\int_0^L \mathrm{e}^{(U(x')-U(0)/k_BT}dx' = \tilde{W}_{st}(0) = C\mathrm{e}^{-U(0)/k_BT} \tag{29.26}$$

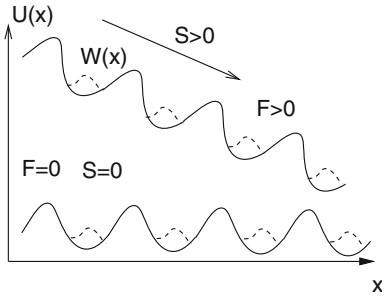

Fig. 29.1 Periodic potential with external force

which shows that there is zero flux[2] (Fig. 29.1)

$$\tilde{S} = 0 \tag{29.27}$$

and no average velocity

$$< v >= 0. \tag{29.28}$$

From

$$\tilde{S}_{st} = -\frac{k_B T}{\eta}\frac{\partial}{\partial x}\tilde{W}_{st}(x) - \frac{1}{\eta}\tilde{W}_{st}(x)\frac{\partial}{\partial x}\left(U(x) - x F_{ext}\right) \tag{29.29}$$

we find

$$\eta\tilde{S}\frac{1}{\tilde{W}(x)} = -\frac{\partial}{\partial x}(k_B T \ln \tilde{W}(x) + U + U_{ext}) \tag{29.30}$$

which can be interpreted in terms of a chemical potential [194]

$$\mu(x) = k_B T \ln \tilde{W}(x) + U(x) + U_{ext}(x) \tag{29.31}$$

as

$$\frac{\partial}{\partial x}\mu(x) = -\frac{\eta\tilde{S}}{\tilde{W}(x)} = -\eta v_d(x) \tag{29.32}$$

where the right side gives the energy which is dissipated by a particle moving in a viscous medium.

[2]The integrand is strictly positive, hence, the integral can not vanish.

29.2 A Simple Sawtooth Ratchet

We consider a simplified model with a sawtooth potential (Fig. 29.2)

$$U(x) = U_m \frac{x}{L}. \tag{29.33}$$

For simplification, we introduce the abbreviations

$$\xi = \frac{F_{ext} L - U_m}{k_B T}$$

$$\phi = \frac{F_{ext} L}{k_B T} \quad \rho = \frac{U_m}{k_B T}$$

$$\sigma = \frac{\eta \tilde{S}}{k_B T} \tag{29.34}$$

and measure length in units of the period by setting $L = 1$.

From (29.20)

$$\tilde{W}(x) = \mathrm{e}^{x\xi} \left(C - \sigma \int_0^x \mathrm{e}^{-\xi x'} dx' \right) = C\mathrm{e}^{x\xi} + \sigma \frac{1 - \mathrm{e}^{x\xi}}{\xi} \tag{29.35}$$

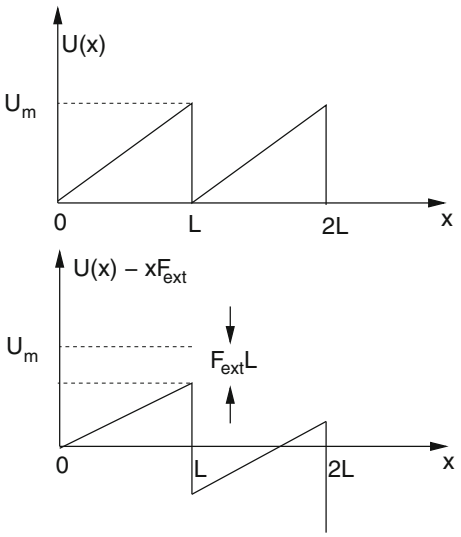

Fig. 29.2 Sawtooth potential

The constant can be determined by normalizing the probability

$$1 = \int_0^1 \tilde{W}(x)dx = \frac{\sigma\xi + (\mathrm{e}^{\xi} - 1)(C\xi - \sigma)}{\xi^2} \tag{29.36}$$

from which

$$\tilde{W}_0 = C = \frac{\xi^2 + \sigma(\mathrm{e}^{\xi} - 1 - \xi)}{\xi(\mathrm{e}^{\xi} - 1)}. \tag{29.37}$$

At $x = 1$ the potential is discontinuous

$$\tilde{W}(1 + \epsilon) = \mathrm{e}^{\phi}\left(C + \sigma\frac{\mathrm{e}^{-\xi} - 1}{\xi}\right) \tag{29.38}$$

and from the periodicity condition

$$C = \mathrm{e}^{\phi}\left(C + \sigma\frac{\mathrm{e}^{-\xi} - 1}{\xi}\right) \tag{29.39}$$

we obtain (Fig. 29.4)

$$0 = \frac{\xi^2 + \sigma(\mathrm{e}^{\xi} - 1 - \xi)}{\xi(\mathrm{e}^{\xi} - 1)}\left(1 - \mathrm{e}^{-\phi}\right) + \sigma\frac{\mathrm{e}^{-\xi} - 1}{\xi} \tag{29.40}$$

$$\sigma = \frac{(\phi - \rho)^2(\mathrm{e}^{\phi} - 1)}{\rho - \phi - 1 + \mathrm{e}^{\phi-\rho} + \mathrm{e}^{\phi}(\phi - \rho) + \mathrm{e}^{\rho} - \mathrm{e}^{\phi}}. \tag{29.41}$$

Without external force the probability density is given by the exponential (Fig. 29.3)

$$\tilde{W}(x) = C\mathrm{e}^{\xi x} = \frac{\rho}{(1 - \mathrm{e}^{-\rho})}\mathrm{e}^{-\rho x}. \tag{29.42}$$

If the potential barrier is smaller than thermal energy

$$\begin{aligned}\sigma &\approx \frac{(\phi^2 - 2\rho\phi)(\mathrm{e}^{\phi} - 1)}{\mathrm{e}^{\phi}(\phi - \rho - 1 + 1 - \rho + \rho^2/2 + \dots) - 1 - \phi + \rho + 1 + \rho + \rho^2/2 + \dots} \\ &\approx \frac{(\phi^2 - 2\rho\phi)(\mathrm{e}^{\phi} - 1)}{(\phi - 2\rho)(\mathrm{e}^{\phi} - 1)} \approx \phi\end{aligned} \tag{29.43}$$

or

$$\tilde{S} \approx \frac{1}{\eta}F_{ext}. \tag{29.44}$$

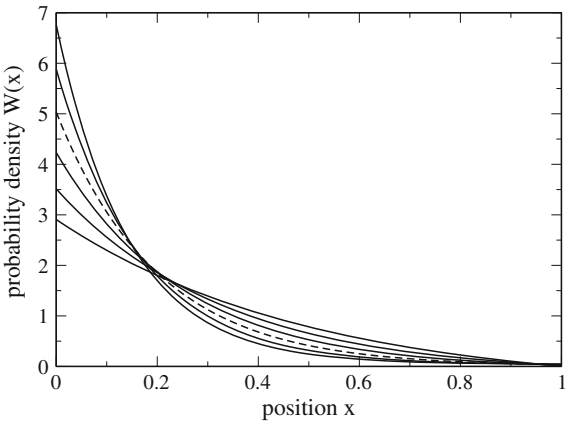

Fig. 29.3 Probability density of the sawtooth ratchet. The probability density calculated from (29.35), (29.37), (29.41) is shown for $\rho = 5$ and $\phi = -2, -1, 0, 1, 2$. For $\phi = 0$ it is given by (29.42) (broken curve)

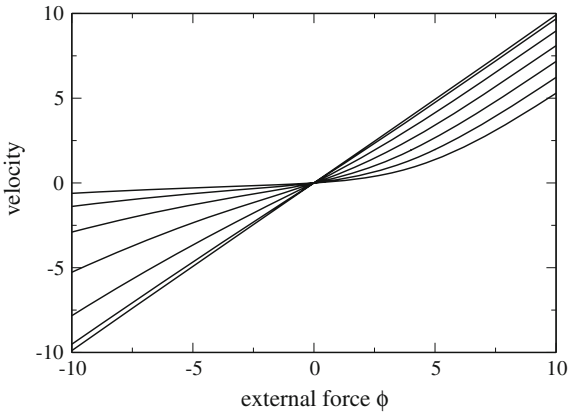

Fig. 29.4 Force–velocity relation of the sawtooth ratchet. The velocity $< v >= S$ from (29.41) is shown as a function of the external force ϕ for different potential barriers $\rho = 0.5, 1, 2, 3, 4, 5, 6$

Linearization for small forces gives

$$\begin{aligned} s\sigma &\approx \frac{(\rho^2 - 2\phi\rho)(\phi + \dots)}{(1 + \phi + \dots)(\phi - \rho - 1 + \mathrm{e}^{-\rho}) - 1 - \phi + \rho + \mathrm{e}^{\rho}} \\ &\approx \frac{\rho^2\phi}{(\phi - \rho - 1 + \mathrm{e}^{-\rho}) + \phi(-\rho - 1 + \mathrm{e}^{-\rho}) - 1 - \phi + \rho + \mathrm{e}^{\rho}} \\ &\approx \frac{\rho^2\phi}{-2 + \mathrm{e}^{-\rho} + \mathrm{e}^{\rho}} \end{aligned} \tag{29.45}$$

or after resubstitution

$$\tilde{S} = \frac{1}{\eta} \frac{(\frac{U_m}{k_B T})^2}{\mathrm{e}^{U_m/k_B T} + \mathrm{e}^{-U_m/k_B T} - 2} F_{ext}. \tag{29.46}$$

29.3 Ratchets in the Low Temperature Limit

Now, we consider a ratchet with smooth potential and assume that the external force is not too strong such that the potential has a well-defined minimum inside the period and a maximum at the boundary (Fig. 29.5).

We expand the potential around the extremal points

$$U(x) \approx U_m - \frac{\omega_m^2}{2} x^2 \quad \text{for } x \approx 0 \tag{29.47}$$

$$U(x) \approx U_0 + \frac{\omega_0^2}{2}(x - x_0)^2 \quad \text{for } x \approx x_0 \tag{29.48}$$

$$U(x) \approx U_m - \frac{\omega_m^2}{2}(x - L)^2 \quad \text{for } x \approx L. \tag{29.49}$$

For small external force the extrema of the effective potential are approximately given by

$$U(x) - xF_{ext} \approx U_m + \frac{F_{ext}^2}{2\omega_m^2} - \frac{\omega_m^2}{2}\left(x + \frac{F_{ext}}{\omega_m^2}\right)^2$$

$$\approx \tilde{U_m} - \frac{\omega_m^2}{2}\tilde{x}^2 \quad \text{for } x \approx 0 \tag{29.50}$$

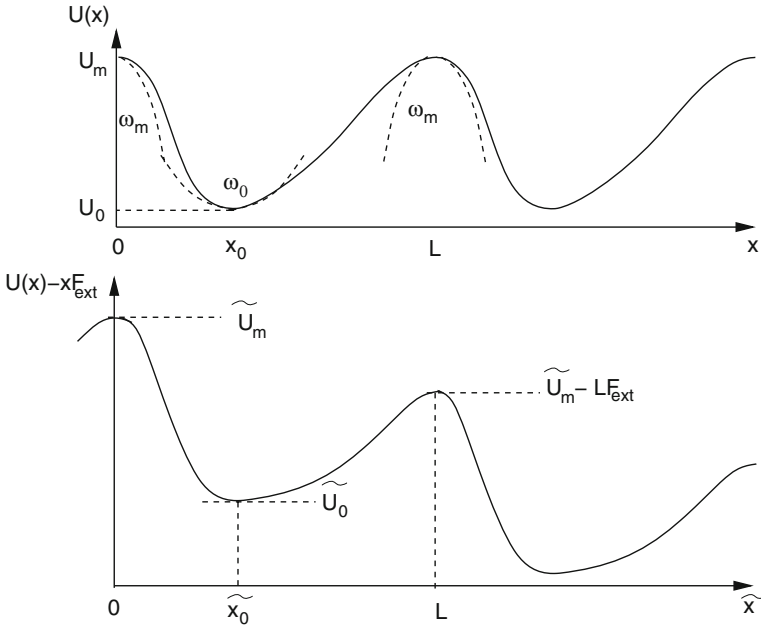

Fig. 29.5 Ratchet in the limit of low temperature and low force

with

$$\tilde{x} = x - x_m = x - \left(-\frac{F_{ext}}{\omega_m^2}\right) \quad \tilde{U}_m = U_m + \frac{F_{ext}^2}{2\omega_m^2} \tag{29.51}$$

by

$$\begin{aligned} U(x) - xF_{ext} &\approx U_0 - \frac{F_{ext}^2}{2\omega_0^2} - x_0 F_{ext} + \frac{\omega_0^2}{2}\left(x - x_0 - \frac{F_{ext}}{\omega_0^2}\right)^2 \\ &\approx U_0 - \frac{F_{ext}^2}{2\omega_0^2} - x_0 F_{ext} + \frac{\omega_0^2}{2}\left(\tilde{x} - x_0 + \frac{F_{ext}}{\omega_m^2} - \frac{F_{ext}}{\omega_0^2}\right)^2 \\ &\approx \tilde{U}_0 + \frac{\omega_0^2}{2}(\tilde{x} - \tilde{x}_0)^2 \quad \text{for } x \approx x_0 \end{aligned} \tag{29.52}$$

with

$$\tilde{x}_0 = x_0 - \frac{F_{ext}}{\omega_m^2} + \frac{F_{ext}}{\omega_0^2} \quad \tilde{U}_0 = U_0 - \frac{F_{ext}^2}{2\omega_0^2} - x_0 F_{ext}$$

and finally,

$$\begin{aligned} U(x) - xF_{ext} &\approx U_m + \frac{F_{ext}^2}{2\omega_m^2} - LF_{ext} - \frac{\omega_m^2}{2}\left(x - L + \frac{F_{ext}}{\omega_m^2}\right)^2 \\ &\approx \tilde{U}_m - LF_{ext} - \frac{\omega_m^2}{2}(\tilde{x} - L)^2 \quad \text{for } x \approx L. \end{aligned} \tag{29.53}$$

In the limit of low temperature (or high barrier) $\tilde{U}_m - \tilde{U}_0 \gg k_B T$ the probability density is essentially concentrated at the potential minimum $\tilde{x}_0$ and can be approximated as

$$\begin{aligned} \tilde{W} &= \mathrm{e}^{(xF_{ext} - U(x))/k_B T}\left[C - \frac{\eta S}{k_B T}\int_0^x dx' \mathrm{e}^{-(x'F_{ext} - U(x'))/k_B T}\right] \\ &\approx \exp\left\{-\frac{\tilde{U}_0}{k_B T} - \frac{\omega_0^2}{2k_B T}(\tilde{x} - \tilde{x}_0)^2\right\}\left[C - \frac{\eta S}{k_B T}\int_0^\infty d\tilde{x}' \exp\left\{\frac{\tilde{U}_m}{k_B T} - \frac{\omega_m^2}{2k_B T}\tilde{x}'^2\right\}\right] \\ &\approx \exp\left\{-\frac{\tilde{U}_0}{k_B T} - \frac{\omega_0^2}{2k_B T}(\tilde{x} - \tilde{x}_0)^2\right\}\left[C - \frac{\eta S}{k_B T \omega_m}\sqrt{\frac{\pi k_B T}{2}}\mathrm{e}^{\tilde{U}_m/k_B T}\right]. \end{aligned} \tag{29.54}$$

From normalization

$$1 = \int_0^L d\tilde{x}\, \tilde{W}(\tilde{x}) = \frac{1}{\omega_0}\sqrt{2\pi k_B T}\mathrm{e}^{-\tilde{U}_0/k_B T}\left[C - \frac{\eta \tilde{S}}{\omega_m}\sqrt{\frac{\pi}{2k_B T}}\mathrm{e}^{\tilde{U}_m/k_B T}\right]$$

we determine the integration constant

$$C = \frac{\omega_0}{\sqrt{2\pi k_B T}} \mathrm{e}^{U_0/\tilde{k}_B T} + \frac{\eta \tilde{S}}{\omega_m} \sqrt{\frac{\pi}{2k_B T}} \mathrm{e}^{\tilde{U}_m/k_B T}. \tag{29.55}$$

From the periodicity

$$\begin{aligned} &\tilde{W}(0) = \mathrm{e}^{-\tilde{U}_m/k_B T} C \\ &= \tilde{W}(L) = \mathrm{e}^{(LF_{ext}-\tilde{U}_m)/k_B T} \left[C - \frac{\eta \tilde{S}}{\omega_m} \sqrt{\frac{\pi}{2k_B T}} \mathrm{e}^{\tilde{U}_m/k_B T} \left(1 + \mathrm{e}^{-LF_{ext}/k_B T}\right) \right] \end{aligned} \tag{29.56}$$

we find

$$\mathrm{e}^{-\tilde{U}_m/k_B T} C \left(\mathrm{e}^{LF_{ext}/k_B T} - 1\right) = \frac{\eta \tilde{S}}{\omega_m} \sqrt{\frac{\pi}{2k_B T}} \left(1 + \mathrm{e}^{LF_{ext}/k_B T}\right) \tag{29.57}$$

and after substituting C

$$\begin{aligned} &\left(\frac{\omega_0}{\sqrt{2\pi k_B T}} \mathrm{e}^{-(\tilde{U}_m - \tilde{U}_0)/k_B T} + \frac{\eta S}{\omega_m} \sqrt{\frac{\pi}{2k_B T}} \right) \left(\mathrm{e}^{LF_{ext}/k_B T} - 1\right) \\ &= \frac{\eta \tilde{S}}{\omega_m} \sqrt{\frac{\pi}{2k_B T}} \left(1 + \mathrm{e}^{LF_{ext}/k_B T}\right) \end{aligned} \tag{29.58}$$

which can be solved for $\tilde{S}$

$$\tilde{S} = \frac{\omega_0 \omega_m}{2\eta\pi} \mathrm{e}^{-(\tilde{U}_m - \tilde{U}_0)/k_B T} \left(\mathrm{e}^{LF_{ext}/k_B T} - 1\right). \tag{29.59}$$

This can be written as

$$\tilde{S} = k_+ - k_- \tag{29.60}$$

where

$$k_+ = \frac{\omega_0 \omega_m}{2\eta\pi} \mathrm{e}^{-(\tilde{U}_m - \tilde{U}_0 - LF_{ext})/k_B T} \tag{29.61}$$

$$k_- = \frac{\omega_0 \omega_m}{2\eta\pi} \mathrm{e}^{-(\tilde{U}_m - \tilde{U}_0)/k_B T} \tag{29.62}$$

are the Kramers–Smoluchowski escape rates (Chap. 8) from the potential minimum $\tilde{x}_0$ over the barriers on the right and left side (Fig. 29.6).

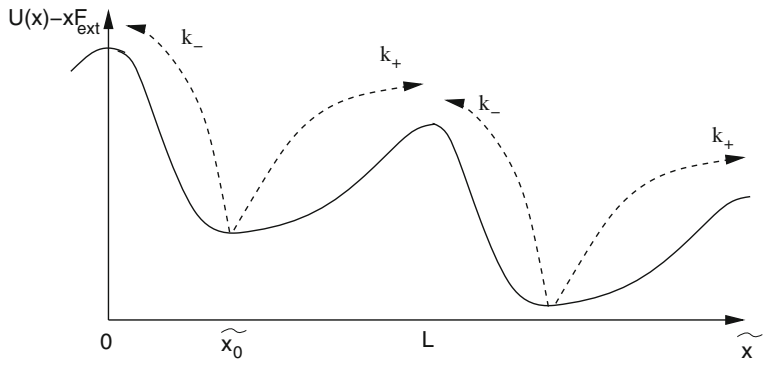

Fig. 29.6 Escape probabilities

Linearization for small force finally gives

$$\tilde{S} \approx \frac{L F_{ext}}{k_B T} \frac{\omega_0 \omega_m}{2\eta\pi} \mathrm{e}^{-(U_m - U_0)/k_B T}. \tag{29.63}$$

29.4 Chemical Transitions

The kinesin molecule consists of a very long (about 100 nm) rod-like part in the middle connecting two ends, one of which is capable to grasp the cargo and one which is composed of two identical "heads" or "motor domains" [195, 196] which proceed along the microtubule in a "step-by-step" fashion [197]. Each head can bind to the microtubule and has its own ATP-binding pocket. The two heads can bind and hydrolize ATP on their own. We assume that the chemistry can be described by a number m of discrete states $i = 1 \cdots m$. A very popular model [198] focuses on a cycle with four states (Fig. 29.7). Detailed models treat both heads explicitly with a total of $4 \times 4 = 16$ states ([192] and references therein) whereas simplified models involve the motion of only one head and require less parameters.

Transitions between the four states are fast compared to the motion of the motor and will be described by chemical kinetics

$$\mathrm{i} \underset{k_{ji}}{\overset{k_{ij}}{\rightleftharpoons}} \mathrm{j}. \tag{29.64}$$

The geometrical configuration will be described by one configuration coordinate x, which is related to the position of the motor along the microtubule. The motion in each state will be described by a Smoluchowski equation (29.6) in a corresponding potential $U_i(x)$ which is assumed to be periodic and asymmetric

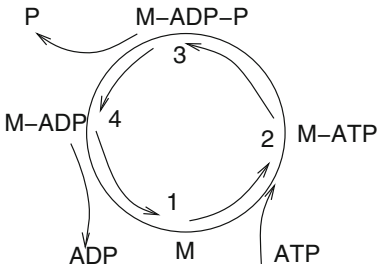

Fig. 29.7 Four-state model of the Chemical cycle. In state (*1*) the head is attached to the microtubule. The transition to state (*2*) involves binding of one ATP molecule from the environment. In state (*3*) ATP has been broken into ADP (adenosine diphosphate) and P (inorganic phosphate). In state (*4*) P is released from the ATP-binding pocket and the head detaches. Then, after some random motion, ADP is released and the head binds again to the microtubule. The head now is back in state (*1*) and an energy amount of about $\Delta\mu = 20 k_B T$ has been released

$$U_i(x+L) = U_i(x) \quad U_i(x) \neq U_i(-x) \tag{29.65}$$

$$\frac{\partial}{\partial t} W_i(x,t) + \frac{\partial}{\partial x} S_i(x,t) = \sum_{i \neq j} \left(k_{ji}(x) W_i(x,t) - k_{ij}(x) W_j(x,t) \right) \tag{29.66}$$

$$S_i(x,t) = -\frac{k_B T}{\eta} \frac{\partial}{\partial x} W_i(x,t) + \frac{1}{\eta} W_i(x,t) \left[F_{ext} - \frac{\partial}{\partial x} U_i(x) \right]. \tag{29.67}$$

The energy source is the hydrolysis reaction

$$\text{ATP} \rightarrow \text{ADP} + \text{P} \tag{29.68}$$

with a free energy change of (Sect. 14.1)[3]

$$\Delta\mu = \mu_{ADP} + \mu_P - \mu_{ATP} = \Delta\mu^0 - k_B T \ln \frac{c_{ATP}}{c_{ADP} c_P}. \tag{29.69}$$

At equilibrium $\Delta\mu = 0$, hence

$$\Delta\mu^0 = k_B T \ln \frac{c^{eq}_{ATP}}{c^{eq}_{ADP} c^{eq}_P} \tag{29.70}$$

and

$$\Delta\mu = -k_B T \ln \frac{c_{ATP}}{c^{eq}_{ATP}} + k_B T \ln \frac{c_{ADP}}{c^{eq}_{ADP}} + k_B T \ln \frac{c_P}{c^{eq}_P}. \tag{29.71}$$

[3] At physiological conditions $\Delta\mu \approx -20 k_B T$.

Each cycle of the motor consumes the energy from hydrolysis of one ATP. Figure 29.7 shows only the state of the motor which is unchanged after completing a full cycle. To describe the chemistry of the coupled motor-environment system properly, we have to keep track of the number of cycles to find the free energy of the system. We use a sequence of states $M_{i,n}$ characterized by the motor state i together with the total number n of completed cycles

$$\ldots \mathrm{M}_{1,0} \underset{k_{2,1}}{\overset{k_{1,2}}{\rightleftharpoons}} \mathrm{M}_{2,0} \underset{k_{3,2}}{\overset{k_{2,3}}{\rightleftharpoons}} \mathrm{M}_{3,0} \underset{k_{4,3}}{\overset{k_{3,4}}{\rightleftharpoons}} \mathrm{M}_{4,0} \underset{k_{1,4}}{\overset{k_{4,1}}{\rightleftharpoons}} \mathrm{M}_{1,1} \underset{k_{2,1}}{\overset{k_{1,2}}{\rightleftharpoons}} \mathrm{M}_{2,1} \underset{k_{3,2}}{\overset{k_{2,3}}{\rightleftharpoons}} \mathrm{M}_{3,1} \cdots \tag{29.72}$$

The effective motor potentials are defined as equilibrium free energies (Fig. 29.8)

$$G_{1,0} = U_1 + k_B T \ln \frac{c_{ATP}}{c_{ATP}^{eq}} \tag{29.73}$$

$$G_{2,0} = U_2 \tag{29.74}$$

$$G_{3,0} = U_3 \tag{29.75}$$

$$G_{4,0} = U_4 + k_B T \ln \frac{c_P}{c_P^{eq}} \tag{29.76}$$

$$G_{1,1} = G_{1,0} - \mu_{ATP} + \mu_{ADP} + \mu_P = G_{1,0} + \Delta\mu \tag{29.77}$$

$$\vdots$$

$$G_{i,n} = G_{i,0} + n\Delta\mu. \tag{29.78}$$

At equilibrium

$$G_{i,n}^{eq} = G_{i,0}^{eq} = U_i \tag{29.79}$$

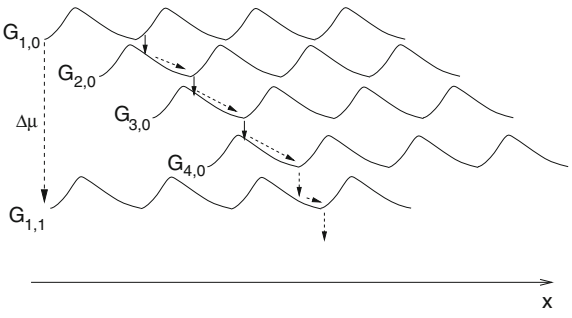

Fig. 29.8 Hierarchy of free energies for the four-state model

and the occupation probabilities are independent of n

$$W_{i,n}^{eq} = N\mathrm{e}^{-U_i/k_BT}. \tag{29.80}$$

The first step

$$M_{1,0} \underset{k_{2,1}}{\overset{k_{1,2}}{\rightleftharpoons}} \mathrm{M}_{2,0} \tag{29.81}$$

involves binding of ATP described by the reaction

$$M + ATP \rightleftharpoons M - ATP. \tag{29.82}$$

From standard reaction kinetics (Sect. 6.3) we expect that the reaction rates have the form

$$r_{\rightarrow} = k_{1,2}^0 c_{ATP} W_M = k_{1,2} W_M \tag{29.83}$$

$$r_{\leftarrow} = k_{2,1} W_{M-ATP} \tag{29.84}$$

where $k_{1,2}^0, k_{2,1}$ do not depend on the ATP concentration. At equilibrium $r_{\rightarrow} = r_{\leftarrow}$ and we find

$$\frac{k_{1,2}^0}{k_{2,1}} = \frac{W_{M-ATP}^{eq}}{c_{ATP}^{eq} W_M^{eq}} = \frac{1}{c_{ATP}^{eq}} \mathrm{e}^{-(G_{2,0}^{eq} - G_{1,0}^{eq})/k_BT} = \frac{1}{c_{ATP}^{eq}} \mathrm{e}^{(U_1 - U_2)/k_BT}. \tag{29.85}$$

For the motor cycle

$$\frac{k_{1,2}}{k_{2,1}} = \frac{c_{ATP}}{c_{ATP}^{eq}} \mathrm{e}^{(U_1 - U_2)/k_BT} = \mathrm{e}^{(G_{1,0} - G_{2,0})/k_BT}. \tag{29.86}$$

The second step corresponds to the chemical reaction

$$M - ATP \rightleftharpoons M - ADP - P \tag{29.87}$$

$$r_{\rightarrow} = k_{2,3} W_{M-ATP} \tag{29.88}$$

$$r_{\leftarrow} = k_{3,2} W_{M-ADP-P} \tag{29.89}$$

$$\frac{k_{2,3}}{k_{3,2}} = \frac{W_{M-ADP-P}^{eq}}{W_{M-ATP}^{eq}} = \mathrm{e}^{(G_2 - G_3)/k_BT} = \mathrm{e}^{(U_2 - U_3)/k_BT}. \tag{29.90}$$

The third step

$$M - ADP - P \rightleftharpoons M - ADP + P \tag{29.91}$$

releases P

$$r_{\rightarrow} = k_{3,4} W_{M-ADP-P} \tag{29.92}$$

$$r_{\leftarrow} = k^0_{4,3} c_P W_{M-ADP} = k_{4,3} W_{M-ADP} \tag{29.93}$$

$$\frac{k_{3,4}}{k^0_{4,3}} = \frac{W^{eq}_{M-ADP} c^{eq}_P}{W^{eq}_{M-ADP-P}} = c^{eq}_P \mathrm{e}^{(U_3-U_4)/k_B T}$$

$$\frac{k_{3,4}}{k_{4,3,}} = \frac{c^{eq}_P}{c_P} \mathrm{e}^{(U_3-U_4)/k_B T} = \mathrm{e}^{(G_3-G_4)}. \tag{29.94}$$

Finally the last step

$$M - ADP + P \rightleftharpoons M + ADP + P \tag{29.95}$$

releases ADP. The motor is in the initial state again but one ATP has been hydrolized and the relevant free energies are

$$G_{4,0} = U_4 + k_B T \ \ln \frac{c_P}{c^{eq}_P} \tag{29.96}$$

$$G_{1,1} = G_{1,0} - \mu_{ATP} + \mu_{ADP} + \mu_P = G_{1,0} + \Delta\mu \tag{29.97}$$

$$r_{\rightarrow} = k_{4,1} W_{M-ADP} \tag{29.98}$$

$$r_{\leftarrow} = k^0_{1,4} W_M c_{ADP} = k_{1,4} W_M \tag{29.99}$$

$$\frac{k_{4,1}}{k^0_{1,4}} = c^{eq}_{ADP} \frac{W^{eq}_M}{W^{eq}_{M-ADP}} = c^{eq}_{ADP} \mathrm{e}^{(U_4-U_1)/k_B T} \tag{29.100}$$

$$\frac{k_{4,1}}{k_{1,4}} = \frac{c^{eq}_{ADP}}{c_{ADP}} \mathrm{e}^{(U_4-U_1)/k_B T}. \tag{29.101}$$

But since

$$U_4 - U_1 + k_B T \ln \frac{c_{ADP}^{eq}}{c_{ADP}} = G_{4,0} - k_B T \ln \frac{c_P}{c_P^{eq}} - \left(G_{1,0} - k_B T \ln \frac{c_{ATP}}{c_{ATP}^{eq}} \right) + k_B T \ln \frac{c_{ADP}^{eq}}{c_{ADP}}$$
$$= G_{4,0} - G_{1,0} + k_B T \left(\ln \frac{c_{ATP}}{c_P c_{ADP}} - \ln \frac{c_{ATP}^{eq}}{c_P^{eq} c_{ADP}^{eq}} \right) = G_{4,0} - G_{1,0} - \Delta\mu = G_{4,0} - G_{1,1}$$

the ratio of the rates is

$$\frac{k_{4,1}}{k_{1,4}} = \mathrm{e}^{(G_{4,0} - G_{1,0} - \Delta\mu)/k_B T} = \mathrm{e}^{(G_{4,0} - G_{1,1})/k_B T}. \tag{29.102}$$

Obviously, the same rates are obtained for any complete cycle

$$M_{1,n} \underset{k_{2,1}}{\overset{k_{1,2}}{\rightleftharpoons}} \mathrm{M}_{2,n} \underset{k_{3,2}}{\overset{k_{2,3}}{\rightleftharpoons}} \mathrm{M}_{3,n} \underset{k_{4,3}}{\overset{k_{3,4}}{\rightleftharpoons}} \mathrm{M}_{4,n} \underset{k_{1,4}}{\overset{k_{4,1}}{\rightleftharpoons}} \mathrm{M}_{1,n+1} \tag{29.103}$$

and we do not need to introduce second indices for the rates.[4] Summing up all cycles

$$W_i = \sum_{n=1}^{4} W_{i,n} \tag{29.104}$$

we end up with the following reaction cycle of the motor

$$\frac{\partial W_1}{\partial t} = -(k_{1,2} + k_{1,4}) W_1 + k_{2,1} W_2 + k_{4,1} W_4$$
$$\frac{\partial W_2}{\partial t} = -(k_{2,1} + k_{2,3}) W_2 + k_{1,2} W_1 + k_{3,2} W_3$$
$$\frac{\partial W_3}{\partial t} = -(k_{3,2} + k_{3,4}) W_3 + k_{2,3} W_2 + k_{4,3} W_4$$
$$\frac{\partial W_4}{\partial t} = -(k_{4,1} + k_{4,3}) W_4 + k_{1,4} W_1 + k_{3,4} W_3. \tag{29.105}$$

Equations (29.86), (29.90), (29.94), (29.102) show that detailed balance holds, if the proper free energies are considered. If, on the other hand, one does not keep track of the number of cycles and tries to assign free energy values, e.g., $G_i = G_{i,0}$ to the four motor states, detailed balance is apparently violated. If we assume furthermore, that only the concentration of ATP is changed away from its equilibrium value, we end up with [192]

[4] E.g. $k_{1,2} = k_{(1,n)\to(2,n)} \ldots k_{4,1} = k_{(4,n)\to(1,n+1)}$.

$$\frac{k_{1,2}}{k_{2,1}} = \frac{c_{ATP}}{c_{ATP}^{eq}} e^{(U_1-U_2)/k_BT} \tag{29.106}$$

$$\frac{k_{2,3}}{k_{3,2}} = e^{(U_2-U_3)/k_BT} \tag{29.107}$$

$$\frac{k_{3,4}}{k_{4,3,}} = \frac{c_P^{eq}}{c_P} e^{(U_3-U_4)/k_BT} \approx e^{(U_3-U_4)/k_BT} \tag{29.108}$$

$$\frac{k_{4,1}}{k_{1,4}} = \frac{c_{ADP}^{eq}}{c_{ADP}} e^{(U_4-U_1)/k_BT} \approx e^{(U_4-U_1)/k_BT}. \tag{29.109}$$

29.5 The Two-State Model

In a simplified two-state model (Fig. 29.9) the cycle is further divided into two substeps combining ATP-binding and hydrolysis

$$\mathrm{M} + \mathrm{ATP} \underset{\alpha_2}{\overset{\alpha_1}{\rightleftharpoons}} \mathrm{M} - \mathrm{ADP} - \mathrm{P} \tag{29.110}$$

as well as the release of ADP and P

$$\mathrm{M} + \mathrm{ADP} + \mathrm{P} \underset{\beta_2}{\overset{\beta_1}{\rightleftharpoons}} \mathrm{M} - \mathrm{ADP} - \mathrm{P}. \tag{29.111}$$

This two-state model has only a small number of parameters, but is very useful to understand the general behavior. It involves a system of two coupled differential equations

$$\frac{\partial}{\partial t} W_1 + \frac{\partial}{\partial x} S_1 = -k_{12} W_1 + k_{21} W_2 \tag{29.112}$$

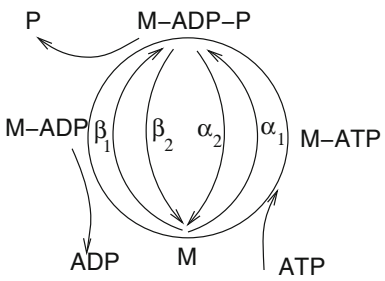

Fig. 29.9 Simplified chemical cycle

$$\frac{\partial}{\partial t}W_2 + \frac{\partial}{\partial x}S_2 = -k_{21}W_2 + k_{12}W_1. \tag{29.113}$$

29.5.1 The Chemical Cycle

Since each cycle consumes the energy from hydrolysis of one ATP, we consider a sequence of states (Fig. 29.10)

$$\cdots \mathrm{M}_{1,0} \underset{\alpha_2}{\overset{\alpha_1}{\rightleftharpoons}} \mathrm{M}_{2,0} \underset{\beta_1}{\overset{\beta_2}{\rightleftharpoons}} \mathrm{M}_{1,1} \underset{\alpha_2}{\overset{\alpha_1}{\rightleftharpoons}} \mathrm{M}_{2,1} \cdots \tag{29.114}$$

For the ATP-binding step

$$M + ATP \rightleftharpoons M - ADP - P \tag{29.115}$$

we have

$$r_{\rightarrow} = k_{(1,n)\rightarrow(2,n)} c_{ATP} W_1 = \alpha_1 W_1 \tag{29.116}$$

$$r_{\leftarrow} = k_{(2,n)\rightarrow(1,n)} W_2 = \alpha_2 W_2 \tag{29.117}$$

$$\frac{k_{(1,n)\rightarrow(2,n)}}{k_{(2,n)\rightarrow(1,n)}} = \frac{W_2^{eq}}{W_1^{eq}} \frac{1}{c_{ATP}^{eq}} = \frac{1}{c_{ATP}^{eq}} \mathrm{e}^{(U_1 - U_2)/k_B T} \tag{29.118}$$

$$\frac{\alpha_1}{\alpha_2} = \frac{c_{ATP}}{c_{ATP}^{eq}} \mathrm{e}^{(U_1 - U_2)/k_B T} = \mathrm{e}^{(G_{1,n} - G_{2,n})/k_B T} \tag{29.119}$$

and for the second step

$$M - ADP - P \rightleftharpoons M + ADP + P \tag{29.120}$$

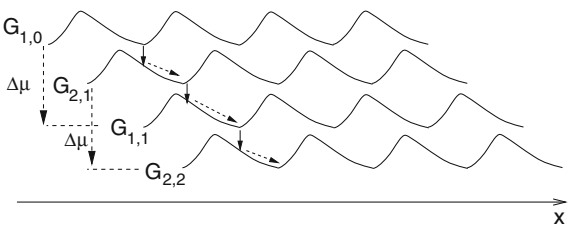

Fig. 29.10 Hierarchy of free energies for the two-state model

$$r_{\rightarrow} = k_{(2,n)\rightarrow(1,n+1)} W_2 = \beta_2 W_2 \tag{29.121}$$

$$r_{\leftarrow} = k_{(1,n+1)\rightarrow(2,n)} c_{ADP} c_P W_1 = \beta_1 W_1 \tag{29.122}$$

$$\frac{k_{(1,n+1)\rightarrow(2,n)}}{k_{(2,n)\rightarrow(1,n+1)}} = \frac{1}{c_P^{eq} c_{ADP}^{eq}} \frac{W_2^{eq}}{W_1^{eq}} = \frac{1}{c_P^{eq} c_{ADP}^{eq}} \mathrm{e}^{(U_1-U_2)/k_B T} \tag{29.123}$$

$$\begin{aligned} \frac{\beta_1}{\beta_2} &= \frac{c_P c_{ADP}}{c_P^{eq} c_{ADP}^{eq}} \mathrm{e}^{(U_1-U_2)/k_B T} \\ &= \mathrm{e}^{(G_{1,n+1}-G_{2,n})/k_B T} = \mathrm{e}^{(G_{1,n}-G_{2,n}+\Delta\mu)/k_B T}. \end{aligned} \tag{29.124}$$

The time evolution of the motor is described by a hierarchy of equations

$$\frac{\partial}{\partial t} W_{1,n} + \frac{\partial}{\partial x} S_{1,n} = -(\alpha_1 + \beta_1) W_{1,n} + \alpha_2 W_{2,n} + \beta_2 W_{2,n-1}.$$

Taking the sum over n

$$W_s = \sum_n W_{s,n} \quad S_s = \sum_n S_{s,n} \tag{29.125}$$

we obtain the two-state model

$$\frac{\partial}{\partial t} W_1 + \frac{\partial}{\partial x} S_1 = -(\alpha_1 + \beta_1) W_1 + (\alpha_2 + \beta_2) W_2 \tag{29.126}$$

$$\frac{\partial}{\partial t} W_2 + \frac{\partial}{\partial x} S_2 = -(\alpha_2 + \beta_2) W_2 + (\alpha_1 + \beta_1) W_1 \tag{29.127}$$

where the transition rates are superpositions

$$k_{21} = \alpha_2 + \beta_2 \tag{29.128}$$

$$k_{12} = \alpha_1 + \beta_1 = \alpha_2 \mathrm{e}^{(U_1-U_2+\Delta\mu)/k_B T} + \beta_2 \mathrm{e}^{(U_1-U_2)/k_B T} \tag{29.129}$$

$$k_{12} = \alpha_1 + \beta_1 = \alpha_2 \frac{c_{ATP}}{c_{ATP}^{eq}} \mathrm{e}^{(U_1-U_2)/k_B T} + \beta_2 \frac{c_P c_{ADP}}{c_P^{eq} c_{ADP}^{eq}} \mathrm{e}^{(U_1-U_2)/k_B T} \tag{29.130}$$

$$= \alpha_2 \mathrm{e}^{(G_{1,n}-G_{2,n})/k_B T} + \beta_2 \mathrm{e}^{(G_{1,n}-G_{2,n}+\Delta\mu)/k_B T}. \tag{29.131}$$

The sum of probabilities $W(x) = W_1(x) + W_2(x)$ and fluxes $S(x) = S_1(x) + S_2(x)$ obey the equations

$$\frac{\partial}{\partial t} W + \frac{\partial}{\partial x} S = 0 \tag{29.132}$$

$$S = -\frac{k_B T}{\eta} \frac{\partial}{\partial x} W(x,t) + \frac{1}{\eta} \left[F_{ext} W(x,t) - \frac{\partial U_1}{\partial x} W_1(x,t) - \frac{\partial U_2}{\partial x} W_2(x,t) \right]. \tag{29.133}$$

In a steady state,

$$\frac{\partial W}{\partial t} = \frac{\partial S}{\partial x} = 0 \tag{29.134}$$

$$W_i(x) = \lambda_i(x) W(x) \quad i = 1, 2 \tag{29.135}$$

where $W_i(x)$ and $\lambda_i(x)$ are periodic.

$$\begin{aligned} S &= -\frac{k_B T}{\eta} \frac{\partial}{\partial x} W(x) + \frac{1}{\eta} \left[F_{ext} - \lambda_1(x) \frac{\partial U_1}{\partial x} - \lambda_2(x) \frac{\partial U_2}{\partial x} \right] W(x) \\ &= -\frac{k_B T}{\eta} \frac{\partial}{\partial x} W(x) + \frac{1}{\eta} \left[F_{ext} - \frac{\partial U_{eff}(x)}{\partial x} \right] W(x) \end{aligned} \tag{29.136}$$

with the effective potential

$$U_{eff}(x) = \int_0^x dx' \quad \left(\lambda_1(x) \frac{\partial U_1}{\partial x} + \lambda_2(x) \frac{\partial U_2}{\partial x} \right) \tag{29.137}$$

which is not necessarily periodic. Due to periodicity of U_i and λ_i

$$\begin{aligned} U_{eff}(x+L) &= U_{eff}(x) + \int_x^{x+L} dx' \quad \left(\lambda_1(x) \frac{\partial U_1}{\partial x} + \lambda_2(x) \frac{\partial U_2}{\partial x} \right) \\ &= U_{eff}(x) + \Delta U \end{aligned} \tag{29.138}$$

with

$$\Delta U = U_{eff}(L) - U_{eff}(0). \tag{29.139}$$

Consider

$$U_{eff}^p(x) = U_{eff}(x) - \frac{\Delta U}{L} x \tag{29.140}$$

which is periodic

$$U^p_{eff}(x+L) = U_{eff}(x+L) - \Delta U(1+\frac{x}{L}) = U^p_{eff}(x). \tag{29.141}$$

Formally, integration then gives the reduced flux (29.25)

$$\tilde{S} = \frac{k_B T}{\eta}(1-\mathrm{e}^{(\Delta U - L F_{ext})/k_B T})\left[\int_0^L dx\, \mathrm{e}^{(xF_{ext}-U_{eff}(x))/k_B T}\int_x^{x+L} dx' \mathrm{e}^{-(x'F_{ext}-U_{eff}(x'))/k_B T}\right]^{-1}. \tag{29.142}$$

Without external force, the flux vanishes if the effective potential is periodic ($\Delta U = 0$). This is especially the case for a symmetric system with $U_{1,2}(-x) = U_{1,2}(x)$, where the steady state distributions $W_{1,2}(x)$ are also symmetric and the velocity

$$< v >= -\frac{1}{\eta}\int_0^L dx \left(W_1 \frac{\partial U_1}{\partial x} + W_2 \frac{\partial U_2}{\partial x}\right) \tag{29.143}$$

vanishes, since the forces are antisymmetric functions (Fig. 29.11). Only for asymmetric systems can the effective potential become nonperiodic ($\Delta U \neq 0$) and the motor develop an average force.

At equilibrium, $\Delta\mu = 0$ and the rates obey detailed balance

$$\frac{k_{12}(x)}{k_{21}(x)} = \mathrm{e}^{(G^{eq}_{1,n} - G^{eq}_{2,n})/k_B T} = \mathrm{e}^{-(U_2(x)-U_1(x))/k_B T} \tag{29.144}$$

which indicates that the system is not chemically driven and is only subject to thermal fluctuations. The steady state is then again given by

$$W_i = N\mathrm{e}^{-U_i(x)/k_B T} \tag{29.145}$$

$$\lambda_1 = \frac{W_1}{W_1+W_2} = \frac{1}{1+\mathrm{e}^{(U_1(x)-U_2(x))/k_B T}} \tag{29.146}$$

$$\lambda_2 = \frac{W_2}{W_1+W_2} = \frac{1}{1+\mathrm{e}^{-(U_1(x)-U_2(x))/k_B T}} \tag{29.147}$$

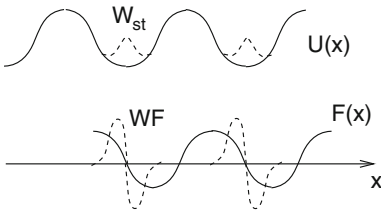

Fig. 29.11 Symmetric system

and the effective potential is

$$\begin{aligned} U_{eff}(x) &= \int_0^x dx' \left(\frac{1}{1+\mathrm{e}^{(U_1(x)-U_2(x))/k_BT}} \frac{\partial U_1}{\partial x} + \frac{1}{1+\mathrm{e}^{-(U_1(x)-U_2(x))/k_BT}} \frac{\partial U_2}{\partial x} \right) \\ &= \int_0^x dx' \left(\frac{\mathrm{e}^{-U_1/k_BT}}{\mathrm{e}^{-U_1/k_BT}+\mathrm{e}^{-U_2(x))/k_BT}} \frac{\partial U_1}{\partial x} + \frac{\mathrm{e}^{-U_2/k_BT}}{\mathrm{e}^{-U_2/k_BT}+\mathrm{e}^{-U_1(x)/k_BT}} \frac{\partial U_2}{\partial x} \right) \\ &= -k_BT \int_0^x dx \ \frac{\partial}{\partial x} \ln\left(\mathrm{e}^{-U_1/k_BT}+\mathrm{e}^{-U_2(x))/k_BT}\right) \\ &= -k_BT \ln\left(\mathrm{e}^{-U_1(x)/k_BT}+\mathrm{e}^{-U_2(x))/k_BT}\right) + k_BT \left(\mathrm{e}^{-U_1(0)/k_BT}+\mathrm{e}^{-U_2(0))/k_BT}\right) \end{aligned} \tag{29.148}$$

which is obviously periodic, hence there is no flux. For $\Delta\mu > 0$ the system is chemically driven and spontaneous motion with $v \neq 0$ can occur.

The ATP consumption rate

$$r = \int_0^L dx(\alpha_1 \tilde{W}_1 - \alpha_2 \tilde{W}_2) \tag{29.149}$$

is generally not zero for a symmetric system, since $\alpha_{1,2}$ are symmetric functions. Therefore, two conditions have to be fulfilled for spontaneous motion to occur: the system must be chemically driven ($\Delta\mu \neq 0$) and it must have polar symmetry. If we assume again, that only the ATP concentration is changed from its equilibrium value,

$$\frac{\beta_1}{\beta_2} = \frac{c_P c_{ADP}}{c_P^{eq} c_{ADP}^{eq}} \mathrm{e}^{(U_1-U_2)/k_BT} \approx \mathrm{e}^{(U_1-U_2)/k_BT} \tag{29.150}$$

$$\begin{aligned} (\alpha_1+\beta_1) &= \beta_2 \mathrm{e}^{(U_1-U_2)/k_BT} + \alpha_2 \frac{c_{ATP}}{c_{ATP}^{eq}} \mathrm{e}^{(U_1-U_2)/k_BT} \\ &= (\alpha_2+\beta_2)\mathrm{e}^{(U_1-U_2)/k_BT} \left(1 + \frac{\alpha_2}{\alpha_2+\beta_2}\left(\frac{c_{ATP}}{c_{ATP}^{eq}} - 1\right)\right). \end{aligned} \tag{29.151}$$

Introducing as a measure of the deviation from equilibrium the quantity

$$\Omega = \frac{\alpha_2}{\alpha_2+\beta_2}\left(\frac{c_{ATP}}{c_{ATP}^{eq}} - 1\right)\mathrm{e}^{(U_1-U_2)/k_BT} \tag{29.152}$$

the rhs of (29.126) becomes

$$\begin{aligned} &-(\alpha_1+\beta_1)W_1 + (\alpha_2+\beta_2)W_2 \\ &= (\alpha_2+\beta_2)\left(W_2 - W_1 \mathrm{e}^{(U_1-U_2)/k_BT} - \Omega W_1\right). \end{aligned} \tag{29.153}$$

In the limit of large concentration $c_{ATP}/c_{ATP}^{eq} \gg 1$, Ω becomes proportional to the concentration ratio

$$\Omega(x) \approx \mathrm{e}^{-\Delta U(x)/k_B T} \frac{\alpha_2(x)}{\alpha_2(x)+\beta_2(x)} \frac{c_{ATP}}{c_{ATP}^{eq}} \tag{29.154}$$

whereas close to equilibrium in the limit $\Delta\mu \neq 0$ but $|\Delta\mu| \ll k_B T$

$$\Delta\mu \approx -k_B T \ln \frac{c_{ATP}}{c_{ATP}^{eq}} \approx -k_B T \ln \left(1 + \frac{\Delta c_{ATP}}{c_{ATP}^{eq}}\right) \approx -k_B T \frac{\Delta c_{ATP}}{c_{ATP}^{eq}} \tag{29.155}$$

$$\Omega(x) \approx \mathrm{e}^{-\Delta U(x)/k_B T} \frac{\alpha_2(x)}{\alpha_2(x)+\beta_2(x)} \frac{(-\Delta\mu)}{k_B T}. \tag{29.156}$$

29.5.2 The Fast Reaction Limit

If the chemical reactions are faster than the diffusive motion, then there is always a local equilibrium

$$\frac{W_1(x,t)}{W_2(x,t)} = \frac{k_{21}(x)}{k_{12}(x)} \tag{29.157}$$

and the total probability $W = W_1 + W_2$ obeys the equation

$$\frac{\partial}{\partial t} W = \frac{k_B T}{\eta} \frac{\partial^2}{\partial x^2} W + \frac{1}{\eta} \frac{\partial}{\partial x} \left(\frac{\partial}{\partial x} (U_1 W_1 + U_2 W_2) \right)$$

$$\frac{\partial}{\partial t} W = \frac{k_B T}{\eta} \frac{\partial^2}{\partial x^2} W + \frac{1}{\eta} \frac{\partial}{\partial x} \left(\frac{\partial}{\partial x} \left(\frac{k_{21}}{k_{12}+k_{21}} U_1 + \frac{k_{12}}{k_{12}+k_{21}} U_2 \right) W \right) \tag{29.158}$$

which describes motion in the average potential.

29.5.3 The Fast Diffusion Limit

If the diffusive motion is faster than the chemical reactions the motor can work as a Brownian ratchet (Fig. 29.12). In the time between chemical reactions equilibrium is established in both states

$$W_{st}^0 = c_{1,2} \mathrm{e}^{-U_{1,2}(x)/k_B T} \tag{29.159}$$

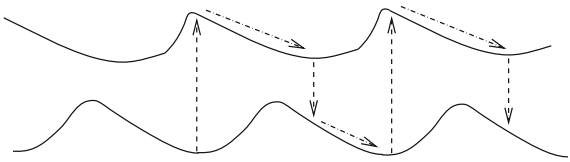

Fig. 29.12 Brownian ratchet

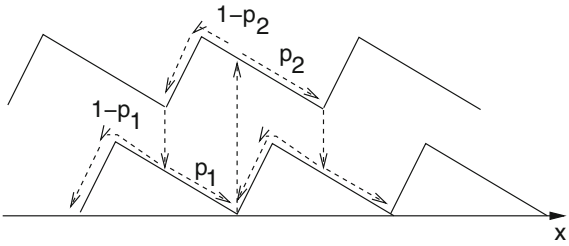

Fig. 29.13 Fast diffusion limit far from equilibrium

If the barrier height is large and the equilibrium distribution is confined around the minima, the diffusion process can be approximated by a simpler rate process. Every ATP consumption corresponds to a transition to the second state. Then the system moves to one of the two neighboring minima with probabilities p_2 and $1 - p_2$, respectively. From here, it makes a transition back to the first state. Finally, it moves right or left with probability p_1 and $1 - p_1$, respectively (Fig. 29.13).

During this cycle, the system proceeds in a forward direction with probability

$$p_+ = p_1 p_2 \tag{29.160}$$

backwards with probability

$$p_- = (1 - p_1)(1 - p_2) \tag{29.161}$$

or it returns to its initial position with probability

$$p_0 = p_2(1 - p_1) + p_1(1 - p_2). \tag{29.162}$$

The average displacement per consumed ATP is

$$< x > \approx L(p_+ - p_-) = L(p_1 + p_2 - 1) \tag{29.163}$$

and the average velocity is

$$v = r < x > . \tag{29.164}$$

In the presence of an external force, the efficiency can thus be estimated as

$$\eta = \frac{-F_{ext}}{\Delta\mu} < x > . \tag{29.165}$$

29.5.4 Operation Close to Thermal Equilibrium

For constant T and μ_i the local heat dissipation is given by

$$T\sigma(x) = \sum_k \left(F_{ext} - \frac{\partial U_k}{\partial x} \right) S_k + r(x)\Delta\mu. \tag{29.166}$$

In a stationary state the total heat dissipation is

$$\Pi = \int T\sigma(x)dx = F_{ext}v + r\Delta\mu \tag{29.167}$$

since

$$\int \frac{\partial U}{\partial x} S dx = -\int U(x)\frac{\partial S}{\partial x}dx = 0. \tag{29.168}$$

Under the action of an external force F_{ext} the velocity and the hydrolysis rate are functions of the external force and $\Delta\mu$

$$v = v(F_{ext}, \Delta\mu)$$

$$r = r(F_{ext}, \Delta\mu). \tag{29.169}$$

Close to equilibrium linearization gives

$$v = \lambda_{11}F_{ext} + \lambda_{12}\Delta\mu$$

$$r = \lambda_{21}F_{ext} + \lambda_{22}\Delta\mu. \tag{29.170}$$

The rate of energy dissipation is given by mechanical plus chemical work

$$\Pi = F_{ext}v + r\Delta\mu = \lambda_{11}F_{ext}^2 + \lambda_{22}\Delta\mu^2 + (\lambda_{12} + \lambda_{21})F_{ext}\Delta\mu \tag{29.171}$$

which must be always positive due to the second law of thermodynamics. This is the case if

$$\lambda_{11} > 0, \lambda_{22} > 0 \quad \text{and } \lambda_{11}\lambda_{22} - \lambda_{12}\lambda_{21} > 0. \tag{29.172}$$

The efficiency of the motor can be defined as

$$\eta = \frac{-F_{ext}\, v}{r\,\Delta\mu} = \frac{-\lambda_{11} F_{ext}^2 - \lambda_{12} F_{ext}\,\Delta\mu}{\lambda_{22}\Delta\mu^2 + \lambda_{21} F_{ext}\,\Delta\mu}$$

$$\eta = -\frac{\lambda_{11} a^2 + \lambda_{12} a}{\lambda_{22} + \lambda_{21} a} \qquad a = \frac{F_{ext}}{\Delta\mu}\,. \tag{29.173}$$

It vanishes for zero force but also for $v = 0$ and has a maximum at (Figs. 29.14, 29.15)

$$a = \frac{\sqrt{1 - \frac{\lambda_{12}\lambda_{21}}{\lambda_{11}\lambda_{22}}} - 1}{\frac{\lambda_{21}}{\lambda_{22}}} \qquad \eta_{max} = \frac{(1 - \sqrt{1 - \Lambda})^2}{\Lambda} \qquad \Lambda = \frac{\lambda_{12}\lambda_{21}}{\lambda_{11}\lambda_{22}}\,. \tag{29.174}$$

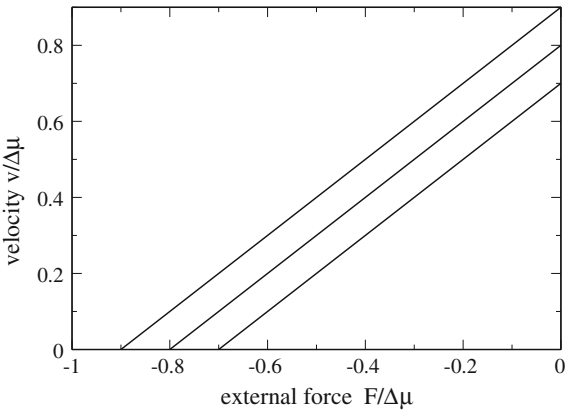

Fig. 29.14 Velocity–force relation

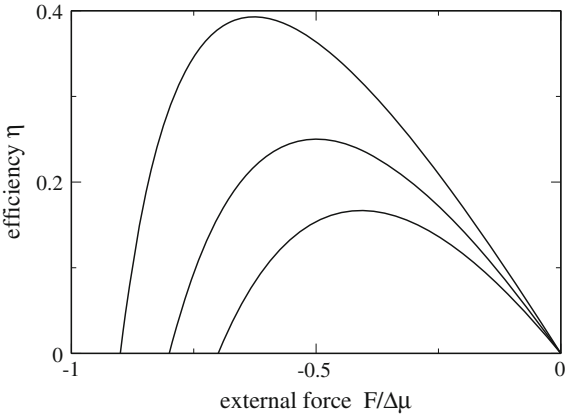

Fig. 29.15 Efficiency of the motor

29.6 Ratchet with Localized Reactions

The analytical treatment of the ratchet model simplifies considerably if it is assumed that the chemical transitions take place only at a number n of certain well-defined configurations $x_\alpha, \quad \alpha = 1 \ldots n$. The transition rates have the form [190]

$$k_{i,j}(x) = \sum_\alpha \omega_{i,j}^\alpha \delta(x - x_\alpha) \tag{29.175}$$

and in the stationary state ($\frac{\partial W_i}{\partial t} = 0$) integration of

$$\begin{aligned} \frac{\partial \tilde{S}_i(x)}{\partial x} &= \sum_{i \neq j} \left(k_{ji}(x) \tilde{W}_i(x,t) - k_{ij}(x) \tilde{W}_j(x,t) \right) \\ &= \sum_{i \neq j} \sum_\alpha \delta(x - x_\alpha) \left(\omega_{ji}^\alpha \tilde{W}_i(x) - \omega_{ij}^\alpha(x) \tilde{W}_j(x) \right) \end{aligned} \tag{29.176}$$

gives piecewise constant fluxes (Fig. 29.16)

$$\tilde{S}_i(x) = \tilde{S}_i(0^-) + \sum_{i \neq j} \sum_\alpha \theta(x - x_\alpha) \left(\omega_{ji}^\alpha \tilde{W}_i(x_\alpha) - \omega_{ij}^\alpha(x) \tilde{W}_j(x_\alpha) \right). \tag{29.177}$$

Equation (29.177) provides a linear relation between $m \times n$ probability densities $\tilde{W}_i(x_\alpha)$ and $m \times n$ flux values $\tilde{S}_i(x_1^+) \ldots \tilde{S}_i(x_n^+)$. However, as the flux sum is constant

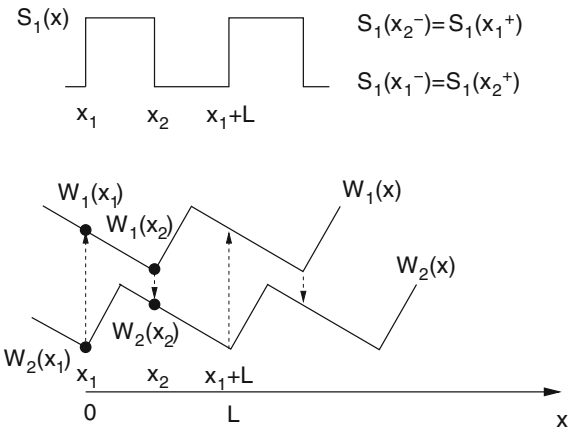

Fig. 29.16 Ratchet with localized reactions. The figure shows an example for the case of $m = 2$ states and $n = 2$ reactive configurations. In a stationary state, there are four unknown values of the probability densities $\tilde{W}_{1,2}(x_{1,2})$ and four unknown values of the fluxes $\tilde{S}_{1,2}(x_{1,2}^-)$. The number of flux values reduces due to the condition $\tilde{S}_1(x) + \tilde{S}_2(x) = \tilde{S} = \text{const}$

$\sum_{i=1}^{m} \tilde{S}_i(x_j^+) = \tilde{S}$ we can eliminate $(n-1)$ variables. Equation (29.177) then provides $(m-1)\times n$ homogeneous linear equations for the $m\times n+(m-1)\times n+1$ variables $\tilde{W}_{1\ldots m}(x_{1\ldots n})$, $\tilde{S}_{1\ldots(m-1)}(x^+_{1\ldots n})$, $\tilde{S}$. Integration of the stationary gradient

$$\begin{aligned}\frac{\partial}{\partial x}\tilde{W}_i(x) &= \frac{1}{k_BT}K_i(x)\tilde{W}_i(x) - \frac{\eta}{k_BT}\tilde{S}_i \\ &= -\frac{1}{k_BT}\frac{\partial(U_i - xF_{ext})}{\partial x}\tilde{W}_i(x) - \frac{\eta}{k_BT}\tilde{S}_i\end{aligned} \tag{29.178}$$

then gives

$$\begin{aligned}\tilde{W}_i(x) &= \tilde{W}_i(x_\alpha)\mathrm{e}^{[U_i(x)-U_i(x_\alpha)-(x-x_\alpha)F_{ext}]/k_BT} \\ &- \frac{\eta}{k_BT}\int_{x_\alpha}^{x}\tilde{S}_i(x')\mathrm{e}^{[U_i(x)-U_i(x')+(x-x')F_{ext}]/k_BT}\end{aligned} \tag{29.179}$$

from which further $m\times n$ homogeneous equations are obtained $(x_{n+1} = x_1 + L)$

$$\begin{aligned}\tilde{W}_i(x_{\alpha+1}) &= \tilde{W}_i(x_\alpha)\mathrm{e}^{[U_i(x_{\alpha+1})-U_i(x_\alpha)-(x_{\alpha+1}-x_\alpha)F_{ext}]/k_BT} \\ &- \frac{\eta\tilde{S}_i(x_\alpha^+)}{k_BT}\int_{x_\alpha}^{x_{\alpha+1}}\mathrm{e}^{[U_i(x_{\alpha+1})-U_i(x')+(x_{\alpha+1}-x')F_{ext}]/k_BT}.\end{aligned} \tag{29.180}$$

Finally, the normalization of the probability

$$\int_0^L \sum_{i=1}^{m}\tilde{W}_i(x)dx = 1 \tag{29.181}$$

provides one more but inhomogeneous equation and we end up with an inhomogeneous system of $(2m-1)\times n+1$ equations for the same number of variables which can be solved by linear algebra.

For the two-state model we consider two reactive configurations $x = 0, x = a$ (Fig. 29.17) with

$$k_{1,2}(x) = \omega^0_{1,2}\delta(x) + \omega^a_{12}\delta(x-a) \tag{29.182}$$

$$k_{2,1}(x) = \omega^0_{2,1}\delta(x) + \omega^a_{2,1}\delta(x-a). \tag{29.183}$$

For a stationary state this leads to a system of two equations

$$\frac{\partial}{\partial x}\tilde{S}_1(x) = \delta(x)\left[\tilde{W}_2(0)\omega^0_{21} - \tilde{W}_1(0)\omega^0_{12}\right] + \delta(x-a)\left[\tilde{W}_2(a)\omega^a_{21} - \tilde{W}_1(a)\omega^a_{21}\right] \tag{29.184}$$

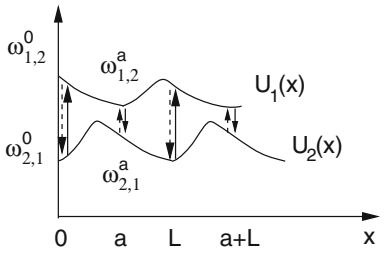

Fig. 29.17 Localized reactions

$$\frac{\partial}{\partial x}\tilde{S}_2(x) = -\frac{\partial}{\partial x}\tilde{S}_1(x). \tag{29.185}$$

Integration gives the fluxes as stepwise functions

$$\begin{aligned}\tilde{S}_1(x) &= \tilde{S}_1(0^-) + \theta(x)\left[\tilde{W}_2(0)\omega^0_{21} - \tilde{W}_1(0)\omega^0_{12}\right] + \theta(x-a)\left[\tilde{W}_2(a)\omega^a_{21} - \tilde{W}_1(a)\omega^a_{21}\right] \\ &= \tilde{S}_1(0^+) + \theta(x-a)\Delta\tilde{S}\end{aligned} \tag{29.186}$$

$$\begin{aligned}\tilde{S}_2(x) &= \tilde{S}_2(0^-) - \theta(x)\left[\tilde{W}_2(0)\omega^0_{21} - \tilde{W}_1(0)\omega^0_{12}\right] - \theta(x-a)\left[\tilde{W}_2(a)\omega^a_{21} - \tilde{W}_1(a)\omega^a_{21}\right] \\ &= \tilde{S}_2(0^+) - \theta(x-a)\Delta\tilde{S}\end{aligned} \tag{29.187}$$

with

$$\Delta\tilde{S} = \tilde{W}_2(a)\omega^a_{21} - \tilde{W}_1(a)\omega^a_{21} = -\left[\tilde{W}_2(0)\omega^0_{21} - \tilde{W}_1(0)\omega^0_{12}\right] \tag{29.188}$$

which provides two linear equations.

From (29.179) we find

$$\begin{aligned}\tilde{W}_i(x) &= \tilde{W}_i(0)\mathrm{e}^{[U_i(x)-U_i(0)-xF_{ext}]/k_BT} \\ &- \eta\frac{\tilde{S}_i(0^+)}{k_BT}\int_0^x dx'\mathrm{e}^{[U_i(x)-U_i(x')+(x-x')F_{ext}]/k_BT} \quad 0 < x < a\end{aligned} \tag{29.189}$$

$$\begin{aligned}\tilde{W}_i(x) &= \tilde{W}_i(a)\mathrm{e}^{[U_i(x)-U_i(a)-(x-a)F_{ext}]/k_BT} \\ &- \eta\frac{\tilde{S}_i(0^+) \pm \Delta\tilde{S}}{k_BT}\int_a^x \mathrm{e}^{[U_i(x)-U_i(x')+(x-x')F_{ext}]/k_BT} \quad a < x < L\end{aligned} \tag{29.190}$$

providing the four equations

$$\tilde{W}_i(a) = \tilde{W}_i(0)\mathrm{e}^{[U_i(a)-U_i(0)-aF_{ext}]/k_BT} - \eta\frac{\tilde{S}_i(0^+)}{k_BT}\int_0^a dx'\mathrm{e}^{[U_i(a)-U_i(x')+(a-x')F_{ext}]/k_BT} \tag{29.191}$$

$$\tilde{W}_i(0) = \tilde{W}_i(a)\mathrm{e}^{[U_i(0)-U_i(a)-(L-a)F_{ext}]/k_BT} - \eta\frac{\tilde{S}_i(0^+) \pm \Delta\tilde{S}}{k_BT}\int_a^L \mathrm{e}^{[U_i(0)-U_i(x')+(L-x')F_{ext}]/k_BT}. \tag{29.192}$$

Together with the normalization condition, we end up with seven equations for seven variables

$$\tilde{S}_1(0^+),\ \tilde{S}_2(0^+),\ \Delta\tilde{S},\ \tilde{W}_1(0),\ \tilde{W}_2(0),\ \tilde{W}_1(a),\ \tilde{W}_2(a). \tag{29.193}$$

Problems

29.1 Deviation from Equilibrium

Make use of the detailed balance conditions

$$\frac{\alpha_1}{\alpha_2} = \mathrm{e}^{(\Delta\mu-\Delta U)/k_BT}$$
$$\frac{\beta_1}{\beta_2} = \mathrm{e}^{-\Delta U/k_BT}$$

and calculate the quantity

$$\Omega = \frac{k_{12}}{k_{21}} - \mathrm{e}^{-\Delta U/k_BT} = \frac{\alpha_1+\beta_1}{\alpha_2+\beta_2} - \mathrm{e}^{-\Delta U/k_BT}.$$

Use the approximation

$$\Delta\mu = \Delta\mu^0 + k_BT\ln\frac{C(ATP)}{C(ADP)C(P)}$$

and express Ω in terms of the equilibrium constant

$$K_{eq} = \mathrm{e}^{\Delta\mu^0/k_BT}.$$

Consider the limiting cases

$$\Delta\mu \neq 0 \text{ but } |\Delta\mu| \ll k_BT$$

and

$$|\Delta\mu| \gg k_BT$$

Chapter 30
Discrete Ratchet Models

Simplified molecular motor models describe the motion of the protein as a hopping process combined with a cyclical transition between internal motor states. We discuss a linear model with two internal states and derive the velocity–force relation.

30.1 Linear Discrete Ratchets

The motion of the protein is described as a hopping process between positions x_n combined with transitions between different states of the motor

$$\mathrm{M}_{1,x_n} \rightleftharpoons \mathrm{M}_{2,x_n} \ldots \rightleftharpoons \mathrm{M}_{N,n_1} \rightleftharpoons \mathrm{M}_{1,x_{n+1}} \ldots \tag{30.1}$$

For example, the four-state model of the ATP hydrolysis can be easily translated into such a scheme (Fig. 30.1)

30.2 Linear Model with Two Internal States

Fisher considers a linear periodic process with two internal states [199]

$$\ldots \mathrm{M}_{1,x_n} \underset{\alpha_2}{\overset{\alpha_1}{\rightleftharpoons}} \mathrm{M}_{2,x_n} \underset{\beta_2}{\overset{\beta_1}{\rightleftharpoons}} \mathrm{M}_{1,x_{n+1}} \ldots \tag{30.2}$$

P.O.J. Scherer and S.F. Fischer, *Theoretical Molecular Biophysics*,
Biological and Medical Physics, Biomedical Engineering,
DOI 10.1007/978-3-662-55671-9_30

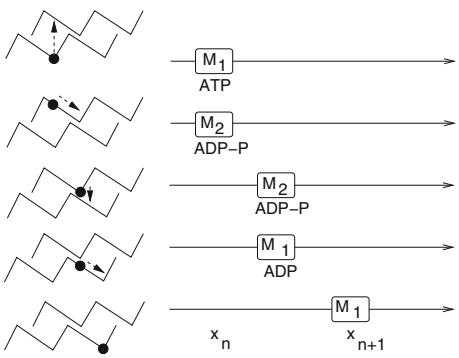

Fig. 30.1 Discrete motor model

The Master equation is

$$\begin{aligned}\frac{\mathrm{d}}{\mathrm{d}t}P_{1n} &= -(\alpha_1+\beta_2)P_{1n} + \alpha_2 P_{2n} + \beta_1 P_{2,n-1}\\ \frac{\mathrm{d}}{\mathrm{d}t}P_{2n} &= -(\alpha_2+\beta_1)P_{2n} + \alpha_1 P_{1n} + \beta_2 P_{1,n+1}\end{aligned} \tag{30.3}$$

and the stationary solution corresponds to the zero eigenvalue of the matrix

$$\begin{pmatrix} -\alpha_1-\beta_2 & \alpha_2+\beta_1 \\ \alpha_1+\beta_2 & -\alpha_2-\beta_1 \end{pmatrix}. \tag{30.4}$$

From the left and right eigenvectors

$$L_0 = \begin{pmatrix} 1 & 1 \end{pmatrix} \quad R_0 = \begin{pmatrix} \alpha_2+\beta_1 \\ \alpha_1+\beta_2 \end{pmatrix} \tag{30.5}$$

we have

$$P_{1,st} = \frac{\alpha_2+\beta_1}{\alpha_2+\beta_1+\alpha_1+\beta_2} \quad P_{2,st} = \frac{\alpha_1+\beta_2}{\alpha_1+\beta_2+\alpha_2+\beta_1} \tag{30.6}$$

and the stationary current is

$$S = \alpha_1 P_{1,st} - \alpha_2 P_{2,st} = \frac{\alpha_1\beta_1 - \alpha_2\beta_2}{\alpha_1+\beta_2+\alpha_2+\beta_1}. \tag{30.7}$$

With the definition of

$$\omega = \frac{\alpha_2\beta_2}{\alpha_1+\alpha_2+\beta_1+\beta_2} \tag{30.8}$$

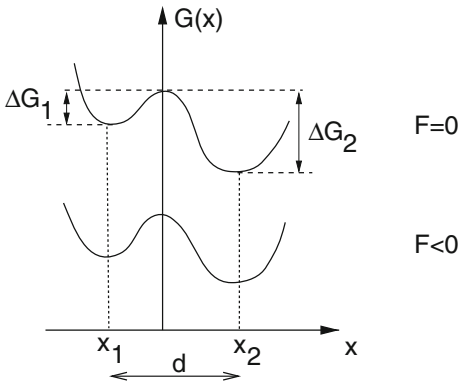

Fig. 30.2 Influence of the external force. The external force changes the activation barriers which become approximately $\Delta G_1(F) = \Delta G_1(0) - x_1 F$, $\Delta G_2(F) = \Delta G_2(0) + x_2 F$

and

$$\Gamma = \frac{\alpha_1 \beta_1}{\alpha_2 \beta_2} = \mathrm{e}^{\Delta\mu/k_B T} \tag{30.9}$$

the current can be written as

$$S = (\Gamma - 1)\omega. \tag{30.10}$$

Consider now application of an external force corresponding to an additional potential energy

$$U_n = -F_{ext} n d. \tag{30.11}$$

Assuming that the motion corresponds to the transition $\mathrm{M}_{2,n} \rightleftharpoons \mathrm{M}_{1,n+1}$ the corresponding rates will become dependent on the force (Fig. 30.2)

$$\begin{aligned} \beta_1 &= \beta_1^0 \mathrm{e}^{\Theta F d/k_B T} \\ \beta_2 &= \beta_2^0 \mathrm{e}^{-(1-\Theta) F d/k_B T}. \end{aligned} \tag{30.12}$$

Here, Θ is the so-called splitting parameter. The force-dependent current is

$$S = \left(\mathrm{e}^{\Delta\mu/k_B T + F d/k_B T} - 1\right) \frac{\alpha_2 \beta_2^0 \mathrm{e}^{-(1-\Theta) F d/k_B T}}{\alpha_1 + \alpha_2 + \beta_1^0 \mathrm{e}^{\Theta F d/k_B T} + \beta_2^0 \mathrm{e}^{-(1-\Theta) F d/k_B T}} \tag{30.13}$$

which vanishes for the stalling force

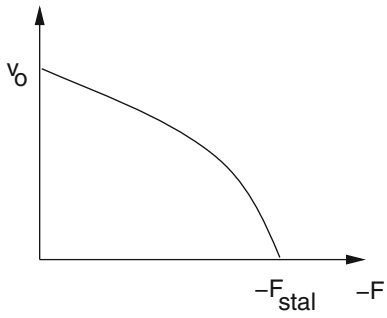

Fig. 30.3 Velocity–force relation

$$F_{stal} = -\frac{\Delta\mu}{d}. \tag{30.14}$$

Close to equilibrium, we expand (Fig. 30.3)

$$\Gamma - 1 = \mathrm{e}^{\Delta\mu/k_BT + Fd/k_BT} - 1 = \mathrm{e}^{(1-F/F_{stal})\Delta\mu/k_BT} - 1 \approx (1 - F/F_{stal})\frac{\Delta\mu}{k_BT} \tag{30.15}$$

$$\omega \approx \omega^0 \left(1 - \frac{Fd}{k_BT}\frac{(\beta_1^0 + (\alpha_1 + \alpha_2)(1-\Theta))}{(\alpha_1 + \alpha_2 + \beta_1^0 + \beta_2^0)}\right). \tag{30.16}$$

Part IX
Appendix

Appendix A
The Grand Canonical Ensemble

Consider an ensemble of M systems which can exchange energy as well as particles with a reservoir. For large M, the total number of particles $N_{tot} = M\overline{N}$ and the total energy $E_{tot} = M\overline{E}$ have well-defined values since the relative widths decrease as

$$\frac{\sqrt{\overline{N_{tot}^2} - \overline{N_{tot}}^2}}{\overline{N_{tot}}} \sim \frac{1}{\sqrt{M}} \quad \frac{\sqrt{\overline{E_{tot}^2} - \overline{E_{tot}}^2}}{\overline{E_{tot}}} \sim \frac{1}{\sqrt{M}} \tag{A.1}$$

Hence, also the average number and energy can be assumed to have well-defined values (Fig. A.1)

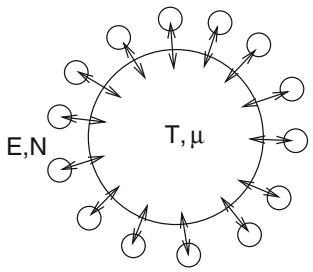

Fig. A.1 Ensemble of systems exchanging energy and particles with a reservoir

P.O.J. Scherer and S.F. Fischer, *Theoretical Molecular Biophysics*,
Biological and Medical Physics, Biomedical Engineering,
DOI 10.1007/978-3-662-55671-9

A.1 Grand Canonical Distribution

We distinguish different microstates j which are characterized by the number of particles N_j and the energy E_j. The number of systems in a certain microstate j will be denoted by n_j. The total number of particles and the total energy of the ensemble in a macrostate with n_j systems in the state j are

$$N_{tot} = \sum_j n_j N_j \quad E_{tot} = \sum_j n_j E_j \tag{A.2}$$

and the number of systems is

$$M = \sum_j n_j \tag{A.3}$$

The number of possible representations is given by a multinomial coefficient

$$W(\{n_j\}) = \frac{M!}{\prod_j n_j!}. \tag{A.4}$$

From Stirling's formula, we have

$$\ln W \approx \ln(M!) - \sum_j (n_j \ln n_j - n_j). \tag{A.5}$$

We search for the maximum of (A.5) under the restraints imposed by (A.2), (A.3). To this end, we use the method of undetermined factors (Lagrange method) and consider the variation

$$\begin{aligned} 0 &= \delta \left(\ln W - \alpha \left(\sum_j n_j - M \right) - \beta \left(\sum_j n_j E_j - E_{tot} \right) - \gamma (\sum_j n_j N_j - N_{tot}) \right) \\ &= \sum_j \delta n_j \left(- \ln n_j - \alpha - \beta E_j - \gamma N_j \right). \end{aligned} \tag{A.6}$$

Since the n_j now can be varied independently, we find

$$n_j = \exp(-\alpha - \beta E_j - \gamma N_j). \tag{A.7}$$

The unknown factors α, β, γ have to be determined from the restraints. First, we have

$$\sum_j n_j = \mathrm{e}^{-\alpha} \sum_j \mathrm{e}^{-\beta E_j - \gamma N_j} = M. \tag{A.8}$$

With the grand canonical partition function

$$\Xi = \sum_j \mathrm{e}^{-\beta E_j - \gamma N_j} \tag{A.9}$$

the probability of a certain microstate is given by

$$P(E_j, N_j) = \frac{n_j}{\sum_j n_j} = \frac{\mathrm{e}^{-\beta E_j - \gamma N_j}}{\Xi} \tag{A.10}$$

and further

$$\mathrm{e}^{-\alpha} = \frac{M}{\Xi}. \tag{A.11}$$

From

$$\sum_j n_j E_j = \frac{M}{\Xi} \sum_j E_j \mathrm{e}^{-\beta E_j - \gamma N_j} = E_{tot} \tag{A.12}$$

we find the average energy per system

$$\overline{E} = \frac{\sum n_j E_j}{M} = -\frac{\partial}{\partial \beta} \ln \Xi \tag{A.13}$$

and similarly from

$$\sum_j n_j N_j = \frac{M}{\Xi} \sum_j N_j \mathrm{e}^{-\beta E_j - \gamma N_j} = N_{tot} \tag{A.14}$$

the average particle number of a system

$$\overline{N} = \frac{\sum n_j N_j}{M} = -\frac{\partial}{\partial \gamma} \ln \Xi. \tag{A.15}$$

Equations (A.13), (A.15) determine the parameters β, γ implicitly and then α follows from (A.11).

A.2 Connection to Thermodynamics

Entropy is given by

$$\begin{aligned} S &= -k \sum P(E_j, N_j) \ln P(E_j, N_j) = -k \sum P(E_j, N_j)(-\beta E_j - \gamma N_j - \ln \Xi) \\ &= k\beta \overline{E} + k\gamma \overline{N} + k \ln \Xi. \end{aligned} \tag{A.16}$$

From thermodynamics, the Duhem–Gibbs relation is known which states for the free enthalpy

$$G = U - TS + pV = \mu N \tag{A.17}$$

where $U = \overline{E}$ and S, V, N are the thermodynamic averages. Solving for the entropy, we have

$$S = \frac{U + pV - \mu N}{T} \tag{A.18}$$

and comparison with (A.16) shows that

$$\beta = \frac{1}{k_B T} \quad \gamma = -\frac{\mu}{k_B T} \tag{A.19}$$

$$k_B T \ln \Xi = pV. \tag{A.20}$$

The summation over microstates j with energy E_j and N_j particles can be replaced by a double sum over energies $E_i(N)$ and particle number N to give

$$\Xi = \sum_{E,N} \mathrm{e}^{-\beta(E(N)-\mu N)} \tag{A.21}$$

which can be written as a sum over canonical partition functions with different particle numbers

$$\Xi = \sum_{N} \mathrm{e}^{\beta\mu N} \sum_{E} \mathrm{e}^{-\beta E(N)} = \sum_{N} \mathrm{e}^{\beta\mu N} Q(N). \tag{A.22}$$

Appendix B
Classical Approximation of Quantum Motion

In quantum mechanics, the motion of a particle (which could be a whole molecule) in an external potential is described by the time-dependent Schrödinger equation

$$i\hbar\dot{\psi}(\mathbf{r},t) = H\psi(\mathbf{r},t) = \left[-\frac{\hbar^2}{2m}\nabla^2 + V(\mathbf{r})\right]\psi(\mathbf{r},t). \tag{B.1}$$

A special kind of solution is a localized wavepacket, which can be approximated as a classical particle as long as dispersion of the wavepacket is negligible. The classical position and momentum are given by the expectation values

$$< \mathbf{r} >=< \psi(\mathbf{r},t)\mathbf{r}\psi(\mathbf{r},t) >=< \psi(\mathbf{r},t)\mathbf{r}\psi(\mathbf{r},t) > \tag{B.2}$$

$$< \mathbf{r} >=< \psi(\mathbf{r},t)\mathbf{p}\psi(\mathbf{r},t) >=< \psi(\mathbf{r},t)\frac{\hbar}{\mathrm{i}}\nabla\psi(\mathbf{r},t) > \tag{B.3}$$

which obey the equations of motion (Ehrenfest theorem)

$$\begin{aligned} < \dot{\mathbf{r}} >&= \frac{1}{\mathrm{i}\hbar} < \psi(\mathbf{r},t)(\mathbf{r}H - H\mathbf{r})\psi(\mathbf{r},t) > \\ &= \frac{1}{m} < \psi(\mathbf{r},t)\frac{\hbar}{\mathrm{i}}\nabla\psi(\mathbf{r},t) >= \frac{< \mathbf{p} >}{m} \end{aligned} \tag{B.4}$$

$$< \dot{\mathbf{p}} >= \frac{1}{\mathrm{i}\hbar} < \psi(\mathbf{r},t)(\mathbf{p}H - H\mathbf{p})\psi(\mathbf{r},t) >= - < \nabla V(\mathbf{r}) > . \tag{B.5}$$

If the variation of the potential gradient over the width of the wavepacket is negligible[1] these look like Newton's equations with a classical force

$$\mathbf{F} = - < \nabla V(\mathbf{r}) >\approx -\nabla V(< \mathbf{r} >). \tag{B.6}$$

[1] Or in some special cases like the harmonic oscillator.

P.O.J. Scherer and S.F. Fischer, *Theoretical Molecular Biophysics*,
Biological and Medical Physics, Biomedical Engineering,
DOI 10.1007/978-3-662-55671-9

For the harmonic oscillator with Hamiltonian

$$\hat{H} = \hbar\omega\left(\hat{a}^\dagger\hat{a} + \frac{1}{2}\right) \tag{B.7}$$

and eigenfunctions $|n>$obeying

$$\begin{aligned}&\hat{H}|n> = \hbar\omega\left(n+\frac{1}{2}\right)|n>\\ &\hat{a}|n> = \sqrt{n}|n-1> \quad \hat{a}^\dagger|n> = \sqrt{n+1}|n+1>\end{aligned} \tag{B.8}$$

a dispersionless Gaussian wavepacket is provided by the coherent oscillator state (Glauber state)[2]

$$\varphi_\alpha(x,t) = e^{-|\alpha|^2/2}\sum_{n=0}^{\infty} \mathrm{e}^{-\mathrm{i}(n+1/2)\omega t}\frac{\alpha^n}{\sqrt{n!}}|n> \tag{B.9}$$

which for any complex α solves the time dependent Schrödinger equation since

$$\mathrm{i}\hbar\dot{\varphi}_\alpha(x,t) = \hat{H}\varphi_\alpha(x,t) = e^{-|\alpha|^2/2}\sum \hbar\omega\left(n+\frac{1}{2}\right)\mathrm{e}^{-\mathrm{i}(n+1/2)\omega t}\frac{\alpha^n}{\sqrt{n!}}|n>. \tag{B.10}$$

Furthermore, it is an eigenfunction of $\hat{a}$ as can be seen from

$$\begin{aligned}\hat{a}\varphi_\alpha(x,t) &= e^{-|\alpha|^2/2}\sum_{n=1}^{\infty}\mathrm{e}^{-\mathrm{i}(n+1/2)\omega t}\frac{\alpha^n}{\sqrt{n!}}\sqrt{n}|n-1>\\ &= \mathrm{e}^{-\mathrm{i}\omega t}\alpha\varphi_\alpha(x,t)\end{aligned} \tag{B.11}$$

from which we find the expectation values

$$<\varphi_\alpha(x,t)\hat{a}\varphi_\alpha(x,t)> = \mathrm{e}^{-\mathrm{i}\omega t}\alpha \tag{B.12}$$

$$<\varphi_\alpha(x,t)\hat{a}^\dagger\varphi_\alpha(x,t)> = \mathrm{e}^{\mathrm{i}\omega t}\alpha^* \tag{B.13}$$

$$\overline{n} = <\varphi_\alpha(x,t)\hat{a}^\dagger\hat{a}\varphi_\alpha(x,t)> = |\alpha|^2 \tag{B.14}$$

$$\overline{H} = \hbar\omega\left(|\alpha|^2+\frac{1}{2}\right). \tag{B.15}$$

The coherent state is not an eigenfunction of the Hamiltonian. The number of excitations is not sharp. Its variance is

$$\mathrm{Var}(n) = <\varphi_\alpha(x,t)(\hat{a}^\dagger\hat{a})^2\varphi_\alpha(x,t)> - |\alpha|^4 = |\alpha|^2 \tag{B.16}$$

[2]Coherent states are normalized but not orthogonal.

hence the relative uncertainty decreases as $1/\sqrt{\overline{n}}$. Average position and momentum oscillate

$$\overline{x} = \frac{x_0}{\sqrt{2}} 2\Re(\alpha e^{-i\omega t}) = x_0\sqrt{2}|\alpha|\cos(\omega t - \arg(\alpha)) \tag{B.17}$$

$$\overline{p} = \frac{\hbar}{x_0}\sqrt{2}\Im(\alpha(t)) = -\frac{\hbar}{x_0}\sqrt{2}|\alpha|\sin(\omega t - \arg(\alpha)) \tag{B.18}$$

where the characteristic length is

$$x_0 = \sqrt{\frac{\hbar}{m\omega}}. \tag{B.19}$$

For large $\overline{n}$, the values of position and momentum become well defined and the oscillator behaves classically with an amplitude

$$x_0\sqrt{2}|\alpha| = x_0\sqrt{2\overline{n}} = \sqrt{\frac{\overline{H}}{\frac{m\omega^2}{2}}}. \tag{B.20}$$

The quantized electromagnetic field is a sum of harmonic oscillators. The Fourier component of the vector potential

$$\mathbf{A} = \sum_{\mathbf{k},\lambda} \sqrt{\frac{\hbar\omega_k}{2\varepsilon_0 V}} \frac{1}{\omega_k} \left(\hat{a}_{k,\lambda}\mathbf{e}_{k,\lambda}e^{i\mathbf{kr}} + \hat{a}^\dagger_{k,\lambda}\mathbf{e}^*_{\mathbf{k},\lambda}e^{-i\mathbf{kr}}\right) \tag{B.21}$$

therefore has to be replaced in the classical limit (B.12)–(B.14) by

$$\begin{aligned}\mathbf{A} &= \sum_{\mathbf{k},\lambda} \sqrt{\frac{\overline{n}\hbar\omega_k}{2\varepsilon_0 V}} \frac{1}{\omega_k} \left(\mathbf{e}_{k,\lambda}e^{i(\mathbf{kr}-\omega_k t)} + \mathbf{e}^*_{\mathbf{k},\lambda}e^{-(i\mathbf{kr}-\omega_k t)}\right) \\ &= \sum_{\mathbf{k},\lambda} A_0(\omega_k, \mathbf{k}) \left(\mathbf{e}_{k,\lambda}e^{i(\mathbf{kr}-\omega_k t)} + \mathbf{e}^*_{\mathbf{k},\lambda}e^{-(i\mathbf{kr}-\omega_k t)}\right)\end{aligned} \tag{B.22}$$

and the amplitude is in classical approximation

$$A_0(\omega_k, \mathbf{k}) = \sqrt{\frac{u(\omega_k, \mathbf{k})}{2\varepsilon_0\omega_k^2}}. \tag{B.23}$$

Appendix C
Time Correlation Function of the Displaced Harmonic Oscillator Model

In the following we evaluate the time correlation function of the displaced harmonic oscillator model (19.14)

$$f_r(t) = \left\langle \mathrm{e}^{-\mathrm{i}t\omega_r b_r^\dagger b_r} \mathrm{e}^{\mathrm{i}t\omega_r (b_r^\dagger + g_r)(b_r + g_r)} \right\rangle .$$

C.1 Evaluation of the Time Correlation Function

To proceed we need some theorems which will be derived afterward.

Theorem 1: A displacement of the oscillator potential energy minimum can be formulated as a canonical transformation

$$\hbar\omega_r (b_r^\dagger + g_r)(b_r + g_r) = \mathrm{e}^{-g_r (b_r^\dagger - b_r)} \hbar\omega_r b_r^\dagger b_r \mathrm{e}^{g_r (b_r^\dagger - b_r)} . \tag{C.1}$$

With the help of this relation the single-mode correlation function becomes

$$F_r(t) = \left\langle \mathrm{e}^{-\mathrm{i}t\omega_r b_r^\dagger b_r} \mathrm{e}^{-g_r (b_r^\dagger - b_r)} \mathrm{e}^{\mathrm{i}t\omega_r b_r^\dagger b_r} \mathrm{e}^{g_r (b_r^\dagger - b_r)} \right\rangle . \tag{C.2}$$

The first three factors can be interpreted as another canonical transformation. To this end we apply

Theorem 2: The time dependent boson operators are given by

$$\mathrm{e}^{-\mathrm{i}\omega_r t b_r^\dagger b_r} b_r^\dagger \mathrm{e}^{\mathrm{i}\omega_r t b_r^\dagger b_r} = b_r^\dagger \mathrm{e}^{-\mathrm{i}\omega_r t} \tag{C.3}$$

$$\mathrm{e}^{-\mathrm{i}\omega_r t b_r^\dagger b_r} b_r \mathrm{e}^{\mathrm{i}\omega_r t b_r^\dagger b_r} = b_r \mathrm{e}^{\mathrm{i}\omega_r t} \tag{C.4}$$

P.O.J. Scherer and S.F. Fischer, *Theoretical Molecular Biophysics*,
Biological and Medical Physics, Biomedical Engineering,
DOI 10.1007/978-3-662-55671-9

to find

$$F_r(t) = \left\langle \exp\left(-g_r(b_r^\dagger \mathrm{e}^{-\mathrm{i}\omega_r t} - b_r \mathrm{e}^{\mathrm{i}\omega_r t})\right) \exp\left(g_r(b_r^\dagger - b_r)\right)\right\rangle. \tag{C.5}$$

The two exponentials can be combined due to

Theorem 3: If the commutator of two operators A and B is a c-number then

$$\mathrm{e}^{A+B} = \mathrm{e}^A \mathrm{e}^B \mathrm{e}^{-\frac{1}{2}[A,B]}. \tag{C.6}$$

The commutator is

$$-g_r^2[b_r^\dagger \mathrm{e}^{-\mathrm{i}\omega_r t} - b_r \mathrm{e}^{\mathrm{i}\omega_r t}, b_r^\dagger - b_r] = -g_r^2(\mathrm{e}^{-\mathrm{i}\omega_r t} - \mathrm{e}^{\mathrm{i}\omega_r t}) \tag{C.7}$$

and we have

$$F_r(t) = \exp\left(-\frac{1}{2}g_r^2(\mathrm{e}^{-\mathrm{i}\omega_r t} - \mathrm{e}^{\mathrm{i}\omega_r t})\right)\left\langle \exp\left(-g_r b_r^\dagger(\mathrm{e}^{-\mathrm{i}\omega_r t} - 1) + g_r b_r(\mathrm{e}^{\mathrm{i}\omega_{tr}} - 1)\right)\right\rangle. \tag{C.8}$$

The remaining average is easily evaluated due to

Theorem 4: For a linear combination of b_r and $b_r^\dagger$ the second order cumulant expansion is exact

$$\left\langle \mathrm{e}^{\mu b^\dagger + \tau b}\right\rangle = \mathrm{e}^{\frac{1}{2}\langle(\mu b^\dagger + \tau b)^2\rangle} = \mathrm{e}^{\mu\tau\langle b^\dagger b + 1/2\rangle}. \tag{C.9}$$

The average square is

$$\begin{aligned}
&\left\langle \left(b_r^\dagger(\mathrm{e}^{-\mathrm{i}\omega_r t} - 1) - b_r(\mathrm{e}^{\mathrm{i}\omega_r t} - 1)\right)^2\right\rangle g_r^2 \\
&= -g_r^2(2 - \mathrm{e}^{\mathrm{i}\omega_r t} - \mathrm{e}^{-\mathrm{i}\omega_r t})\left\langle b_r^\dagger b_r + b_r b_r^\dagger\right\rangle \\
&= -g_r^2(2 - \mathrm{e}^{\mathrm{i}\omega_r t} - \mathrm{e}^{-\mathrm{i}\omega_r t})(2\overline{n}_r + 1)
\end{aligned} \tag{C.10}$$

with the average phonon number[3]

$$\overline{n}_r = \frac{1}{\mathrm{e}^{\beta\hbar\omega_r} - 1}. \tag{C.11}$$

Finally we have

$$\begin{aligned}
F_r(t) &= \exp\left(-\frac{1}{2}g_r^2(2 - \mathrm{e}^{\mathrm{i}\omega_r t} - \mathrm{e}^{-\mathrm{i}\omega_r t})(2\overline{n}_r + 1) - \frac{1}{2}g_r^2(\mathrm{e}^{-\mathrm{i}\omega_r t} - \mathrm{e}^{\mathrm{i}\omega_r t})\right) \\
&= \exp\left(g_r^2\left[(\mathrm{e}^{\mathrm{i}\omega_r t} - 1)(\overline{n}_r + 1) + (\mathrm{e}^{-\mathrm{i}\omega_r t} - 1)\overline{n}_r\right]\right)
\end{aligned} \tag{C.12}$$

[3] In the following we use the abbreviation $\beta = 1/k_B T$.

or, using trigonometric functions

$$F_r(t) = \exp\left(g_r^2\left[(\cos\omega_r t - 1 + \mathrm{i}\sin\omega_r t)(\overline{n}_r + 1) + (\cos\omega_r t - 1 - \mathrm{i}\sin\omega_r t)\overline{n}_r\right]\right)$$
$$= \exp\left(g_r^2(\overline{n}_r + 1)(\cos\omega_r t - 1) + \mathrm{i}g_r^2\sin\omega_r t\right). \tag{C.13}$$

C.2 Boson Algebra

C.2.1 Derivation of Theorem 1

Consider the following unitary transformation

$$A = \mathrm{e}^{-g(b^\dagger - b)} b^\dagger b \mathrm{e}^{g(b^\dagger - b)} \tag{C.14}$$

and make a series expansion

$$A = A(0) + g\frac{\mathrm{d}A}{\mathrm{d}g} + \frac{1}{2}g^2\frac{\mathrm{d}^2A}{\mathrm{d}g^2}\cdots \tag{C.15}$$

The derivatives are

$$\frac{\mathrm{d}A}{\mathrm{d}g}|_{g=0} = [b^\dagger b, b^\dagger - b] = b^\dagger[b, b^\dagger] + [b^\dagger, -b]b$$
$$= (b + b^+) \tag{C.16}$$

$$\frac{\mathrm{d}^2A}{\mathrm{d}g^2}|_{g=0} = [[b^\dagger b, b^\dagger - b], b^\dagger - b]$$
$$= [b + b^\dagger, b^\dagger - b,] = 2 \tag{C.17}$$

$$\frac{\mathrm{d}^nA}{\mathrm{d}g^n}|_{g=0} = 0 \quad \text{for } n \geq 3 \tag{C.18}$$

and the series is finite

$$A = b^\dagger b + g(b^\dagger + b) + g^2 = (b^\dagger + g)(b + g). \tag{C.19}$$

Hence for any of the normal modes

$$\hbar\omega_r(b_r^\dagger + g_r)(b_r + g_r) = \mathrm{e}^{-g_r(b_r^\dagger - b_r)}\hbar\omega_r b_r^\dagger b_r \mathrm{e}^{g_r(b_r^\dagger - b_r)}. \tag{C.20}$$

C.2.2 Derivation of Theorem 2

Consider

$$A = \mathrm{e}^{\tau b^\dagger b} b \mathrm{e}^{-\tau b^\dagger b} \quad \text{with } \tau = -\mathrm{i}\omega t. \tag{C.21}$$

Make again a series expansion

$$\frac{\mathrm{d}A}{\mathrm{d}\tau} = [b^+ b, b] = -b \tag{C.22}$$

$$\frac{\mathrm{d}^2 A}{\mathrm{d}\tau^2} = [b^+ b, -b] = b \quad \text{etc.} \tag{C.23}$$

$$A = b\left(1 - \tau + \frac{\tau^2}{2} - \cdots\right) = b\left(1 + \mathrm{i}t\omega + \frac{(\mathrm{i}t\omega)^2}{2} + \cdots\right) = b\,\mathrm{e}^{\mathrm{i}\omega t}. \tag{C.24}$$

Hermitian conjugation gives

$$\mathrm{e}^{-\mathrm{i}\omega t b^\dagger b} b^+ \mathrm{e}^{\mathrm{i}\omega t b^\dagger b} = b^\dagger \mathrm{e}^{-\mathrm{i}\omega t}. \tag{C.25}$$

C.2.3 Derivation of Theorem 3

Consider the operator

$$f(\tau) = \mathrm{e}^{-B\tau} \mathrm{e}^{-A\tau} \mathrm{e}^{(A+B)\tau} \tag{C.26}$$

as a function of the c-number τ. Differentiation gives

$$\begin{aligned} \frac{df(\tau)}{d\tau} &= \mathrm{e}^{-B\tau}(-A - B)\mathrm{e}^{-A\tau}\mathrm{e}^{(A+B)\tau} + \mathrm{e}^{-B\tau}\mathrm{e}^{-A\tau}(A + B)\mathrm{e}^{(A+B)\tau} \\ &= \mathrm{e}^{-B\tau}[\mathrm{e}^{-A\tau}, B]\mathrm{e}^{(A+B)\tau}. \end{aligned} \tag{C.27}$$

Now if the commutator $[A, B]$ is a c-number then

$$[A^n, B] = A[A^{n-1}, B] + [A, B]A^{n-1} = \cdots n[A, B]A^{n-1} \tag{C.28}$$

and therefore

$$\begin{aligned} [\mathrm{e}^{-A\tau}, B] &= \sum_{n=0}^{\infty} \frac{(-\tau)^n}{n!}[A^n, B] = \sum_n \frac{(-\tau)^n}{(n-1)!} A^{n-1}[A, B] \\ &= -\tau[A, B]\mathrm{e}^{-A\tau} \end{aligned} \tag{C.29}$$

and (C.27) gives

$$\frac{df(\tau)}{d\tau} = -\tau[A, B]e^{-B\tau}e^{-A\tau}e^{(A+B)\tau} = -\tau[A, B]f(\tau) \tag{C.30}$$

which is for the initial condition $f(0) = 1$ solved by

$$f(\tau) = \exp\left(-\frac{\tau^2}{2}[A, B]\right). \tag{C.31}$$

Substituting $\tau = 1$ finally gives

$$e^{-B}e^{-A}e^{(A+B)} = e^{-\frac{1}{2}[A,B]}. \tag{C.32}$$

C.2.4 Derivation of Theorem 4

This derivation is based on (200). For one single oscillator consider the linear combination

$$\mu b^\dagger + \tau b = A + B \tag{C.33}$$

$$[A, B] = -\mu\tau. \tag{C.34}$$

Application of (C.32) gives

$$\left\langle e^{\mu b^\dagger + \tau b}\right\rangle = \left\langle e^{\mu b^\dagger}e^{\tau b}\right\rangle e^{\mu\tau/2} \tag{C.35}$$

and after exchange of A and B

$$\left\langle e^{\mu b^\dagger + \tau b}\right\rangle = \left\langle e^{\tau b}e^{\mu b^\dagger}\right\rangle e^{-\mu\tau/2}. \tag{C.36}$$

Combination of the last two equations gives

$$\left\langle e^{\tau b}e^{\mu b^\dagger}\right\rangle = \left\langle e^{\mu b^\dagger}e^{\tau b}\right\rangle e^{\mu\tau}. \tag{C.37}$$

Using the explicit form of the averages we find

$$Q^{-1}\,\mathrm{tr}\left(e^{-\beta\hbar\omega b^\dagger b}e^{\tau b}e^{\mu b^\dagger}\right) = Q^{-1}\,\mathrm{tr}\left(e^{-\beta\hbar\omega b^\dagger b}e^{\mu b^\dagger}e^{\tau b}\right)e^{\mu\tau} \tag{C.38}$$

and due to the cyclic invariance of the trace operation the right side becomes

$$= Q^{-1}\mathrm{tr}(e^{\tau b}e^{-\beta\hbar\omega b^\dagger b}e^{\mu b^\dagger})e^{\mu\tau} \tag{C.39}$$

which can be written as

$$= Q^{-1}\mathrm{tr}(\mathrm{e}^{-\beta\hbar\omega b^\dagger b}\mathrm{e}^{+\beta\hbar\omega b^\dagger b}\mathrm{e}^{\tau b}\mathrm{e}^{-\beta\hbar\omega b^\dagger b}\mathrm{e}^{\mu b^\dagger})\mathrm{e}^{\mu\tau}$$

$$= \left\langle \mathrm{e}^{+\beta\hbar\omega b^\dagger b}\mathrm{e}^{\tau b}\mathrm{e}^{-\beta\hbar\omega b^\dagger b}\mathrm{e}^{\mu b^\dagger}\right\rangle \mathrm{e}^{\mu\tau}. \tag{C.40}$$

Application of (C.3) finally gives the relation

$$\left\langle \exp(\tau b)\exp(\mu b^\dagger)\right\rangle = \left\langle \exp\left(\tau\mathrm{e}^{-\beta\hbar\omega}b\right)\exp\left(\mu b^\dagger\right)\right\rangle \mathrm{e}^{\mu\tau} \tag{C.41}$$

which can be iterated to give

$$\begin{aligned}\left\langle \exp(\tau b)\exp(\mu b^\dagger)\right\rangle &= \left\langle \exp\left(\tau\mathrm{e}^{-2\beta\hbar\omega}b\right)\exp\left(\mu b^\dagger\right)\right\rangle \mathrm{e}^{\mu\tau(1+\mathrm{e}^{-\beta\hbar\omega})} = \cdots \\ &= \left\langle \exp\left(\tau\mathrm{e}^{-(n+1)\beta\hbar\omega}b\right)\exp\left(\mu b^\dagger\right)\right\rangle \mathrm{e}^{\mu\tau(1+\mathrm{e}^{-\beta\hbar\omega}+\cdots+\mathrm{e}^{-n\beta\hbar\omega})}\end{aligned} \tag{C.42}$$

and in the limit $n \to \infty$

$$\left\langle \exp(\tau b)\exp(\mu b^\dagger)\right\rangle = \left\langle \exp(\mu b^\dagger)\right\rangle \exp\left(\frac{\mu\tau}{1-\mathrm{e}^{-\beta\hbar\omega}}\right) = \exp\left(\frac{\mu\tau}{1-\mathrm{e}^{-\beta\hbar\omega}}\right) \tag{C.43}$$

since only the zero-order term of the expansion of the exponential gives a nonzero contribution to the average. With the average number of vibrations

$$\overline{n} = \frac{1}{\mathrm{e}^{\beta\hbar\omega}-1} \tag{C.44}$$

we have

$$\left\langle \exp(\tau b)\exp(\mu b^\dagger)\right\rangle = \exp\left(\mu\tau(\overline{n}+1)\right) \tag{C.45}$$

and finally

$$\left\langle \mathrm{e}^{\mu b^\dagger+\tau b}\right\rangle = \mathrm{e}^{\mu\tau(\overline{n}+1/2)}. \tag{C.46}$$

The average of the square is

$$\left\langle (\mu b^\dagger+\tau b)^2\right\rangle = \mu\tau\left\langle b^\dagger b + b\,b^\dagger\right\rangle = \mu\tau(2\overline{n}+1) \tag{C.47}$$

which shows the validity of the theorem.

Appendix D
Complex Cotangent Function

The cotangent of an imaginary argument can be written as

$$\cot(iy) = \frac{\cosh y}{i \sinh y} = -i \coth y \tag{D.1}$$

which for large $|y|$ approximates

$$\cot(iy) \to -i \quad \text{sign}(y). \tag{D.2}$$

For a complex argument we write (Fig. D.1)

$$\cot(x + iy) = \frac{1 + i \coth y \cot x}{i \coth y - \cot x} \tag{D.3}$$

which for large y approximates

$$\frac{1 + i \frac{1+e^{-2y}}{1-e^{-2y}} \cot x}{i \frac{1+e^{-2y}}{1-e^{-2y}} - \cot x} = -i + \frac{2i(\cot x + 1)}{i - \cot x} e^{-2y} + \cdots \tag{D.4}$$

P.O.J. Scherer and S.F. Fischer, *Theoretical Molecular Biophysics*,
Biological and Medical Physics, Biomedical Engineering,
DOI 10.1007/978-3-662-55671-9

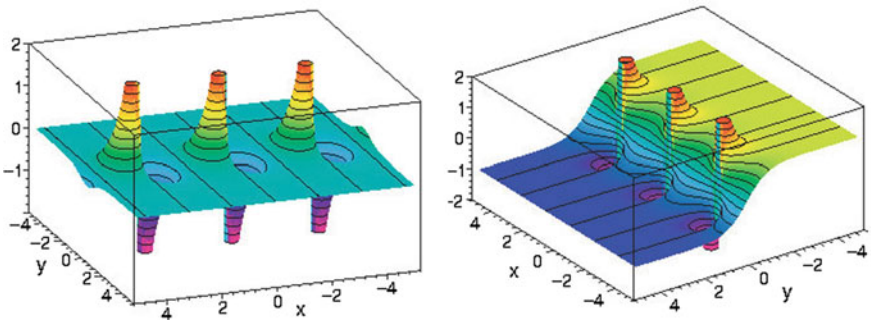

Fig. D.1 Complex cotangent function. Real (*left*) and imaginary (*right*) part of $\cot(x + iy)$ are shown

and for large negative y

$$\frac{1 - i\frac{1+e^{2y}}{1-e^{2y}}\cot x}{-i\frac{1+e^{2y}}{1-e^{2y}} - \cot x} = i + \frac{2i(\cot x - i)}{i + \cot x}e^{2y} + \cdots \tag{D.5}$$

Appendix E
The Saddle Point Method

The saddle point method is an asymptotic method to calculate integrals of the type

$$\int_{-\infty}^{\infty} e^{\phi(x)} dx \tag{E.1}$$

If the function $\phi(x)$ has a maximum at x_0 then the integrand also has a maximum there and the integral can be approximated by expanding the exponent around x_0

$$\phi(x) = \phi(x_0) + \frac{1}{2} \frac{d^2\phi(x)}{dx^2}_{|x_0} (x - x_0)^2 + \cdots \tag{E.2}$$

as a Gaussian integral

$$\int_{-\infty}^{\infty} e^{\phi(x)} dx \approx e^{\phi(x_0)} \sqrt{\frac{2\pi}{|\phi''(x_0)|}}. \tag{E.3}$$

The method can be extended to integrals in the complex plane

$$\int_C e^{\phi(z)} dz = \int_C e^{\Re(\phi(z))} e^{i\Im(\phi(z))} dz. \tag{E.4}$$

If the integration contour is deformed such that the imaginary part is constant (stationary phase), then (Fig. E.1)

$$\int_C e^{\phi(z)} dz = e^{i\Im(\phi(z_0))} \int_{C'} e^{\Re(\phi(z))} dz. \tag{E.5}$$

P.O.J. Scherer and S.F. Fischer, *Theoretical Molecular Biophysics*,
Biological and Medical Physics, Biomedical Engineering,
DOI 10.1007/978-3-662-55671-9

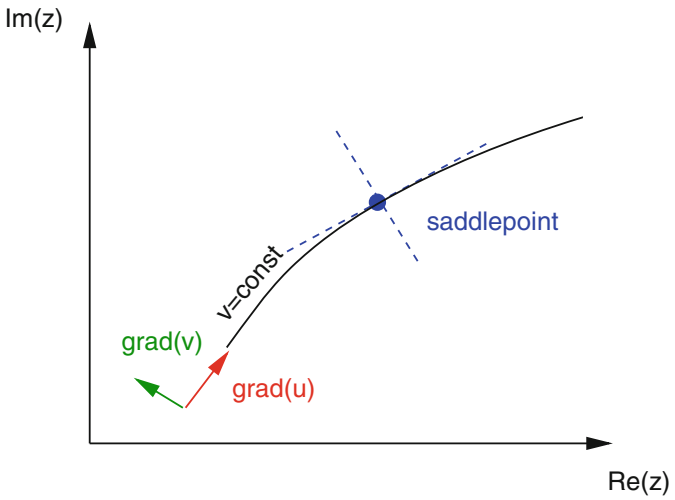

Fig. E.1 Saddle point method

The contour C' and the expansion point are determined from

$$\phi'(z_0) = 0 \tag{E.6}$$

$$\phi(z) = u(z) + iv(z) = u(z) + iv(z_0). \tag{E.7}$$

Now consider the imaginary part as a function of (x, y). The gradient is according to Cauchy and Riemann

$$\nabla v(x, y) = (\frac{\partial v}{\partial x}, \frac{\partial v}{\partial y}) = (-\frac{\partial u}{\partial y}, \frac{\partial u}{\partial x}) \tag{E.8}$$

which is perpendicular to the gradient of the real part

$$\nabla u(x, y) = (\frac{\partial u}{\partial x}, \frac{\partial u}{\partial y}) \tag{E.9}$$

which gives the direction of steepest descent. The method is known as saddle point method since a maximum of the real part always is a saddle point. From the expansion

$$\phi(z) = \phi(z_0) + \frac{1}{2}\phi''(z_0)(z - z_0)^2 + \cdots \tag{E.10}$$

and

$$dz^2 = dx^2 - dy^2 + 2idx\,dy \tag{E.11}$$

we find

$$\begin{aligned}\Re(\phi(z)) &= \Re(\phi(z_0)) - \frac{1}{2}\left(\Re(\phi''(z_0))(dx^2 - dy^2) - 2\Im(\phi''(z_0))dx\,dy\right)\\ &= \Re(\phi(z_0)) - \frac{1}{2}(dx, dy)\begin{pmatrix}\Re(\phi'') & -\Im(\phi'')\\ -\Im(\phi'') & -\Re(\phi'')\end{pmatrix}\begin{pmatrix}dx\\ dy\end{pmatrix}.\end{aligned} \tag{E.12}$$

The eigenvalues of the matrix are

$$\pm\sqrt{\Re(\phi'')^2 + \Im(\phi'')^2} = \pm|\phi''| \tag{E.13}$$

and the eigenvectors

$$\begin{pmatrix}dx\\ dy\end{pmatrix} \propto \begin{pmatrix}1\\ \frac{\Re(\phi'')\pm|\phi''|}{\Im(\phi'')}\end{pmatrix}. \tag{E.14}$$

Similarly, the imaginary part

$$\begin{aligned}\Im(\phi(z)) &= \Im(\phi(z_0)) + \Re(\phi''(z_0))dxdy + \frac{1}{2}\Im(\phi''(z_0))(dx^2 - dy^2)\\ &= \Im(\phi(z_0)) + \frac{1}{2}(dx, dy)\begin{pmatrix}\Im(\phi'') & \Re(\phi'')\\ \Re(\phi'') & -\Im(\phi'')\end{pmatrix}\begin{pmatrix}dx\\ dy\end{pmatrix}.\end{aligned} \tag{E.15}$$

The direction of stationary phase is given by

$$dy = \frac{\Re(\phi'') \pm |\phi''|}{\Im(\phi'')}dx \tag{E.16}$$

hence is along the eigenvectors of the real part.

Solutions

Problems of Chap. 1

1.1 Gaussian Polymer Model

$$\Delta\mathbf{r}_i = \mathbf{r}_i - \mathbf{r}_{i-1} \quad i = 1 \cdots N$$

(a)

$$P(\Delta\mathbf{r}_i) = \frac{1}{b^3}\sqrt{\frac{27}{8\pi^3}} \exp\left\{-\frac{3(\Delta\mathbf{r}_i)^2}{2b^2}\right\}$$

is the normalized probability function with

$$\int_{-\infty}^{\infty} P(\Delta\mathbf{r}_i) d^3\Delta\mathbf{r}_i = 1 \quad \int_{-\infty}^{\infty} \Delta\mathbf{r}_i^2 P(\Delta\mathbf{r}_i) d^3\Delta\mathbf{r}_i = b^2$$

(b)

$$\mathbf{r}_N - \mathbf{r}_0 = \sum_{i=1}^{N} \Delta\mathbf{r}_i$$

$$P\left(\sum_{i=1}^{N} \Delta\mathbf{r}_i = \mathbf{R}\right) = \int_{-\infty}^{\infty} d^3\Delta\mathbf{r}_1 \cdots \int_{-\infty}^{\infty} d^3\Delta\mathbf{r}_N \prod_{i=1}^{N} P(\Delta\mathbf{r}_i)\delta\left(\mathbf{R} - \sum_{i=1}^{N} \Delta\mathbf{r}_i\right)$$

$$= \int \frac{1}{(2\pi)^3} d^3\mathbf{k} e^{i\mathbf{k}\mathbf{R}} \int_{-\infty}^{\infty} d^3\Delta\mathbf{r}_1 \cdots \int_{-\infty}^{\infty} d^3\Delta\mathbf{r}_N \left(\frac{1}{b^3}\sqrt{\frac{27}{8\pi^3}}\right)^N$$

P.O.J. Scherer and S.F. Fischer, *Theoretical Molecular Biophysics*,
Biological and Medical Physics, Biomedical Engineering,
DOI 10.1007/978-3-662-55671-9

$$\times \prod \exp\left\{-\frac{3\Delta\mathbf{r}_i^2}{2b^2} - \mathrm{i}\mathbf{k}\Delta\mathbf{r}_i\right\}$$

$$= \int \frac{1}{(2\pi)^3} d^3\mathbf{k} \mathrm{e}^{\mathrm{i}\mathbf{k}\mathbf{R}} \left[\left(\frac{1}{b^3}\sqrt{\frac{27}{8\pi^3}}\right)\int_{-\infty}^{\infty} d^3\Delta\mathbf{r} \exp\left\{-\frac{3\Delta\mathbf{r}^2}{2b^2} - \mathrm{i}\mathbf{k}\Delta\mathbf{r}\right\}\right]^N$$

$$= \int \frac{1}{(2\pi)^3} d^3\mathbf{k} \mathrm{e}^{\mathrm{i}\mathbf{k}\mathbf{R}} \exp(-\frac{Nb^2}{6}\mathbf{k}^2)$$

$$= \frac{1}{b^3}\sqrt{\frac{27}{8\pi^3 N^3}} \exp\left\{-\frac{3\mathbf{R}^2}{2Nb^2}\right\}$$

(c)

$$\exp\left\{-\frac{1}{k_B T}\left(\frac{f}{2}\sum \Delta\mathbf{r}_i^2 - \kappa \sum \Delta\mathbf{r}_i\right)\right\} = \prod_i \exp\left\{-\frac{1}{k_B T}\left(\frac{f}{2}\Delta\mathbf{r}_i^2 - \kappa\Delta\mathbf{r}_i\right)\right\}$$

$$\frac{f}{2k_B T} = \frac{3}{2b^2} \rightarrow f = \frac{3k_B T}{b^2}$$

(d)

$$x_N - x_0 = \frac{N\kappa}{f} \quad y_N - y_0 = z_N - z_0 = 0$$

$$L = x_N - x_0 = \frac{N\kappa b^2}{3k_B T}$$

1.2 Three-dimensional Polymer Model

(a)

$$Nb^2$$

(b)

$$b^2\left(N\frac{1+x}{1-x} + \frac{2x(x^2-1)}{(1-x)^2}\right) \quad \text{with } x = \cos\theta$$

$$\approx Nb^2\frac{1+\cos x}{1-\cos x}$$

(c)

$$Nb^2 \frac{(1+\cos\theta_1)(1+\cos\theta_2)}{1-\cos\theta_1\cos\theta_2}$$

(d) $N \gg a/b$ with the coherence length

$$a = b\frac{1+\cos x}{(1-\cos x)\cos\frac{x}{2}}$$

(e)

$$Nb^2\left(\frac{4}{\theta^2}-1\right)-b^2\left(\frac{4}{\theta^2}-\frac{8}{\theta^4}\right)$$

1.3 Two-Component Model

(a)

$$\kappa = -k_B T \frac{1}{l_\alpha - l_\beta} \ln\left(\frac{Ml_\alpha - L}{L - Ml_\beta}\right)$$

$$-k_B T\left(\frac{1}{2Ml_\alpha - 2L} + \frac{1}{2Ml_\beta - L} + \frac{l_\alpha - l_\beta}{12(L-Ml_\beta)^2} - \frac{l_\alpha - l_\beta}{12(Ml_\alpha - L)^2}\right)$$

The exact solution can be written with the digamma function Ψ which is well known by algebra programs as

$$\kappa = -k_B T \frac{1}{l_\alpha - l_\beta}\left(-\Psi\left(\frac{L-Ml_\beta}{l_\alpha - l_\beta}+1\right)+\Psi\left(\frac{Ml_\alpha - L}{l_\alpha - l_\beta}\right)\right)$$

The error of the asymptotic expansion is largest for $L \approx Ml_\alpha$ or $L \approx Ml_\beta$. The following table compares the relative errors of the Stirling approximation and the higher order asymptotic expansion for $M = 1000$ and $l_\beta/l_\alpha = 2$

L/l_α	Stirling	asympt. expansion
1000.2	0.18	0.13
1000.5	0.11	0.009
1001	0.065	0.00094
1005	0.019	$2.5{*}10^{-6}$

(b)

$$Z(\kappa, M, T) = \left(\mathrm{e}^{\frac{\kappa l_\alpha}{k_B T}} + \mathrm{e}^{\frac{\kappa l_\beta}{k_B T}}\right)^M$$

$$\overline{L} = M\frac{l_\alpha e^{\frac{\kappa l_\alpha}{k_B T}} + l_\beta e^{\frac{\kappa l_\beta}{k_B T}}}{e^{\frac{\kappa l_\alpha}{k_B T}} + e^{\frac{\kappa l_\beta}{k_B T}}}$$

$$\overline{L^2} = \overline{L}^2 + M e^{\kappa(l_\alpha + l_\beta)/k_B T}\left(\frac{l_\alpha - l_\beta}{e^{\kappa l_\alpha/k_B T} + e^{\kappa l_\beta/k_B T}}\right)^2$$

$$\sigma^2 = M e^{\kappa(l_\alpha + l_\beta)/k_B T}\left(\frac{l_\alpha - l_\beta}{e^{\kappa l_\alpha/k_B T} + e^{\kappa l_\beta/k_B T}}\right)^2$$

$$\frac{\sigma}{\overline{L}} \sim \frac{1}{\sqrt{N}}$$

$$\frac{\partial\sigma}{\partial\kappa} = 0 \text{ for } (l_\alpha + l_\beta) = 2\frac{l_\alpha e^{\kappa l_\alpha/k_B T} + l_\beta e^{\kappa l_\beta/k_B T}}{e^{\kappa l_\alpha/k_B T} + e^{\kappa l_\beta/k_B T}}$$

hence for

$$\kappa = 0$$

$$\frac{\partial^2\sigma^2}{\partial\kappa^2}(\kappa = 0) = -\frac{M}{k(k_B T)^2}(l_\alpha - l_\beta)^2 < 0 \rightarrow \text{ maximum}$$

also a maximum of σ since the square root is monotonous.

Problems of Chap. 2

2.1 Osmotic Pressure of a Polymer Solution

$$\mu_\alpha(P,T) - \mu_\alpha^0(P,T) = k_B T\left(\ln(1-\phi_\beta) + (1-\frac{1}{M})\phi_\beta + \chi\phi_\beta^2\right)$$

$$\mu_\alpha^0(P',T) - \mu_\alpha^0(P,T) = \mu_\alpha(P,T) - \mu_\alpha^0(P,T) = -\Pi\frac{\partial\mu_\alpha^0(P,T)}{\partial P}$$

$$\Pi = -\left(\frac{\partial\mu_\alpha^0(P,T)}{\partial P}\right)^{-1} k_B T\left(\ln(1-\phi_\beta) + (1-\frac{1}{M})\phi_\beta + \chi\phi_\beta^2\right)$$

For the pure solvent

$$\mu_\alpha^0 = \frac{G}{N_\alpha}$$

$$dG = -SdT + VdP + \mu_\alpha^0(P,T)dN$$

$$\frac{\partial \mu_\alpha^0}{\partial P}\Big|_{T,N_\alpha} = \frac{V}{N_\alpha}$$

$$\Pi = -\frac{N_\alpha}{V}k_BT\left(-\phi_\beta - \frac{1}{2}\phi_\beta^2 - \frac{1}{3}\phi_\beta^3 + \cdots + (1-\frac{1}{M})\phi_\beta + \chi\phi_\beta^2\right)$$

$$= \frac{N_\alpha k_B T}{V}\left(\frac{1}{M}\phi_\beta + (\frac{1}{2}-\chi)\phi_\beta^2 + \cdots\right)$$

$$\chi = \frac{\chi_0 T_0}{T}$$

high T:

$$\frac{1}{2} - \chi > 0 \quad \Pi > 0 \text{ good solvent}$$

low T:

$\Pi < 0$ bad solvent, possibly phase separation

2.2 Polymer Mixture

$$\Delta F = Nk_BT\left(\frac{\phi_1}{M_1}\ln\phi_1 + \frac{\phi_2}{M_2}\ln\phi_2 + \chi\phi_1\phi_2\right)$$

$$\phi_{2,c} = \frac{1}{1+\sqrt{\frac{M_2}{M_1}}}$$

$$\chi_c = \frac{1}{2}(\sqrt{M_1}+\sqrt{M_2})(\frac{1}{M_2\sqrt{M_1}} + \frac{1}{M_1\sqrt{M_2}})$$

symmetric case

$$\phi_c = \frac{1}{2}$$

$\chi_c = \dfrac{2}{M}$ can be small, demixing possible

Problems of Chap. 4

4.1 Membrane Potential

$$\Phi_I = B\mathrm{e}^{\kappa x} \quad \Phi_{II} = B\left(1 + \frac{\epsilon_W}{\epsilon_M}\kappa x\right) \quad \Phi_{III} = V - B\mathrm{e}^{-\kappa(x-L)}$$

$$B = \frac{V}{2 + \frac{\epsilon_W}{\epsilon_M}\kappa L}$$

$Q/A = \epsilon_W \kappa B$ per area A

$$C/A = \frac{Q/A}{V} = \frac{\epsilon_W \kappa}{2 + \frac{\epsilon_W}{\epsilon_M}\kappa L} = \frac{1}{\frac{2}{\epsilon_w \kappa} + \frac{L}{\epsilon_M}}$$

4.2 Ion Activity

$$k_B T \ln \gamma^c = k_B T \ln \frac{a}{c} = -\frac{Z^2 \mathrm{e}^2}{8\pi\epsilon} \frac{\kappa}{1 + \kappa R}$$

$$\ln \gamma_+^c = \ln \gamma_-^c = -\frac{1}{k_B T} \frac{Z^2 \mathrm{e}^2}{8\pi\epsilon} \frac{\kappa}{1 + \kappa R}$$

$$\ln \gamma_\pm^c = -\frac{1}{k_B T} \frac{Z^2 \mathrm{e}^2}{16\pi\epsilon} \left(\frac{\kappa}{1 + \kappa R_+} + \frac{\kappa}{1 + \kappa R_-} \right)$$

$\kappa \to 0$ for dilute solution

$$\ln \gamma_\pm^c \to -\frac{1}{k_B T} \frac{Z^2 \mathrm{e}^2 \kappa}{8\pi\epsilon}$$

Problems of Chap. 5

5.1 Abnormal Titration Curve

$$\Delta G(B, B) = 0$$

$$\Delta G(BH^+, B) = \Delta G_{1,int}$$

$$\Delta G(B, BH^+) = \Delta G_{2,int}$$

$$\Delta G(BH^+, BH^+) = \Delta G_{1,int} + \Delta G_{2,int} + W_{1,2}$$

$$\Xi = 1 + \mathrm{e}^{-\beta(\Delta G_{1,int}-\mu)} + \mathrm{e}^{-\beta(\Delta G_{2,int}-\mu)} + \mathrm{e}^{-\beta(\Delta G_{1,int}+\Delta G_{2,int}-W+2\mu)}$$

$$\overline{s_1} = \frac{\mathrm{e}^{-\beta(\Delta G_{1,int}-\mu)} + \mathrm{e}^{-\beta(\Delta G_{1,int}+\Delta G_{2,int}-W+2\mu)}}{\Xi}$$

$$\overline{s_2} = \frac{\mathrm{e}^{-\beta(\Delta G_{2,int}-\mu)} + \mathrm{e}^{-\beta(\Delta G_{1,int}+\Delta G_{2,int}-W+2\mu)}}{\Xi}$$

Problems of Chap. 6

6.1 pH-Dependence of Enzyme Activity

$$\frac{r}{r_{max}} = \frac{1}{1 + (1 + \frac{c_{H+}}{K})\frac{K_M}{c_S}}$$

$$K = \frac{c_{H+}c_{S-}}{c_{HS}} \quad c_s = c_{S-} + c_{HS}$$

6.2 Polymerization at the End of a Polymer

$$c_{iM} = K c_M c_{(i-1)M} = \cdots = \frac{(K c_M)^i}{K}$$

$$< i >= \frac{\sum_{i=1}^{\infty} i(K c_M)^i}{\sum_{i=1}^{\infty}(K c_M)^i} = \frac{1}{1 - K c_M} \text{ for } K c_M < 1$$

6.3 Primary Salt Effect

$$r = k_1 c_X$$

$$K = \frac{c_X}{c_A c_B} \exp\left\{-\frac{Z_A Z_B \mathrm{e}^2 \kappa}{4\pi\epsilon k_B T}\right\}$$

$$c_X = K c_A c_B \exp\left\{\frac{Z_A Z_B \mathrm{e}^2 \kappa}{4\pi\epsilon k_B T}\right\}$$

Problems of Chap. 7

7.1 Smoluchowski Equation

$$P(t + \Delta t, x) = \mathrm{e}^{\Delta t \frac{\partial}{\partial t}} P(t, x)$$

$$w^{\pm}(x \pm \Delta x) P(t, x \pm \Delta x) = \mathrm{e}^{\pm \Delta x \frac{\partial}{\partial x}} w^{\pm}(x) P(t, x)$$

$$\mathrm{e}^{\Delta t \frac{\partial}{\partial t}} P(t, x) = \mathrm{e}^{\Delta x \frac{\partial}{\partial x}} w^{+}(x) P(t, x) + \mathrm{e}^{-\Delta x \frac{\partial}{\partial x}} w^{-}(x) P(t, x)$$

$$P(t, x) + \Delta t \frac{\partial}{\partial t} P(t, x) + \cdots = (w^{+}(x) + w^{-}(x)) P(x, t)$$

$$+\Delta x \frac{\partial}{\partial x}(w^{+}(x) - w^{-}(x)) P(x, t) + \frac{\Delta x^2}{2} \frac{\partial^2}{\partial x^2}(w^{+}(x) + w^{-}(x)) P(x, t) + \cdots$$

$$\frac{\partial}{\partial t} P(t, x) = \frac{\Delta x}{\Delta t} \frac{\partial}{\partial x}(w^{+}(x) - w^{-}(x)) P(x, t) + \frac{\Delta x^2}{\Delta t} \frac{\partial^2}{\partial x^2} P(x, t) + \cdots$$

$$D = \frac{\Delta x^2}{\Delta t} \quad K(x) = -\frac{k_B T}{\Delta x}(w^{+}(x) - w^{-}(x))$$

7.2 Eigenvalue Solution to the Smoluchowski Equation

$$-\frac{k_B T}{m\gamma} \mathrm{e}^{-U/k_B T} \left(\frac{\partial}{\partial x} \mathrm{e}^{U/k_B T} W\right)$$

$$= -\frac{k_B T}{m\gamma} \mathrm{e}^{-U/k_B T} \left(\mathrm{e}^{U/k_B T} \frac{\partial W}{\partial x} + \mathrm{e}^{U/k_B T} W \frac{1}{k_B T} \frac{\partial U}{\partial x} \right)$$

$$= -\frac{k_B T}{m\gamma} \frac{\partial W}{\partial x} - \frac{1}{m\gamma} \frac{\partial U}{\partial x} W = S$$

$$\mathfrak{L}_{FP} W = -\frac{\partial}{\partial x} S = \frac{\partial}{\partial x} \frac{k_B T}{m\gamma} \mathrm{e}^{-U/k_B T} \left(\frac{\partial}{\partial x} \mathrm{e}^{U/k_B T} W \right)$$

$$\mathfrak{L}_{FP} = \frac{k_B T}{m\gamma} \frac{\partial}{\partial x} \mathrm{e}^{-U/k_B T} \frac{\partial}{\partial x} \mathrm{e}^{U/k_B T}$$

$$\mathfrak{L} = \mathrm{e}^{U/2k_B T} \mathfrak{L}_{FP} \mathrm{e}^{-U/2k_B T} = \mathrm{e}^{U/2k_B T} \frac{k_B T}{m\gamma} \frac{\partial}{\partial x} \mathrm{e}^{-U/k_B T} \frac{\partial}{\partial x} \mathrm{e}^{U/2k_B T}$$

$$\mathfrak{L}^H = \mathrm{e}^{U/2k_B T} \left(-\frac{\partial}{\partial x} \right) \mathrm{e}^{-U/k_B T} \left(-\frac{\partial}{\partial x} \right) \frac{k_B T}{m\gamma} \mathrm{e}^{U/2k_B T} = \mathfrak{L}$$

since

$$\frac{k_B T}{m\gamma} = \text{ const}$$

For an eigenfunction ψ of $\mathfrak{L}$ we have

$$\lambda\psi = \mathfrak{L}\psi = \mathrm{e}^{U/2k_B T} \mathfrak{L}_{FP} \mathrm{e}^{-U/2k_B T} \psi$$

hence

$$\mathfrak{L}_{FP} \left(\mathrm{e}^{-U/2k_B T} \psi \right) = \lambda \left(\mathrm{e}^{-U/2k_B T} \psi \right)$$

gives an Eigenfunction of the Focker-Planck operator to the same eigenvalue λ. A solution of the Smoluchowski equation is then given by

$$W(x, t) = \mathrm{e}^{\lambda t} \mathrm{e}^{-U/2k_B T} \psi(x)$$

The Hermitian operator is very similar to the harmonic oscillator in second quantization

$$\mathfrak{L} = \frac{k_B T}{m\gamma} \left(\mathrm{e}^{U/2k_B T} \frac{\partial}{\partial x} \mathrm{e}^{-U/2k_B T} \right) \left(\mathrm{e}^{-U/2k_B T} \frac{\partial}{\partial x} \mathrm{e}^{U/2k_B T} \right)$$

$$= \frac{k_B T}{m\gamma}\left(\frac{\partial}{\partial x} - \frac{1}{2k_B T}\frac{\partial U}{\partial x}\right)\left(\frac{\partial}{\partial x} + \frac{1}{2k_B T}\frac{\partial U}{\partial x}\right)$$

$$= \frac{k_B T}{m\gamma}\left(\frac{\partial}{\partial x} - \frac{m\omega^2}{2k_B T}x\right)\left(\frac{\partial}{\partial x} + \frac{m\omega^2}{2k_B T}x\right)$$

$$= -\frac{\omega^2}{\gamma}\left(\sqrt{\frac{k_B T}{m\omega^2}}\frac{\partial}{\partial x} - \frac{1}{2}\sqrt{\frac{m\omega^2}{k_B T}}x\right)\left(\sqrt{\frac{k_B T}{m\omega^2}}\frac{\partial}{\partial x} + \frac{1}{2}\sqrt{\frac{m\omega^2}{k_B T}}x\right)$$

$$= -\frac{\omega^2}{\gamma}\left(\frac{\partial}{\partial \xi} - \frac{1}{2}\xi\right)\left(\frac{\partial}{\partial \xi} + \frac{1}{2}\xi\right) = -\frac{\omega^2}{\gamma}b^+ b$$

with boson operators

$$b^+ b - b b^+ = 1.$$

From comparison with the harmonic oscillator we know the eigenvalues

$$\lambda_n = -\frac{\omega^2}{\gamma}n \quad n = 0, 1, 2, \cdots$$

The ground state obeys

$$a\psi_0 = \left(\frac{\partial}{\partial x} + \frac{1}{2k_B T}\frac{\partial U}{\partial x}\right)\psi_0 = 0$$

with the solution

$$\psi_0 = \mathrm{e}^{-U(x)/2k_B T}.$$

This corresponds to the stationary solution of the Smoluchowski equation

$$W = \sqrt{\frac{m\omega^2}{2\pi k_B T}}\mathrm{e}^{-U(x)/k_B T}.$$

7.3 Diffusion Through a Membrane

$$k_{AB} = k_A + k_B$$

$$0 = \frac{\mathrm{d}\overline{N}}{\mathrm{d}t} = \sum_{N=}^{M}\frac{\mathrm{d}P_N}{\mathrm{d}t}N = -\sum_{N=1}^{M}k_{AB}MNP_N + \sum_{N=1}^{N}(k_{AB} - 2k_m)N^2 P_N$$

$$+\sum_{N=2}^{M} k_{AB} M N P_{N-1} - \sum_{N=2}^{M} k_{AB}(N-1) N P_{N-1}$$

$$+\sum_{N=1}^{M-1} 2k_m N(N+1) P_{N+1}$$

$$\approx -k_{AB} M \overline{N} + (k_{AB} - 2k_m)\overline{N^2} + k_{AB} M(1+\overline{N}) - k_{AB}(\overline{N^2} + \overline{N}) + 2k_m(\overline{N^2} - \overline{N})$$

$$= k_{AB} M - k_{AB} \overline{N} - 2k_m \overline{N}$$

$$\overline{N} = M \frac{k_A + k_B}{k_A + k_B + 2k_m}$$

$$0 = \frac{\mathrm{d}\overline{N^2}}{\mathrm{d}t} = \sum N^2 \frac{\mathrm{d}P_N}{\mathrm{d}t} = -\sum_{N=1}^{M} k_{AB} M N^2 P_N + \sum_{N=1}^{N} (k_{AB} - 2k_m) N^3 P_N$$

$$+\sum_{N=2}^{M} k_{AB} M N^2 P_{N-1} - \sum_{N=2}^{M} k_{AB}(N-1) N^2 P_{N-1}$$

$$+\sum_{N=1}^{M-1} 2k_m N^2 (N+1) P_{N+1}$$

$$\approx -k_{AB} M \overline{N^2} + (k_{AB} - 2k_m)\overline{N^3} + k_{AB} M(\overline{N^2} + 2\overline{N} + 1)$$

$$-k_{AB}(\overline{N^3} + 2\overline{N^2} + \overline{N}) + 2k_m(\overline{N^3} - 2\overline{N^2} + \overline{N})$$

$$= +k_{AB} M(2\overline{N} + 1) - k_{AB}(2\overline{N^2} + \overline{N}) + 2k_m(-2\overline{N^2} + \overline{N})$$

$$= k_{AB} M + \overline{N}(2k_{AB} M - k_{AB} + 2k_m) - \overline{N^2}(2k_{AB} + 4k_m)$$

$$\overline{N^2} = \frac{k_{AB} M + (2k_{AB} M - k_{AB} + 2k_m) M \frac{k_{AB}}{k_{AB} + 2k_m}}{2k_{AB} + 4k_m}$$

$$= \frac{2k_{AB} k_m}{(k_{AB} + 2k_m)^2} M + \frac{k_{AB}^2}{(k_{AB} + 2k_m)^2} M^2$$

and the variance is

$$\overline{N^2} - \overline{N}^2 = \frac{2k_m k_{AB}}{(k_{AB} + 2k_m)^2} M = \frac{2k_m}{k_{AB} M} \overline{N}^2.$$

The diffusion current from $A \to B$ is

$$J = \frac{\mathrm{d}N_A}{\mathrm{d}t} - \frac{\mathrm{d}N_B}{\mathrm{d}t} = \sum_N (-k_A(M-N)P_N + k_m N P_N) - \sum_N (-k_B(M-N)P_N + k_m N P_N)$$

$$= \sum_N (k_B - k_A)(M-N)P_N = (k_B - k_A)(M - \overline{N}).$$

Problems of Chap. 9

9.1 Dichotomous Model

$\lambda_1 = 0$

$$\mathbf{L}_1 = (1\ 1\ 1\ 1) \quad \mathbf{R}_1 = \begin{pmatrix} 0 \\ 0 \\ \beta \\ \alpha \end{pmatrix} \quad \frac{(\mathbf{L}_1 \mathbf{P}_0)}{(\mathbf{L}_1 \mathbf{R}_1)} = \frac{1}{\alpha + \beta}$$

$\lambda_2 = -(\alpha + \beta)$

$$\mathbf{L}_2 = (\alpha\ -\beta\ \alpha\ -\beta)\, \mathbf{R}_2 = \begin{pmatrix} 0 \\ 0 \\ -1 \\ 1 \end{pmatrix} \quad \frac{(\mathbf{L}_2 \mathbf{P}_0)}{(\mathbf{L}_2 \mathbf{R}_2)} = 0$$

$$\lambda_{3,4} = -\frac{k_- + k_+ + \alpha + \beta}{2} \pm \frac{1}{2}\sqrt{(\alpha+\beta)^2 + (k_+ - k_-)^2 + 2(\beta - \alpha)(k_- - k_+)}$$

fast fluctuations:

$$\lambda_3 = -\frac{\alpha}{\alpha + \beta} k_- - \frac{\beta}{\alpha + \beta} k_+ + O(k^2)$$

$$\mathbf{L}_3 \approx (1,1,0,0) \quad \mathbf{R}_3 \approx \begin{pmatrix} \beta \\ \alpha \\ -\beta \\ -\alpha \end{pmatrix} \quad \frac{(\mathbf{L}_3\mathbf{P}_0)}{(\mathbf{L}_3\mathbf{R}_3)} \approx \frac{1}{\alpha+\beta}$$

$$\lambda_4 = -(\alpha+\beta) - \frac{\alpha}{\alpha+\beta}k_+ - \frac{\beta}{\alpha+\beta}k_- + O(k^2)$$

$$\mathbf{L}_4 \approx (-\alpha,\beta,0,0) \quad \mathbf{R}_4 \approx \begin{pmatrix} 1 \\ -1 \\ 1 \\ -1 \end{pmatrix} \quad \frac{(\mathbf{L}_4\mathbf{P}_0)}{(\mathbf{L}_4\mathbf{R}_1)} \approx 0$$

$$\mathbf{P}(t) \approx \begin{pmatrix} 0 \\ 0 \\ \frac{\beta}{\alpha+\beta} \\ \frac{\alpha}{\alpha+\beta} \end{pmatrix} + \begin{pmatrix} \frac{\beta}{\alpha+\beta} \\ \frac{\alpha}{\alpha+\beta} \\ -\frac{\beta}{\alpha+\beta} \\ -\frac{\alpha}{\alpha+\beta} \end{pmatrix} \mathrm{e}^{\lambda_3 t} \quad \rightarrow P(D^*) = \mathrm{e}^{\lambda_3 t}$$

slow fluctuations:

$$\lambda_3 \approx -k_+ - \alpha$$

$$\mathbf{L}_3 \approx (k_+ - k_-, -\beta, 0, 0) \quad \mathbf{R}_3 \approx \begin{pmatrix} k_+ - k_- \\ -\alpha \\ -(k_+ - k_-) \\ \alpha \end{pmatrix} \quad \frac{\mathbf{L}_3\mathbf{P}_0}{\mathbf{L}_3\mathbf{R}_3} \approx \frac{\beta}{\alpha+\beta}\frac{1}{k_+ - k_-}$$

$$\lambda_4 \approx -k_- - \beta$$

$$\mathbf{L}_4 \approx (\alpha, k_+ - k_-, 0, 0)\mathbf{R}_4 \approx \begin{pmatrix} \beta \\ k_+ - k_- \\ -\beta \\ -(k_+ - k_-) \end{pmatrix} \quad \frac{\mathbf{L}_4\mathbf{P}_0}{\mathbf{L}_4\mathbf{R}_4} \approx \frac{\alpha}{\alpha+\beta}\frac{1}{k_+ - k_-}$$

$$\mathbf{P}(t) \approx \begin{pmatrix} 0 \\ 0 \\ \frac{\beta}{\alpha+\beta} \\ \frac{\alpha}{\alpha+\beta} \end{pmatrix} + \frac{\beta}{\alpha+\beta}\begin{pmatrix} 1 \\ 0 \\ -1 \\ 0 \end{pmatrix} \mathrm{e}^{-(k_+ + \alpha)t} + \frac{\alpha}{\alpha+\beta}\begin{pmatrix} 0 \\ 1 \\ 0 \\ -1 \end{pmatrix} \mathrm{e}^{-(k_- + \beta)t}$$

$$P(D^*) \approx \frac{\beta}{\alpha+\beta} \mathrm{e}^{-(k_+ + \alpha)t} + \frac{\alpha}{\alpha+\beta} \mathrm{e}^{-(k_- + \beta)t}$$

Problems of Chap. 10

10.1 Entropy Production

$$0 = dH = TdS + Vdp + \sum_k \mu_k dN_k$$

$$TdS = -\sum_k \mu_k dN_k = -\sum_j \sum_k \mu_k \nu_{kj} d\xi_j = \sum_j A_j d\xi_j$$

$$\frac{\mathrm{d}S}{\mathrm{d}t} = \sum_j \frac{A_j}{T} r_j$$

Problems of Chap. 11

11.1 ATP Synthesis

At chemical equilibrium

$$0 = A = -\sum \nu_k \mu_k$$

$$= \mu^0(ADP) + k_B T \ln c(ADP) + \mu^0(POH) + k_B T \ln c(POH) + 2k_B T \ln c(H^+_{out}) + 2e\Phi_{out}$$

$$-\mu^0(ATP) - k_B T \ln c(ATP) - \mu^0(H_2O) - k_B T \ln c(H_2O) - 2k_B T \ln c(H^+_{in}) - 2e\Phi_{in}$$

$$k_B T \ln K = -\Delta G^0 = \mu^0(ADP) - \mu^0(ATP) + \mu^0(POH) - \mu^0(H_2O)$$

$$= k_B T \ln \frac{c(ATP)c(H_2O)c^2(H^+_{in})}{c(ADP)c(POH)c^2(H^+_{out})} + 2e(\Phi_{in} - \Phi_{out})$$

$$= k_B T \ln \frac{c(ATP)c(H_2O)}{c(ADP)c(POH)} + 2k_B T \ln \frac{c(H^+_{in})}{c(H^+_{out})} + 2e(\Phi_{in} - \Phi_{out})$$

Problems of Chap. 15

15.1 Transition State Theory

$$\mathrm{A{+}B} \underset{}{\overset{K^{\ddagger}}{\rightleftharpoons}} [\mathrm{AB}]^{\ddagger} \overset{k^{\ddagger}}{\rightarrow} \mathrm{P}$$

$$k = k^{\ddagger} c_{[AB]^{\ddagger}} = k^{\ddagger} K^{\ddagger} c_A c_B$$

$$K^{\ddagger} = \frac{c_{[AB]^{\ddagger}}}{c_A c_B} = \frac{q_{[AB]^{\ddagger}}}{q_A q_B} \mathrm{e}^{-\Delta H^{\ddagger}/k_B T} = q_x \frac{q^{\ddagger}_{[AB]^{\ddagger}}}{q_A q_B} \mathrm{e}^{-\Delta H^{\ddagger}/k_B T}$$

$$q_x = \frac{\sqrt{2\pi m k_B T}}{h} \delta x$$

$$k^{\ddagger} = \frac{v^{\ddagger}}{\delta x} = \frac{1}{\delta x} \sqrt{\frac{k_B T}{2\pi m}}$$

$$k = \frac{1}{\delta x} \sqrt{\frac{k_B T}{2\pi m}} \frac{\sqrt{2\pi m k_B T}}{h} \delta x \frac{q^{\ddagger}_{[AB]^{\ddagger}}}{q_A q_B} \mathrm{e}^{-\Delta H^{\ddagger}/k_B T} c_A c_B$$

$$= \frac{k_B T}{h} \frac{q^{\ddagger}_{[AB]^{\ddagger}}}{q_A q_B} \mathrm{e}^{-\Delta H^{\ddagger}/k_B T} c_A c_B$$

15.2 Harmonic Transition State Theory

$$k = v < \delta(x - x^{\ddagger}) >= \sqrt{\frac{k_B T}{2\pi m}} \frac{\int_{-\infty}^{\infty} \mathrm{e}^{-m\omega^2 x^2/2k_B T} \delta(x - x^{\ddagger})}{\int_{-\infty}^{\infty} \mathrm{e}^{-m\omega^2 x^2/2k_B T}}$$

$$= \sqrt{\frac{k_B T}{2\pi m}} \frac{\mathrm{e}^{-m\omega^2 x^{\ddagger 2}/2k_B T}}{\sqrt{\frac{2\pi k_B T}{m\omega^2}}}$$

$$= \frac{\omega}{2\pi} \mathrm{e}^{-\Delta E/k_B T}$$

Problems of Chap. 16

16.1 Marcus Cross Relation

$$\begin{array}{ll} \mathrm{A{+}A^- \rightarrow A^-{+}A} & \lambda_A = 2\Delta E(A_{eq} \rightarrow A^-_{eq}) \\ \mathrm{D{+}D^+ \rightarrow D^+{+}D} & \lambda_D = 2\Delta E(D_{eq} \rightarrow D^+_{eq}) \\ \mathrm{A{+}D \rightarrow A^-{+}D^+} & \lambda_{AD} = \Delta E(A_{eq} \rightarrow A^-_{eq}) + \Delta E(D_{eq} \rightarrow D^+_{eq}) = \frac{\lambda_A+\lambda_D}{2} \end{array}$$

$$k_A = \frac{\omega_A}{2\pi} \mathrm{e}^{-\lambda_A/4k_BT}$$

$$k_B = \frac{\omega_B}{2\pi} \mathrm{e}^{-\lambda_B/4k_BT}$$

$$K_{AD} = \mathrm{e}^{-\Delta G/k_BT}$$

$$k_{AD} = \frac{\omega_{AD}}{2\pi} \exp\left\{-\frac{(\lambda_{AD}+\Delta G)^2}{4\lambda_{AD}k_BT}\right\}$$

$$= \frac{\omega_{AD}}{2\pi} \exp\left\{-\frac{\lambda_A+\lambda_D}{8k_BT} - \frac{\Delta G}{2k_BT} - \frac{\Delta G^2}{4\lambda_{AD}k_BT}\right\}$$

$$= \sqrt{k_Ak_BK_{AD}} \sqrt{\frac{\omega^2_{AD}}{\omega_A\omega_D}} \exp\left\{-\frac{\Delta G^2}{4\lambda_{AD}k_BT}\right\}$$

Problems of Chap. 18

18.1 Absorption Spectrum

$$\alpha = \frac{1}{2\pi\hbar} \int dt \sum_{i,f} \mathrm{e}^{\mathrm{i}\omega t} < i| \sum \frac{\mathrm{e}^{-\beta H}}{Q} \mathrm{e}^{-\mathrm{i}\omega_i t} \mu f > \mathrm{e}^{\mathrm{i}\omega_f t} < f\mu i >$$

$$= \frac{1}{2\pi\hbar} \int dt \mathrm{e}^{\mathrm{i}\omega t} < \mathrm{e}^{-\mathrm{i}Ht/\hbar} \mu \mathrm{e}^{\mathrm{i}Ht/\hbar} \mu >$$

$$= \frac{1}{2\pi\hbar} \int dt \mathrm{e}^{\mathrm{i}\omega t} < \mu(0)\mu(t) >$$

$$\approx \frac{|\mu_{eg}|^2}{2\pi\hbar}\int dt \mathrm{e}^{\mathrm{i}\omega t} < \mathrm{e}^{-\mathrm{i}H_g t/\hbar}\mathrm{e}^{\mathrm{i}H_e t/\hbar} >_g$$

Problems of Chap. 20

20.1 Motional Narrowing

$$(s+\mathrm{i}\omega_1)(s+\mathrm{i}\omega_2)+(\alpha+\beta)(s+\mathrm{i}\overline{\omega})$$

$$= -\left(\Omega+\frac{\Delta\omega}{2}\right)\left(\Omega-\frac{\Delta\omega}{2}\right)-\mathrm{i}\omega_c\Omega$$

$$\Omega = \omega - \overline{\omega}$$

$$\Omega^2 - \frac{\Delta\omega^2}{4} + \mathrm{i}\omega_c\Omega = 0$$

$$\left(\Omega+\frac{\mathrm{i}\omega_c}{2}\right)^2 = \frac{\Delta\omega^2}{4} - \frac{\omega_c^2}{4}$$

For $\omega_c \ll \Delta\omega$ the poles are approximately at

$$\Omega_p = -\frac{\mathrm{i}\omega_c}{2} \pm \frac{\Delta\omega}{2}$$

and two lines are observed centered at the unperturbed frequencies $\overline{\omega} \pm \Delta\omega/2$ and with their width determined by ω_c. For $\omega_c = \Delta\omega$ the two poles coincide at

$$\Omega_p = -\frac{\mathrm{i}\omega_c}{2}$$

and a single line at the average frequency $\overline{\omega}$ appears. For $\omega_c \gg \Delta\omega$ one pole approaches zero according to

$$\Omega_p = -\mathrm{i}\frac{\Delta\omega^2}{4\omega_c}$$

which corresponds to a sharp line at the average frequency $\overline{\omega}$. The other pole approaches infinity as

$$\Omega_p = -\mathrm{i}\omega_c.$$

It contributes a broad line at $\overline{\omega}$ which vanishes in the limit of large ω_c (Fig. 1).

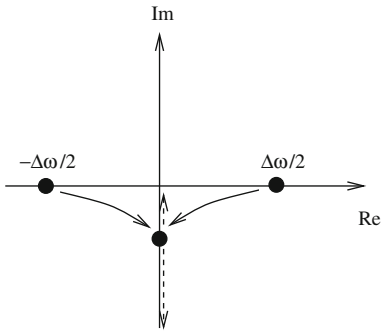

Fig. 1 Poles of the lineshape function

Problems of Chap. 21

21.1 Crude Adiabatic Model

$$\frac{\partial C}{\partial Q} = \begin{pmatrix} -s & c \\ -c & -s \end{pmatrix} \frac{\partial \zeta}{\partial Q} \quad C^\dagger \frac{\partial C}{\partial Q} = \begin{pmatrix} 0 & 1 \\ -1 & 0 \end{pmatrix} \frac{\partial \zeta}{\partial Q}$$

$$\frac{\partial^2 C}{\partial Q^2} = \begin{pmatrix} -s & c \\ -c & -s \end{pmatrix} \frac{\partial^2 \zeta}{\partial Q^2} - C \left(\frac{\partial \zeta}{\partial Q} \right)^2$$

$$C^\dagger \frac{\partial^2 C}{\partial Q^2} = \begin{pmatrix} 0 & 1 \\ -1 & 0 \end{pmatrix} \frac{\partial^2 \zeta}{\partial Q^2} - \left(\frac{\partial \zeta}{\partial Q} \right)^2$$

$$\int dr\, C^\dagger \Phi^\dagger \frac{\partial^2}{\partial Q^2} \Phi C = C^\dagger \frac{\partial^2 C}{\partial Q^2} + 2 C^\dagger \frac{\partial C}{\partial Q} \frac{\partial}{\partial Q} + \frac{\partial^2}{\partial Q^2}$$

$$= \frac{\partial^2}{\partial Q^2} + \begin{pmatrix} 0 & 1 \\ -1 & 0 \end{pmatrix} \frac{\partial^2 \zeta}{\partial Q^2} - \left(\frac{\partial \zeta}{\partial Q} \right)^2 + 2 \begin{pmatrix} 0 & 1 \\ -1 & 0 \end{pmatrix} \frac{\partial \zeta}{\partial Q} \frac{\partial}{\partial Q}$$

$$\int dr\, C^\dagger \Phi^\dagger (T_{el} + V_0 + \Delta V) \Phi C =$$

$$C^\dagger E C + C^\dagger \int dr \Phi^\dagger \Delta V \Phi \quad C = C^\dagger \begin{pmatrix} \overline{E}(Q) - \frac{\Delta E(Q)}{2} & V(Q) \\ V(Q) & \overline{E}(Q) + \frac{\Delta E(Q)}{2} \end{pmatrix} C$$

$$\int dr\, C^\dagger \Phi^\dagger H\, \Phi\, C =$$

$$= -\frac{\hbar^2}{2m} \frac{\partial^2}{\partial Q^2} + C^\dagger \begin{pmatrix} \overline{E}(Q) - \frac{\Delta E(Q)}{2} & V(Q) \\ V(Q) & \overline{E}(Q) + \frac{\Delta E(Q)}{2} \end{pmatrix} C + \frac{\hbar^2}{2m} \left(\frac{\partial \zeta}{\partial Q} \right)^2$$

$$-\frac{\hbar^2}{2m}\begin{pmatrix}0 & 1\\ -1 & 0\end{pmatrix}\left(\frac{\partial^2\zeta}{\partial Q^2}+2\frac{\partial\zeta}{\partial Q}\frac{\partial}{\partial Q}\right)$$

$$\cos\zeta\sin\zeta=\frac{V(Q)}{\sqrt{4V(Q)^2+\Delta E(Q)^2}}\quad \cos\zeta^2-\sin\zeta^2=\frac{\Delta E(Q)}{\sqrt{4V(Q)^2+\Delta E(Q)^2}}$$

$$\frac{\partial}{\partial Q}(cs)^2=2cs(c^2-s^2)\frac{\partial\zeta}{\partial Q}=\frac{2V\Delta E}{4V^2+\Delta E^2}\frac{\partial\zeta}{\partial Q}$$

$$\frac{\partial}{\partial Q}(cs)^2=\frac{\partial}{\partial Q}\frac{V^2}{4V^2+\Delta E^2}$$

$$=\frac{2V}{4V^2+\Delta E^2}\frac{\partial V}{\partial Q}-\frac{V^2}{(4V^2+\Delta E^2)^2}\left(2\Delta E\frac{\partial\Delta E}{\partial Q}+8V\frac{\partial V}{\partial Q}\right)$$

$$\frac{\partial\zeta}{\partial Q}=\frac{\Delta E}{4V^2+\Delta E^2}\frac{\partial V}{\partial Q}-\frac{V}{4V^2+\Delta E^2}\frac{\partial\Delta E}{\partial Q}\approx\frac{1}{\Delta E}\frac{\partial V}{\partial Q}$$

$$\frac{\partial^2\zeta}{\partial Q^2}=\frac{\Delta E\frac{\partial^2 V}{\partial Q^2}-V\frac{\partial^2\Delta E}{\partial Q^2}}{4V^2+\Delta E^2}-\left(\Delta E\frac{\partial V}{\partial Q}-V\frac{\partial\Delta E}{\partial Q}\right)\frac{2\Delta E\frac{\partial\Delta E}{\partial Q}+8V\frac{\partial V}{\partial Q}}{(4V^2+\Delta \mathrm{e}^2)^2}$$

$$\approx\frac{1}{\Delta E}\frac{\partial^2 V}{\partial Q^2}-\frac{2}{\Delta E^2}\frac{\partial\Delta E}{\partial Q}\frac{\partial V}{\partial Q}$$

$$\widetilde{H}\approx-\frac{\hbar^2}{2m}\frac{\partial^2}{\partial Q^2}+\begin{pmatrix}\overline{E}-\sqrt{4V^2+\Delta E^2} & \\ & \overline{E}+\sqrt{4V^2+\Delta E^2}\end{pmatrix}$$

$$+\frac{\hbar^2}{2m}\frac{1}{\Delta E^2}\left(\frac{\partial V}{\partial Q}\right)^2-\frac{\hbar^2}{2m}\begin{pmatrix}0 & 1\\ -1 & 0\end{pmatrix}\left(\frac{1}{\Delta E}\frac{\partial^2 V}{\partial Q^2}-\frac{2}{\Delta E^2}\frac{\partial\Delta E}{\partial Q}\frac{\partial V}{\partial Q}+\frac{2}{\Delta E}\frac{\partial V}{\partial Q}\frac{\partial}{\partial Q}\right)$$

Problems of Chap. 22

22.1 Ladder Model

$$\mathrm{i}\hbar\dot{C}_0=V\sum_{j=1}^{n}C_j$$

$$\mathrm{i}\hbar\dot{C}_j=E_jC_j+VC_0$$

$$C_j = u_j \mathrm{e}^{\frac{E_j}{\mathrm{i}\hbar}t}$$

$$\mathrm{i}\hbar \dot{u}_j \mathrm{e}^{\frac{E_j}{\mathrm{i}\hbar}t} = VC_0$$

$$u_j = \frac{V}{\mathrm{i}\hbar}\int^t \mathrm{e}^{-\frac{E_j}{\mathrm{i}\hbar}t'} C_0(t')dt'$$

$$C_j = \frac{V}{\mathrm{i}\hbar}\int^t \mathrm{e}^{\mathrm{i}\frac{E_j}{\hbar}(t-t')} C_0(t')dt'$$

$$E_j = \alpha + j * \hbar\Delta\omega$$

$$\dot{C}_0 = \frac{V}{\mathrm{i}\hbar}\sum_{j=1}^{n} C_j = -\frac{V^2}{\hbar^2}\sum\int^t \mathrm{e}^{\mathrm{i}(j\Delta\omega+\alpha/\hbar)(t-t')} C_0(t')dt'$$

$$\omega = j\Delta\omega + \frac{\alpha}{\hbar}$$

$$\sum_{j=-\infty}^{\infty} \mathrm{e}^{\mathrm{i}(j\Delta\omega+\alpha/\hbar)(t-t')}\Delta j \;\rightarrow\; \int_{-\infty}^{\infty} \mathrm{e}^{i\omega(t-t')}\frac{d\omega}{\Delta\omega} = \frac{2\pi}{\Delta\omega}\delta(t-t')$$

$$\dot{C}_0 = -\frac{2\pi V^2}{\Delta\omega}C_0 = -\frac{2\pi V^2}{\hbar}\rho(E)C_0$$

$$\rho(E) = \frac{1}{\hbar\Delta\omega} = \frac{1}{\Delta E}$$

Problems of Chap. 23

23.1 Hückel Model with Alternating Bonds

(a)

$$\alpha \mathrm{e}^{\mathrm{i}kn} + \beta \mathrm{e}^{\mathrm{i}(kn+\chi)} + \beta' \mathrm{e}^{\mathrm{i}(kn+k+\chi)} = \mathrm{e}^{\mathrm{i}kn}\left(\alpha + \beta \mathrm{e}^{\mathrm{i}\chi} + \beta' \mathrm{e}^{\mathrm{i}(k+\chi)}\right)$$

$$\alpha \mathrm{e}^{\mathrm{i}(kn+\chi)} + \beta' \mathrm{e}^{\mathrm{i}(kn-k)} + \beta \mathrm{e}^{\mathrm{i}kn} = \mathrm{e}^{\mathrm{i}(kn+\chi)}\left(\alpha + \beta' \mathrm{e}^{-\mathrm{i}(k+\chi)} + \beta \mathrm{e}^{-\mathrm{i}\chi}\right)$$

(b)

$$\beta \mathrm{e}^{\mathrm{i}\chi} + \beta' \mathrm{e}^{\mathrm{i}(k+\chi)} = \beta' \mathrm{e}^{-\mathrm{i}(k+\chi)} + \beta \mathrm{e}^{-\mathrm{i}\chi}$$

$$e^{2i\chi} = \frac{\beta' e^{-ik} + \beta}{\beta' e^{ik} + \beta} = e^{-ik} \frac{\beta' e^{-ik/2} + \beta e^{ik/2}}{\beta' e^{ik/2} + \beta e^{-ik/2}} = e^{-ik} \frac{\left(\beta' e^{-ik/2} + \beta e^{ik/2}\right)^2}{\beta'^2 + \beta^2 + 2\beta\beta' \cos k}$$

$$e^{i\chi} = \pm e^{-ik/2} \frac{\beta' e^{-ik/2} + \beta e^{ik/2}}{\sqrt{\beta'^2 + \beta^2 + 2\beta\beta' \cos k}}$$

$$\lambda = \alpha + \beta e^{i\chi} + \beta' e^{i(k+\chi)} = \alpha \pm \frac{\beta\beta' e^{-ik} + \beta^2 + \beta'^2 + \beta\beta' e^{ik}}{\sqrt{\beta'^2 + \beta^2 + 2\beta\beta' \cos k}}$$

$$= \alpha \pm \sqrt{\beta'^2 + \beta^2 + 2\beta\beta' \cos k}$$

(c)

$$0 = \Im\left(e^{i\chi + i(N+1)k}\right) = \Im\left(\pm e^{-ik/2} \frac{\beta' e^{-ik/2} + \beta e^{ik/2}}{\sqrt{\beta'^2 + \beta^2 + 2\beta\beta' \cos k}} e^{i(N+1)k}\right)$$

$$= \pm \Im\left(\frac{\beta' e^{iNk} + \beta e^{i(N+1)k}}{\sqrt{\beta'^2 + \beta^2 + 2\beta\beta' \cos k}}\right)$$

$$0 = \beta' \sin(Nk) + \beta \sin(N+1)k)$$

(d) For a linear polyene with 2N-1 carbon atoms use again eigenfunctions

$$c_{2n} = \sin(kn) = \Im(e^{ikn})$$

$$c_{2n-1} = \sin(kn + \chi) = \Im(e^{i(kn+\chi)})$$

and chose the k-values such that

$$\Im(e^{iNk}) = \sin(Nk) = 0$$

Problems of Chap. 25

25.1 Special Pair Dimer

$$\begin{pmatrix} c & -s \\ s & c \end{pmatrix} \begin{pmatrix} -\Delta/2 & V \\ V & \Delta/2 \end{pmatrix} \begin{pmatrix} c & s \\ -s & c \end{pmatrix}$$

is diagonalized if

$$(c^2 - s^2)V = cs\Delta$$

or with $c = \cos\chi$, $s = \sin\chi$

$$\tan(2\chi) = \frac{2V}{\Delta}$$

$$c^2 - s^2 = \cos 2\chi = \frac{1}{\sqrt{1 + \frac{4V^2}{\Delta^2}}} \geq 0$$

$$2cs = \sin(2\chi) = \frac{1}{\sqrt{1 + \frac{\Delta^2}{4V^2}}} \geq 0.$$

The eigenvalues are (Fig. 2)

$$E_\pm = \pm\left(\frac{\Delta}{2}(c^2 - s^2) + 2csV\right)$$

$$= \pm\left(\frac{\Delta}{2}\frac{1}{\sqrt{1 + \frac{4V^2}{\Delta^2}}} + V\frac{1}{\sqrt{1 + \frac{\Delta^2}{4V^2}}}\right) = \pm\frac{1}{2}\sqrt{\Delta^2 + 4V^2}.$$

The transition dipoles are

$$\mu_+ = s\mu_a + c\mu_b$$

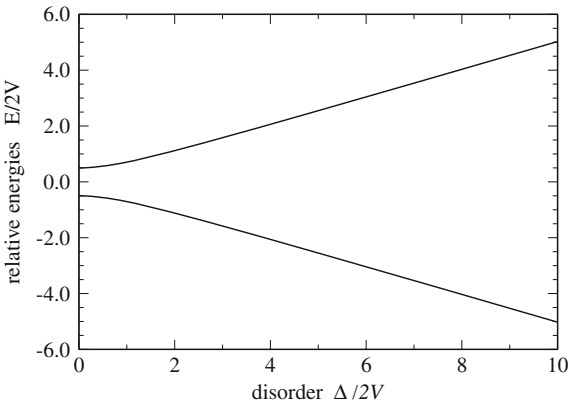

Fig. 2 Energy splitting of the two dimer bands

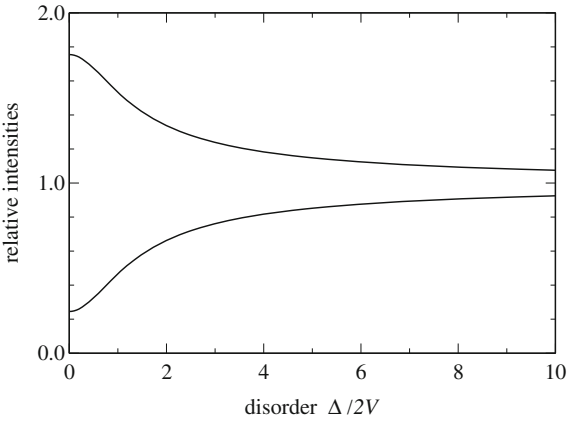

Fig. 3 Intensities of the two dimer bands

$$\mu_- = c\mu_a - s\mu_b$$

and the intensities (for $|\mu_a| = |\mu_b| = \mu$)

$$|\mu_\pm|^2 = \mu^2(1 \pm 2cs\cos\alpha) = \mu^2(1 \pm \frac{\cos\alpha}{\sqrt{1+\frac{\Delta^2}{4V^2}}})$$

with (Fig. 3)

$$\cos\alpha = -0.755.$$

25.2 LHC II

$$|n;\alpha>=\frac{1}{3}\sum_k \mathrm{e}^{-\mathrm{i}kn}|k;\alpha>$$

$$\sum_{n=1}^{9} E_\alpha |n;\alpha><n;\alpha| = \sum_{n=1}^{9} E_\alpha \frac{1}{9}\sum_{k,k'} \mathrm{e}^{-i(k-k')n}|k;\alpha><k';\alpha|$$

$$= \delta_{k,k'} E_\alpha |k;\alpha><k;\alpha|$$

$$\sum_{n=1}^{9} E_\alpha |n;\beta><n;\beta| \sum_{n=1}^{9} E_\alpha \frac{1}{9}\sum_{k,k'} \mathrm{e}^{-i(k-k')n}|k;\beta><k';\beta|$$

$$= \delta_{k,k'} E_\alpha |k;\beta><k;\beta|$$

$$\sum_{n=1}^{9} V_{dim}|n;\alpha><n;\beta| = \sum_{n=1}^{9} V_{dim}\frac{1}{9}\sum_{k,k'} \mathrm{e}^{-i(k-k')n}|k;\alpha><k';\beta|$$

$$= \delta_{k,k'} V_{dim}|k;\alpha><k;\beta|$$

$$\sum_{n=1}^{9} V_{\beta\alpha,1}|n;\alpha><n-1;\beta| = \sum_{n=1}^{9} V_{\beta\alpha,1}\mathrm{e}^{-\mathrm{i}k}\frac{1}{9}\sum_{k,k'} \mathrm{e}^{-i(k-k')n}|k;\alpha><k';\beta|$$

$$= \delta_{k,k'} V_{\beta\alpha,1}\mathrm{e}^{-\mathrm{i}k}|k;\alpha><k;\beta|$$

$$\sum_{n=1}^{9} V_{\beta\alpha,1}|n;\beta><n+1;\alpha| = \sum_{n=1}^{9} V_{\beta\alpha,1}\mathrm{e}^{\mathrm{i}k}\frac{1}{9}\sum_{k,k'} \mathrm{e}^{-i(k-k')n}|k;\beta><k';\alpha|$$

$$= \delta_{k,k'} V_{\beta\alpha,1}\mathrm{e}^{\mathrm{i}k}|k;\beta><k;\alpha|$$

$$\sum_{n=1}^{9} V_{\alpha\alpha,1}(|n;\alpha><n+1;\alpha| + h.c.) = \sum_{n=1}^{9} V_{\alpha\alpha,1}\mathrm{e}^{\mathrm{i}k}\frac{1}{9}\sum_{k,k'} \mathrm{e}^{-i(k-k')n}|k;\alpha><k';\alpha| + h.c.$$

$$= \delta_{k,k'} 2V_{\alpha\alpha,1}\cos k|k;\alpha><k;\alpha|$$

$$H_{\alpha\alpha}(k) = E_\alpha + 2V_{\alpha\alpha 1}\cos k$$

$$H_{\beta\beta}(k) = E_\beta + 2V_{\beta\beta 1}\cos k$$

$$H_{\alpha\beta}(k) = V_{dim} + \mathrm{e}^{-\mathrm{i}k}V_{\beta\alpha,1}$$

$$H_{\beta\alpha}(k) = V_{dim} + \mathrm{e}^{\mathrm{i}k}V_{\beta\alpha,1}$$

$$H(k) = \begin{pmatrix} E_\alpha + 2V_{\alpha\alpha 1}\cos k & V + \mathrm{e}^{-\mathrm{i}k}W \\ V + \mathrm{e}^{\mathrm{i}k}W & E_\beta + 2V_{\beta\beta 1}\cos k \end{pmatrix} = \overline{E}_k + \begin{pmatrix} -\Delta_k/2 & V + \mathrm{e}^{-\mathrm{i}k}W \\ V + \mathrm{e}^{\mathrm{i}k}W & \Delta_k/2 \end{pmatrix}$$

Perform a canonical transformation with

$$S = \begin{pmatrix} c & -s\mathrm{e}^{-\mathrm{i}\chi} \\ s\mathrm{e}^{\mathrm{i}\chi} & c \end{pmatrix}.$$

$S^\dagger\, H\, S$ becomes diagonal if

$$c^2(V + \mathrm{e}^{\mathrm{i}k}W) - s^2\mathrm{e}^{2\mathrm{i}\chi}(V + \mathrm{e}^{-\mathrm{i}k}W) + cs\mathrm{e}^{\mathrm{i}\chi}\Delta_k = 0.$$

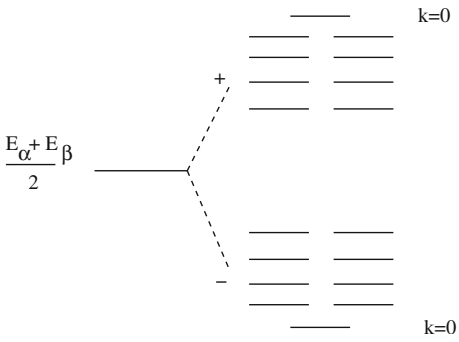

Fig. 4 Energy levels of LHII

Chose χ such that

$$V + e^{ik} W = \text{sign} V |V + e^{ik} W| e^{i\chi} = U(k) e^{i\chi}$$

and solve

$$(c^2 - s^2) U + cs \Delta_k = 0$$

by[4]

$$c^2 - s^2 = -\text{sign}\left(\frac{U}{\Delta}\right) \frac{1}{\sqrt{1 + \frac{4U^2}{\Delta^2}}} \quad cs = \frac{\left|\frac{U}{\Delta}\right|}{\sqrt{1 + \frac{4U^2}{\Delta^2}}}.$$

The eigenvalues are (Fig. 4)

$$E_\pm(k) = \overline{E}_k \pm \text{sign} V \frac{1}{2} \sqrt{\Delta^2 + 4U^2}$$

$$= \frac{E_\alpha + E_\beta}{2} + (V_{\alpha\alpha 1} + V_{\beta\beta 1}) \cos k$$

$$\pm \text{sign} V \sqrt{\left(\frac{E_\alpha - E_\beta + 2(V_{\alpha\alpha 1} - V_{\beta\beta 1}) \cos k}{2}\right)^2 + V^2 + W^2 + 2VW \cos k}$$

$$\mu_{k,+} = c \frac{1}{3} \sum_n e^{ikn} \mu_{n\alpha} + s e^{i\chi} \frac{1}{3} \sum_n e^{ikn} \mu_{n\beta}$$

[4]The sign is chosen such that for $|\Delta| \ll |U|$ the solution becomes $c = s = 1/\sqrt{2}$.

$$= c\frac{1}{3}\sum_n e^{ikn} S_9^n \mu_{0\alpha} + s e^{i\chi}\frac{1}{3}\sum_n e^{ikn} S_9^n R_z(2\nu + \phi_\beta - \phi_\alpha)\mu_{0,\alpha}$$

$$= \frac{1}{3}\sum_n e^{ikn} \begin{pmatrix} \cos\frac{2\pi}{9}n & -\sin\frac{2\pi}{9}n & \\ \sin\frac{2\pi}{9}n & \cos\frac{2\pi}{9}n & \\ & & 1 \end{pmatrix} \left(c + s e^{i\chi} \begin{pmatrix} \cos\epsilon & -\sin\epsilon & \\ \sin\epsilon & \cos\epsilon & \\ & & 1 \end{pmatrix} \right) \mu_0 \begin{pmatrix} \sin\theta \\ 0 \\ \cos\theta \end{pmatrix}.$$

The sum over n again gives the selection rules

$k = 0$ z-polarisation

$k = \pm\frac{2\pi}{9}$ circular xy-polarisation.

The second factor gives for z-polarization

$$\mu = 3\mu_0(c + s e^{i\chi})\cos\theta$$

$$|\mu|^2 = 9\mu_0^2(1 + 2cs\ \cos\chi)\cos^2\theta$$

with

$$\cos^2\theta \approx 0.008$$

and for polarization in the xy plane

$$\mu = 3\mu_0 \sin\theta \begin{pmatrix} c\ + s e^{i\chi}\cos\epsilon \\ s e^{i\chi}\sin\epsilon \end{pmatrix}$$

$$|\mu|^2 = 9\mu_0^2 \sin^2\theta(1 + 2\cos\epsilon\, cs\cos\chi)$$

with

$$\sin^2\theta \approx 0.99 \quad \cos\epsilon \approx -0.952.$$

The intensities of the (k,-) states are

$$|\mu_z|^2 = 9\mu_0^2(1 - 2cs\ \cos\chi)\cos^2\theta$$

$$|\mu_\perp|^2 = 9\mu_0^2 \sin^2\theta(1 - 2\cos\epsilon\, cs\cos\chi).$$

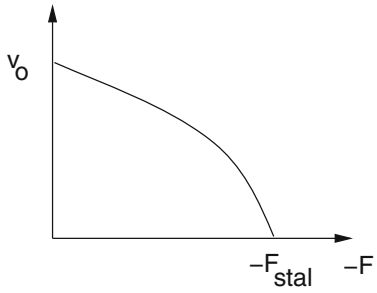

25.3 Exchange Narrowing

$$P(\delta E_k = X) = \int d\delta E_1 d\delta E_2 \cdots P(\delta E_1) P(\delta E_2) \cdots \delta(X - \frac{\sum \delta E_n}{N})$$

$$P(\delta E_k = X) = \frac{1}{2\pi} \int dt \int \delta E_1 d\delta E_2 \cdots \frac{1}{\Delta\sqrt{\pi}} \mathrm{e}^{-\delta E_1^2/\Delta^2} \cdots \mathrm{e}^{\mathrm{i}t(X - \sum \delta E_n/N)}$$

$$= \frac{1}{2\pi} \int dt\, \mathrm{e}^{\mathrm{i}tX} \left(\frac{1}{\Delta\sqrt{\pi}} \int \delta E_1 \mathrm{e}^{-\delta E_1^2/\Delta^2 - it\delta E_1/N} \right)^N$$

$$= \frac{1}{2\pi} \int dt\, \mathrm{e}^{\mathrm{i}tX} \mathrm{e}^{-\Delta^2 t^2/4N}$$

$$= \frac{\sqrt{N}}{\sqrt{\pi}\Delta} \mathrm{e}^{-X^2 N/\Delta^2}.$$

Problems of Chap. 29

29.1 Deviation from Equilibrium

$$\Omega = \mathrm{e}^{-\Delta U/k_B T} (1 - \mathrm{e}^{\Delta\mu/k_B T}) \frac{\alpha_2}{\alpha_2 + \beta_2}$$

$$\Omega(x) = \mathrm{e}^{(\Delta\mu^0 - \Delta U(x))/k_B T} \frac{\alpha_2(x)}{\alpha_2(x) + \beta_2(x)} \left(K_{eq} - \frac{C(ATP)}{C(ADP)C(P)} \right).$$

For $\Delta\mu \neq 0$ but $\Delta\mu \ll k_B T$ Ω becomes a linear function of $\Delta\mu$

$$\Omega(x) \to -\mathrm{e}^{-\Delta U(x)/k_B T} \frac{\alpha_2(x)}{\alpha_2(x) + \beta_2(x)} \frac{\Delta\mu}{k_B T}$$

whereas in the opposite limit $\Delta\mu \gg k_B T$ it becomes proportional to the concentration ratio

$$\Omega(x) \to -\mathrm{e}^{-\Delta U(x)/k_B T} \frac{\alpha_2(x)}{\alpha_2(x) + \beta_2(x)} \mathrm{e}^{\Delta\mu^0/k_B T} \frac{C(ATP)}{C(ADP)C(P)}.$$

References

1. T.L. Hill, *An Introduction to Statistical Thermodynamics* (Dover publications, New York, 1986)
2. S.Cocco, J.F.Marko, R.Monasson, arXiv:cond-mat/0206238v1
3. C. Storm, P.C. Nelson, Phys. Rev. E **67**, 51906 (2003)
4. K.K. Mueller-Niedebock, H.L. Frisch, Polymer **44**, 3151 (2003)
5. C. Leubner, Eur. J. Phys. **6**, 299 (1985)
6. P.J. Flory, J. Chem. Phys. **10**, 51 (1942)
7. M.L. Huggins, J. Phys. Chem. **46**, 151 (1942)
8. M. Feig, C.L. Brooks III, Curr. Opinion Struct. Biol. **14**, 217 (2004)
9. B. Roux, T. Simonson, Biophys. Chem **78**, 1 (1999)
10. A. Onufriev, Ann. Rep. Comp. Chem. **4**, 125 (2008)
11. M. Born, Z. Phys. **1**, 45 (1920)
12. B. Bagchi, D.W. Oxtoby, G.R. Fleming, Chem. Phys. **86**, 257 (1984)
13. D. Bashford, D. Case, Ann. Rev. Phys. Chem. **51**, 29 (2000)
14. W.C. Still, A. Tempczyk, R.C. Hawley, T. Hendrickson, JACS **112**, 6127 (1990)
15. G.D. Hawkins, C.J. Cramer, D.G. Truhlar, Chem. Phys. Lett. **246**, 122 (1995)
16. M. Schaefer, M. Karplus, J. Phys. Chem. **100**, 1578 (1996)
17. Wonpil Im, M.S. Lee, C.L. Brooks III, J. Comput. Chem. **24,** 1691 (2003)
18. F. Fogolari, A. Brigo, H. Molinari, J. Mol. Recognit. **15**, 377 (2002)
19. A.I. Shestakov, J.L. Milovich, A. Noy, J. Colloid Interface Sci. **247**, 62 (2002)
20. B. Lu, D. Zhang, J.A. McCammon, J. Chem. Phys. **122**, 214102 (2005)
21. P. Koehl, Curr. Opin. Struct. Biol. **16**, 142 (2006)
22. P. Debye, E. Hueckel, Phys. Z. **24**, 305 (1923)
23. G. Gouy, Comt. Rend. **149**, 654 (1909)
24. G. Gouy, J. Phys. **9**, 457 (1910)
25. D.L. Chapman, Phil. Mag. **25**, 475 (1913)
26. O. Stern, Z. Elektrochem. **30**, 508 (1924)
27. A.-S. Yang, M. Gunner, R. Sampogna, K. Sharp, B. Honig, Proteins **15**, 252 (1993)
28. M. Schaefer, M. Sommer, M. Karplus, J. Phys. Chem. B **101**, 1663 (1997)
29. R.A. Raupp-Kossmann, C. Scharnagl, Chem. Phys. Lett. **336**, 177 (2001)
30. H. Risken, *The Fokker-Planck Equation* (Springer, Berlin, 1989)
31. H.A. Kramers, Physica **7**, 284 (1941)
32. P.O.J. Scherer, Chem. Phys. Lett. **214**, 149 (1993)
33. E.W. Montroll, H. Scher, J. Stat. Phys. **9**, 101 (1973)
34. E.W. Montroll, G.H. Weiss, J. Math. Phys. **6**, 167 (1965)

P.O.J. Scherer and S.F. Fischer, *Theoretical Molecular Biophysics*,
Biological and Medical Physics, Biomedical Engineering,
DOI 10.1007/978-3-662-55671-9

35. A.A. Zharikov, P.O.J. Scherer, S.F. Fischer, J. Phys. Chem. **98**, 3424 (1994)
36. A.A. Zharikov, S.F. Fischer, Chem. Phys. Lett. **249**, 459 (1995)
37. S.R. de Groot, P. Mazur, *Irreversible Thermodynamics* (Dover publications, New York, 1984)
38. D.G. Miller, Faraday Discuss. Chem. Soc. **64**, 295 (1977)
39. R. Paterson, Faraday Discuss. Chem. Soc. **64**, 304 (1977)
40. D.E. Goldman, J. Gen. Physiol. **27**, 37 (1943)
41. A.L. Hodgkin, A.F. Huxley, J. Physiol. **117**, 500 (1952)
42. J. Kenyon, How to solve and program the Hodgkin-Huxley equations, http://134.197.54.225/department/Faculty/kenyon/HodgkinHuxley/pdfs/HH_Program.pdf
43. K. Banerjee, B. Das, G. Gangopadhyay, J. Chem. Phys. **138**, 165102 (2013)
44. S. Marzen, H.G. Garcia, R. Philips, J. Mol, Biol. **425**, 1433 (2013)
45. V.J. Hilser, J.O. Wrabl, H.N. Motlagh, Annu. Rev. Biophys. **41**, 585 (2012)
46. J. Monod, J. Wyman, J.P. Changeux, J. Mol. Biol. **12**, 88 (1965)
47. D.E Koshland Jr., G. Nemethy, D. Filmer, Biochemsitry **5**, 365 (1966)
48. J. Vreeken, *A friendly introduction to reaction-diffusion systems*, Internship paper (AILab Zurich, 2002)
49. E. Pollak, P. Talkner, Chaos **15**, 026116 (2005)
50. P.W. Atkins, Phys. Chem. (Freeman & Company, 2006)
51. W.J. Moore, *Basic Physical Chemistry* (Prentice–Hall, 1983)
52. F.T. Gucker, R.L. Seifert, *Physical Chemistry* (W.W. Norton & Company, New York, 1966)
53. S. Glasstone, K.J. Laidler, H. Eyring, *The Theory of Rate Processes* (McGraw-Hill, New York, 1941)
54. K.J. Laidler, *Chemical Kinetics*, 3rd edn. (Harper and Row, New York, 1987)
55. G.A. Natanson, J. Chem. Phys. **94**, 7875 (1991)
56. R.A. Marcus, Ann. Rev. Phys. Chem. **15**, 155 (1964)
57. R.A. Marcus, N. Sutin, Biochim. Biophys. Acta **811**, 265 (1985)
58. R.A. Marcus, Angew. Chem. Int. Ed. Engl. **32**, 1111 (1993)
59. A.M. Kuznetsov, J. Ulstrup, *Electron Transfer in Chemistry and Biology* (Wiley, New York, 1998), p. 49
60. M. Born, K. Huang, *Dynamical Theory of Crystal Lattices* (Oxford University, New York, 1954)
61. J. Deisenhofer, H. Michel, Science **245**, 1463 (1989)
62. J. Deisenhofer, O. Epp, K. Miki, R. Huber, H. Michel, Nature **318**, 618 (1985)
63. J. Deisenhofer, O. Epp, K. Miki, R. Huber, H. Michel, J. Mol. Biol. **180**, 385 (1984)
64. H. Michel, J. Mol. Biol. **158**, 567 (1982)
65. MOLEKEL 4.0, P. Fluekiger, H.P. Luethi, S. Portmann, J. Weber, Swiss National Supercomputing Centre CSCS, Manno (Switzerland, 2000)
66. M. Bixon, J. Jortner, J. Chem. Phys. **48**, 715 (1968)
67. S. Fischer, J. Chem. Phys. **53**, 3195 (1970)
68. K.F. Freed, J. Jortner, J. Chem. Phys. **52**, 6272 (1970)
69. E.N. Economou, *Green's Functions in Quantum Physics* (Springer, Berlin, 1978)
70. A. Nitzan, J. Jortner, J. Chem. Phys. **56**, 3360 (1972)
71. Y. Fujimura, H. Kono, T. Nakajima, J. Chem. Phys. **66**, 199 (1977)
72. S. Matsika, P. Krause, Annu. Rev. Phys. Chem. **62**, 621 (2011)
73. B.R. Henry, W. Siebrand, J. Chem Phys. **54**, 1072 (1971)
74. W. Siebrand, M.Z. Zgierski, Chem. Phys. Lett. **35**, 151 (1975)
75. E.A. Gasilovitch et al., Opt. Spectrosc. **105**, 208 (2008)
76. C.M. Marian, WIREs Comput. Mol. Sci. **2**, 187 (2012)
77. P.W. Anderson, J. Phys. Soc. Jpn. **9**, 316 (1954)
78. R. Kubo, J. Phys. Soc. Jpn. **6**, 935 (1954)
79. R.Kubo, in *Fluctuations, Relaxations and Resonance in Magnetic Systems, D.ter Haar* (New York, Plenum, 1962)
80. M. Baer, Chem. Phys. Lett. **35**, 112 (1975)
81. M. Baer, Molec. Phys. **40**, 1011 (1980)

82. M. Baer, Chem. Phys. **259**, 123 (2000)
83. M. Baer, Phys. Rep. **358**, 75 (2002)
84. G.A. Worth, L.S. Cederbaum, Annu. Rev. Phys. Chem. **55**, 127 (2004)
85. T. Pacher, C.A. Mead, L.S. Cederbaum, H. Köppel, J. Chem. Phys. **91**, 7057 (1989)
86. Conical Intersections, ed. by W. Domcke, D.R. Yarkony, H. Köppel (World Scientific, Singapore, 2004)
87. M. Desouter-Lecomte, J.C. Leclerc, J.C. Lorquet, Chem. Phys. **9**, 147 (1975)
88. H. Köppel, W. Domcke, L.S. Cederbaum, Adv. Chem. Phys. **57**, 59 (1984)
89. C.A. Mead, D.G. Truhlar, J. Chem. Phys. **77**, 6090 (1982)
90. A.D. McLachlan, Mol. Phys. **4**, 417 (1961)
91. T.G. Heil, A. Dalgarno, J. Phys. B **12**, 557 (1979)
92. L.D. Landau, Phys. Z. Sowjetun. **1**, 88 (1932)
93. C. Zener, Proc. Roy. Soc. A **137**, 696 (1932)
94. W. Domcke, H. Köppel, L.S. Cederbaum, Mol. Phys. **43**, 851 (1983)
95. G.J. Atchity, S.S. Xantheas, K. Ruedenberg, J. Chem. Phys. **95**, 1862 (1991)
96. G. Herzberg, H.C. Longuet-Higgins, Discuss. Faraday Soc. **35**, 77 (1963)
97. H.C. Longuet-Higgins, U. Opik, M.H.L. Price, R.A. Sack, Proc. R. Soc. A - Math. Phys. **244**, 1 (1958)
98. M.V. Berry, Proc. R. Soc. A - Math. Phys. **392**, 45 (1984)
99. R. Gherib, Ilya G. Ryabinkin, A.F. Izmaylov, arXiv:1501.06816v2 [physics.chem-ph] 3 Mar 2015
100. C.A. Langhoff, G.W. Robinson, Mol. Phys. 26, 249 (1973). Mol. Phys. **29**, 61 (1975)
101. F. Metz, Chem. Phys. **9**, 121 (1975)
102. H. Scheer, W.A. Svec, B.T. Cope, M.H. Studler, R.G. Scott, J.J. Katz, JACS **29**, 3714 (1974)
103. A. Streitwieser, *Molecular Orbital Theory for Organic Chemists* (Wiley, New York, 1961)
104. J.E. Lennard-Jones, Proc. R. Soc. Lond. Ser. A **158** (1937)
105. B. Hudson, B. Kohler, Synth. Metals **9**, 241 (1984)
106. B.S. Hudson, B.E. Kohler, K. Schulten, in *E.C*, ed. by Excited States (Lin (Academic, New York, 1982), pp. 1–95
107. B.E. Kohler, C. Spangler, C. Westerfield, J. Chem. Phys. **89**, 5422 (1988)
108. T. Polivka, J.L. Herek, D. Zigmantas, H.-E. Akerlund, V. Sundstrom, Proc. Natl. Acad. Sci. USA **96**, 4914 (1999)
109. B.E. Kohler, J. Chem. Phys. **93**, 5838 (1990)
110. W.T. Simpson, J. Chem. Phys. **17**, 1218 (1949)
111. H. Kuhn, J. Chem. Phys. **17**, 1198 (1949)
112. M. Gouterman, J. Mol. Spectrosc. **6**, 138 (1961)
113. M. Gouterman, J. Chem. Phys. **30**, 1139 (1959)
114. M. Gouterman, G.H. Wagniere, L.C. Snyder, J. Mol. Spectrsoc. **11**, 108 (1963)
115. C. Weiss, *The Porphyrins*, vol. III (Academic press, 1978), p. 211
116. D. Spangler, G.M. Maggiora, L.L. Shipman, R.E. Christofferson, J. Am. Chem. Soc. **99** (1977)
117. M.W. Schmidt, K.K. Baldridge, J.A. Boatz, S.T. Elbert, M.S. Gordon, J.J. Jensen, S. Koseki, N. Matsunaga, K.A. Nguyen, S. Su, T.L. Windus, M. Dupuis, J.A. Montgomery, J. Comput. Chem. **14**, 1347 (1993)
118. B.R. Green, D.G. Durnford, Ann. Rev. Plant Physiol. Plant Mol. Biol. **47**, 685 (1996)
119. H.A. Frank et al., Pure Appl. Chem. **69**, 2117 (1997)
120. R.J. Cogdell et al., Pure Appl. Chem. **66**, 1041 (1994)
121. T. Förster, Ann. Phys. **2**, 55 (1948)
122. T. Förster, Disc. Faraday Trans. **27**, 7 (1965)
123. D.L. Dexter, J. Chem. Phys. **21**, 836 (1953)
124. D.L. Andrews, Chem. Phys. **135**, 195 (1989)
125. R.C. Hilborn, Am. J. Phys. **50**, 982 (1982). (Revised 2002)
126. S.H. Lin, Proc. R. Soc. Lond. Ser. A **335**, 51 (1973)
127. S.H. Lin, W.Z. Xiao, W. Dietz, Phys. Rev. E **47**, 3698 (1993)
128. E.W. Knapp, P.O.J. Scherer, S.F. Fischer, BBA **852**, 295 (1986)

129. P.O.J. Scherer, S.F. Fischer, in *Chlorophylls*, ed. by H. Scheer (CRC Press, Boca Raton, 1991), pp. 1079–1093
130. R.J. Cogdell, A. Gall, J. Koehler, Quart. Rev. Biophys. **39**(227), 227 (2006)
131. M. Ketelaars et al., Biophys. J. **80**, 1591 (2001)
132. M. Matsushita et al., Biophys. J. **80**, 1604 (2001)
133. K. Sauer, R.J. Cogdell, S.M. Prince, A. Freer, N.W. Isaacs, H. Scheer, Photochem. Photobiol. **64**, 564 (1996)
134. A. Freer, S. Prince, K. Sauer, M. Papitz, A. Hawthorntwaite-Lawless, G. McDermott, R. Cogdell, N.W. Isaacs, in *The Antenna Complex of the Photosynthetic Bacterium Rhodopseudomonas Acidophila Structure*, vol. 4 (London, 1996), p. 449
135. M.Z. Papiz, S.M. Prince, A. Hawthorntwaite-Lawless, G. McDermott, A. Freer, N.W. Isaacs, R.J. Cogdell, Trends Plant Sci. **1**, 198 (1996)
136. G. McDermott, S.M. Prince, A. Freer, A. Hawthorntwaite-Lawless, M. Papitz, R. Cogdell, Nature **374**, 517 (1995)
137. N.W. Isaacs, R.J. Cogdell, A. Freer, S.M. Prince, Curr. Opin. Struct. Biol. **5**, 794 (1995)
138. E.E. Abola, F.C. Bernstein, S.H. Bryant, T.F. Koetzle, J. Weng, Protein Data Bank, in *Crystallographic Databases - Information Content, Software Systems, Scientific Applications*, eds. by F.H. Allen, G. Bergerhoff, R. Sievers, (Data Commission of the International Union of Crystallography, Bonn, 1987)p. 107
139. F.C. Bernstein, T.F. Koetzle, G.J.B. Williams, E.F. Meyer Jr., M.D. Brice, J.R. Rodgers, O. Kennard, T. Shimanouchi, M. Tasumi, J. Mol. Biol. **112**, 535 (1977)
140. R. Sayle, E.J. Milner-White, Trends Biochem. Sci. (TIBS) **20**, 374 (1995)
141. Y. Zhao, M.-F. Ng, G. Chen, Phys. Rev. E **69**, 032902 (2004)
142. H. van Amerongen, R. van Grondelle, J. Phys. Chem. B **105**, 604 (2001)
143. C. Hofmann, T.J. Aartsma, J. Köhler, Chem. Phys. Lett. **395**, 373 (2004)
144. S.E. Dempster, S. Jang, R.J. Silbey, J. Chem. Phys. **114**, 10015 (2001)
145. S. Jang, R.J. Silbey, J. Chem. Phys. **118**, 9324 (2003)
146. K. Mukai, S. Abe, Chem. Phys. Lett. **336**, 445 (2001)
147. R.G. Alden, E. Johnson, V. Nagarajan, W.W. Parson, C.J. Law, R.G. Cogdell, J. Phys. Chem. B **101**, 4667 (1997)
148. V. Novoderezhkin, R. Monshouwer, R. van Grondelle, Biophys. J. **77**, 666 (1999)
149. M.K. Sener, K. Schulten, Phys. Rev. E **65**, 31916 (2002)
150. M. Fujitsuka, T. Majima, PCCP **14**, 11234 (2012)
151. J.C. Genereux, J.K. Barton, Chem. Rev. **110**, 1642 (2010)
152. M. Bixon, B. Giese, S. Wessely, T. Langenbacher, M.E. Michel-Beyerle, J. Jortner, PNAS **96**, 11713 (1999)
153. M. Gutman, Structure **12**, 1123 (2004)
154. P. Mitchell, Biol. Rev. Camb. Philos. Soc. **41**, 445 (1966)
155. H. Luecke, H.-T. Richter, J.K. Lanyi, Science **280**, 1934 (1998)
156. R. Neutze et al., BBA **1565**, 144 (2002)
157. D. Borgis, J.T. Hynes, J. Chem. Phys. **94**, 3619 (1991)
158. A. Warshel, S. Creighton, W.W. Parson, J. Phys. Chem. **92**, 2696 (1988)
159. M. Plato, C.J. Winscom, in *The Photosynthetic Bacterial Reaction Center*, ed. by J. Breton, A. Vermeglio (Plenum, New York, 1988), p. 421
160. P.O.J. Scherer, S.F. Fischer, Chem. Phys. **131**, 115 (1989)
161. L.Y. Zhang, R.A. Friesner, Proc. Natl. Acad. Sci. USA **95**, 13603 (1998)
162. S.F. Fischer, R.P. van Duyne, Cem. Phys. **5**, 183 (1974)
163. E.W. Schlag, S. Schneider, S.F. Fischer, Ann. Rev. Phys. Chem. **12**, 465 (1971)
164. P. Huppman, T. Arlt, H. Penzkofer, S. Schmidt, M. Bibikova, B. Dohse, D. Oesterhelt, J. Wachtveitl, W. Zinth, Biophys. J. **82**, 3186 (2002)
165. C. Kirmaier, D. Holten, Proc. Natl. Acad. Sci. **97**, 3522 (1990)
166. M. Bixon J. Jortner, Adv. Chem. Phys. **106**, 35 (1999)
167. H. Sumi, T. Kakitani, Chem. Phys. Lett. **252**, 85 (1996)

168. K. Wynne, G. Haran, G.D. Reid, C.C. Moser, P.L. Dutton, R.M. Hochstrasser, J. Phys. Chem **100**, 5140 (1990)
169. C. Kirmaier, D. Holten, W.W. Parson, Biochim. Biophys. Acta **810**, 33 (1985)
170. P.O.J. Scherer, S.F. Fischer, Spectrochimica acta Part A **54**, 1191 (1998)
171. P.O.J. Scherer, S.F. Fischer, in *Perspectives in Photosynthesis*, ed. by J. Jortner, P. Pullmann (Kluwer, 1990), p. 361
172. F.Y. Jou, G. Freeman, Can. J. Chem. **54**, 3694 (1996)
173. A.A. Zharikov, S.F. Fischer, J. Chem. Phys. **124**, 054506 (2006)
174. L.M. McDowell, C. Kirmaier, D. Holten, J. Phys. Chem. **95**, 3379 (1991)
175. C. Kirmaier, C. He, D. Holten, Biochem. **40**, 12132 (2001)
176. J.L. Martin, G.R. Fleming, J. Lambry, Biochem. **27**, 8276 (1988)
177. J.L. Martin, J. Breton, A.J. Hoff, A. Migus, A. Antonetti, Proc. Natl. Acad. Sci. U.S.A. **83**, 957 (1986)
178. P.O.J. Scherer, S.F. Fischer, in *Chlorophylls*, ed. by H. Scheer (CRC Press, Boca Raton, 1991), p. 1079
179. J.L. Chuang, S.G. Boxer, D. Holten, C. Kirmaier, Biochemistry **45**, 3845 (2006)
180. T. Arlt, S. Schmidt, W. Kaiser, C. Lauterwasser, M. Meyer, H. Scheer, W. Zinth, Proc. Natl. Acad. Sci. USA **90**, 11757 (1993)
181. V.A. Shuvalov, A.G. Yakolev, FEBS Lett. **540**, 26 (2003)
182. T.R. Middendorf, L.T. Mazzola, K. Lao, M.A. Steffen, S.G. Boxer, Biocim et Biophys. Acta **1143**, 223 (1993)
183. P.O.J. Scherer, S.F. Fischer, Chem. Phys. Lett. **141**, 179 (1987)
184. P. Huppman, S. Spörlein, M. Bibikova, D. Oesterhelt, J. Wachtveitl, W. Zinth, J. Phys. Chem A **107**, 8302 (2003)
185. F. Juelicher, in *Transport and Structure: Their Competitive Roles in Biophysics and Chemistry*. Lecture Notes in Physics, ed. by S.C. Müller, J. Parisi, W. Zimmermann (Springer, Berlin, 1999)
186. A. Parmeggiani, F. Juelicher, A. Ajdari, J. Prost, Phys. Rev. E **60**, 2127 (1999)
187. F. Jülicher, A. Ajdari, J. Prost, Rev. Mod. Phys. **69**, 1269 (1997)
188. F. Jülicher, J. Prost, Progr. Theor. Phys. Suppl. **130**, 9 (1998)
189. J. Prost, J.F. Chauwin, L. Peliti, A. Ajdari, Phys. Rev. Lett. **72**, 2652 (1994)
190. R. Lipowski, T. Harms, Eur. Biophys, J. **29**, 452 (2000)
191. R. Lipowski, in Stochastic Processes, in *Physics, Chemistry and Biology*, Lecture Notes in Physics, ed. by J.A. Freund, T. Pöschel, vol. 557, (Springer, Berlin, 2000), pp. 21–31
192. P. Reimann, Phys. Rep. **361**, 57 (2002)
193. D. Keller, C. Bustamante, Biophys. J. **78**, 541 (2000)
194. Hong Qian, J. Math. Chem. **27**, 219 (2000)
195. J. Howard, Annu. Rev. Physiol. **58**, 703 (1996)
196. S.M. Block, J. Cell Biol. **140**, 1281 (1998)
197. K. Svodoba, C.F. Schmidt, B.J. Schnapp, S.M. Block, Nature **365**, 721 (1993)
198. S. Leibler, D.A. Huse, J. Cell Biol. **121**, 1357 (1993)
199. M.E. Fisher, A.B. Kolomeisky, arXiv:cond-mat/9903308v1
200. Mermin, J. Math. Phys. **7**, 1038 (1966)

Index

P.O.J. Scherer and S.F. Fischer, *Theoretical Molecular Biophysics*,
Biological and Medical Physics, Biomedical Engineering,
DOI 10.1007/978-3-662-55671-9